HORIZON
NUCLEAR POWER

WYLFA NEWYDD

ENERGY WORKING FOR BRITAIN

Wylfa Newydd Project

6.4.32 ES Volume D - WNDA Development App D8-7 - Surface water and groundwater modelling results (Part 7/7)

PINS Reference Number: EN010007

Application Reference Number: 6.4.32

June 2018

Revision 1.0

Regulation Number: 5(2)(a)

Planning Act 2008
Infrastructure Planning (Applications: Prescribed Forms and Procedure) Regulations 2009

Horizon Internal DCRM Number: WN0902-JAC-PAC-APP-00019

[This page is intentionally blank]

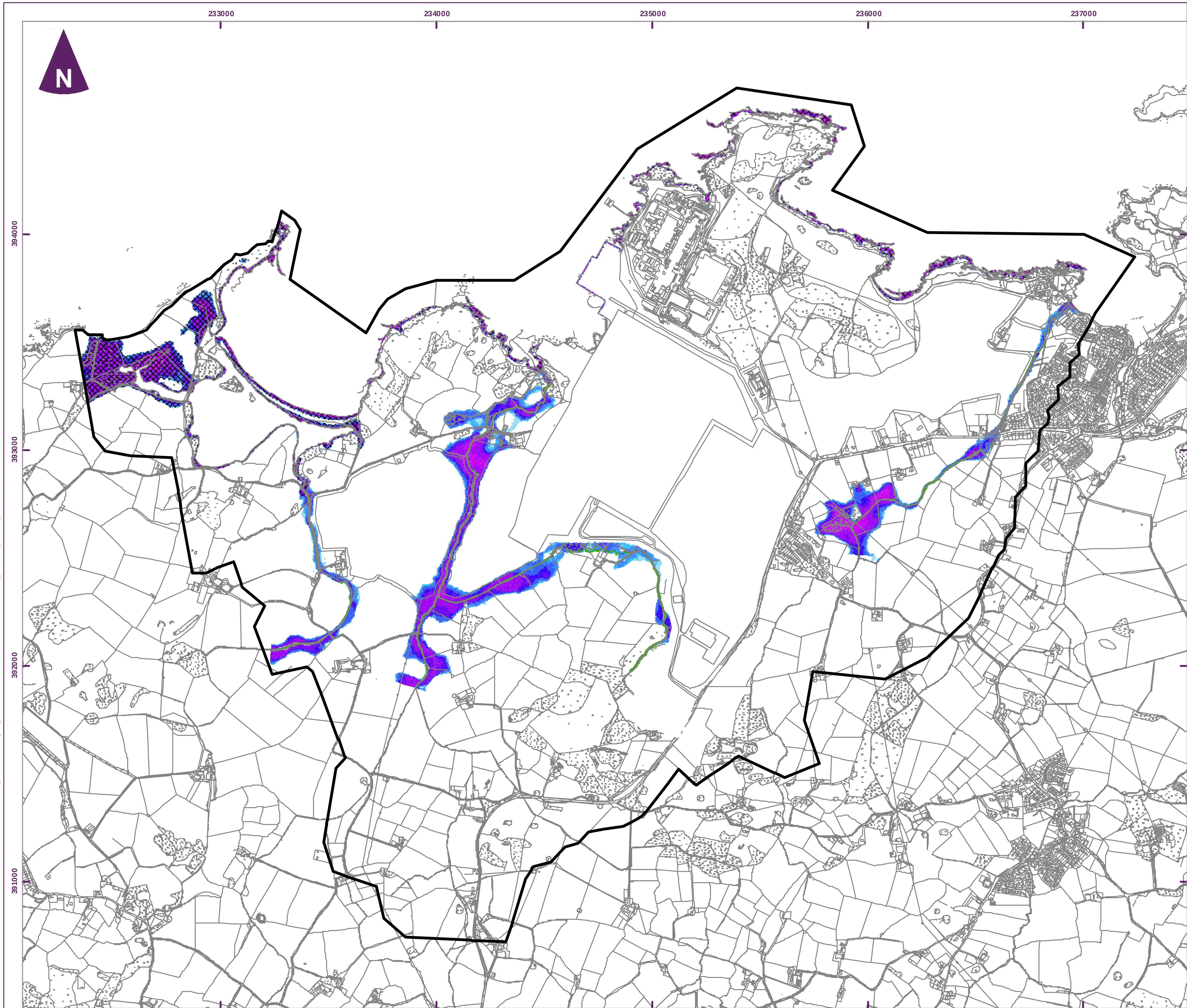

Key

Peak flood depth (m)
Reference Point 5
1 : 1000 year AEP fluvial
Climate change 2180s - reasonably foreseeable

- 0.01 - 0.05
- 0.05 - 0.10
- 0.10 - 0.25
- 0.25 - 0.50
- 0.50 - 0.75
- 0.75 - 1.00
- 1.00 - 1.50
- 1.50 - 2.00
- > 2.00
- Model boundary
- MHWS Extent 2180s
- Model river centreline

Notes:
The depths represent the maximum depth achieved. The flood prediction does not represent a moment in time as maximum depths can be achieved at different times.

Model run date: 10/05/2017
Corresponding data:
35989-C1277i2_DCO_Phase5_F1000_2180sRF.xlsx

Meters
0 250 500 750 1,000
Scale at A3

Wylfa Newydd
DCO
Hydraulic Modelling

amec foster wheeler

Figure 91
DCO Reference Point 5 peak fluvial depth 1:1000 year AEP climate change 2180s - reasonably foreseeable

file: H:\Projects\35989 Wylfa NNB Modelling\Design\Task 28 - Hydrological Modelling\Figures DCO\MXDs\35989-Lon420i2 - DCO_Phase5_F1000_2180sRF.mxd

NOT PROTECTIVELY MARKED

May 2017 35989-Lon420i2 caldi

Appendix C
Topography comparison

This Appendix presents a selection of figures which were created to compare the surveyed topography associated with cross sections along the reaches (filled in brown) to the 1m LIDAR DTM grid (purple line). This was used to verify the use of the LiDAR data to support the 1D river reach modelling, notably bank levels. Most sections show good agreement between the LiDAR elevation and the surveyed elevation of the banks. There are no consistent differences or trends between sections, suggesting the LiDAR has no systematic offset, and is representative of the ground topography.

Table C.1 Comparison sections along Afon Cafnan

Afon Cafnan section 'CAFN_00' 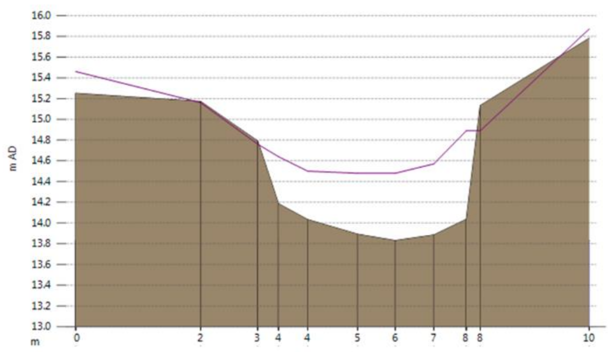	**Afon Cafnan section 'CAFN_10'** 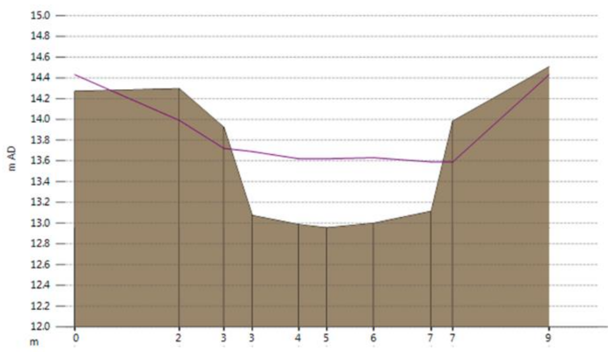
Afon Cafnan section 'CAFN_15' 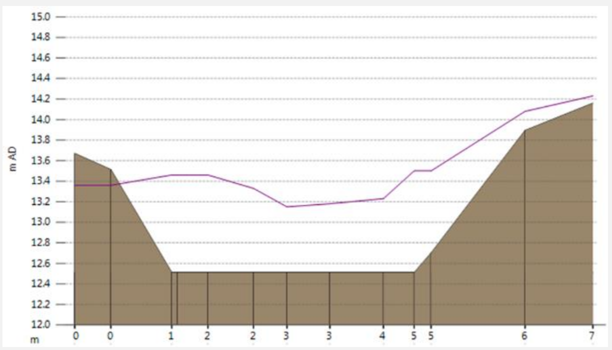	Afon Cafnan section 'CAFN_25' 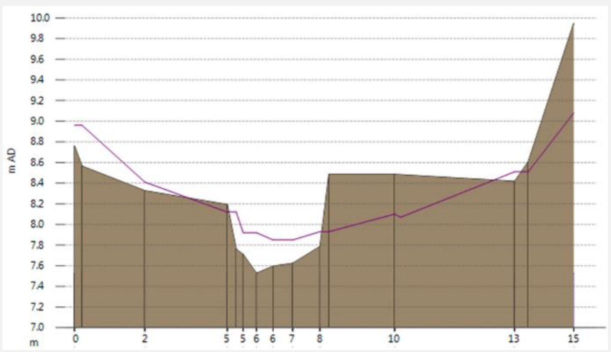
Afon Cafnan section 'CAFN_30' 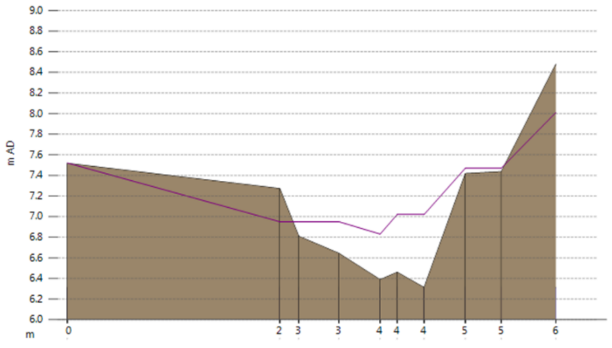	Afon Cafnan section 'CAFN_40' 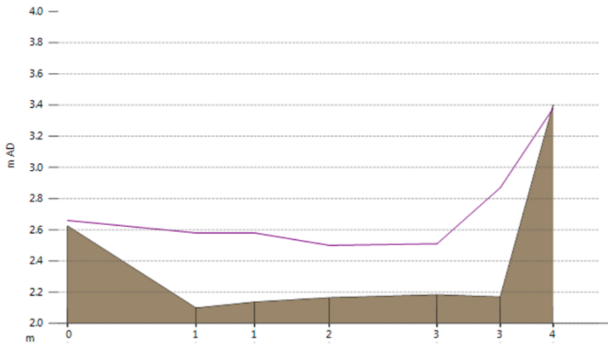

Table C.2 Comparison sections along Caerdegog Isaf

Caerdegog Isaf section 'CAER_01n'

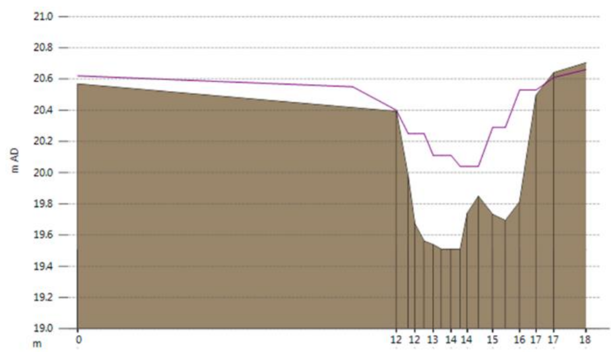

Caerdegog Isaf section 'CAER_04n'

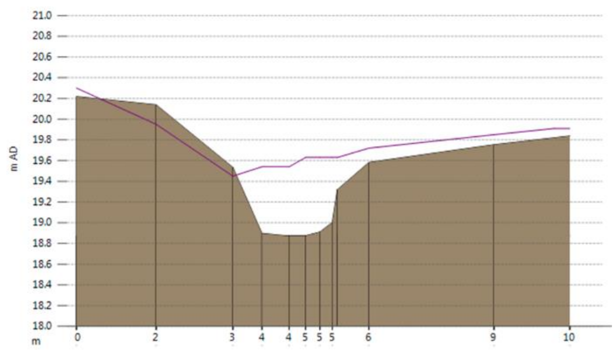

Caerdegog Isaf section 'CAER_12n'

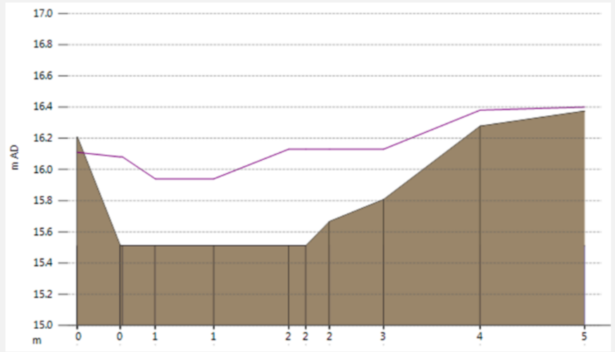

Caerdegog Isaf section 'CAER_18n'

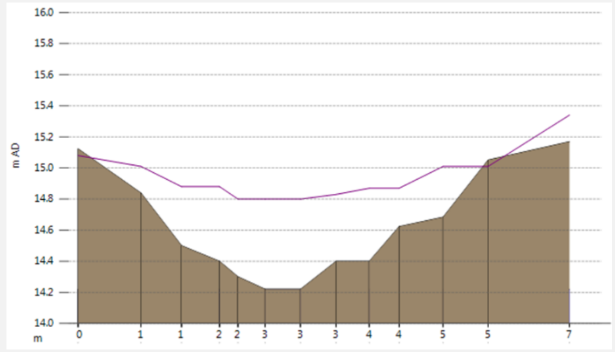

Table C.3 Comparison sections along Cemaes Stream

Cemaes Stream section 'CEMA_02n'

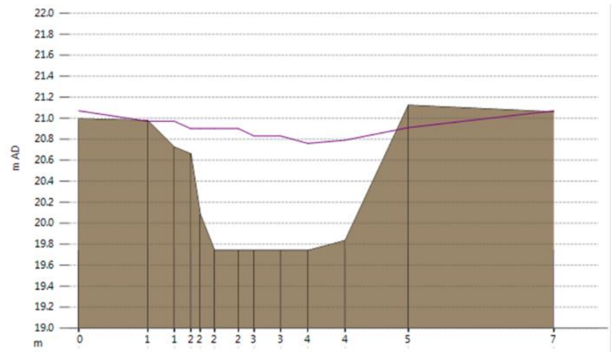

Cemaes Stream section 'CEMA_10n'

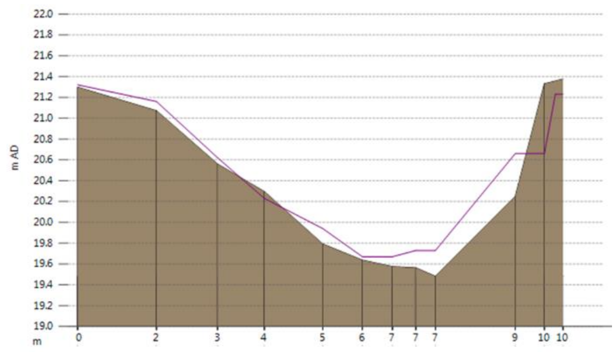

Cemaes Stream section ‘CEMA_14n’	Cemaes Stream section ‘CEMA_20n’
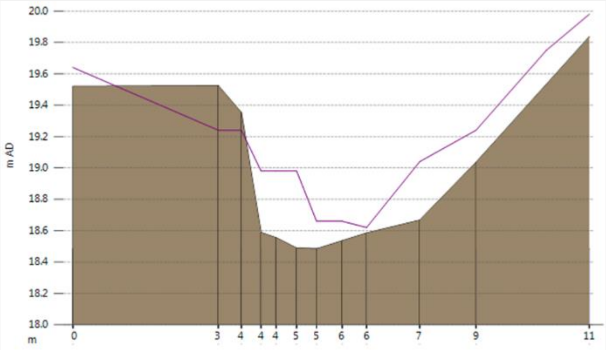	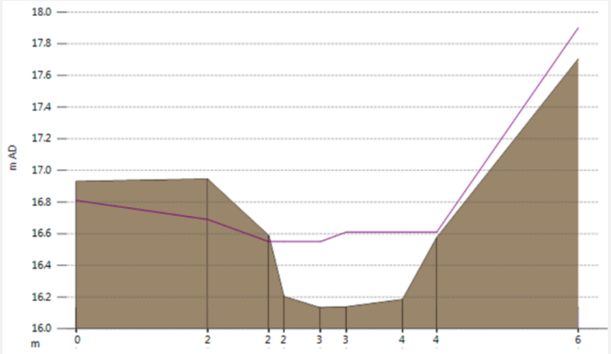

Table C.4 Comparison sections along Cemlyn Stream

Cemlyn Stream section ‘CEML_13’	Cemlyn Stream section ‘CEML_08’
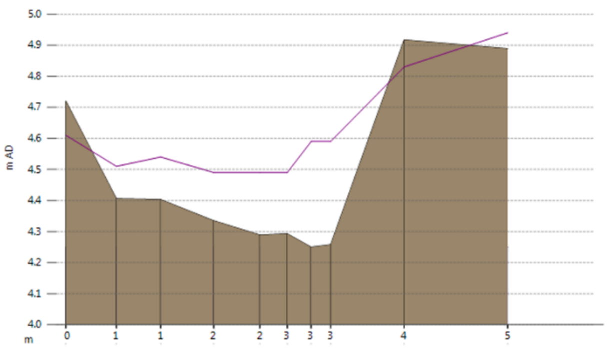	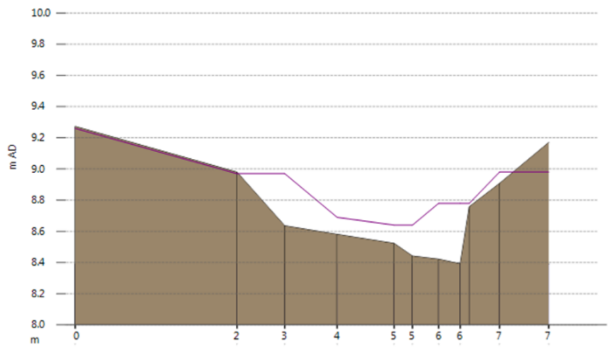
Cemlyn Stream section ‘CEML_04’	Cemlyn Stream section ‘CEML_01’
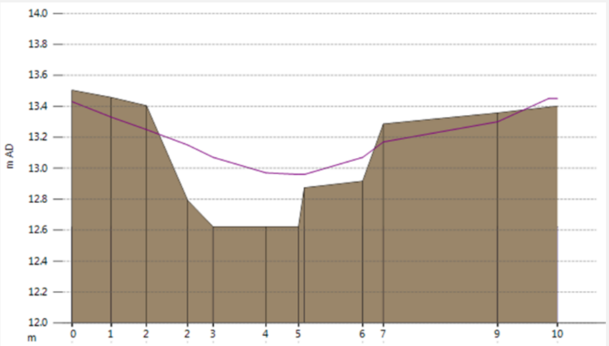	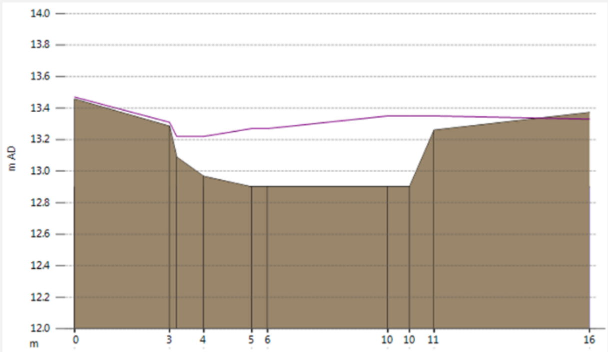

Appendix D
River reach roughness representation

Manning's roughness values have been determined using definitions detailed in Chow (1959). The table below shows a selection of cross sections from the baseline model, the roughness values chosen for the cross sections, along with associated photographs taken on site.

Watercourse	Model section	Manning's n roughness values used	Photograph
Cemlyn Stream	XS0	0.07	
Cemlyn Stream	XS1	0.035 (floodplain) and 0.07	
Cemlyn Stream	XS3	0.035 (floodplain) and 0.07	
Cemlyn Stream	XS4	0.035 (floodplain) and 0.07	

Watercourse	Model section	Manning's n roughness values used	Photograph
Cemlyn Stream	XS6	0.035 (floodplain) and 0.07	 
Cemlyn Stream	XS10	0.035 (floodplain) and 0.05	
Cemlyn Stream	XS13	0.035 (floodplain) and 0.07	
Cemlyn Stream	XS15	0.035 (floodplain), 0.02 (tree/scrub lined bank) and 0.07	

Watercourse	Model section	Manning's n roughness values used	Photograph
Cemlyn Stream	XS19	0.035 (floodplain), and 0.07	
Caerdegog Isaf	XS0	0.05 (floodplain), and 0.07	 4
Caerdegog Isaf	XS3	0.05 (floodplain), and 0.07	
Caerdegog Isaf	XS7	0.035 (floodplain), and 0.07	
Caerdegog Isaf	XS11	0.035 (floodplain), and 0.045	

Watercourse	Model section	Manning's n roughness values used	Photograph
Caerdegog Isaf	XS13	0.035 (floodplain), and 0.07	
Caerdegog Isaf	XS14	0.1 (floodplain), and 0.07	
Caerdegog Isaf	XS15	0.035 (floodplain), and 0.07	
Caerdegog Isaf	XS19	0.035 (floodplain), and 0.045	
Afon Cafnan	XS0	0.05 (scrub-lined bank), and 0.04	

Watercourse	Model section	Manning's n roughness values used	Photograph
Afon Cafnan	XS4	0.05 (scrub-lined bank), and 0.04	
Afon Cafnan	XS10	0.04	
Afon Cafnan	XS20	0.04	
Afon Cafnan	XS26	0.04 -0.05	
Afon Cafnan	XS31/XS32	0.05	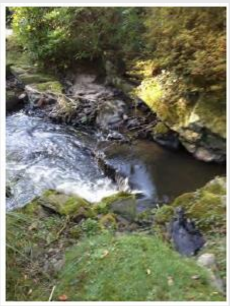

Watercourse	Model section	Manning's n roughness values used	Photograph
Afon Cafnan	XS36	0.05	
Cemaes Stream	XS0	0.05 (floodplain), and 0.075	
Cemaes Stream	XS6	0.05 (floodplain), and 0.045	
Cemaes Stream	XS9/XS10	0.05	
Cemaes Stream	XS17	0.07	

Watercourse	Model section	Manning's n roughness values used	Photograph
Cemaes Stream	XS20	0.05 (rough grass bank), 0.04	

Appendix E
Hydrology factual report

Horizon Nuclear Power

Wylfa Newydd Main Site, Anglesey, NW Wales

Hydrology Assessment Report

September 2017

Amec Foster Wheeler UK Limited

Report for

Horizon Nuclear Power
Sunrise House
1420 Charlton Court
Gloucester Business Park
Delta Way
Gloucester
GL3 4AE

Main contributors

Peter Duffell
Lianne Grogan
Bidur Ghimire

Issued by

....
Peter Duffell

Approved by

....
Bidur Ghimire

Amec Foster Wheeler

Floor 12
25 Canada Square
Canary Wharf
London E14 5LB
United Kingdom
Tel +44 (0) 203 215 1610

Doc Ref. 35989C1415_V3

\\att5-fs7\shared2\projects\35989 wlyfa nnb modelling\design\task 45 dco rev2\task sheet 4 - mainsite\overall reporting\appendix e\x-mod-207017-0000-aa40-rpt-0001 appendix e v3_final.docx

Copyright and non-disclosure notice

Third-party disclaimer

Management systems

This document has been produced by Amec Foster Wheeler Environment & Infrastructure UK Limited in full compliance with the management systems, which have been certified to ISO 9001, ISO 14001 and OHSAS 18001 by LRQA.

Document revisions

No.	Details	Date
1	Draft	07/06/2017
2	Post Stage 2.4 Peer Review	13/09/2017
3	January 2018 Final	22/01/2018

Contents

1. About this report

1.1 Purpose and applicability

Hydraulic modelling is being undertaken to support various assessments being undertaken to underpin the Environmental Statement (ES), Flood Consequence Assessment (FCA), Habitat Regulations Assessment (HRA) and water discharge permit applications associated with the Wylfa Newydd nuclear new build project. This report has been produced for the purpose of describing the pluvial and fluvial hydrology assessment undertaken to support hydraulic modelling for the Wylfa Newydd Main Site. This report details the methodologies applied, the data inputs and the assumptions made in the process, and provides the hydrological inputs to the Main Site InfoWorks ICM hydraulic model (referred to hereafter as the 'InfoWorks ICM hydraulic model'). The scope of this report is confined to describing how hydrological inputs have been developed for model scenarios representing baseline conditions and the proposed construction and operation phases.

1.2 Responsible parties

Both Amec Foster Wheeler and Horizon Nuclear Power have specific responsibilities to deliver as part of the hydrology assessment. These are described in Table 1.1.

Table 1.1 Responsible party descriptions

Responsible party	Description
Amec Foster Wheeler	Are responsible for all the hydrology assessments undertaken to calculate inflows to the hydraulic modelling. Amec Foster Wheeler are also responsible for all the hydraulic modelling documented in this report. Amec Foster Wheeler are not responsible for, and have no involvement in, the development of the scope of the proposed construction and operation phases or the design of any mitigation measures which are proposed and incorporated in the hydraulic modelling.
Horizon Nuclear Power	Are responsible for providing scheme designs for incorporation into the hydraulic modelling.

1.3 Scope

The scope of the work documented in this report is confined to:

- describing the surface water context around Wylfa Newydd Main Site;
- presenting the method for hydrological assessment;
- testing of specific input parameters, such as season and storm duration, to confirm appropriate parameters for the assessment; and
- documentation of a factual account of the approaches deployed and the results produced by the hydrological assessment for the required model scenarios.

Interpretation and assessment of the results is outside the scope of this report.

1.4 Structure of this report

The remainder of this report is structured as follows:

- Section 2 describes the hydrological context;

- Section 3 presents the required model scenarios, including consideration of climate change;
- Section 4 describes the methodology; and
- Section 5 provides the results of the hydrological assessment, for use in the InfoWorks ICM hydraulic model.
- Section 6 provides details and summary results of FEH sensitivity testing into the permeable catchment adjustment.

2. Hydrology context

2.1 Watercourses

There are three surface water catchments within the InfoWorks ICM hydraulic model area: the Cemlyn Stream in the west; the Afon Cafnan and tributary Caerdegog Isaf in the centre; and the Cemaes Stream in the east. The area of land immediately around the existing Wylfa Power Station, to the west of the Cemaes Stream and northeast of the Afon Cafnan catchment, does not contain any significant watercourses and drains directly to the Irish Sea. All three watercourses flow generally northwards and outflow to the Irish Sea (at Cemlyn Bay, Porth y Pistyll and Cemaes Bay, respectively). The upstream areas of these catchments extend outside (south of) the InfoWorks ICM hydraulic model boundary.

The catchments associated with each of these three watercourses are referred to hereafter as ‘watercourse catchments’ to distinguish them from the sub-catchments created for the hydrological assessment. The three watercourse catchments, including the Caerdegog Isaf, are displayed on Figure 2.1 (at the end of Section 2) to their outfall at the Irish Sea and catchment descriptors from Flood Estimation Handbook (FEH) Web Service (CEH, 2016) are given in Table 2.1.

Table 2.1 Watercourse catchment descriptors from FEH Web Service

Descriptor	Cemlyn Stream	Afon Cafnan	Cemaes Stream
National Grid Reference (NGR) at Downstream Point of Catchment	SH 33350 93000	SH 34500 93350	SH 36900 93700
Catchment Area (km^2)	2.72	9.98	2.73
BFIHOST	0.477	0.465	0.425
SAAR (mm/year)	937	969	951
FARL	1	0.95	1
SPRHOST	40.1	40	40.32
URBEXT2000	0.0055	0.0021	0.0191
PROPWET	0.45	0.45	0.45

Source: FEH Web Service (CEH, 2016)

These catchment descriptors were reviewed as part of the hydrology assessment, described in Section 4.3.

2.2 Sub-catchments

The watercourse catchments were split into sub-catchments for representation in the InfoWorks ICM hydraulic model for two reasons: to isolate the Caerdegog Isaf tributary from the Afon Cafnan; and to isolate parts of the catchments in which construction and operation works are to take place. This allows changes in river flows to be applied only in the affected river reaches and not in the whole catchment, as well as more specifically representing works areas. This approach results in several sub-catchments being nested within each watercourse catchment.

A total of eight sub-catchments were identified (numbered 2–9) as listed in Table 2.2. These sub-catchments are shown with the watercourse catchments on Figure 2.1 and with topography on Figure 2.2. As the assessment progressed Sub-catchment 1, representing the Cemlyn Stream, was replaced by Sub-catchments 8 and 9 to isolate works downstream of Nanner Bridge, and consequently is not discussed further. The downstream hydrology assessment points for Sub-catchments 2 to 9 are also shown on Figure 2.1.

Table 2.2 Description of sub-catchments

Catchment	Watercourse	Location	DCO Catchment ID	Downstream NGR	Rationale
Cemlyn Stream	Cemlyn Stream	Upstream of Nanner Bridge	Sub-catchment 9	SH 33450 92100	Isolate area without works
		Downstream of Nanner Bridge	Sub-catchment 8	SH 33350 93000	Residual area with works
Afon Cafnan	Afon Cafnan	Upstream reach	Sub-catchment 3	SH 33950 92250	Isolate area without works
		Downstream reach	Sub-catchment 2	SH 34500 93350	Residual area with works
	Caerdegog Isaf	Upstream reach	Sub-catchment 5	SH 34950 92550	Isolate Caerdegog Isaf and split works area within
		Downstream reach	Sub-catchment 4	SH 34050 92300	Isolate Caerdegog Isaf and split works area within
Cemaes Stream	Cemaes Stream	Upstream of A5025	Sub-catchment 7	SH 36500 93000	Split work area within
		Downstream of A5025	Sub-catchment 6	SH 36900 93700	Split work area within

The model scenarios to be applied to the sub-catchments are defined in Section 3. The derivation of sub-catchment descriptors and the parameters applied to them to derive rainfall depths and flows for the model scenarios are described in Section 4.

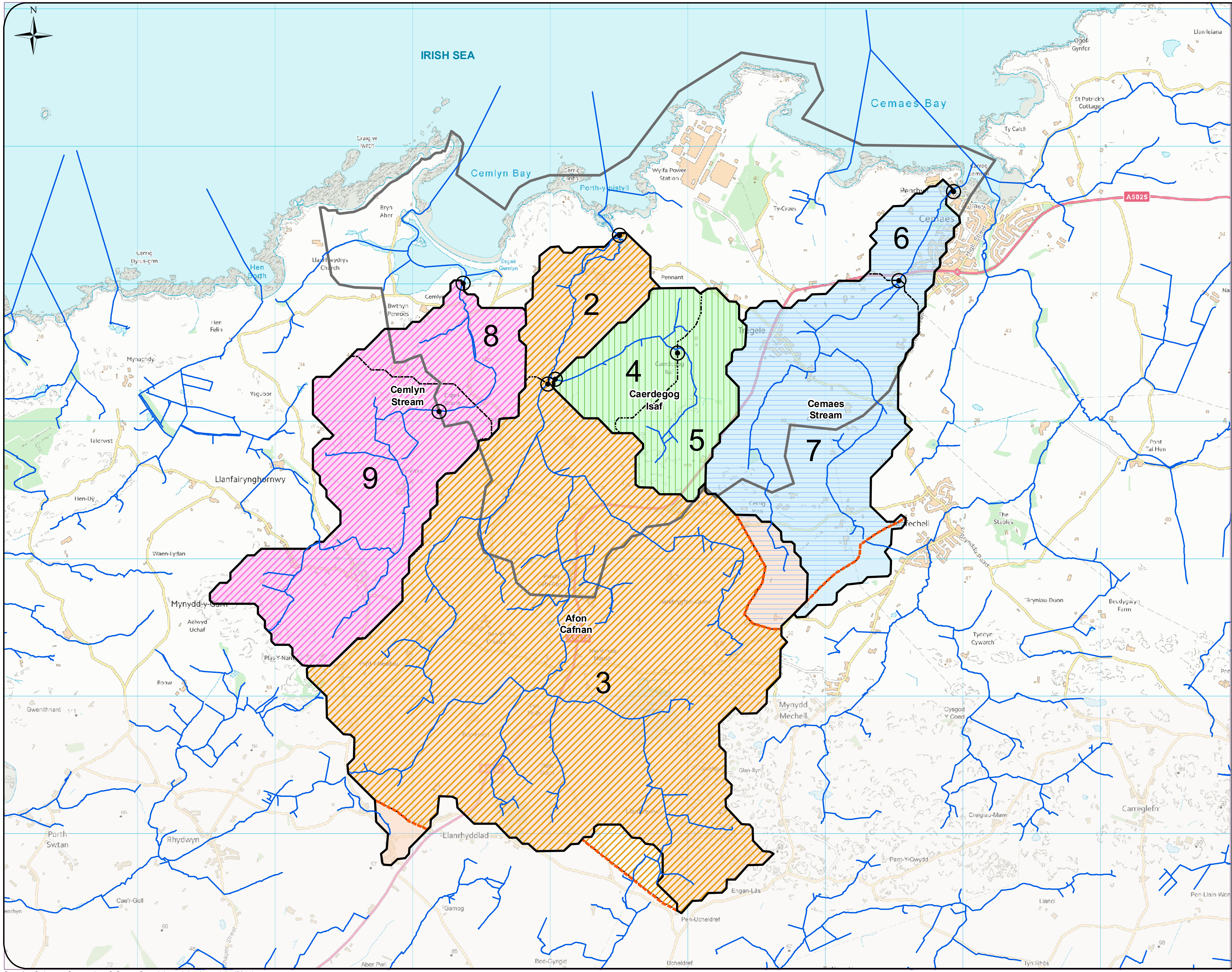

LEGEND

Hydraulic model boundary

Detailed river network

Downstream sub-catchment hydrology assessment points

FEH Hydrology Catchments

Afon Cafnan

Caerdegog Isaf

Cemaes Stream

Cemlyn Stream

FEH Catchment boundaries amended with Panorama 50m data

2-9 Sub-catchments

Figure 2.1
Hydrology catchments & assessment points

Wylfa Newydd Main Site
DCO Hydrology Assessment Report

Scale: 1:25,000
When printed at A3
0 200 400 600 800 1,000 M

HORIZON NUCLEAR POWER

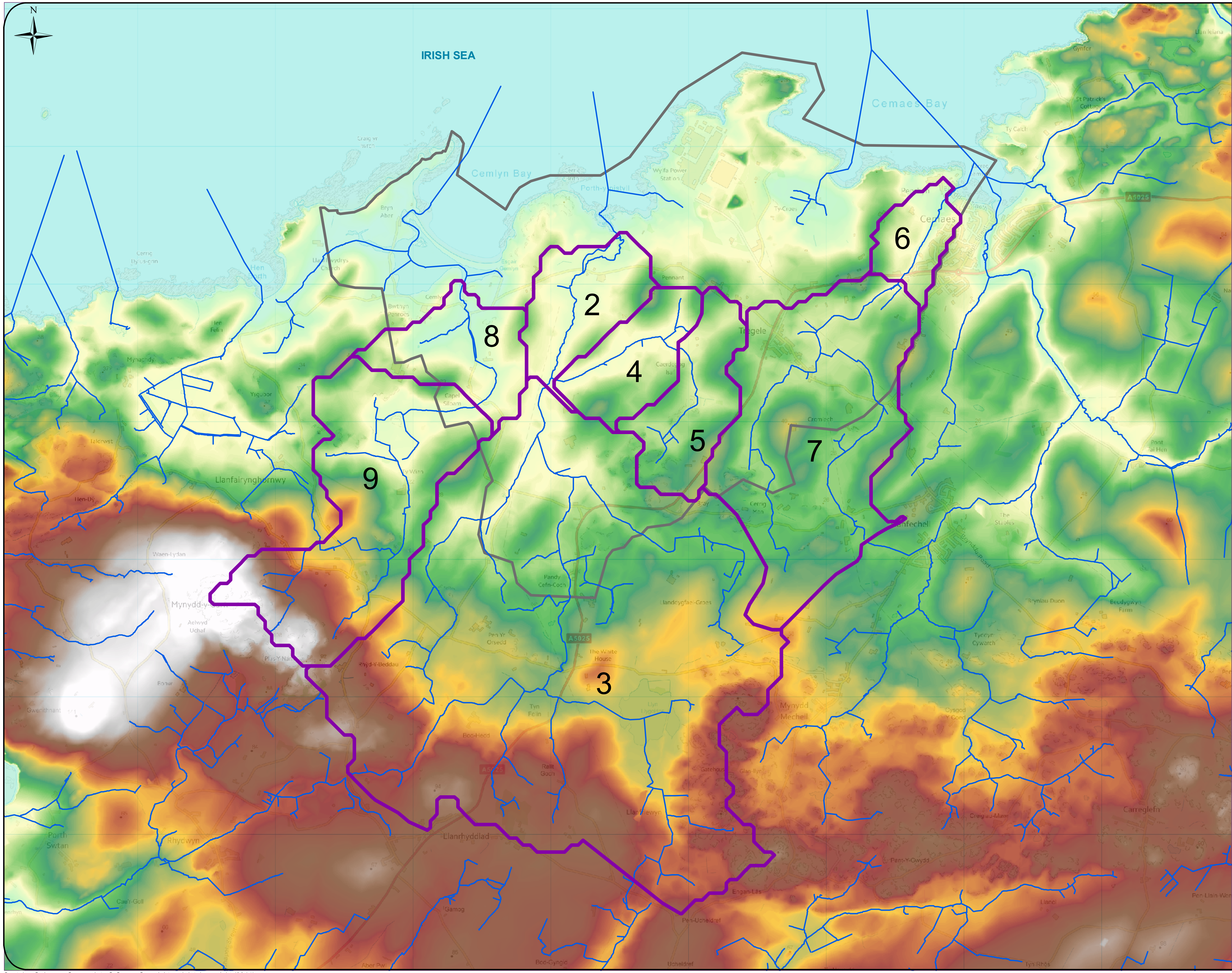

LEGEND

Hydraulic model boundary

Detailed river network

Ground Level

Value

High : 168.85

Low : -2.1

2-9 Sub-catchments

Figure 2.2
Phase 1 Baseline topography with sub-catchments

Scale: 1:25,000
When printed at A3

0 200 400 600 800 1,000 M

HORIZON NUCLEAR POWER

3. Scenarios

This section describes the hydrology assessment scenarios required to support the hydraulic modelling. The required scenarios to be assessed include variations on flood sources, physical scenarios, epochs, climate change scenarios and event frequencies. These are defined as follows:

- **Physical scenario** = Phase of development:
  - Phase 1 Baseline – prior to any works. This is an essential requirement so as to provide a description of the environment against which subsequent phases can be compared;
  - Phase 4 (reference Point 4) Construction – most extensive phase in construction;
  - Phase 5 (reference Point 5) Operation – normal operational state. This phase will persist for 60+ years.
- **Flood source** = Type of flood risk. Pluvial and fluvial flood sources were considered independently. Fluvial scenarios were carried out in order to assess the risk of flooding associated with watercourses in the vicinity of the proposed development, with critical event durations defined in terms of catchment characteristics for upstream catchments, whereas pluvial scenarios were run with short event durations in order to evaluate the impact of changes in surface properties and landforms arising from the development itself;
- **Event frequency** = Annual exceedance probability (AEP) of flood event. Four events are being considered consisting of the 1:2 year, 1:30 year, 1:100 year and 1:1,000 year AEP events. ONR (2014a) recommend consideration of the 1:10,000 year event for nuclear new build. However whilst this event may be required for the Nuclear Safety Licence Application, it is not required for the Development Consent Order Application. As such the 1:10,000 year AEP event is outside the scope of this report. Excluding the modelling of the 1:1,000 year AEP has been justified on the basis that, the nuclear island will be hydraulically separated from the surrounding landscape. Water from the surrounding landscape will not be permitted to flow onto the nuclear island and water from the nuclear island will not be permitted to flow off the nuclear island into the wider environment. The drainage infrastructure that will be implemented to achieve this are being developed separately and are outside the scope of this assessment.;
- **Epoch** = Future time period:
  - 2020s representing the current time period;
  - 2080s representing the end of site operational lifetime;
  - 2180s representing the end of site decommissioning/full site lifetime (in line with Office for Nuclear Regulation (ONR) and Environment Agency (EA) guidance (ONR and EA, 2016)); and
- **Climate change approach** = Level of conservatism required. Derivation of the uplift factor, dependent on epoch and flood source, is presented in Section 3.1.

Hydrology assessment scenarios required to support the hydraulic modelling are presented in Table 3.1. Landform changes for the pluvial modelling were represented in the InfoWorks ICM hydraulic model and therefore pluvial hydrology is only required for Phase 1 Baseline as rainfall is not affected by changes to the physical scenario.

Table 3.1 Hydrology assessment scenarios

Physical scenario	Event frequency (1:X) (AEP)	Epoch	Climate change approach	Flood source	Storm duration	Climate change uplift
Phase 1 Baseline	2, 30, 100, 1000	2020s	Reasonable foreseeable	Pluvial	0.5 and 1.1 hour	5%
				Fluvial	Critical	15%
	2, 30, 100, 1000	2080s	Reasonable foreseeable	Pluvial	0.5 and 1.1 hour	20%
				Fluvial	Critical	30%
	2, 30, 100, 1000	2180s	Reasonable foreseeable	Pluvial	0.5 and 1.1 hour	50%
				Fluvial	Critical	110%
	100, 1000	2080s	Credible maximum	Pluvial	0.5 and 1.1 hour	40%
				Fluvial	Critical	75%
Phase 4 Construction	2, 30, 100, 1000	2020s	Reasonable foreseeable	Fluvial	Critical	15%
Phase 5 Operation	2, 30, 100, 1000	2080s	Reasonable foreseeable	Fluvial	Critical	30%
	2, 30, 100, 1000	2180s	Reasonable foreseeable	Fluvial	Critical	110%
	100, 1000	2080s	Credible maximum	Fluvial	Critical	75%

3.1 Climate change

To account for the potential effects of climate change an uplift factor was applied to rainfall depths used to derive the rainfall intensity inputs for the pluvial hydraulic modelling. Separate climate change uplifts were applied to flows used as input for the fluvial hydraulic modelling. This factor varied depending on the assessment epoch of interest, the level of conservatism required and the flood source.

Current guidance in relation to climate change allowances

Guidance on climate change allowances for river flows for Wales was provided by the 2016 guidance document Flood Consequence Assessments: Climate change allowances (Welsh Government, 2016), and by the 2011 guidance document Adapting to Climate Change: Guidance for Flood and Coastal Erosion Risk Management Authorities in Wales (Welsh Government, 2011).

The 2016 guidance was targeted specifically at assessment of future flood risks within the planning process, and contained the most up-to-date fluvial climate change allowances by catchment for Wales. The site catchments are located in the West Wales river basin district (RBD). Therefore fluvial climate change allowances for the West Wales RBD, were taken from the 2016 guidance.

For the extreme yet credible (H++) climate change scenario, the 2016 guidance referred to the climate change allowances included in the 2011 guidance, since no new research on the H++ scenario had been carried out in the intervening period.

Pluvial climate change allowances were taken from the 2011 guidance, as the 2016 guidance did not contain climate change allowances for change in extreme rainfall. The climate change allowances for change in extreme rainfall were applicable across all of Wales.

The appropriate pluvial and fluvial climate change allowances (Welsh Government, 2011 and 2016, respectively) are provided in Table 3.2 and Table 3.3. There is no H++ allowance for change in extreme precipitation (pluvial).

Table 3.2 Pluvial climate change allowances for Wales (from 1961-1990 baseline)

Allowance category	2020s	2080s
Lower end estimate	0%	10%
Central estimate	5%	20%
Upper end estimate	10%	40%
H++	No guidance	No guidance

Source: Welsh Government, 2011.

Table 3.3 Fluvial climate change allowances for the West Wales river basin district (from 1961-1990 baseline)

Allowance category	2020s	2080s
Lower end estimate	5%	15%
Central estimate	15%	30%
Upper end estimate	25%	75%
H++	40%	110%

Source: Welsh Government, 2016, except for the H++ values which are from Welsh Government, 2011.

Climate change approach

In order to account for the effects of climate change, and in line with the above guidance, the following climate change scenarios have been identified, based on epoch and level of conservatism, for hydrological analysis:

- A 'reasonably foreseeable 2020s' scenario. The pluvial and fluvial climate change factors for this were based on the central estimate of climate change for the 2020s.
- A 'reasonably foreseeable 2080s' scenario. The pluvial and fluvial climate change factors for this were based on the central estimate of climate change for the 2080s. This was in line with the principles set out in statutory planning policy for new nuclear developments and external hazards assessment guidance for nuclear site licensing (DECC, 2011; ONR, 2014a, 2014b; ONR and EA, 2016).
- A 'credible maximum 2080s' scenario. The pluvial and fluvial climate change factors for this were based on the upper estimate of climate change for the 2080s, in line with the relevant policies and guidance referenced above. This was applied as a sensitivity test for the 2080s epoch.
- A 'reasonably foreseeable 2180s' scenario. The fluvial climate change factor for this was based on the H++ estimate of climate change for the 2080s. Since there are no H++ climate change allowances for extreme precipitation, the pluvial uplift was an additional 10% above that for the

2080s credible maximum. This was applied as a sensitivity test for the 2180s epoch representing the far future.

The choice of climate change allowances as detailed above was in line with the 2016 guidance, which recommended that the central estimate for the 2080s should be used to assess the potential impact of climate change as part of a flood consequence assessment, and that in addition an assessment of risk made using the upper end estimate. This approach has been followed here for the 2080s.

In addition the guidance stated that the use of the H++ scenario should be considered for contingency planning for those development which are "*very sensitive to flood risk and have lifetimes beyond the end of the century … Examples include major infrastructure projects*". Wylfa Newydd Main Site met all these criteria, being a significant infrastructure with an extended lifespan exceeding 100 years. Therefore, the H++ scenario for fluvial uplift has been applied as the 'reasonably foreseeable' climate uplift for the 2180s time epoch.

There were no pluvial H++ climate uplift values available in the current guidance. There was also no guidance on pluvial uplift values for time periods beyond the 2080s, as current climate change projections do not extend beyond 2100. In the absence of any research-based guidance on this issue, an additional 10% uplift was used for the 2180s, on top of the available 2080s uplift values. It is recognised that this approach is somewhat arbitrary and subject to significant uncertainty, but the provision of an additional uplift allows for some sensitivity testing of how much worse pluvial flood risk could become over the decommissioning period.

Uplift factors

A summary of the climate change uplift values is displayed in Table 3.4.

Table 3.4 Pluvial and fluvial climate change uplifts

Physical Scenario	Epoch	Climate change approach	Allowance category	Pluvial	Fluvial
Phase 1 Baseline Phase 4 Construction	2020s	Reasonable foreseeable	Central estimate, 2020s	5%	15%
Phase 1 Baseline Phase 5 Operation	2080s	Reasonable foreseeable	Central estimate, 2080s	20%	30%
Phase 1 Baseline Phase 5 Operation	2180s	Reasonable foreseeable	H++, 2080s	50% [1]	110%
Phase 1 Baseline Phase 5 Operation	2080s	Credible maximum	Upper estimate, 2080s	40%	75%

Source: Welsh Government, 2011 and 2016.
[1] In the absence of an H++ scenario for pluvial climate change allowances available in current guidance, an additional 10% was added to the pluvial upper end estimate for the 2080s in Wales.

4. Hydrology methodology

A working draft of the hydrology methodology was produced on 19 October 2016 and underwent an iterative process of internal project team review and revision. The final working draft was provided to Horizon Nuclear Power for issue to NRW on 29 March 2017. This was presented to NRW at a meeting on 12 April 2017.

4.1 Introduction

This section describes hydrology methodology used to derive the pluvial hyetographs and fluvial hydrographs, which were calculated as inputs for separate and independent fluvial and pluvial modelling scenarios. This includes a description of input data, derivation of catchment descriptor and urbanisation parameters, determination of peak flow method, rainfall parameters, storm durations and seasonal storm profiles. A summary of final input parameters for derivation of rainfall depths and flows follows at the end of the section.

The remainder of Section 4 is structured as follows:

- Section 4.2 presents the data used in the hydrology assessment;
- Section 4.3 describes and justifies the derivation of catchment descriptor and urbanisation parameter values, identifying the final values to be used in the hydrology assessment;
- Section 4.4 identifies potential peak flow methods from guidance, sets out criteria and process for comparing methods, presents results and conclusions of comparison and determines the most appropriate peak flow method;
- Section 4.5 describes and justifies the rainfall data used, the area it was applied to and any adjustments made to it;
- Section 4.6 describes and justifies the derivation of storm durations based on catchment descriptors, presents those values and confirms the critical storm duration based on InfoWorks ICM hydraulic model results of representing various catchment based storm durations;
- Section 4.7 describes and justifies the critical seasonal storm profile; and
- Section 4.8 summarises which parameters were used to derive rainfall depths and flows and how these were represented in the InfoWorks ICM hydraulic model.

4.2 Input data

Data used in the hydrology assessment is presented in Table 4.1.

Table 4.1 Hydrology assessment input data

Data	Source	Date obtained	Purpose
Digital catchment and sub catchment boundaries	Centre for Ecology and Hydrology (CEH) FEH Web Service https://fehweb.ceh.ac.uk/	Various (March, October 2016)	Catchment boundary definition
Catchment descriptors	CEH FEH Web Service https://fehweb.ceh.ac.uk/	Various (May, June, October 2016)	Catchment descriptor information; manipulated where necessary to determine descriptors for sub catchments; amended where necessary to account for refined catchment boundaries
FEH13 rainfall (depth – duration – frequency) data	CEH FEH Web Service https://fehweb.ceh.ac.uk/	Various (May, June, October 2016)	Rainfall inputs for pluvial scenarios (direct input to hydraulic model) and fluvial scenarios (input to ReFH v2.2).
LiDAR (Light Detecting and Ranging) data (1m resolution)	NRW	September 2013	For checking and amending FEH catchment boundaries where necessary; defining sub catchment boundaries.
Panorama 50m data	Ordnance Survey		For checking and amending FEH catchment boundaries where necessary; defining sub catchment boundaries. This data type was only used to plug small gaps that existed in the LiDAR data coverage.
Design description of the proposed construction and operation works	Horizon Nuclear Power	April 2016	For determining changes to sub-catchment characteristics DPLBAR[1] and DPSBAR[2] to reflect the proposed works.
OS Mastermap 1:10,000 scale	Ordnance Survey	October 2014	Baseline mapping
Climate change uplift factor	Adapting to Climate Change: guidance for flood and coastal erosion risk management authorities in Wales (Welsh Government, 2011) Flood consequence assessments: climate change allowances (Welsh Government, 2016)	November 2016	Climate change uplift factor applied to rainfall and flow for future epochs

4.3 Catchment descriptor and urbanisation parameter derivation

Phase 1 Baseline catchment boundaries

Catchment boundaries for the watercourse catchments associated with Cemlyn Stream, Afon Cafnan and Cemaes Stream were downloaded from the Centre for Ecology and Hydrology (CEH) FEH Web Service (CEH, 2016). The watercourse catchments were reviewed as part of the DCO hydrology development. The

[1] Mean of distances between each node on the catchment terrain grid and the catchment outlet, in kilometres. Used to characterise catchment size and configuration.
[2] This landform descriptor (mean drainage path slope) provides an index of watercourse catchment steepness. It was developed for the Flood Estimation Handbook and is calculated as the mean of all inter-nodal slopes. The index is expressed in metres per kilometre with values ranging from >300 in mountainous terrain to <25 in the flattest parts of the country.

FEH catchment boundaries were mapped in GIS and compared with ground elevation data, principally comprising of LiDAR data, but supplemented by OS Panorama data[3] where gaps in the LiDAR were present.

At three locations the boundary defined by FEH was found to be slightly inaccurate and was corrected in line with the ground elevation data. This resulted in slight changes to the upstream boundaries of the Afon Cafnan and Cemaes Stream, the divide between the Afon Cafnan and Cemaes Stream catchments, and along the boundary between Sub-catchments 4 and 5. The watercourse catchments, showing adjusted catchment boundaries, and the sub-catchments are shown in Figure 2.1.

Phase 1 Baseline catchment descriptors

Catchment descriptors were needed for all sub-catchments. The descriptors required in the analysis are defined below:

- AREA = Catchment drainage area (km^2);
- BFIHOST = Baseflow index;
- DPLBAR = Index describing catchment size and drainage path configuration (km);
- DPSBAR = Index of catchment steepness (m/km);
- PROPWET = Index of proportion of time that soils are wet;
- SAAR = 1961-1990 standard-period average annual rainfall (mm); and
- URBEXT2000 = FEH index of fractional urban extent.

For Phase 1 Baseline, the catchment descriptors were taken directly from the FEH Web Service (CEH, 2016) for upstream Sub-catchments 3, 5, 7 and 9. Catchment descriptors (AREA, DPLBAR, DPSBAR and URBEXT) were modified to account for amendments to the sub-catchment boundary for Sub-catchments 3, 5 and 7. For Phase 1 Baseline, the catchment descriptors were derived for downstream Sub-catchments 2, 4, 6 and 8. Catchment boundaries were derived by subtracting upstream sub-catchments from watercourse catchments in GIS. Sub-catchment descriptors were modified or derived as a function of area. The method for modifying catchment descriptors is described in Table 4.2. The resultant catchment descriptors are shown in Table 4.3.

[3] OS Panorama data has since been withdrawn, however, changes made using this topographic data set are still considered appropriate given the minor nature of the changes made.

Table 4.2 Catchment descriptor and urbanisation parameter modification methods

Catchment descriptor	Phase 1 Baseline	Phase 4 Construction and Phase 5 Operation
Area	Upstream sub-catchments modified from FEH Web Service (CEH, 2016) based on topography using GIS software. Downstream sub-catchments were derived by subtraction of upstream areas from watercourse catchment areas.	Catchment boundary altered, using GIS software, to reflect changes in topography from proposed design.
BFIHOST	This was determined by back calculation using area weighting of upstream and downstream catchments, as described in Section 7.2.2 of FEH Volume 5 (IoH, 1999).	Unaltered from Phase 1. Although changes in land use would influence the BFIHOST value for Phase 4 Construction, the precise influence is problematic to calculate and expected to be limited relative to the extent of the sub-catchment.
DPLBAR	For each sub-catchment this value was determined in GIS by calculating the drainage length to the downstream outlet for each node in a 50m ground elevation model, and taking the mean of all values. The method for deriving DPLBAR is detailed in Section 3.2.2 of FEH Volume 5 (IoH, 1999). Note: value for Sub-catchment 8 was determined by FEH Vol 5 Equation 7.1 (IoH, 1999): $DPLBAR = AREA^{0.548}$	For each sub-catchment this value was determined in GIS by calculating the drainage length to the downstream outlet for each node in a 50m ground elevation model, and taking the mean of all values. The method for deriving DPLBAR is detailed in Section 3.2.2 of FEH Volume 5 (IoH, 1999).
DPSBAR	Was determined in a similar way to DPLBAR by calculating the steepest downstream slope to an adjacent node for each node in a 50m ground elevation model, and taking the mean of the slope values. The method for deriving DPSBAR is detailed in Section 3.4.1 of FEH Volume 5 (IoH, 1999). Note: value for Sub-catchment 8 was determined by back calculation using area weighting of upstream and downstream catchments, as described in Section 7.2.2 of FEH Volume 5 (IoH, 1999).	For each sub-catchment this value was determined in GIS by calculating the steepest downstream slope to an adjacent node for each node in a 50m ground elevation model, and taking the mean of the slope values. The method for deriving DPSBAR is detailed in Section 3.4.1 of FEH Volume 5 (IoH, 1999).
PROPWET	All the watercourse catchments downloaded from FEH Web Service (CEH, 2016) had a PROPWET value of 0.45, so this value was assigned to the sub-catchments too.	Unaltered from Phase 1.
SAAR	Determined by back calculation using area weighting of upstream and downstream catchments, as described in Section 7.2.2 of FEH Volume 5 (IoH, 1999).	Unaltered from Phase 1.
URBEXT2000	Determined by back calculation using area weighting of upstream and downstream catchments, as described in Section 7.2.2 of FEH Volume 5 (IoH, 1999).	URBEXT2000 = Urban Area / (Catchment Area x 1.567) (Based on equation from URBEXT2000 – A new FEH catchment descriptor (Bayliss, 2006)).
Urban Area	Not modified.	Determined by adding all new impermeable areas to the existing Urban Area. Existing Urban Area = URBEXT2000 x Catchment Area x 1.567 (Based on equation from URBEXT2000 – A new FEH catchment descriptor (Bayliss, 2006)).
Imperviousness Factor	Not modified. Default value of 0.3 (Wallingford HydroSolutions, 2016).	Impervious factor determined using area weighting of impervious factors, based on a value of 0.8 representing new impermeably areas and the default value of 0.3 for all unchanged areas.

Table 4.3 Phase 1 Baseline modified catchment descriptors

Sub-catchment	Parameters	Downstream NGR	Area (km^2)	BFIHOST	DPLBAR	DPSBAR	PROPWET	SAAR	URBEXT2000	Urban Area (km^2)	Imperviousness factor
2	Derived	SH 34500 93350	0.66	0.521	0.82	36.22	0.45	913	0.000	0	0.3
3	Modified[1]	SH 33950 92250	7.87	0.455	2.83	48.30	0.45	978	0.003	0.03	0.3
4	Derived	SH 34050 92300	0.59	0.528	0.84	44.62	0.45	937	0.000	0	0.3
5	Modified[1]	SH 34950 92550	0.71	0.464	0.72	42.21	0.45	944	0.000	0	0.3
6	Derived	SH 36900 93700	0.35	0.513	0.49	44.68	0.45	931	0.149	0.08	0.3
7	Modified[1]	SH 36500 93000	2.49	0.414	2.03	36.97	0.45	955	0.000	0	0.3
8	Derived	SH 33350 93000	0.675	0.537	0.81	51.40	0.45	928	0.000	0	0.3
9	From FEH	SH 33450 92100	2.04	0.457	1.76	75.90	0.45	940	0.006	0.02	0.3

Notes: [1] For these sub-catchments the FEH catchment boundaries were modified slightly based on detailed ground elevation data

Phase 4 Construction and Phase 5 Operation catchment boundaries and descriptors

Design plans for Phase 4 Construction and Phase 5 Operation involve topographical and permeability changes. As a result of the topographical changes, the sub-catchment boundaries were altered and associated catchment descriptors (AREA, DPSBAR and DPLBAR) were adjusted. A comparison of sub-catchment boundaries which were altered (Sub-catchments 2, 4, 5, 6, 7 and 8) for all three physical scenarios is shown on Figure 4.1 (at the end of Section 4). Additionally, urbanisation parameters were modified to represent additional roads, buildings and soil mounds being constructed, as follows:

- Urban area/Adjusted urban area (km^2) = Mapped new areas of hardstanding or equivalent within the sub-catchment; and
- Imperviousness factor = Proportion of urban area, which is impervious (default is 0.3).

During Phase 4 Construction, mounds were treated as impermeable surfaces whilst compacted and un-vegetated. During Phase 5 Operation, mounds were treated as permeable surfaces once established. URBEXT2000 was re-calculated as a function of adjusted urban area. The method for modifying the area and urbanisation parameters is described in Table 4.2. The resultant catchment descriptors are shown in Table 4.4 and Table 4.5 for Phase 4 Construction and Phase 5 Operation, respectively.

Table 4.4 Phase 4 Construction modified catchment descriptors and urbanisation parameters

Sub-catchment	Parameters	Area (km^2)	BFIHOST	DPLBAR	DPSBAR	PROPWET	SAAR	URBEXT2000	Adjusted Urban Area (km^2)	Imperviousness factor
2	Modified from Phase 1	0.51	0.521	0.80	40.75	0.45	913	0.36	0.284	0.8
3	No change from Phase 1	7.87	0.455	2.83	48.30	0.45	978	0.003	0.03	0.3
4	Modified from Phase 1	0.44	0.528	0.70	40.08	0.45	937	0.1	0.068	0.8
5	Modified from Phase 1	0.55	0.464	0.82	37.84	0.45	944	0.21	0.180	0.8
6	Modified from Phase 1	0.36	0.513	0.53	59.94	0.45	931	0.37	0.208	0.6
7	Modified from Phase 1	2.42	0.414	1.98	37.42	0.45	955	0.01	0.046	0.8
8	Modified from Phase 1	0.70	0.537	0.76	47.23	0.45	928	0.14	0.152	0.8
9	No change from Phase 1	2.04	0.457	1.76	75.90	0.45	940	0.006	0.02	0.3

Note: Parameters unchanged from Phase 1 included as grey text

Table 4.5 Phase 5 Operation modified catchment descriptors and urbanisation parameters

Sub-catchment	Parameters	Area (km^2)	BFIHOST	DPLBAR	DPSBAR	PROPWET	SAAR	URBEXT2000	Adjusted Urban Area (km^2)	Imperviousness factor
2	Modified from Phase 1	0.51	0.521	0.85	41.0	0.45	913	0	0	0.3
3	No change from Phase 1	7.87	0.455	2.83	48.30	0.45	978	0.003	0.03	0.3
4	Modified from Phase 1	0.45	0.528	0.69	38.6	0.45	937	0.04	0.026	0.8
5	Modified from Phase 1	0.70	0.464	0.72	42.2	0.45	944	0.03	0.034	0.8
6	Modified from Phase 1	0.37	0.513	0.48	56.3	0.45	931	0.149	0.08	0.3
7	Modified from Phase 1	2.48	0.414	2.05	38.4	0.45	955	0	0.002	0.8
8	Modified from Phase 1	0.68	0.537	0.73	46.8	0.45	928	0	0	0.3
9	No change from Phase 1	2.04	0.457	1.76	75.90	0.45	940	0.006	0.02	0.3

Note: Parameters unchanged from Phase 1 included as grey text

4.4 Peak flow method

Determination of peak flows for fluvial modelling required identification of the most appropriate method. Current guidance from Natural Resources Wales (NRW), in the form of Technical Guidance: Flood

Estimation (NRW, 2016), identifies two recommended methods to estimate flow for events up to and including a 1:1000 year AEP event:

- Flood Estimation Handbook (FEH) statistical method; and
- Revitalised Flood Hydrograph (ReFH, Version 2.2) method.

The FEH statistical method uses QMED and AMAX data from a group of gauged catchments, which are hydrologically similar to the target catchment. The ReFH2.2 method uses catchment descriptors from the target catchment.

NRW's preferred approach for estimating peak flows up to and including the 1:100 year AEP event was the FEH statistical method. However, this had several limitations when compared with the ReFH2.2 method.

The InfoWorks ICM model required inputs of full hydrographs for small catchments, for the following events frequencies: 1:2, 1:30, 1:100 and 1:1000 year AEP. The ReFH2.2 method provides full hydrographs, whereas the FEH statistical method only provides peak flows. Consequently, if the FEH statistical method were used for flood peaks, the ReFH2.2 method would also need to be applied to yield a hydrograph, which would then be scaled to the FEH statistical peak flow.

Furthermore, using the FEH statistical method to derive hydrologically similar pooling groups for small catchments can be problematic, as most donor gauges are in large catchments. By contrast ReFH2.2 can be reliably used for small catchments.

The ReFH2.2 method can reliably be used to calculate the 1:1,000 year AEP event. The FEH statistical method cannot reliably be used to calculate the 1:1000 year AEP event, due to the inability to derive a hydrologically similar pooling group of sufficient size (FEH Vol. 2 Section 16.5 recommends pooling groups should have at least 5T data points, where T is the event return period of interest, meaning that more than 5000 AMAX data points would be required to reliably estimate the 1:1000 year AEP event). The FEH statistical method therefore relies on applying a ratio method, whereby the flood growth factor from ReFH2.2 is applied the FEH 1:100 year AEP peak flow estimate.

For the requirements of this analysis, the FEH statistical method presented several limitations in reliability, accuracy and practicability. This made the ReFH2.2 method more preferable. However, it was also important to ensure a reasonable degree of conservatism in resulting estimates when selecting a peak flow methodology. Therefore, if the FEH statistical method produced notably greater peak flows than the ReFH2.2 method, it would be chosen as the most appropriate method for further hydrological assessment. If not the ReFH2.2 method will be chosen.

Peak flows were calculated using both methods, for four event frequencies (1:2, 1:30, 1:100 and 1:1,000 year AEP). Calculations were undertaken for Sub-catchment 3, as this was the sub-catchment with the greatest area (7.9km^2) and therefore was the most likely catchment to achieve an acceptable fit with a pooling group under the FEH statistical method. Phase 1 Baseline catchment descriptors were used and no climate change uplift was applied, as it was the relative difference between the peak flows from each method that was of interest.

FEH statistical method set-up

The FEH statistical method uses pooled data from gauging stations around the UK which have similar catchment characteristics to derive a growth curve, and applies this to a mean annual maximum flood (QMED) estimate.

The QMED for Sub-catchment 3 was calculated from catchment descriptors, according to the standard FEH regression based catchment parameter equation in the Flood Estimation Guidelines (Environment Agency, 2015) (page 39 of 110). Donor gauges were considered to refine the QMED value from catchment descriptors, however, none were considered appropriate. The only gauge on Anglesey[4] was not considered suitable for QMED calculation, based on initial concerns raised by NRW[5] and subsequent discussions at the 9 July 2016 meeting as well as the National River Flow Archive entry for the station (CEH, 2017) which

[4] 102001 Cefni at Bodffordd SH429768
[5] Letter to Bryony Stocking of Horizon Nuclear Power Ltd. from NRW dated 26 January 2015. Wylfa Newydd – NRW comments on A5025 bypass flood modelling methodology statement for Valley & Llanfachraeth

indicates the weir is susceptible to blockage. Two additional gauges in mainland Wales[6], close to Anglesey in Snowdonia, were also not suitable as donors, as their catchments were not comparable to Sub-catchment 3, having greater slopes and rainfall. Therefore, QMED from catchment descriptors was brought forward, adjusted for urbanisation, according the updated equation (Kjeldsen, 2010) and used in the flood frequency curve development.

To develop the flood frequency curve, WINFAP-FEH 3 software was used, together with the latest HIFLOWS dataset (version 4.1 as of May 2016). Using WINFAP, a pooling group of gauges, based on hydrological similarity was identified. Gauges from the pooling group were reviewed and two stations removed due to short record and uncertainty identified about high flows. Furthermore, gauges in highly permeable catchments (SPRHOST<20%) were reviewed and non-flood years removed (Annual Maximum (AMAX) values less than half of QMED). An additional gauge was added to the pooling group, to ensure the refined pooling group had more than 500 years of data. The refined pooling group was tested for heterogeneity and found to be acceptably homogenous.

Curve fitting to the refined pooling group was tested for goodness of fit. The Generalised Logistic (GL) distribution provided a better fit that the Generalised Extreme Value (GEV) distribution, although both gave an acceptable fit (GL Z value = 0.3235; GEV Z value = -1.1195). Growth factors from both distributions were then multiplied by QMED to produce peak flow values for events up to and including the 1:100 year AEP event. This allowed comparison of peak flows from both distributions, to determine which was the most conservative. To derive the FEH statistical 1:1000 year AEP peak flow, the ratio method was applied, based on both distributions and both seasons from ReFH2.2. This resulted in four peak flow estimates for the 1:1,000 year AEP event, which were compared to determine which was the most conservative. These flow estimates are presented below in Table 4.6

ReFH2.2 method set-up

The ReFH2.2 software was used with Sub-catchment 3 catchment descriptors and FEH13 depth duration frequency (DDF) rainfall data. Default values were used for all other parameters, including storm duration, time step, seasonal correction factor (SCF) and aerial reduction factor (ARF). An initial assumption was made that the ReFH2.2 default critical storm duration as calculated from catchment descriptors was robust, in terms of yielding the highest peak levels at points of interest in the subject catchments. This assumption was subjected to sensitivity analysis for storm duration and found to be sound, as reported in section 4.6 of this report and additional sensitivity testing using the hydraulic model is detailed in Section 7.7 of the main report).

Wallingford Hydrosolutions advised that the winter seasonal storm profile was most appropriate for rural catchments. However, conservatism was considered the most important factor for the purposes of this analysis. As such both winter and summer seasons were used. Resultant peak flows were compared to determine which was the most conservative.

Results

The peak flows for both the FEH statistical and ReFH2.2 methods for Sub-catchment 3 are presented in Table 4.6. All peak flows were compared to determine the most conservative method.

[6] 65006 Seiont at Peblig Mill SH493621, 65004 Gwrfai at Bontnewydd SH484599

Table 4.6 Peak flows (m^3/s) for Sub-catchment 3 using FEH statistical and ReFH2.2 methods

	FEH statistical				ReFH2.2	
Event	**Generalised logistic growth factor**	**Generalised logistic peak flow (m^3/s)**	**Generalised extreme value growth factor**	**Generalised extreme value peak flow (m^3/s)**	**Winter season peak flow (m^3/s)**	**Summer season peak flow (m^3/s)**
1:2 year AEP	1	2.98	1	2.98	2.93	3.73
1:30 year AEP	2.357	7.02	2.397	7.14	6.44	8.57
1:100 year AEP	3.232	9.63	3.144	9.36	9.24	12.52
1:1000 year AEP	n/a	n/a	n/a	n/a	15.79	21.97
1:1000 year AEP ratio method (summer)	n/a	16.89	n/a	16.43	n/a	n/a
1:1000 year AEP ratio method (winter)	n/a	16.45	n/a	16.00	n/a	n/a

As mentioned earlier in this section, the ReFH2.2 was the preferred method for estimating peak flows, due to the limitations of the FEH statistical method. The results also show that the ReFH2.2 (summer season) gave the greatest peak flows for all events and is therefore the most conservative method. As such the ReFH2.2 (summer season) method was considered the most appropriate method for flow estimation for all fluvial modelling scenarios.

This decision was subject to an assumption: When using ReFH2.2, the season that gives the most conservative hydrograph peak flows, also results in the most conservative representation of flooding in the hydraulic model. This assumption was later tested (s.4.7) and found to be sound.

4.5 Rainfall parameters

Pluvial

ReFH2.2, with FEH13 DDF data, was used to determine hyetographs for pluvial modelling. FEH13 rainfall data were obtained for all 1km^2 grid cells across the InfoWorks ICM hydraulic model domain at the site. An analysis of the rainfall data showed that spatial variability of rainfall depths across the InfoWorks ICM hydraulic model domain was less than 1mm for the 1:100 year AEP event. As rainfall was not affected by physical scenarios and had negligible spatial variability for a given event frequency and storm duration, it was appropriate for all rainfall depth estimation for pluvial modelling to be carried out with rainfall data from a single grid square: National Grid Reference (NGR) SH 34001 91000.

Within ReFH2.2, plot scale equations were used with a nominal area of 1km^2 (Wallingford HydroSolutions, 2016). An SCF was applied to rainfall depths, calculated based on location, season, duration and event. ReFH2.2 also calculated an ARF, which is inversely proportional to catchment area. An ARF reduces the point rainfall estimates to a catchment average rainfall depth, accounting for the likelihood that rainfall depth will fall throughout the whole of the storm duration and across the whole catchment. ARF was not applied to rainfall depths, since this factor would have been slightly less than and very close to 1.0 for each sub-catchment. Omitting the ARF allowed for the same rainfall to be applied across the whole of the InfoWorks ICM hydraulic model domain. The net result is a slightly conservative estimate of rainfall inputs across the InfoWorks ICM hydraulic model domain.

Fluvial

ReFH2.2, with FEH13 DDF data, was used to determine hydrographs for fluvial modelling. FEH13 rainfall data were used for each sub-catchment. Rainfall depths for the upstream sub-catchments were obtained directly from FEH Web Service (Sub-catchments 3, 5, 7 and 9) as part of the catchment descriptor information. For downstream sub-catchments, rainfall depths from adjacent catchments were used. Sub-catchment 3 DDF data was used for Sub-catchment 2. Sub-catchment 5 DDF data was used for Sub-catchment 4. Sub-catchment 7 DDF data was used for Sub-catchment 6. Cemlyn Stream DDF data was used for sub-catchment 8. This approach was justified because there was negligible spatial variability in rainfall depths.

SCF and ARF were both applied to rainfall depths. It was appropriate to apply ARF for fluvial modelling, as catchment specific rainfall data were used.

Summary

The rainfall parameters used for both pluvial and fluvial modelling are summarised in Table 4.7. The same rainfall parameters were used to estimate rainfall depths and flows for every model scenario. Because rainfall depth estimation for pluvial modelling is not sub-catchment specific, the use of catchment descriptors and urbanisation parameters (as outlined in Section 4.3) is only relevant to flow estimation for fluvial modelling.

Table 4.7 Rainfall parameters summary

Flood source	Rainfall data	Area applied to	Seasonal correction factor (SCF)	Aerial reduction factor (ARF)
Pluvial	FEH13 DDF for single grid square (SH 34001 91000)	Entire InfoWorks ICM hydraulic model area	Applied	Not applied
Fluvial	FEH13 DDF for each main catchment	Each sub-catchment	Applied	Applied

4.6 Storm duration derivation

Pluvial

Pluvial flood risk is generally associated with short, intense storms. Early pluvial modelling (not reported), using now superseded hydrology, was undertaken for a wide range of storm durations (summer profile 0.5, 1, 3, 6 and 24-hour) which showed the greatest flood risk was associated with the shorter storm durations. Therefore only the 0.5 and 1 hour storm durations were used to derive pluvial hydrology for the current hydrology assessment. Further pluvial storm duration sensitivity tests, using ReFH2.2 were undertaken (see Section .7.6, Main Report). These sensitivity tests show that peak flood depths in the hydraulic model had low sensitivity to pluvial storm duration, but the 0.5 and 1 hr durations resulted in marginally greater peak flood depths overall. Therefore, confidence can be added to the use of the 0.5 and 1 hr storm durations to derive pluvial hydrology.

The number of time steps used to derive a hyetograph is not prescribed, but too few results in a blocky shape and too many can result in odd oscillations in the rainfall. A time step of 0.1 hours was determined to result in a suitable shape for both storm durations and therefore was applied to both storm durations, to allow direct comparison. These parameters were used for all model scenarios.

Fluvial

Fluvial flood risk is generally associated with longer storms and is influenced by the physical nature of the catchment particularly as significant attenuation in the system can mean a peak volume event results in greater flooding than a peak flow event. For this reason, it is necessary to identify a critical storm duration based on catchment descriptors, which is then confirmed using the InfoWorks ICM hydraulic model.

For fluvial modelling, critical storm durations were calculated based on catchment descriptors for watercourse catchments (Wallingford HydroSolutions, 2016). The watercourse catchment critical storm durations were applied to the corresponding sub-catchments. Therefore, the watercourse catchments were considered independently and used different storm durations. However, all the sub-catchments within a given watercourse catchment were considered together and used the same storm duration. The reasoning behind this approach is that the sub-catchments within a watercourse catchment were hydraulically linked, but the watercourse catchments were not hydraulically linked to each other.

An appropriate time step should be 5-20% of the storm duration and must be an odd denominator of the storm duration (Wallingford HydroSolutions, 2016). Infoworks ICM software required all catchments to have the same time step. It was also useful for comparison for all storm durations to have the same time step. As such an appropriate time step (0.5 hour) was chosen on the basis of the storm durations being modelled.

To determine if the watercourse catchment critical storm duration based on catchment descriptors was robust, hydrology based on both a longer and shorter storm duration was also derived. These additional storm durations were chosen based on half (0.5D) and double (2D) the critical storm duration based on catchment descriptors, while maintaining the requirement of an odd division by the 0.5 hour time step. Critical storm duration from catchment descriptors and associated InfoWorks ICM hydraulic model run parameters are summarised in Table 4.8. For all three storm durations, hydrographs were derived for the 1:100 year AEP event with climate change representing 2020s reasonable foreseeable, summer season for Phase 1 Baseline.

Table 4.8 Storm duration for watercourse catchments

	Cemlyn Stream	Afon Cafnan	Cemaes Stream
Critical storm duration (D) from catchment descriptors	3.5 hour	5.5 hour	5.5 hour
0.5 D	2.5 hour	2.5 hour	2.5 hour
2 D	6.5 hour	10.5 hour	10.5 hour
Time step	0.5 hour	0.5 hour	0.5 hour
Applies to sub-catchments	8, 9	2, 3, 4, 5	6, 7

Hydrographs for each sub-catchment were represented in the InfoWorks ICM hydraulic model. Depth and flow were recorded across five output lines and are presented in Table 4.9. Output lines are presented on Figure 4.2.

Table 4.9 Storm duration comparison InfoWorks ICM hydraulic model results

	Peak flow (m^3/s)			Peak depth (m)		
Results line	**0.5 x D**	**D**	**2 x D**	**0.5 x D**	**D**	**2 x D**
RLine_105	4.04	4.22	4.12	0.23	0.24	0.24
RLine_53	0.85	0.91	0.88	0.42	0.43	0.42
RLine_69	0.67	0.79	0.68	0.33	0.37	0.34
RLine_71	1.08	1.24	1.04	0.39	0.41	0.38
RLine_96	0.66	1.27	1.17	0.74	0.82	0.83

D = Critical storm duration as determined by watercourse catchment descriptors

Figure 4.2 InfoWorks ICM hydraulic model output locations

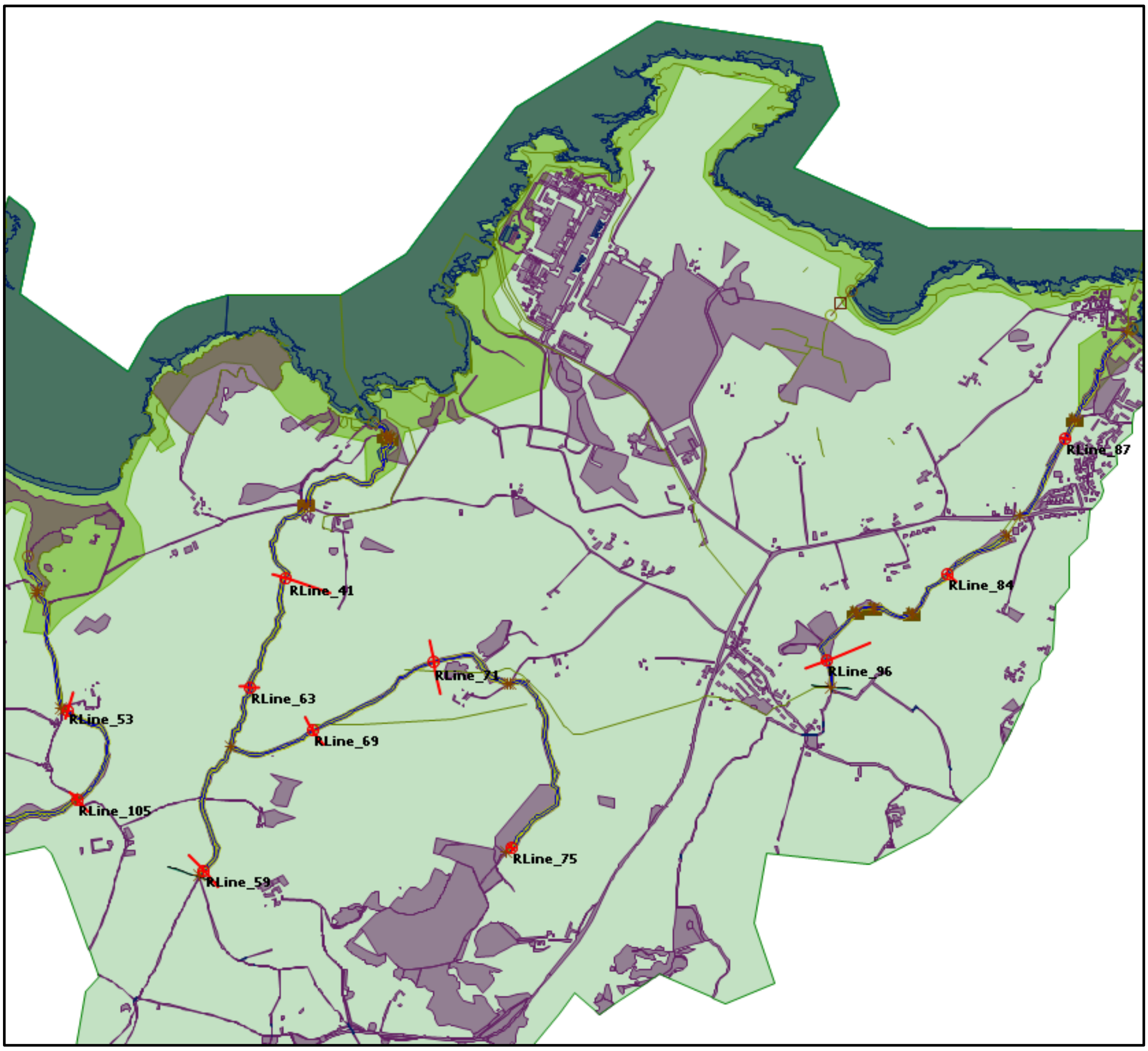

The storm duration from catchment descriptors (D) resulted in the greatest peak flows at every output location and the greatest peak depths at all, but one output location. Upstream on the Cemaes Stream near Tregele, the depth was marginally lower for D than the 2 x D storm duration (RLine_96). As the D storm duration resulted in the greatest flows and depths, apart from one only slightly lower depth location, it was concluded that watercourse catchment critical storm duration based on catchment descriptors was robust and appropriate for use in flow estimation for fluvial modelling for all model scenarios. Further sensitivity testing of the fluvial storm duration was undertaken, with more durations tested for greater granularity (see Section.7.7, Main Report). These sensitivity tests showed that peak flood depths in the hydraulic model had low sensitivity to fluvial storm duration, but the D storm duration resulted in marginally greater peak flood depths overall. Therefore confidence can be added to the use of the D storm duration, for use in flow estimation for fluvial modelling.

Construction and operation design plans result in catchment descriptor modifications in some sub-catchments, which could change the critical storm duration. However, as these changes affect a relatively small area compared to the watercourse catchment, they are unlikely to significantly change the critical storm duration for the watercourse catchment. Therefore, the same critical storm durations (D) were applied to all physical scenarios present day and future.

4.7 Seasonal storm profile

The ReFH2.2 method uses a seasonal storm profile. The summer season was determined to represent a conservative approach to peak flow (Section 4.4), however, it is necessary to confirm this provides the peak flows and depths for both the fluvial and pluvial events as represented independently in the InfoWorks ICM hydraulic model. For both seasons, inputs were derived for the 1:100 year AEP event with climate change representing 2020s reasonable foreseeable for Phase 1 Baseline. Storm duration and time step for the pluvial comparison used 0.5 hour and for the fluvial comparison used D as determined in Section 4.6 (5.5 hour or 3.5 hour, as appropriate to the watercourse catchment).

For pluvial modelling, rainfall depth hyetographs were converted into rainfall intensity hyetographs, as required by the InfoWorks ICM hydraulic model. For pluvial modelling, significant depth and flow were recorded across seven of eleven output lines and are presented in Table 4.10. For fluvial modelling, flow hydrographs for each sub-catchment were represented in the InfoWorks ICM hydraulic model. For fluvial modelling, depth and flow were recorded across five output lines and are presented in Table 4.10. Output lines are presented on Figure 4.3.

Table 4.10 Season comparison InfoWorks ICM hydraulic model results

		Peak flow (m^3/s)		Peak depth (m)	
Source	**Results line**	**Summer**	**Winter**	**Summer**	**Winter**
Pluvial	RLine_41	0.92	0.17	0.16	0.03
	RLine_53	0.35	0.07	0.29	0.13
	RLine_59	2.46	1.37	0.54	0.41
	RLine_63	0.03	0.02	0.02	0.01
	RLine_69	0.79	0.16	0.37	0.18
	RLine_71	1.25	0.32	0.37	0.15
	RLine_96	0.20	0.12	0.11	0.09
Fluvial	RLine_105	4.22	2.64	0.24	0.19
	RLine_53	0.91	0.45	0.43	0.34
	RLine_69	0.79	0.28	0.37	0.22
	RLine_71	1.24	0.55	0.41	0.26
	RLine_96	1.27	0.42	0.82	0.67

For both pluvial and fluvial modelling, the summer season resulted in the greatest depth and flow in the InfoWorks ICM hydraulic model. It was therefore concluded that summer was the critical season and most appropriate for use in rainfall depth estimation for pluvial modelling and flow estimation for fluvial modelling, for all model scenarios.

4.8 Summary of design hydrology input parameters

Pluvial modelling

Rainfall depth hyetographs were derived for the 1:2, 1:30, 1:100 and 1:1,000 year AEP events based on the final pluvial input parameters summarised in Table 4.11. The depth hyetographs were uplifted by the appropriate climate change, as identified in Table 3.1. Rainfall depth hyetographs were divided by the time step, to derive the corresponding rainfall intensity hyetograph and exported in the format required by the InfoWorks ICM software. Rainfall intensity hyetographs were input into the hydraulic model at every grid square within the model extent. No hydrological inflows were specified to represent the effect of rainfall falling on areas upstream of the model domain. Therefore, arguably, the total effect of the pluvial event represented in model scenarios on flood flows and levels in watercourses running through the model domain may be underrepresented for those watercourses with an inflow at the upstream edge of the model domain. However, the omission of upstream flow boundaries for the pluvial scenarios was considered appropriate for two reasons:

- The purpose of pluvial modelling was to represent the localised change in runoff as a result of the construction and operation phases, as compared to the baseline;
- The effect of rainfall in the upper catchments is already represented in the fluvial modelling. Moreover, the fluvial critical storm durations are greater than the longest pluvial critical storm durations. Therefore, any representation of the cumulative effect of rainfall in the upper catchment represented in the pluvial modelling would be less conservative than that already represented in the fluvial modelling.

Table 4.11 Pluvial model inputs

Parameter	Input basis	Detail provided in
Method	ReFH2.2 hyetograph	Section 4.5
Rainfall depths	FEH13 DDF for single grid square (SH 34001 9100)	Section 4.5
SCF	As calculated by ReFH2.2	Section 4.5
ARF	1	Section 4.5
Storm duration	0.5 hour and 1.1 hour	Section 4.6
Season	Summer	Section 4.7

Fluvial modelling

Flow hydrographs were derived for the 1:2, 1:30, 1:100 and 1:1,000 year AEP events based on the final fluvial input parameters summarised in Table 4.12. Catchment descriptors were adjusted to reflect changes made to sub-catchment area, DPLBAR, DPSBAR and urbanisation parameters as part of the Phase 4 Construction and Phase 5 Operation works as described in Table 4.4 and Table 4.5, respectively. The flow hydrographs were uplifted by the appropriate climate change, as identified in Table 3.1. Flow hydrographs were split into specific reaches and exported in the format required by the InfoWorks ICM software.

Table 4.12 Fluvial model inputs

Parameter	Input basis	Detail provided in
Method	ReFH2.2 hyetograph	Section 4.4 and 4.5
Rainfall depths	FEH13 DDF for sub-catchment	Section 4.5
SCF	As calculated by ReFH2.2	Section 4.5
ARF	As calculated by ReFH2.2	Section 4.5
Storm duration	5.5 hour (Afon Cafnan), 5.5 hour (Cemaes Stream), 3.5 hour (Cemlyn Stream) applied to each sub-catchment within each watercourse catchment	Section 4.6
Season	Summer	Section 4.7

Catchment descriptors	Over-written to reflect landform changes for Phase 4 Construction and Phase 5 Operation	Table 4.4 and Table 4.5
Urbanisation	Over-written to reflect landform changes for Phase 4 Construction and Phase 5 Operation	Table 4.4 and Table 4.5

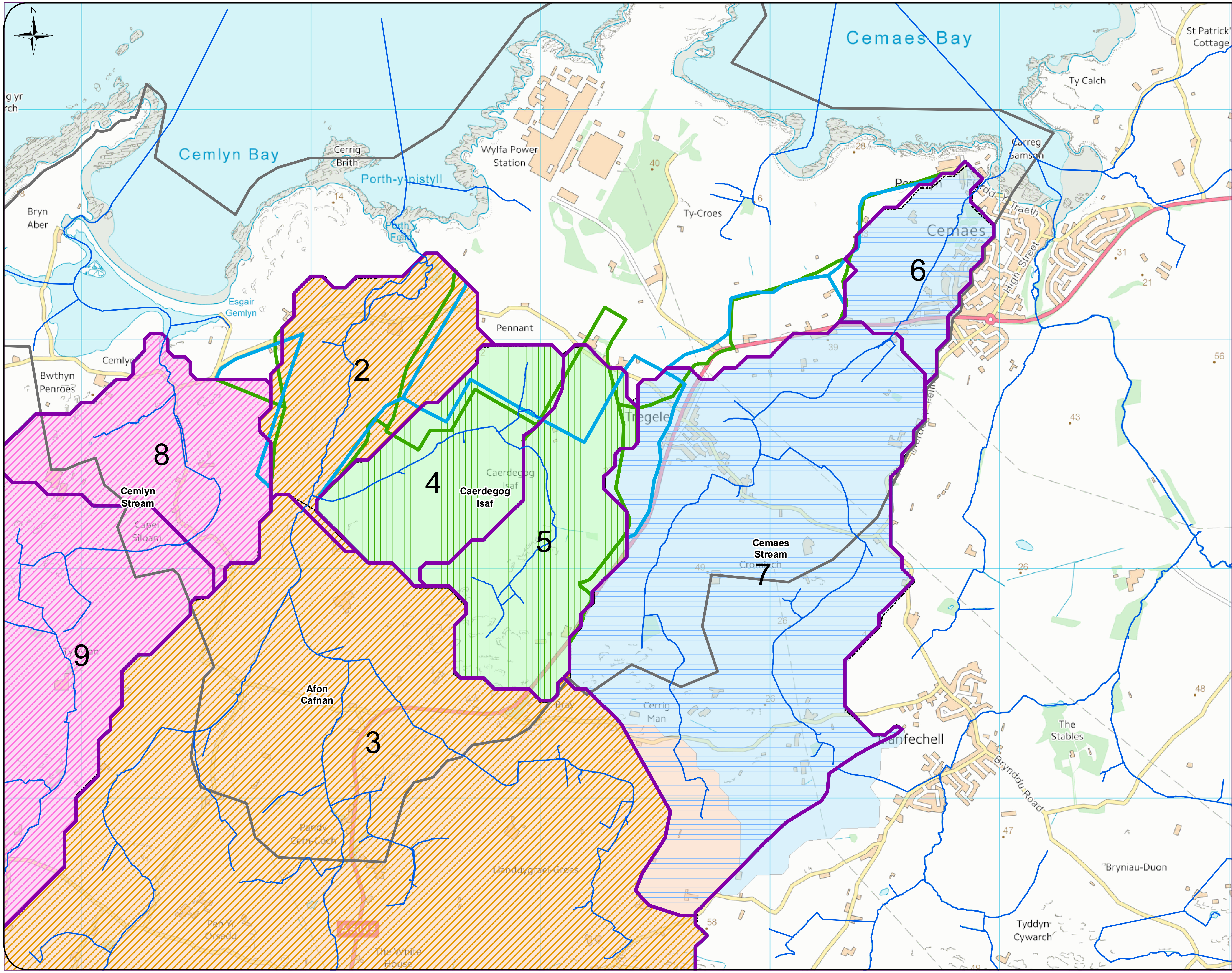

LEGEND

- Hydraulic model boundary
- Phase 1 Baseline
- Phase 4 Construction
- Phase 5 Operation
- Detailed river network

FEH Hydrology Catchments

- Afon Cafnan
- Caerdegog Isaf
- Cemaes Stream
- Cemlyn Stream

2-9 Sub-catchments

Figure 4.1
Hydrology sub-catchments for all physical scenarios

Scale: 1:15,000
When printed at A3
0 200 400 600 M

HORIZON NUCLEAR POWER

5. Hydrology assessment results

5.1 Pluvial estimates

Rainfall hyetographs were produced for the Phase 1 Baseline only as rainfall is not affected by changes to the physical scenario. Landform changes for the pluvial modelling were represented in the InfoWorks ICM hydraulic model. Total rainfall depth estimates, based on the methodology outlined in this report (Section 4), are presented in Table 5.1.

Table 5.1 Total rainfall depths (mm) for all model scenarios

		Event frequency			
Storm duration	**Model scenario**	**1:2 year AEP**	**1:30 year AEP**	**1:100 year AEP**	**1:1000 year AEP**
0.5 hour	2020s reasonably foreseeable	9.2	23.4	35.6	62.5
	2080s reasonably foreseeable	10.5	26.7	40.7	71.4
	2080s credible maximum	NA	NA	47.4	83.3
	2180s reasonably foreseeable	13.1	33.4	50.8	89.2
1.1 hour	2020s reasonably foreseeable	12.3	31.7	48.6	85.7
	2080s reasonably foreseeable	14.0	36.2	55.5	98.0
	2080s credible maximum	NA	NA	64.7	114.3
	2180s reasonably foreseeable	17.5	45.3	69.4	122.5

The InfoWorks ICM software requires rainfall inputs in an intensity format. Rainfall depths were converted to intensity and are reproduced as follows:

- for the 2020s reasonable foreseeable 0.5 hour events in Figure 5.1;
- for the 2020s reasonable foreseeable 1.1 hour events in Figure 5.2;
- for the 2080s reasonable foreseeable / credible maximum 0.5 hour events in Figure 5.3;
- for the 2080s reasonable foreseeable / credible maximum 1.1 hour events in Figure 5.4;
- for the 2180s reasonable foreseeable 0.5 hour events in Figure 5.5; and
- for the 2180s reasonable foreseeable 1.1 hour events in Figure 5.6.

Figure 5.1 Pluvial hyetographs for 0.5 hour storm duration 2020s reasonable foreseeable

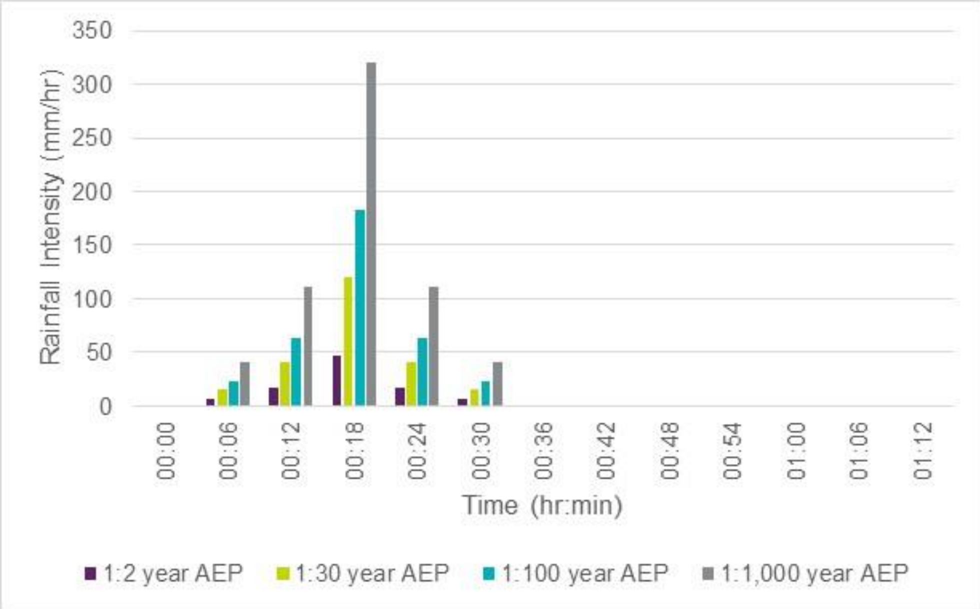

Figure 5.2 Pluvial hyetographs for 1.1 hour storm duration 2020s reasonable foreseeable

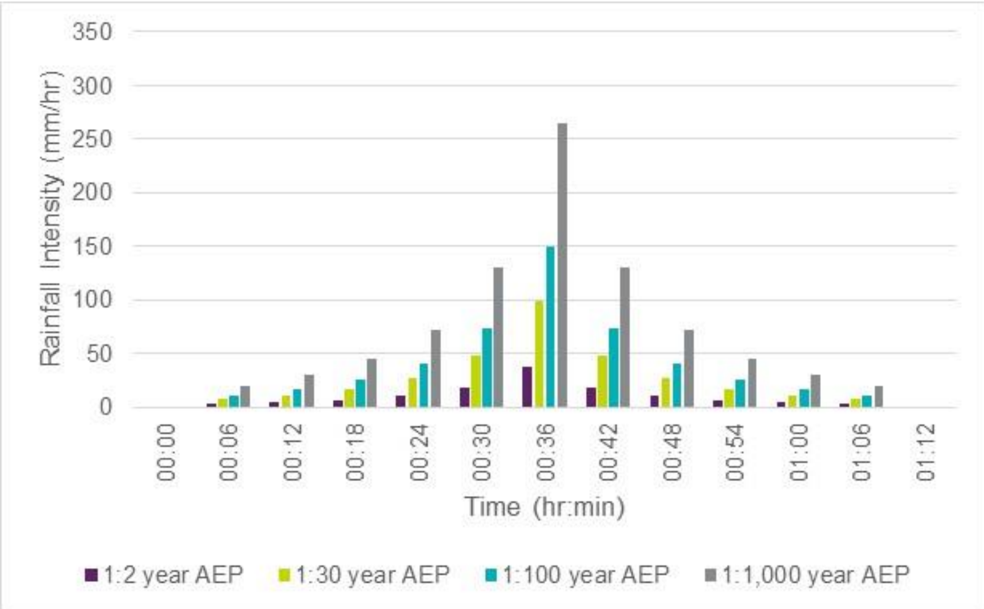

Figure 5.3 Pluvial hyetographs for 0.5 hour storm duration 2080s reasonable foreseeable and credible maximum

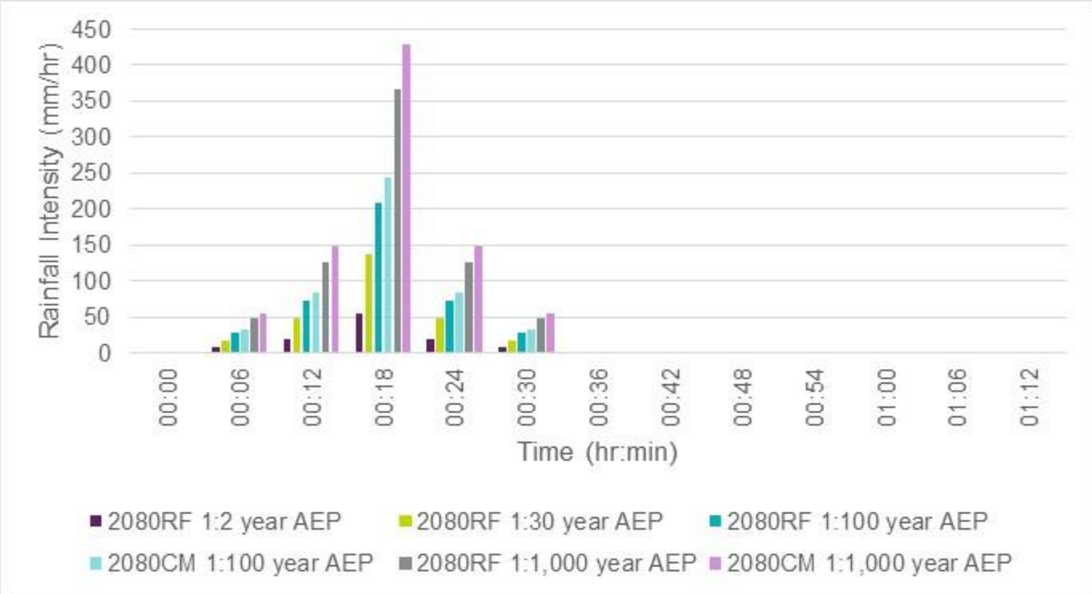

Figure 5.4 Pluvial hyetographs for 1.1 hour storm duration 2080s reasonable foreseeable and credible maximum

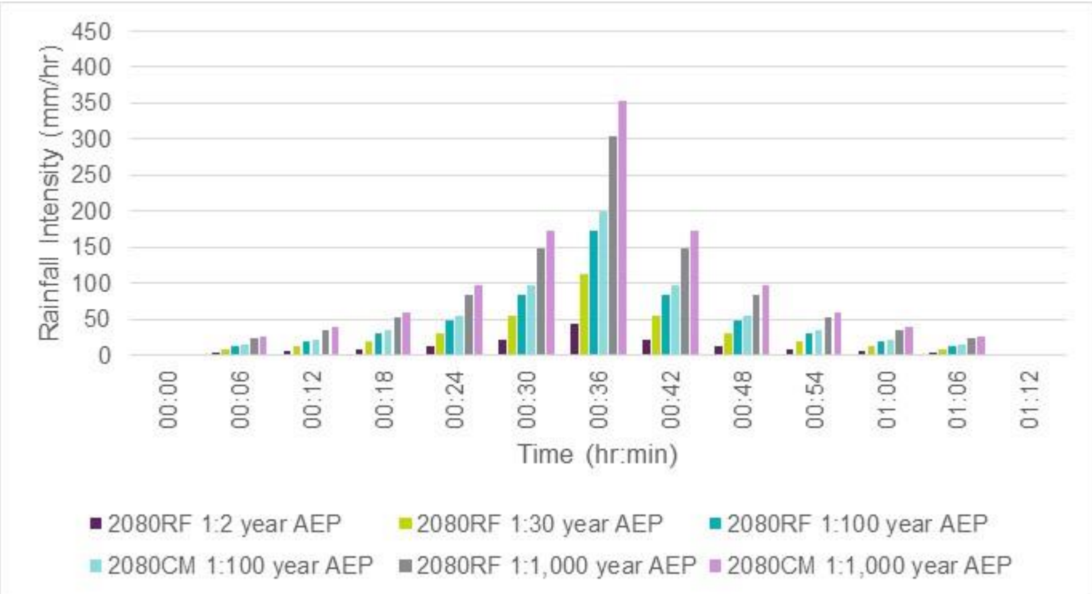

Figure 5.5 Pluvial hyetographs for 0.5 hour storm duration 2180s reasonable foreseeable

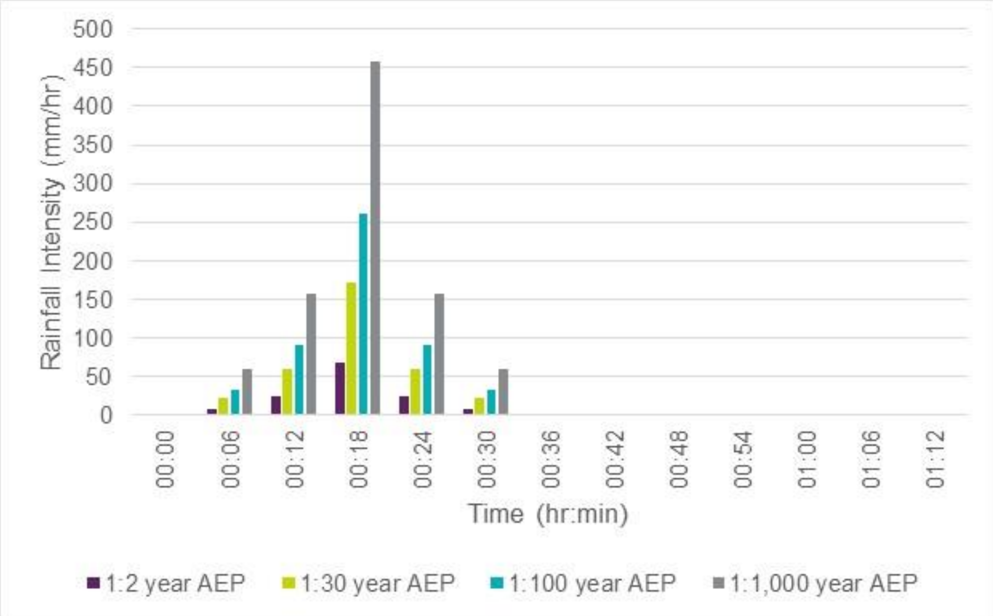

Figure 5.6 Pluvial hyetographs for 1.1 hour storm duration 2180s reasonable foreseeable

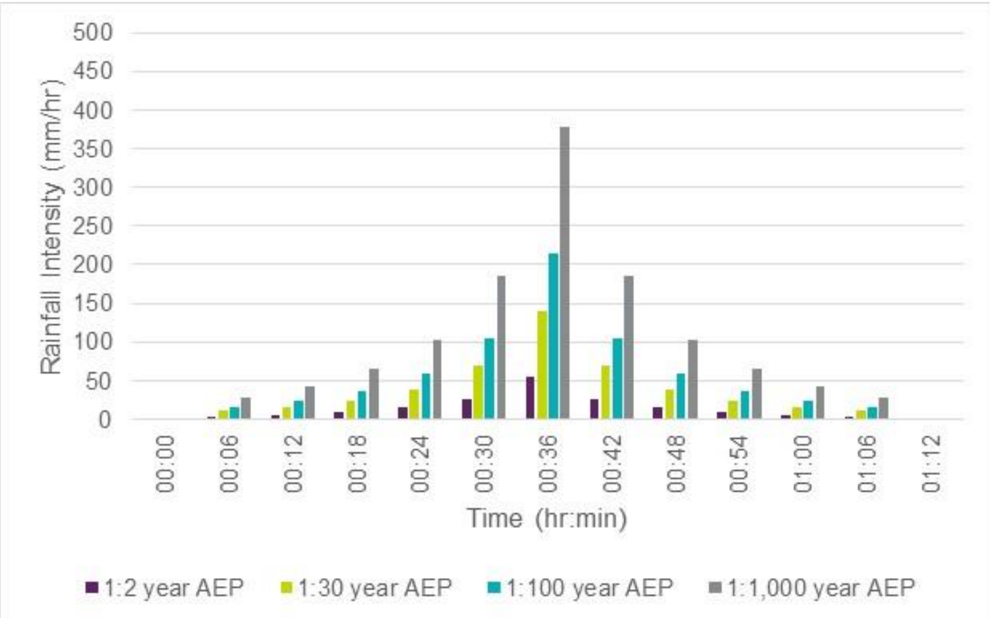

5.2 Fluvial estimates

Phase 1 Baseline

Flow hydrographs were produced for Phase 1 Baseline based on the methodology outlined in this report (Section 4). Peak flows are presented in Table 5.2.

Table 5.2 Phase 1 Baseline peak flows (m^3/s) including climate change allowance

		Sub-catchment							
Model scenario	**Event frequency**	**2**	**3**	**4**	**5**	**6**	**7**	**8**	**9**
2020s reasonable foreseeable	1:2 year AEP	0.4	4.5	0.4	0.6	0.3	1.8	0.4	1.4
	1:30 year AEP	1.0	10.0	0.9	1.4	0.7	4.1	1.0	3.4
	1:100 year AEP	1.4	14.5	1.3	2.0	1.0	6.0	1.5	5.0
	1:1000 year AEP	2.5	25.2	2.3	3.6	1.7	10.3	2.7	9.0
2080s reasonable foreseeable	1:2 year AEP	0.5	5.1	0.4	0.7	0.3	2.0	0.5	1.6
	1:30 year AEP	1.1	11.3	1.0	1.6	0.8	4.6	1.1	3.8
	1:100 year AEP	1.6	16.4	1.5	2.2	1.1	6.7	1.7	5.6
	1:1000 year AEP	2.9	28.5	2.6	4.0	1.9	11.7	3.1	10.1
2180s maximum credible	1:100 year AEP	2.2	22.1	2.0	3.1	1.5	9.1	2.3	7.6
	1:1000 year AEP	3.9	38.3	3.5	5.4	2.6	15.7	4.2	13.6
2180s reasonable foreseeable	1:2 year AEP	0. 8	8.2	0.7	1.1	0.5	3.3	0.8	2.6
	1:30 year AEP	1.8	18.3	1.6	2.5	1.2	7.5	1.8	6.1
	1:100 year AEP	2.6	26.5	2.4	3.7	1.8	10.9	2.7	9.1
	1:1000 year AEP	4.6	46.0	4.2	6.5	3.1	18.9	5.0	16.3

Hydrographs are reproduced for the 1:100 year AEP events as follows:

- for the 1:100 year AEP 2020s reasonable foreseeable events in **Error! Not a valid bookmark self-reference.**;
- for the 1:100 year AEP 2080s reasonable foreseeable events in Figure 5.8;
- for the 1:100 year AEP 2080s credible maximum events in Figure 5.9; and
- for the 1:100 year AEP 2180s reasonable foreseeable events in Figure 5.10.

Hydrographs for the other events were derived for the modelling, but have not been reproduced in the report as there is no difference from the 1:100 year AEP events apart from scaling to the peaks presented in Table 5.2.

Figure 5.7 Phase 1 Baseline fluvial hydrographs for 1:100 year AEP 2020s reasonable foreseeable

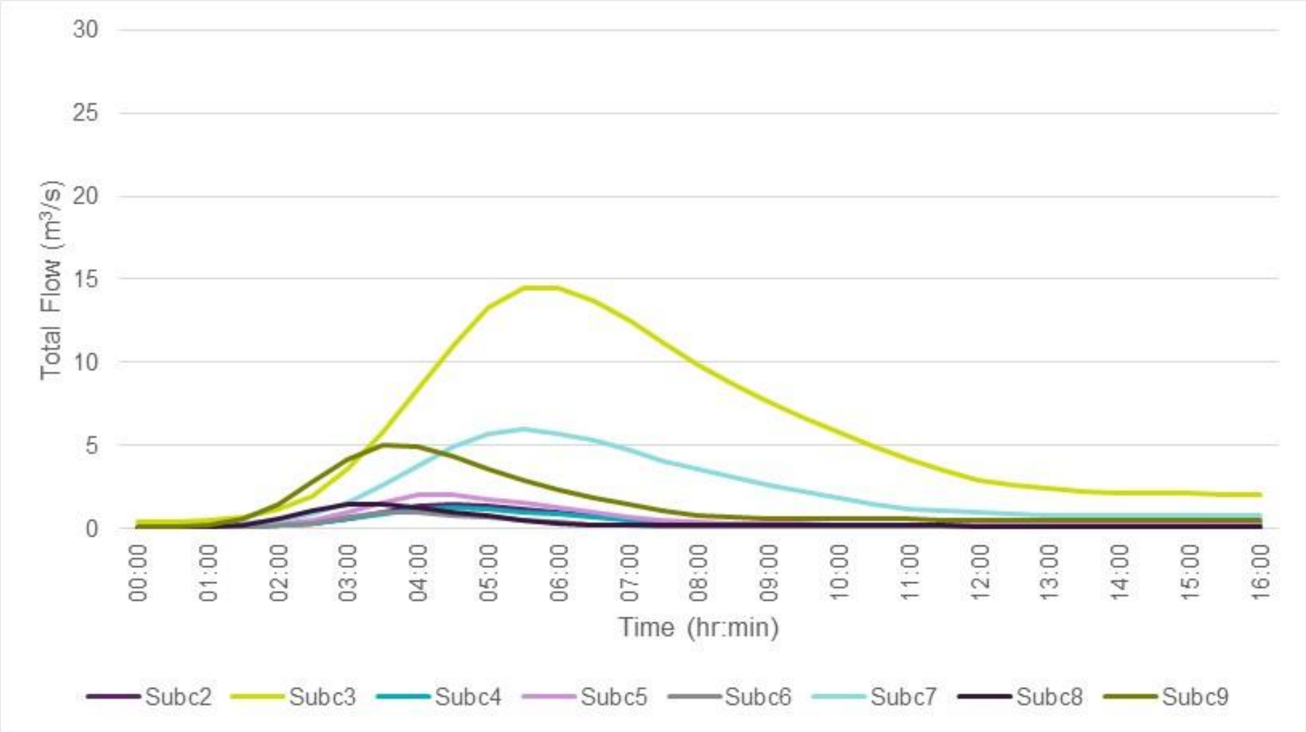

Figure 5.8 Phase 1 Baseline fluvial hydrographs for 1:100 year AEP 2080s reasonable foreseeable

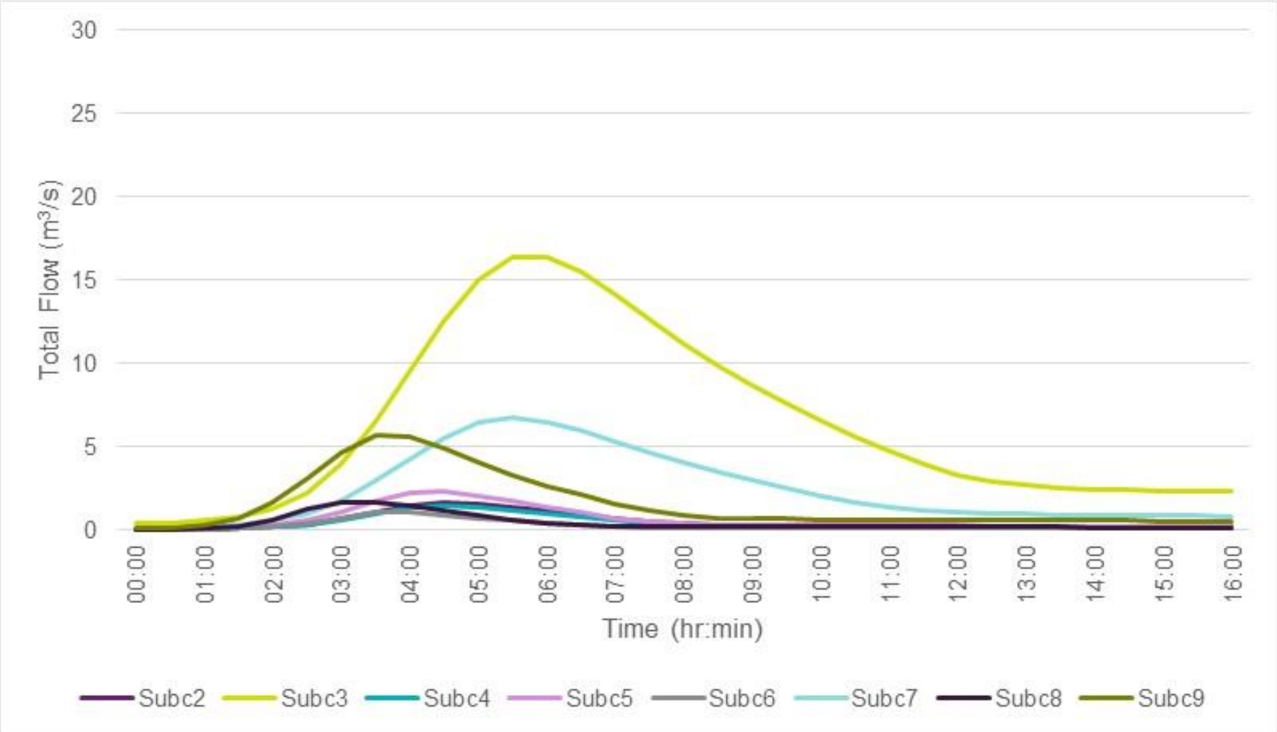

Figure 5.9 Phase 1 Baseline fluvial hydrographs for 1:100 year AEP 2080s credible maximum

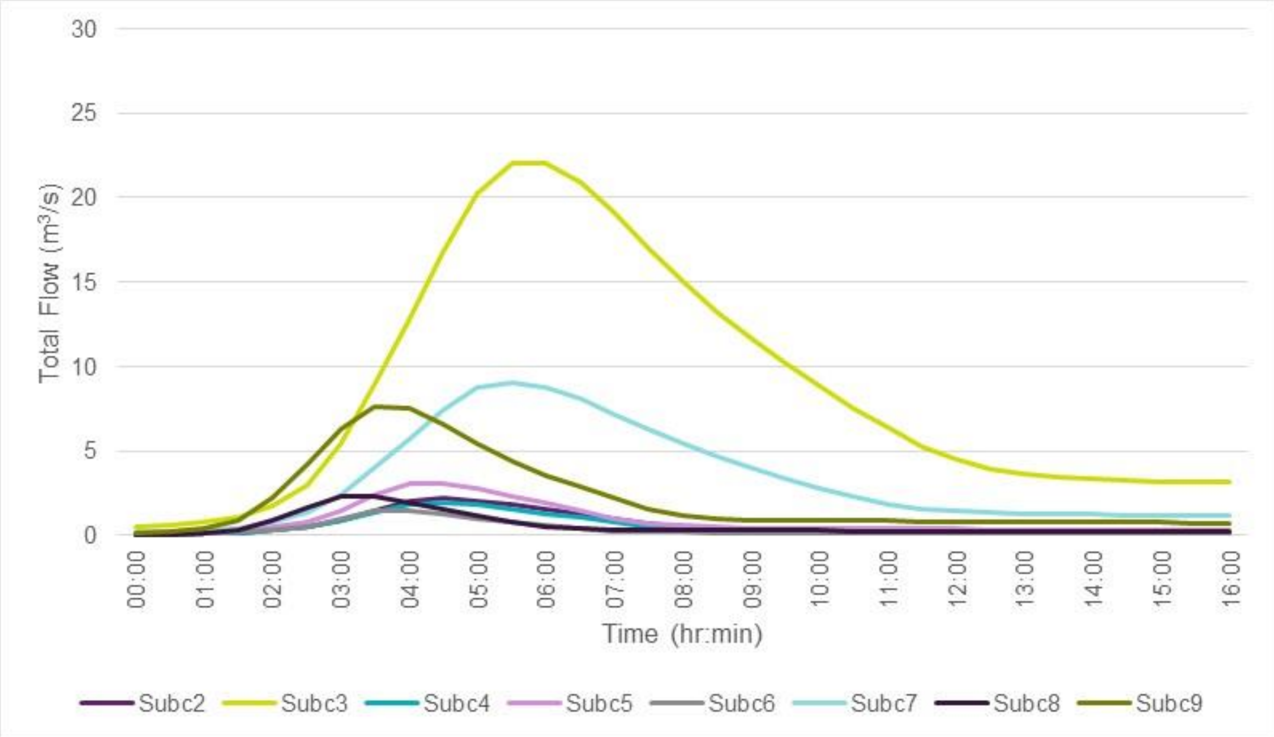

Figure 5.10 Phase 1 Baseline fluvial hydrographs for 1:100 year AEP 2180s reasonable foreseeable

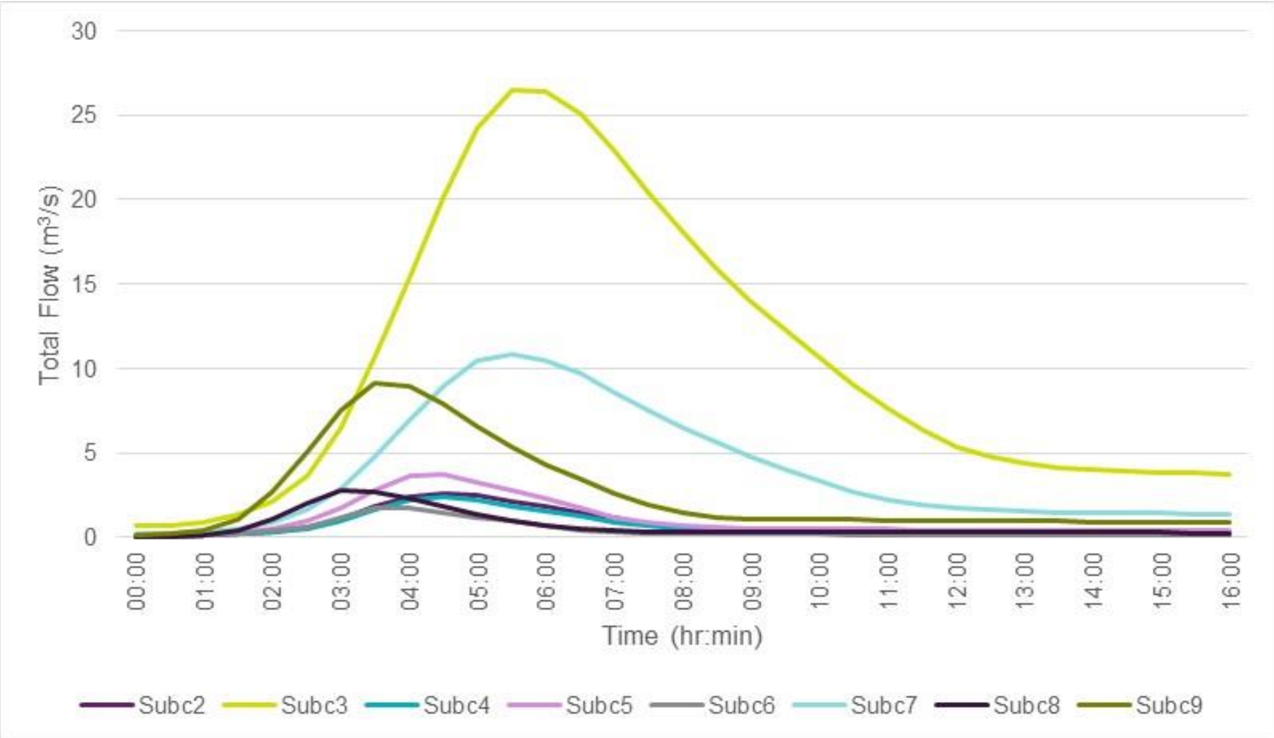

Phase 4 Construction

Flow hydrographs were produced for Phase 4 Construction based on the methodology outlined in this report (Section 4). Peak flows are presented in Table 5.3. Note that Sub-catchments 3 and 9 had the same catchment descriptors and urbanisation parameters for all physical scenarios, as there was no proposed works in these sub-catchments, and therefore the flows are unchanged from those derived for Phase 1 Baseline.

Table 5.3 Phase 4 Construction peak flows (m^3/s) including climate change allowance

		Sub-catchment							
Model scenario	**Event frequency**	**2**	**3**	**4**	**5**	**6**	**7**	**8**	**9**
2020s reasonable foreseeable	1:2 year AEP	0.6	4.5	0.4	0.6	0.5	1.8	0.6	1.4
	1:30 year AEP	1.4	10.0	0.8	1.3	1.0	4.0	1.3	3.4
	1:100 year AEP	1.9	14.5	1.1	1.8	1.4	5.9	2.0	5.0
	1:1000 year AEP	3.1	25.2	1.9	3.0	2.4	10.2	3.4	9.0

Hydrographs are reproduced for the 1:100 year AEP 2020s reasonable foreseeable events in **Error! Not a valid bookmark self-reference.**. Hydrographs for the other events were derived for the modelling, but have not been reproduced in the report as there is no difference from the 1:100 year AEP events apart from scaling to the peaks presented in
Table 5.3.

Figure 5.11 Phase 4 Construction fluvial hydrographs for 1:100 year AEP 2020s reasonable foreseeable

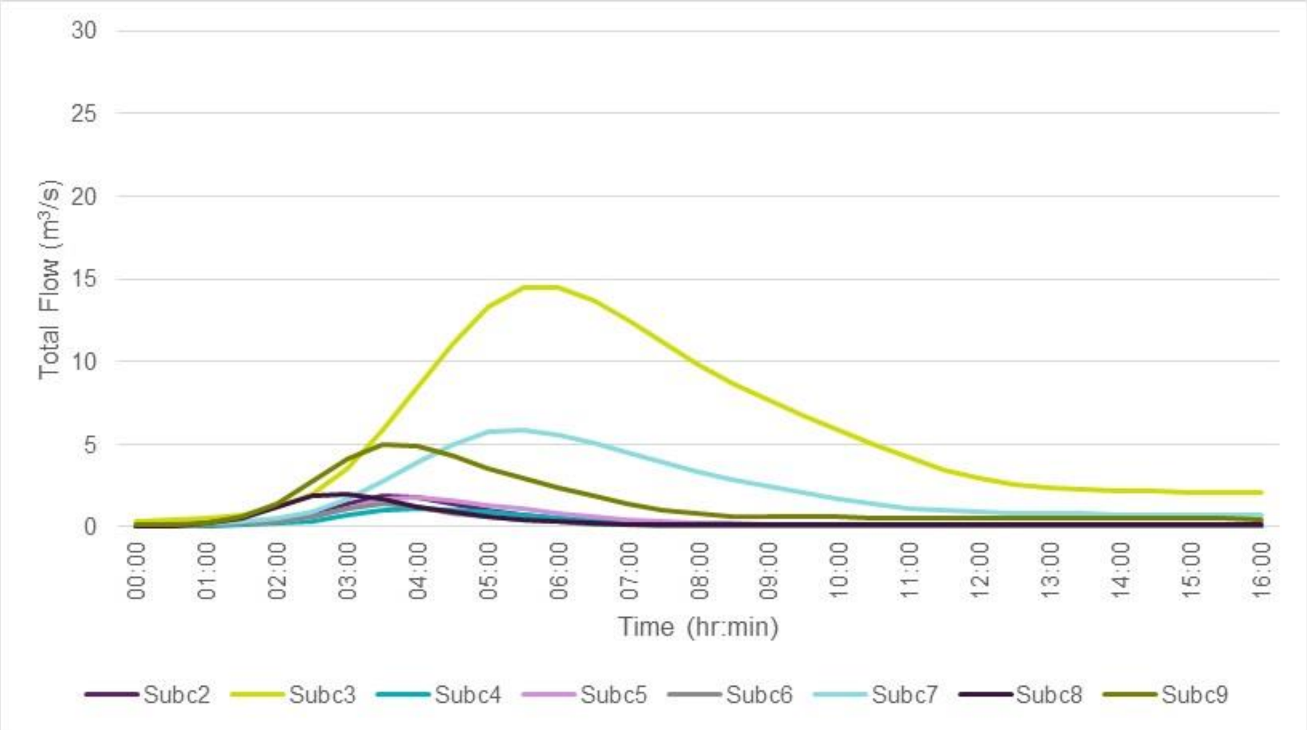

Phase 5 Operation

Flow hydrographs were produced for Phase 5 Operation based on the methodology outlined in this report (Section 4). Peak flows are presented in **Error! Not a valid bookmark self-reference.**. Note that Sub-catchments 3 and 9 had the same catchment descriptors and urbanisation parameters for all physical scenarios, as there was no proposed works in these sub-catchments, and therefore the flows are unchanged from those derived for Phase 1 Baseline.

Table 5.4 Phase 5 Operation peak flows (m³/s) including climate change allowance

		Sub-catchment							
Model scenario	**Event frequency**	**2**	**3**	**4**	**5**	**6**	**7**	**8**	**9**
2080s reasonable foreseeable	1:2 year AEP	0.4	5.1	0. 4	0.7	0.4	2.0	0.5	1.6
	1:30 year AEP	0.9	11.3	0.8	1.6	0.8	4.6	1.2	3.8
	1:100 year AEP	1.3	16.4	1.2	2.3	1.2	6.7	1.8	5.6
	1:1000 year AEP	2.2	28.5	2.1	4.0	2.0	11.7	3.2	10.1
2180s maximum credible	1:100 year AEP	1.7	22.1	1.6	3.1	1.6	9.1	2.4	7.6
	1:1000 year AEP	3.0	38.3	2.8	5.3	2.7	15.7	4.3	13.6
2180s reasonable foreseeable	1:2 year AEP	0.6	8.2	0.6	1.1	0.6	3.3	0.8	2.6
	1:30 year AEP	1.4	18.3	1.3	2.6	1.3	7.5	1.9	6.1
	1:100 year AEP	2.1	26.5	1.9	3.7	1.9	10.9	2.8	9.1
	1:1000 year AEP	3.6	46.0	3.3	6.4	3.3	18.9	5.1	16.3

Hydrographs are reproduced for the 1:100 year AEP events as follows:

- for the 1:100 year AEP 2080s reasonable foreseeable in Figure 5.12;
- for the 1:100 year AEP 2080s credible maximum in Figure 5.13; and
- for the 1:100 year AEP 2180s reasonable foreseeable in Figure 5.14.

Hydrographs for the other events were derived for the modelling, but have not been reproduced in the report as there is no difference from the 1:100 year AEP events apart from scaling to the peaks presented in Table 5.4.

Figure 5.12 Phase 5 Operation fluvial hydrographs for 1:100 year AEP 2080s reasonable foreseeable

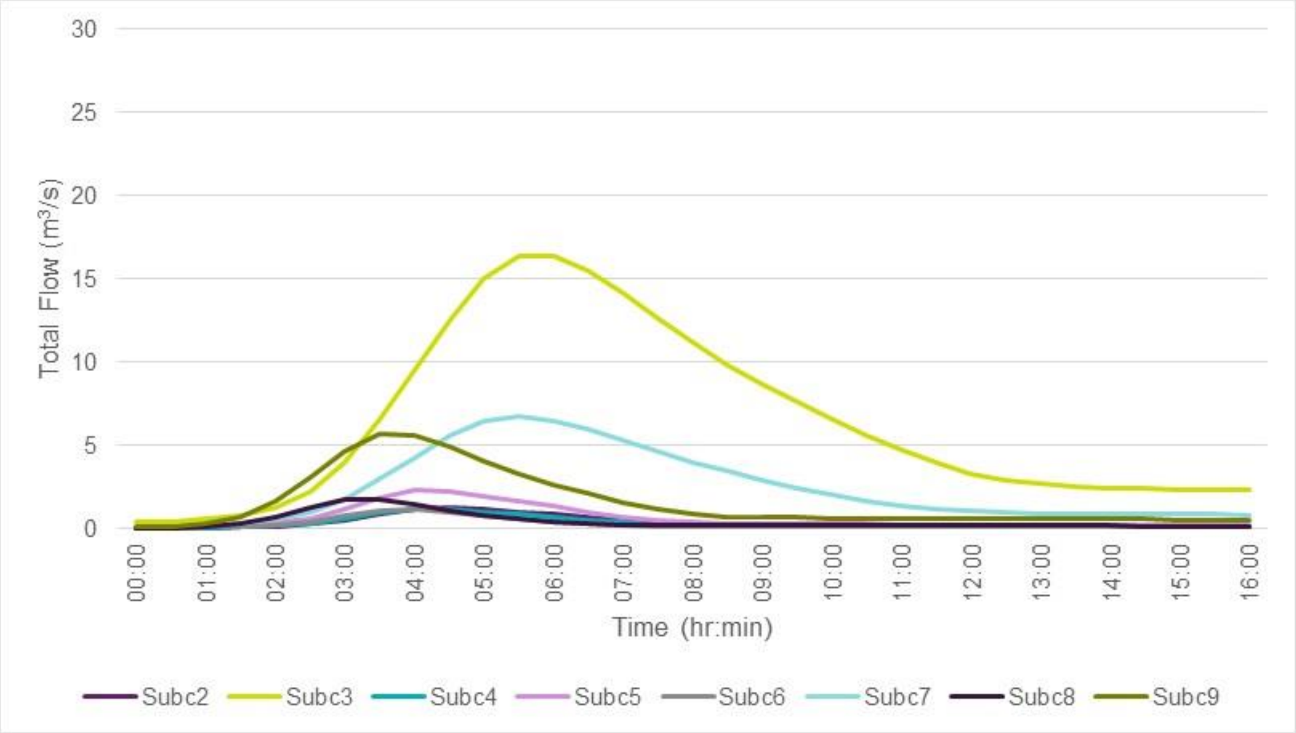

Figure 5.13 Phase 5 Operation fluvial hydrographs for 1:100 year AEP 2080s credible maximum

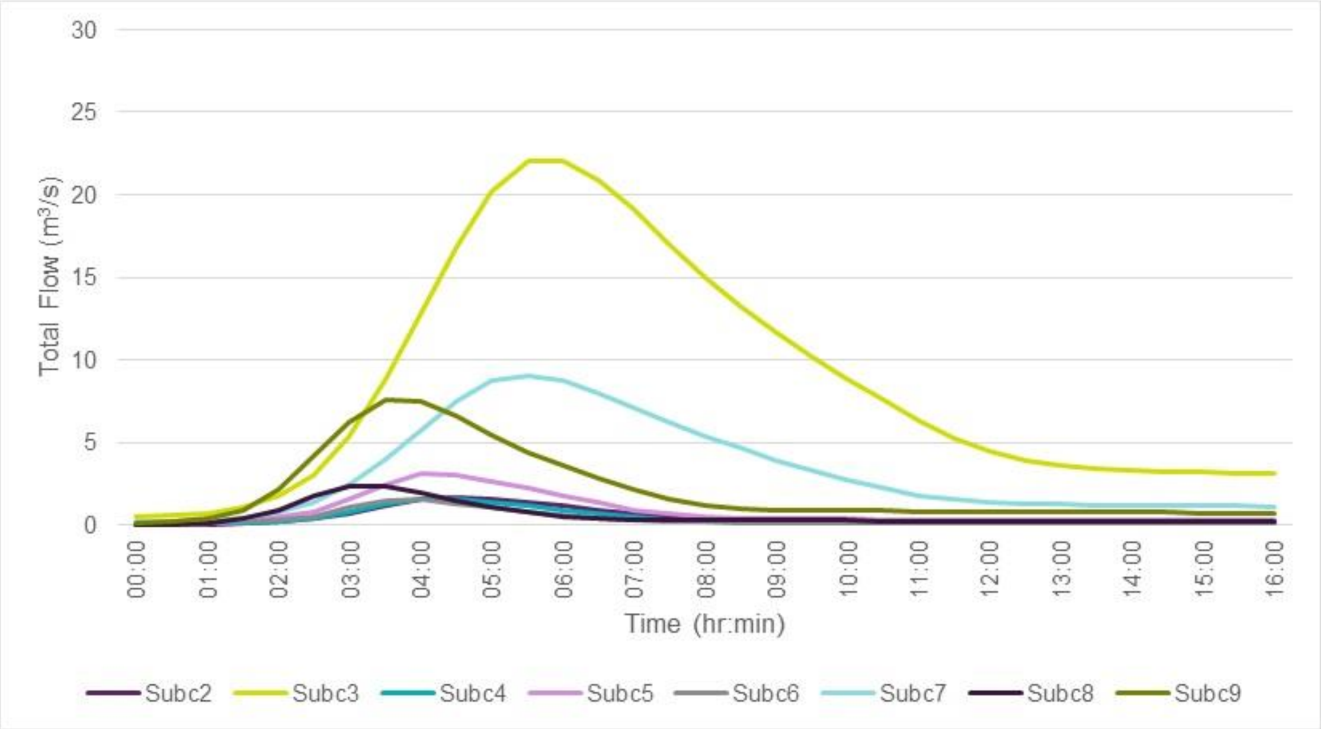

Figure 5.14 Phase 5 Operation fluvial hydrographs for 1:100 year AEP 2180s reasonable foreseeable

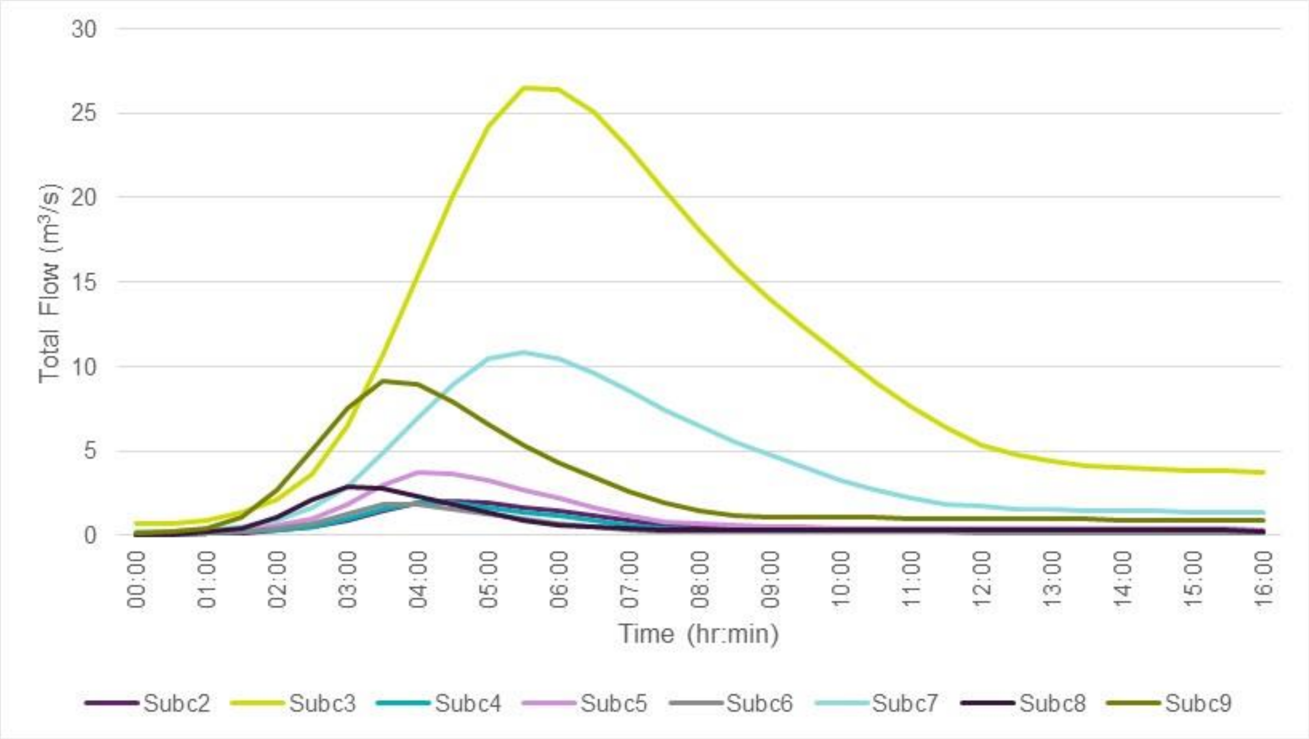

6. Sensitivity to permeable catchment adjustment

In Section 4.4 of this report, the FEH statistical peak flood values were derived from a pooling group with the removal of non-flood data from AMAX series of permeable catchments. The growth curve was derived considering all AMAX data as flood-year values irrespective of the non-flood year proportion. The aim of this test was to look into the effect of permeable catchment adjustment on the flood growth curve as prescribed in Chapter 19 of Flood Estimation Handbook Volume 3. The adjustment is applied to account for the non-flood years that usually appears in the AMAX data series of permeable catchments. This adjustment assumes Generalised Logistic distribution of AMAX data and hence growth factor for 1:2 year AEP event flood (QMED) is preserved to be 1 as recommended in FEH methods.

The pooling group for this test was taken same as that was used in section 4.4 (presented in Table 6.1 below). The growth curve derived for sub-catchment 3 from the pooling group was adjusted for permeable catchment in which statistical parameters L-CV and L-SKEW are adjusted for stations having SPRHOST less than 20%. Two such stations (26802 and 44008) were undergone for the adjustment. The adjusted flood growth factors and corresponding peak flow values were derived for a range of frequency events. A comparison of results for 1:100 year, 1:30 year and 1:2 year AEP events are presented in Section 6.1.

Table 6.1 FEH Statistical pooling group for sub-catchment 3

Station number	Station Name	Number of obs.	SDM	L-CV	L-SKEW	QMED
27051	Crimple @ Burn Bridge)	42	0.917	0.221	0.149	4.539
45816	Haddeo @ Upton)	21	1.006	0.313	0.404	3.522
28033	Dove @ Hollinsclough)	35	1.118	0.259	0.417	4.666
47022	Tory Brook @ Newnham Park)	21	1.217	0.255	0.072	7.331
25019	Leven @ Easby)	36	1.263	0.345	0.383	5.538
26802	Gypsey Race @ Kirby Grindalythe)	15	1.307	0.284	0.270	0.109
25011	Langdon Beck @ Langdon)	28	1.356	0.238	0.318	15.878
206006	Annalong @ Recorder)	48	1.509	0.189	0.052	15.330
25003	Trout Beck @ Moor House)	41	1.511	0.174	0.285	15.164
27010	Hodge Beck @ Bransdale Weir)	41	1.527	0.224	0.293	9.420
203046	Rathmore Burn @ Rathmore Bridge)	32	1.534	0.133	0.100	10.821
44008	South Winterbourne @	35	1.575	0.414	0.336	0.448

	Winterbourne Steepleton)					
49003	de Lank @ de Lank)	48	1.774	0.23	0.220	13.985
27032	Hebden Beck @ Hebden)	48	1.808	0.206	0.265	3.923
51002	Horner Water @ West Luccombe)	33	1.811	0.395	0.312	10.600

Source: HiFlows Dataset v.4.1, WINFAP v.3.0

6.1 Sensitivity test results

The FEH Statistical permeable adjusted peak flow is compared to the original results from the peak flow method in Table 6.2.

Table 6.2 FEH Statistical peak flows (m^3/s) for Sub-catchment 3

	FEH Statistical Peak flow				
Annual Exceedance Probability (AEP)	**Flood years only growth factor***	**Flood years only peak flow (m^3/s)**	**Permeable-adjusted growth factor**	**Permeable-adjusted peak flow (m^3/s)**	**Peak flow percentage change (%)**
1:2 year	1	2.98	1	2.98	0.0
1:30 year	2.357	7.02	2.376	7.08	0.8
1:100 year	3.232	9.63	3.262	9.72	0.9

*Source for flood years only values -Table 4.6.

The results show that the permeable catchment adjustment has an effect of increasing the peak flow. The increment is less than 1% for the range of AEP considered. This is considered to be negligible and proves to be insensitive to the adjustment. It is because of having very small number of non-flood years relative to the total number of AMAX data in the pooing group. The growth factors and corresponding peak flows reported in section 4.4 are reasonable and appropriate.

References

Bayliss, A.C. et al, 2006. *URBEXT2000 – A new FEH catchment descriptor, R&D Technical Report FD1919/TR.*

CEH, 2007. *Flood Estimation Handbook. Supplementary Report No. 1: The revitalised FSR/FEH rainfall-runoff method*. Centre for Ecology and Hydrology (CEH), Wallingford, 2007.

CEH, 2016. *FEH Web Service*. Available online at: https://fehweb.ceh.ac.uk/

CEH, 2017. *National River Flow Archive*. Available online at: http://nrfa.ceh.ac.uk/data/search

DECC, 2011. *National Policy Statement for Nuclear Power Generation (EN-6)*. Department for Energy and Climate Change, The Stationary Office, London, July 2011. Available online at: https://www.gov.uk/government/publications/national-policy-statements-for-energy-infrastructure.

EA, 2015. *Flood Estimation Guidelines*. Environment Agency, issued 21/01/15. Technical Guidance 197_08.

Institute of Hydrology, 1999. *Flood Estimation Handbook*. Institute of Hydrology, 1999. Wallingford, Oxon, 5 Volumes.

Kjeldsen, 2010. *Modelling the impact of urbanization on flood frequency relationships in the UK*. Hydrology Research, 41 (5). Pp. 391-405.

NRW, 2016. *Technical Guidance: Flood Estimation*. Natural Resources Wales, GPG 102.

ONR, 2014a. *Technical Assessment Guide (TAG) for External Hazards (TAG-13)*. Office for Nuclear Regulation, September 2014. Document ID: NS-TAST-GD-013, Revision 5. Available online at: http://www.onr.org.uk/operational/tech_asst_guides/ns-tast-gd-013.pdf.

ONR, 2014b. *Safety Assessment Principles for Nuclear Facilities*. Office for Nuclear Regulation, November 2014. Available online at: http://www.onr.org.uk/saps/saps2014.pdf

ONR and EA, 2016. *Joint Advice Note: Principles for Flood and Coastal Erosion Risk Management (for new nuclear power stations)*. Office for Nuclear Regulation and Environment Agency. Report reference: 16/02/18 Flood Risk Principles, Issue 6, 18 February 2016. Draft for Sign off – official. Approved by EA on 24 March 2016.

Stewart et al., 2013. *Reservoir Safety – Long Return Period Rainfall. Defra R&D Technical Report WS 194/2/39/TR, Vol 1 (Part 2)*. Available online at: http://evidence.environment-agency.gov.uk/FCERM/Libraries/FCERM_Project_Documents/long_return_part_2.sflb.ashx

Wallingford HydroSolutions, 2016. *The Revitalised Flood Hydrograph Model ReFH 2.2: Technical Guidance*. Wallingford HydroSolutions, Wallingford, 2016. Available online at: http://files.hydrosolutions.co.uk/refh2/ReFH2_Technical_Report.pdf

Welsh Government, 2011. *Adapting to Climate Change: guidance for flood and coastal erosion risk management authorities in Wales*. Available online at: http://gov.wales/docs/desh/publications/111231floodingclimatechangeen.pdf

Welsh Government, 2016. *Flood Consequence Assessments: climate change allowances*. Available online at: http://gov.wales/topics/planning/policy/policyclarificationletters/2016/cl-03-16-climate-change-allowances-for-planning-purposes/?lang=en

NOT PROTECTIVELY MARKED

Horizon Nuclear Power

Wylfa Newydd: Groundwater and Stream Flow Impact Modelling

Hydrogeology Modelling Factual Report

January 2018

Amec Foster Wheeler

Technical Note for

Horizon Nuclear Power
Sunrise House
1420 Charlton Court
Gloucester Business Park
Gloucester
GL3 4AE

Main contributors

Rob Soley
Josh Hall
Tim Lewis
Will Witterick

Amec Foster Wheeler

Floor 12
25 Canada Square
Canary Wharf
London E14 5LB
United Kingdom
Tel +44 (0) 203 215 1610

DMDC ref: 207017-0000-AA40-RPT-0007_005

\\att5-fs7.global.amec.com\shared2\Projects\35989 Wlyfa NNB Modelling\Design\Task 44 - Rev1 GW modelling\Deliverables\207017-0000-AA40-RPT-0007 Jan 18 GW Mod report data - i5 Final\X-MOD-207017-0000-AA40-RPT-0007 i5_Final.docx

Copyright and non-disclosure notice

Third-party disclaimer

Management systems

This document has been produced by Amec Foster Wheeler Environment & Infrastructure UK Limited in full compliance with the management systems, which have been certified to ISO 9001, ISO 14001 and OHSAS 18001 by LRQA.

Contents

Glossary of terms and definitions

TERM	DEFINITION
4R	Computer code to calculate daily Rainfall to Routed Runoff and Recharge (Heathcote et al, 2004).
AE	Actual Evaporation, as realised from rainfall, the soil and plants.
ArcGIS (ESRI)	Geographical Information System – software package for manipulating spatial data developed by the software house ESRI.
Drift	In this report this refers to the superficial geological sediments of glacial origin overlying the bedrock. These comprise the great majority of the superficial deposits except for recent alluvium, peat, beach deposits and soils. The shallow groundwater in them is represented at interflow in the 4R model for Wylfa Newydd, with underlying bedrock groundwater in MODFLOW
Effective Rainfall	This is the proportion of rainfall which is hydrologically effective, entering the surface water or groundwater flow systems rather than being lost back to the atmosphere through evapotranspiration. In the 4R model for Wylfa Newydd, total effective rainfall = Rapid Runoff over the surface + shallow superficial deposit Interflow + bedrock Recharge.
Evapotranspiration	The combined evaporation of water from the soil, the plants drawing water from it, and from open water. Can be reported at a Potential rate which would occur when there is no restriction on the water available to evaporate from the soil, or a rate Actually realised, depending on the ability of the plants to draw water from the soil.
FAO paper 56	Food and Agriculture Organisation Paper 56 describing soil moisture calculations for irrigation demands. This calculation approach has been adopted by the Environment Agency and written into the 4R code as a groundwater modelling industry standard for calculating evapotranspiration and the components of effective rainfall.
FDC	Flow Duration Curve: a statistical summary of daily flows plotted against the percentage of the time they are exceeded.
HNP	Horizon Nuclear Power.
Hydraulic conductivity	The rate of flow across a unit area of ground driven by a unit hydraulic head gradient, expressed in m/d. Regional flow rates within the Wylfa Newydd MODFLOW single layer model depend on the horizontal hydraulic conductivity which is profiled to vary with depth (referred to as VKD), and on the saturated depth over which these horizontal conductivities are integrated into the transmissivity. In this report, ‘hydraulic conductivity’ is used interchangeably with the term ‘permeability’ which is more generally understood.
Interflow	Shallow groundwater circulation and discharge back to the surface after evapotranspiration losses. In the 4R code this water has passed through the soil into the interflow linear store from which a fixed proportion is released each day, re-entering the surface routing network within a cell and combining with rapid runoff.
LIDAR	Ground elevation data captured by light detecting and ranging technology carried on light aircraft.
ModelMap	A GIS package illustrating model spatial datasets.
NRFA	National River Flow Archive.

TERM	DEFINITION
Permeability	A parameter defining the ease with which groundwater can flow through the ground – here used interchangeably with the term hydraulic conductivity which is defined more formally above.
PE	Potential Evapotranspiration, calculated from meteorological variables.
Rapid Runoff	Proportion of rainfall lost as runoff at the ground surface. In the 4R code this enters the surface routing network between model cells and the proportion generated depends on the daily rainfall intensity and soil moisture deficit at the time. So high intensity storm events when the soils are already wet will generate a higher proportion of rapid runoff in the routed surface drainage network.
RAW	Readily Available Water (FAO56 Parameter for soil moisture calculations).
Recharge	Water leaving the superficial deposits interflow store in 4R and accumulated for separate bedrock groundwater modelling in MODFLOW.
Reference Points 1, 4 and 5	These are the three phases which have been characterised; the Baseline (Reference Point 1) , Construction (Reference Point 4) and Operation (Reference Point 5) .
Release factor	The proportion of the water volume held in one of 4R's stores which is released into the surface drainage network each day. E.g. an interflow release factor of 0.1 means 10 % of the volume of water in the store is released each day back into surface routing each day.
REW	Readily Evaporable Water (FAO56 Parameter for soil moisture calculations) (Allen et al, 1998).
Superficial deposits	The sediments overlying the bedrock – mostly glacial Drift deposits, together with thinner peat, alluvium, beach deposits and soils.
Soil moisture deficit	A soil moisture deficit is developed by evapotranspiration of water from the soil. It represents the depth of water required to raise the soil moisture content back up to a capacity when additional water can be released from the soil as interflow or recharge.
TAW	Total Available Water (FAO56 Parameter for soil moisture calculations) (Allen et al, 1998).
TEW	Total Evaporable Water (FAO56 Parameter for soil moisture calculations) (Allen et al, 1998).
Transmissivity	The rate of flow through a unit width of the groundwater system driven by a unit hydraulic gradient, expressed in units of m^2/d. Calculated by integrating the profile of horizontal hydraulic conductivity with depth. A higher transmissivity means water can flow more easily, with less driving groundwater level gradient, than a lower transmissivity.
VKD	A profile defining the variation of horizontal hydraulic conductivity with saturated depth within a MODFLOW groundwater model layer. In the Wylfa Newydd model this profile is used to set a zone of more transmissive bedrock down to a depth of 5 m below rockhead, with the underlying bedrock assumed to be less permeable based on the combined analysis of investigation hydrotesting data.

1. Introduction

1.1 Purpose and applicability of this report

Horizon Nuclear Power Ltd (HNP) commissioned Amec Foster Wheeler to carry out groundwater and stream flow modelling for Environment Impact Assessment and Permitting to support the Wylfa Newydd Development Consent Order (DCO). The construction works involve extensive landform re-profiling of the superficial deposits together with associated drainage management for sediment control. The works also involve excavation and dewatering in the bedrock, so the model is required to predict the potential drawdown risks to receptors comprising wetland Sites of Special Scientific Interest and streams and private abstraction boreholes, in combination with the impacts of soil surface and catchment area changes on stream and ditch flows. The associated risks of the intrusion of saline water into the inland freshwater groundwater body must also be considered.

The Wylfa Newydd DCO model combines simulation of surface and near-surface processes carried out using the 4R code (Rainfall to Routed Runoff and Recharge, Heathcote *et al.*, 2004), with a bedrock groundwater simulation using the USGS MODFLOW code – a standard combination of modelling tools used extensively by the Environment Agency for regional groundwater modelling studies.

This report provides a factual account of the modelling methods and tools used to generate surface and shallow subsurface drainage daily flow and flow impact outputs, together with bedrock groundwater level drawdown impact predictions as part of the DCO. The report also presents the assumptions made and any limitations with the approaches used, and summarises the predicted impacts on groundwater level and surface flow receptors. This final version of the report has been amended in response to comments from Natural Resources Wales (NRW) discussed at a draft consultation workshop held in Cardiff on 28 June 2017, and provided following NRW formal review. It also incorporates impact predictions derived from additional engineering variant scenarios modelled during November/December 2017 to ensure that the more refined construction and completion design proposals have been represented.

The model impact predictions will be separately interpreted in the Environmental Impact Assessment for DCO in the context of the Wylfa Newydd Development Area and the sensitivity of associated hydro-ecological and private groundwater supply receptors, as well as supporting the application for a dewatering licence and associated discharge permits by HNP for consideration by Natural Resources Wales (NRW). This report does not include an assessment of the significance of impacts in the context of the receptor-scale conceptual understanding - it is a factual account of the modelling undertaken.

1.2 Responsible parties

The Amec Foster Wheeler staff responsible for this hydrogeological modelling work are listed as follows:

RESPONSIBLE PARTY	DESCRIPTION
Rob Soley	Hydrogeology Technical Lead
Tim Lewis	Hydrogeology Technical Reviewer
Will Witterick	Lead Modeller
Joshua Hall	4R Modeller
Tim Power	Task Manager
John Rampley	Task Director

1.3 Report contents and associated model output summary

It is important to emphasise that the primary purpose of this report is to provide a factual account of the numerical modelling work carried out. This work has incorporated the data available from previous reports detailing the hydrogeological investigations, testing, monitoring, analysis and conceptualisation of the Wylfa Newydd site and two of the key SSSI receptors – Tre'r Gof and Cae Gwyn (Jacobs 2016, Jacobs 2017, Horizon, 2017), and has also been designed to predict impacts on the Cemlyn Bay Lagoon SSSI. Some further conceptual synthesis has been required to summarise and simplify the hydro-testing data for numerical modelling purposes (as described in Section 3), but these previous reports provide a more comprehensive account of the field-based data and understanding, which is not repeated here. The model predictions have, in turn, helped to inform refinement of the reported conceptual understanding.

Section 2 of this report introduces the background to the Wylfa Newydd groundwater and river flow modelling, including the previous reporting. This includes the pressures and receptors to be considered, the objectives and spatial extent of the modelling, and the methodology proposals which have been presented to, and reviewed by, NRW previously.

Section 3 summarises the data synthesis and conceptualisation which underpins the numerical model design and parameterisation for the existing baseline and predicted future phase site conditions.

Section 4 presents the baseline model construction, parameterisation and calibration, in comparison with field measurements of stream flows and groundwater levels. It includes consideration of model sensitivity related to uncertainty around how much recharge may be entering and flowing through the bedrock - using alternative high and low recharge and transmissivity models compared with a Central (historical calibration) model. It also describes how the models representing site conditions at the height of construction (Reference Point 4), and during operation of the new power station (Reference Point 5) have been built by changing the boundary conditions assumed for the baseline models. Engineering variant scenarios have been run to consider how local deepening of the excavation and subsequent shotcreting of its walls and floor might affect predicted groundwater level and surface flow impacts. The alternative higher and lower bedrock recharge and transmissivity models have also been used to explore the sensitivity of the calibration and impact predictions to the simplified parameterisation assumptions.

Section 5 summarises the predicted construction dewatering rates needed to inform abstraction licensing, and the locations where time series of outflows from the drainage system are provided to inform discharge consenting. It also provides an overview of the predicted impacts associated with the differences between the Baseline, Reference Point 4 and Reference Point 5 models – explaining how they have been processed and where the details can be found in the appendices.

A brief factual summary of the work completed is finally included in **Section 6**, followed by a list of reference reports.

Figures have been embedded in or close to the text describing them for ease of review and understanding - to summarise modelling approaches, parameter distributions, calibration output and predicted impact post-processing formats. Comprehensive data collation, model build plans and outputs are also provided into six appendices at the back of the report as follows:

- **Appendix A:** Borehole hydro-test data;
- **Appendix B:** Baseline model build plans;
- **Appendix C:** Groundwater level and stream flow data compared with baseline historical model calibration;
- **Appendix D:** Predictive scenario model plans for Reference Point 4 (construction) and Reference Point 5 (operation);
- **Appendix E:** Environmental impact predictions – bedrock groundwater level drawdown and stream flow duration curves; and
- **Appendix F:** Digital results file listing.

The digital modelling files listed in Appendix F include a 'ModelMap' ArcGIS collation of all the drawdown predictions, together with the model build and parameter distributions to facilitate closer scrutiny of any locations as required. Similarly, the time series flow and dewatering predictions are collated in spreadsheets intended to allow analysis and plotting at a variety of scales, as required by the reviewer.

2. Modelling background, aims and area

2.1 Wylfa Newydd hydrogeology, pressures and receptors

Jacobs' (2016) Hydrogeology Baseline report for the Wylfa Newydd Development Area (boundary shown on figure 2.1) summarises previous reporting and the findings of borehole, geological and pumping test investigations. Fractured and generally low permeability bedrock is overlain by low permeability glacial till and alluvial superficial deposits. Most of the effective rainfall (i.e. the water not returned to the atmosphere by evapotranspiration) becomes surface runoff or travels through relatively shallow recharge, flow and discharge pathways in the superficial deposits and bedrock outcrops towards the streams and rivers which drain the catchments around the site. These flow pathways will be impacted by the landform re-profiling, forced drainage and sediment control works planned through the construction phases of the development.

There is also some recharge to a bedrock groundwater system which testing suggests is most permeable close to the rockhead (see Section 3 for further analysis). During autumn 2015, two pumping tests (figure 2.1) were carried out to investigate the possible response of bedrock groundwater to abstraction pressure over a longer time scale than the previous programme of hydro-testing associated with the ground investigation boreholes (Jacobs, 2016). The first borehole tested (PW1 which is located in the area proposed for deep excavations and dewatering) had low yield (~0.7 l/s) and only localised drawdown, but yields from the second borehole (PW2 to the east of the proposed excavation) were higher (9 l/s falling to 3.8 l/s) with drawdown responses noted up to 300 m away. These findings confirm that a bedrock groundwater impact pathway warrants further investigation and modelling, even if the regional connectivity and yield of the fractures through which flow occurs is expected to reduce with time as the upper more permeable zones are dewatered during the construction works. Further analysis of the variability of bedrock hydraulic conductivity measurements is presented in Section 3.

The excavation and dewatering to prepare for the construction of the reactor basements, intakes and other works will result in bedrock groundwater level drawdown. This could potentially induce saline intrusion and have an impact on wetlands (i.e. groundwater dependent terrestrial ecosystems) and stream baseflow where superficial deposits are thin or absent. It could also impact the few private groundwater abstractions located outside the Development Area (figure 2.1). There are two wetland SSSI receptors of particular interest. Most of the Tre'r Gof SSSI sits on thick, low permeability tills in a glacial kettle hole feature approximately 900 m north east of the proposed excavations for the reactor units. There will be marked changes in the landforms, catchments and drainage around Tre'r Gof and these are likely to dominate the potential impacts on the water balance of this wetland. The reported conceptualisation for this receptor (Horizon, 2017) accepts that bedrock drawdown impacts associated with the reactor excavations may result in some localised bedrock groundwater inflow reductions around the margins of Tre'r Gof where the Drift is thinner, but asserts that the associated risks to the shallow water table and dependent vegetation are likely to be relatively small. The Cae Gwyn SSSI is located around 1,000 m to the south west of the proposed excavation, at a higher elevation where the superficial deposits are thinner or absent (i.e. the bedrock outcrops). Monitoring at Cae Gwyn suggest that this site is at least partly supported by bedrock groundwater, particularly during the wetter winter months (Jacobs, 2017) – so the dewatering risks warranted closer modelling scrutiny alongside the field monitoring of baseline conditions. Impact risks to a third SSSI (Cemlyn Bay, some 1,500 m west of the excavation) – in particular, the naturally impounded brackish coastal lagoon there – are also considered in the model. Drawdown risks to surrounding private water supplies also need to be assessed.

Once Wylfa Newydd is completed and operational, the long term groundwater level consequences of drainage to the lowest impounded elevation within the permeable backfill material (6m AOD), and the completion of a relatively impermeable platform need to be predicted.

2.2 DCO modelling aims

The stream flow, drawdown and saline intrusion impact predictions reported here are based on a model which combines calculations of daily rainfall to routed runoff and shallow interflow (using the 4R code) with a simulation of recharge to, flow through, and discharge from, groundwater in the bedrock (using the MODFLOW code). The model also provides predictions of dewatering and surface drainage flow rates to underpin applications for a dewatering abstraction licence and surface water discharge consents needed to cover construction phase operations. Figure 2.1 shows the approximate location of the reactor units which will be the focus of excavation and dewatering, the SSSIs (Tre'r Gof, Cae Gwyn and Cemlyn Bay) and private groundwater abstraction receptors within a distance of 1.5 km from the excavation.

Figure 2.1 Wylfa Newydd Development Area, private groundwater abstractions, wetland receptors and pumping test locations

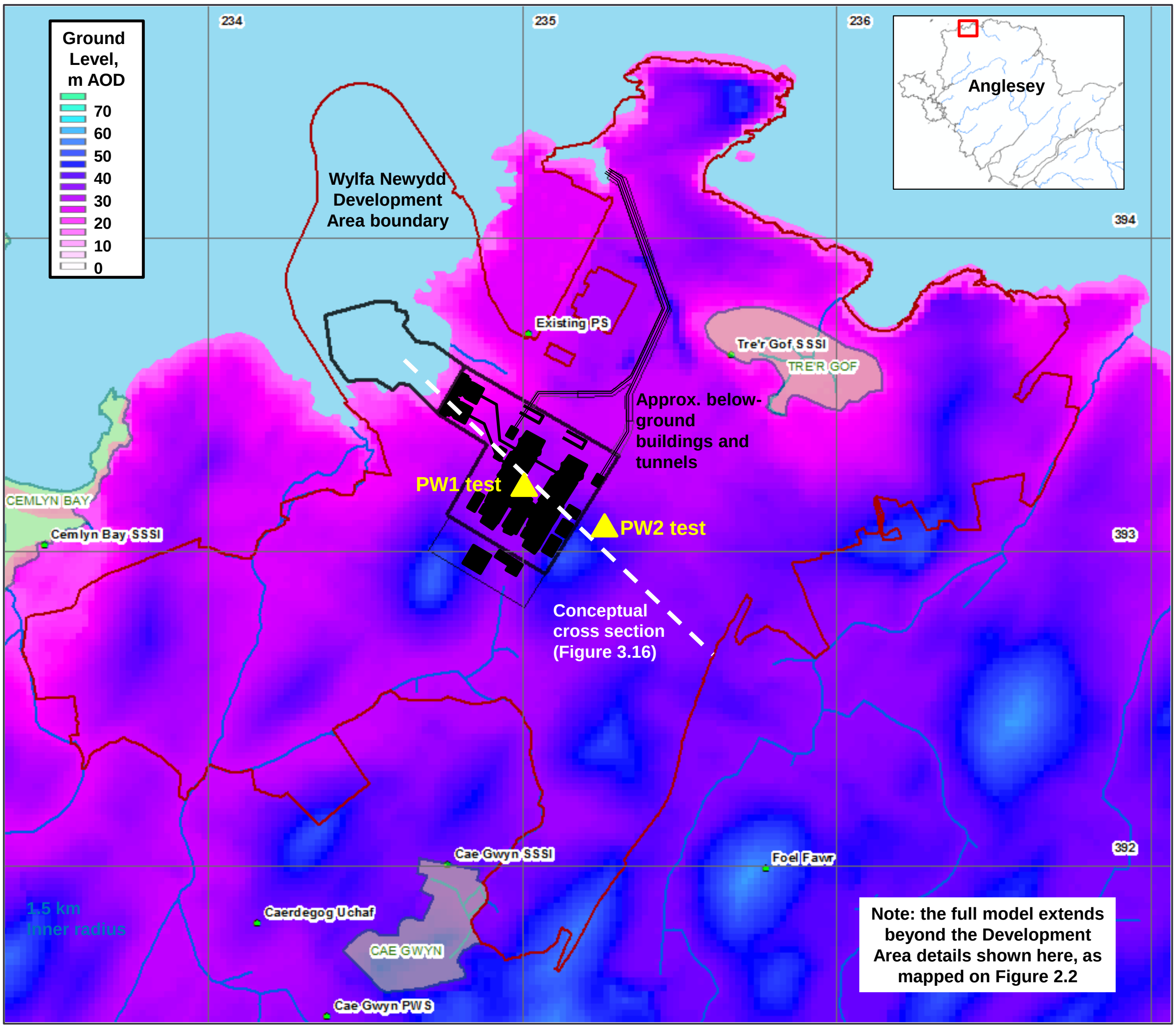

In summary, the functional objectives of this modelling work include the ability to predict the impacts of:

- landform re-profiling, land surface and vegetation changes and drainage management on surface flows across the site, during construction and for the long term operation – using the 4R code;
- excavation dewatering on bedrock groundwater/surface water interactions with streams and drains – using MODFLOW in combination with the near surface impacts represented in 4R;
- excavation dewatering on bedrock groundwater flows to the coast or the potential for saline water to be drawn inland;

- excavation dewatering on bedrock groundwater levels at Cae Gwyn, Tre'r Gof and Cemlyn Bay SSSIs and at private groundwater abstractions; and
- long term passive drainage of the permeable backfill around the sub-surface structures for the operational life of the power station.

The model also provides initial estimates of the range of daily pumping rates required to keep the Reference Point 4 Construction excavations dewatered – combining predicted groundwater inflows with the direct rainfall-recharge into the pit which will dominate the daily peak pumping requirements during storm events (no runoff into the excavation is simulated – it is all intercepted by perimeter drains). Time series surface flow estimates are also extracted from the Reference Point 4 model for the locations where discharges from the managed drainage system flow into receiving watercourse – to help inform consent applications.

This modelling work is NOT intended to consider:

- Extreme, short duration flooding events. Extreme pluvial and fluvial flows have been addressed and reported under a separate modelling task. The modelling work described here operates on a daily soil moisture balance, runoff and interflow calculation time step and is based upon historical meteorological, hydrological and hydrogeological data. As such, it is intended to consider the range of historical meteorological conditions that have occurred over a 50+ year period from 1960, rather than more extreme events lasting hours or minutes with longer return periods. We have, however, confirmed that the peak simulated flows from this work are consistent with the 1 in 50 year event peak flows from the pluvial and fluvial modelling.
- The consequences of climate change or drought events more severe than those experienced in the historical climate record from 1960. This historical record does include some significant drought periods which have been selected as a focus for output analysis but the focus of this modelling work is to predict the impacts of the construction and operational phases on the water and hydro-ecological regimes experienced by the environmental receptors over timescales of weeks, months and years - in comparison with the current baseline. In the flood modelling work it is important to consider short term extreme rainfall events beyond those experienced in the historical record in order to ensure that the drainage design is appropriate. But there is no similar imperative for this hydrogeological modelling work which aims to predict longer term groundwater drawdown and stream flow duration curve impacts.
- Sediment entrainment or surface water quality simulation. The work only considers surface flows at a daily average time interval. The construction phase model does incorporate a simple representation of the influence which settlement lagoon management can be expected to have in capturing runoff peaks to control sediment. But, whilst the model also includes a routing network for surface flows which could be developed further in future to help predict the fate of pollution spills, it is not intended as a platform to consider issues of sediment entrainment and transport capacity.

2.3 Spatial extent of the combined 4R and MODFLOW models

The 4R and MODFLOW models for the Baseline (Reference Point 1), Construction (Reference Point 4) and Operation (Reference Point 5) all cover an area shown in figure 2.2. This is the same as previous 4R modelling carried out to predict the flow impacts associated with site clearance soil stripping (Reference Point 2). It includes the catchments draining to the Tre'r Gof and Cae Gwyn wetlands, the Cemlyn Bay SSSI brackish/freshwater coastal lagoon, and the construction sites for the reactors and associated developments. Llyn Llygeirian is located in modelled catchment headwaters around 2 km south of the Development Area boundary - well beyond any potential hydrological impacts. The models are constructed on a common regular grid of 20 m by 20 m cells and combine to simulate surface flows across a routed network of streams and drainage channels, interacting with bedrock groundwater levels. The impacts of the earthworks, landform, drainage and surface vegetation changes, excavation and dewatering are predicted by comparing outputs from the Construction and Operation phase models against the current Baseline condition.

Figure 2.2 Area covered by Wylfa Newydd 4R and MODFLOW model grids (20m x 20m cells) showing the Wylfa Newydd Development Area and the SSSI receptors which have been a focus for impact predictions

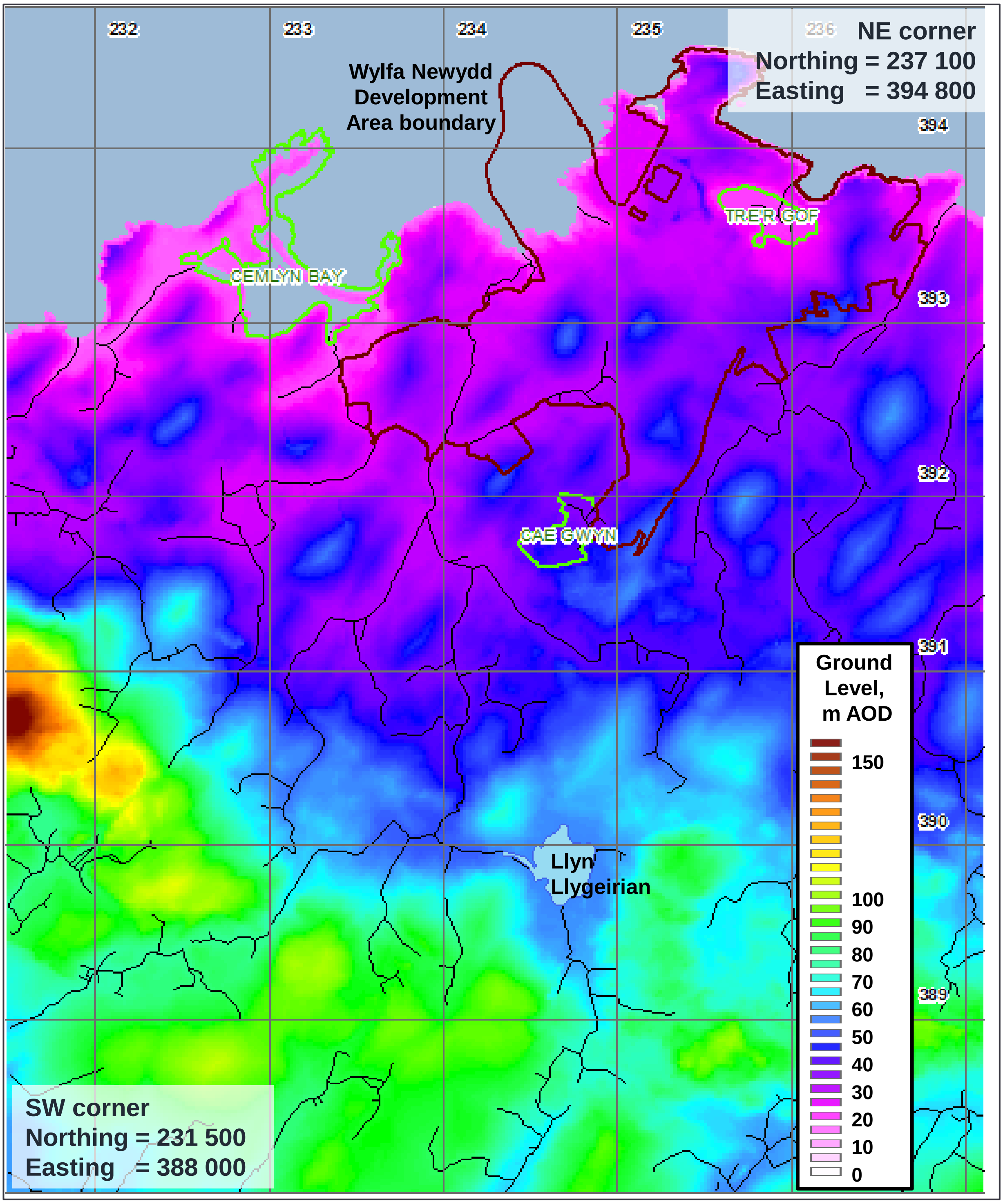

3. Hydrogeological data synthesis and conceptualisation

3.1 Data collation

The data inputs for the DCO groundwater and stream flow modelling are summarised below in Table 3.1.

Table 3.1 Summary of modelling input data sources

Input Data	Data source
Rainfall	Daily totals from RAF Valley Met Office station (~16km to the south) for 1 January 1960 to 31 July 2016. Previously analysed in comparison with Wylfa site monitoring in Amec Foster Wheeler, 2015 NSMHHA Report 200383-000-000-RPT-0003 Revision 5 issue 3.
Reference Potential Evapotranspiration	Calculated from daily max and min temperature and wind speed data from RAF Valley for 1 January 1960 to 31 July 2016.
Land use (baseline)	CORINE Land Cover 2006 data, version 17.
Soil texture	BGS Soil Parent Material Model data
Geology mapping (solid and Drift)	BGS 1:50k
Superficial deposit thickness and rockhead grid covering the whole model area (to extend site investigation data understanding)	BGS national model dataset
Surface routing (baseline)	Cell by cell downhill routing derived from OS Terrain 5 data and Natural Resources Wales LiDAR 2015 topographic elevation data, and forced to align with natural blue line mapped streams or drainage plans.
Ground investigation reports, borehole data and rockhead surface for the site	Reports, data and modelled site geology surfaces provided by HNP. Jacobs (2016) Borehole logs used to modify BGS rockhead.
Hydro-testing data (hydraulic conductivity) derived from short term BH and 2 longer term pumping tests	Summary reports and data provided by HNP (Jacobs, 2016)
Flow and groundwater level monitoring data across the site, including Tre'r Gof and Cae Gwyn	Monitoring data supplied by HNP, (reported in Jacobs, 2016)
Flow data, Afon Cefni at Bodffordd Gauging Station	National River Flow Archive data to provide a longer term indication of daily flow variability from a reliable gauging station located in a nearby Anglesey catchment (~18km to the south) with similar geology.
Baseline reports (hydrogeology, Tre'r Gof), and the location of known private groundwater supplies and any other environmental receptors to be considered	Summary reports and data provided by HNP (Jacobs, 2016, Horizon, 2017)
Detailed landform (topography) and drainage design plans for Reference Points 4 and 5 in digital formats	HNP Reference Point 4 from [5151821-ATK-XX-ZZ-M2-L-001 to 005 Rev 4.0.dwg] and Reference Point 5 from [20170331 ACAD-WN-ATK-EW_MUND-ZZ-M2-C-0002_Prop_Landform_Ref_5-Model]
Specification of proposed excavations, deep structures, backfill and dewatering assumptions for Ref Points 4 and 5.	HNP [Modelling Assumptions Log Version 4 – [35989-C1107_v4 Model Input Statement_Phase_4 and 5_01-06-17]

The focus of this modelling work is to quantify the potential environmental and abstraction receptor impacts of the landform re-profiling, drainage and dewatering associated with the construction Reference Point 4, and the longer term passive groundwater drainage around the reactors. For this purpose it is assumed that the meteorological variation which exists within the historical 1960 to 2016 daily time series being modelled will adequately contextualise the range of predicted impacts on surface flows and the groundwater system – without the need to explicitly consider climate change influences.

3.2 Initial data analysis and conceptual model development

Based on the review of previous reports and analysis of the available data, a conceptual hydrogeological model of the site was developed to underpin the numerical model design. This section summarises the available topographical, Drift thickness, surface flow, groundwater level and hydro-testing data, and explains the choice of model design based on the planned site works and predicted impact objectives of the modelling. A more detailed analysis of the large amount of hydro-testing (permeability) data is also included to inform the conceptually simplified parameter assumptions used in the numerical model (Section 3.3). A comprehensive description of both 4R and MODFLOW components of the baseline numerical model is provided in Section 4.

Topography, geological mapping and glacial Drift thickness

Detailed investigation drilling across the development site has provided high resolution information on the hard fractured bedrock geology which will be excavated to provide the reactor foundations and the superficial deposits which will be extensively re-profiled and re-distributed. These data have been presented separately in the Jacobs (2016) hydrogeological baseline report. However, in order to build a groundwater and stream flow model extended to cover all of the surface water catchments draining onto the development site or potentially impacted wetland receptors, it has been necessary to collate ground elevation data from Ordnance Survey Terrain 5 and Natural Resources Wales LiDAR sources and to combine this with digital Solid and Drift geology 1:50,000 map datasets available from the British Geological Survey (BGS).

Figure 3.1 presents a series of high resolution three dimensional topographic drape images based on the 5 m gridded OS Terrain 5 ground elevation data in which the vertical dimension is exaggerated to 10 times the horizontal in order to emphasise landform characteristics. The ground surface is coloured according to:

a. The ground elevation, in m Above Ordnance Datum (m AOD).

b. The surface mapping of glacial Drift superficial deposits, with bedrock outcrops left uncoloured. The boundaries of the three SSSIs are also labelled.

c. The thickness of Drift deposits indicated by the BGS national digital superficial deposits thickness dataset (available on a coarser 50 m grid).

Figure 3.1 3D topography and Drift thickness images

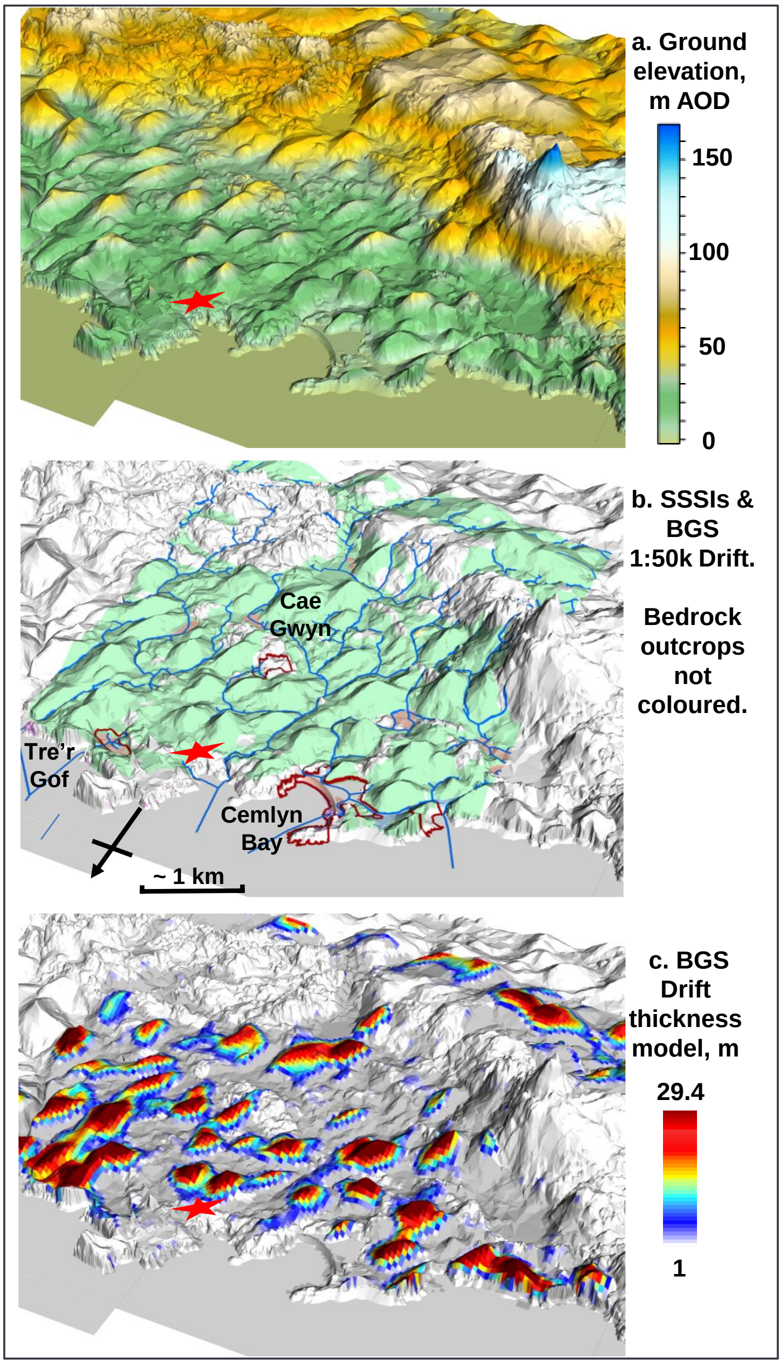

The viewpoint for all three drapes looks south eastward and the location of the Wylfa Newydd proposed reactors is approximately indicated with a red star.

There is extensive Drift coverage across most of the development site and surrounding the SSSIs. This is predominantly low permeability glacial Till left by retreating ice sheets. The BGS 1:50k mapping shows the solid metamorphic Cambrian age bedrock to outcrop forming the crest of the ridge of higher ground to the south west. Bedrock is also exposed around the coastal margin and cliffs, and in smaller exposures inland.

However, low permeability glacial Till cover of at least 1 m thick is extensive across the development site and thicknesses can approach 30 m according to the site investigation data, and the BGS Drift model, in a series of oval-shaped 'drumlin' mounds. These sit on a rockhead surface which has been smoothed and levelled by glacial erosion. The drumlin mounds tend to be slightly elongated along a north east – south west orientation. Figure 4.4 also presents maps of the superficial deposit thickness.

Ground investigation has shown the Tre'r Gof SSSI to be located mostly on relatively thick low permeability Drift sitting within a deep 'kettle hole' depression in the rockhead surface (Jacobs, 2016b). Direct interaction with bedrock groundwater is considered to be localised around the margins of the wetland (where the Drift is thinner), with the hydro-ecology of the plant species present more dependent on rainfall inputs to a shallow nutrient-poor water table in the peat which is held up by the surface water channels draining to its impounded outflow point to the sea.

Cae Gwyn, by contrast, sits at a higher elevation, adjacent to bedrock outcrops, and water levels in the peat close to the surface lie within much shallower bedrock depressions – this SSSI water table is in closer hydraulic continuity with bedrock groundwater (Jacobs, 2017).

The gravel berm which impounds the freshwater or brackish lagoon at Cemlyn Bay is a distinctive feature which is associated with the European Habitats Directive level designation of this SSSI and is clearly apparent in the figure 2.2 images. Surface water inflows to the lagoon probably dominate its water balance, in combination with interaction, through the gravel berm, with the sea. But it is also understood to interact with groundwater within the superficial deposits and possibly also with the bedrock around and beneath it.

The relatively coarsely gridded BGS Drift thickness data have been kriged to the finer OS Terrain grid in order to calculate a continuous rockhead surface across the model area. This was necessary because the analysis of hydro-testing permeability data indicated that there are marked increases in bedrock permeability close to the rockhead surface - presumably associated with weathering and the opening of fractures due to erosion and stress relief. Figure 3.2 shows the OS Terrain ground level and the rockhead elevation map derived from it by removing the kriged BGS Drift thickness and illustrates how much of the landform mounding between the bedrock hills to the south and the coastline is related to the glacial drumlins.

Figure 3.2 Ground and rockhead elevation maps

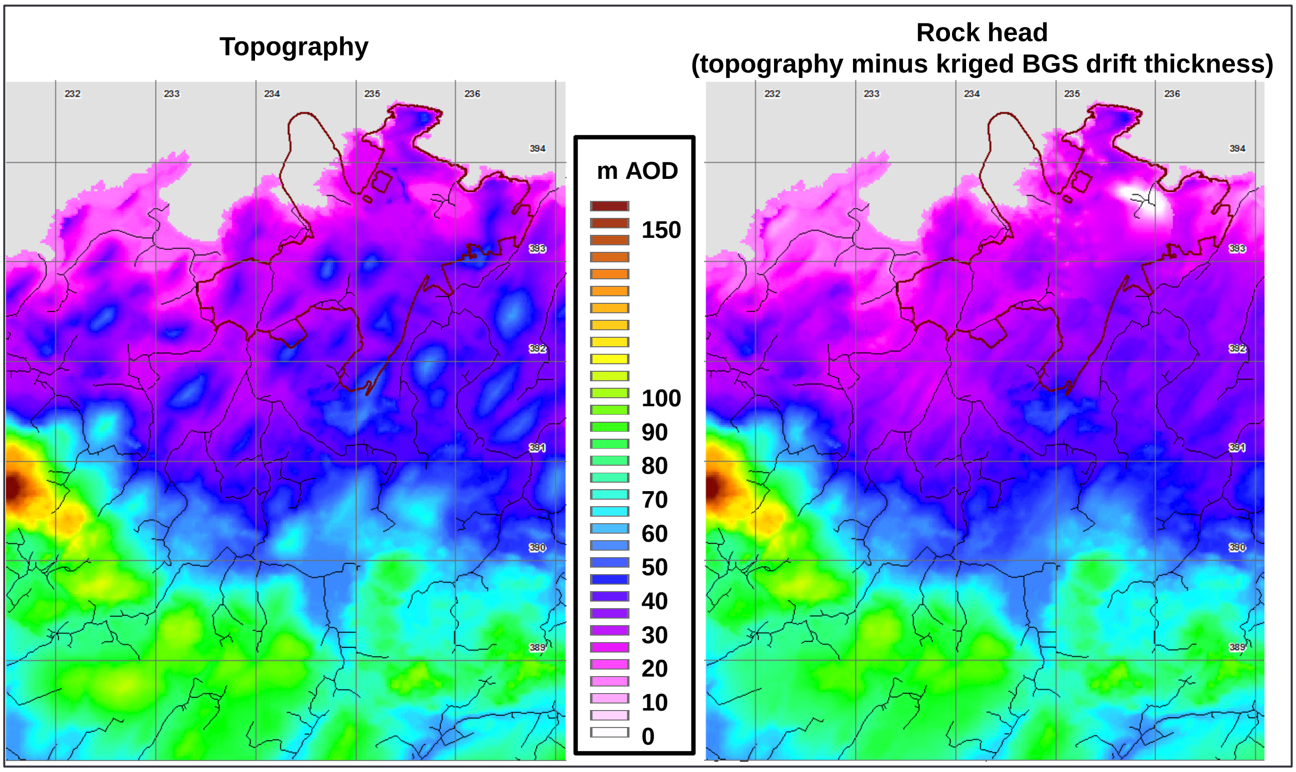

Within the area where more detailed ground investigation data are available, further modifications to the land elevation, Drift thicknesses and associated rockhead estimates were made (based on the borehole logs which penetrate the rockhead) before they were used to inform the numerical groundwater model build. In addition, targeted manual corrections were made to the rockhead elevation under Tre'r Gof, since interpolation of available measured elevations did not reproduce the 'bedrock depression' feature that is known to exist at Tre'r Gof.

Stream flow gauging data and impact analysis sites

Jacobs (2016b) describe the installation of five flumes around the Tre'r Gof SSSI as part of the hydrological baseline characterisation investigations. Four of these (VN1 to VN4, as referred to elsewhere, at surface flow receptor locations TG1 to TG4) measure flows onto the wetland and the fifth (VN5 as referred to elsewhere at flow receptor TG5) measures flow off it - northwards to the coast. Their location is mapped in figure 3.3 together with the two other sites where flumes (Flume A and Flume B) have been installed more recently to gauge flows continuously on the Nant Caerdegog Isaf tributary of the Afon Cafnan, and the Nant Cemlyn respectively. The model area has been set to include all of the surface water catchments to these gauged points so that they can be used for flow calibration purposes. It also covers the entire catchment areas for the environmental receptors including Cemlyn Bay, Tre'r Gof, Cae Gwyn and the stream network on which a number of flow impact analysis points have been located (figure 3.3 – including the Nant Cemaes and Nant Caerdegog Isaf streams).

Figure 3.3 Surface water flow calibration and receptor impact analysis locations

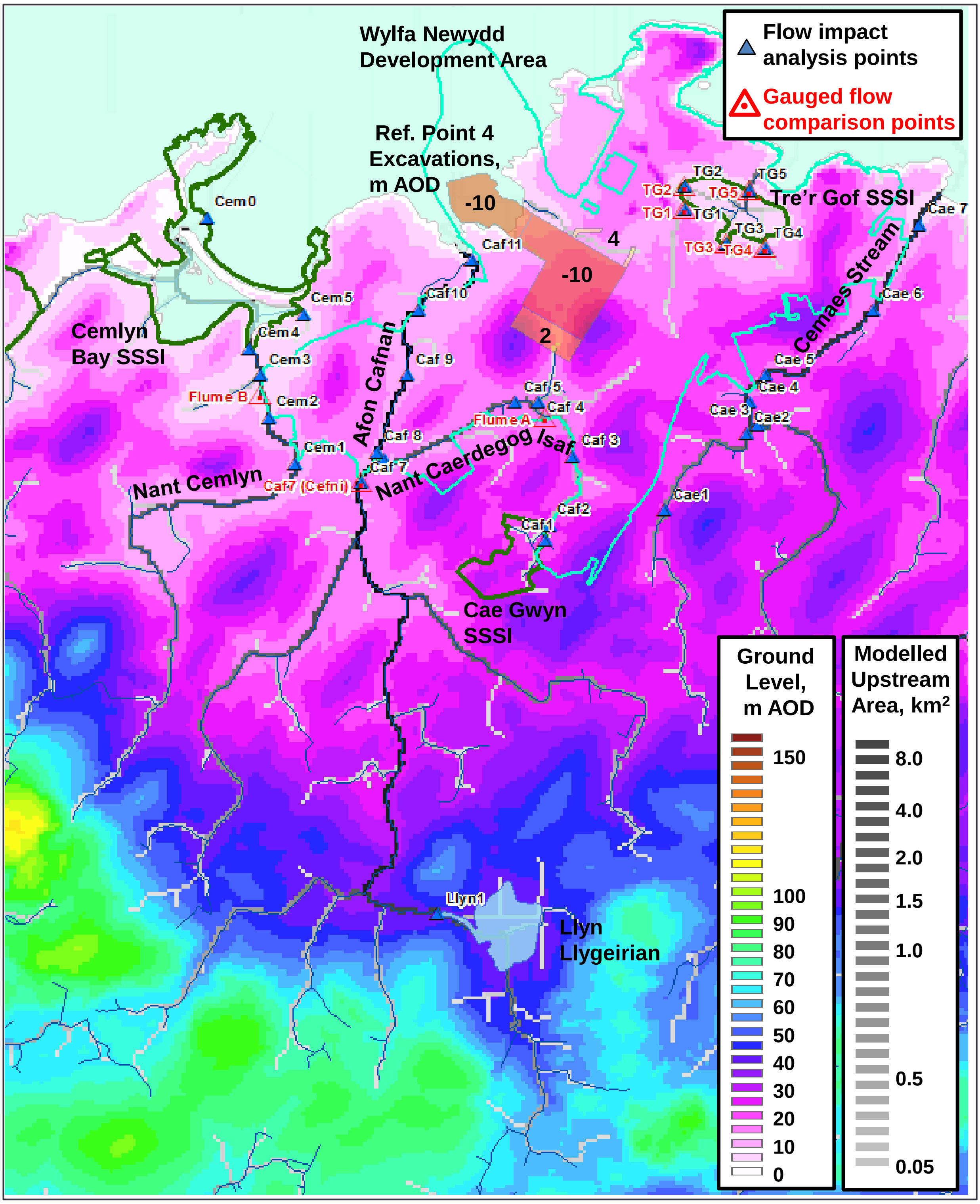

Figure 3.8 provides a larger scale Development Area view of the colour flood topography and upstream routed area details on figure 3.3. The baseline existing ground surface elevations are mapped on the 20 m regular model grid and have been used in association with the blue line stream network to define a routing network as part of the 4R rainfall to routed runoff and recharge model. The light to darker grey model cell

colouring overlying the topography shows how the total modelled upstream surface area accumulates down this stream network. Figure 3.3 also shows the blue line boundary of the Wylfa Newydd Development Area, and the outline and depths of the excavations which, together with re-profiled land forms and surface drainage routing, have been modelled to predict the potential impacts of Reference Point 4 construction on the flow receptors, SSSIs and bedrock groundwater levels.

All of the flow records gauged within or close to the Wylfa Newydd site are of relatively short duration and variable quality. The Tre'r Gof site records start in 2012 but have a break during 2014 before renewed monitoring in 2015 and 2016 – to the end of the data collation period in July 2016. Flume A and B flows (and associated spot gaugings) are only available from autumn 2015 (figure 3.4).

Figure 3.4 Gauge flow time series used for model calibration (located on figure 3.3)

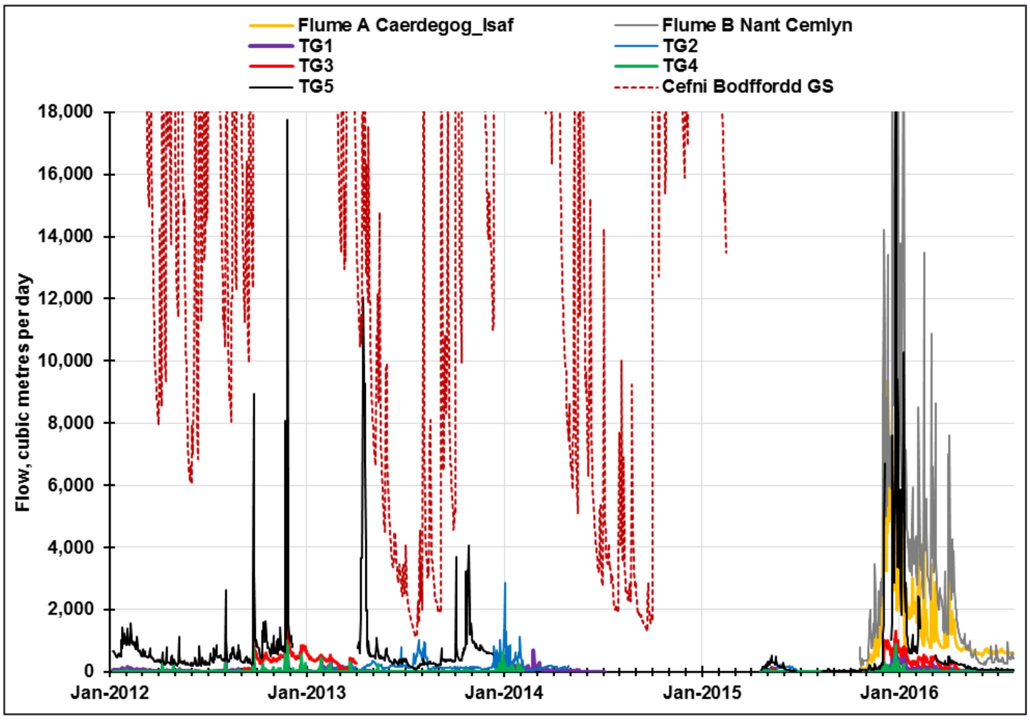

In order to allow for comparison of simulated flow response characteristics against a longer term and more reliable record, National River Flow Archive data available for the Afon Cefni at Bodffordd gauging station were also collected. This station has gauged flows from a much larger catchment (21.7 km^2) 19 km to the south at the centre of Anglesey, starting in 1988. It is accepted that both the rainfall and catchment response characteristics of the Afon Cefni will differ from those local to Wylfa. However, it was still considered helpful to compare the available Bodffordd record (also shown on figure 3.4) against flows simulated in the Afon Cafnan at site Caf7 (figure 3.3) by scaling according to the ratio of mean simulated and gauged flows - in order to review the credibility of the flow response range characteristics in the broader Anglesey context.

Comparison of gauged flows between the Tre'r Gof monitoring points in figure 3.4 suggests that the inflow record for TG2 may in part be unreliable as it contains improbable step changes and periods when it exceeds the outflows gauged more credibly at TG5 (e.g. apparently during the summer of 2013). The contributing areas to the smaller catchment inflow gauges (TG2 and 4 all have less than 0.1 km^2 upstream according to the modelled routing) are also poorly defined because the connectivity of surface ditches and the capture zones of shallow Drift groundwater seepages draining into them are not well constrained. TG1 inflows are also unexpectedly small based on the modelled upstream area – which may indicate that there is shallow groundwater flow beneath or around the gauge. As the total contributing surface catchment area to these gauging sites increases, the correlation with flows is expected to become more predictable. So the total Tre'r Gof outflow catchment record TG5, and the Flumes A and B on the Nant Caerdegog Isaf and Nant Cemlyn streams respectively are of most value for the calibration of the 4R-MODFLOW numerical model described in Section 4 (where each record is plotted at a larger scale, e.g. see Figure 4.12). Comparison of the time series from Flumes A and B in figure 3.4, and with check spot flow gaugings included on calibration plots in Section 4 also suggests that the summer 2016 Flume A rating curve is overestimating flows.

In order to further compare the flow records available for calibration, they have been divided by their modelled or reported upstream surface catchment areas, and then plotted as per unit area flow duration curves (Figure 3.5). The Nant Cemlyn Flume B curve and higher parts of the Flume A and TG3 curves are closest to that for the much larger Bodffordd gauged catchment. The TG2 curve is also comparable suggesting that the obvious errors apparent in the time series perhaps relate to an issue with timing.

Figure 3.5 Flow per unit area duration curves for the gauged records, 2012 to 2016

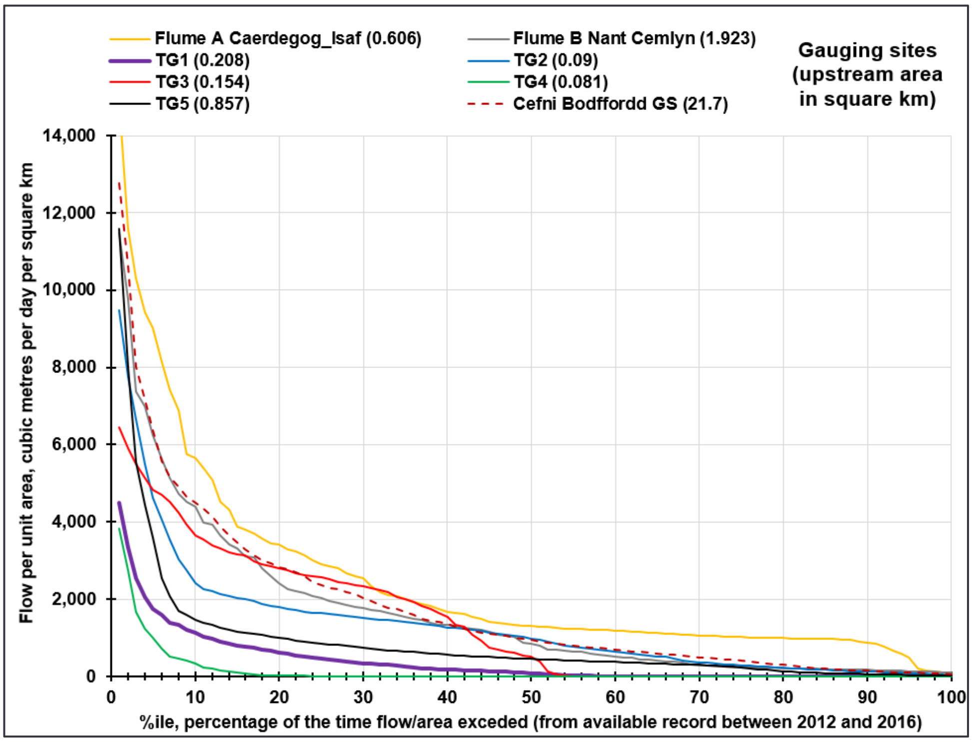

The lower portions of the TG3 record fall to zero much sooner than the Bodffordd response, and low flows at Flume A are apparently much more resilient– suggesting these flow ranges may be less reliable. The curve for TG5 is generally lower than Bodffordd, probably reflecting lower rainfall of the lower elevation north east coastal location, although the lower 30% of flows per unit area are similar. The curves for TG1 and TG4 are extremely low which probably indicates that the effective catchment for these sites is in reality less than assumed in the modelled routing, and/or that there is perhaps shallow Drift groundwater flow beneath the gauges.

Whilst this assessment of the flow gauge records highlights the caution which should be associated with their use for model calibration, they are the only flow data available for this purpose. It is also important to note that the 4R model described in Section 4 is not intended to capture baseline hydrogeological variability within the superficial deposits on a small scale (which is not well known anyway), beyond a simple understanding of their thickness on the 20 m modelled grid. Its purpose is rather to credibly represent the *changes* in catchment area, runoff responses, surface flow patterns and recharge which can be expected to result from the landform re-profiling associated with the Wylda Newydd development.

Groundwater level data

In addition to the surface flow gauging data discussed above, there are many groundwater level monitoring sites fitted with data loggers to collect daily data (alongside manual check dips). These high resolution data provide important insight into the response of the groundwater system to recharge and pumping stresses. Analysis of these data has fed into the development of the conceptual understanding, as well as the data being used for comparison with levels simulated by the numerical model during refinement and calibration of the baseline model. Appendix C tabulates and maps the location of the 96 records used for comparison with modelled levels. These include all of the available bedrock records (because the MODFLOW model simulates bedrock groundwater flows and levels), and a few selected wetland water table monitoring sites.

Figure 3.6 plots all the daily averaged groundwater monitoring data from the Development Area for the period from August 2015 to January 2016 to illustrate the quantity of information available, and to pick out some of the initial understanding which can be derived from these data. Rainfall is included at the top of the plot, and data from monitored intervals within the superficial deposits are plotted separately from bedrock groundwater level elevations. Most of the superficial and bedrock hydrographs exhibit recharge (rising) responses to rainfall over the period mid-November to mid-January. Several superficial and bedrock groundwater hydrographs show a stepped rise in levels (typically around 2 m) around 5 December 2015 – the day after 25 mm of rainfall was recorded nearby at RAF Valley. One of the superficial deposit hydrographs highlighted as a thicker blue line in Figure 3.6 shows a much larger groundwater rise during this recharge event taking levels from 3 m below ground to 1.8 m above ground. This record is from BH311CP, located 30 m from the coast to the north east of Tre’r Gof, which has a monitored screened interval in the deep superficial deposits (23 to 25 m below the ground level of 12 mAOD). Whilst the timing of this stepped response is in line with other hydrographs its magnitude seems implausible given the more muted response to subsequent recharge events. Levels were generally flat or slowly recessing in the preceding period despite rainfall events of similar magnitude, emphasising the importance of the simulation of evaporative losses and soil moisture deficits which is carried out within 4R.

Figure 3.6 Groundwater levels and rainfall measured between August 2015 and January 2016

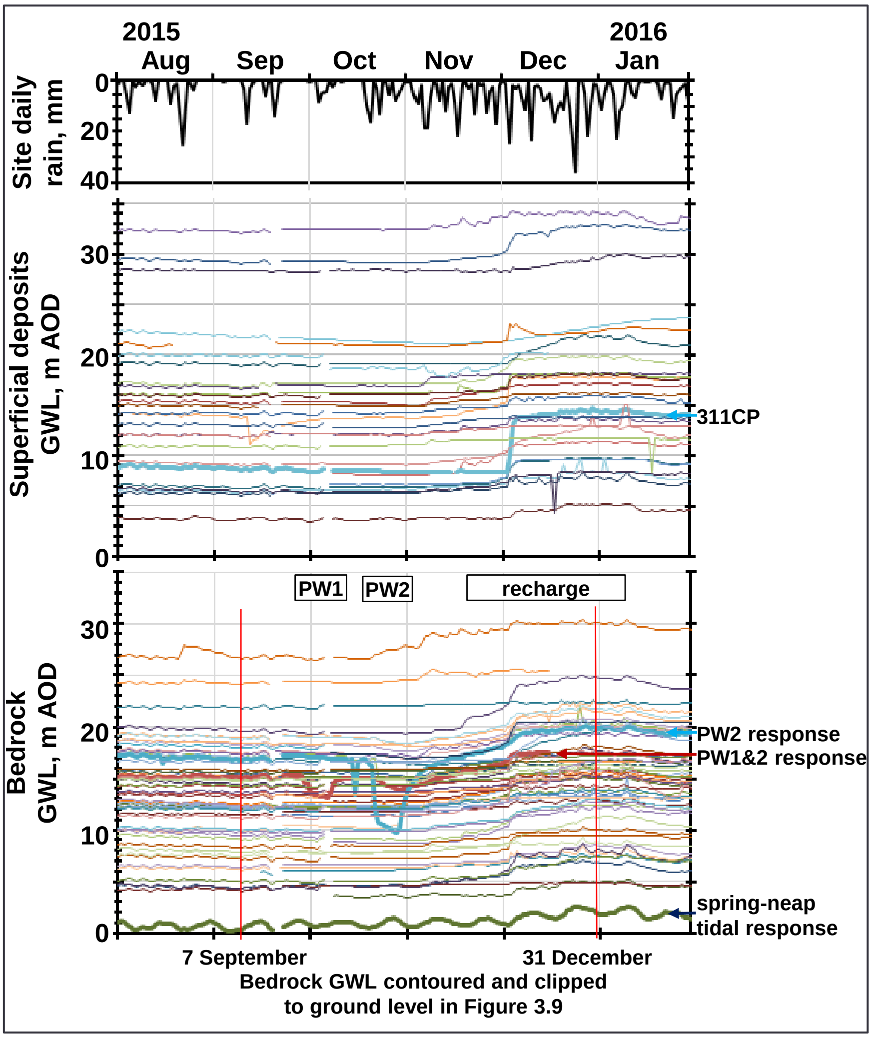

One of the bedrock hydrographs – plotted and labelled in figure 3.6 as a thickened brown line (BH787R) – is only 36 m from the first borehole pumping test (PW1) and is the only hydrograph to show a clear response. It also responds to a lesser extent to the pumping of the second, more distant borehole tested (PW2). Monitored responses to the second, higher yield pumping test (later in October 2015), were more widespread (c. 300m) – most notably in the labelled thick blue hydrograph (BH801R).

The lowest elevation bedrock groundwater level hydrograph on the plot (labelled thick green) is located 30 m from the coast. Although the daily resolution of the data does not show the twice daily tidal cycle, a clear neap – spring tidal signal is evident. The more comprehensive data review presented in the Jacobs Baseline Hydrogeology report suggests that such tidal responses are only seen in data monitored within approximately 50 m of the coast.

Superficial deposit and bedrock groundwater level contour maps from the Hydrogeology Baseline Report are presented in figure 3.7 for the September and December 2015 periods, selected to maximise data coverage before and after the noted recharge response. These maps support the interpretation that patterns of groundwater flow remain similar between seasons, and that there is both a north-easterly gradient driving bedrock flow towards the coast beneath Tre'r Gof, and a north-westerly gradient from Cae Gwyn towards Cemlyn Bay. They also highlight the locally higher levels apparent where superficial deposit monitoring exists in the low permeability drumlin features.

Figure 3.7 Groundwater level (m AOD) contour maps (adapted from Jacobs Baseline Hydrogeology Report)

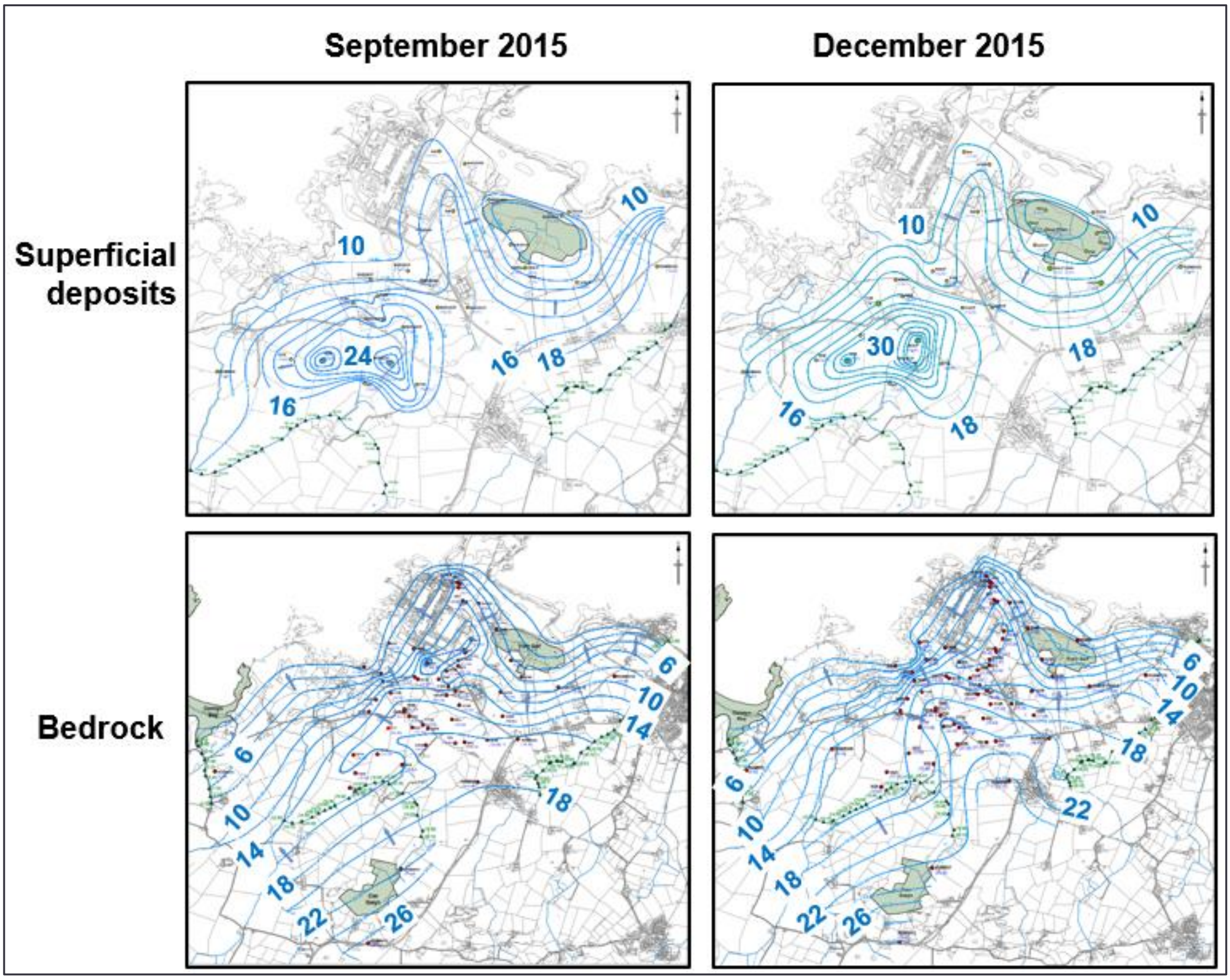

The MODFLOW model described in Section 4 has been designed to simulate flow and groundwater levels in the bedrock only, water in the superficial deposits being represented in 4R – so additional analysis and calibration attention has focused on the bedrock groundwater level monitoring. Bedrock simulated groundwater levels located beneath the shallower Drift water table piezometers on Cae Gwyn and Tre'r Gof SSSIs have also been extracted for comparative plots although it is important to emphasise that the Drift groundwater is not explicitly represented in the MODFLOW model.

The locations of the monitored borehole and piezometer records used for comparison with simulated bedrock groundwater levels from the baseline historical model are shown in figure 3.8 which includes a simple summary of the historical model calibration, as discussed in section 4.6. These provide locally detailed coverage across the site investigation area only. Each monitored hydrograph has been plotted in the calibration appendix C – together with the ground level and rockhead elevations derived from the associated borehole information, and the model simulated levels. A selection, distributed across the site, have been collated together to facilitate calibration review in Section 4 figures (locations shown on figure 3.8). Figure 3.8 also maps the location of the bedrock groundwater level receptor impact analysis cells at the three SSSIs, the Existing Power Station site and at three private groundwater supplies (Caerdegog Uchaf, Cae Gwyn, and Foel Fawr). In addition to tabulated data for these receptor cells, bedrock groundwater level drawdown maps are presented in plan and GIS formats so that predicted impacts can be derived for any location.

Figure 3.8 Bedrock groundwater level calibration and receptor impact analysis locations

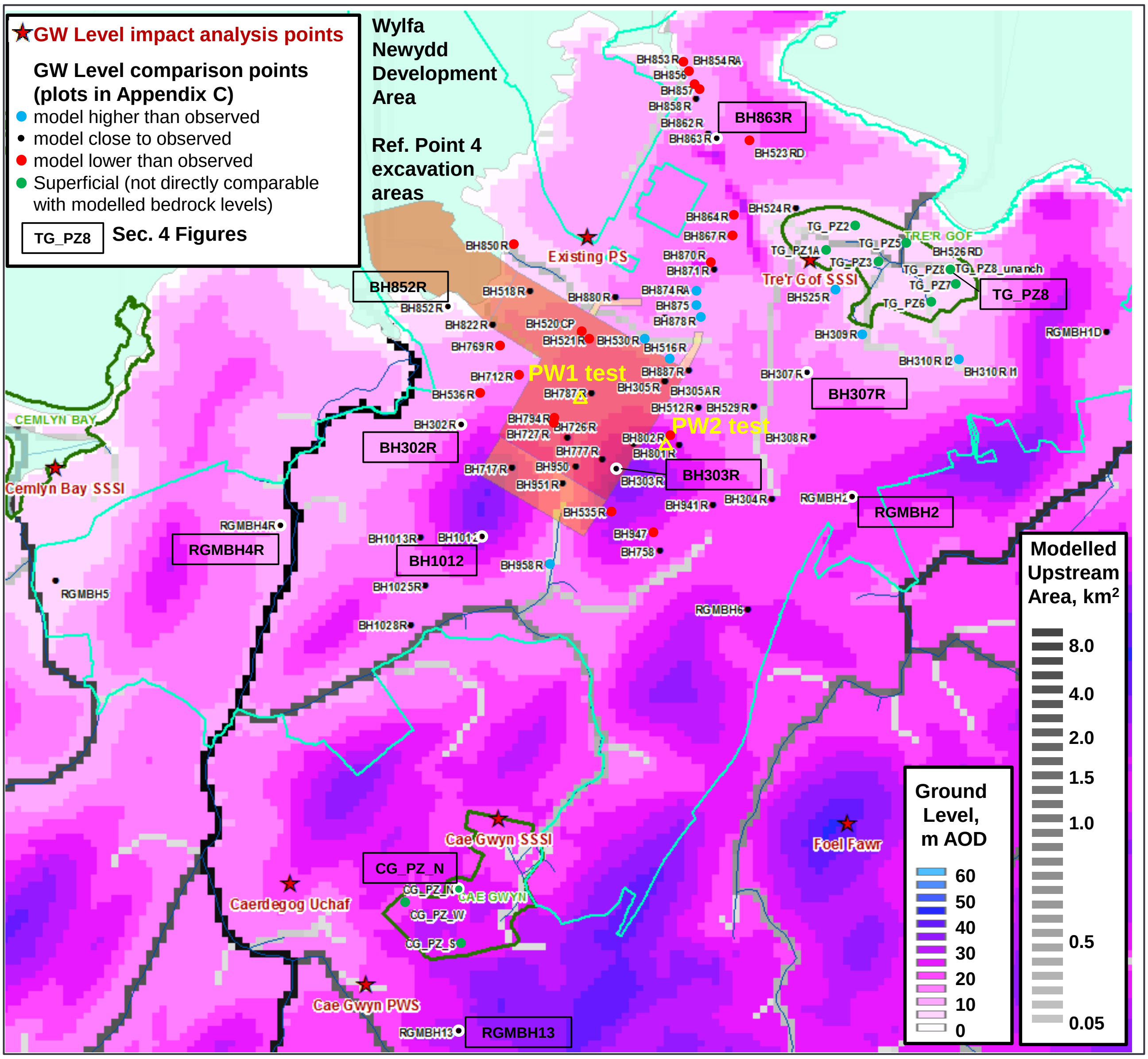

As part of the quality assurance process to review and prepare the bedrock groundwater level records for use in model calibration, the bedrock monitored data shown in figure 3.6 have been kriged and contoured onto the model grid for every day between August 2015 and January 2016. Each of these grids has been compared with, and minimised by, ground elevations so that interpolated areas where bedrock groundwater levels may be above the surface are apparent from the change in shape of the otherwise smooth contours. Figure 3.9 shows two of these interpolated groundwater level maps for periods selected because of their comprehensive and reliable data coverage (figure 3.6) from before the recharge response (7 September 2015), and after it (31 December 2015).

Figure 3.9 Bedrock high and low groundwater level contour maps, minimised to ground level

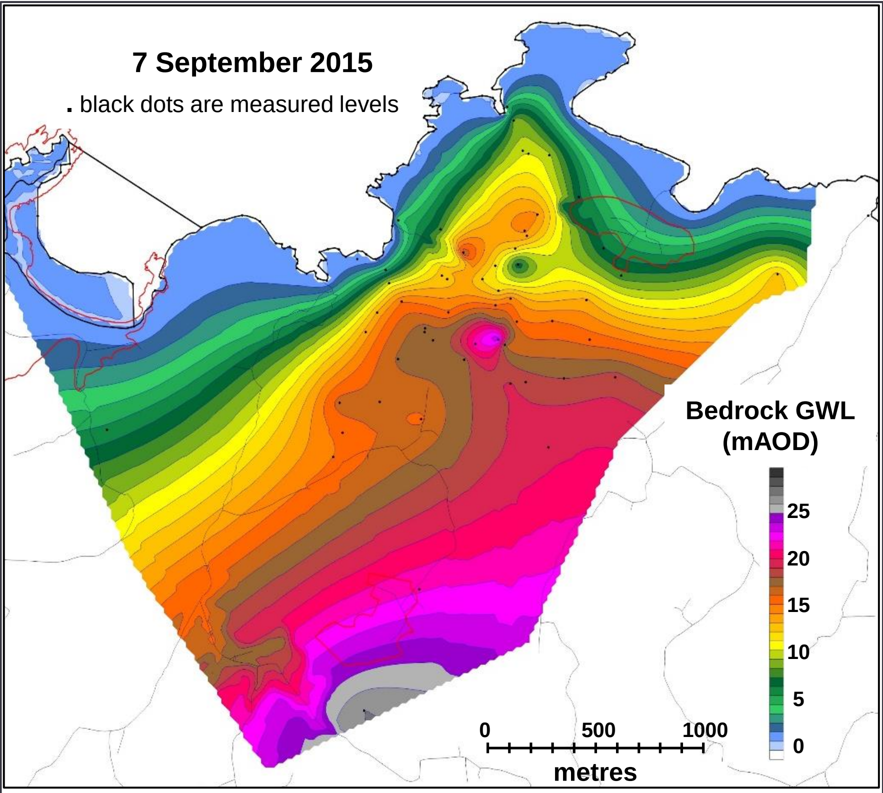

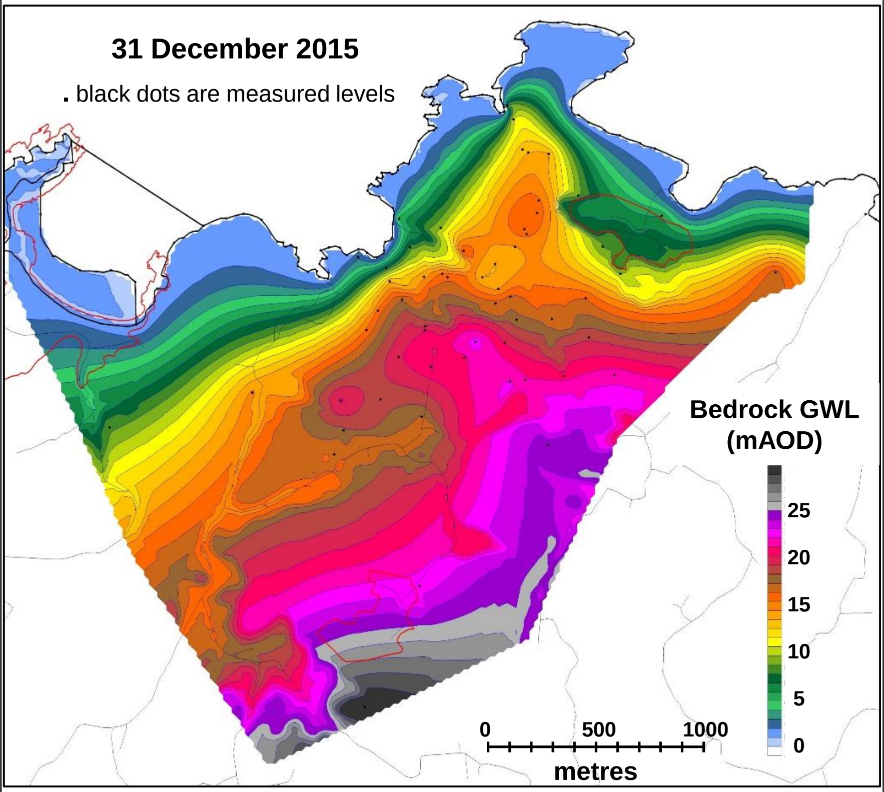

Both of these more detailed maps include additional sea level control (assumed to be at 0 m AOD) around the coast and show groundwater elevations and inferred bedrock gradients and flow directions which are similar to the analysis previously presented (the lower two graphs of Figure 3.7). Away from the borehole monitoring locations (marked with black dots), the extrapolated contours should be viewed with caution. Indeed, groundwater level calibration should be limited to the comparison of time series observation and simulated data, informed by the ground level and rockhead context which is also included in the Appendix C plots.

The Appendix C analysis shows that very few bedrock groundwater levels fall to more than 7 m below the rockhead. This is in line with the analysis of borehole hydro-testing data (presented in the next section) which suggests that aggregated permeabilities in the Cambrian and pre-Cambrian bedrock are typically only enhanced in the upper 5 to 10 metres below rockhead.

Nonetheless, the dry period (September 2015) interpolated levels generally remain below ground level in areas where there is good surrounding data coverage suggesting that transmissivities are sufficient to drain small residual groundwater flows within the bedrock, rather than forcing local discharge to the surface drainage network.

The influence of topographic control (implying local drainage) is much more apparent following recharge (December 2015) when groundwater levels are higher, although the underlying patterns of flow through the bedrock on broader scales are very similar. During both periods groundwater levels to the south of Cae Gwyn remain high – recharge to the bedrock in this topographically elevated area is expected to be relatively high because the Drift is thin or absent.

Analysis of pumping tests and single borehole hydro-testing permeability data

During autumn 2015, two pumping tests were carried out to investigate the response of bedrock groundwater to abstraction pressure over a longer time scale than the programme of hydro-testing associated with the ground investigation boreholes (Jacobs, 2016). The monitored response to these tests has been highlighted previously in figure 3.6, and in the associated text, and they are located on figure 3.8. The first borehole tested (PW1) had low yield (~0.7 l/s, maintained over a period of 8 days) and only localised drawdown but yields from the second borehole (PW2) were higher (9 l/s falling gradually to 3.8 l/s over a 9 day period) with drawdown responses noted up to 300 m away. These findings confirm that a bedrock groundwater impact pathway warrants the modelling investigations reported here, even if the regional connectivity and yield of the fractures through which flow occurs is very variable and is also expected to reduce with time as the upper more permeable zones are dewatered during construction works.

A considerably greater number of shorter term, smaller scale single borehole hydraulic conductivity tests have been conducted in the boreholes drilled in various phases of ground investigation at and around the Wylfa site (Jacobs, 2016), including the bedrock monitoring boreholes mapped in Figure 3.6. Different methodologies have been employed including single packer, double packer, rising head and falling head tests. Typically, these tests have been conducted over lengths of open hole of a few metres, with results that have been reported in the appropriate site investigation reports.

These tests can in theory provide valuable information to support the parameterisation of the groundwater model. It must be remembered however that the Cambrian and pre-Cambrian bedrock at Wylfa is primarily a fractured medium, and the test results will strongly depend on the nature of the fractures within the test interval. Apart from some information for the boreholes themselves, the precise distribution, nature and connectivity of the fractures on a wider scale can never be fully known.

Hydraulic properties must of course be specified for the whole of the model domain. At this catchment scale, or the scale of the large volumes of rock which will be excavated during construction, the bedrock may be appropriately approximated as a porous medium, and it is possible to analyse the large amount of borehole hydro-testing data to help inform the choice of model parameters. Based on the analysis of the available data described below, the expectation for most areas is that fracture development, and therefore hydraulic conductivity, will be enhanced over a relatively shallow zone close to rockhead, and that below this zone hydraulic conductivity will be a relatively uniform low value.

Bedrock hydraulic conductivity data for individual boreholes are presented in Appendix A. Only boreholes for which rockhead elevation is known, and which have more than one test value, are shown, since the vertical profile of hydraulic conductivity is of primary interest. The borehole profiles give an indication of variations with depth at distinct points, but of greater relevance to the understanding of water movement at the catchment or excavation scale, are methods of analysis that consider all the data together.

Initial analysis investigated whether there are clear spatial (areal) patterns to the variation of parameter values. The geological characterisation of faulting and fracture zone in the bedrock suggests there may be some anisotropy in bulk hydraulic conductivity which might suggest that groundwater flow is more restricted south to north than it is east-west. However, the estimate of saturated transmissivity derived from the hydraulic conductivity profiles shown in Appendix A did not reveal any clear patterns of spatial dependence that might allow informed interpolation between, and extrapolation away from, the borehole data points.

In the absence of any apparent systematic and predictable spatial (areal) variation in bedrock hydraulic parameters, analysis then focussed on deriving the most appropriate ‘representative’ vertical profile of hydraulic conductivity for use in the bedrock groundwater model. In order to cover a broader range of the hydraulic conductivity parameters derived from the tests, alternative models with higher and lower transmissivity and bedrock recharge were also developed to consider the sensitivity of impact predictions around the central calibration model.

Figure 3.10 shows an initial summary of all available test results from boreholes for which both rockhead and tested interval elevations are known (mostly 471 bedrock interval tests but also showing 12 results from superficial deposit intervals).

Figure 3.10 Distribution of hydraulic conductivity measurements from all tests where the tested interval and rockhead elevations are both known

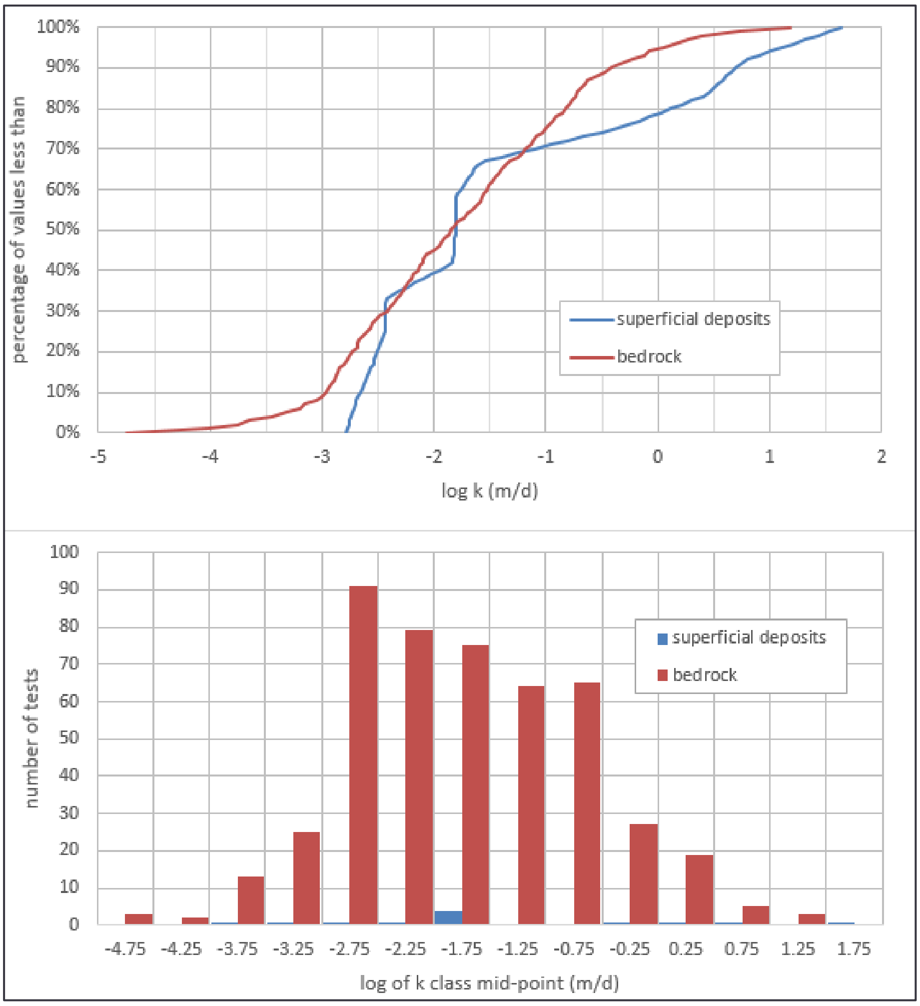

It is appropriate to present these summary data on a logarithmic scale, otherwise the plots are dominated by the few high values.

It is clear that 90% of bedrock values lie below $10^{-0.5}$ m/d, i.e. 0.3 m/d.

Figure 3.11 shows the bedrock test interval results in their vertical context, plotted against depth below rockhead: note that this does not include all of the data summarised above, since rockhead elevation is unknown for some boreholes.

The same information is plotted at two different scales to aid clarity and understanding. The pink data markers are the hydraulic conductivity derived from each test. Each blue line connects the test results for an individual borehole.

This clearly shows the wide scatter of data at all depths below rockhead.

Figure 3.11 Variation of bedrock hydraulic conductivity measurements with depth below rockhead

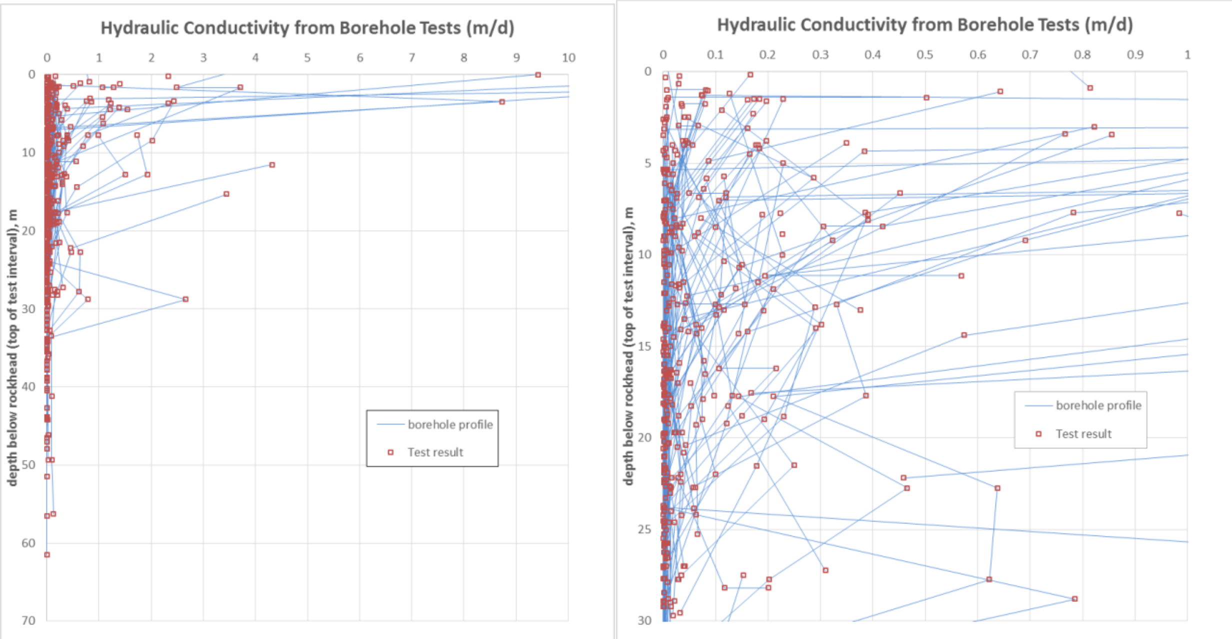

In order to develop a representative vertical profile to underpin simplified model parameterisation, the data were divided into classes based on depth below rockhead. Within each depth class, the geometric mean was found, and is shown on Figure 3.12 on both arithmetic and logarithmic scales. Two calculations were undertaken, grouping the data into 1 m intervals and 2 m intervals.

Figure 3.12 Geometric mean of bedrock hydraulic conductivity measurements with depth below rockhead

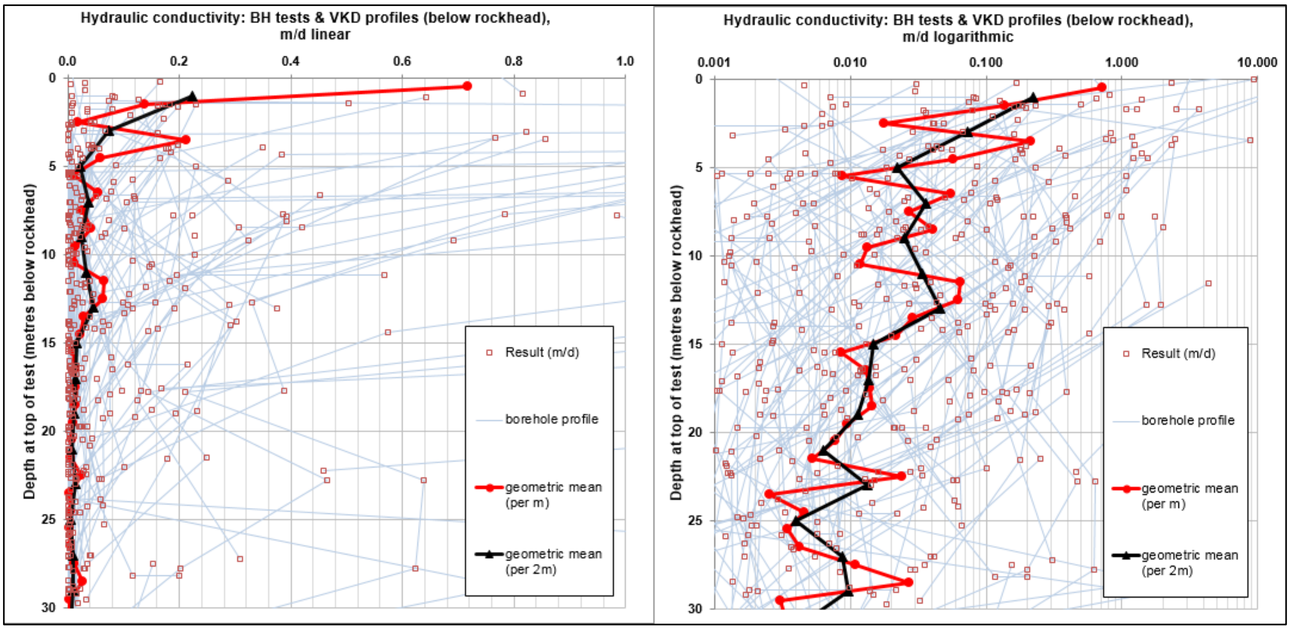

These plots show that hydraulic conductivity is typically higher in the top 5-15 m below rockhead.

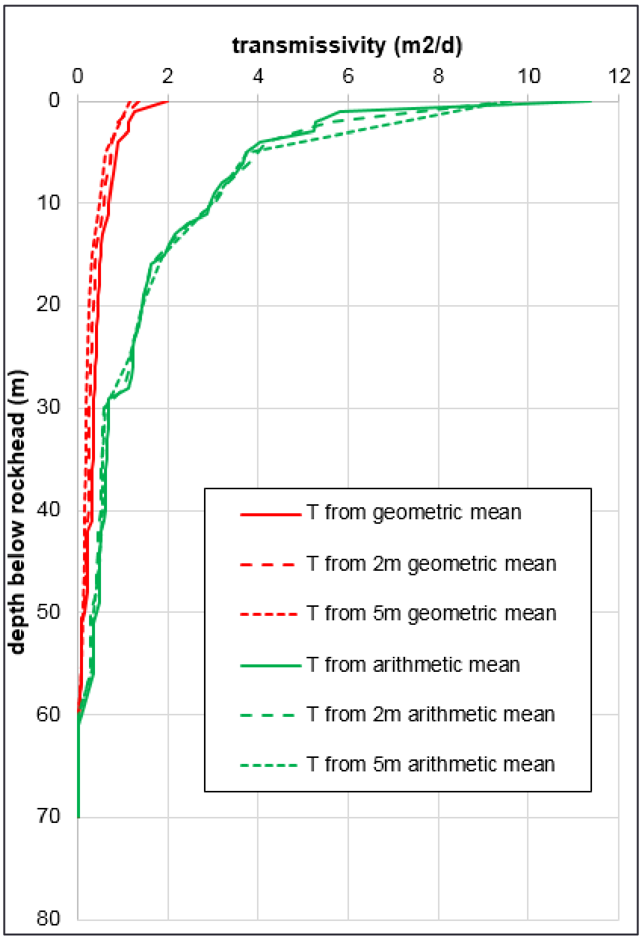

Figure 3.13 Average transmissivity values derived from borehole bedrock hydraulic conductivity measurements

The analysis was extended to work out transmissivity based on the data groupings described: in addition a 5 m data grouping was also used (Figure 3.13). This also includes results from the calculation based on arithmetic mean for reference, although it is considered that the arithmetic mean values are subject to considerable bias by the presence of a small number of large data values, and calculations based on geometric mean values are more appropriate.

Although the transmissivity calculated from arithmetic mean values shows some increase from around 30 m depth upward, examination of the data show that this is the result of a small number of (regionally unrepresentative) higher data values at this depth (see the left hand graph of Figure 3.11). Locally connected fracture networks of higher conductivity like this could be expected to be associated with the short term higher yields evident from the second pumping test. However, the main increase in transmissivity identified by the geometric mean is from 5 to 10 m depth upwards.

Consideration of this analysis, together with examination of observed groundwater levels which tend to recess toward the elevation at which hydraulic conductivity begins to increase (i.e. there are very few groundwater level hydrographs which fall to more than 7 m below rockhead), led to the adoption in the groundwater model of a bedrock hydraulic conductivity profile with the 'inflection point' at 5 m below rockhead, which produced a credible modelled simulation of bedrock groundwater levels.

Section 4.5 explains how alternative models have been used to explore uncertainties in the bedrock groundwater recharge and hydraulic conductivity profile assumptions. The Central calibration and variant sensitivity modelled profiles of hydraulic conductivity are shown together with the hydro-test data in Figure 3.14, and the equivalent transmissivity profiles are plotted in Figure 3.15.

Figure 3.14 Measured and simulated bedrock hydraulic conductivity profiles

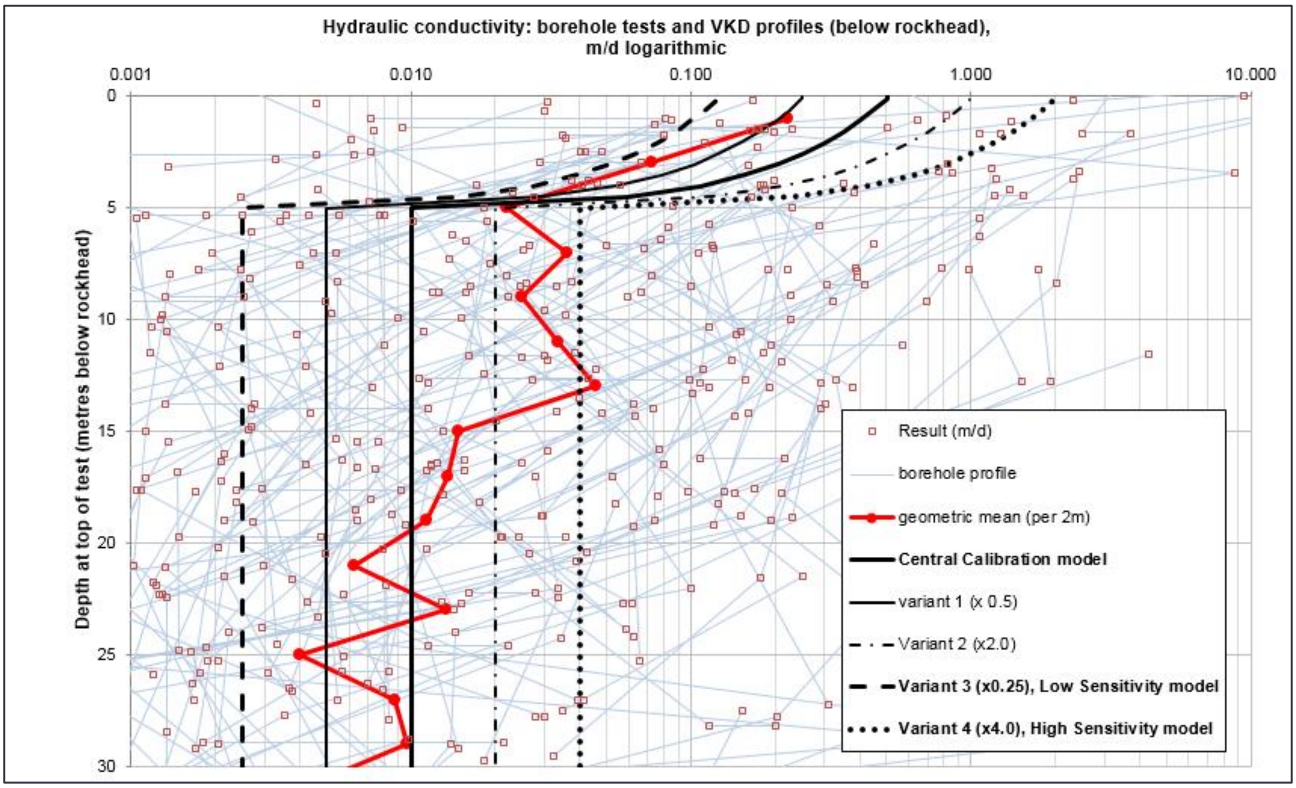

Figure 3.15 Measured and simulated bedrock transmissivity profiles

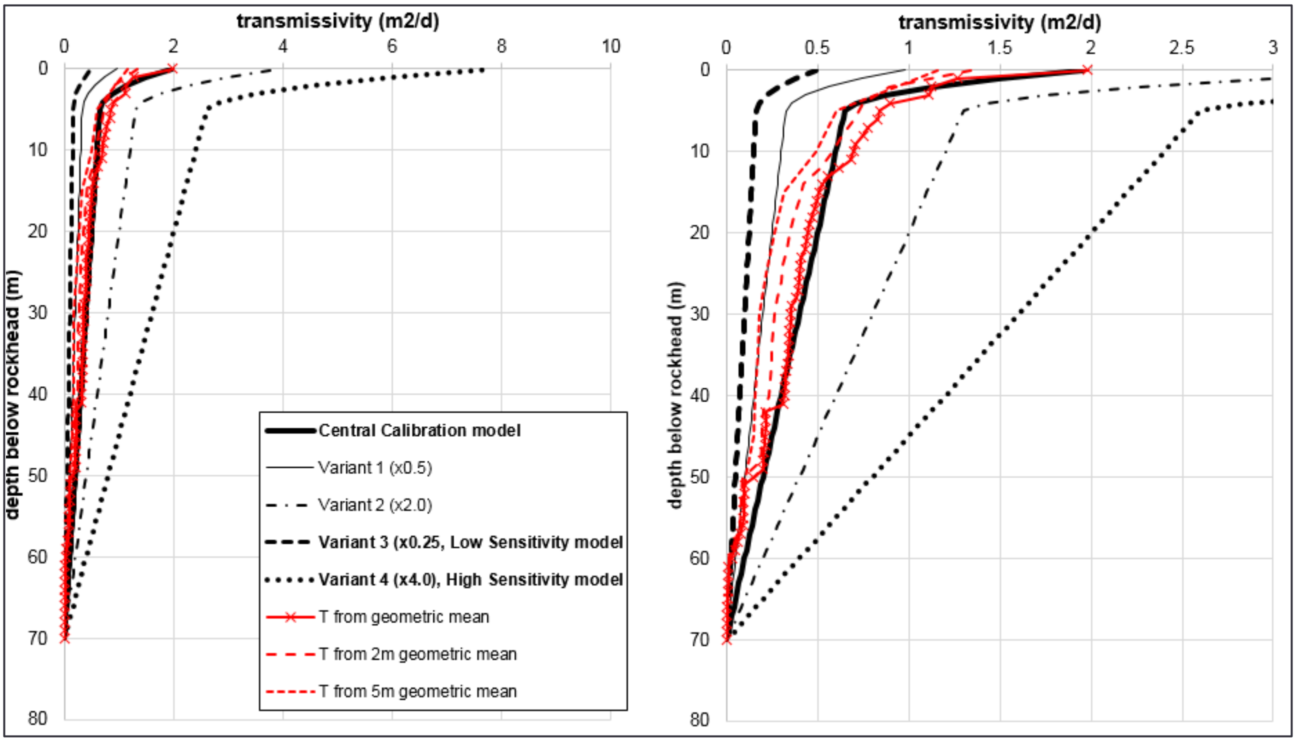

It can be seen that the Central profile used in the calibrated baseline model is a realistic representation of the data, and that the variant models - used with higher (variant 4) or lower (variant 3) bedrock recharge assumptions as part of the model sensitivity analysis (Section 4) - encompass the range of measured values.

3.3 Conceptualisation summary for numerical modelling

The analysis of groundwater levels and bedrock permeability described above, builds on the hydrogeological conceptualisation previously presented in the Jacobs Baseline report - including the schematic cross section copied into Figure 3.16. The baseline situation includes a gradient driving bedrock and superficial groundwater flow towards the sea which follows the topography and steepens by the coast. The drumlin of superficial deposits (and the 'perched' shallow groundwater within it) will be removed to enable the final platform for the reactors to be founded within the bedrock, and the deepest excavation will be below sea level (the floor generally at -10 mAOD, with locally deeper parts down to -18 mAOD). Ground investigation boreholes have demonstrated that the frequency and aperture of fracturing in the bedrock decreases with depth below rockhead. Transmissivity profiles based on the geometric mean of sampled test data have been included on the right of the cross section, plotted together with the Central and variant modelled profiles against a depth below rockhead axis.

Faulting and fracture zones probably result in localised preferential groundwater flow pathways within the bedrock which will be encountered during excavation – as evidenced by the higher yielding second pumping test. However, the hydro-test results suggest that bulk permeabilities are generally very low at depth. The location of fracture zones is poorly understood, and engineering interventions would be deployed locally as and if needed to reduce short term inflows into the excavation. Variant MODFLOW models with hydraulic conductivities which are four times or one quarter the central profile have been used to explore the uncertainty in bulk bedrock parameters.

Figure 3.16 Conceptual cross section* from Jacobs Hydrogeology Baseline Report with hydraulic conductivity test results and a range of transmissivity profiles which have been modelled in MODFLOW (*line mapped on figure 2.1)

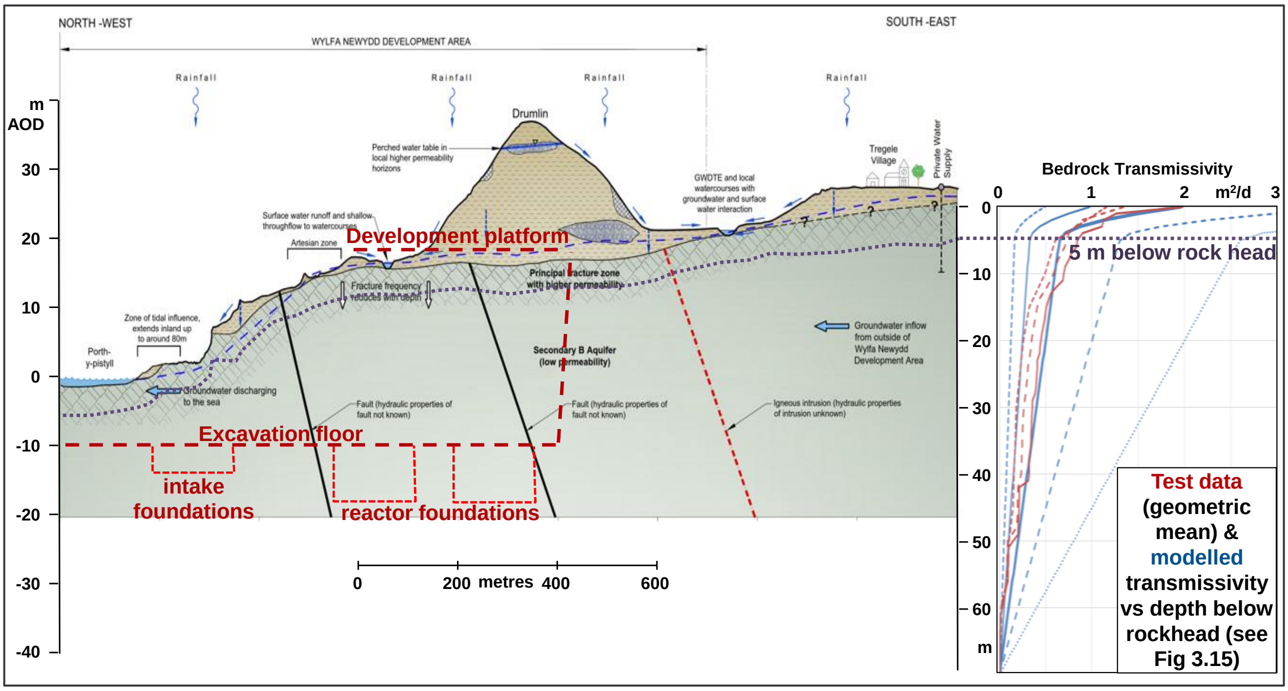

Recharge to the MODFLOW bedrock groundwater model is calculated in the 4R code which also incorporates routed surface water runoff and shallow groundwater interflow within the superficial deposits (to ensure that all the effective rainfall is modelled). The influence of earthworks landform re-profiling, mounding and drainage management is best dealt with within 4R, and is expected to dominate impacts on surface water flow receptors, together with much smaller changes in bedrock groundwater – surface water interaction represented in MODFLOW. Both components of the numerical model are described in Section 4.

4. Numerical modelling assumptions and process

4.1 Introduction

The DCO Wylfa-Newydd groundwater and stream flow models are a set of three separate models representing baseline (present day) conditions of the site and the catchments draining onto and across it, and future predictive Reference Point 4 (Construction) and Reference Point 5 (completion/operation) scenarios.

The models share a common spatial extent, as shown in figure 2.2, which extends from the coast in the north to the area south of Llanrhyddlad, and from Cemlyn Bay in the west to Cemaes Bay in the east. The models all utilise a regular 20 m grid, and cover the time period of historical daily rainfall and potential evaporation from 1 January 1960 to 31 July 2016. All model runs have been carried out using a combination of the 4R code for surface routed runoff and Drift shallow interflow processes, with MODFLOW used to simulate flow, storage and discharge from the Cambrian and pre-Cambrian bedrock.

The principal function of the models to date is to predict the impacts of changes at the site during the course of construction and operation on groundwater levels and on surface flows to the SSSIs at Tre’r Gof, Cae Gwyn and Cemlyn Bay, and in surrounding watercourses.

Each successive model therefore comprises a suite of input files that describe these changes from the baseline. Comparison of the predicted surface flows from each model at defined points in the landscape enables the prediction of the impact of the construction phases on bedrock groundwater and surface drainage and flows into the SSSIs at Tre’r Gof, Cae Gwyn, and Cemlyn Bay.

Following the description of input data and conceptual synthesis in Section 3, this section presents the numerical modelling assumptions and process, as follows:

- The processes represented in the 4R – MODFLOW code combination.
- The baseline model build and parameterisation assumptions.
- Historical calibration, uncertainty and sensitivity analysis, including the development of 2 variant models with relatively ‘High’ or ‘Low’ bedrock recharge and transmissivity compared to the ‘Central’ calibration model.
- Baseline historical comparisons of simulated and measured bedrock groundwater level and stream flow time series.
- The changes made to baseline model build and boundary conditions for the Reference Point 4 and Reference Point 5 predictive models.
- The use of the Central, Low and High sensitivity models to generate a range of potential impact predictions.

The section describes the numerical modelling process with reference to many tables and figures within the text, and also references a comprehensive collation of model build plans and calibration outputs in appendices as follows:

- Appendix B Baseline model build plans.
- Appendix C Time series comparisons of the historical baseline simulation bedrock groundwater levels and gauged flows.
- Appendix D Model build plans for Reference Point 4 and Reference Point 5 predictive models.

4.2 4R and MODFLOW modelling components and run numbers

Figure 4.1 shows how the two modelling codes combine to simulate surface water and groundwater flow processes.

Figure 4.1 Schematic of the rainfall to evapotranspiration, routed runoff and shallow interflow processes represented in 4R, and the bedrock groundwater recharge, flow and discharge processes simulated by MODFLOW

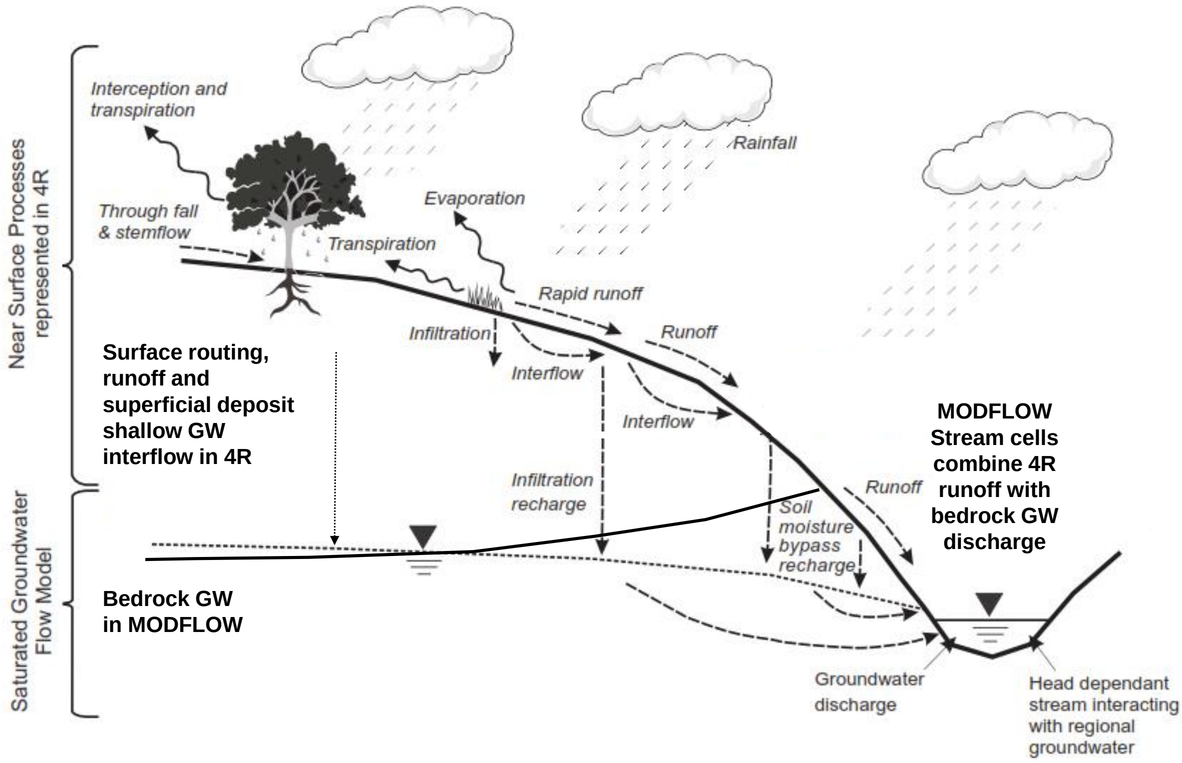

4R (Rainfall Routing to Runoff and Recharge, Heathcote et al, 2004) is a numerical modelling framework for the prediction of surface and shallow subsurface flows. The model simulates a daily soil moisture balance including evapotranspiration losses and the generation of surface runoff, interflow and deeper infiltration (recharge) of water, together with the surface routing of rapid runoff and interflow through the environment. For the Wylfa DCO modelling, 4R also calculates bedrock recharge and directly generates input files for the MODFLOW model of groundwater flow processes.

4R deals with most of the anticipated impacts of landform re-profiling, vegetation changes and site drainage on surface and near-surface flows. It includes a slow “interflow” path from interfluves to valley bottoms, to simply represent the topographically routed flow through the Drift, soil mounds and shallow wetland water tables. This surface routed water is added into MODFLOW Stream input files. 4R also simulates the infiltration of deeper bedrock Recharge input files so that MODFLOW can calculate any effects on bedrock groundwater flows or levels arising from construction activities such as excavation and dewatering.

The process of model build, refinement and predictive scenario use is recorded in a Run Log and it is important to specify the model run numbers from which outputs are derived in order to access the full details of the underlying parameter and boundary assumptions. For the Wylfa modelling work, component 4R and MODFLOW transient models have been built to represent different scenarios (historical baseline calibration, and baseline, Reference Point 4 and Reference Point 5 predictive scenarios). Beyond the models representing the preferred Central calibration assumptions for recharge and bedrock transmissivity, two variants have also been developed to consider the uncertainty around the proportion of water recharging and flowing through the bedrock – so there are also High and Low recharge/transmissivity sensitivity models.

Table 4.1 summarises each of the scenarios and the time discretisation of MODFLOW stress periods. It also lists all of the 4R and MODFLOW (MF) run numbers for the associated Central, Low and High sensitivity models which are reported here for the Wylfa DCO. Runs are elsewhere referred to simply according to the scenario and sensitivity model used (e.g. Reference Point 4 Central recharge/transmissivity run).

Table 4.1 includes additional engineering variant predictive scenarios run in November/December 2017 to consider the impacts associated with refined construction proposals including a locally deepened excavation (Reference Point 4 variant) with a shotcreted and perimeter drain completion (Reference Point 5 variant).

Table 4.1 4R and MODFLOW run numbers for the Wylfa Newydd 2017 DCO groundwater and stream flow modelling

			Recharge and Transmissivity Sensitivity Models					
			Central		Low		High	
Scenario	**Includes**	**MF periods***	**4R**	**MF**	**4R**	**MF**	**4R**	**MF**
Historical Baseline Calibration	Pumping tests included	3 per month from 1960 to 2009 then daily from January 2010 to July 2016	136	050	139v2	053v2	140	054
Baseline Scenario	No pumping tests	Daily from January 1960 to July 2016	141	055	142v2	056v2	143	057
Ref Point 4 Scenario	Mid-construction: reprofiled soil mounds, managed drainage & dewatered inland and seaward excavations	Daily from January 1960 to July 2017	153	075	152	074	154	076
Ref Point 5 Scenario	Operational: final landforms, largely impermeable platform and passively drained backfilled excavation	Daily from January 1960 to July 2018	159	072	158	071	160	073
Ref Point 4 (Deeper Variant)	Mid-construction: reprofiled soil mounds, managed drainage & dewatered inland (locally deepened) and seaward excavations	Daily from January 1960 to July 2017	161	077	162	078	163	079
Ref Point 5 (Shotcreted Variant)	Operational: final landforms, largely impermeable platform and passively drained backfilled excavation with shotcreted walls and an outer perimeter drain	Daily from January 1960 to July 2018	159	080	158	081	160	082

* all runs have the same historical sequence of daily rainfall and potential evaporation inputs to 4R

4.3 Baseline model build assumptions

Many of the input data for both 4R and MODFLOW models are spatial in nature, and these have been collated into a ModelMap GIS file (WylDCOModelMap.mxd) which accompanies this report. It is part of the digital files transferred with the modelling results. Appendix B includes a gallery of Baseline Model Plans printed from this GIS, focusing on the Wylfa Site area of the model. These plans include the GIS 'Table of Contents' to help users of the report and data to find and review local details as required. It has also been used to collate all the maps summarising the modelling process and outputs within the report.

The ModelMap is a standard ArcGIS project which serves a number of purposes:

- Collation and QA of spatial data.
- Production of input files for the models.
- Visualisation of the model inputs and outputs.
- Interpretation and understanding of the causes of model scenario differences.

The ModelMap is organised by the Baseline, Construction and Completion phases modelled, with additional information concerning the geology and geography of the model area. For each phase, including the baseline, the following layers are included:

- Elevation of the ground surface at each phase (which influences the routing network and catchments).
- Routing of surface water rapid runoff and interflow, in the form of lines linking model cells.
- Routed Area, showing the total upstream area contributing to the flow in each cell.
- Long-Term Average 4R model outputs showing the spatial distribution of average interflow and rapid runoff in mm/a.
- Soil and Land Use, the parameter determining evapotranspiration losses in the soil zone. Zones are delineated for urban hardstanding areas (including the power plant), soil mounds and stripped areas, and vegetated areas (grassland and woodland). Vegetated areas are further divided into heavy soils of clay-loam type and light soils of sand-loam type.
- Slope and Soil Surface, the parameters used to determine rapid runoff behaviour. Each cell is categorised by its slope (in degrees), with a distinction also being drawn between bare soil and covered soil.
- Interflow Release Coefficients, values governing the rate of interflow release i.e. proportion of subsurface water released into surface streams each day. Depends on the distance to surface drainage – so higher values adjacent to streams produce more rapid release.
- Drift Thickness, where the surface coverage has been divided into conceptual types to control the proportion of water assumed to recharge the bedrock MODFLOW layer, through a combination of water released from, and bypassing, the soil moisture store.
- Artificial Drainage, showing the toe drains, sediment settlement lagoons and sub-surface pipes incorporated into the Reference Point 4 model.
- MODFLOW Stream cell, General Head Boundary (seabed) and Drain cell distributions and parameter assumptions.
- MODFLOW output bedrock head distributions and drawdown rasters for Reference Point 4 and 5 models, and engineering variant models, compared with the Baseline scenario.

Full details of the model build assumptions are contained in the model input files themselves which can accessed through the Run Log.

Explanatory summaries of the parameter and process dependencies and range of values are provided in the table 4.2 (for 4R) and table 4.3 (for MODFLOW) on the following pages.

Table 4.2 4R processes and parameter assumptions (input data sources provided in table 3.1)

Process/Parameter	Baseline Description	Sensitivity	Ref Point 4	Ref Point 5
Routing and catchments	Based on LiDAR and OS Terrain data, with known watercourses 'forced'.	No	Includes mounds & excavation, managed drainage & sediment lagoon storage (smoothing runoff peaks)	Includes final landform, drainage blanket routing water under mound to the south east of Tre'r Gof (figure 5.11)
Soil - Land use	Categories include: Existing Power station - 90% runoff Urban (Cemaes) - 30% runoff Pasture–clay loam Pasture–sandy loam Woodland–clay loam	No	Excavation - 100% runoff Bare soil - less evaporation Others as baseline	Concrete - 100% runoff Power station - 90% runoff Others as baseline
Evapotranspiration	FAO "TAW" parameter (Total Available Water) based on upland grazing land, in the range 116mm to 135mm. Woodland TAW in the range 199mm to 474mm.	No	Less evaporation from bare soil and excavation	Less evaporation from platform
Rapid runoff daily release factor	Based on slope, with categories (degrees) <1, 1 to 3, 3 to 5, >5. Rapid runoff release factor in the range 0.25 (shallow slopes) to 0.85 (steep slopes).	No	Changes with landform slope	Changes with landform slope
Drift interflow daily release factor	Interflow release factor of 0.005 (i.e. slow release) in areas with thick drift (drumlins and within Tre'r Gof). Elsewhere, the daily interflow release factor is a linear function of distance to watercourse in the range 0.001 (at >200m distance) to 0.1 (20m distance).	No	Changes with distance to managed drainage	Changes with final landform Drift drainage path lengths
Bedrock recharge	All cells include both a Drift interflow calculation and a bedrock recharge calulation, with the proportion dependent on the thickness of the superficial deposits. Bedrock recharge includes infiltration after soil moisture evaporation, subject to daily limits, combined with recharge which bypasses the soil moisture store.	Yes - variant models consider higher and lower proportions of bedrock recharge, with associated changes to Drift interflow amounts	Changes with re-distribution of mounds.	Changes according to final landform
Surface water abstractions and discharges	Surface water abstractions and discharges, and leakage of mains supply water assumed zero everywhere	No	None	None

The latest version of the 4R code (version 41w) has been used for all of the Wylfa DCO modelling.

Both 4R and MODFLOW models are built on a common regular grid of 20 m x 20 m cells which has 340 rows (north to south) and 280 columns (east to west), covering the area mapped in figure 2.2.

Table 4.3 MODFLOW packages and parameter assumptions

Process/Parameter	Baseline Description	Sensitivity	Reference Point 4	Reference Point 5
Runoff and recharge inputs	4R rapid runoff + interflow accumulated into Stream cells down routing network. 4R recharge added into Bedrock groundwater flow simulation	Yes - variant models consider higher and lower proportions of bedrock recharge, with associated changes to Drift interflow amounts	Changes from 4R	Changes from 4R
Single bedrock layer geometry	Top of layer set at rockhead. Bottom of layer set 70 m below. The base is well below the floor of the excavation, hydraulic conductivities are very low, and flow is assumed to be negligible below this depth.	No	Excavation locally lowers top of layer by up to 30 m. Base remains fixed	Top of layer (including permeable backfill) locally set at platform level
Stream boundary cells	Initiated when upstream routed area >8,300m2, set typically at ground elevation, with further cells added locally during calibration (e.g. on Cae Gwyn) to control heads. Stream cell conductance to control bedrock GW to SW flow rates set according to drift thickness, ranging from 250m2/d at Bedrock outcrop down to 0.5m2/d where the Drift is thickest. These conductance parameter ranges have been adjusted through comparison with observed groundwater level data and stream flow data during calibration. They also extend across the Cemlyn Bay lagoon, and Llyn Llygeirian to simulate GW - SW flow.	No	Distribution, elevation and conductance change with routing, mound elevations and made ground thickness. Stream cells used to simulate the dewatering of the excavation floor - combining GW discharge with effective rainfall-runoff.	Distribution, elevation and conductance change with final routing, elevations and made ground thickness.
General Head boundary cells	Covers the sea bed to represent potential interaction with Bedrock groundwater. Set in the model at a mean sea level elevation of 0.01 mAOD, with a conductance of 10m2/d. Real sea level varies tidally and the mean is slowly rising above Ordnance Datum due to climate change. (Now around 0.2m higher than OD at Newlyn).	No	Sea bed boundary cells removed in the seaward excavation area, behind the coffer dam	As Baseline
Drain boundary cells	Not used	No	Not used	Set behind the impermeable concrete intakes at 6 mAOD to passively drain the permeable excavation backfill
Groundwater abstraction Well boundary cells	The two pumping tests in 2015 are included in the historical calibration run but excluded from all other scenarios. Private supply well abstraction rates have been assumed to be negligible in all models.	No	None	None
Bedrock hydraulic conductivity	Set to be variable using Variable Hydraulic Conductivity with Depth functionality (VKD). K increases within 5m of rockhead, based on the analysis of hydrotesting data described in Section 4.	Yes - profiles changed to 1/4 and 4 times the central calibration values, associated with Low and High Recharge assumptions	Excavation assumed to locally remove permeable zone near rockhead.	VKD inflection point set locally at the floor of the excavation with K above increasing rapidly to represent the permeable backfill (5m/d).
Bedrock storage and specific yield	When bedrock head is above the top of the layer, storage assumed =9x10-4. When head is within the layer, specific yield = 0.07. In areas where bedrock is at outcrop or beneath shallow soils based on BGS mapping or site investigations (e.g. parts of the Cae Gwyn SSSI), storage is set to specific yield (i.e. the bedrock is always unconfined). These storage parameters have been adjusted through comparison with observed groundwater level data during calibration. The predictions of long term construction and completion drawdown from the model are not sensitive to storage parameters.	No	no changes	no changes. In reality the backfill is likely to have a higher specific yield than the bedrock, and the foundations will be impermeable. But the estimates of long term groundwater levels and passive drainage flows are not sensitive to storage.

The MODFLOW USG ('Unstructured Grids") code has been used for the Wylfa DCO modelling. A regular 20 m grid has been used for simplicity of pre- and post-processing and visualisation but the USG version includes access to all of the latest coding options if they should be required in future (e.g. grid refinement around areas of specific interest, where data availability justifies this). It has been further adapted by Amec Foster Wheeler for application on previous regional modelling projects to include the Environment Agency's 'Variable Hydraulic Conductivity with Depth' (VKD) functionality in order to incorporate the data-based profiles described in Section 4.

Figure 4.2 on the next page shows the full extent of the 4R-MODFLOW model. It maps the Baseline topographic elevation grid which influences the 4R surface routing network, together with the following Baseline model MODFLOW boundary condition cells:

- Stream cells which accumulate combined rapid surface runoff and Drift interflow, and also simulate surface drainage interaction with the groundwater in the underlying MODFLOW bedrock layer – providing the main route for water to leave the bedrock. These have also been extended across the Cemlyn Bay lagoon, and Llyn Llygeirian in the southern upper catchment draining to the Afon Cafnan.
- General Head Boundary cells across the sea bed which allow discharge of bedrock groundwater directly to the sea.

4R calculations are carried out across the whole model area but MODFLOW cells beyond the Cemlyn Bay, Cemaes and Cafnan surface water catchments are set as inactive (i.e. these are no flow boundaries).

Figure 4.2 also shows the outline boundaries of the Wylfa Newydd Development Area, and the three SSSI receptors which have been a focus for impact predictions.

Figure 4.2 Baseline model boundary conditions

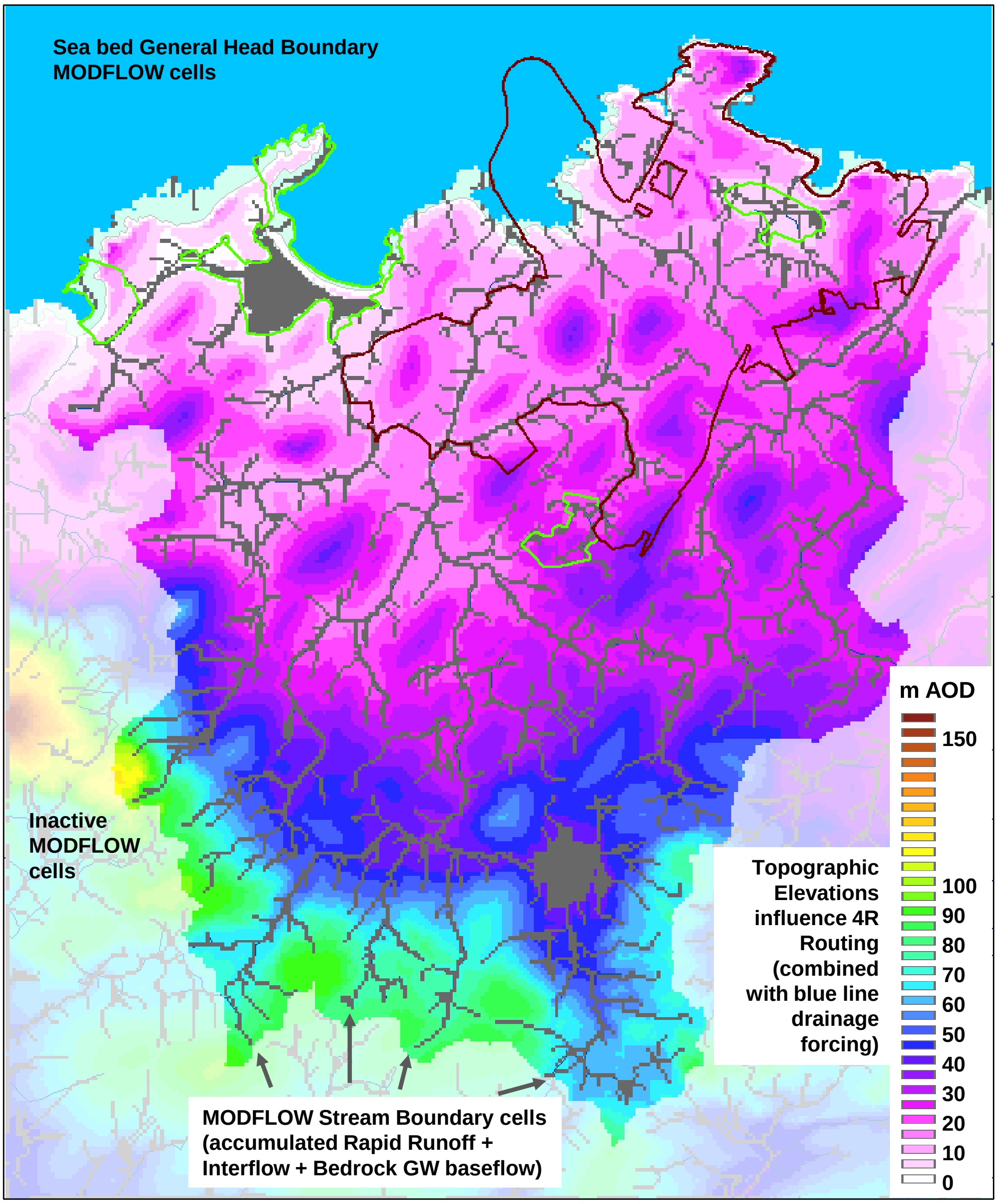

Figure 4.3 provides more detailed mapping of the Wylfa Newydd Development Area at the north of the model and has the same extent as the series of model build and output plans collated in appendix B which include national grid reference lines for locational purposes but also show the Table of Contents of the ModelMap GIS in order to help users find the digital data layers for local review. Figure 4.3 includes the same MODFLOW boundary conditions as presented previously (active-inactive bedrock groundwater cells, Stream cells and sea bed General Head Boundary cells) but also maps the surface network used by 4R to route surface rapid runoff and Drift interflow into and down the MODFLOW Stream cells. This can be seen to have been derived from the topographic elevation grid shown beneath it (e.g. with radial flow away from the glacial drumlin mounds) but has also been forced to follow blue line streams where these have been mapped.

The locations of Stream cells which correspond to the sites of flow gauge records used for model calibration comparisons are also shown on figure 4.3. The available flow data has have been presented and discussed previously around figures 3.3, 3.4 and 3.5.

Figure 4.3 Detailed Site baseline routing network, Stream and General Head Boundary cells and flow gauges (see figure 4.2 for key)

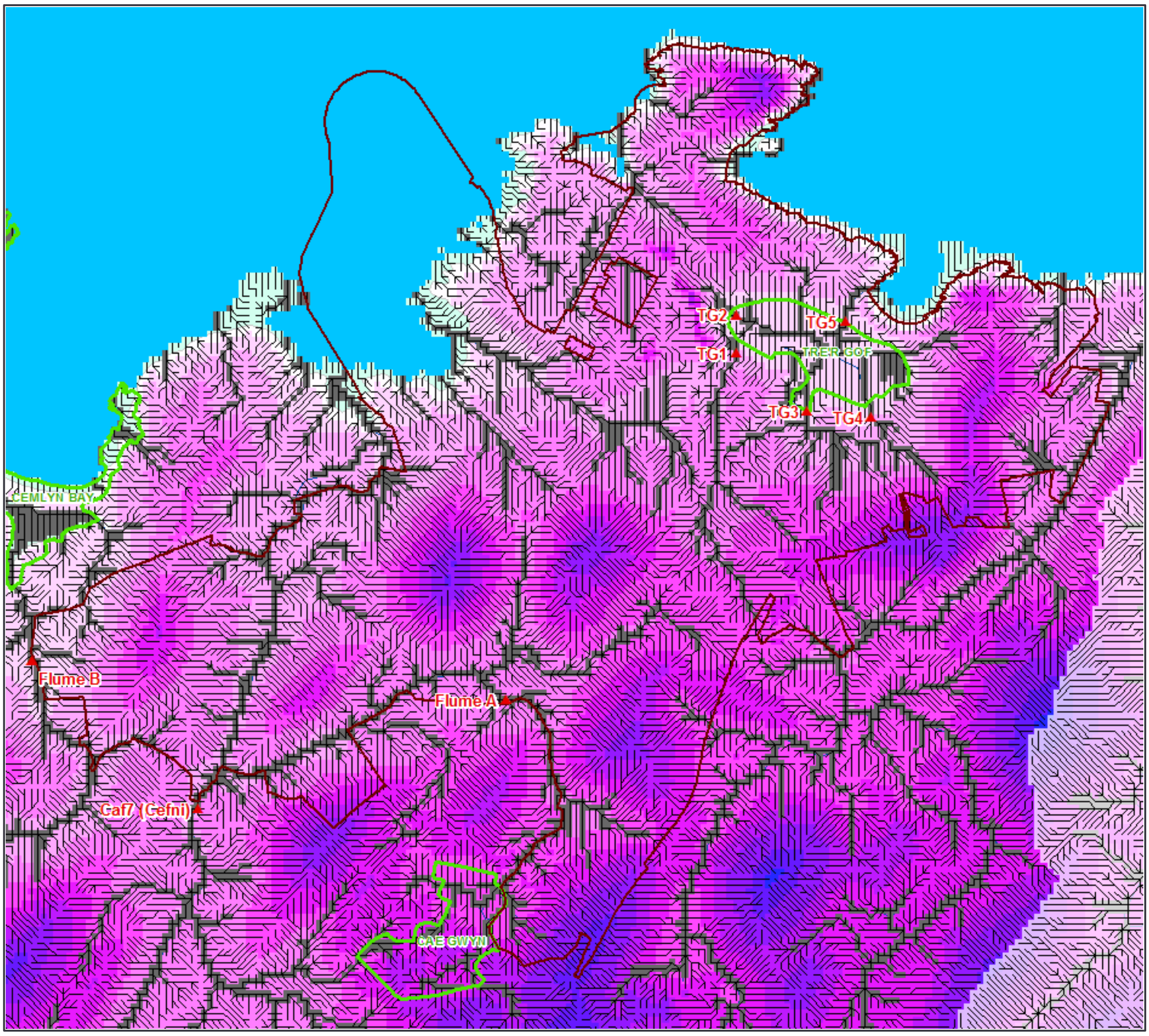

The elevation of the top of the 70 m thick MODFLOW bedrock layer has been set at rockhead – the top right map in figure 4.4. This was derived by subtracting the Drift thickness grid (bottom right map) from the ground surface (top left). As discussed previously around figures 3.1 and 3.2, the Drift thickness is mostly based on the BGS model which includes the drumlin features, and mapping of bedrock outcrop areas where there is only thin soil or peat cover (as around Cae Gwyn). However, the rockhead surface has also been modified according to site investigation so that it includes, for example, the Drift-filled kettle hole depression feature beneath Tre'r Gof which is not present in the BGS national Drift thickness model. Drilling at Tre'r Gof has proved superficial deposits to a depth of 25 mbgl but few boreholes have reached the rockhead so its surface topology is not well known. For modelling purposes it has been assumed that the kettle hole depression is deepest in the centre of the SSSI with thinner superficial deposits around its margins. The parameterisation of bedrock groundwater – surface water interaction uses this thickness to influence the ease with which bedrock groundwater can flow into the drainage network across the wetland. This means there is potential for changes in simulated bedrock groundwater levels around the wetland to influence flows of water into it (although these flow rates are small in comparison with the surface flows (into the SSSI) and direct rainfall (onto the the SSSI) which have a more direct influence on the shallow wetland water table).

Figure 4.4 Baseline topography and rockhead elevations, Drift thickness and land use

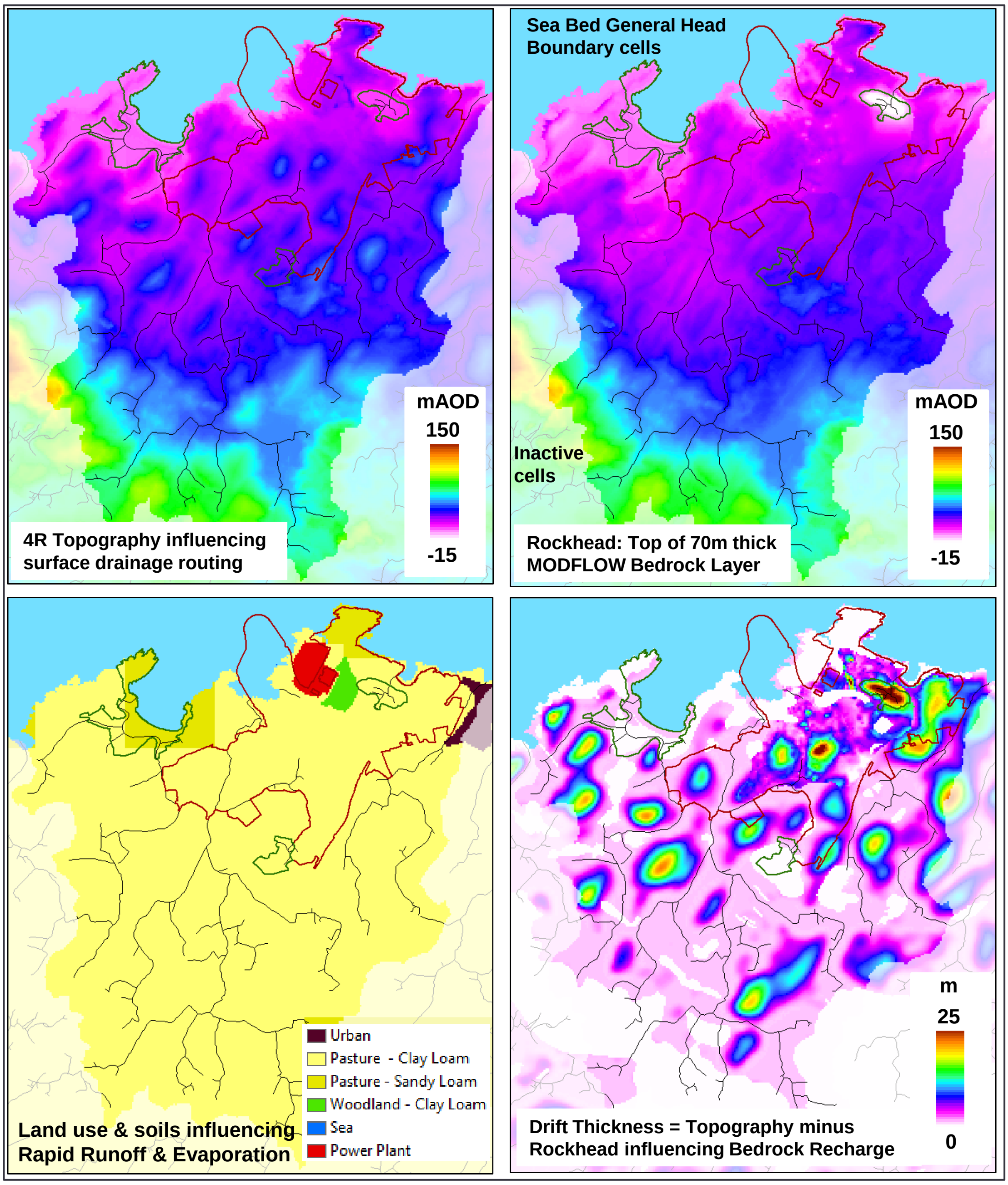

The bottom left map on figure 4.4 shows the baseline distribution of soil-land use combinations which influence the daily 4R calculation of rapid runoff (the proportion of rainfall minus potential evaporation assumed to enter the surface routing network, bypassing the soil moisture store), and also the amounts of evapotranspiration from that store – by grass (pasture – the dominant land use) or at higher rates by trees (woodland). The Existing Power Station is assumed to be 90 % impermeable – generating the highest rates of rapid runoff. The village of Cemaes in the north-west has a lower proportion of rapid runoff (34 % - a percentage commonly assumed for urban and sub-urban areas in regional groundwater flow models built for the Environment Agency).

4.4 Baseline model calibration process and outputs

The historical climate inputs from January 1960 to July 2016 were run through the baseline existing catchment model build summarised in Section 4.3 and appendix B, with output groundwater levels and stream flows compared against the measured hydrographs discussed around figures 3.3 to 3.9. Through a process of iterative review and refinement, constrained within the simple conceptualisation and bedrock parameter ranges set out in figures 3.10 to 3.16, the calibration of the model was gradually improved. The final historical calibration runs (4R Run 136 combined with MODFLOW Run 50 – table 4.1) incorporate the two pumping tests carried out during autumn 2015 so that monitored and simulated responses could be compared. However, it is important to note that, as described in Section 3, there are no clearly defined areal patterns in bedrock hydraulic conductivity, so local parameter adjustments have been avoided. The main focus for MODFLOW refinement and parameter exploration has been to consider the effects of alternative VKD profiles based on the analysis of the hydro-test data presented in Section 3, as well as introducing credible assumptions for confined and unconfined storage. Where modelled heads rise above the top of the layer in mapped bedrock outcrop areas (i.e. into overlying shallow soil or peat deposits), confined storage has been set to the unconfined specific yield value so that groundwater level variability is more credibly subdued (e.g. as at Cae Gwyn). Additional Stream cells have also been added in similar locations to prevent heads rising unrealistically above the ground surface.

Figure 4.5 maps the long term average baseline components of effective rainfall calculated by 4R as inputs to MODFLOW Stream cells (combined rapid runoff and shallow Drift interflow) and bedrock layer recharge (combining a mix of water passing through and bypassing the soil moisture store, which has been refined through comparison against groundwater level hydrographs).

Figure 4.5 Baseline calibration 4R surface runoff and bedrock recharge added into MODFLOW

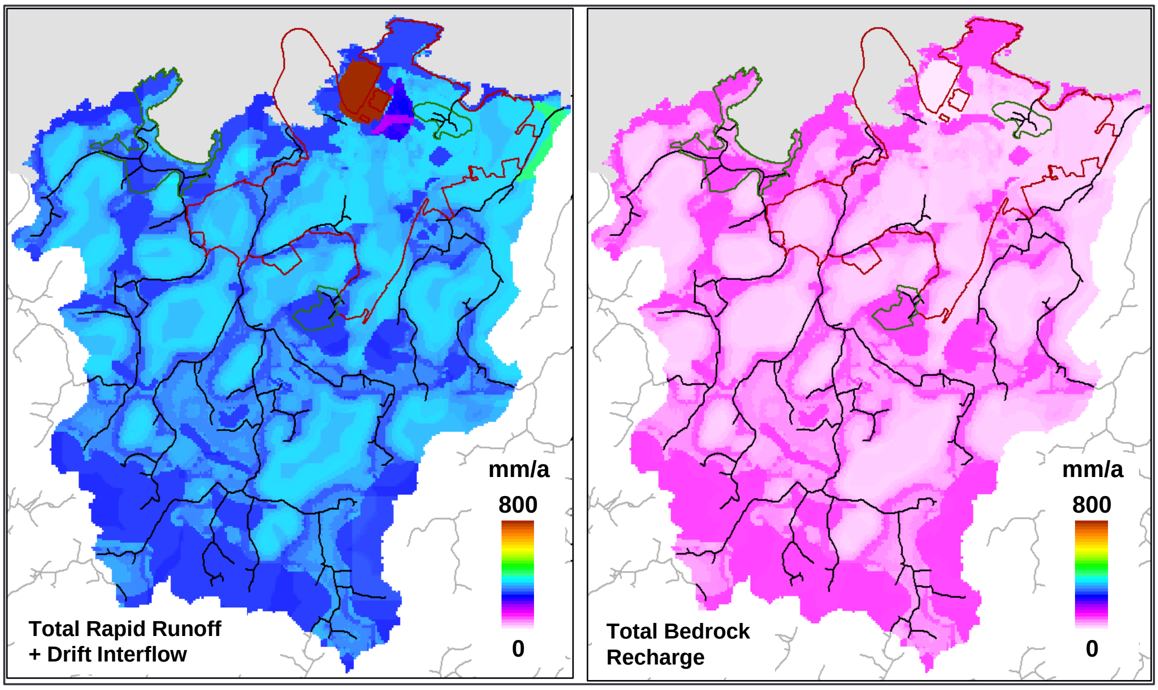

Both maps in figure 4.5 are plotted on the same long term average scale so it is clear that the surface and Drift components of effective rainfall handled within 4R are dominant, in comparison with the much lower rates of recharge through the low permeability Drift to the very low permeability underlying bedrock. The higher runoff from the Existing Power Station is also clear, as is the influence of Drift thickness (figure 4.4) on the distribution of bedrock recharge – more in outcrop areas and less beneath the drumlins and at Tre'r Gof. Bedrock recharge within the Wylfa Newydd Development Area simulated by the Central calibrated 4R model ranges between 30 and 100 mm/a.

The main outputs reviewed from MODFLOW are time series of simulated bedrock groundwater levels and surface stream flows, compared with field measurements. A comprehensive collation of these baseline historical calibration plots is included in appendix C, with selected hydrographs presented and discussed in Section 4.6.

Simulated bedrock groundwater levels from the predictive baseline scenario model are also post-processed into grids and coloured raster maps (figure 4.6). In order to understand seasonal variations, such maps are prepared for a representative dry period (30 September 1991) and a wet period (31 December 2000) – as a basis for drawdown comparisons with the Reference Point 4 construction and Reference Point 5 completion scenarios.

The patterns of bedrock groundwater flow implied by both wet and dry period piezometric maps are very similar, although the influence of local surface drainage is more evident in the locally convergent contours following recharge when groundwater levels are higher. This is particularly apparent in the upper and middle catchment watercourses.

Cae Gwyn is located just north of an area of high bedrock groundwater levels with less local drainage control so there is more variation between summer and winter simulated heads.

Approaching the coast, there is more bedrock discharge directly to the sea in the baseline scenario. This is unsurprising given the relatively steep slopes and cliffs which characterise much of the coastline. The model also credibly simulates the conceptual understanding based on field investigations that there are bedrock groundwater gradients driving flow northwards to the sea beneath and around the superficial deposit filled kettle hole under Tre'r Gof, as well as creating the potential for upward flow through these deposits to the shallow water table and drainage network within the wetland itself. The simulated bedrock groundwater inflows to the SSSI are small in comparison with the surface flows and rainfall onto it. At the Cemlyn Bay SSSI, bedrock groundwater levels are held close to the elevation of the lagoon. Bedrock groundwater discharge through the Drift into the MODFLOW Stream cells representing the lagoon is simulated in the model.

Other baseline model outputs summarised in Section 5 include the General Head Boundary flow interactions with the sea which confirm that, in the absence of any significant excavation, dewatering or other significant groundwater abstraction pressures, there are no existing saline intrusion risks.

Figure 4.6 Baseline bedrock groundwater levels simulated by MODFLOW for a dry and wet period, with the Wylfa Newydd Development Area and receptor SSSIs also mapped

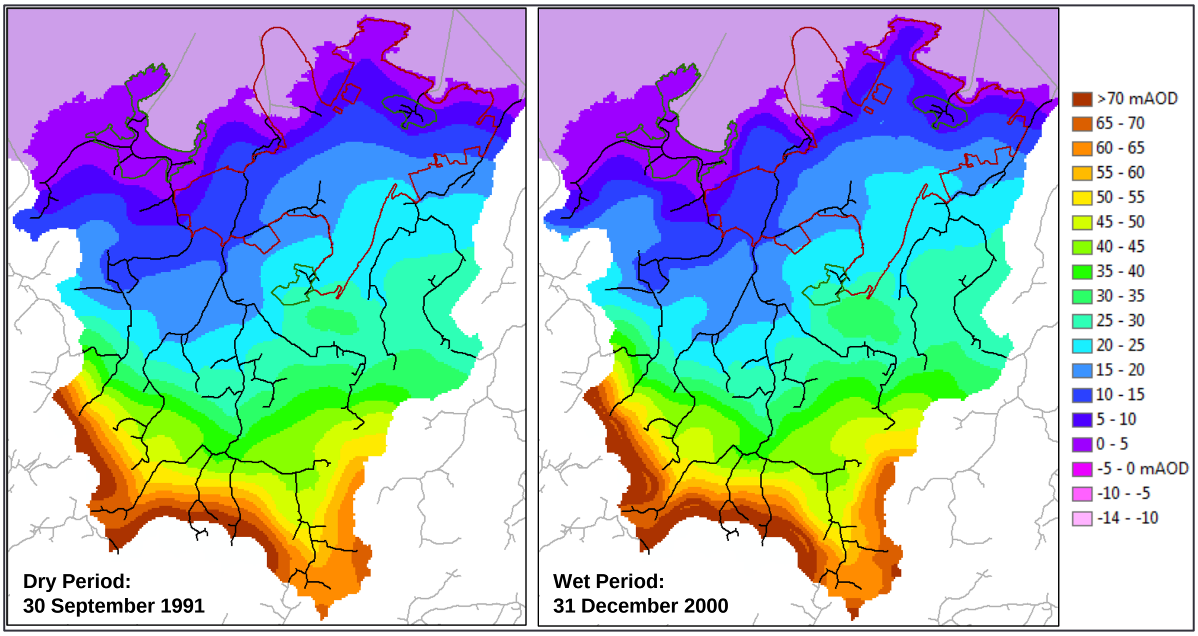

4.5 Uncertainties and model sensitivity analysis

There are many uncertainties associated with local scale parameter variability within the ground. This variability is best avoided, or at least simplified, when building models, which should be as simple as is justified by the questions being asked, and the conceptual understanding of the hydrogeology. However, whilst the calibrated historical simulation is deemed to be credible enough to be fit for predictive use (see Sections 4.6 and 4.7), it is worth building sensitivity models to explore alternative assumptions in order to provide a range of possible prediction outputs around the Central model.

For the Wylfa Newydd Development Area, it is not possible to explicitly measure how much recharge gets into and flows through the bedrock. The Section 3 analysis of hydro-test data has also highlighted that a range of bedrock hydraulic conductivity values will be encountered within the generalised expectation of significantly lower permeability at depths of more than 5 or 10 m below rockhead. These uncertainties can be expected to make a difference to the drawdown predictions associated with the excavation and dewatering and have therefore driven the development of alternative sensitivity models which assume High or Low recharge to the bedrock through the Drift relative to the Central calibrated model described above (figure 4.7). Four variants were initially derived by changing the influence of Drift thickness on recharge to the underlying bedrock, from which the highest and lowest variants were carried forward in the sensitivity analysis. Equivalent changes were made to the bedrock VKD profiles assumed in MODFLOW.

Figure 4.7 Bedrock recharge and transmissivity sensitivity modelling and baseline groundwater levels

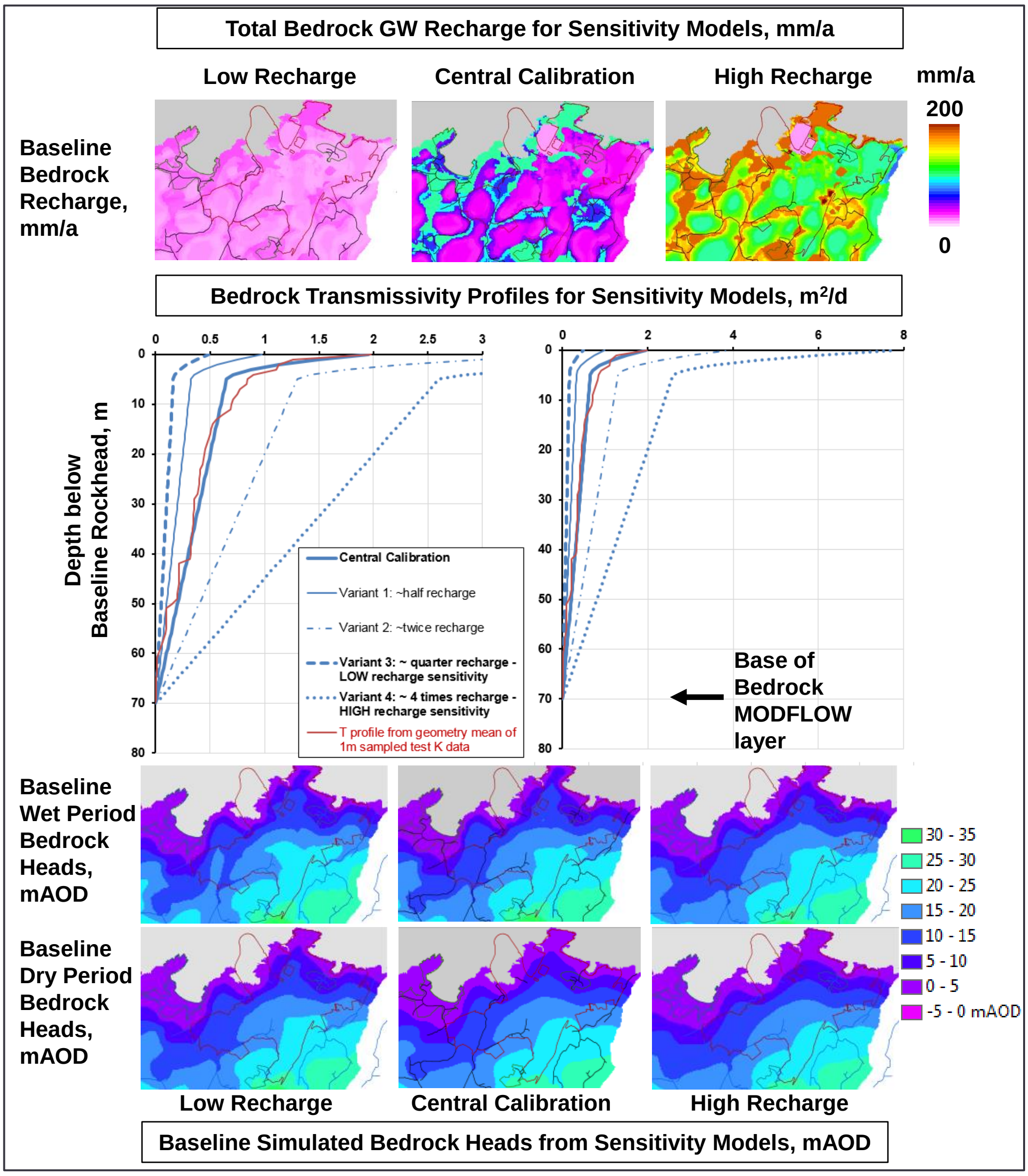

So the historical calibration scenario (baseline catchments, historical climate, and pumping test stresses) has also been run through sensitivity models with the Low and High variant recharge distributions and associated VKD profiles. Regional bedrock head maps for all three models are quite similar (figure 4.7) because both recharge and transmissivity have been varied together in an attempt to produce models with an equivalent degree of calibration fit.

The presentation of simulated heads and flows from the three sensitivity models, alongside the measured hydrographs (in the following Section 4.6) shows that this attempt to produce equally valid alternative calibrations has not been entirely successful. The Central model remains the most credible overall. However, the variants are still considered helpful in broadening the potential range of predicted impacts on heads and flows.

4.6 Comparisons of measured and simulated bedrock groundwater levels and stream flow

Daily average monitored groundwater levels are compared with hydrographs simulated in the MODFLOW bedrock cells in figures 4.8, 4.9 and 4.10. These include 11 hydrographs, located and clearly labelled on figure 3.8, which have been selected from the comprehensive collation observed and modelled data for all available bedrock and wetland SSSI sites in appendix C to provide good areal coverage across the site, representing a range of hydrogeological situations.

Each of the hydrograph plots includes the ground level and, where known, the elevation of the rockhead to indicate whether the measured and simulated water levels are confined (above the rockhead, within the overlying Drift), or lie unconfined within the bedrock (below the rockhead). In each of the figures, the plots are presented from top to bottom in order of decreasing ground elevation and locations with a variety of Drift thicknesses have been included.

Monitored daily average groundwater levels are presented in black, with the Central calibrated model behind (a blue line), and the Low (orange) and High (green) sensitivity model hydrographs at the back. This colouring scheme has been applied to other simulated hydrographs in the remainder of the report, wherever possible, to facilitate review through consistent familiarity.

The three hydrographs grouped in Figure 4.8 are presented together because they have relatively long period records – from 2010 to 2016. Figure 4.9 includes a further six hydrographs from investigation sites with shorter records (2015 and 2016). The monitored borehole intervals for all of these data are within the Cambrian or pre-Cambrian bedrock, so a direct comparison can be made with the MODFLOW simulated bedrock layer hydrographs. The head scale for the hydrographs in both of these figures is also fixed, although m AOD ranges vary, so that the amplitudes of groundwater level fluctuations between them can be compared.

The monitored data in Figure 4.10, however, relate to Drift piezometers located at the Tre'r Gof and Cae Gwyn SSSIs. A direct comparison cannot, therefore be made with the simulated bedrock heads in the model at these same locations. These plots have been included because of the focus of hydro-ecological impact assessment at these important receptor sites, as well as the need to inform model impact predictions by an awareness of the relationship between simulated bedrock levels and the SSSI ground and shallow water table elevations. Both of these hydrographs are plotted with an expanded head scale, compared with the plots in the previous two figures, in order to show more detail.

The Figure 3.8 map of all the appendix C groundwater level hydrograph locations includes a simple colour coded summary of the comparison between simulated and observed levels at the boreholes with monitored intervals in the bedrock. Boreholes where simulated levels are close to observed are indicated by black points, with blue points mapped where modelled levels are higher than observed, and red points where they are lower. There is reasonable coverage of acceptably matched observations (black points) across the site, and more locations where simulated levels are too low (red) compared with too high (blue).

Some of the locations where levels are two low (e.g. to the north of the existing power station) suggest that the influence of the sea level general head boundary in the model may be too strong in comparison with observed levels which are closer to the higher ground levels in this area. Where simulated levels are too high (by up to 3.5 m) and observed levels lie within the superficial deposits, the transmissivity of the bedrock may locally be higher than modelled e.g. there could be a case for lowering the modelled VKD inflection point a further 3.5 m below rockhead.

No attempt has been made to introduce areal zonation into the model parameterisation in order to refine and improve the local calibration in these areas – e.g. the VKD profile inflection point is set at 5 m below rockhead everywhere because this produces the best overall match with bedrock groundwater levels. Locally lowering this inflection point to increase the depth of more transmissive bedrock could improve the comparison of simulated baseline historical levels with observed but is unlikely to significantly change the distribution of predicted drawdown impacts due to the excavation. The excavation floor will mostly be at -10m AOD and is expected to dewater the surrounding zone of more permeable shallow bedrock whether this is this is 5 m or 8.5 m below rockhead.

Figure 4.8 Monitored and simulated historical bedrock groundwater level hydrograph examples, 2010 to 2016 (located on Figure 3.8)

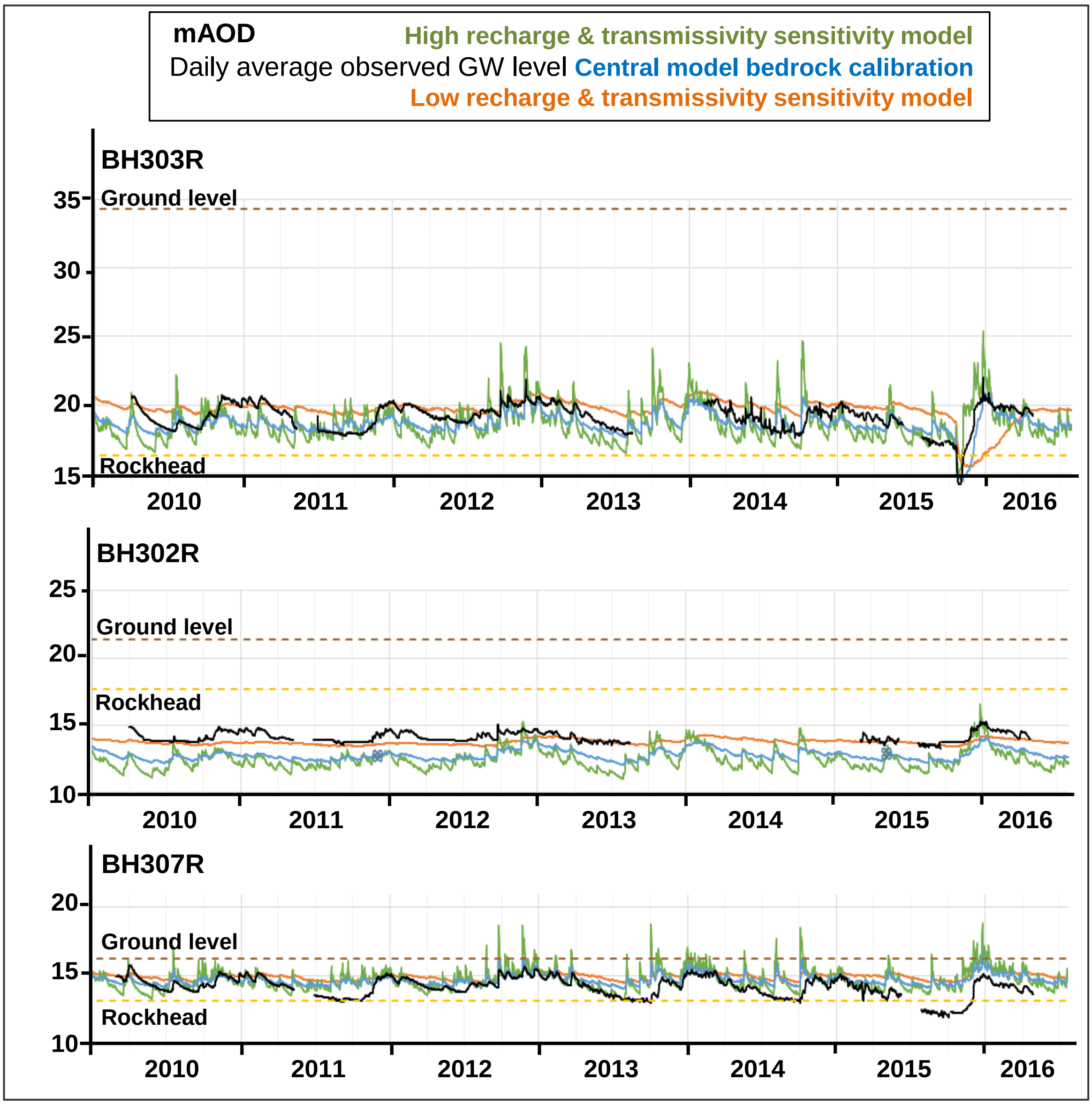

In Figure 4.8 the observed hydrograph for BH303R is reasonably well matched by the Central calibration model in terms of both short term and seasonal fluctuations, as well as average levels. Here the superficial deposits are very thick and the bedrock monitored groundwater level lies within them. During autumn 2015, both observed and simulated Central hydrographs show a similar response to the pumping test. Although average levels for the variant Low and High models are similar, the Low hydrograph is smoother and more sluggish than the observed pumping test response, and the High model hydrograph (within the Drift) is too peaky in terms of short term recharge signals, and recovers too rapidly after the pumping test.

Ground level is lower at BH302R, the Drift is thinner, and the monitored head is within the bedrock. Whilst the amplitude of annual and shorter term head fluctuations is well matched by the Central model, absolute simulated levels are 2 m too low. Here the Low recharge and transmissivity sensitivity model is a closer match. The High variant model unconfined hydrograph (i.e. where the water level is within the bedrock) is less peaky than the other two situations where the piezometric surface is within the superficial deposits but amplitudes are still greater than observed.

Observed heads at BH307R have a similar elevation and amplitude as BH302R, although the ground level is lower, and the heads are mostly just above rockhead in the thin Drift (falling below rockhead only in autumn 2015). This borehole is located in between the planned excavation and Tre'r Gof (Figure 3.8). All three sensitivity models simulate heads around the observed elevation but the Central model is the best fit.

Figure 4.9 Monitored and simulated historical bedrock groundwater level hydrograph examples, 2015 to 2016 (located on Figure 3.8)

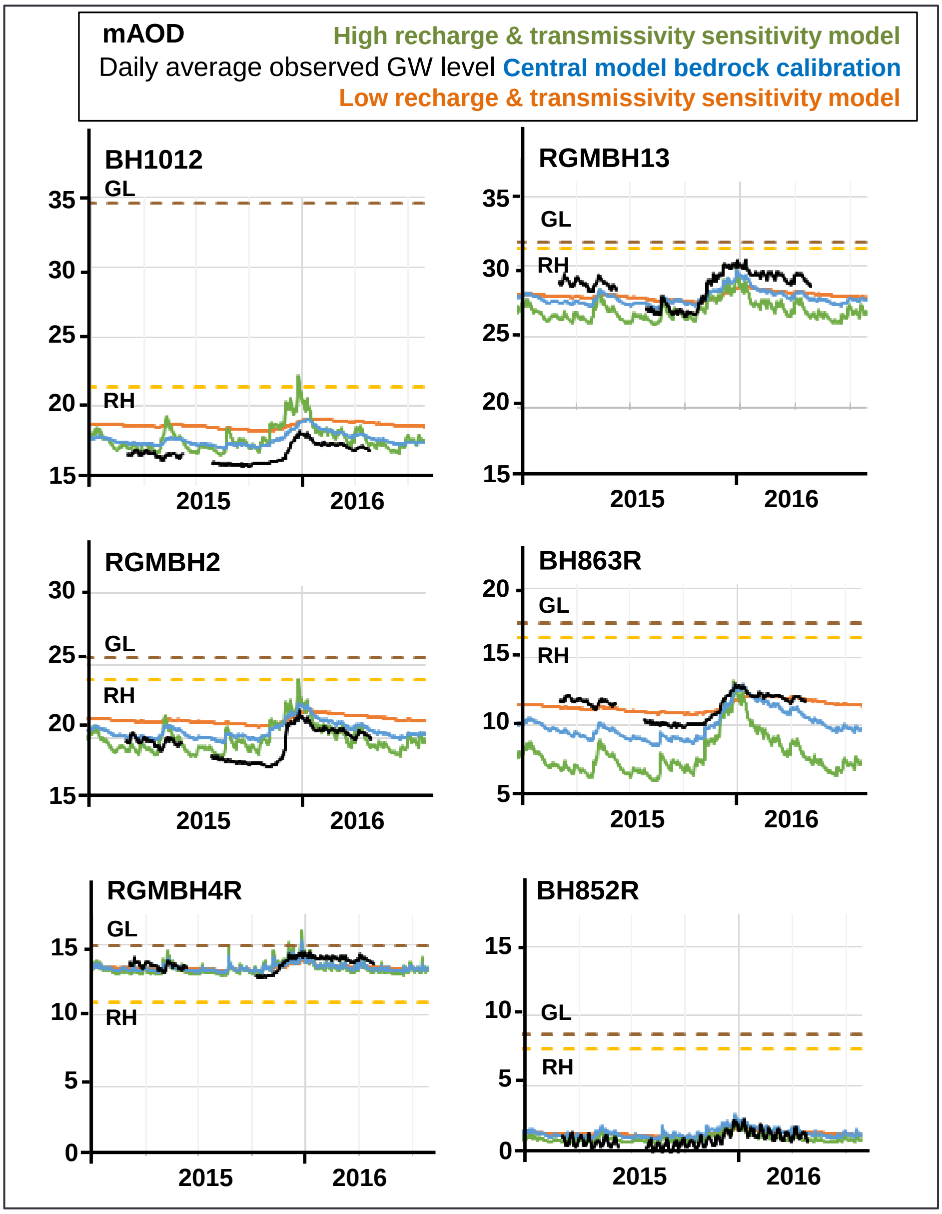

As noted in Section 3, it is apparent in Figures 4.8 and 4.9 (and through appendix C) that monitored bedrock water levels do not generally fall more than 6 or 7 m below rockhead. For example, both BH302R in Figure 4.8 and BH863R in Figure 4.9 are relatively close to the coast (~300 m inland), but heads within the bedrock are still well above nearby sea level. This is further evidence, beyond that from the hydro-testing data analysis, that regionally effective permeability is only typically enhanced in the upper ~5 m of the bedrock. Only very close to the coast (~50 m inland) at BH852R are bedrock heads clearly influenced by interaction with the sea – this is the only observed hydrograph with tidal influences (albeit that the daily averages plotted here just show neap-spring cycles).

The observed hydrographs plotted in Figure 4.8 are generally credibly matched by the Central model simulation. As previously noted, hydrographs simulated by the Low recharge and transmissivity model tend to be too smooth whereas those from the High variant are too peaky. The higher transmissivities of this variant model also connect BH863R too well with the nearby sea bed General Head Boundaries to the north, pulling down minimum heads below the field data.

Figure 4.10 Monitored SSSI Drift piezometer and simulated historical bedrock groundwater level hydrograph examples, 2015 to 2016 (located on Figure 3.8)

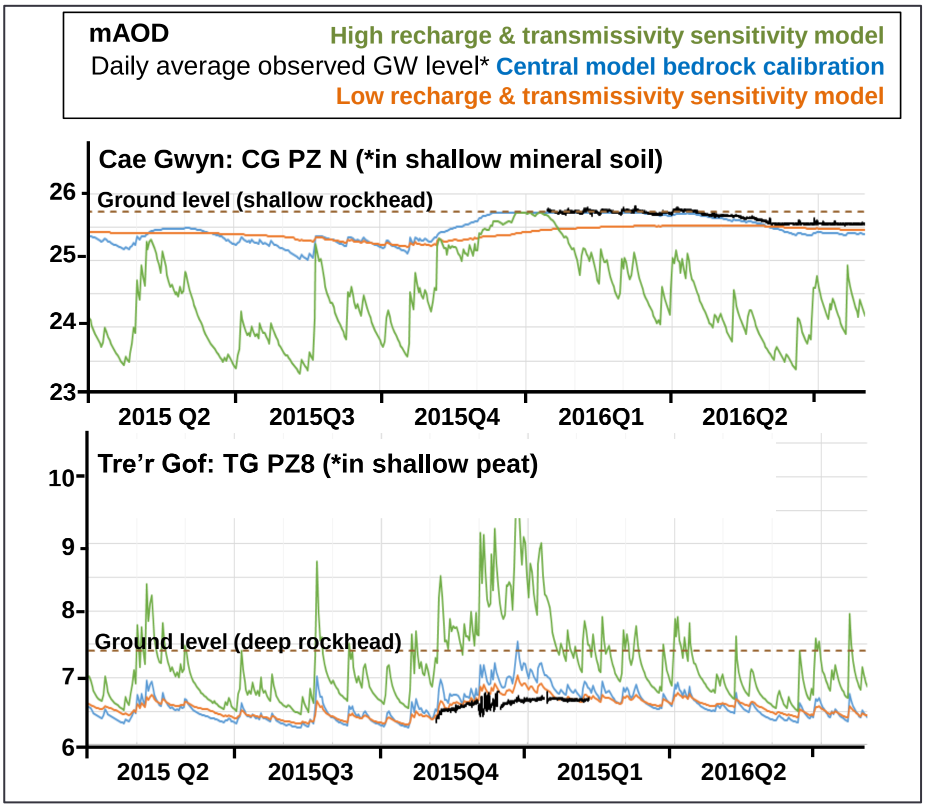

It is important to note that the m AOD scale used for Figure 4.10 is enlarged by 5 times in comparison with the preceding figures.

The elevation of the rockhead is not recorded for either of the Tre'r Gof or Cae Gwyn shallow piezometer records plotted on Figure 4.10. However, it is known that in some parts of the Cae Gwyn SSSI, peat and mineral soil sits directly on the bedrock at a shallow depth – there are high elevation outcrops surrounding this receptor – whereas the Drift confining the bedrock at Tre'r Gof is much thicker and less permeable.

At Cae Gwyn, the Drift is thin with relatively little resistance for flow between bedrock and Drift groundwater levels so it is encouraging that the simulated bedrock heads of the Central calibration model are reasonably close to the monitored shallow soil piezometer record. The CG_PZ_N soil hydrograph clearly shows the influence of local drainage overflow during the 2015/2016 winter and spring months with a gradual recession through May and June 2016. This is well matched by the Central calibration model – showing Stream cell elevations have been set appropriately, and that the transmissivity assumed is more credible than the High variant simulated hydrograph which falls too rapidly away from the drainage constraint. The failure of the Low variant hydrograph to reach the local Stream elevations also suggests that recharge in this sensitivity model is probably too low in this area of thin or no Drift.

At Tre'r Gof, the deeply confined bedrock head simulation cannot be directly compared with the monitored shallow water table in the peat. Both the Central and Low variant models seem consistent with the conceptual understanding of the SSSI with bedrock flow beneath and around the kettle hole feature towards the sea. The High recharge and transmissivity model, by contrast simulates rapid winter confined head rises to artesian levels – up to 3 m above the ground surface – which appears less credible.

The calibration of the sensitivity models with respect to the available surface flow gauging data discussed in Section 3 (and located on Figures 3.3 and 4.3) is presented in Figure 4.11 – the four gauge comparison Stream cells with the largest upstream catchment areas, and in Figure 4.12 – the four Tre'r Gof inflow gauges where the effective contributing catchments are much smaller and less certain. These figures illustrate the main features of the Central model calibration, and differences compared to flows simulated in the sensitivity variant models. The same Baseline calibration data are also plotted at larger scales in appendix C.

Both the Central calibration and Low recharge and transmissivity models provide a credible match to gauged flows at all four of the sites in Figure 4.11 (the orange time series for the Low sensitivity model is generally hidden behind the blue time series for the Central calibration model). Short term daily flow responses, the contrast between summer and winter flows and rates of recession are all reasonable. The hydrographs for the High variant however suggest that too much water is being generated by the larger proportion of bypass recharge assumed, making peak flows too high, and forcing excessive recharge through the bedrock so that recession rates are too slow and summer flows too high.

This suggests that it is appropriate for much of the effective rainfall to be routed to runoff and interflow within 4R which can provide a good representation of the likely flow impacts associated with landform re-profiling.

The range of flows simulated at the VN3 and VN2 Tre'r Gof inflow flumes (Figure 4.12) by the Central and Low sensitivity models is a reasonable match to the gauged ranges, although there are clearly timing errors in the early data for VN2. The gauged flows for VN1 and VN4 are much less than their 4R assumed contributing surface catchment areas would imply, as discussed around Figures 3.4 and 3.5. But these gauged flows are a small fraction of those presented in Figure 4.8, and the credible simulation of the VN5 outflow suggests that the overall rates of flow onto and off the SSSI are reasonably represented in the Central and Low models.

4.7 Summary of the credibility of the Central and sensitivity models

The Central calibration model is considered to be a credible representation of the conceptual understanding and data presented in Section 3, and also compares reasonably (but not perfectly) with many (but not all) of the available hydrometric records. The Low recharge and transmissivity variant model produces a similar calibration of surface flows, but bedrock groundwater level responses are too smooth and slow. The High recharge and transmissivity model is the least credible of the three based on comparisons with measured heads and flows. However, in order to provide a range of predictions which is more likely to envelope the conditions actually encountered during construction and operation of the site, all three models have been carried forward to represent the predictive Reference Point 4 and Reference Point 5 scenarios.

Figure 4.11 Gauged and simulated historical stream flows from sites with larger catchments, 2012 to 2016

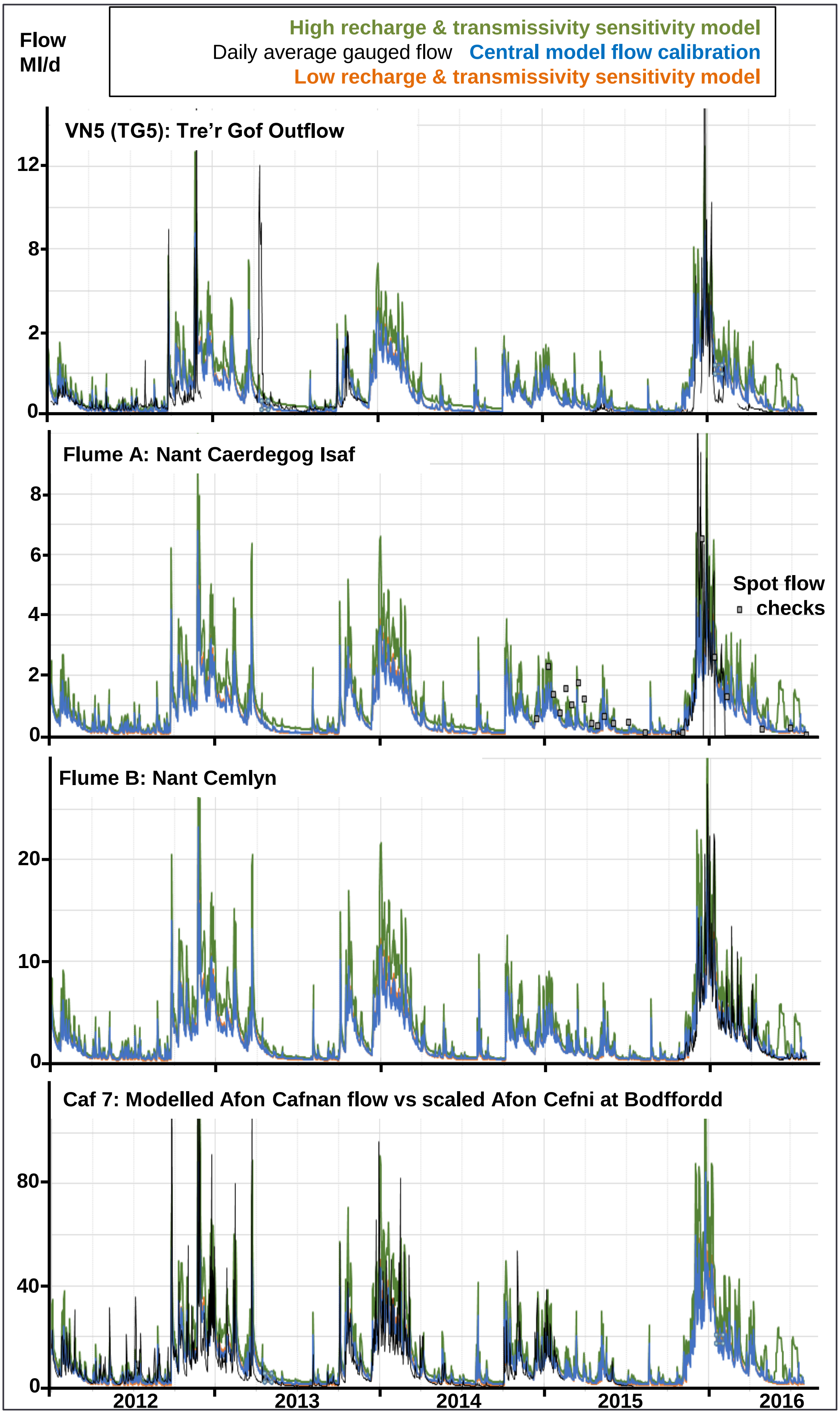

Figure 4.12 Gauged and simulated historical stream flows from Tre'r Gof inflow sites, 2012 to 2016

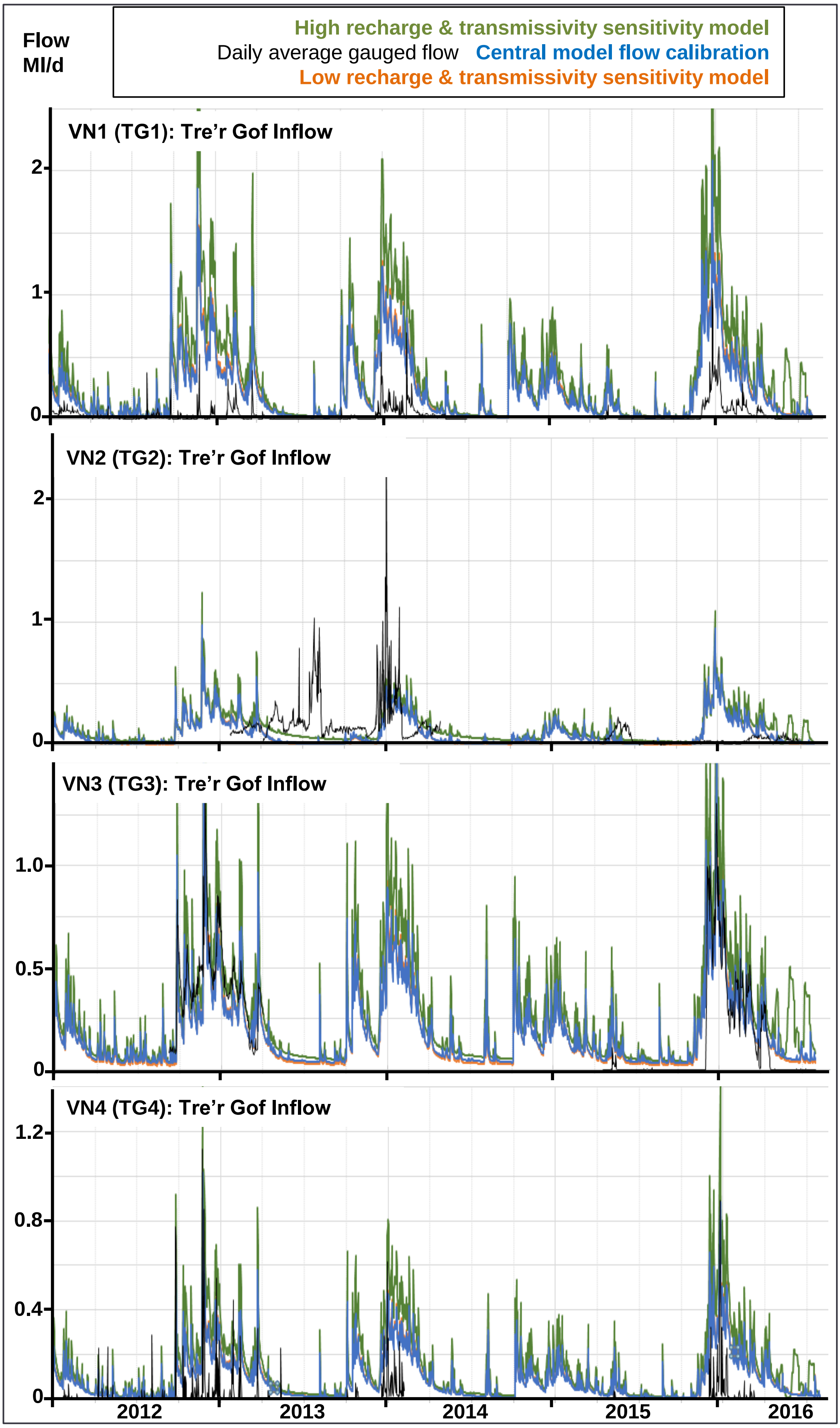

4.8 Reference Point 4 (construction) and Reference Point 5 (operation) predictive scenario modelling

Predictive scenario models have been built based on the Baseline sensitivity models, incorporating changes in boundary conditions, structure and parameterisation for mid construction Reference Point 4 and completion/operational Reference Point 5. Run numbers are listed in Table 4.1 and each scenario run has fixed boundary conditions throughout the simulation of responses to historical rainfall and potential evaporation climate drivers i.e. no attempt has been made to simulate the earthworks being moved, the excavation being dug and then backfilled etc. This is appropriate for the Baseline and Reference Point 5 completion scenarios but is a very precautionary simulation for the Reference Point 4 construction which will only have impacts in the short term whilst works are ongoing. Post-processing interpolation between these scenarios has taken account of a possible schedule of works when considering predicted impacts on stream flow duration curves (described in Section 5). But the Reference Point 4 predictions of bedrock drawdown from the model should certainly be viewed as precautionary because of the short time for which the excavation will be dug before it is shotcreted and then backfilled. The Reference Point 5 completion model is also precautionary in terms of the extent of predicted bedrock groundwater level drawdown impacts because no attempt has been made to represent the barrier effect associated with the shotcrete which would, in reality, reduce groundwater inflows. Figure 4.13 maps the excavation extent, dewatered floor elevations and backfill assumptions modelled.

Figure 4.13 Excavation and dewatering assumptions for the Reference Point 4 and 5 scenario models

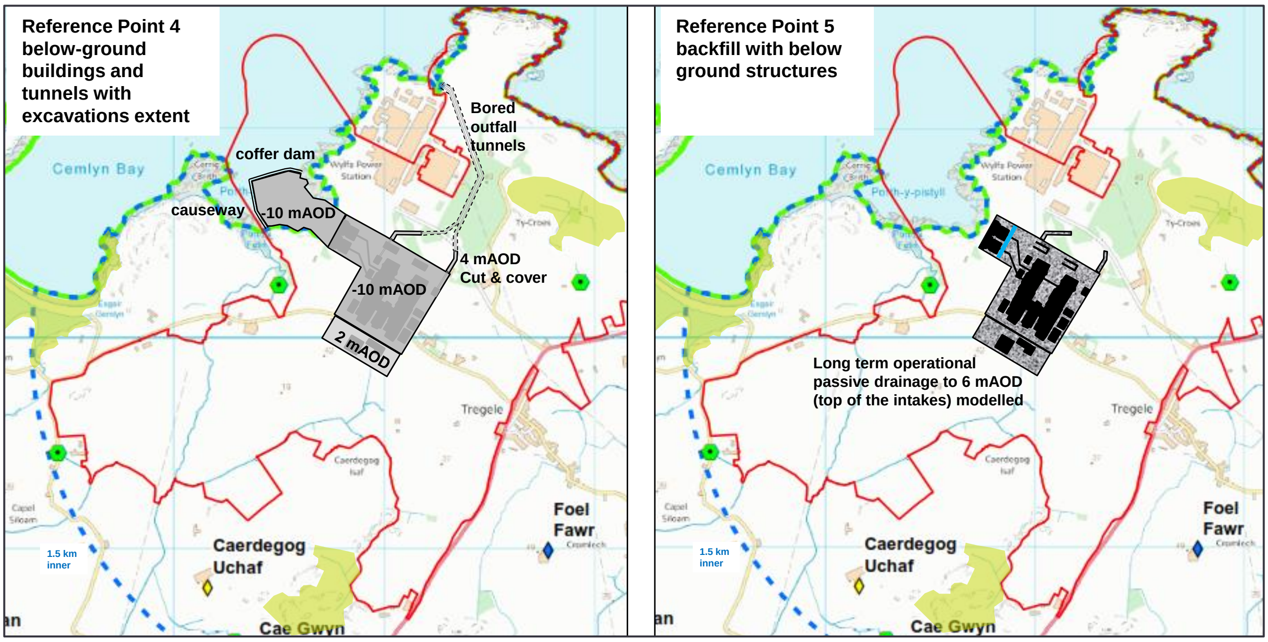

The Reference Point 4 excavations are likely to be dug as a single void in order to construct the proposed reactor and associated foundations. The initial Reference Point 4 model (figure 4.13) assumed that the base floor elevation of the excavation would be a uniform -10m AOD. This excavation will extend beyond the coast behind a coffer dam to ensure continuous inflow to the cooling water intakes even during low spring tides. A much shallower (4 mAOD) dewatered cut and cover excavation will be used to install the outfalls adjacent to the excavation but the remaining outfall tunnels to the north will be bored and are unlikely to have any significant groundwater level or flow impact

During November/December 2017 a review of more detailed excavation drawings found that the initially modelled extent and depth assumptions remain broadly valid, but that there will be locally deeper areas of the excavation floor. An engineering variant of the initial Reference Point 4 model was therefore run to simply incorporate the deeper areas of the excavation which the newer construction design requires for the intake works (-13.5m AOD) and foundation works (down to -18m AOD) – as shown in figure 4.14.

Figure 4.14 Excavation and ground elevation assumptions for the locally deepened engineering variant of the Reference Point 4 scenario model

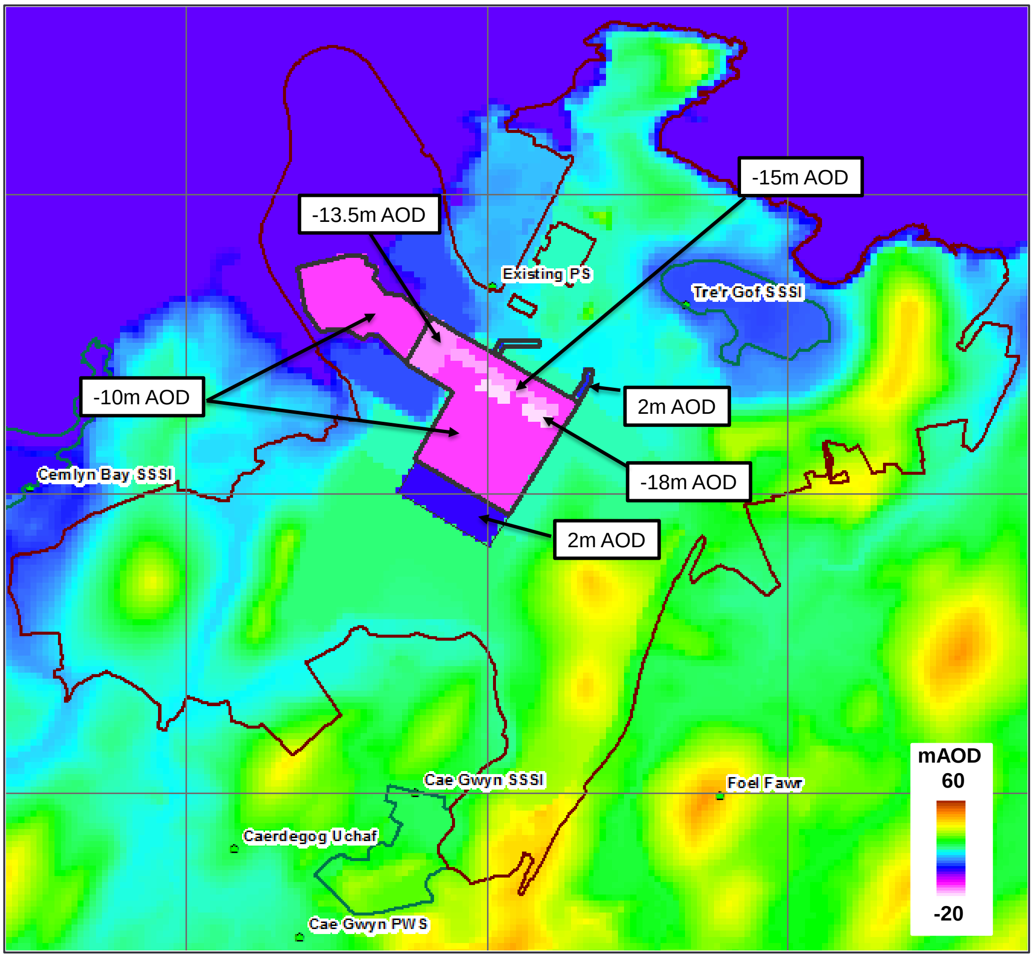

During Reference Point 5, long term active dewatering of the backfilled excavation is not required, so passive drainage to drains set at an elevation of 6m AOD at the back of the impermeable concrete intakes has been modelled (figure 4.13). The initial Reference Point 5 model does not include the barrier effect of shotcreting the walls, or laying the concrete floor slab, or the impermeable foundation structures so the model results are more conservative than would otherwise be the case. The backfill material in the Reference Point 5 model is assumed to be highly permeable crushed rock, and 10% of the completed platform surface has been assumed to allow recharge into it, with the remaining effective rainfall managed through surface drainage.

During November/December 2017, an engineering variant of this initial Reference Point 5 model was also run to incorporate the shotcreting of the excavation walls and floor intended to reduce bedrock inflows into the backfill, together with a surrounding perimeter drain to keep groundwater levels below finished ground level. A MODFLOW horizontal flow barrier was inserted into the model for this purpose with additional Drain boundaries cells outside it set at at an elevation 2 m below ground level (or at sea level adjacent to the coast).

The Section 5 presentation of modelled construction and completion scenario impacts includes predictions from both the initial Reference Point 4 and 5 models (which are the same as presented in the 2017 version of this report), and also, in Section 5.8, the engineering variant model versions (locally deeper excavation Reference Point 4 and shotcreted/perimeter drained Reference Point 5 scenarios). The additional engineering variant models are not intended to reflect the final design exactly, but instead to indicate the sensitivity of the groundwater level and surface flow impact predictions to changes in the local depth of the excavation and/or to engineering construction methods and completion details.

Beyond the bedrock excavation and backfill assumptions set out in figures 4.13 and 4.14, there are many other changes built into the Reference Point 4 and 5 models. These are set out in table 4.2 (for 4R) and table 4.3 (for MODFLOW) and are further illustrated in figure 4.15. This figure presents a collation of many of the Central calibration model build and output layers taken from ModelMap GIS for the Baseline, Reference Point 4 and Reference Point 5 scenarios. More detailed larger scale plans of these layers are also included in appendix D which presents a collation of predictive scenario maps equivalent to the Baseline model build in appendix B. In figure 4.14 they are pulled together to make comparisons between them easier to understand, and to link the changes made in the input build assumptions with the consequential impacts on the modelled outputs.

The rows of maps for the model build assumptions show:

- Ground elevations and upstream routed areas equivalent to figure 3.3: shows the landform re-profiling, excavations, mounding and managed drainage in Reference Point 4, and the completed flat platform in Reference Point 5. Catchment areas and flow rates will be impacted as a result of these changes.
- Soil and land use changes: with extensive bare soil mounds (lower evaporation) and an excavation floor assumed to generate 100 % rapid runoff in Reference Point 4, and a 90 % impermeable platform for the new power station in Reference Point 5. It should be noted that the Site Campus which will be constructed for worker accommodation during construction to the north of Tre’r Gof and east of the Existing Power Station has not been represented in the Reference Point 4 model. This will include some impermeable roof and road way areas but will also incorporate soakaways designed to limit runoff and promote local recharge. It is not associated with any major landform re-profiling which would change catchment divides, so its broader scale impact on the split between recharge and runoff, or on the inflows to Tre’r Gof from the north should be negligible.
- Slope changes influencing the speed at which rapid runoff is assumed to be released into the routing network.
- Drift interflow release assumptions in 4R also changes as the distance to the drainage network is modified through the construction period.
- The thickness of the Drift or made ground mounds will be significantly re-distributed, which is expected to result in changes in the split between Drift interflow and bedrock recharge rates.

Consequential changes are apparent in the final three rows of model outputs:

- Combined rapid runoff and interflow generated by 4R for adding onto the MODFLOW Stream cell network.
- Bedrock recharge added by 4R into the MODFLOW groundwater simulation.
- Dry period (30 September 1991) bedrock groundwater levels simulated by MODFLOW – showing the influence of the Reference Point 4 excavation and dewatering, and the Reference Point 5 passive drainage.

Figure 4.15 Predictive scenario modelling parameter inputs, assumptions and outputs for the Central model

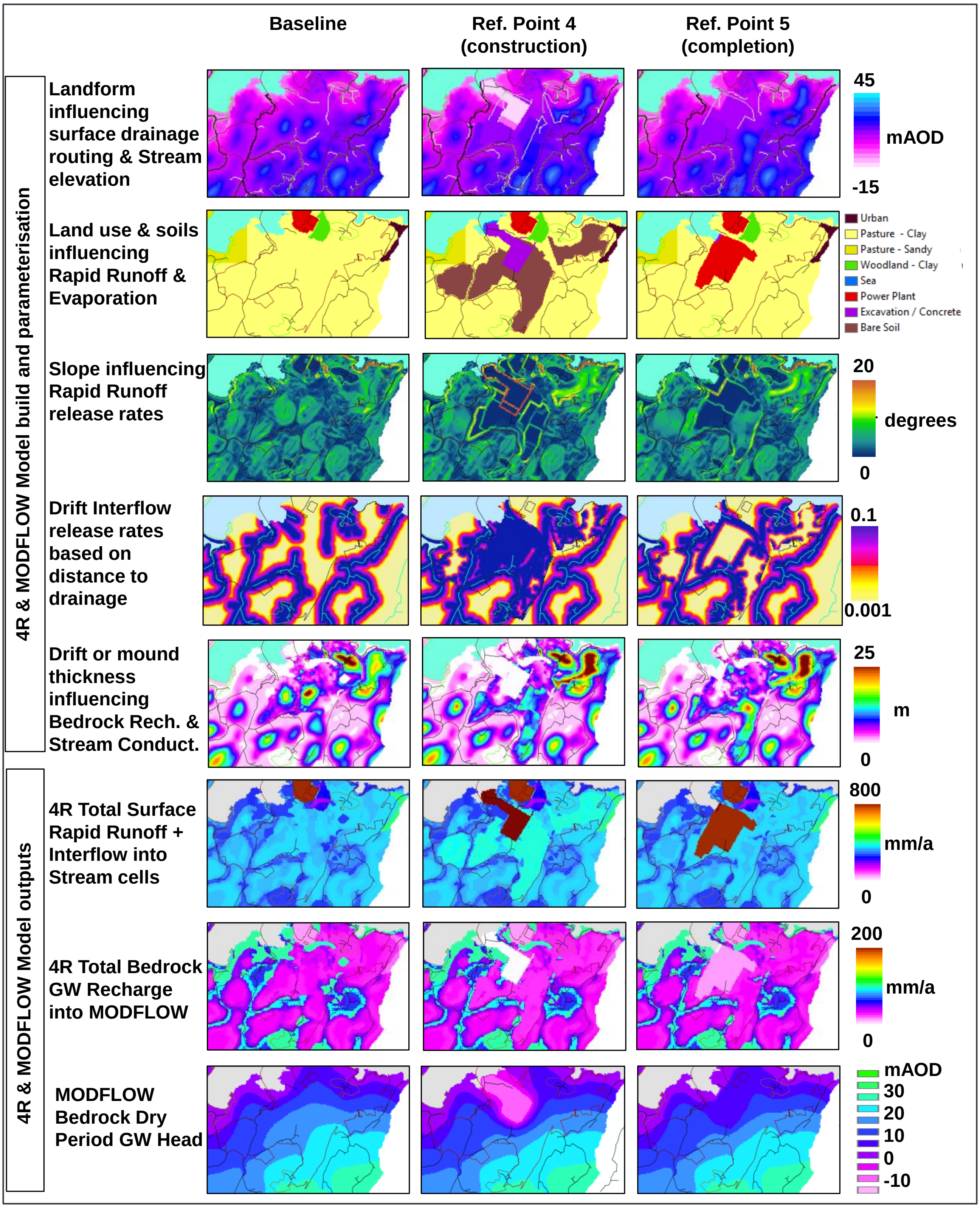

Modelling the managed drainage network

During the construction period, the runoff from the stripped soil and earthworks mounds will be collected in a series of toe drains which have been designed to carry storm flow responses from extreme events, routing the water into settlement lagoons where the sediment is removed before managed discharge of the water back into surrounding watercourses or the sea. The locations of these discharge points and lagoons have been schematically built into the 4R routing network of the Reference Point 4 models as simple linear routed runoff stores – releasing a proportion of the water stored in them each day (set to 0.2 - e.g. 20 %). The Reference Point 4 model routing also includes underground pipes connecting drainage between non-adjacent cells. These are shown as schematic arrows and reflected in the upstream routed area in ModelMap layers - full details are presented in the model build plans in appendix D (and also in figure 5.1).

Figure 4.16 shows the influence of these sediment lagoons built into the model simulation, comparing the inflows upstream of a lagoon to the outflows downstream of it. The soil stripping and steeper slopes built into the Reference Point 4 models result in 'flashier' rapid runoff peaks flowing into the lagoon compared with the baseline model. Outflows downstream are 'smoother', with lower peaks and slower subsequent recessions which will be essential to the successful functioning of these lagoons for sediment removal. Similar effects are simulated at all the lagoon locations.

Figure 4.16 The simulated flow impact of a sediment lagoon in the 4R model

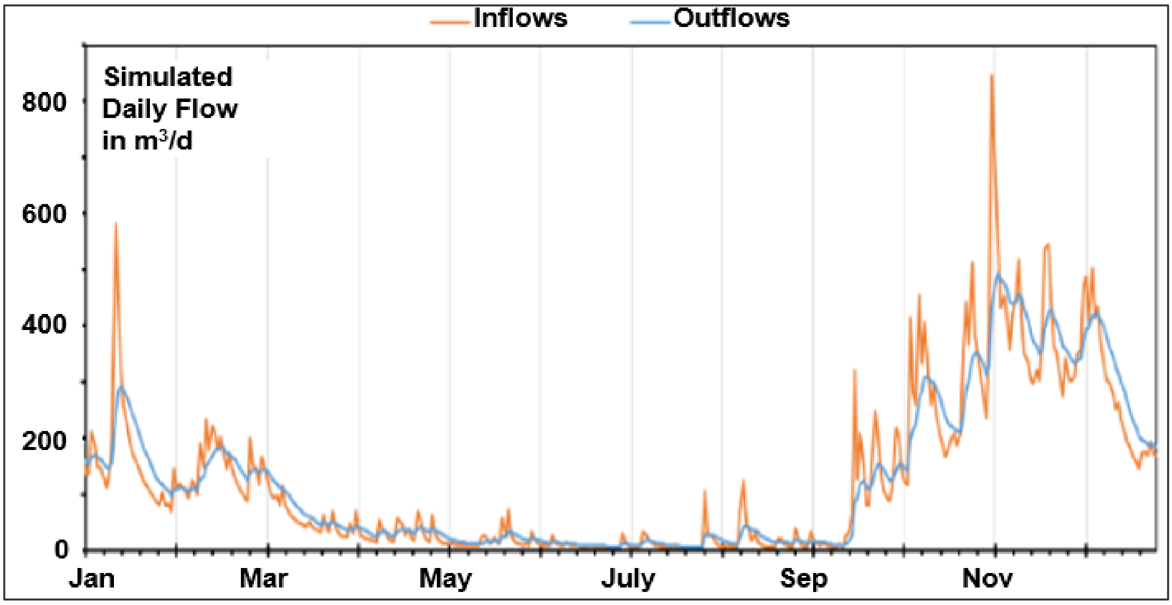

It is acknowledged that this simple linear store representation will not reflect how the lagoons are actually managed in detail, but it is important to build in some representation of their attenuating effects which will be essential for the management of suspended solids and which will also have related consequences on the timing and rates of discharges. Time series of simulated outflows from the lagoons, and in the associated receiving watercourses, have been used to help inform the design of appropriate discharge consents (being prepared by others) which will be required from NRW.

The Reference Point 4 MODFLOW models represent the dewatering of the excavation areas by covering their floor with Stream boundary cells set at -10 m AOD (or to the locally deeper elevations shown for the engineering variant of this model in figure 4.14). The runoff from surrounding areas has been forced around the excavations, and the Stream cells within the excavations are routed to two points located to accumulate water from the inland and seaward areas separately – to facilitate post processing and reporting of these two separate component areas. Stream cells have been used for this purpose across the floor of the excavations because they combine the rapid runoff associated with direct rainfall into the excavation with the inflow of bedrock groundwater, accounting for each separately to provide the total flow which would need to be managed each day.

The appendix D model build plans for the Reference Point 5 models show that there is no actively managed system of toe drains or sediment lagoons assumed for the long term operation of the site. However, in order to preserve the Baseline catchment draining towards Tre'r Gof from the south and east, the mounding in that area will be placed on a permeable drainage blanket. This is intended to promote infiltration of runoff from the south-eastern slopes of the mound so that it can flow north-westward within the drainage blanket under the mound and back to Tre'r Gof. This design has been simply represented by displacements built into the 4R routing network incorporating simple linear stores to smooth flow relocated to the TG3 and TG4 inflow points to Tre'r Gof such that their overall contributing catchment area remains close to the Baseline situation.

The Reference Point 5 MODFLOW models include a row of Drain boundary cells set at an elevation of 6 m AOD set within the permeable backfill at the north-west end of the excavation on the landward side of the intake structures. The concrete intakes themselves are assumed to provide an impermeable barrier separating the backfilled excavation from the sea, and the Reference Point 5 4R models have been adjusted such that rainfall onto them all becomes rapid runoff (i.e. there is no recharge to the concrete). The backfilled excavation has been modelled in MODFLOW using a VKD profile with an inflection point set at -10 m AOD to distinguish the high permeability fill (hydraulic conductivity assumed to be 5 m/d) above, from the low permeability bedrock below. The initial Reference Point 5 MODFLOW model does not incorporate any barrier effect which would be associated with the shotcreting of the walls and floor of the excavation – so predicted drawdown impacts in the surrounding bedrock can be viewed as precautionary. The impermeable foundation structures within the excavation are also not explicitly represented in the initial Reference Point 5 model. The engineering variant Reference Point 5 model does include a simple representation of the shotcreted walls and floor, together with a perimeter drain.

The bedrock head outputs from the Central calibration Baseline, initial Reference Point 4 and Reference Point 5 models have been presented previously at the bottom of figure 4.14, and time series flows simulated from these runs at the TG3 inflow to Tre'r Gof are plotted below. This environmental flow receptor point has been selected for illustration of the changing response characteristics simulated not just because it is represents one of the better calibrations, but because its upstream catchment area has been kept close to the Baseline in the Reference Point 4 models by discharges from the managed drainage system and in the Reference Point 5 models by the re-routing of water from the south through the drainage blanket such that contributing catchment areas are similar to the Baseline condition. The attenuation of peak runoff flows due to the management of the sediment lagoons is therefore apparent.

Figure 4.17 Time series scenario flows example for Tre'r Gof inflow, TG3

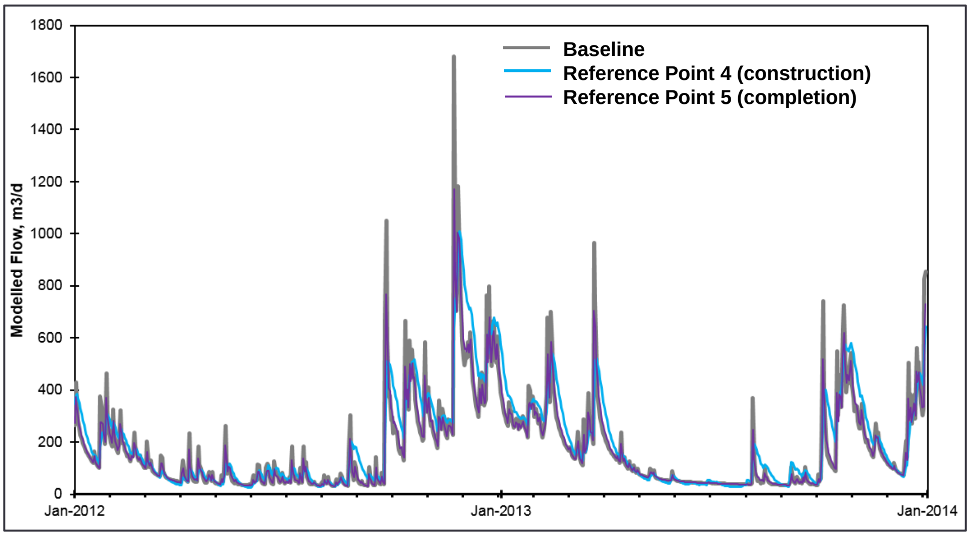

Using the sensitivity analysis models to assess predictive uncertainty

The preceding figures in this section illustrating the changes made to build the Reference Point 4 and 5 models have been drawn from the Central calibration model which provides the most credible Baseline simulation.

Figure 4.18 shows that both Low and High recharge and transmissivity sensitivity models have also been adapted and re-built in the same way. The distribution of bedrock recharge across the Site for all three sensitivity models in each of the three scenarios is mapped at the top of figure 4.18 against a common scale. The maximum ~30 m depth of the excavation floor (in Reference Point 4) and the permeable backfill (in Reference Point 5) below rockhead has also been marked on the alternative Baseline transmissivity profiles, although this will vary. At the coast, for example, where rockhead is at ground and sea level, only the upper 10 m of the transmissivity profile will be removed in the excavation.

Figure 4.18 Bedrock recharge output from the 3 sensitivity models for each of the 3 scenarios, with the associated MODFLOW transmissivity profiles

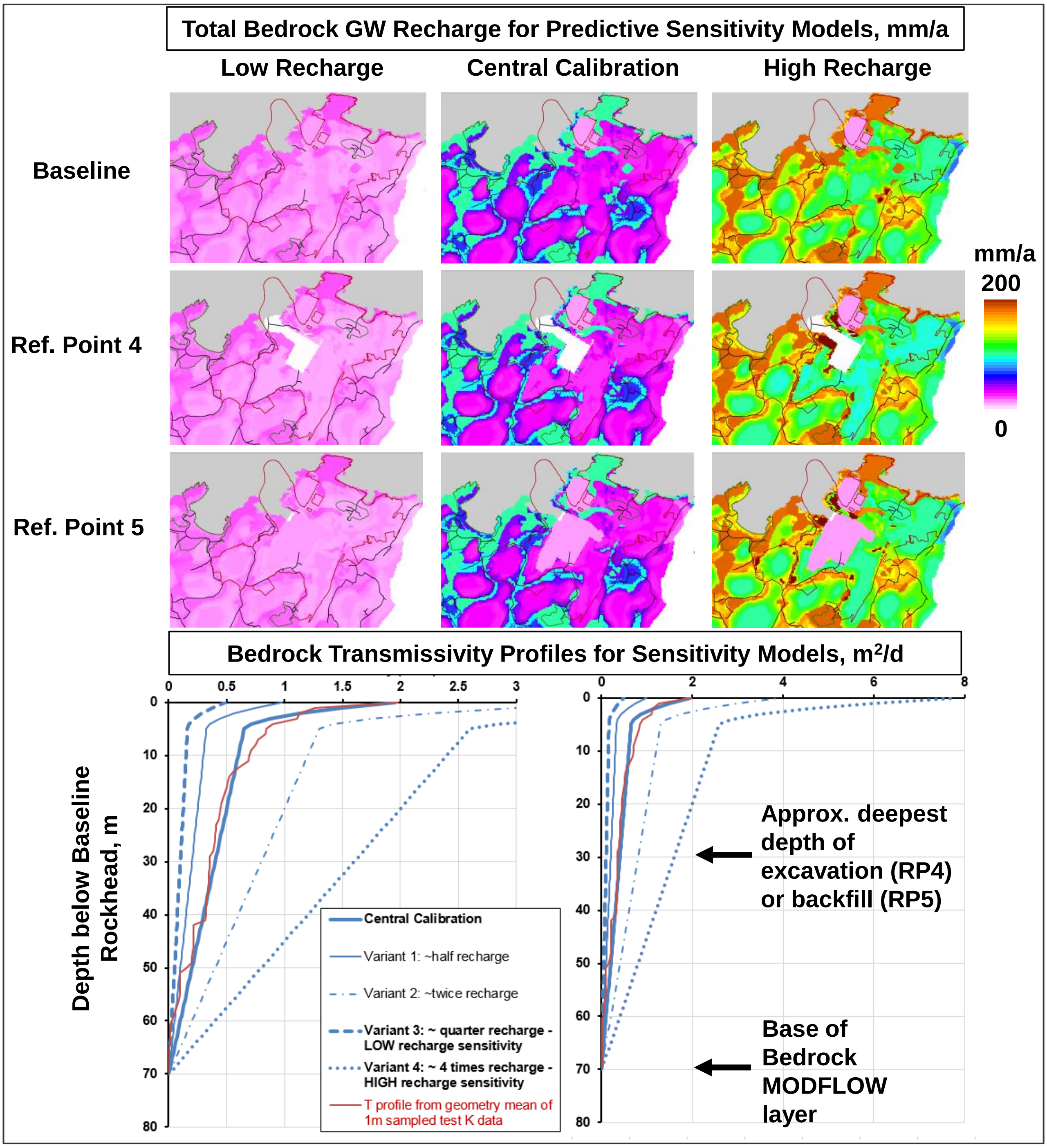

Although the Low and High variant models are a poorer representation of the Baseline understanding, this approach acknowledges key uncertainties regarding the split of water between the Drift and the bedrock and allows a range of output predictions to be presented from the modelling work in Section 5.

5. Bedrock groundwater level and Stream flow impact predictions

5.1 Introduction and structure of digital data transfer

This Section initially presents and summarises the output predictions from the modelling work originally presented in the 2017 issue of this report – assuming an excavation floor at -10m AOD for Reference Point 4, and no shotcreting or outer perimeter drain for Reference Point 5, as follows:

- Reference Point 4 flow time series for drainage discharge consenting and excavation dewatering (Section 5.2).
- Bedrock groundwater level drawdown impacts (Section 5.3).
- Changes in bedrock groundwater inflow to SSSIs (Section 5.4).
- Saline intrusion risks (Section 5.5).
- Reference Point 5 passive drainage from the backfilled excavation (Section 5.6).
- Surface water receptor flow duration curve impacts (Section 5.7).

During November/December 2017, review of the detailed excavation plans and completion proposals prompted the development of engineering variant models to explore the sensitivity of the predicted impacts to design changes. The engineering variant Reference Point 4 model includes locally deepened excavation areas, and the variant Reference Point 5 model assumes that the walls and floor of the excavation are shotcreted to prevent bedrock groundwater inflow, with an outer perimeter drain to prevent flooding around the excavation. The predicted impacts associated with these engineering variants are collated in Section 5.8, and compared with the maps, time series plots and tables presented in the previous sections.

Appendix E includes a comprehensive collation of groundwater level drawdown plans, and surface water receptor flow duration curve impact plots, but the other outputs are plotted in figures within this section. Appendix F provides the digital directory structure within which all the output predictions from the modelling work have been transferred to HNP for interpretation and incorporation into the DCO submission.

Throughout the presentation of the model calibration and scenario impact predictions in this report, we have included outputs from the Central calibration model alongside those from the two alternative sensitivity models based on Low or High bedrock recharge and transmissivity assumptions. **In reviewing these results it is important to bear in mind, as explained in Section 3, that the Central model provides the most credible calibration and predictions, and that the groundwater flow and impact predictions associated with the High recharge and transmissivity model are particularly precautionary, being based on a simulation which is much less plausible. Other assumptions in the initial modelling are also deliberately precautionary (i.e. will simulate greater levels of drawdown), including the decision not to represent any of the bedrock grouting or shotcreting works which will be engineered in the course of construction. The engineering variant model predictions presented in Section 5.8 are intended to illustrate the influence of these design assumptions.**

5.2 Reference Point 4 flow time series for discharge consenting and dewatering

Figure 5.1 Location of Reference Point 4 sediment lagoons, discharge and dewatering Stream cells

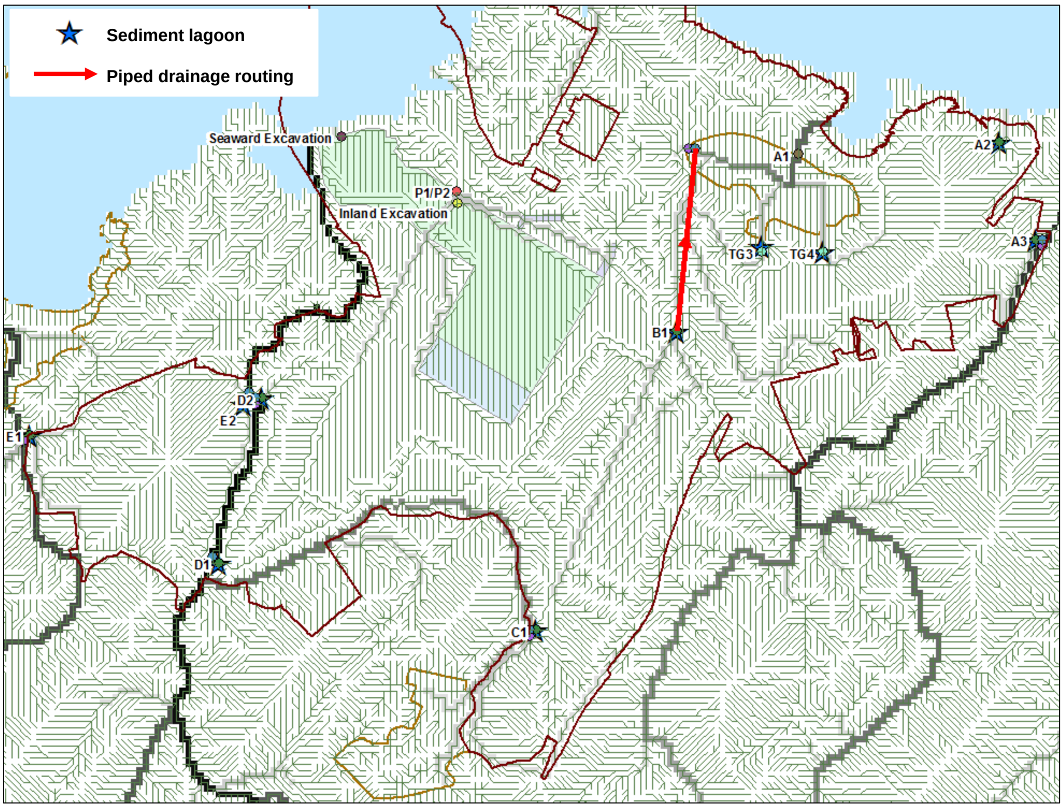

Figure 5.1 shows the location of the Reference Point 4 construction sediment lagoons and points P1/P2 from which discharges will need to be consented by NRW.

Time series of daily flows associated with both the discharges and the receiving watercourses have been provided to HNP to help inform the consent requirements.

The outline design for the drainage ditch running along the south and east of Tre'r Gof incorporates overflows to maintain some flows into the SSSI. The Reference Point 4 model routing mapped on figure 5.1 assumes that the drainage network will incorporate the ability to manage controlled releases from sediment lagoons onto the wetland at the baseline inflow points TG3 and TG4. Alternative drainage assumptions could be modelled which route water from the south and east around Tre'r Gof to a sediment lagoon at discharge point A1.

Figure 5.1 also plots and labels the location of two Reference Point 4 Stream cells (P1/P2) which accumulate the dewatering flows from the **inland** and **seaward** components of the **excavation**. Total dewatering requirements are dominated by the rapid runoff of effective rainfall falling into the excavations but also include the bedrock groundwater inflows (rates of which are low compared to the rapid runoff), which are accounted for separately.

Figure 5.2 presents these time series, which have been provided to HNP to inform the abstraction licence (environmental permit) which will need to be applied for. As discussed in Section 4, these indicate the potential for inflows in the short-term period when the excavation has reached its maximum depth, and before its walls have been concreted in preparation for construction of the power station foundations. The transient changes in groundwater dewatering around the inland excavation over the first ~5 years are the result of imposing the lower Stream cell drainage instantaneously at the beginning of the run on starting heads set initially at ground level.

Figure 5.2 Simulated dewatering rates for the Reference Point 4 inland and seaward excavations

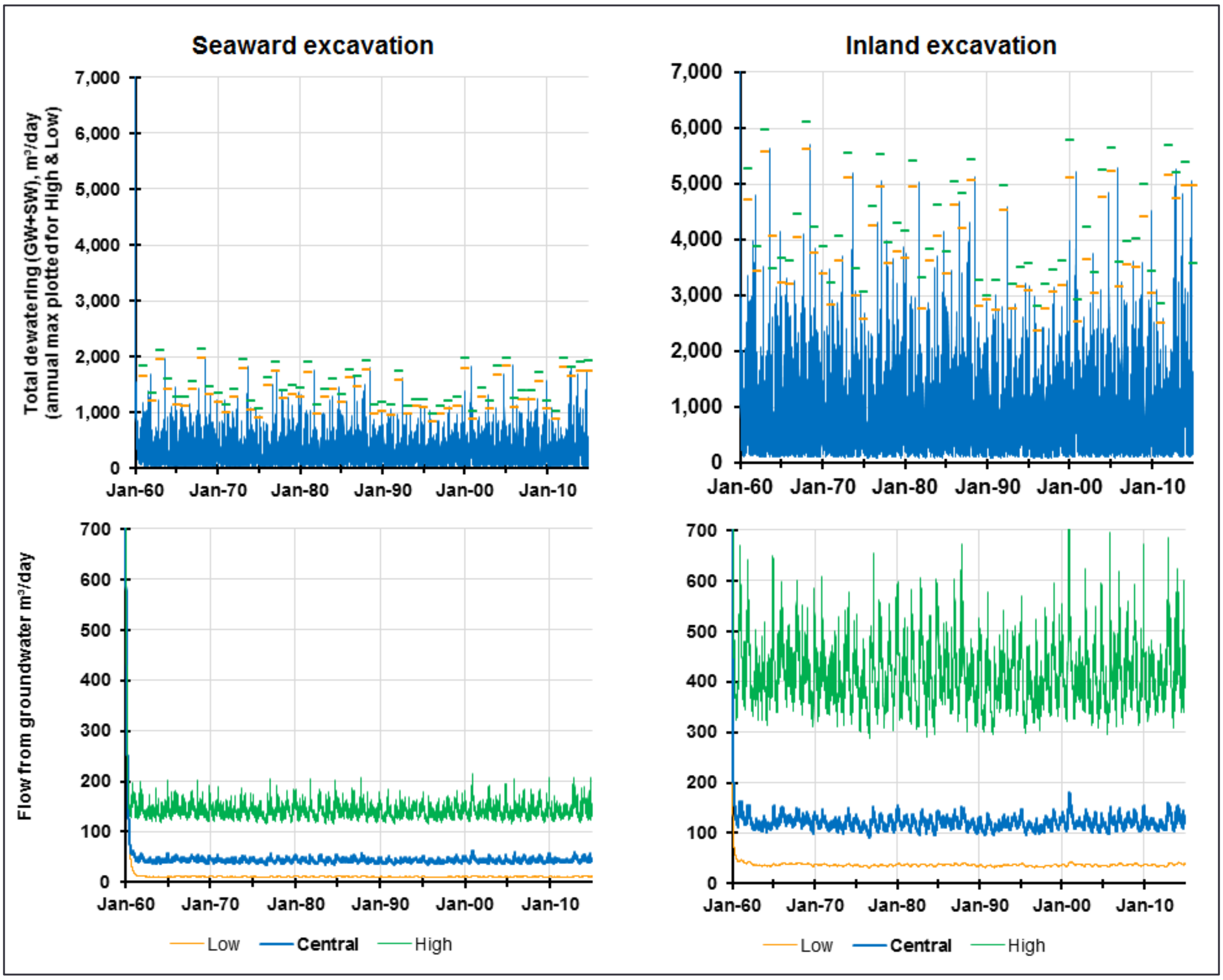

In reality, wherever excavation breaks into locally more permeable fissure zones, which can be expected, engineering intervention such as grouting would be used to keep the workings dry and reduce the need for pumping. Grouting and shotcreting have not been built into the model scenarios so the predictions of groundwater inflows and drawdown can be viewed as conservative. As also discussed in Section 4, the predictions from the Central calibration model should be considered as the most credible for the bulk properties of the bedrock. The higher recharge and transmissivity variant sensitivity model is less credible and its predictions should be considered as a very precautionary upper limit for shorter term groundwater inflow estimates before engineering interventions are applied.

The most important influence on the rates of pumping required from the excavation will be the rainfall experienced during the construction period. The model provides daily average flow estimated based on the climate sequence experienced between 1960 and 2016. If a sub-daily understanding of potential hourly runoff peaks associated with more extreme rainfall events which might occur during construction is required, reference would need to be made to the separate surface water flood modelling work being undertaken.

5.3 Bedrock groundwater level drawdown impacts

A comprehensive set of bedrock groundwater drawdown plans, calculated as Baseline minus Reference Point 4 or Reference Point 5 heads, are collated in appendix E for each of the three sensitivity models, for the two periods selected to represent dry and wet conditions (30 September 1991 and 30 December 2000 respectively).

These maps are also presented alongside each other in figures 5.3 and 5.4 below. The drawdown associated with the Reference Point 4 excavation and dewatering, and the Reference Point 5 passive drainage of the permeable backfill is clear. As would be expected, the areal extent of these impacts is broader in the High recharge and transmissivity variant – noting the previous comments that this simulation should be viewed as an unlikely and precautionary basis for predictions. The drawdown impacts extend more broadly during dry periods than during higher groundwater level winter recharge periods.

As set out at the start of this section, it is important to note that the extent of the long term drawdown predicted by the Reference Point 5 model would be much more limited if the impermeable barrier effects of concreting the floor and the walls of the excavation prior to backfill were built in.

In some locations, bedrock groundwater levels in the Reference Point 4 and 5 scenarios are predicted to rise relative to the Baseline, particularly during wetter, high groundwater level winter periods. These are sites where mound emplacement has been associated with the removal of stream cells controlling drainage, or with local stream cells being set at a higher elevation – so groundwater levels could rise to higher elevations than in the Baseline situation (in which groundwater level rise would be truncated by discharge to the surface water courses).

Figure 5.3 Simulated bedrock groundwater level drawdown relative to the baseline for a dry period (30 September 1991)

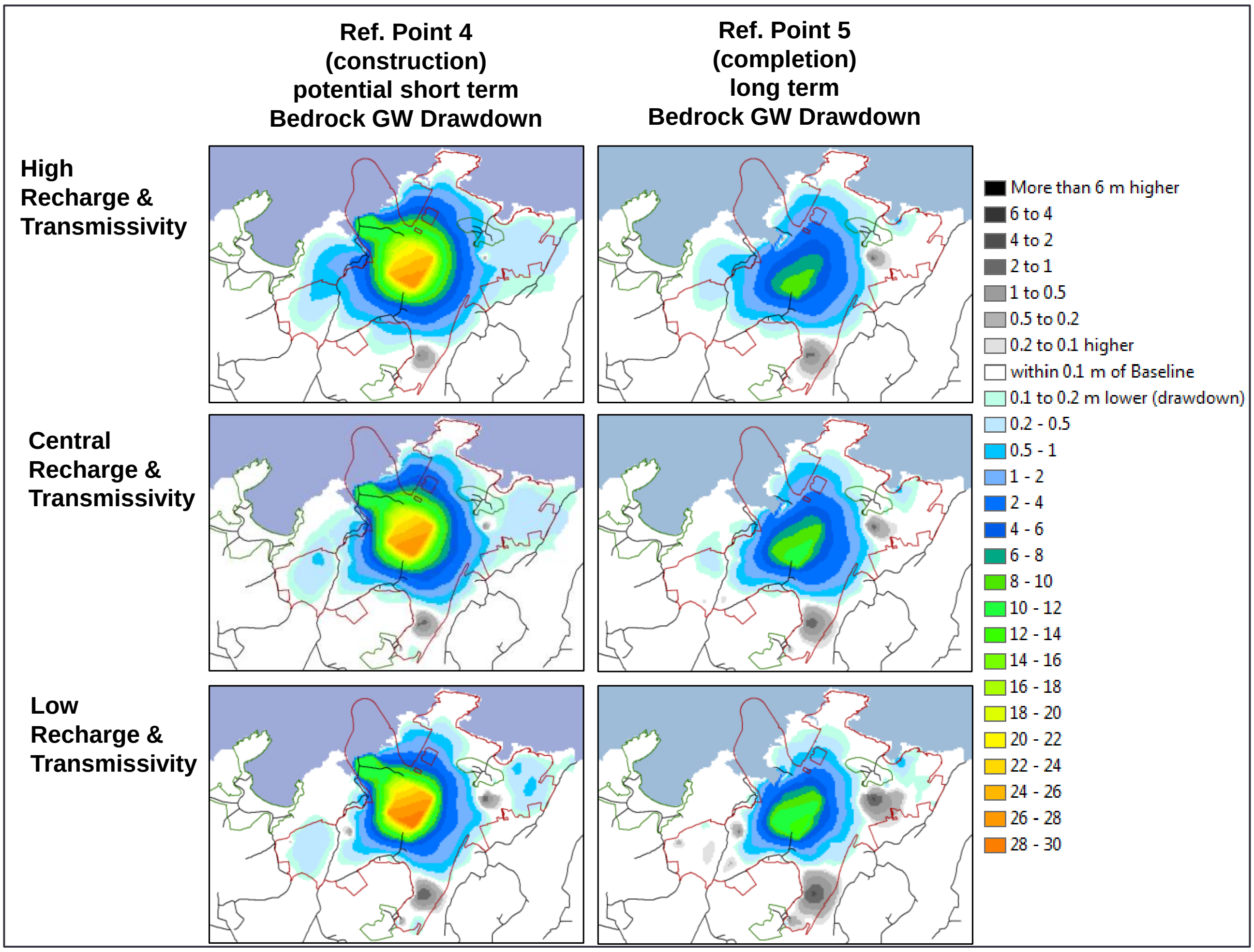

Figure 5.4 Simulated bedrock groundwater level drawdown relative to the baseline for a wet period (31 December 2000)

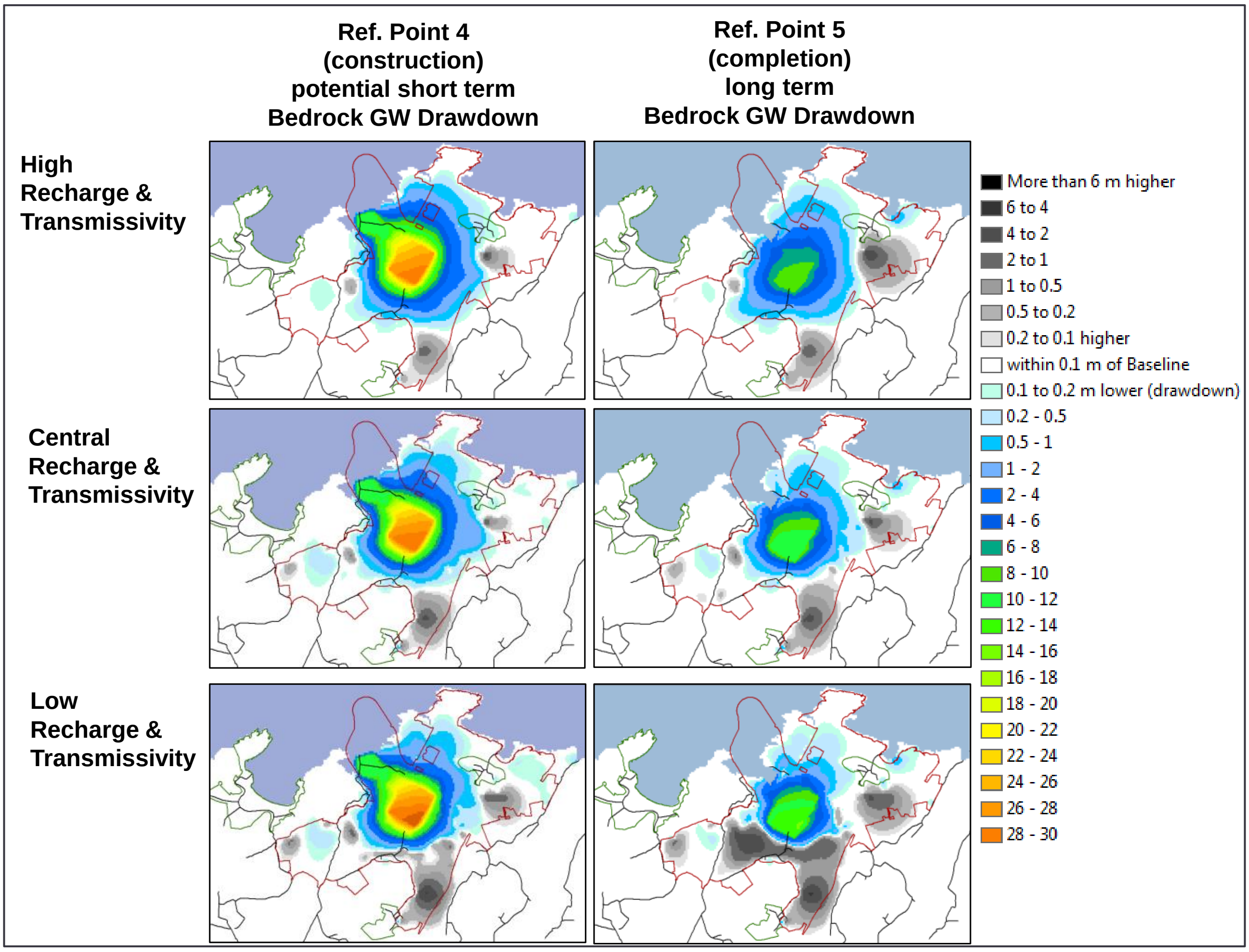

The appendix E plans also include the location of model cells selected to report groundwater level and drawdown predictions at the SSSIs, the existing power station, and at local private supply wells (also included in the report on figure 3.8). These data are listed in table 5.1 and included in the digital data transfer to HNP for further DCO interpretation.

Table 5.1 Simulated bedrock groundwater levels and drawdown at receptor cells

Dry period = 30/9/91, Wet period = 31/12/2000			Recharge and Transmissivity Sensitivity Models					
All bedrock head elevations in m AOD			Central		Low		High	
Scenario	**Groundwater receptor cell**	**Model Cell Row_Col**	**Dry**	**Wet**	**Dry**	**Wet**	**Dry**	**Wet**
Baseline	Caerdegog Uchaf private supply	150_133	17.67	18.43	18.02	18.94	17.58	18.24
	Foel Fawr private supply	141_214	25.37	26.79	26.36	28.06	25.35	26.18
	Cae Gwyn PWS	164_144	20.98	21.19	20.92	21.14	20.96	21.25
	Existing Power Station	56_177	7.70	9.96	8.97	11.52	6.57	9.20
	Nearest Magnox potentially susceptible building	41_182	5.28	7.20	7.89	8.50	3.16	6.45
	Tre'r Gof SSSI	59_209	7.64	8.98	7.27	8.10	8.15	9.97
	Cae Gwyn SSSI	140_164	22.48	22.94	22.71	23.26	22.21	22.77
	Cemlyn Bay SSSI	89_99	1.78	1.88	1.75	1.90	1.74	1.79
Ref Point 4 Construction (short term only)	Caerdegog Uchaf private supply	150_134	17.66	18.42	18.01	18.93	17.55	18.21
	Foel Fawr private supply	141_215	25.36	26.78	26.36	28.05	25.30	26.18
	Cae Gwyn PWS	164_145	20.97	21.19	20.91	21.13	20.95	21.27
	Existing Power Station	56_178	-1.23	5.63	3.38	9.15	-3.51	1.71
	Nearest Magnox potentially susceptible building*	41_182	2.34	5.83	6.68	7.51	0.30	4.70
	Tre'r Gof SSSI	59_210	6.76	8.47	6.88	7.73	6.20	9.13
	Cae Gwyn SSSI	140_165	22.47	22.94	22.70	23.27	22.17	22.79
	Cemlyn Bay SSSI	89_100	1.78	1.88	1.75	1.90	1.74	1.78
Ref Point 5 Operation	Caerdegog Uchaf private supply	150_135	17.67	18.43	18.02	18.94	17.58	18.24
	Foel Fawr private supply	141_216	25.38	26.81	26.36	28.06	25.36	26.19
	Cae Gwyn PWS	164_146	20.98	21.19	20.92	21.14	20.96	21.25
	Existing Power Station	56_179	5.92	9.04	7.97	10.90	4.85	7.79
	Nearest Magnox potentially susceptible building*	41_182	4.49	6.70	7.65	8.15	2.40	5.96
	Tre'r Gof SSSI	59_211	7.18	8.87	7.08	7.97	7.45	9.71
	Cae Gwyn SSSI	140_166	22.48	22.94	22.71	23.26	22.22	22.77
	Cemlyn Bay SSSI	89_101	1.78	1.88	1.75	1.90	1.74	1.79

* NB the model does not include parameters representing any sub-surface structures beneath the Magnox buildings.

Dry period = 30/9/91, Wet period = 31/12/2000			Recharge and Transmissivity Sensitivity Models					
All bedrock drawdown in metres (Baseline - Scenario)			Central		Low		High	
Scenario	**Groundwater receptor cell**	**Model Cell Row_Col**	**Dry**	**Wet**	**Dry**	**Wet**	**Dry**	**Wet**
Ref Point 4 Construction (short term only)	Caerdegog Uchaf private supply	150_134	0.01	0.02	0.01	0.01	0.03	0.03
	Foel Fawr private supply	141_215	0.01	0.02	0.00	0.01	0.05	-0.01
	Cae Gwyn PWS	164_145	0.01	0.00	0.01	0.01	0.01	-0.02
	Existing Power Station	56_178	8.92	4.33	5.60	2.38	10.08	7.49
	Nearest Magnox potentially susceptible building*	41_182	2.95	1.37	1.21	0.98	2.85	1.75
	Tre'r Gof SSSI	59_210	0.88	0.51	0.40	0.37	1.95	0.84
	Cae Gwyn SSSI	140_165	0.02	0.00	0.01	0.00	0.04	-0.02
	Cemlyn Bay SSSI	89_100	0.00	0.00	0.00	0.00	0.00	0.00
Ref Point 5 Operation	Caerdegog Uchaf private supply	150_135	0.00	0.00	0.00	0.00	0.00	0.00
	Foel Fawr private supply	141_216	-0.01	-0.01	0.00	0.00	-0.01	-0.02
	Cae Gwyn PWS	164_146	0.00	0.00	0.00	0.00	0.00	0.00
	Existing Power Station	56_179	1.78	0.91	1.00	0.62	1.71	1.41
	Nearest Magnox potentially susceptible building*	41_182	0.79	0.49	0.24	0.35	0.76	0.49
	Tre'r Gof SSSI	59_211	0.45	0.10	0.19	0.13	0.70	0.26
	Cae Gwyn SSSI	140_166	0.00	0.00	0.00	0.00	0.00	0.00
	Cemlyn Bay SSSI	89_101	0.00	0.00	0.00	0.00	0.00	0.00

5.4 Changes in bedrock groundwater inflow to SSSIs

Changes in bedrock levels can be expected to be associated with changes in groundwater to surface water flows. Changes in bedrock groundwater discharge predicted within the Tre’r Gof, Cae Gwyn and Cemlyn Bay SSSI boundary polygons are collated in table 5.2. These predictions need to be interpreted in the context of other influences on the shallow Drift water tables associated with the dependent wetland plant communities or ecosystems. Cae Gwyn, for example, is at a relatively high elevation close to a bedrock outcrop recharge mound and any model predicted changes in bedrock heads could be expected to be closely linked to changes in the shallow water table over some parts of the wetland. However, table 5.1 shows that predicted bedrock drawdown at Cae Gwyn is negligible. Tre’r Gof is much less directly dependent on bedrock groundwater inflows, but is located at a lower elevation where there is an upward gradient towards the SSSI - predicted bedrock groundwater level drawdown and associated reductions in upward flow are only a small component of the overall water balance for the site. The Central Reference Point 4 model dry period bedrock input reduction of -6.7 m^3/d is around 6% of the Baseline Q95 low flow statistic for the Tre'r Gof outflow TG5 (110 m^3/d).

Table 5.2 Simulated bedrock groundwater discharges to SSSI receptors and differences predicted between scenarios

Dry period = 30/9/91, Wet period = 31/12/2000		Recharge and Transmissivity Sensitivity Models					
Bedrock GW to SW flows across the SSSIs in m^3/d		Central		Low		High	
Scenario	**SSSI Area**	**Dry**	**Wet**	**Dry**	**Wet**	**Dry**	**Wet**
Baseline	Tre'r Gof SSSI	17.1	37.3	7.1	14.0	36.7	83.0
	Cae Gwyn SSSI	10.4	55.2	4.0	10.7	12.4	70.7
	Cemlyn Bay SSSI	81.6	170.2	24.5	47.4	188.2	364.0
Ref. Point 4 Construction (short term)	Tre'r Gof SSSI	10.4	35.0	6.1	13.4	11.3	76.1
	Cae Gwyn SSSI	9.7	53.0	3.7	10.5	11.3	64.9
	Cemlyn Bay SSSI	81.5	170.1	24.5	47.4	187.0	363.8
Ref. Point 5 Operation	Tre'r Gof SSSI	14.2	37.4	6.6	13.8	28.6	85.5
	Cae Gwyn SSSI	9.1	52.1	3.6	10.2	12.3	64.0
	Cemlyn Bay SSSI	81.6	170.0	24.5	47.4	187.6	363.7

Dry period = 30/9/91, Wet period = 31/12/2000		Recharge and Transmissivity Sensitivity Models					
GW to SW flow changes in m3/d (Scenario - Baseline)		Central		Low		High	
Scenario	**SSSI Area**	**Dry**	**Wet**	**Dry**	**Wet**	**Dry**	**Wet**
Ref. Point 4 Construction (short term)	Tre'r Gof SSSI	-6.7	-2.3	-1.0	-0.7	-25.4	-7.0
	Cae Gwyn SSSI	-0.7	-2.2	-0.2	-0.3	-1.1	-5.9
	Cemlyn Bay SSSI	-0.1	-0.1	0.0	0.0	-1.1	-0.2
Ref. Point 5 Operation	Tre'r Gof SSSI	-2.9	0.0	-0.4	-0.2	-8.1	2.4
	Cae Gwyn SSSI	-1.4	-3.1	-0.4	-0.5	-0.1	-6.7
	Cemlyn Bay SSSI	-0.1	-0.2	0.0	0.0	-0.6	-0.3

5.5 Saline intrusion risks (General Head Boundary inflows)

The modelling results show that there are no saline water inflow risks associated with the Baseline or Reference Point 5 scenarios – inland heads remain above sea level and flows are always outwards at the coast.

Figure 5.5 shows the inflows simulated from the sea bed General Head Boundary cells induced by the excavation and dewatering assumptions built into the Reference Point 4 construction model. The observations and caveats discussed in association with the dewatering rate predictions apply to these results as well. In reality, the Reference Point 4 construction phase will not continue indefinitely, and the High sensitivity model predictions should be considered as highly precautionary. The Central model inflow predictions amount to less than 10 m^3/d. It is also relevant to note that most of the seawater which might in reality flow into the bedrock when the excavation is at -10m AOD will end up in the seaward end of the pit itself where the groundwater will already be saline. In other words, by constructing the coffer dam out in the bay and excavating both inland and seaward components of the excavation together, saline intrusion risks - which according to these inflow predictions are very minor anyway because of the low permeability of the bedrock - are reduced yet further. In addition, most locally significant saline inflows would end up in the excavation, rather than in the bedrock surrounding it, being pumped out as part of the dewatering management. Finally, it is important to note that if any locally significant fracture systems were encountered which connected the pit with the sea, these would be quickly grouted up to keep the workings dry.

Figure 5.5 Simulated General Head Boundary inflow time series from the Reference Point 4 models (assuming no shotcreting or grouting of the excavation)

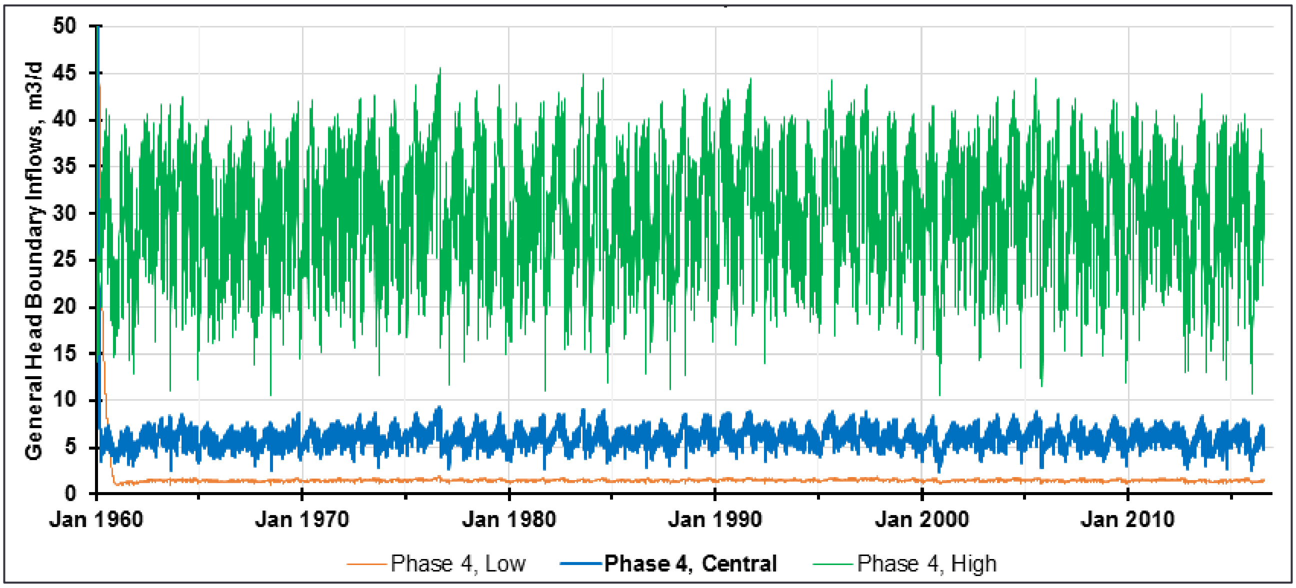

Figure 5.6 maps the Reference Point 4 spatial distribution of flows from the bedrock out to the sea bed General Head Boundaries (in blue), and the boundary cells local to the excavation where flows are reversed – from the sea into the bedrock. Most of these potential inflow risk cells are on the sea bed out in the bay, although the inflowing boundary cells also extend up the coast by ~180 m north of the coffer dam indicating that this is where some saline water may enter part of the freshwater bedrock groundwater system which is not going to be removed by excavation. It is likely that saline water entering the fractured bedrock on its way to the dewatered excavation during the construction phase would be flushed out again by freshwater from inland when the works are finished and a positive seaward hydraulic gradient is re-established.

Figure 5.6 Reference Point 4 simulated General Head Boundary flow and bedrock groundwater level map (for the dry period, 30 September 1991))

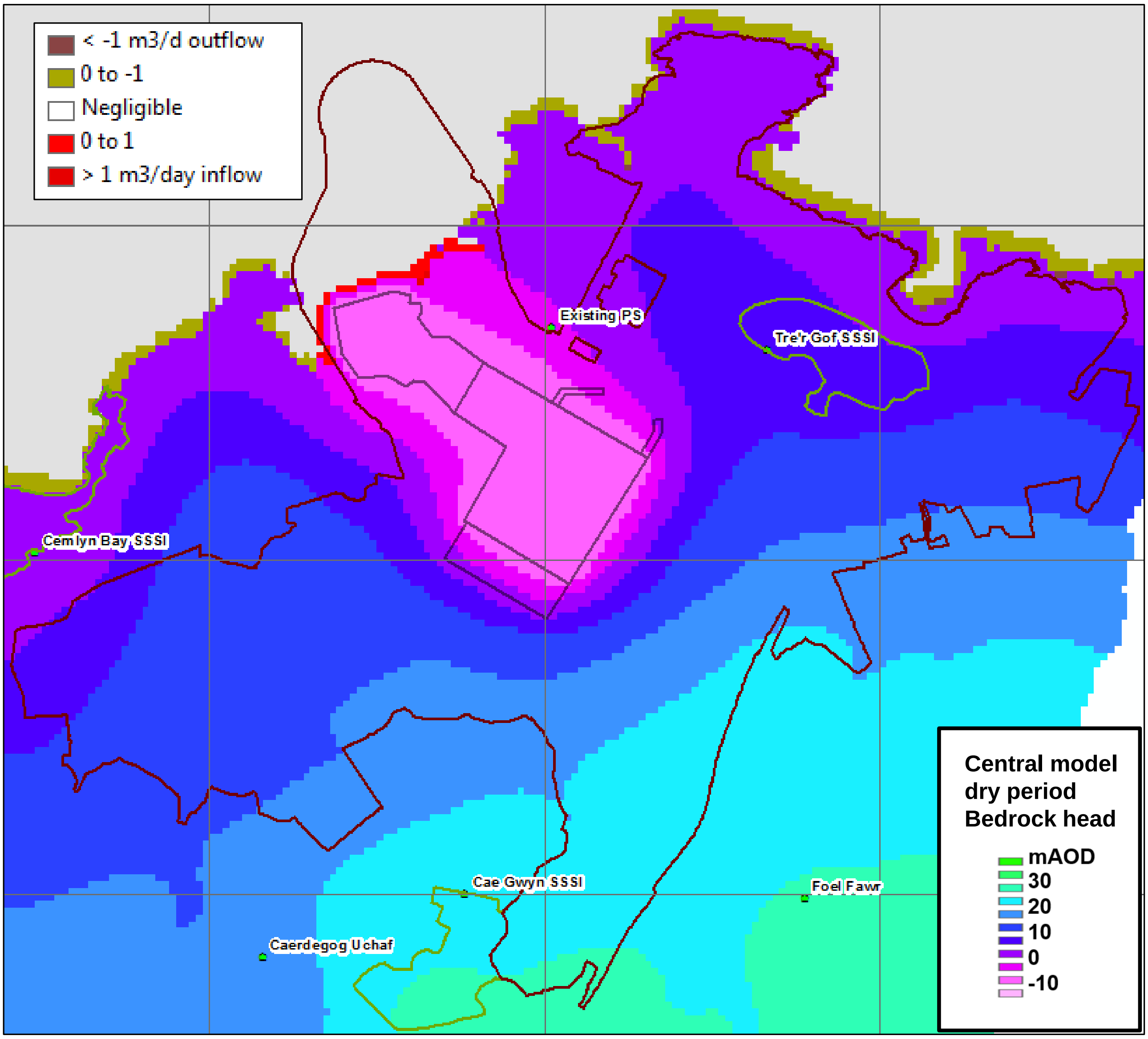

5.6 Reference Point 5 passive drainage from the backfilled excavation

Figure 5.7 shows the location of Reference Point 5 model Drain boundary cells located in the permeable excavation backfill, at the back of the impermeable concrete intake structures, and the dry period groundwater levels simulated by the Central calibration model. These incorporate the impact of the passive drainage on the surrounding bedrock, assuming no shotcreting has been carried out.

There are no Drain boundary cells built into the Baseline or Reference Point 4 construction models.

Figure 5.7 Reference Point 5 passive Drain boundary cells and simulated bedrock groundwater level map (for the dry period, 30 September 1991)

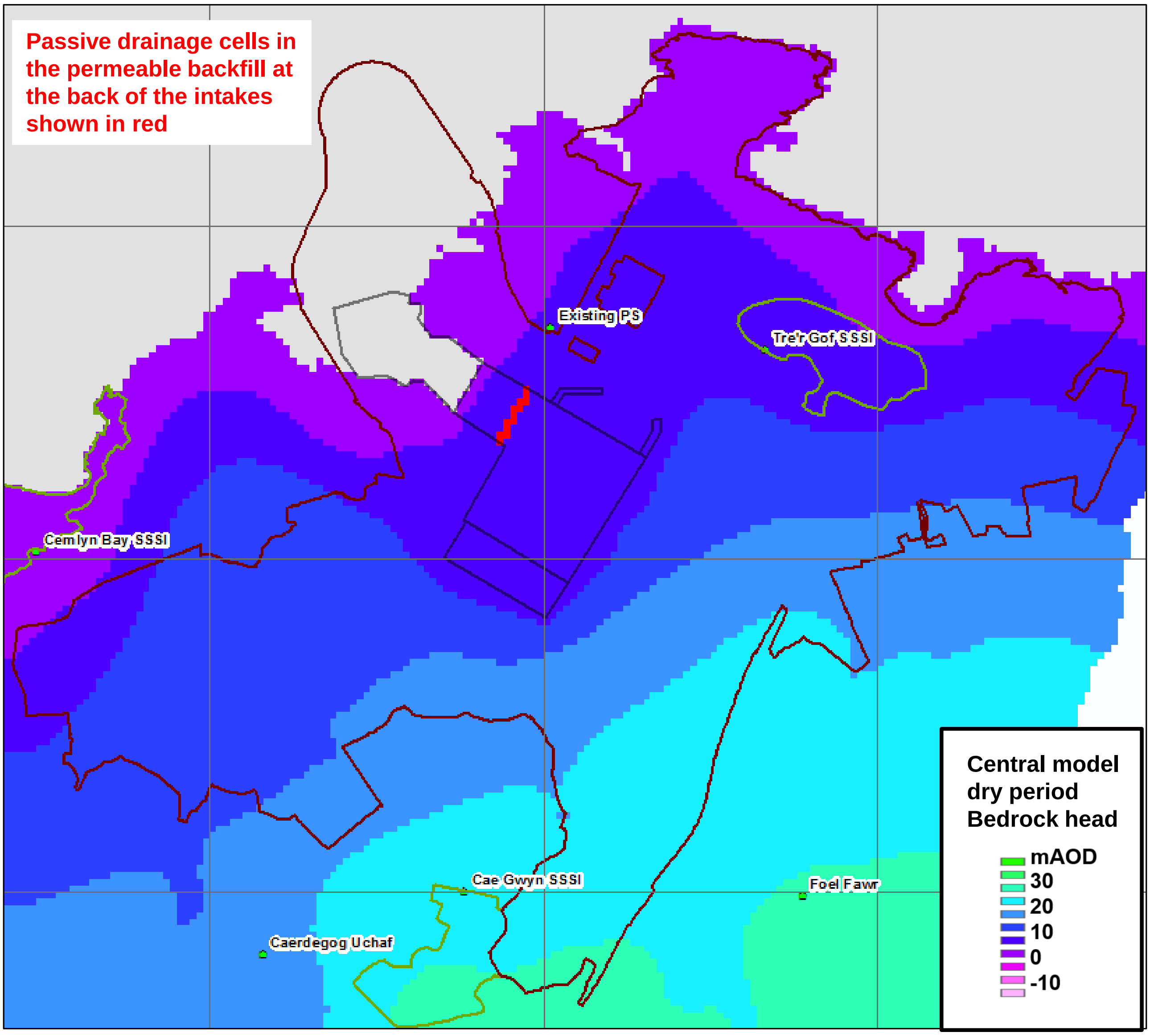

Figure 5.8 plots the flows simulated from the Reference Point 5 model Drain boundary cells mapped in figure 5.7. It is appropriate to ignore the initial 5 years of these results, during which the model is re-equilibrating with the imposition of the Drain boundaries set at 6 m AOD, because Reference Point 5 is a long term operational scenario. After this initial period, drainage predicted by the Central calibration model is typically around 50 to 100 m^3/day and less than 150 m^3/d for most of the time – a combination of inflow from the surrounding bedrock and recharge from the overlying platform area which has been assumed to be 10% permeable (the remaining surface runoff being handled by the drainage system). The previously discussed caveats apply to the predictions of flows from the High bedrock recharge and transmissivity variant model which are roughly twice the Central model rates.

Figure 5.8 Simulated Drain flow time series from the Reference Point 5 backfilled excavation

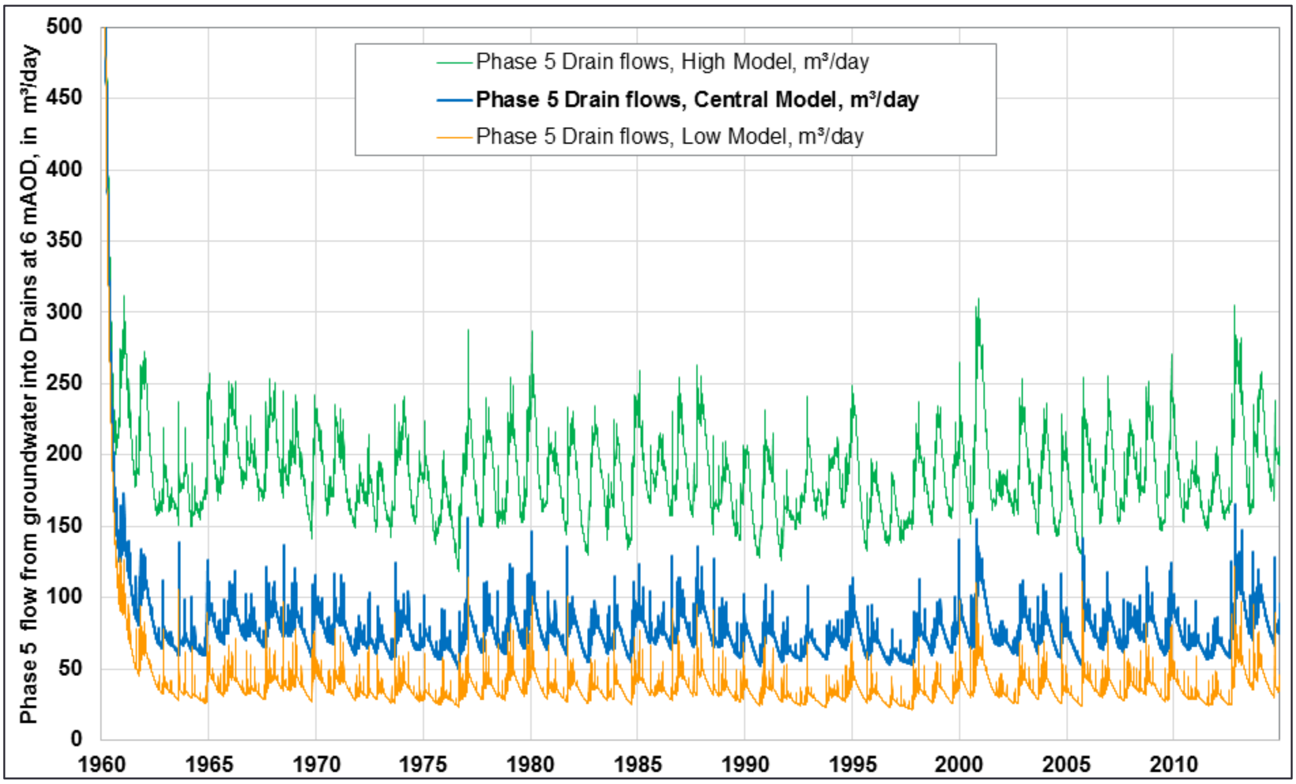

5.7 Surface water receptor flow duration curve impacts

The last set of model predicted impacts sent in digital format to HNP for DCO interpretation focus on the surface water flow receptors where flow regime changes are expected to be dominated by the modified catchments, slopes, land surface characteristics and managed drainage assumptions dealt with in 4R (although bedrock groundwater system impacts simulated in MODFLOW are also incorporated).

The Baseline, Reference Point 4 and Reference Point 5 models are all quasi steady-state, in that they all represent a snapshot at a point in time during the construction schedule extended over the long term. To simulate possible time series of flows in the model area as construction proceeds from one phase to the next, a post-processing spreadsheet tool has been developed which linearly interpolates from one construction phase to the next, and calculates a simulated time series of flows at each point of interest in the catchment as construction proceeds through to completion. The calculations are repeated using rainfall and climate data from three periods in the historical record, representing a relatively “dry” construction period scenario, an “average” scenario and a “wet” scenario (defined according to a 12 year rolling average analysis of hydrologically effective rainfall). The main output from this process is a flow duration curve impact plot which summarises the flow changes experienced through comparison of the long term Baseline and Reference Point 5 time series (the black line on figure 5.8), but also through analysis of flows changing over each of the wet, dry or average 12 year construction periods (the blue, red and green curves respectively). An overall summary of the long-term Reference Point 5 changes in flow, expressed as a percentage of the Baseline flow is provided by the colouring of the x-axis at the bottom of the plot – where red denotes that flows are more than 30 % lower than the Baseline, blue denotes more than 30 % higher than the Baseline etc. This puts the absolute m^3/d flow changes into the context of the Baseline reference condition.

The tool, which is in the form of a macro in an Excel spreadsheet, produces a series of output spreadsheets, each of which includes simulated time series of flows at one of the surface flow receptor cells, and the calculated impact of construction (i.e. scenario flow minus baseline flow) under each of the three climate scenarios. A separate spreadsheet is produced for each point or group of interest. The calculation details may be configured by the reviewer of the spreadsheet so that, for example, different climate periods may be chosen, or assumptions around the durations of the construction phases changed.

Output spreadsheets are named according to the run numbers used as input (i.e. the run numbers corresponding to the Baseline, Reference Point 4 and Reference Point 5 scenarios), and the location for which flows are extracted. Each output spreadsheet contains a number of worksheets, as described in table 5.3.

Table 5.3 Surface water receptor flow duration curve analysis spreadsheet contents

SHEET	CONTENT
QA_content	QA cover sheet
Plots	Main output sheet. Control data, and plots of interpolated flows and impacts, as time series and as flow duration curve summaries. (e.g. figure 5.8 for TG5)
Ref	Reference data: run numbers included in the analysis.
Base	Flow time series from Baseline scenario
Ph4	Flow time series from Reference Point 4 scenario
Ph5	Flow time series from Reference Point 5 scenario
Calcs	Calculation of simulated, interpolated time series of flows under dry, average and wet construction period assumptions
Phase Flows	Plot of simulated flows from each Baseline, Reference Point 4 and Reference Point 5 scenarios (e.g. figure 4.16 for TG3).

The Plots sheet for the Central calibration model predicted flows and impacts at outflow point TG5 are shown in figure 5.9 to illustrate the post-processing approach described. These can be taken as representative of Tre’r Gof as a whole. The managed drainage system in Reference Point 4 includes capture of runoff from the mound to the south east which is discharged onto Tre’r Gof as well as a piped connection from sediment lagoon B1 (figure 5.1) which slightly increases the overall catchment area modelled to the wetland. As a result, the construction period flow duration curve impacts indicate that flows would be generally higher than in the Baseline. The drainage blanket placed under the south-eastern mound is assumed capture and re-route water to inflow points TG3 and TG4 in Reference Point 5 (appendix D, figure 22) but on completion of the works, there will be no managed pipe connections and the drainage from site B1 is assumed to be routed around the platform and into the sea, so there is a small loss in the long-term Reference Point 5 catchment area of ~9% compared with the Baseline. As a result, and in combination with the small loss of bedrock groundwater inputs due to drawdown, the long-term Reference Point 5 flow duration curve is lower than the Baseline by around 10% during lower flow periods (from Q50 down).

Figure 5.9 The Plots sheet illustrating time series and flow duration curve impact analysis processing at TG5, the outflow from Tre'r Gof, from the Central calibration model scenarios

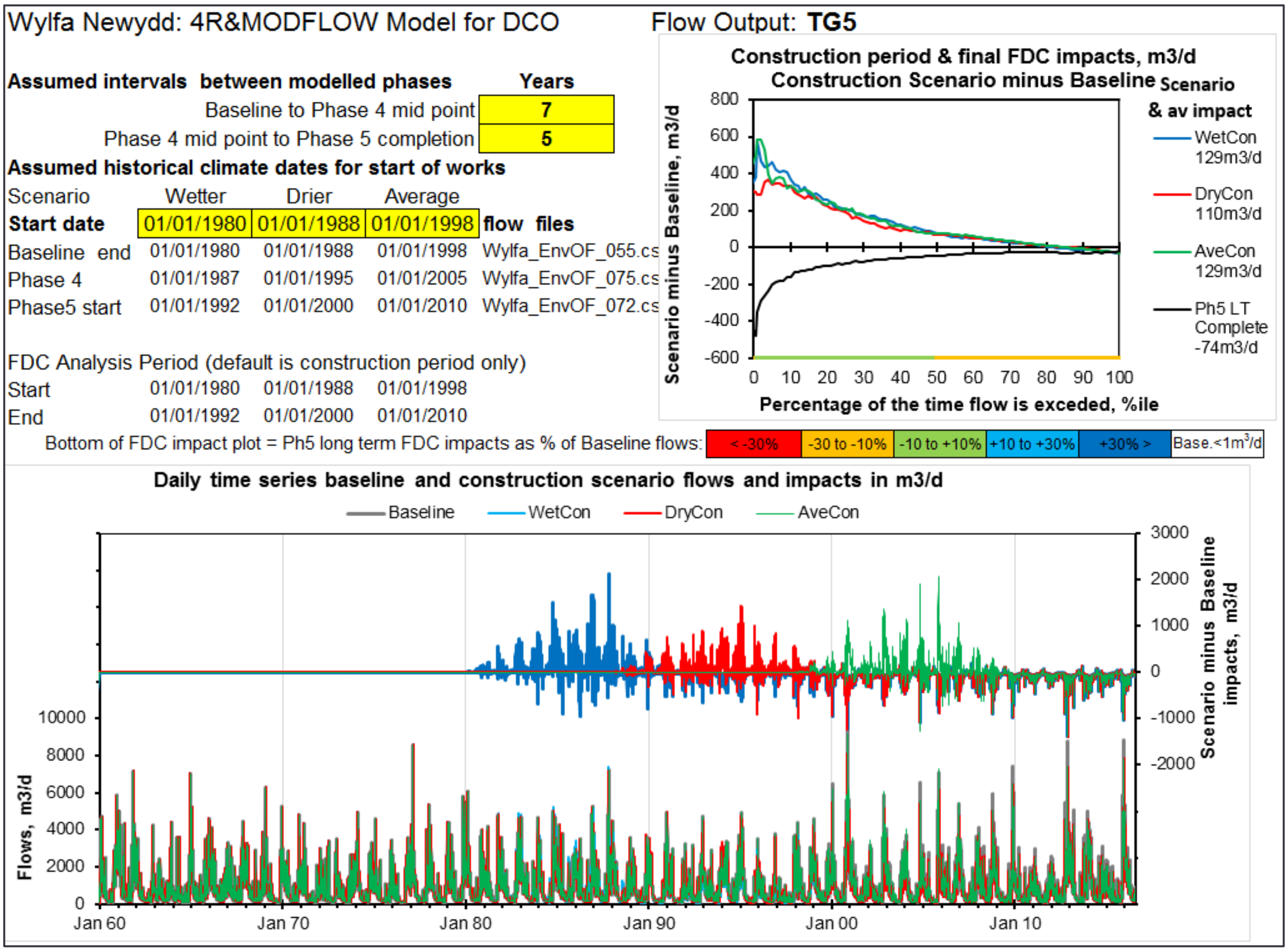

As with the groundwater level drawdown results, complete sets of these flow impact analysis spreadsheets have been generated from the High and Low variant bedrock recharge and sensitivity models, as well as for the most credible Central calibration. To facilitate comparison of these sensitivity predictions, appendix E includes a collation of the flow duration curve impact plots from all three sensitivity models for all the sites. Figure 5.10 illustrates this overview summary format for TG5. The Central model chart is the same as that presented in figure 5.9. The High recharge and transmissivity variant sensitivity model predicted Reference Point 5 impacts would represent a higher proportion of Baseline flows (see colouring on the bottom axis), but the calibration discussion presented in Section 4 suggests this is the least credible of the three models.

Figure 5.10 Example of the appendix E comparison of TG5 flow duration curve impacts plots TG5 based on the Low, Central and High variant recharge and transmissivity sensitivity models

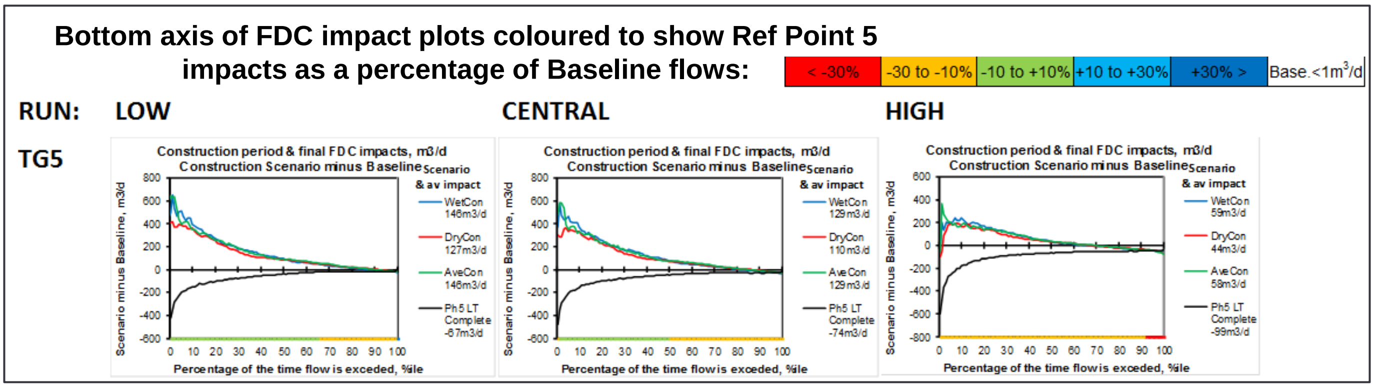

Flow duration curve impact summary plot summaries from the Central model for all of the surface water flow analysis points are mapped alongside each other in the following figures to facilitate interpretation:

- Figure 5.11: Tre'r Gof and Cemaes Stream.
- Figure 5.12: Nant Caerdegog Isaf and Afon Cafnan.
- Figure 5.13: Nant Cemlyn

The impact plots are formatted according to the keys shown in figures 5.9 and 5.10, with the bottom axis coloured according to the black line Reference Point 5 impacts as a percentage of baseline flows.

The maps locate the analysis points which are labelled by the percentage change in 4R model upstream catchment area (100 x [Reference Point 5 area minus Baseline area]/Baseline area), and classified according to the same flow impact colour scheme (e.g. a green point means that the completed upstream surface catchment area is within 10% of the Baseline area). The maps also include the Baseline rivers (light blue lines) and colour flooded elevation indicating the Baseline landform. Comparison with the mapped Reference Point 5 4R routing network and upstream area shows how changes in landform across the Site have been assumed to alter surface drainage directions and catchment areas. The assumed drainage blanket re-routing of runoff from the south east slopes of the mound to the south of Tre'r Gof back to TG3 and TG4 inflows is indicated schematically by orange arrows on figure 4.11, and the location of the backfilled excavation area is included on figure 4.12.

In general, changes in upstream routed surface water catchment area are a clear influence on predicted flow duration curve impacts, combined with less marked reductions in baseflow within these catchments associated with bedrock drawdown.

Figure 5.11 shows the largest losses of surface catchment modelled as draining to Tre'r Gof are at TG1 (28% loss) and TG4 (24% loss). Flow duration curve losses are apparent at these sites, although the lower flow reductions at TG4 are reduced by the slower release of water assumed from the drainage blanket beneath the mound. Although there is no change in the small surface catchment assumed to drain to TG1 from the north west, small losses of bedrock baseflow result in low flow reductions which represent a larger **proportion** of Baseline flows. The impacts plotted at TG5 (and shown on figures 5.9 and 5.10) integrate those mapped at the inflow points: an overall catchment reduction of 9% results in losses across the flow range which combine with bedrock baseflow losses to represent more than 10% of the Baseline lower flow simulation for roughly half of the time. Elsewhere around Tre'r Gof and the Cemaes Stream, Reference Point 5 catchment area and predicted flow changes are within 10% of Baseline. However, shorter term Reference Point 4 flow losses from the Cemaes Stream are predicted because of the management of the drainage network (figure 5.1) to control runoff and sediment releases during the construction period.

Figure 5.11 Central model flow duration curve impacts plots for Tre'r Gof and Cemaes Stream

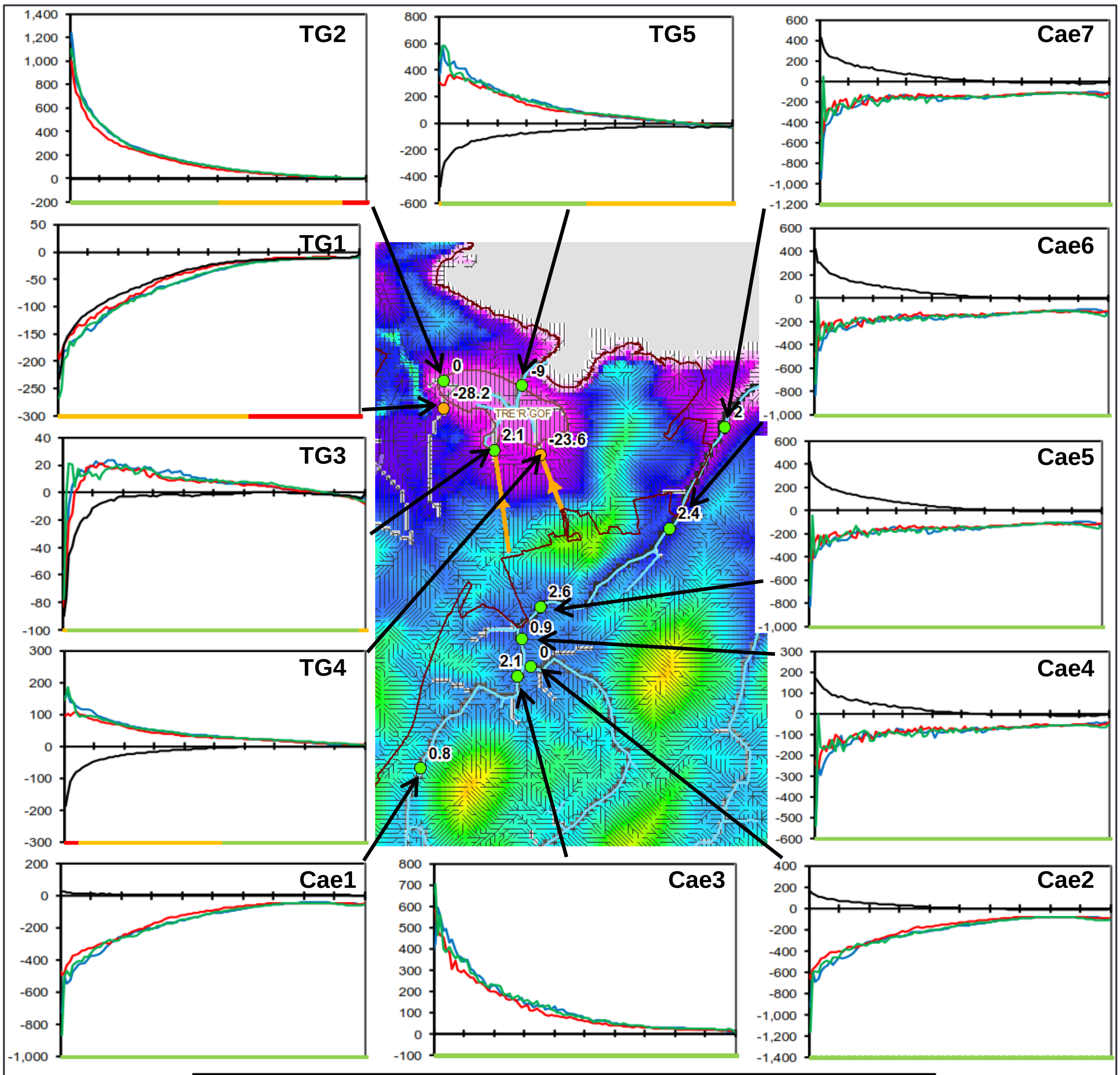

The largest loss of surface catchment is associated with landform changes in the excavation and platform area to the north of the Nant Caerdegog Isaf tributary of the Afon Cafnan, as highlighted by the analysis of flows simulated at Caf4 on figure 5.12. Almost all of the Baseline sub-catchment to Caf4 is lost, which becomes proportionally less marked moving downstream to Caf5 (-33%) and Caf6 (-25%) on the Nant Caerdegog Isaf, and falls to less than 4% on the Afon Cafnan itself. This largely explains the simulated flow duration curve impacts, although there is also an increase in the very small catchment modelled to Caf1 at the headwaters of the Nant Caredegog Isaf.

Figure 5.12 Central model flow duration curve impacts plots for Nant Caerdegog Isaf and Afon Cafnan

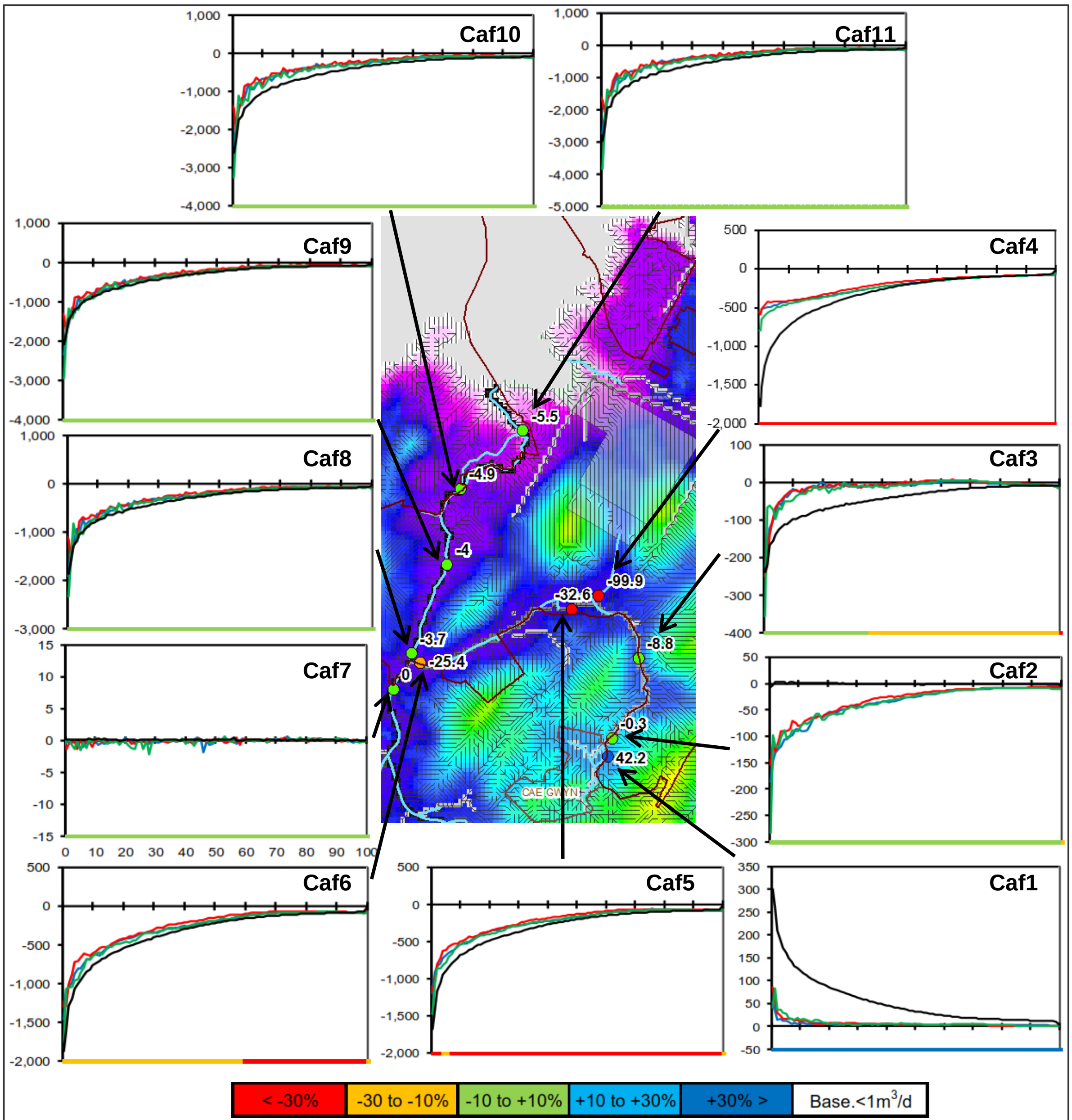

Bottom axis of FDC impact plots coloured to show Ref Point 5 impacts as a percentage of Baseline flows
Map plots Ref Point 5 minus Baseline upstream routed area as % of Baseline area with points labelled as % change, Phase 5 4R routing, and Baseline landform & stream lines

Figure 5.13 Central model flow duration curve impacts plots for Nant Cemlyn

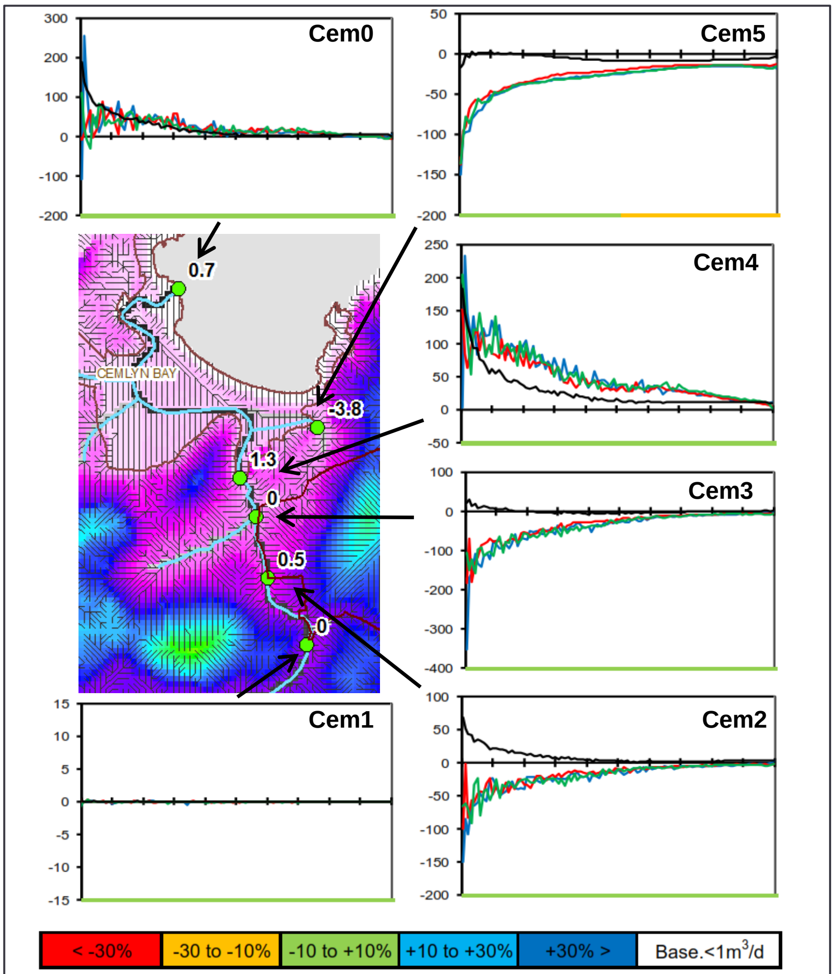

Bottom axis of FDC impact plots coloured to show Ref Point 5 impacts as a percentage of Baseline flows
Map plots Ref Point 5 minus Baseline upstream routed area as % of Baseline area with points labelled as % change, Phase 5 4R routing, and Baseline landform & stream lines

Catchment area and flow changes simulated in the Nant Cemlyn are negligible (figure 5.13), although construction and completion low flow losses represent more than 10% of Baseline predictions at Cem5, located on the small tributary flowing from the east into the Cemlyn lagoon.

5.8 Engineering variant model impact predictions

Engineering variant Reference Point 4 and 5 models

During November/December 2017 a review of more detailed excavation drawings found that the initially modelled extent and depth assumptions remain broadly valid but that there will be locally deeper areas of the excavation floor. An engineering variant of the initial Reference Point 4 model was therefore run to simply incorporate the deeper areas of the excavation which the construction design requires for the intake works (13.5 mAOD) and foundation works (down to -18 mAOD) (as shown in figure 4.14).

At the same time, an engineering variant of the Reference Point 5 model was also built to incorporate the shotcreting of the excavation walls and floor intended to reduce bedrock inflows into the backfill, together with a surrounding perimeter drain to keep groundwater levels below finished ground level

The preceding sections (Sections 5.2 to 5.7) presentation of modelled construction and completion scenario impacts is based on predictions from the initial Reference Point 4 and 5 models (which are the same as presented in the 2017 version of this report). This new section (Section 5.8) provides comparative impacts predicted by the engineering variant model versions (locally deeper excavation Reference Point 4 and shotcreted/perimeter drained Reference Point 5 scenarios). The additional engineering variant models are not intended to reflect the final design exactly but instead to indicate the sensitivity of the groundwater level and surface flow impact predictions to changes in the local depth of the excavation or to engineering completion details.

Bedrock groundwater levels and drawdown impacts

Figure 5.14 maps the dry period bedrock groundwater levels and coastal boundary flows from the Central version of the engineering variant Reference point 4 model including locally deeper excavation.

Figure 5.14 Engineering variant (locally deeper excavation) Reference Point 4 bedrock groundwater levels and simulated General Head Boundary inflows map (for dry period): compare with figure 5.6

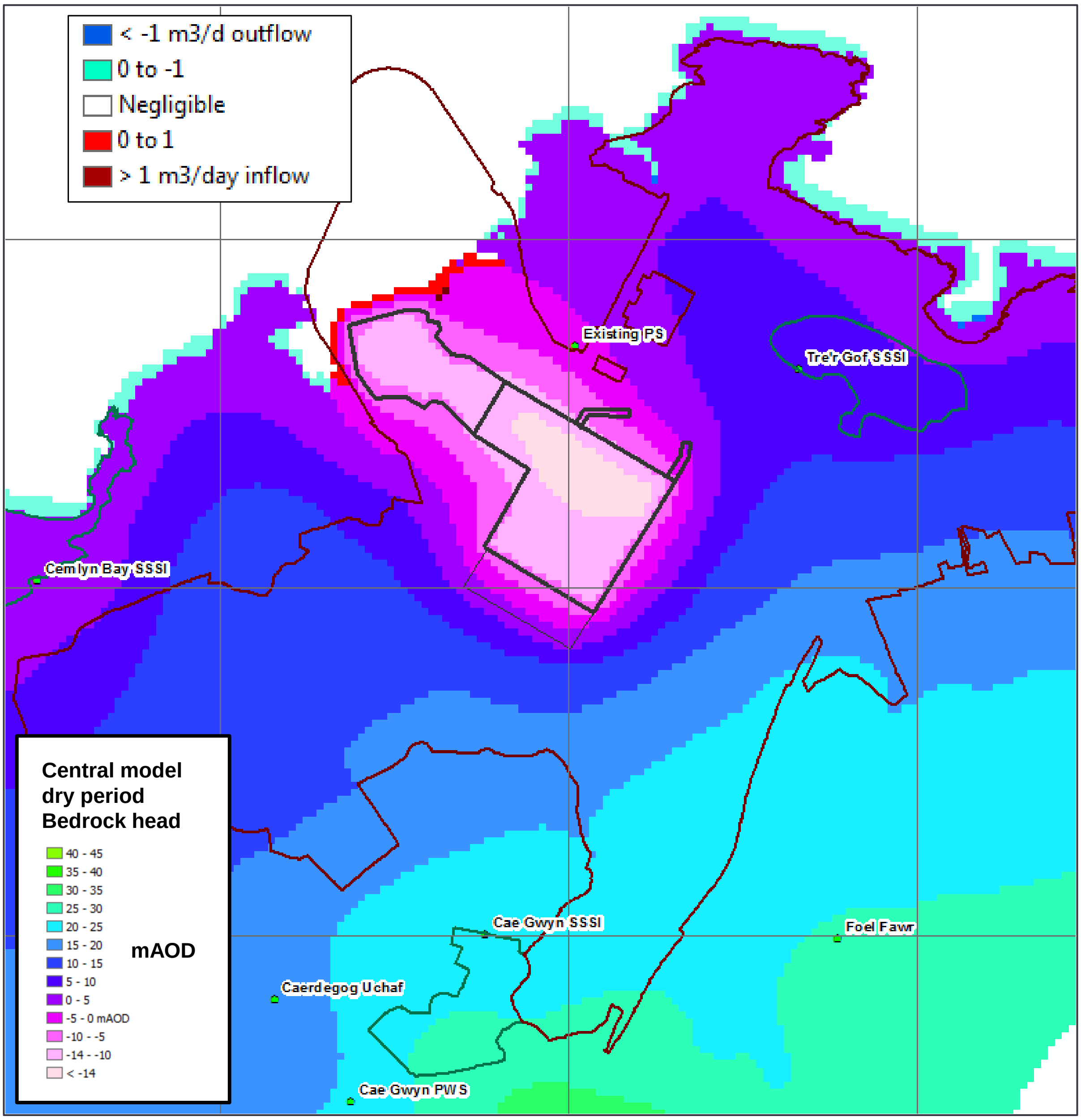

Simulated bedrock groundwater levels in the excavation area are clearly lower than in the equivalent figure 5.6 due to the deeper dewatering assumed for the intake and foundation construction works.

Figure 5,15 shows the bedrock groundwater levels predicted from the engineering variant Reference Point 5 model which assumes the excavation will be shotcreted before backfilling, and also incorporates a perimeter drain around the excavation set at an elevation 2 m below ground level, or at sea level if that is higher (i.e. adjacent to the coast). In some areas the reduced bedrock groundwater inflow to the backfill has resulted in higher groundwater levels outside it, but in other places the perimeter drain lowers groundwater levels in comparison with the initial model assumptions (compare figure 5.15 with figure 5.7).

Figure 5.15 Engineering variant (shotcreted excavation and outer perimeter drain) Reference Point 5 bedrock groundwater levels map (for dry period 30 September 1991): compare with figure 5.7

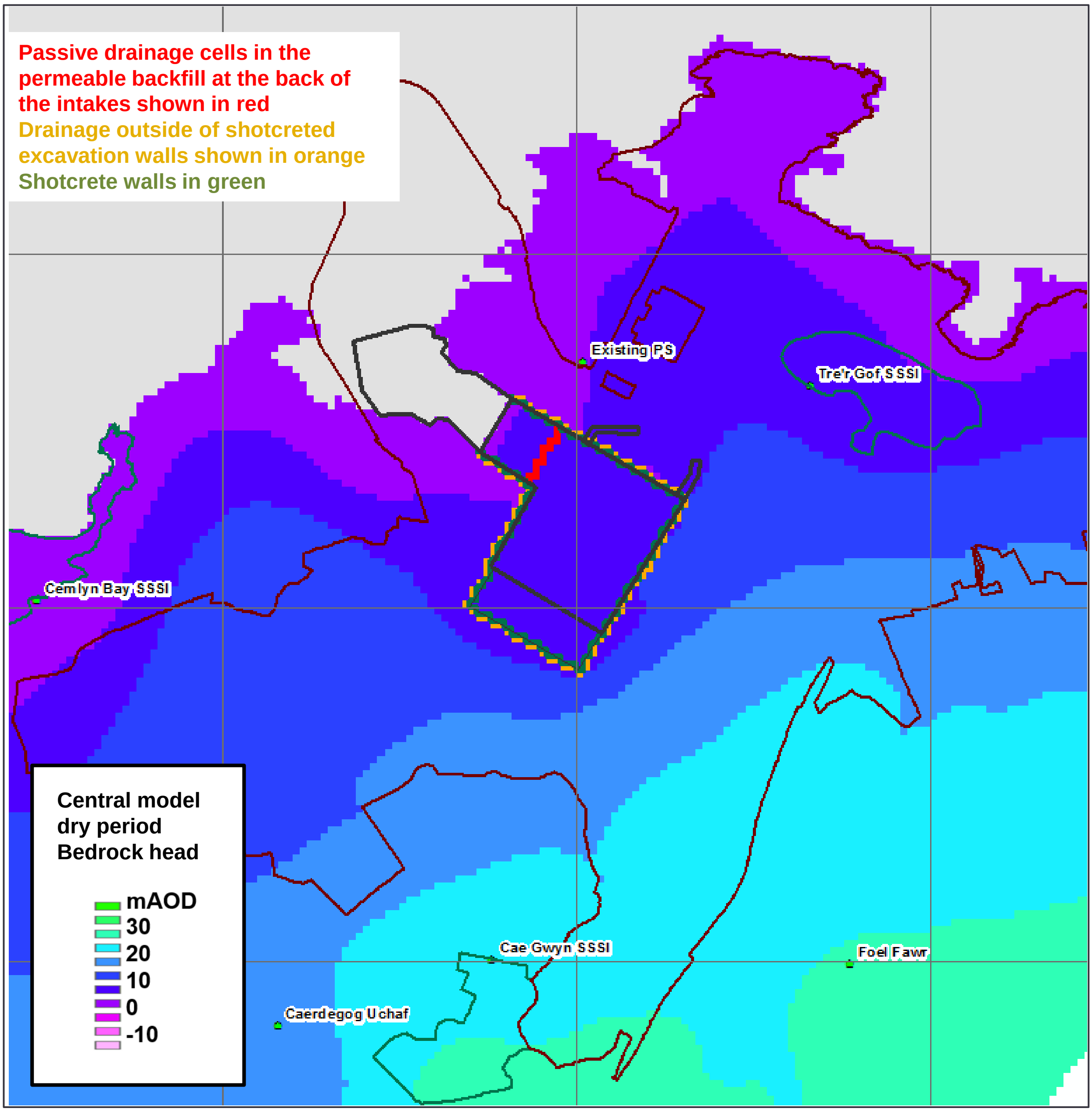

To facilitate more direct comparison of groundwater level impacts, figure 5.16 shows both initial and locally deeper engineering variant Reference Point 4 model dry period drawdown relative to the Baseline.

Figure 5.16 Comparison of initial and engineering variant (locally deeper excavation) maps of Reference Point 4 bedrock groundwater level drawdown relative to the Baseline from the Central parameter model (for dry period 30 September 1991)

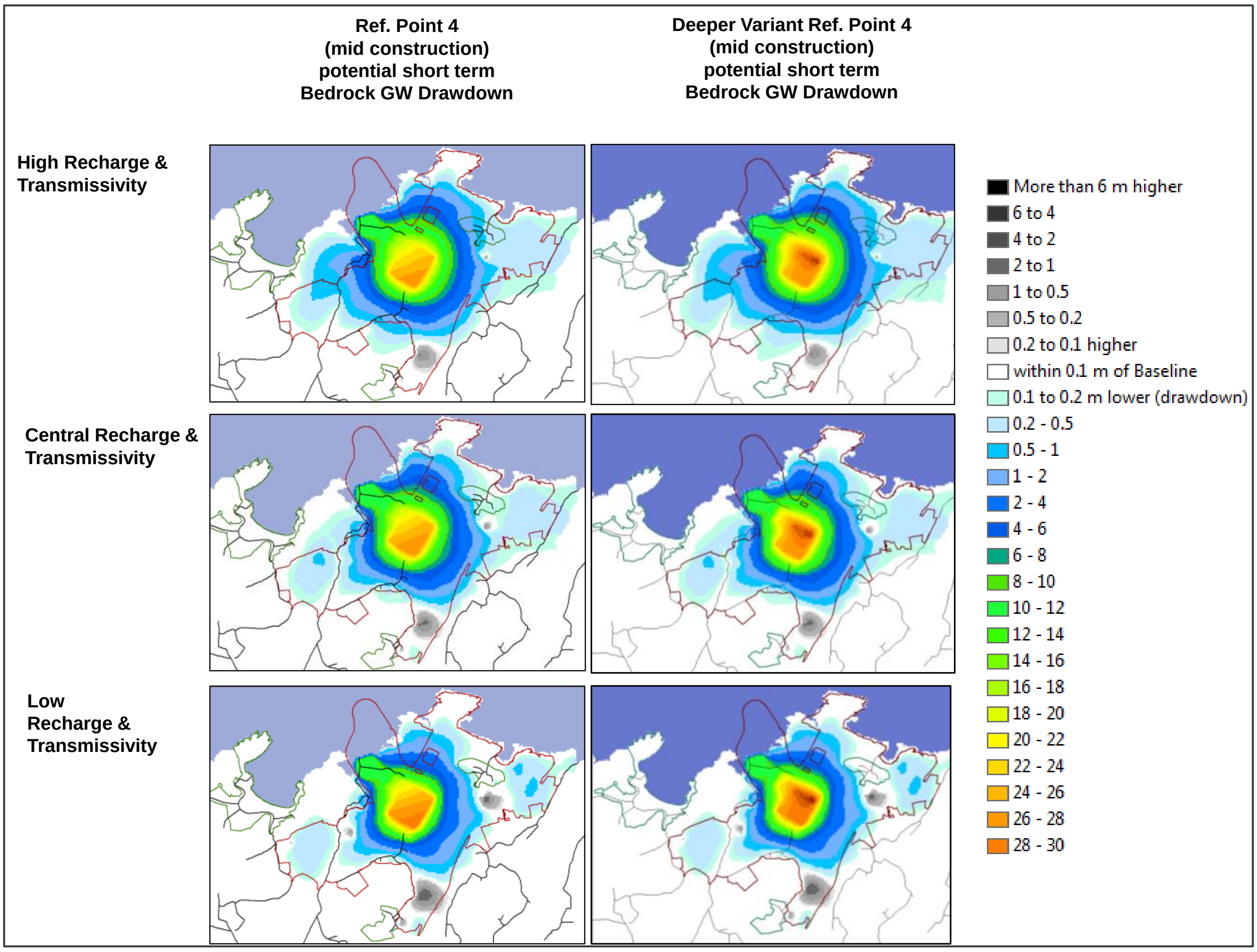

The additional drawdown is clearly apparent in the deeper excavation areas, but the magnitude and patterns of predicted groundwater level impacts are otherwise very similar.

Figure 5.17 Comparison of initial and engineering variant (shotcreted and outer perimeter drain) maps of Reference Point 5 bedrock groundwater level drawdown relative to the Baseline from the Central parameter model (for dry period 30 September 1991)

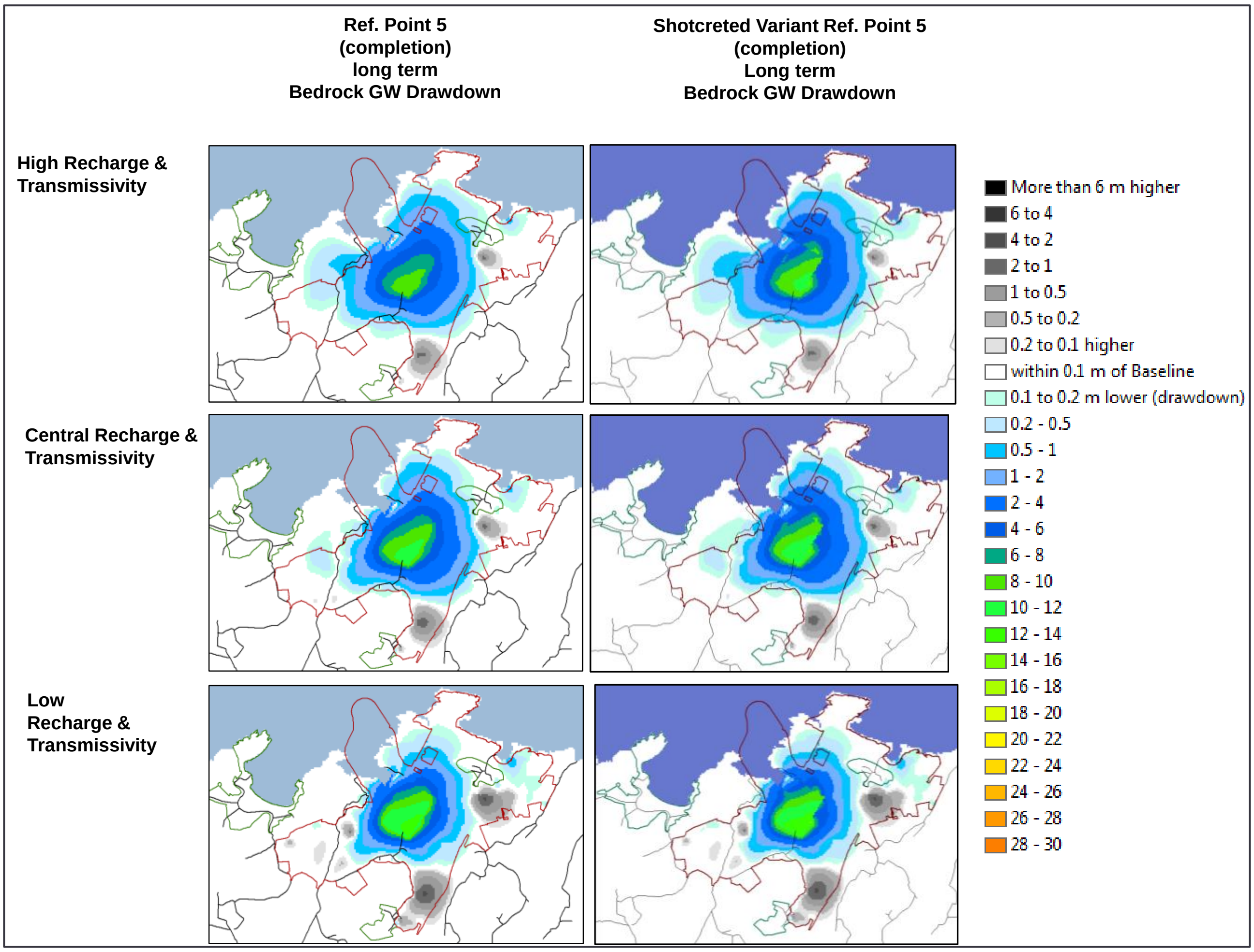

Figure 5.17 is a similar drawdown comparison for the initial and engineering variant Reference Point 5 models. The drawdown consequence of the engineering variant combination of shotcreted groundwater inflow barrier varies in the bedrock around the margins of the excavation. Where the completed ground level next to the platform is close to or below the Baseline topography, the influence of the perimeter drain in pulling surrounding bedrock levels down, outweighs the recovery due to reduced groundwater inflows into the backfilled excavation. The inclusion of a perimeter drain around the impermeable intake works next to the coast also results in more drawdown. Within the backfill itself, the reduced inflow from groundwater means that drawdown is also greater in the shotcreted model, although it is important to acknowledge that, as an excavated, effectively sealed and backfilled ‘box’, the area beneath the platform should no longer be considered part of the bedrock groundwater body flow system. Outside the eastern corner of the backfilled excavation, reduced groundwater inflows due to the shorcreted barrier result in slightly higher bedrock groundwater levels (i.e. reduced drawdown) because perimeter drain elevations are relatively higher.

Groundwater receptor site and SSSI predictions of bedrock groundwater level and flow impact predictions

Table 5.4 lists the groundwater levels and drawdown at the receptor locations for the engineering variant models.

Table 5.4 Simulated bedrock groundwater levels and drawdown at receptor cells based on engineering variant models: compare with table 5.1

Dry period = 30/9/91, Wet period = 31/12/2000	All bedrock head elevations in m AOD		Recharge and Transmissivity Sensitivity Models					
			Central		Low		High	
Scenario	Groundwater receptor cell	Model Cell Row_Col	Dry	Wet	Dry	Wet	Dry	Wet
Baseline	Caerdegog Uchaf private supply	150_133	17.67	18.43	18.02	18.94	17.58	18.24
	Foel Fawr private supply	141_214	25.37	26.79	26.36	28.06	25.35	26.18
	Cae Gwyn PWS	164_144	20.98	21.19	20.92	21.14	20.96	21.25
	Existing Power Station	56_177	7.70	9.96	8.97	11.52	6.57	9.20
	Nearest Magnox potentially susceptible building*	41_182	5.28	7.20	7.89	8.50	3.16	6.45
	Tre'r Gof SSSI	59_209	7.64	8.98	7.27	8.10	8.15	9.97
	Cae Gwyn SSSI	140_164	22.48	22.94	22.71	23.26	22.21	22.77
	Cemlyn Bay SSSI	89_99	1.78	1.88	1.75	1.90	1.74	1.79
Ref Point 4 (Deeper Variant)	Caerdegog Uchaf private supply	150_134	17.66	18.42	18.01	18.93	17.55	18.21
	Foel Fawr private supply	141_215	25.36	26.78	26.36	28.05	25.30	26.18
	Cae Gwyn PWS	164_145	20.97	21.19	20.91	21.13	20.95	21.27
	Existing Power Station	56_178	-2.01	5.09	2.85	8.89	-4.64	1.14
	Nearest Magnox potentially susceptible building*	41_182	2.19	5.78	6.60	7.47	0.08	4.60
	Tre'r Gof SSSI	59_210	6.74	8.46	6.88	7.72	6.13	9.12
	Cae Gwyn SSSI	140_165	22.47	22.94	22.70	23.27	22.17	22.79
	Cemlyn Bay SSSI	89_100	1.78	1.88	1.75	1.90	1.74	1.78
Ref Point 5 (Shotcreted Variant)	Caerdegog Uchaf private supply	150_135	17.66	18.42	18.01	18.93	17.56	18.21
	Foel Fawr private supply	141_216	25.36	26.78	26.36	28.05	25.31	26.18
	Cae Gwyn PWS	164_146	20.97	21.19	20.91	21.13	20.95	21.27
	Existing Power Station	56_179	4.96	8.65	7.47	10.61	3.17	6.92
	Nearest Magnox potentially susceptible building*	41_182	4.31	6.61	7.61	8.11	2.02	5.79
	Tre'r Gof SSSI	59_211	7.21	8.89	7.13	8.02	7.34	9.67
	Cae Gwyn SSSI	140_166	22.47	22.94	22.70	23.27	22.20	22.80
	Cemlyn Bay SSSI	89_101	1.78	1.87	1.75	1.89	1.74	1.78

* NB the model does not include parameters representing any sub-surface structures beneath the Magnox buildings.

Dry period = 30/9/91, Wet period = 31/12/2000	All bedrock drawdown in metres (Baseline - Scenario)		Recharge and Transmissivity Sensitivity Models					
			Central		Low		High	
Scenario	Groundwater receptor cell	Model Cell Row_Col	Dry	Wet	Dry	Wet	Dry	Wet
Ref Point 4 (Deeper Variant)	Caerdegog Uchaf private supply	150_134	0.01	0.02	0.01	0.01	0.03	0.03
	Foel Fawr private supply	141_215	0.01	0.02	0.00	0.01	0.05	-0.01
	Cae Gwyn PWS	164_145	0.01	0.00	0.01	0.01	0.01	-0.02
	Existing Power Station	56_178	9.71	4.86	6.12	2.64	11.20	8.06
	Nearest Magnox potentially susceptible building*	41_182	3.09	1.42	1.29	1.02	3.08	1.85
	Tre'r Gof SSSI	59_210	0.89	0.52	0.40	0.38	2.02	0.85
	Cae Gwyn SSSI	140_165	0.02	0.00	0.01	0.00	0.04	-0.02
	Cemlyn Bay SSSI	89_100	0.00	0.00	0.00	0.00	0.00	0.00
Ref Point 5 (Shotcreted Variant)	Caerdegog Uchaf private supply	150_135	0.01	0.02	0.01	0.01	0.03	0.03
	Foel Fawr private supply	141_216	0.01	0.02	0.00	0.01	0.04	-0.01
	Cae Gwyn PWS	164_146	0.01	0.00	0.01	0.01	0.01	-0.02
	Existing Power Station	56_179	2.74	1.30	1.50	0.91	3.39	2.28
	Nearest Magnox potentially susceptible building*	41_182	0.97	0.58	0.28	0.39	1.14	0.66
	Tre'r Gof SSSI	59_211	0.43	0.09	0.15	0.08	0.81	0.30
	Cae Gwyn SSSI	140_166	0.01	-0.01	0.00	0.00	0.01	-0.03
	Cemlyn Bay SSSI	89_101	0.00	0.01	0.00	0.00	0.00	0.00

Comparison with table 5.1 shows that predicted groundwater levels from the engineering variant models are within 1 cm of the initial scenario models at all the receptor analysis points except for the Existing Power Station, and the Tre'r Gof cell. At the Existing Power Station, close to the excavation, the deeper intake works, and the perimeter drain built into the Reference Point 4 and 5 variant models respectively increase the predicted drawdown (by around 0.8 and 1.0 m respectively for the Central model dry period).

At the Tre'r Gof cell the changes in predicted groundwater level are much smaller – the deeper excavation results in only 2 cm more drawdown during construction, and the shotcreting/perimeter drain assumptions cause operational dry period levels to be 3 cm higher.

Comparison of predicted groundwater inflows to SSSI receptors from the engineering variant models (table 5.5) with the equivalent predictions from the initial models (table 5.2) shows the only apparent change to be a small reduction in Reference Point 4 simulated inflows to Tre'r Gof (e.g. 1 m^3/d for the Central model during the dry period) associated with locally deepening the floor of the excavation.

Table 5.5 Simulated bedrock groundwater discharges to SSSI receptors and differences predicted between scenarios, based on engineering variant models: compare with table 5.2

Dry period = 30/9/91, Wet period = 31/12/2000		Recharge and Transmissivity Sensitivity Models					
Bedrock GW to SW flows across the SSSIs in m^3/d		Central		Low		High	
Scenario	**SSSI Area**	**Dry**	**Wet**	**Dry**	**Wet**	**Dry**	**Wet**
Baseline	Tre'r Gof SSSI	17.1	37.3	7.1	14.0	36.7	83.0
	Cae Gwyn SSSI	10.4	55.2	4.0	10.7	12.4	70.7
	Cemlyn Bay SSSI	81.6	170.2	24.5	47.4	188.2	364.0
Ref Point 4 (Deeper Variant)	Tre'r Gof SSSI	9.3	32.8	6.0	13.4	10.8	76.0
	Cae Gwyn SSSI	9.7	53.0	3.7	10.5	11.3	64.9
	Cemlyn Bay SSSI	81.5	170.1	24.5	47.4	187.0	363.8
Ref Point 5 (Shotcreted Variant)	Tre'r Gof SSSI	14.5	37.6	6.8	13.9	27.5	85.0
	Cae Gwyn SSSI	9.1	52.0	3.6	10.3	11.8	63.2
	Cemlyn Bay SSSI	81.6	170.0	24.5	47.4	187.5	363.7

Dry period = 30/9/91, Wet period = 31/12/2000		Recharge and Transmissivity Sensitivity Models					
GW to SW flow changes in m3/d (Scenario - Baseline)		Central		Low		High	
Scenario	**SSSI Area**	**Dry**	**Wet**	**Dry**	**Wet**	**Dry**	**Wet**
Ref Point 4 (Deeper Variant)	Tre'r Gof SSSI	-7.8	-4.5	-1.0	-0.7	-25.9	-7.1
	Cae Gwyn SSSI	-0.7	-2.2	-0.2	-0.3	-1.1	-5.9
	Cemlyn Bay SSSI	-0.1	-0.1	0.0	0.0	-1.2	-0.2
Ref Point 5 (Shotcreted Variant)	Tre'r Gof SSSI	-2.6	0.2	-0.3	-0.1	-9.2	2.0
	Cae Gwyn SSSI	-1.3	-3.2	-0.4	-0.4	-0.6	-7.5
	Cemlyn Bay SSSI	-0.1	-0.2	0.0	0.0	-0.7	-0.3

Dewatering, coastal boundary and drainage flow time series predictions

Figure 5.18 shows, in comparison with figure 5.2, that locally deepening inland areas of the modelled Reference Point 4 excavation is predicted to result in small increases in the rates of bedrock inflows which would need to be pumped out for dry working in the short term. The average increase predicted for the inland area by the Central model is only 10 m3/d (from 121 to 131 m^3/d on average) which remains negligible in the context of total dewatering requirements of up to 6 Ml/d dominated by rainfall.

Figure 5.18 Simulated dewatering rates from the engineering variant (locally deeper excavation) Reference Point 4 models inland and seaward excavations: compare with figure 5.2

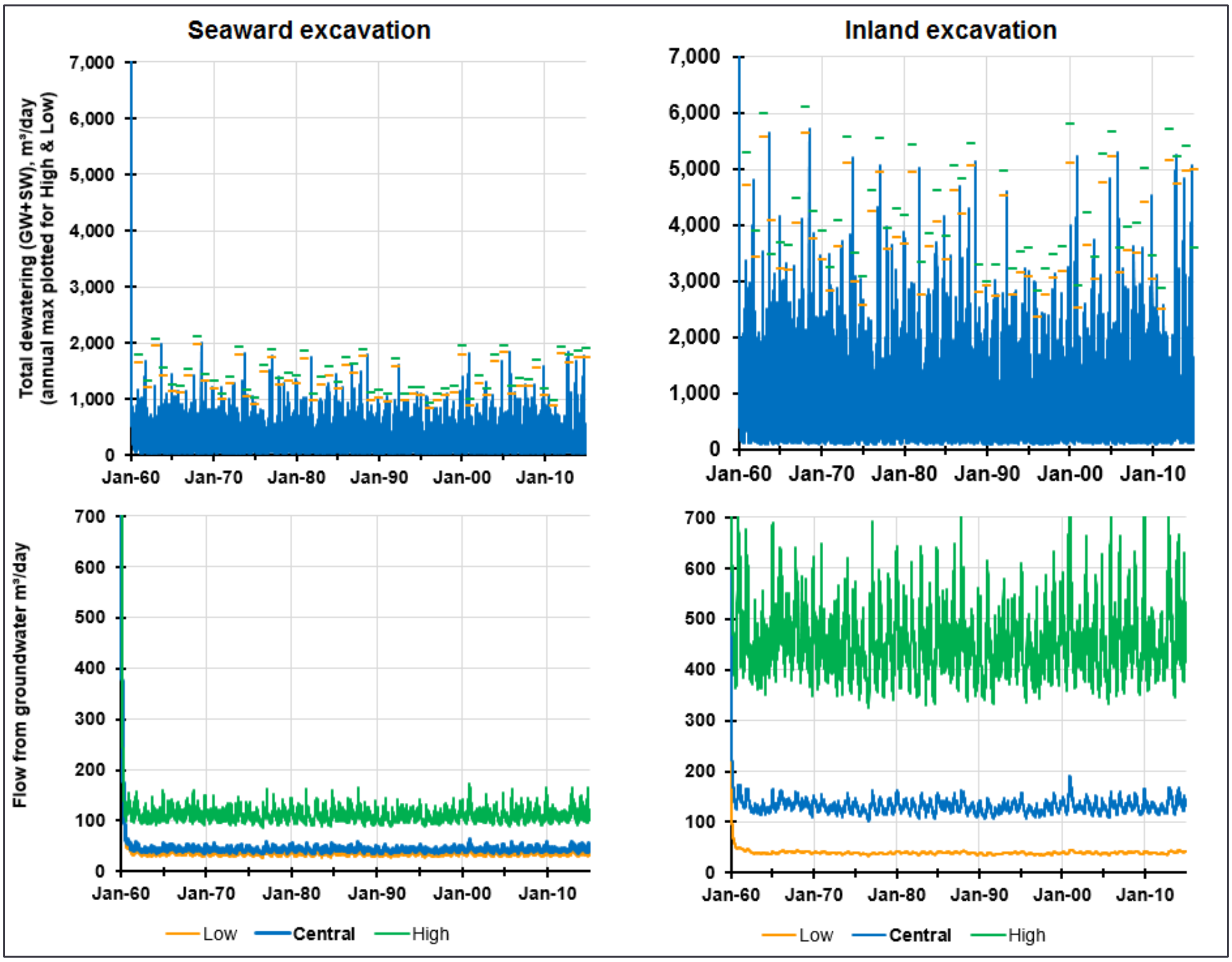

Comparison of figure 5.19 with figure 5.5 shows that changes in the predicted Reference Point 4 General Head Boundary inflows simulated around the coffer dam and coast adjacent to the excavation are negligible. Deepening the excavation for the construction of the intake works can be expected to cause some ingress of poorer quality bedrock groundwater from the seaward bedrock and inland movement of the saline interface but this volume is effectively being removed from the bedrock groundwater body and being replaced by concrete. The additional drawdown simulated in the centre of the deepened areas of the excavation (figures 5.14 and 5.16) could also be associated with changes in local groundwater quality but these should not make any material difference to environmental outcomes because these volumes will be concreted with for foundation and intake works, within the backfilled excavation, beneath the platform of the operational site.

Figure 5.19 Simulated General Head Boundary inflow time series from the engineering variant (locally deeper excavation) Reference Point 4 models: compare with figure 5.5

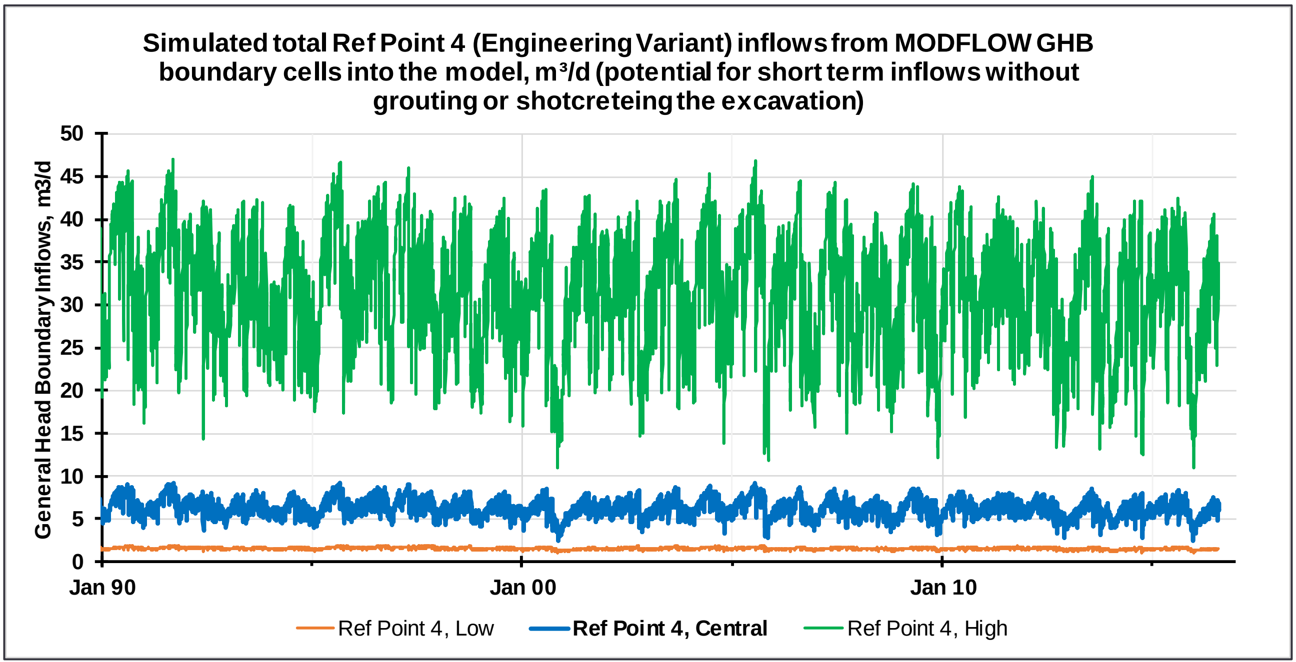

The shotcreting of the excavation walls and floor assumed for the engineering variant Reference Point 5 model greatly reduces the time series of Drain cell flows out of the backfilled excavation (figure 5.20 compared with figure 5.8). If the excavation walls and floor are effectively sealed, only recharge through permeable areas of the overlying platform (assumed to be 10 % of the area) would need to be drained from the backfill.

Figure 5.20 Simulated Drain flow time series from the engineering variant (shotcreted) Reference Point 5 models backfilled excavation: compare with figure 5.8

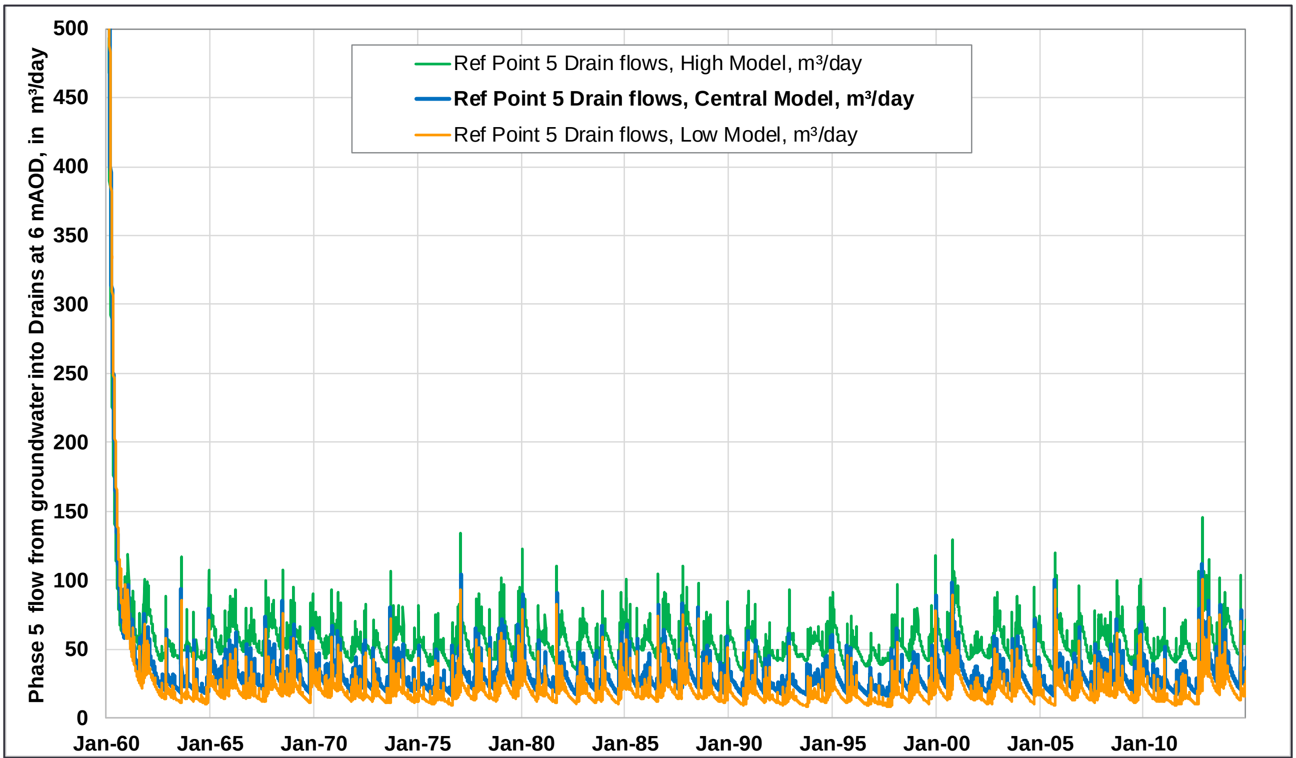

Surface flow duration curve impact predictions

A full set of the flow duration curve impact analysis spreadsheets derived from the engineering variant Reference Point 4 and 5 models are provided digitally with this report, as listed in Appendix F, which can be viewed alongside the initial model versions. However, figure 5.21 demonstrates that these changes in the assumed local depth of the excavation and in the details of completion below ground level make very little difference to the simulated flow duration curve impacts. The patterns of predicted surface flow changes remain very close to those presented in figures 5.11 to 5.13, as described in Section 5.7.

Figure 5.21 Comparison of flow duration curve impact analysis plots for Tre'r Gof outflow point TG5 from the Central parameter initial and engineering variant models

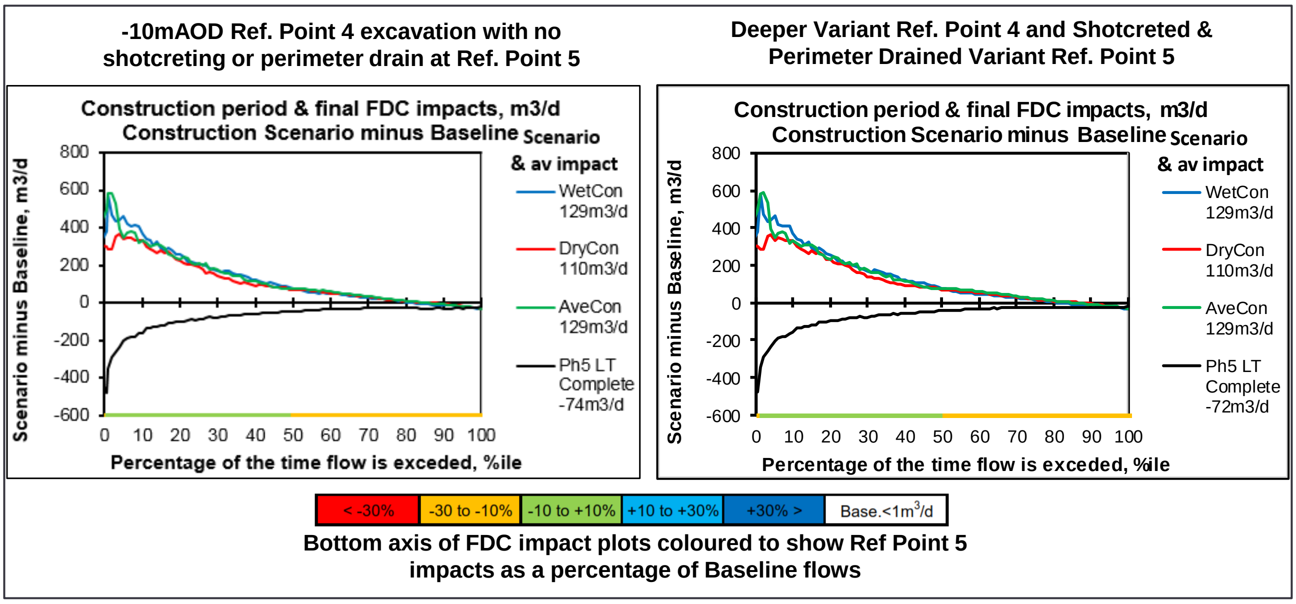

6. Summary

The Wylfa-Newydd 4R and MODFLOW modelling work has provided a set of three sensitivity models (representing Central calibration, Low and High variants of bedrock recharge and transmissivity). These have been applied to an historical calibration simulation, and have been run for each of the Baseline (present day), Reference Point 4 (Construction) and Reference Point 5 (completion/operation) predictive scenarios. Figure 6.1 provides schematic cross sections of these modelled reference points together with maps of the ground elevation differences from the baseline model.

Figure 6.1 Baseline, Reference Points 4 (construction) and 5 (completion) schematic cross sections, and maps of ground elevation differences

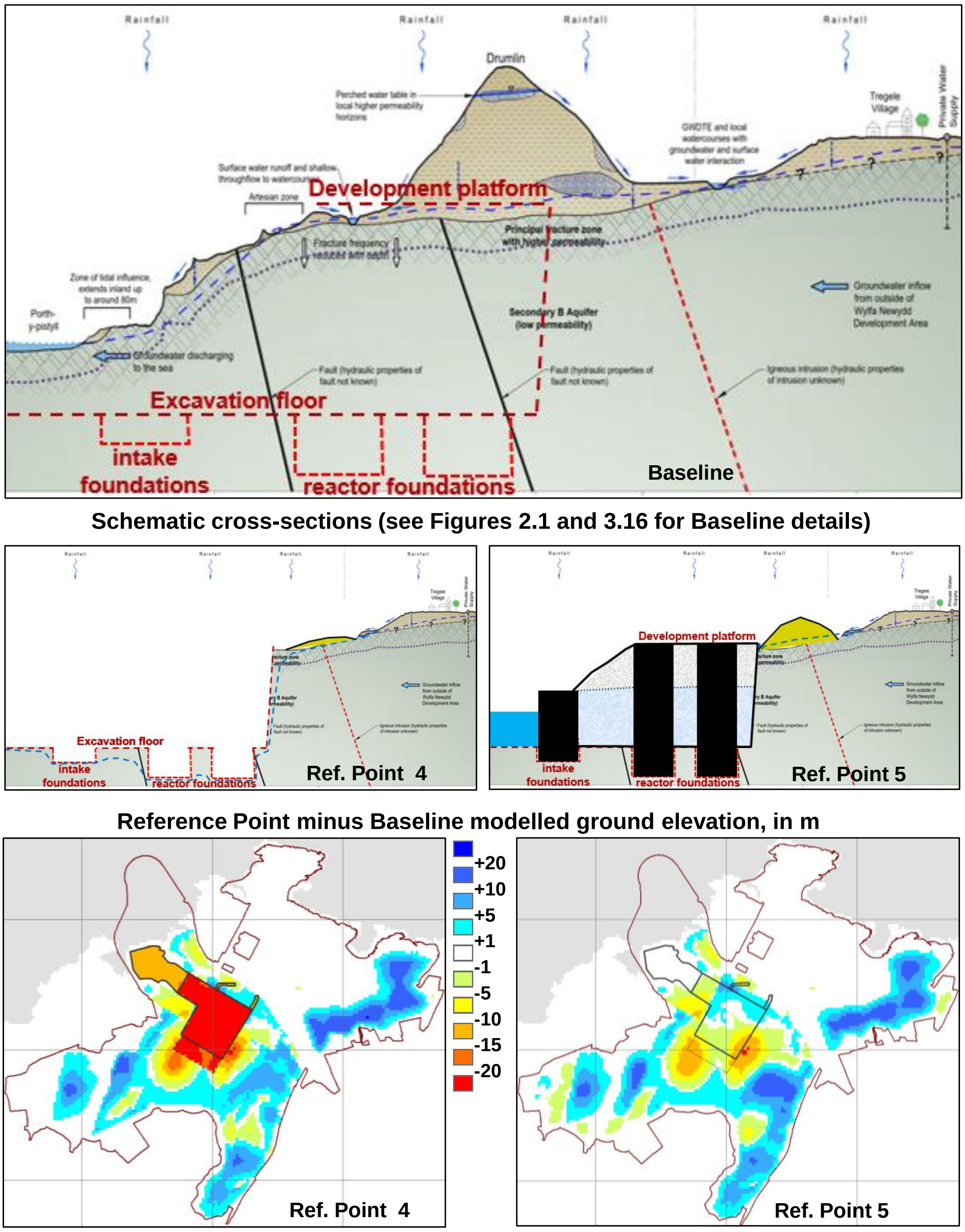

These models represent the different aspects of surface, shallow drainage and bedrock groundwater pressure changes associated with each phase: topography changes, soil stripping, landscape mounds, toe drains, sediment lagoons and changes in land use, bedrock excavation and dewatering.

The Central calibration model is a credible representation of the conceptual understanding of the Site hydrogeology which simulates bedrock heads and surface flows which are a reasonable match much of the available data. The High and Low variant sensitivity models fit less well but acknowledge the uncertainties in the proportions of water flowing through the Drift and the bedrock and provide a bracketed range of predicted outputs around the most likely Central model results.

Engineering variant models have also been run to consider the changes in predicted impacts associated with locally deepening of the Reference Point 4 excavation, and the use of shotcrete to seal it before backfill for Reference Point 5.

Predicted flows, groundwater levels and impacts from the modelling have been presented in a set of appendices and explained through illustrative figures and text within the report. Digital outputs have been transferred to HNP for interpretation associated with the DCO submission.

7. References

Allen, R.G., Pereira, L.S., Raes, D., and Smith, M., 1998. Crop evaporation – Guidelines for computing crop water requirements – FAO Irrigation and drainage paper 56. Food and Agricultural Organisation of the United Nations, Rome, 1998.

Amec Foster Wheeler, July 2015. Wylfa Newydd Nuclear Safety, Meteorological and Hydrological Hazards Assessment (NSMHHA) Report 200383-000-000-RPT-0003 Revision 5 issue 3

Heathcote, J. A., Lewis, R. T. and Soley, R. W, N., 2004. Rainfall routing to runoff and recharge for regional groundwater models. Quarterly Journal of Engineering Geology and Hydrogeology, **37**, 113-130.

Horizon, 2017, Tre'r Gof Hydroecological Assessment, Ref WN034-JAC-PAC-REP-00047 (appendix B8.05 to the Environmental Statement)

Jacobs, 2016, Wylfa Newydd Project, Consultancy Report: Wylfa Newydd Development Area Hydrogeology Baseline for the Wylfa Newydd Project. Updated in January 2018.

Jacobs, 2017, Wylfa Newydd Development, Cae Gwyn SSSI Hydroecological Assessment, Ref WN034-JAC-PAC-REP-00170 (appendix B8.06 to the Environmental Statement)

Appendix A
Borehole hydro-test data

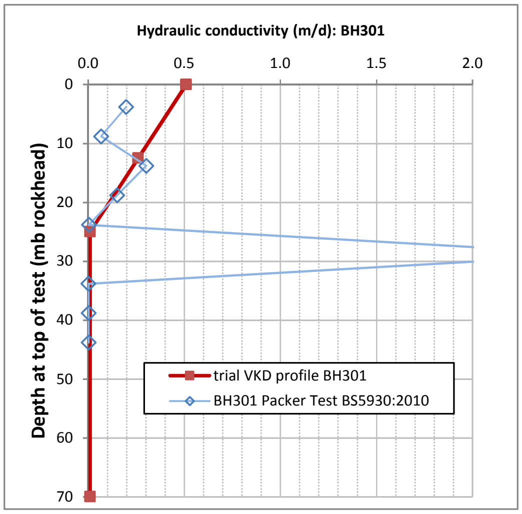

Estimated Estimated profile properties	
kbase (m/d)	0.01
kslope (m/d/m)	0.02
kmax (m/d)	3
inflection point (m)	25
depth at which kmax reached (m)	n/a
saturated transmissivity (m^2/d)	6.95

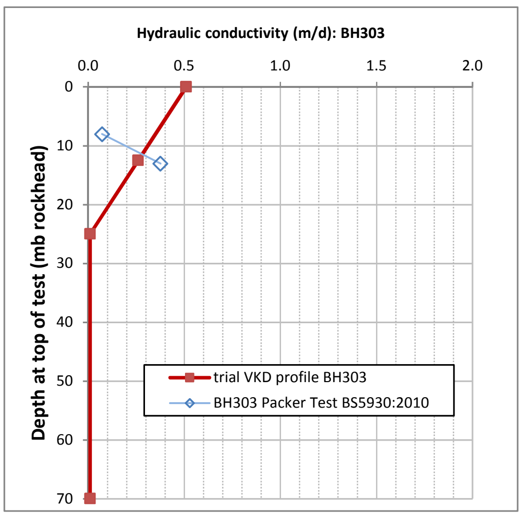

Estimated Estimated profile properties	
kbase (m/d)	0.01
kslope (m/d/m)	0.02
kmax (m/d)	3
inflection point (m)	25
depth at which kmax reached (m)	n/a
saturated transmissivity (m^2/d)	6.95

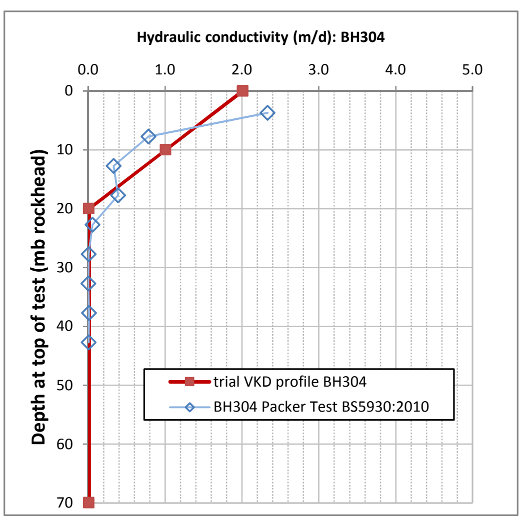

Estimated profile properties	
kbase (m/d)	0.01
kslope (m/d/m)	0.1
kmax (m/d)	3
inflection point (m)	20
depth at which kmax reached (m)	n/a
saturated transmissivity (m^2/d)	20.70

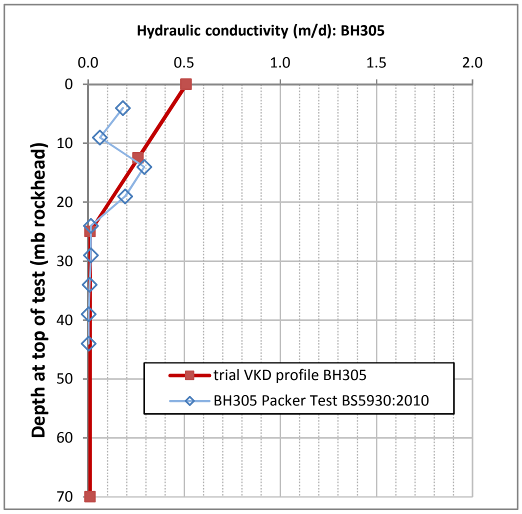

Estimated profile properties	
kbase (m/d)	0.01
kslope (m/d/m)	0.02
kmax (m/d)	3
inflection point (m)	25
depth at which kmax reached (m)	n/a
saturated transmissivity (m^2/d)	6.95

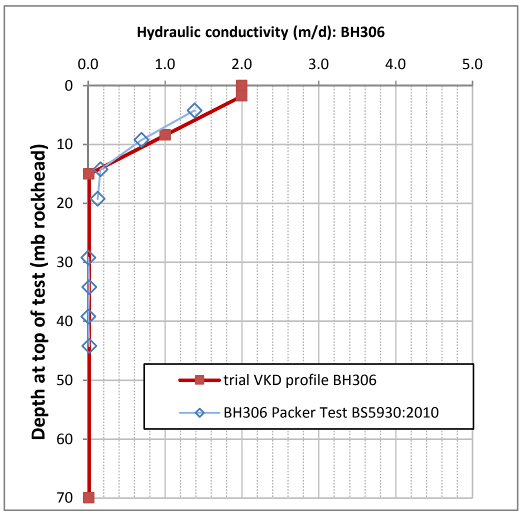

Estimated profile properties	
kbase (m/d)	0.01
kslope (m/d/m)	0.15
kmax (m/d)	2
inflection point (m)	15
depth at which kmax reached (m)	1.73
saturated transmissivity (m^2/d)	17.35

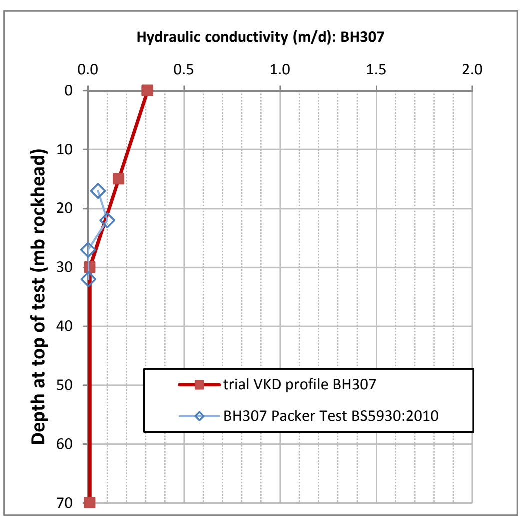

Estimated profile properties	
kbase (m/d)	0.01
kslope (m/d/m)	0.01
kmax (m/d)	2
inflection point (m)	30
depth at which kmax reached (m)	n/a
saturated transmissivity (m^2/d)	5.20

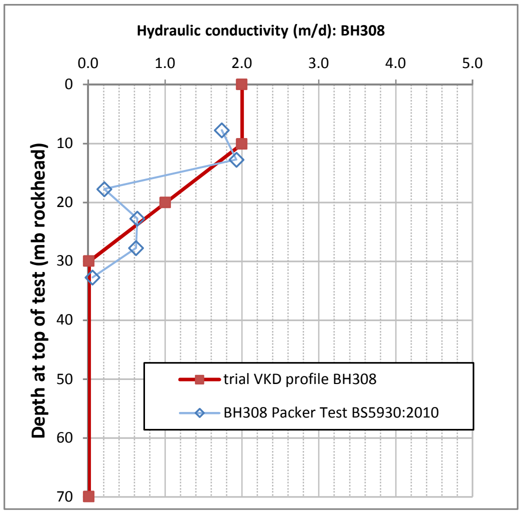

Estimated profile properties	
kbase (m/d)	0.01
kslope (m/d/m)	0.1
kmax (m/d)	2
inflection point (m)	30
depth at which kmax reached (m)	10.10
saturated transmissivity (m^2/d)	40.60

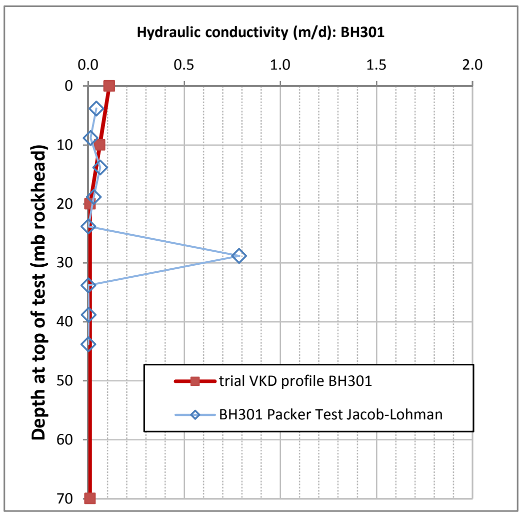

Estimated profile properties	
kbase (m/d)	0.01
kslope (m/d/m)	0.005
kmax (m/d)	3
inflection point (m)	20
depth at which kmax reached (m)	n/a
saturated transmissivity (m^2/d)	1.70

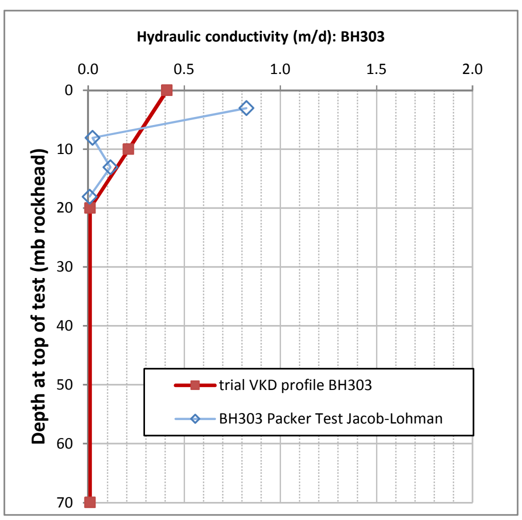

Estimated profile properties	
kbase (m/d)	0.01
kslope (m/d/m)	0.02
kmax (m/d)	3
inflection point (m)	20
depth at which kmax reached (m)	n/a
saturated transmissivity (m^2/d)	4.70

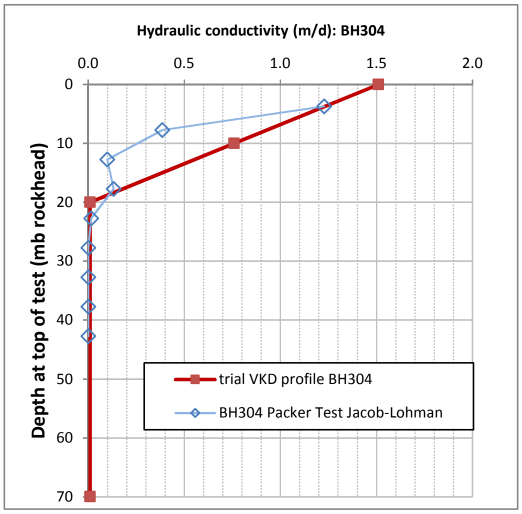

Estimated profile properties	
kbase (m/d)	0.01
kslope (m/d/m)	0.075
kmax (m/d)	3
inflection point (m)	20
depth at which kmax reached (m)	n/a
saturated transmissivity (m^2/d)	15.70

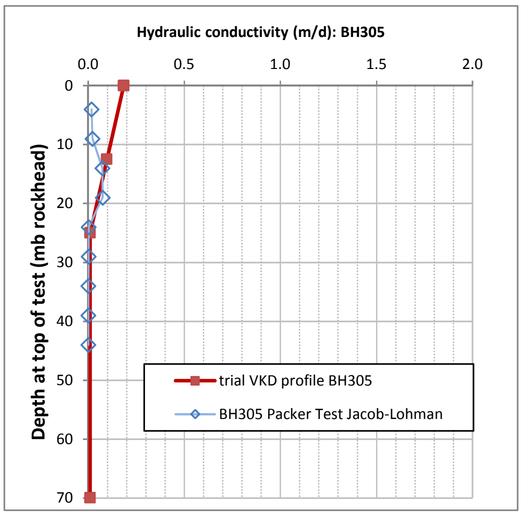

Estimated profile properties	
kbase (m/d)	0.01
kslope (m/d/m)	0.007
kmax (m/d)	3
inflection point (m)	25
depth at which kmax reached (m)	n/a
saturated transmissivity (m^2/d)	2.89

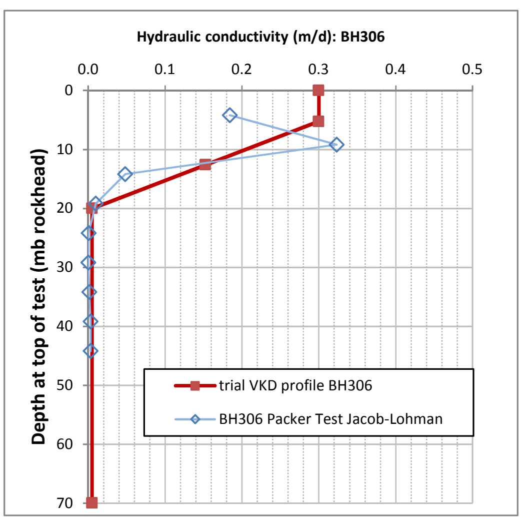

Estimated profile properties	
kbase (m/d)	0.005
kslope (m/d/m)	0.02
kmax (m/d)	0.3
inflection point (m)	20
depth at which kmax reached (m)	5.25
saturated transmissivity (m^2/d)	4.07

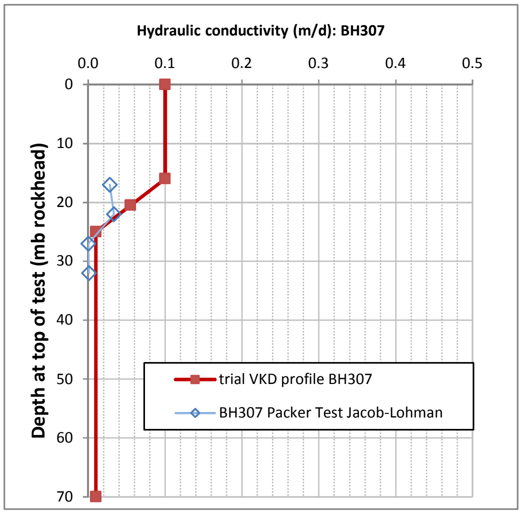

Estimated profile properties	
kbase (m/d)	0.01
kslope (m/d/m)	0.01
kmax (m/d)	0.1
inflection point (m)	25
depth at which kmax reached (m)	16.00
saturated transmissivity (m^2/d)	2.55

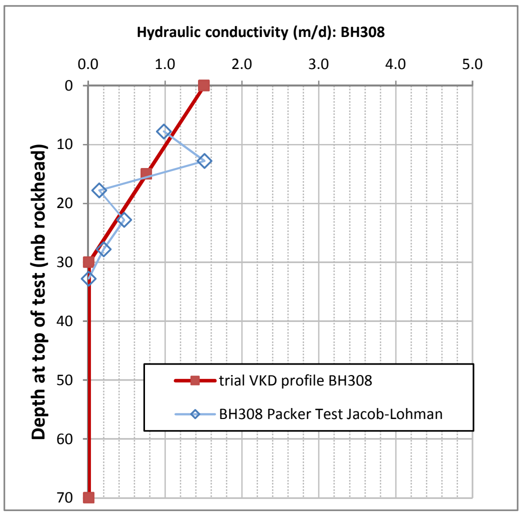

Estimated profile properties	
kbase (m/d)	0.01
kslope (m/d/m)	0.05
kmax (m/d)	2
inflection point (m)	30
depth at which kmax reached (m)	n/a
saturated transmissivity (m^2/d)	23.20

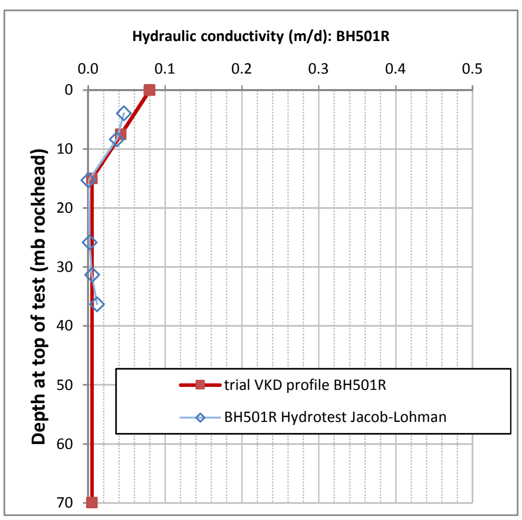

Estimated profile properties	
kbase (m/d)	0.005
kslope (m/d/m)	0.005
kmax (m/d)	2
inflection point (m)	15
depth at which kmax reached (m)	n/a
saturated transmissivity (m^2/d)	0.91

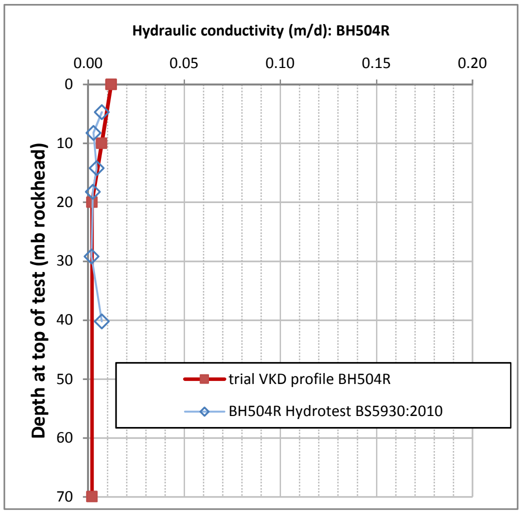

Estimated profile properties	
kbase (m/d)	0.002
kslope (m/d/m)	0.0005
kmax (m/d)	2
inflection point (m)	20
depth at which kmax reached (m)	n/a
saturated transmissivity (m^2/d)	0.24

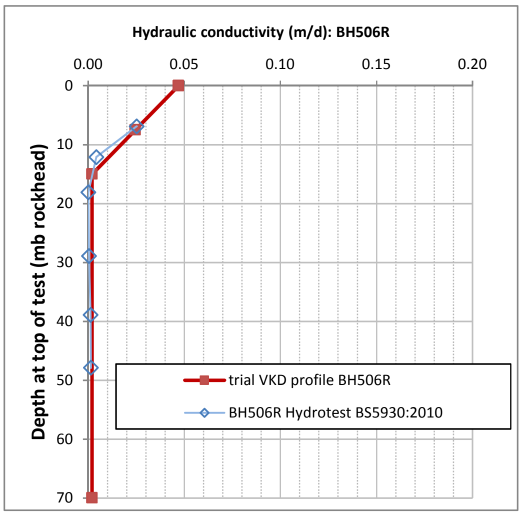

Estimated profile properties	
kbase (m/d)	0.002
kslope (m/d/m)	0.003
kmax (m/d)	2
inflection point (m)	15
depth at which kmax reached (m)	n/a
saturated transmissivity (m^2/d)	0.48

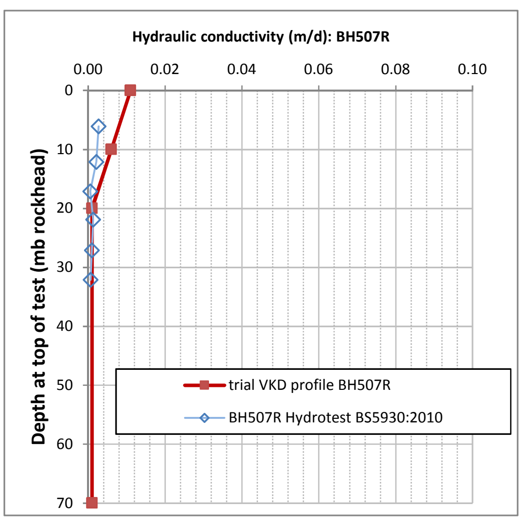

Estimated profile properties	
kbase (m/d)	ition points
kslope (m/d/m)	0
kmax (m/d)	0
inflection point (m)	0
depth at which kmax reached (m)	0.00
saturated transmissivity (m^2/d)	0.00

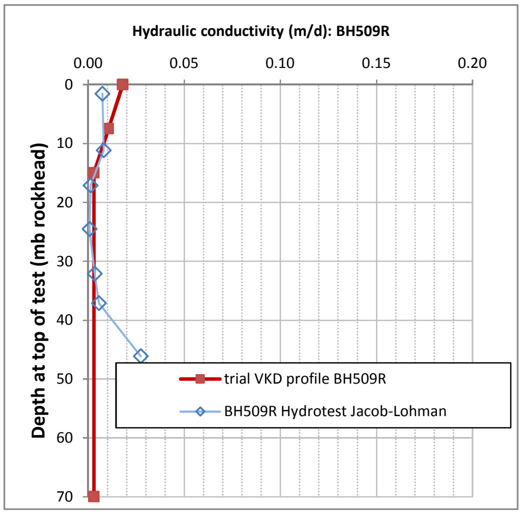

Estimated profile properties	
kbase (m/d)	ition points
kslope (m/d/m)	0
kmax (m/d)	0
inflection point (m)	0
depth at which kmax reached (m)	0.00
saturated transmissivity (m^2/d)	0.00

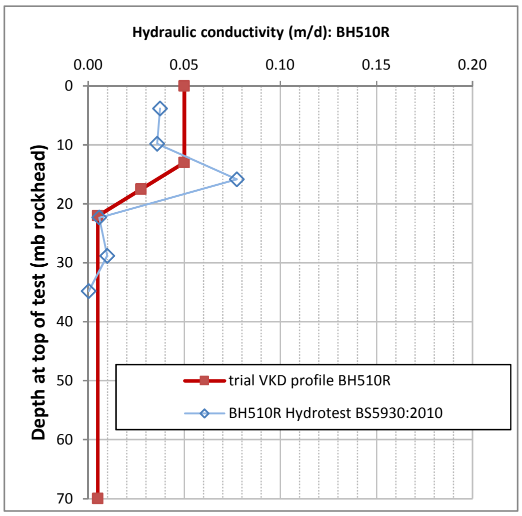

Estimated profile properties	
kbase (m/d)	0.005
kslope (m/d/m)	0.005
kmax (m/d)	0.05
inflection point (m)	22
depth at which kmax reached (m)	13.00
saturated transmissivity (m^2/d)	1.14

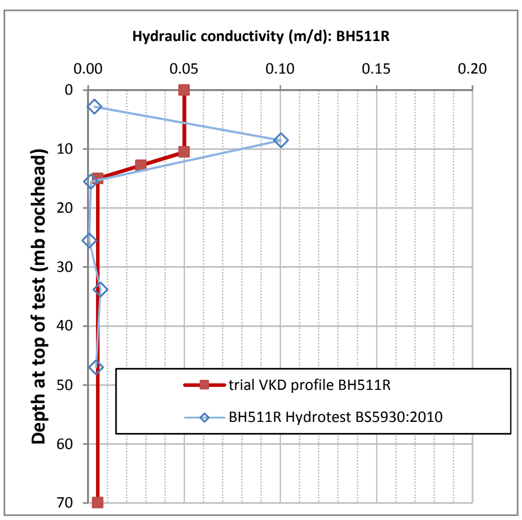

Estimated profile properties	
kbase (m/d)	0.005
kslope (m/d/m)	0.01
kmax (m/d)	0.05
inflection point (m)	15
depth at which kmax reached (m)	10.50
saturated transmissivity (m^2/d)	0.92

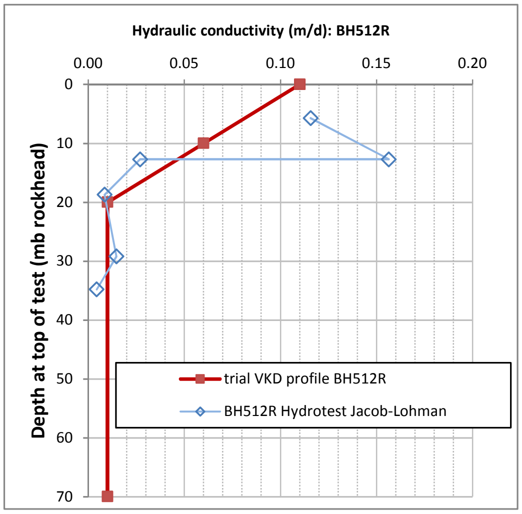

Estimated profile properties	
kbase (m/d)	0.01
kslope (m/d/m)	0.005
kmax (m/d)	2
inflection point (m)	20
depth at which kmax reached (m)	n/a
saturated transmissivity (m^2/d)	1.70

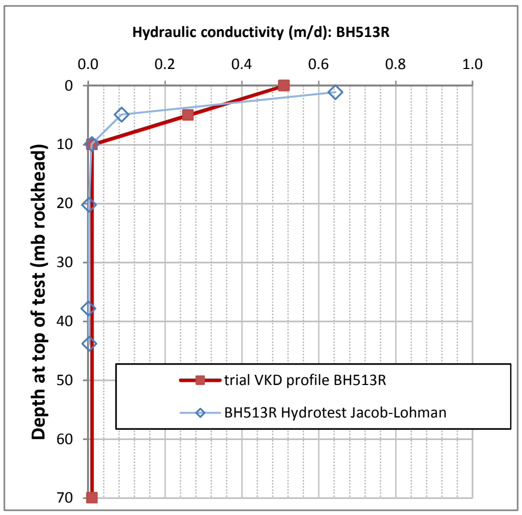

Estimated profile properties	
kbase (m/d)	0.01
kslope (m/d/m)	0.05
kmax (m/d)	1
inflection point (m)	10
depth at which kmax reached (m)	n/a
saturated transmissivity (m^2/d)	3.20

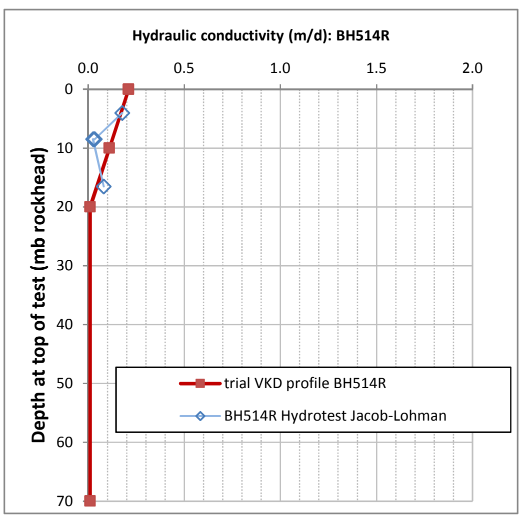

Estimated profile properties	
kbase (m/d)	0.01
kslope (m/d/m)	0.01
kmax (m/d)	1
inflection point (m)	20
depth at which kmax reached (m)	n/a
saturated transmissivity (m^2/d)	2.70

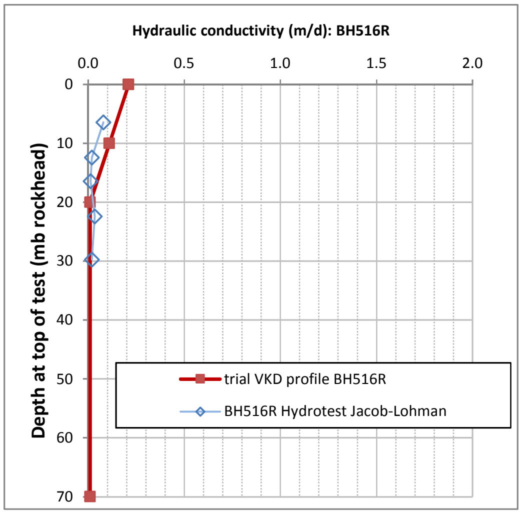

Estimated profile properties	
kbase (m/d)	0.01
kslope (m/d/m)	0.01
kmax (m/d)	1
inflection point (m)	20
depth at which kmax reached (m)	n/a
saturated transmissivity (m^2/d)	2.70

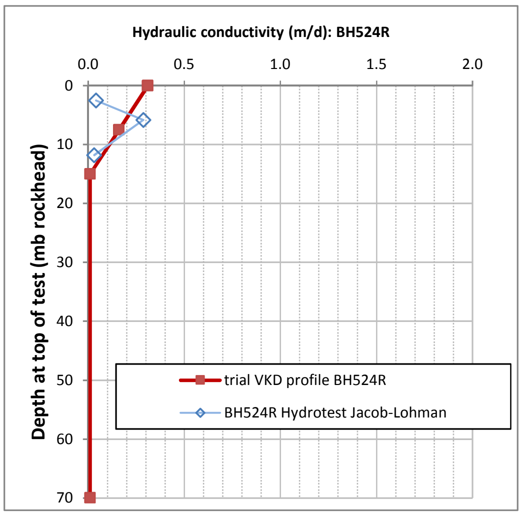

Estimated profile properties	
kbase (m/d)	0.01
kslope (m/d/m)	0.02
kmax (m/d)	1
inflection point (m)	15
depth at which kmax reached (m)	n/a
saturated transmissivity (m^2/d)	2.95

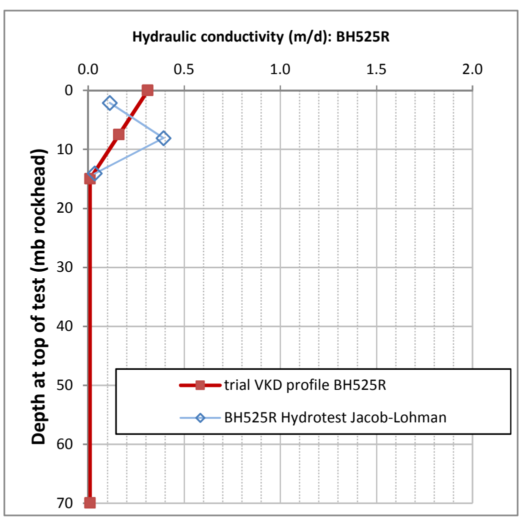

Estimated profile properties	
kbase (m/d)	0.01
kslope (m/d/m)	0.02
kmax (m/d)	1
inflection point (m)	15
depth at which kmax reached (m)	n/a
saturated transmissivity (m^2/d)	2.95

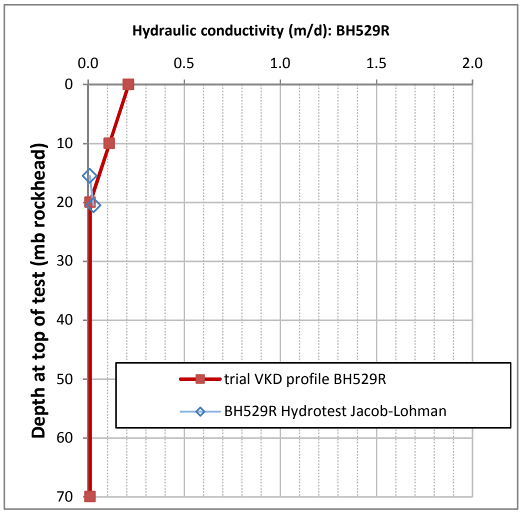

Estimated profile properties	
kbase (m/d)	0.01
kslope (m/d/m)	0.01
kmax (m/d)	1
inflection point (m)	20
depth at which kmax reached (m)	n/a
saturated transmissivity (m^2/d)	2.70

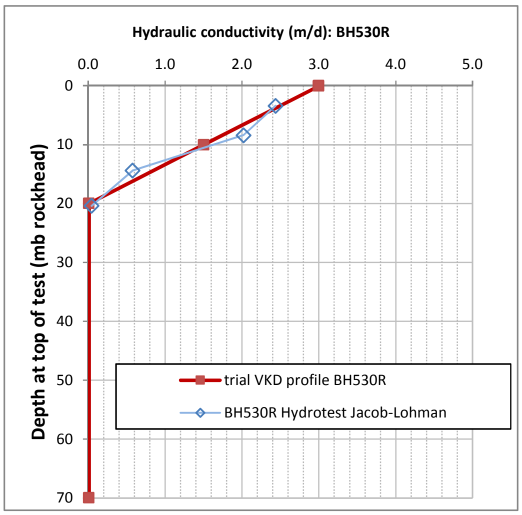

Estimated profile properties	
kbase (m/d)	0.01
kslope (m/d/m)	0.15
kmax (m/d)	3
inflection point (m)	20
depth at which kmax reached (m)	0.07
saturated transmissivity (m^2/d)	30.70

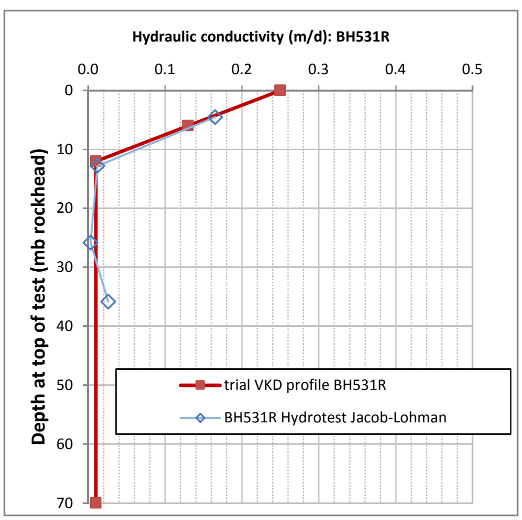

Estimated profile properties	
kbase (m/d)	0.01
kslope (m/d/m)	0.02
kmax (m/d)	1
inflection point (m)	12
depth at which kmax reached (m)	n/a
saturated transmissivity (m^2/d)	2.14

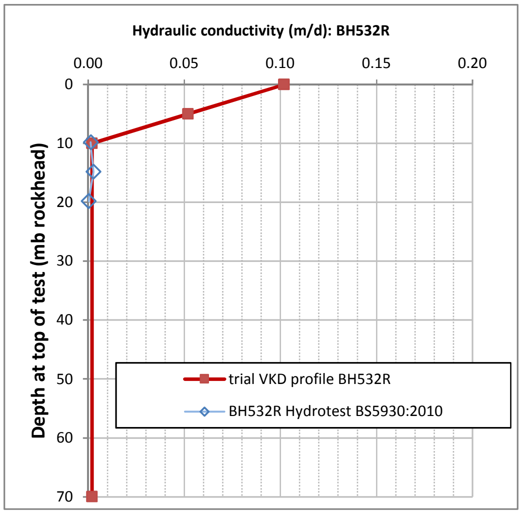

Estimated profile properties	
kbase (m/d)	0.002
kslope (m/d/m)	0.01
kmax (m/d)	1
inflection point (m)	10
depth at which kmax reached (m)	n/a
saturated transmissivity (m^2/d)	0.64

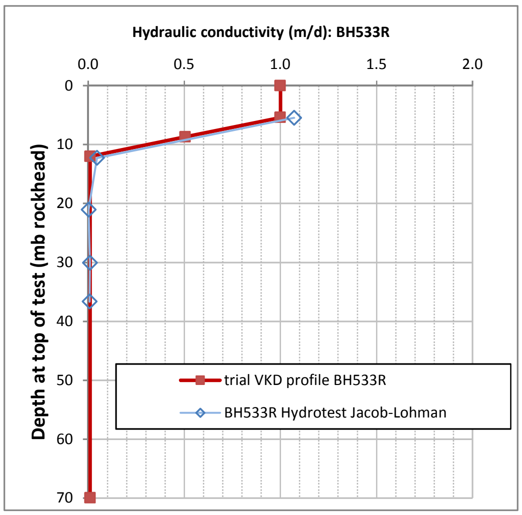

Estimated profile properties	
kbase (m/d)	0.01
kslope (m/d/m)	0.15
kmax (m/d)	1
inflection point (m)	12
depth at which kmax reached (m)	5.40
saturated transmissivity (m^2/d)	9.31

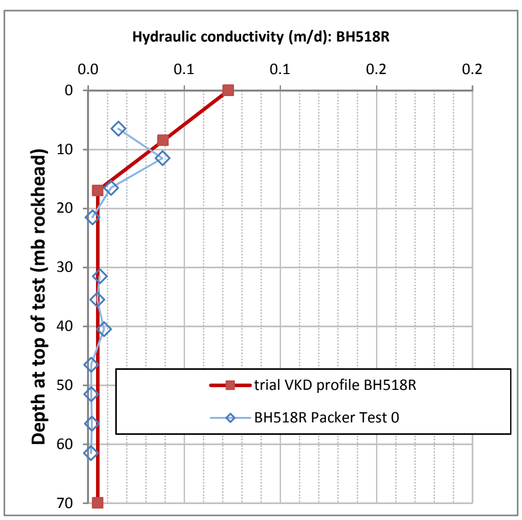

Estimated profile properties	
kbase (m/d)	0.005
kslope (m/d/m)	0.004
kmax (m/d)	1
inflection point (m)	17
depth at which kmax reached (m)	n/a
saturated transmissivity (m^2/d)	0.93

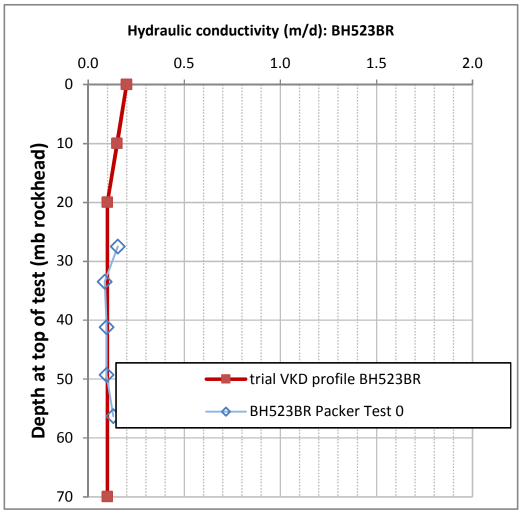

Estimated profile properties	
kbase (m/d)	0.1
kslope (m/d/m)	0.005
kmax (m/d)	1
inflection point (m)	20
depth at which kmax reached (m)	n/a
saturated transmissivity (m^2/d)	8.00

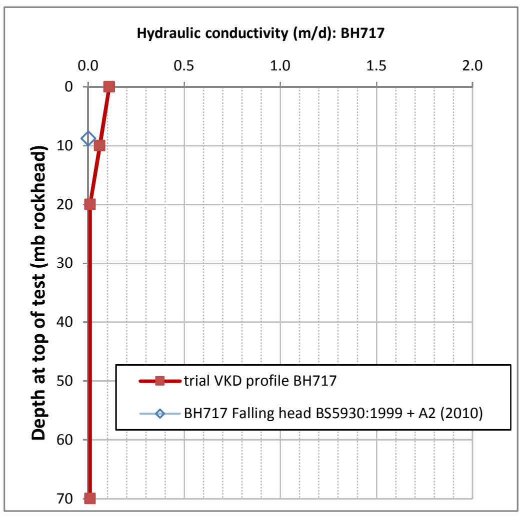

Estimated profile properties	
kbase (m/d)	0.01
kslope (m/d/m)	0.005
kmax (m/d)	1
inflection point (m)	20
depth at which kmax reached (m)	n/a
saturated transmissivity (m^2/d)	1.70

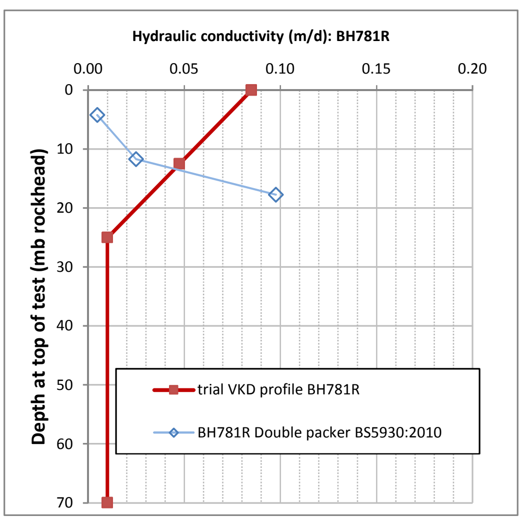

Estimated profile properties	
kbase (m/d)	0.01
kslope (m/d/m)	0.003
kmax (m/d)	1
inflection point (m)	25
depth at which kmax reached (m)	n/a
saturated transmissivity (m^2/d)	1.64

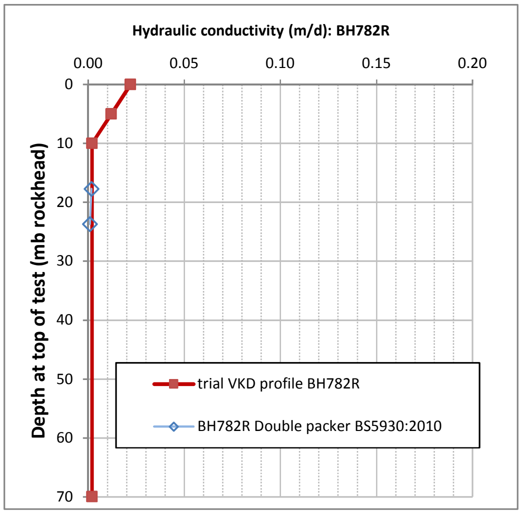

Estimated profile properties	
kbase (m/d)	0.002
kslope (m/d/m)	0.002
kmax (m/d)	1
inflection point (m)	10
depth at which kmax reached (m)	n/a
saturated transmissivity (m^2/d)	0.24

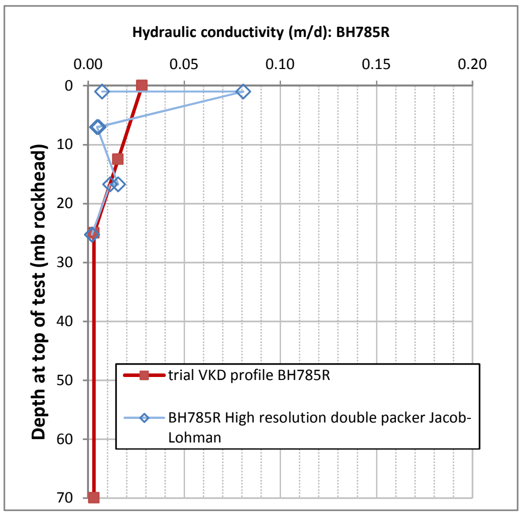

Estimated profile properties	
kbase (m/d)	0.003
kslope (m/d/m)	0.001
kmax (m/d)	1
inflection point (m)	25
depth at which kmax reached (m)	n/a
saturated transmissivity (m^2/d)	0.52

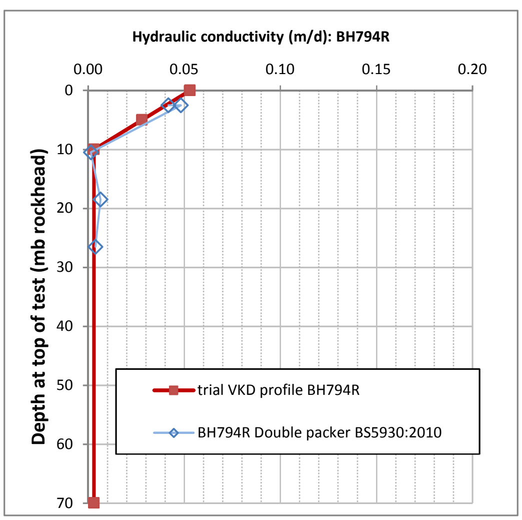

Estimated profile properties	
kbase (m/d)	0.003
kslope (m/d/m)	0.005
kmax (m/d)	1
inflection point (m)	10
depth at which kmax reached (m)	n/a
saturated transmissivity (m^2/d)	0.46

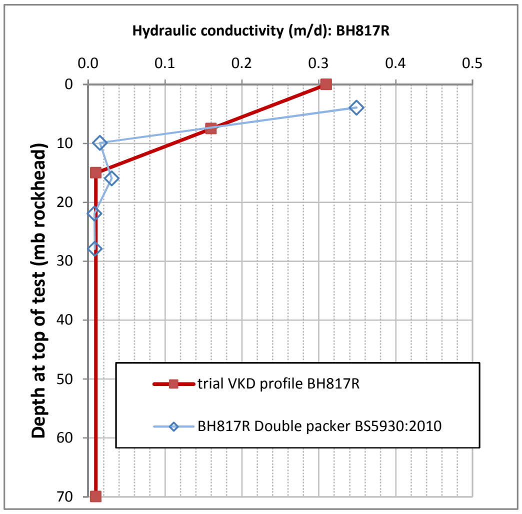

Estimated profile properties	
kbase (m/d)	0.01
kslope (m/d/m)	0.02
kmax (m/d)	1
inflection point (m)	15
depth at which kmax reached (m)	n/a
saturated transmissivity (m^2/d)	2.95

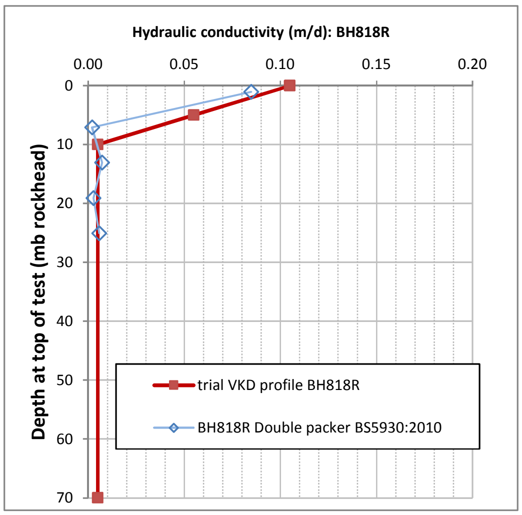

Estimated profile properties	
kbase (m/d)	0.005
kslope (m/d/m)	0.01
kmax (m/d)	1
inflection point (m)	10
depth at which kmax reached (m)	n/a
saturated transmissivity (m^2/d)	0.85

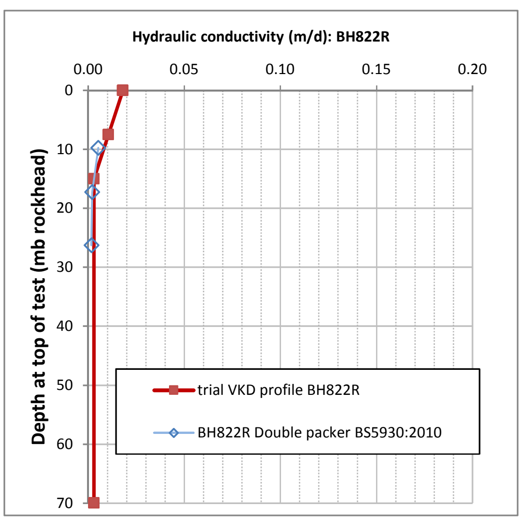

Estimated profile properties	
kbase (m/d)	0.003
kslope (m/d/m)	0.001
kmax (m/d)	1
inflection point (m)	15
depth at which kmax reached (m)	n/a
saturated transmissivity (m^2/d)	0.32

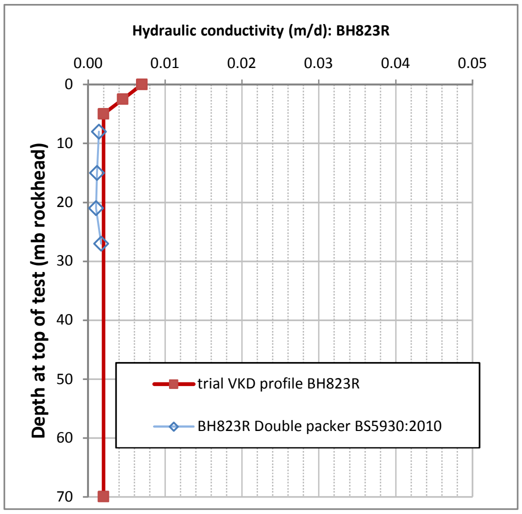

Estimated profile properties	
kbase (m/d)	0.002
kslope (m/d/m)	0.001
kmax (m/d)	1
inflection point (m)	5
depth at which kmax reached (m)	n/a
saturated transmissivity (m^2/d)	0.15

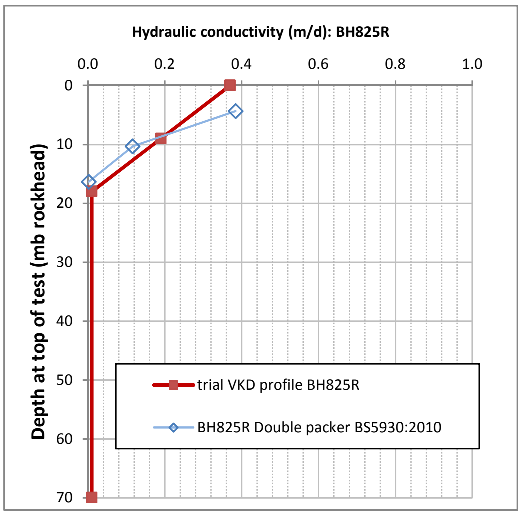

Estimated profile properties	
kbase (m/d)	0.01
kslope (m/d/m)	0.02
kmax (m/d)	1
inflection point (m)	18
depth at which kmax reached (m)	n/a
saturated transmissivity (m^2/d)	3.94

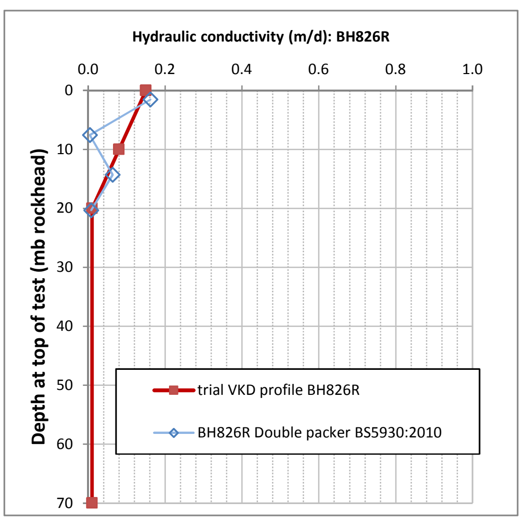

Estimated profile properties	
kbase (m/d)	0.01
kslope (m/d/m)	0.007
kmax (m/d)	1
inflection point (m)	20
depth at which kmax reached (m)	n/a
saturated transmissivity (m^2/d)	2.10

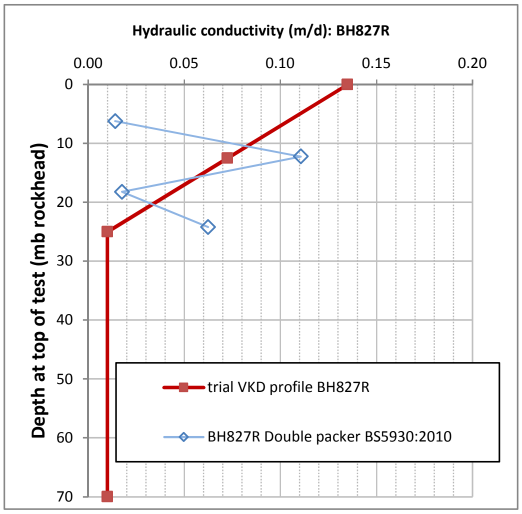

Estimated profile properties	
kbase (m/d)	0.01
kslope (m/d/m)	0.005
kmax (m/d)	1
inflection point (m)	25
depth at which kmax reached (m)	n/a
saturated transmissivity (m^2/d)	2.26

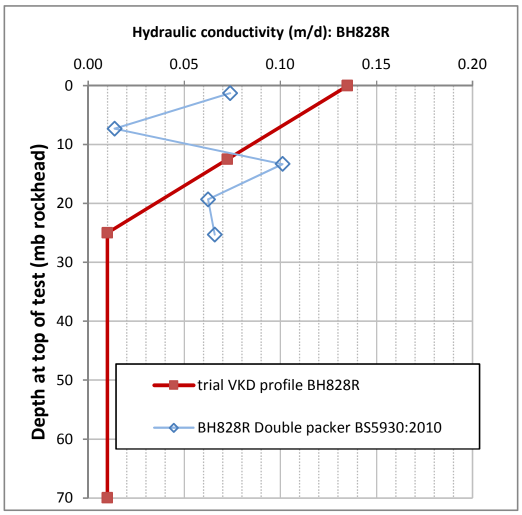

Estimated profile properties	
kbase (m/d)	0.01
kslope (m/d/m)	0.005
kmax (m/d)	1
inflection point (m)	25
depth at which kmax reached (m)	n/a
saturated transmissivity (m^2/d)	2.26

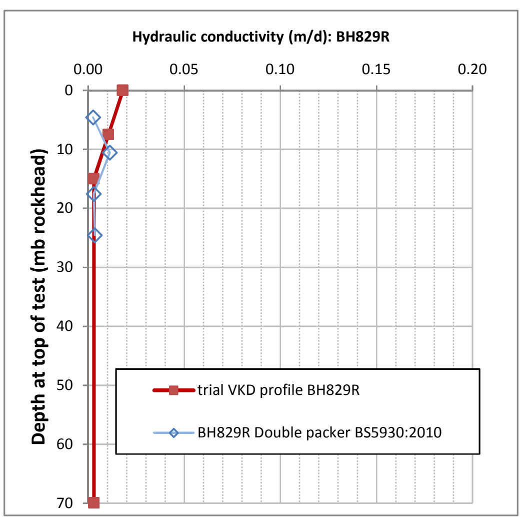

Estimated profile properties	
kbase (m/d)	0.003
kslope (m/d/m)	0.001
kmax (m/d)	1
inflection point (m)	15
depth at which kmax reached (m)	n/a
saturated transmissivity (m^2/d)	0.32

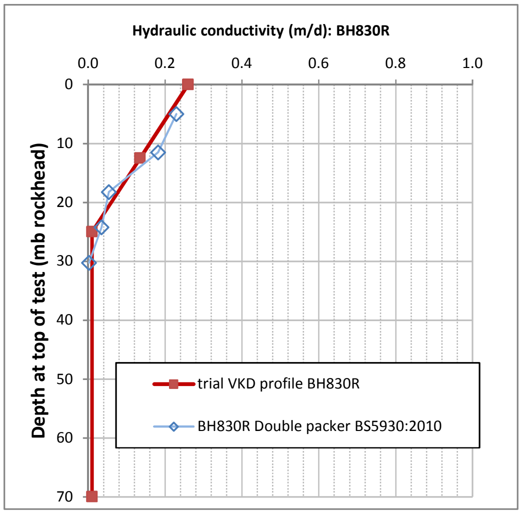

Estimated profile properties	
kbase (m/d)	0.01
kslope (m/d/m)	0.01
kmax (m/d)	1
inflection point (m)	25
depth at which kmax reached (m)	n/a
saturated transmissivity (m^2/d)	3.83

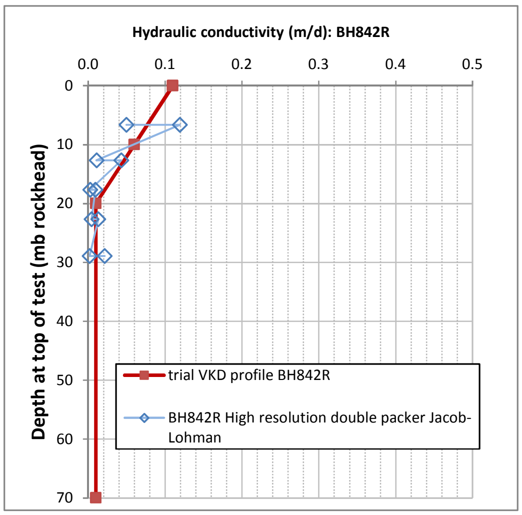

Estimated profile properties	
kbase (m/d)	0.01
kslope (m/d/m)	0.005
kmax (m/d)	1
inflection point (m)	20
depth at which kmax reached (m)	n/a
saturated transmissivity (m^2/d)	1.70

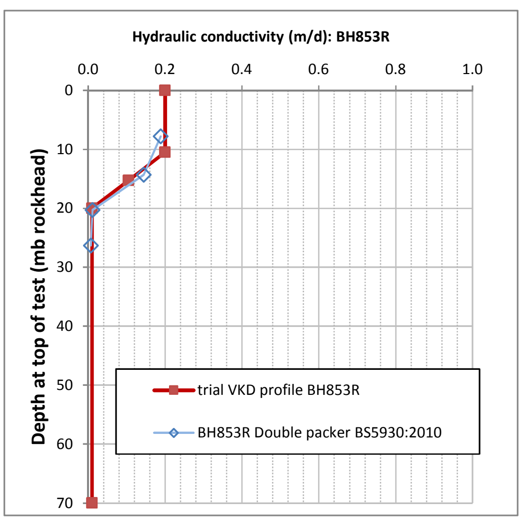

Estimated profile properties	
kbase (m/d)	0.01
kslope (m/d/m)	0.02
kmax (m/d)	0.2
inflection point (m)	20
depth at which kmax reached (m)	10.50
saturated transmissivity (m^2/d)	3.60

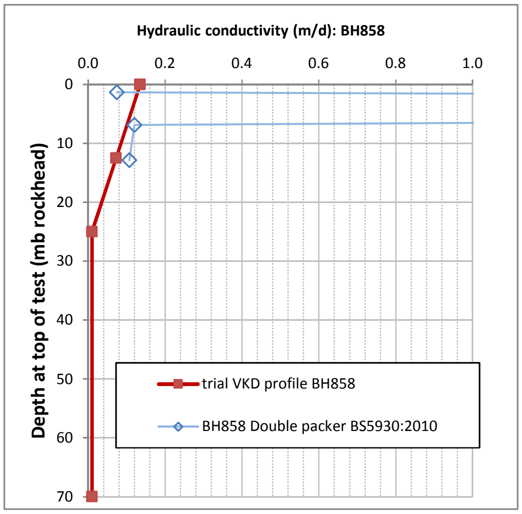

Estimated profile properties	
kbase (m/d)	0.01
kslope (m/d/m)	0.005
kmax (m/d)	1
inflection point (m)	25
depth at which kmax reached (m)	n/a
saturated transmissivity (m^2/d)	2.26

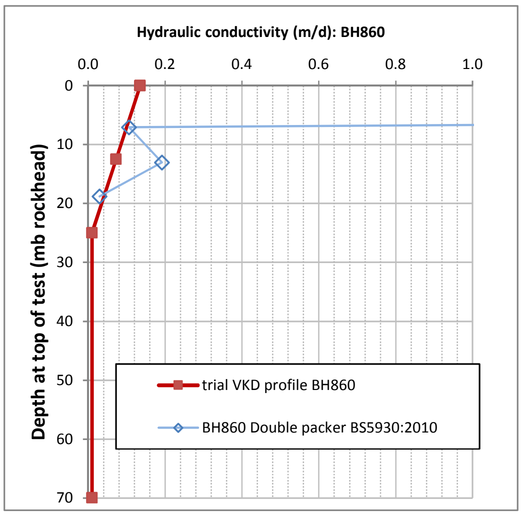

Estimated profile properties	
kbase (m/d)	0.01
kslope (m/d/m)	0.005
kmax (m/d)	1
inflection point (m)	25
depth at which kmax reached (m)	n/a
saturated transmissivity (m^2/d)	2.26

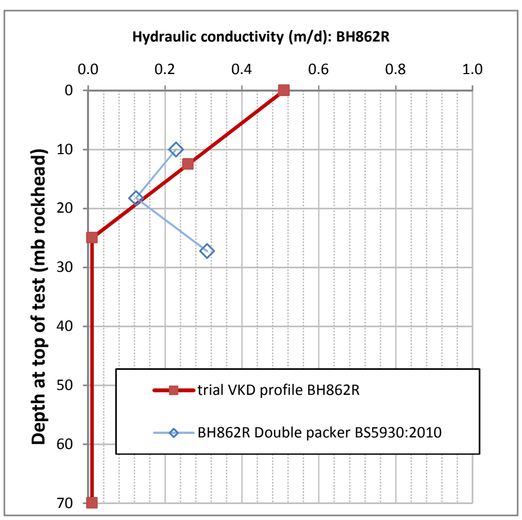

Estimated profile properties	
kbase (m/d)	0.01
kslope (m/d/m)	0.02
kmax (m/d)	1
inflection point (m)	25
depth at which kmax reached (m)	n/a
saturated transmissivity (m^2/d)	6.95

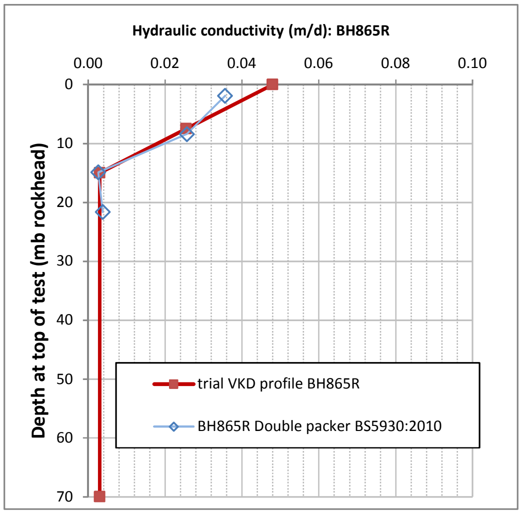

Estimated profile properties	
kbase (m/d)	0.003
kslope (m/d/m)	0.003
kmax (m/d)	1
inflection point (m)	15
depth at which kmax reached (m)	n/a
saturated transmissivity (m^2/d)	0.55

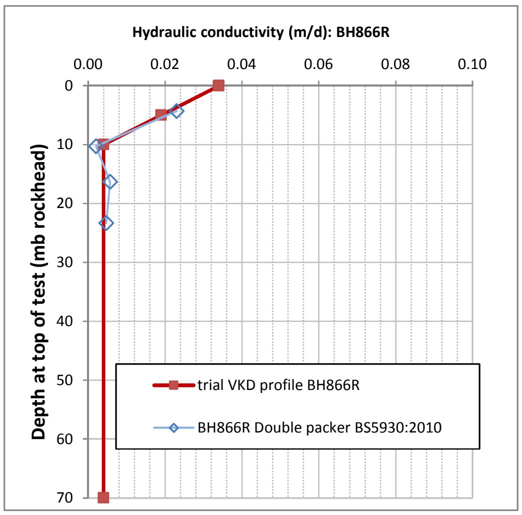

Estimated profile properties	
kbase (m/d)	0.004
kslope (m/d/m)	0.003
kmax (m/d)	1
inflection point (m)	10
depth at which kmax reached (m)	n/a
saturated transmissivity (m^2/d)	0.43

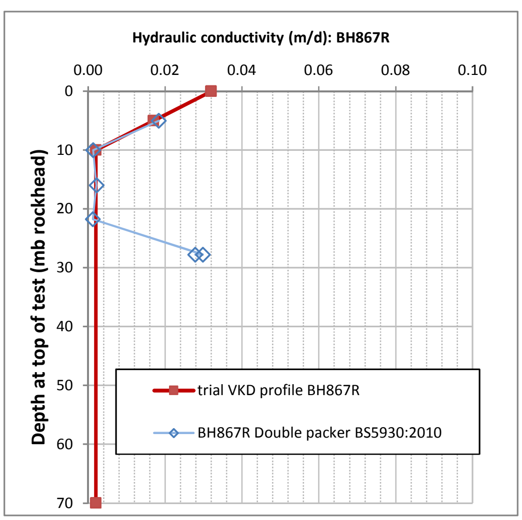

Estimated profile properties	
kbase (m/d)	0.002
kslope (m/d/m)	0.003
kmax (m/d)	1
inflection point (m)	10
depth at which kmax reached (m)	n/a
saturated transmissivity (m^2/d)	0.29

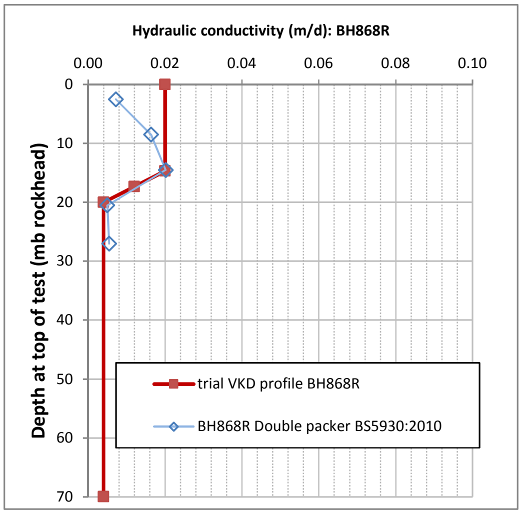

Estimated profile properties	
kbase (m/d)	0.004
kslope (m/d/m)	0.003
kmax (m/d)	0.02
inflection point (m)	20
depth at which kmax reached (m)	14.67
saturated transmissivity (m^2/d)	0.56

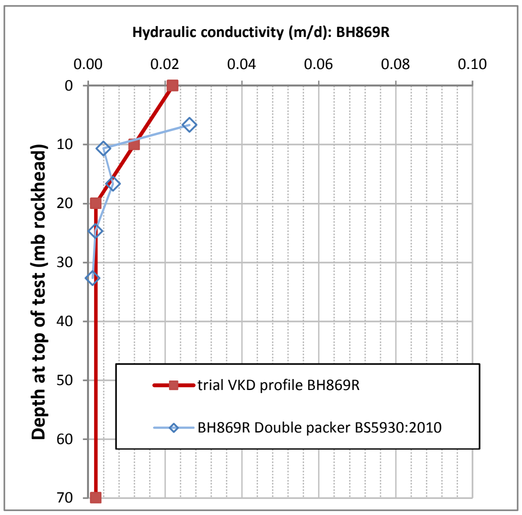

Estimated profile properties	
kbase (m/d)	0.002
kslope (m/d/m)	0.001
kmax (m/d)	1
inflection point (m)	20
depth at which kmax reached (m)	n/a
saturated transmissivity (m^2/d)	0.34

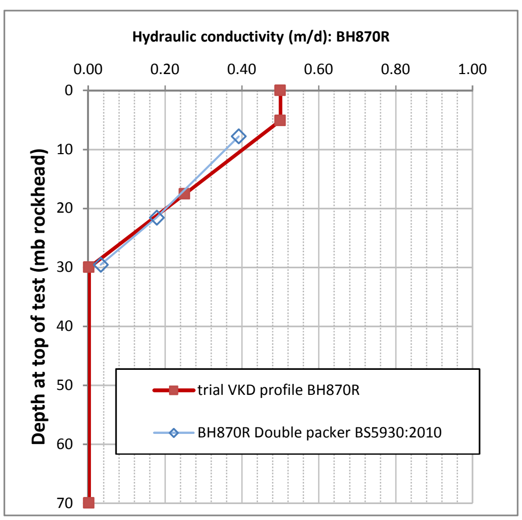

Estimated profile properties	
kbase (m/d)	0.002
kslope (m/d/m)	0.02
kmax (m/d)	0.5
inflection point (m)	30
depth at which kmax reached (m)	5.10
saturated transmissivity (m^2/d)	8.88

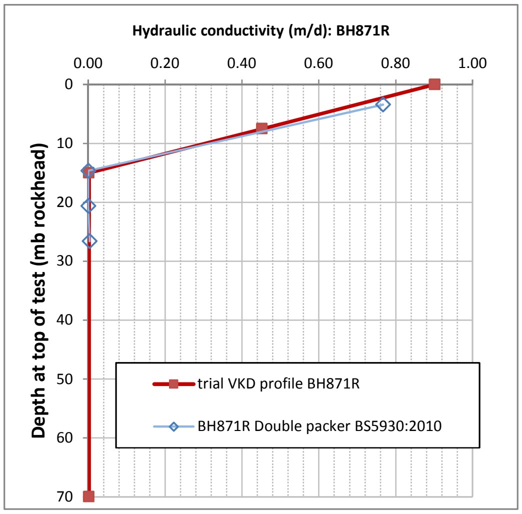

Estimated profile properties	
kbase (m/d)	0.002
kslope (m/d/m)	0.06
kmax (m/d)	1
inflection point (m)	15
depth at which kmax reached (m)	n/a
saturated transmissivity (m^2/d)	6.89

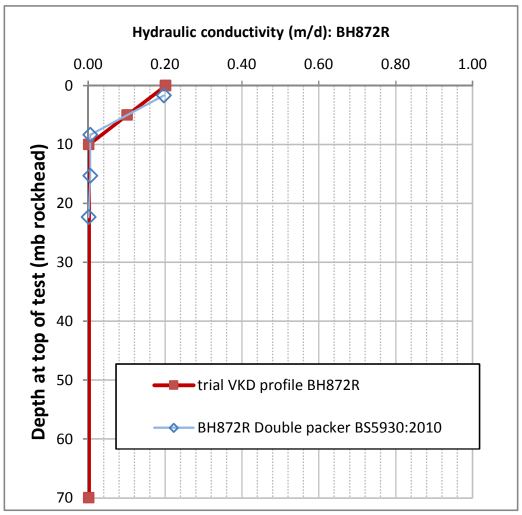

Estimated profile properties	
kbase (m/d)	0.002
kslope (m/d/m)	0.02
kmax (m/d)	1
inflection point (m)	10
depth at which kmax reached (m)	n/a
saturated transmissivity (m^2/d)	1.14

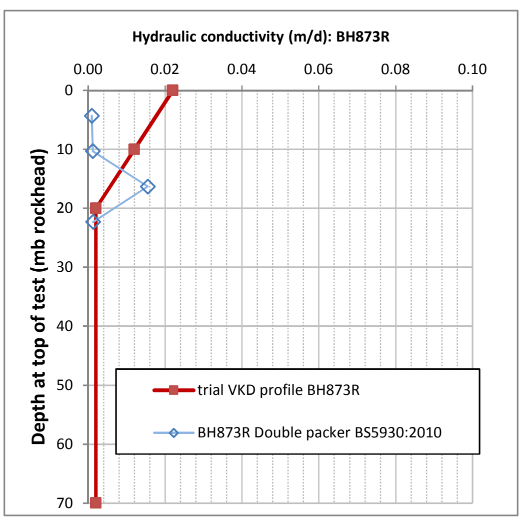

Estimated profile properties	
kbase (m/d)	0.002
kslope (m/d/m)	0.001
kmax (m/d)	1
inflection point (m)	20
depth at which kmax reached (m)	n/a
saturated transmissivity (m^2/d)	0.34

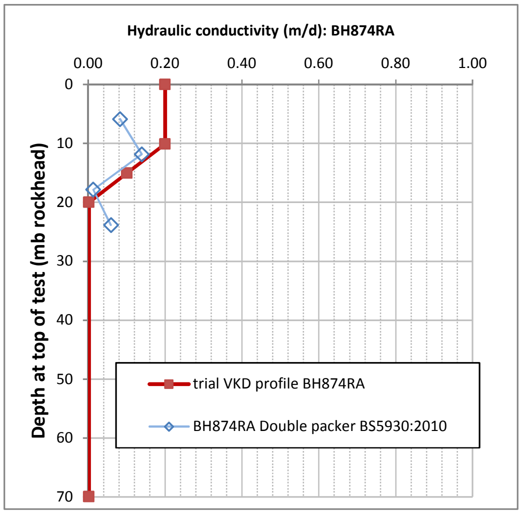

Estimated profile properties	
kbase (m/d)	0.002
kslope (m/d/m)	0.02
kmax (m/d)	0.2
inflection point (m)	20
depth at which kmax reached (m)	10.10
saturated transmissivity (m^2/d)	3.12

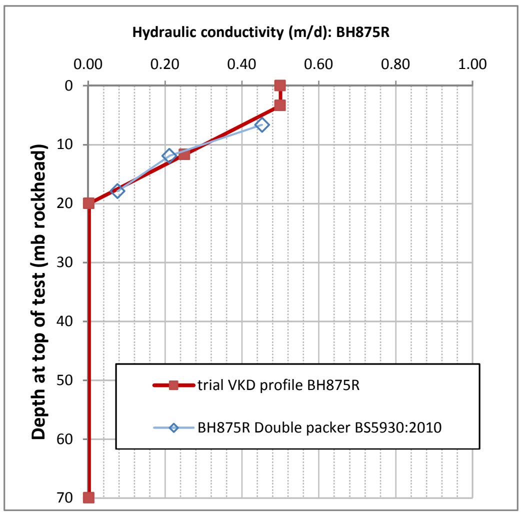

Estimated profile properties	
kbase (m/d)	0.002
kslope (m/d/m)	0.03
kmax (m/d)	0.5
inflection point (m)	20
depth at which kmax reached (m)	3.40
saturated transmissivity (m^2/d)	5.97

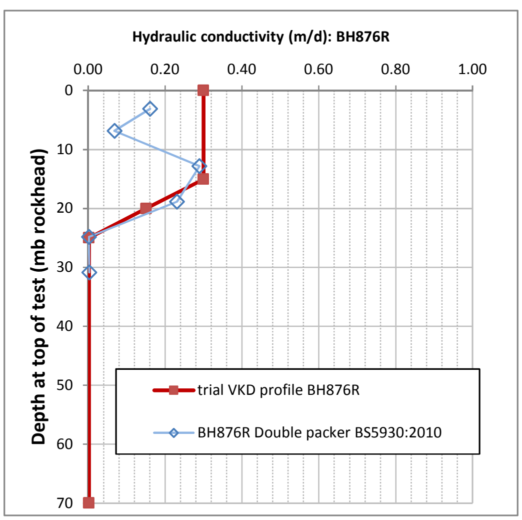

Estimated profile properties	
kbase (m/d)	0.002
kslope (m/d/m)	0.03
kmax (m/d)	0.3
inflection point (m)	25
depth at which kmax reached (m)	15.07
saturated transmissivity (m^2/d)	6.11

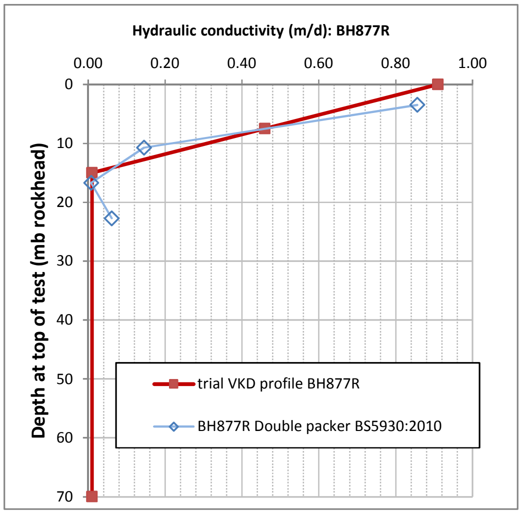

Estimated profile properties	
kbase (m/d)	0.01
kslope (m/d/m)	0.06
kmax (m/d)	1
inflection point (m)	15
depth at which kmax reached (m)	n/a
saturated transmissivity (m^2/d)	7.45

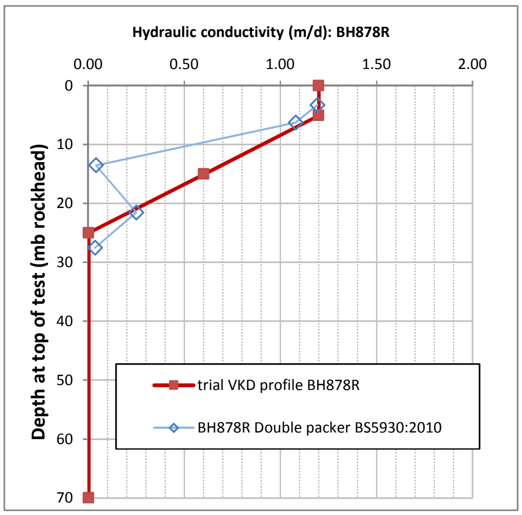

Estimated profile properties	
kbase (m/d)	0.002
kslope (m/d/m)	0.06
kmax (m/d)	1.2
inflection point (m)	25
depth at which kmax reached (m)	5.03
saturated transmissivity (m^2/d)	18.13

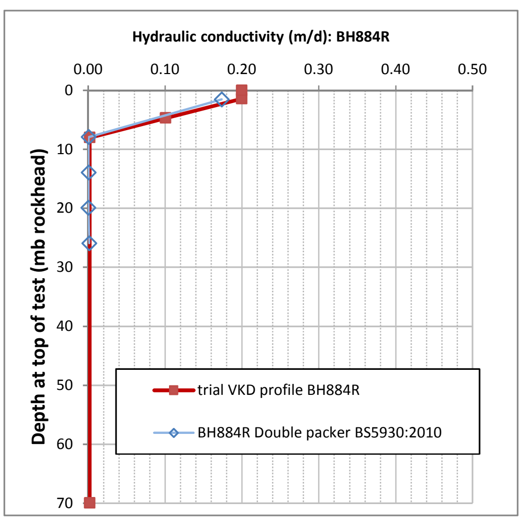

Estimated profile properties	
kbase (m/d)	0.002
kslope (m/d/m)	0.03
kmax (m/d)	0.2
inflection point (m)	8
depth at which kmax reached (m)	1.40
saturated transmissivity (m^2/d)	1.07

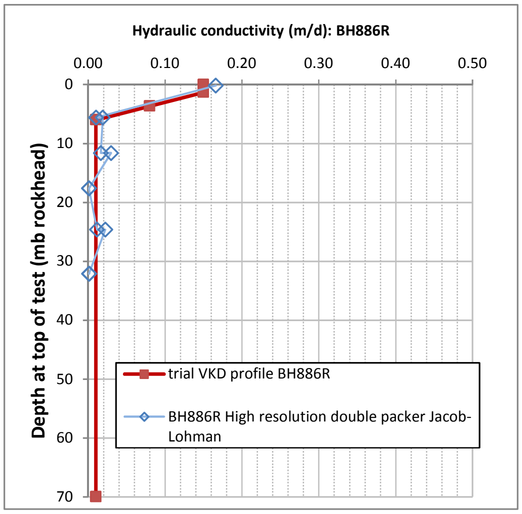

Estimated profile properties	
kbase (m/d)	0.01
kslope (m/d/m)	0.03
kmax (m/d)	0.15
inflection point (m)	6
depth at which kmax reached (m)	1.33
saturated transmissivity (m^2/d)	1.21

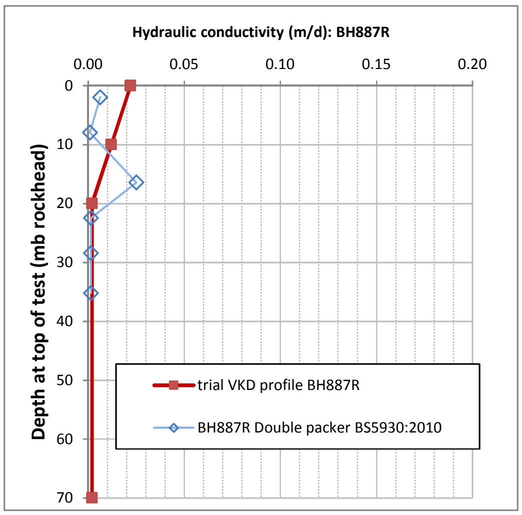

Estimated profile properties	
kbase (m/d)	0.002
kslope (m/d/m)	0.001
kmax (m/d)	0.05
inflection point (m)	20
depth at which kmax reached (m)	n/a
saturated transmissivity (m^2/d)	0.34

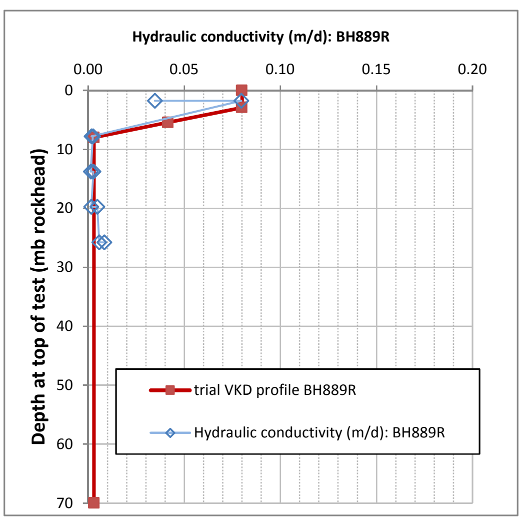

Estimated profile properties	
kbase (m/d)	0.003
kslope (m/d/m)	0.015
kmax (m/d)	0.08
inflection point (m)	8
depth at which kmax reached (m)	2.87
saturated transmissivity (m^2/d)	0.63

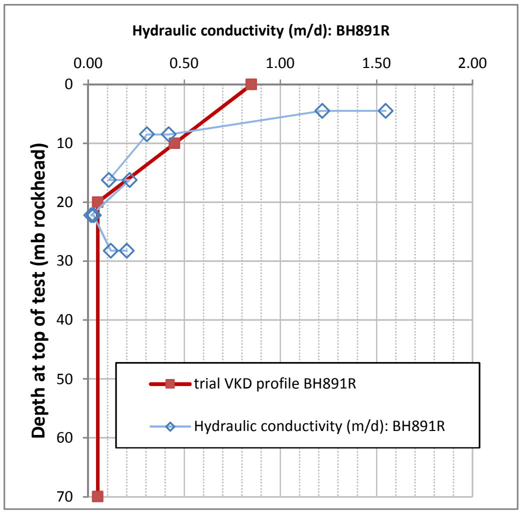

Estimated profile properties	
kbase (m/d)	0.05
kslope (m/d/m)	0.04
kmax (m/d)	1
inflection point (m)	20
depth at which kmax reached (m)	n/a
saturated transmissivity (m^2/d)	11.50

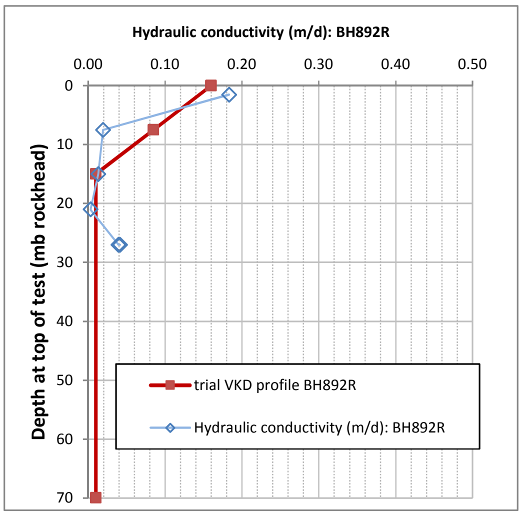

Estimated profile properties	
kbase (m/d)	0.01
kslope (m/d/m)	0.01
kmax (m/d)	1
inflection point (m)	15
depth at which kmax reached (m)	n/a
saturated transmissivity (m^2/d)	1.83

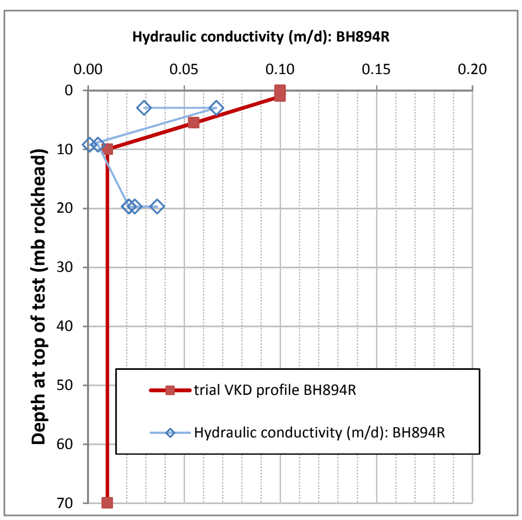

Estimated profile properties	
kbase (m/d)	0.01
kslope (m/d/m)	0.01
kmax (m/d)	0.1
inflection point (m)	10
depth at which kmax reached (m)	1.00
saturated transmissivity (m^2/d)	1.20

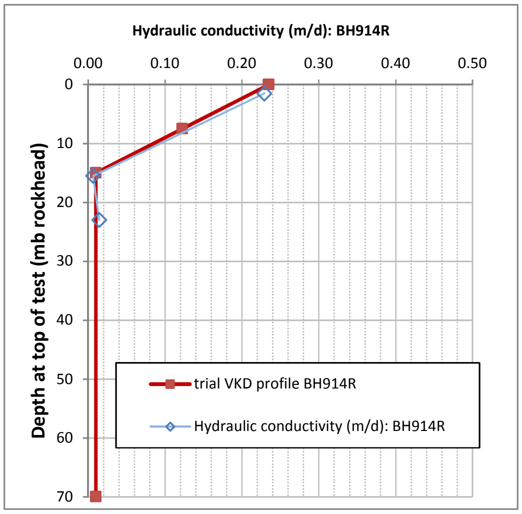

Estimated profile properties	
kbase (m/d)	0.01
kslope (m/d/m)	0.015
kmax (m/d)	0.25
inflection point (m)	15
depth at which kmax reached (m)	n/a
saturated transmissivity (m^2/d)	2.39

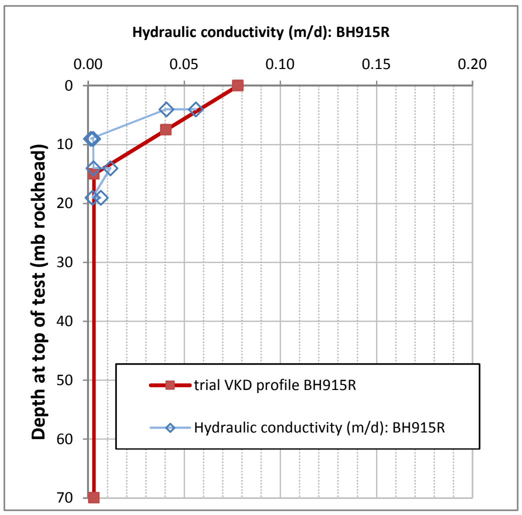

Estimated profile properties	
kbase (m/d)	0.003
kslope (m/d/m)	0.005
kmax (m/d)	0.1
inflection point (m)	15
depth at which kmax reached (m)	n/a
saturated transmissivity (m^2/d)	0.77

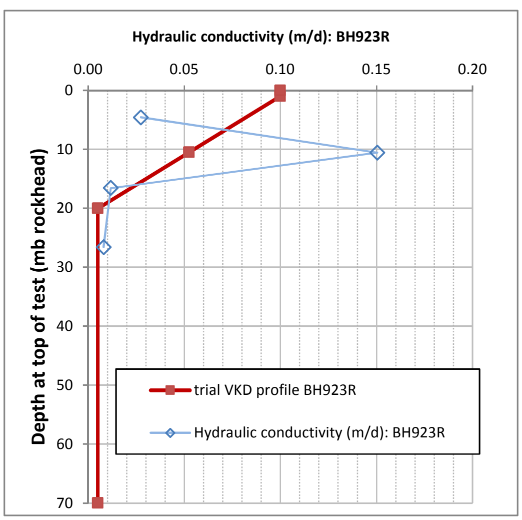

Estimated profile properties	
kbase (m/d)	0.005
kslope (m/d/m)	0.005
kmax (m/d)	0.1
inflection point (m)	20
depth at which kmax reached (m)	1.00
saturated transmissivity (m^2/d)	1.35

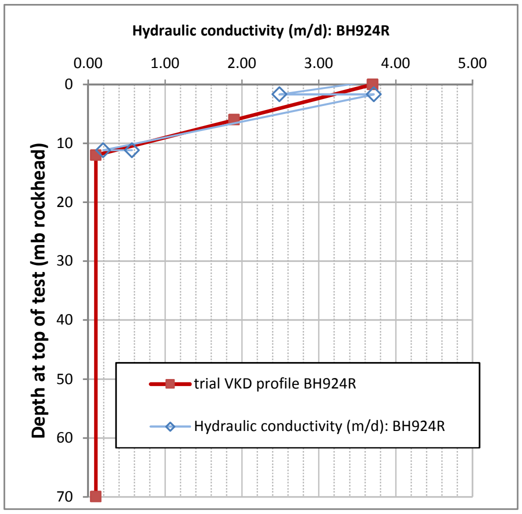

Estimated profile properties	
kbase (m/d)	0.1
kslope (m/d/m)	0.3
kmax (m/d)	5
inflection point (m)	12
depth at which kmax reached (m)	n/a
saturated transmissivity (m^2/d)	28.60

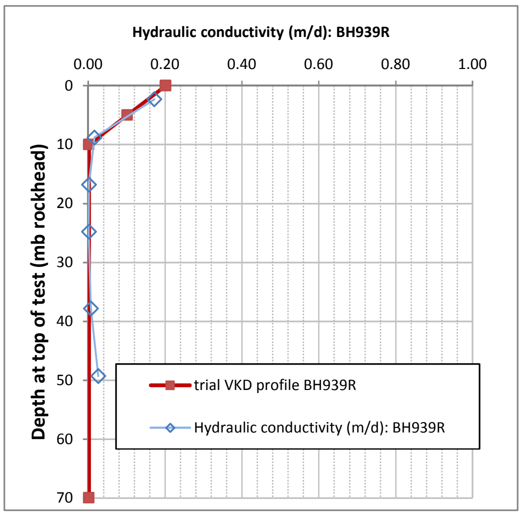

Estimated profile properties	
kbase (m/d)	0.002
kslope (m/d/m)	0.02
kmax (m/d)	1
inflection point (m)	10
depth at which kmax reached (m)	n/a
saturated transmissivity (m^2/d)	1.14

Appendix B
Baseline model build plans

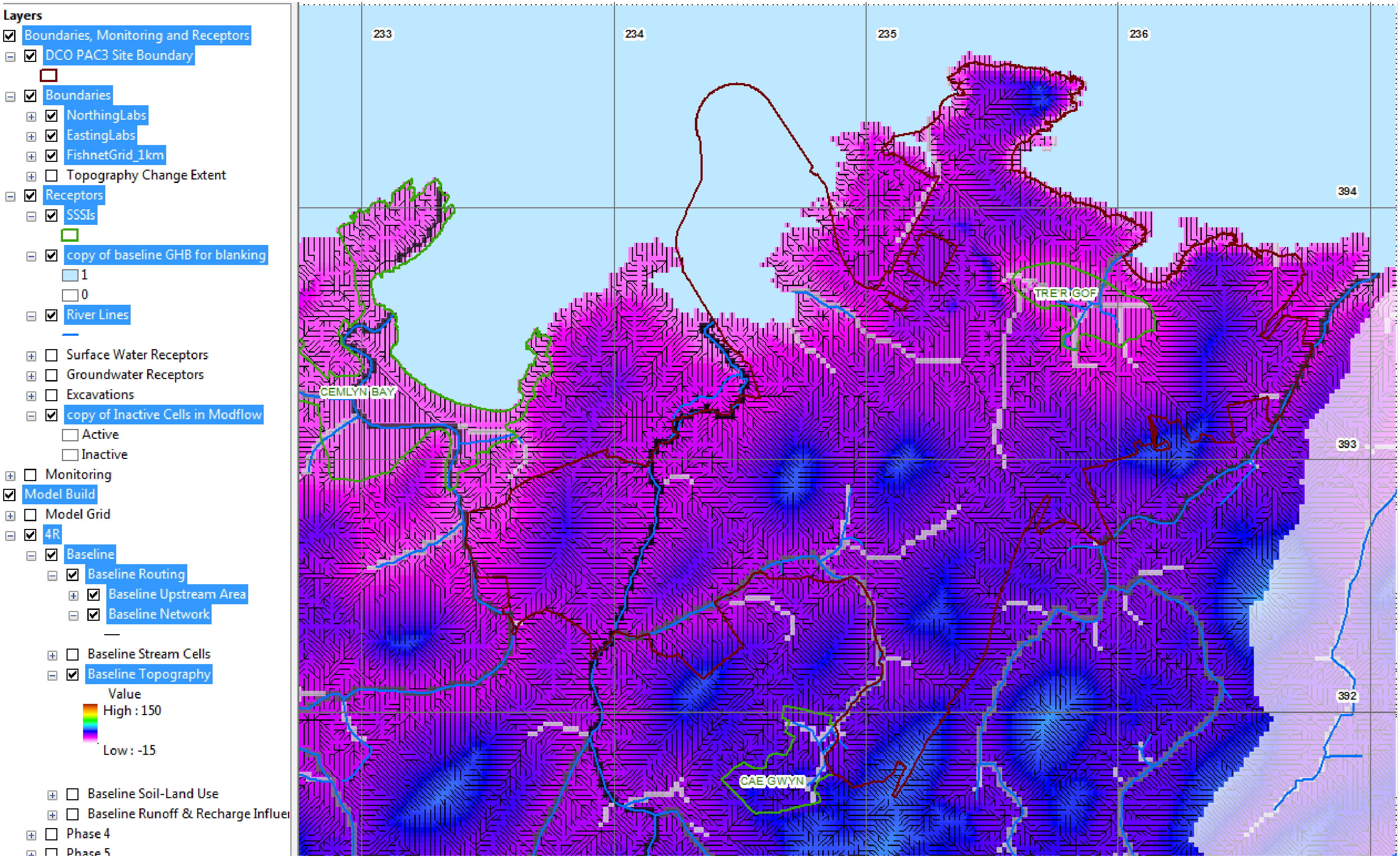

1 **Baseline topography, rivers, SSSI receptors, Site boundary, 4R upstream routed area and detailed routing, MODFLOW General Head Boundary sea bed, and Inactive cell overlay**

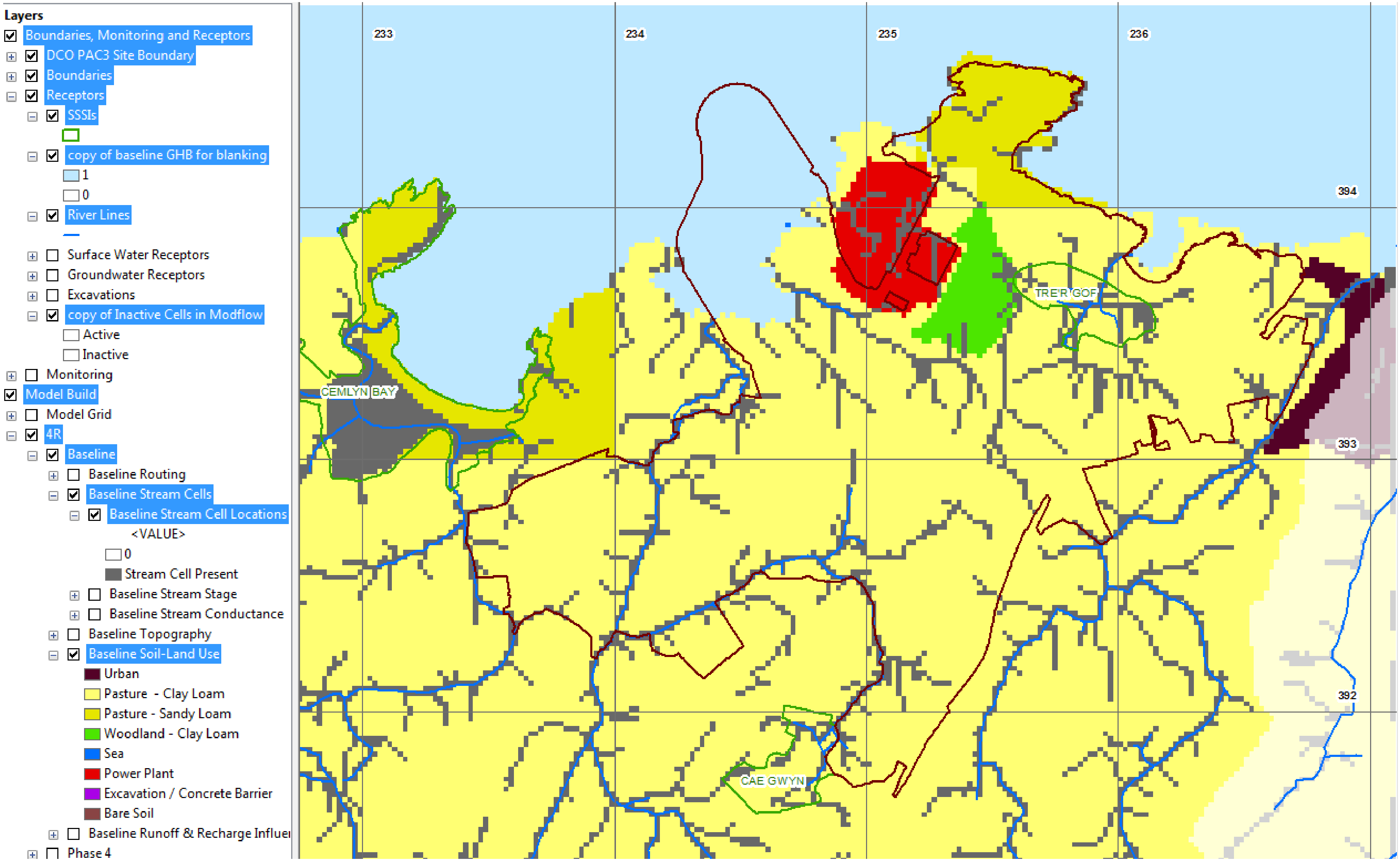

Layers
Boundaries, Monitoring and Receptors
DCO PAC3 Site Boundary
Boundaries
Receptors
SSSIs
copy of baseline GHB for blanking
1
0
River Lines
Surface Water Receptors
Groundwater Receptors
Excavations
copy of Inactive Cells in Modflow
Active
Inactive
Monitoring
Model Build
Model Grid
4R
Baseline
Baseline Routing
Baseline Stream Cells
Baseline Stream Cell Locations
<VALUE>
0
Stream Cell Present
Baseline Stream Stage
Baseline Stream Conductance
Baseline Topography
Baseline Soil-Land Use
Urban
Pasture - Clay Loam
Pasture - Sandy Loam
Woodland - Clay Loam
Sea
Power Plant
Excavation / Concrete Barrier
Bare Soil
Baseline Runoff & Recharge Influe
Phase 4
233
234
235
236
394
393
392
CEMLYN BAY
TRE'R GOF
CAE GWYN

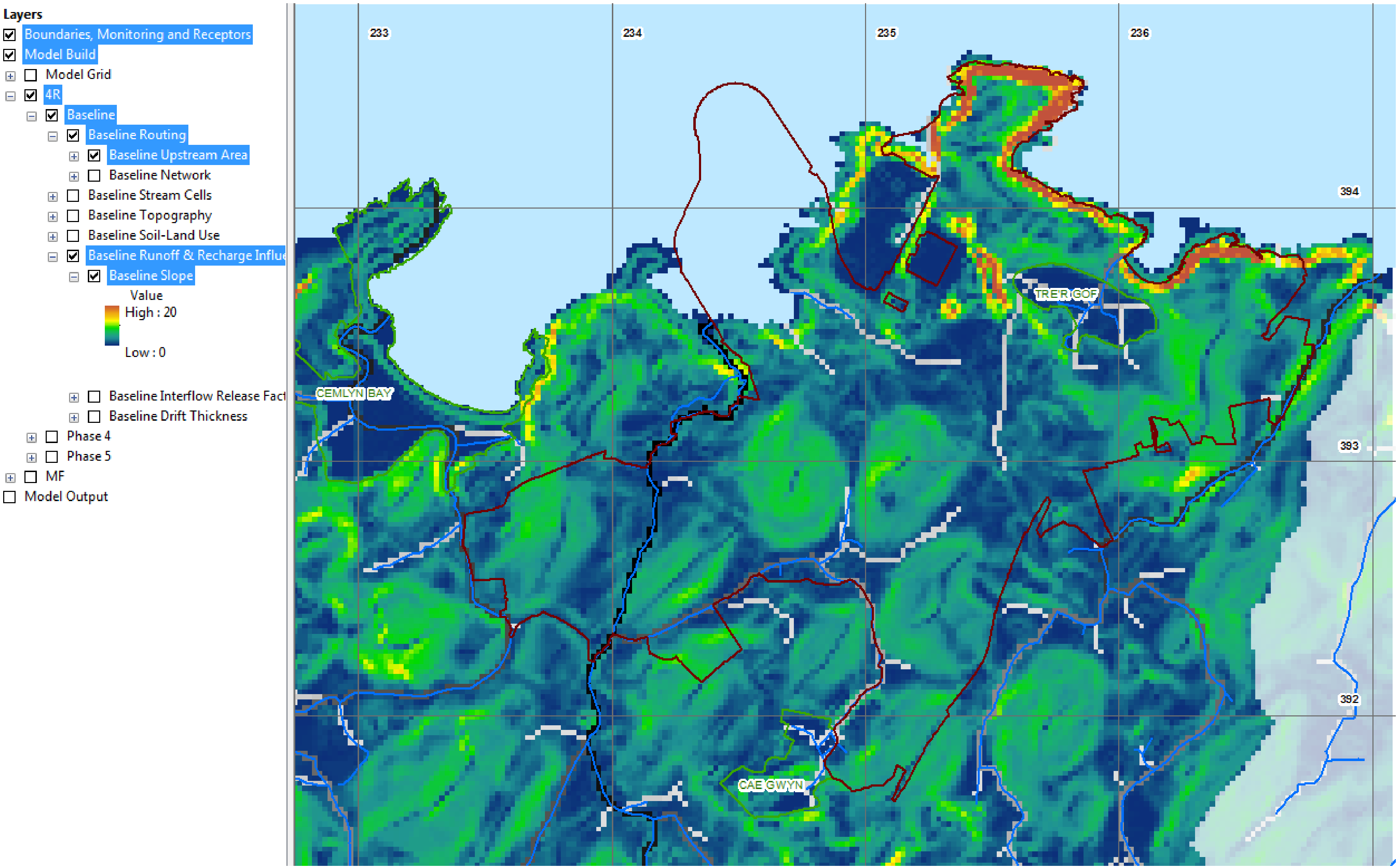

Baseline rivers, SSSI receptors, Site boundary, 4R upstream routed area and slope, MODFLOW General Head Boundary sea bed, and Inactive cell overlay

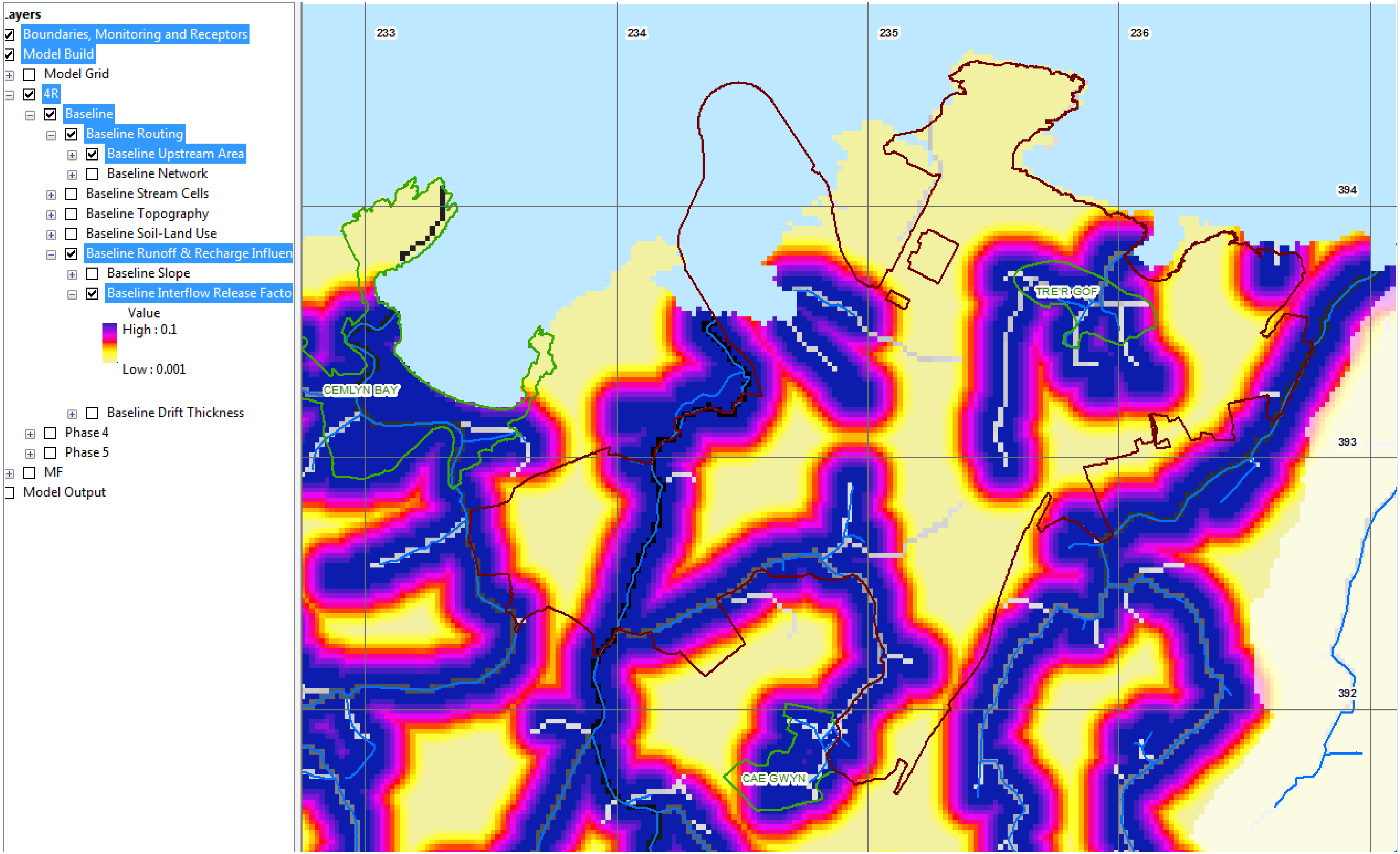

WylDCOGWMod_35989N1403i1 Appendix B, Baseline model build and output plans from 35989X1409Map\WylDCOModelMap.mxd

4

Baseline rivers, SSSI receptors, Site boundary, 4R upstream routed area and interflow release factor, MODFLOW General Head Boundary sea bed, and Inactive cell overlay

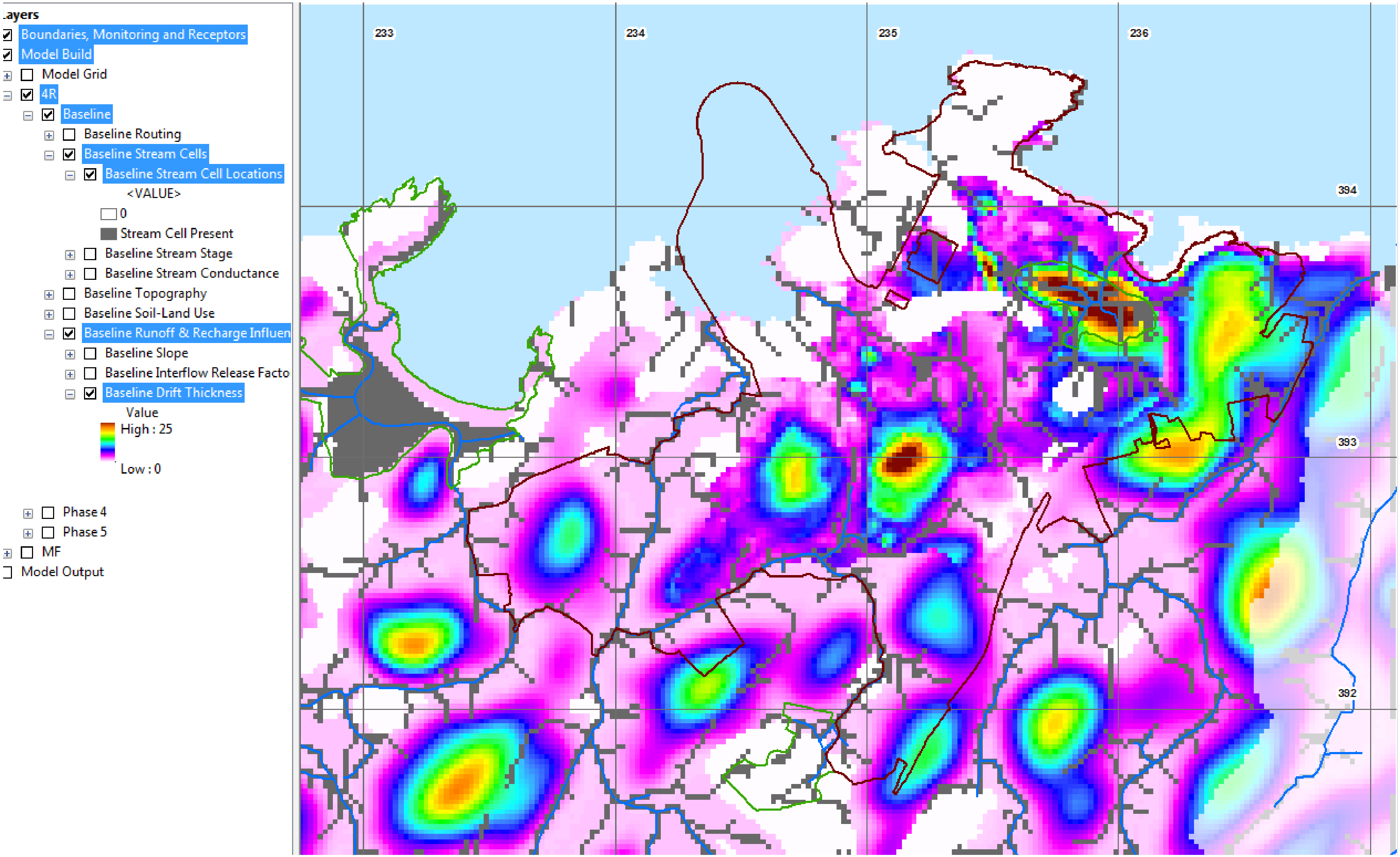

Baseline rivers, SSSI receptors, Site boundary, Drift thickness, MODFLOW General Head Boundary sea bed & Stream cells, and Inactive cell overlay

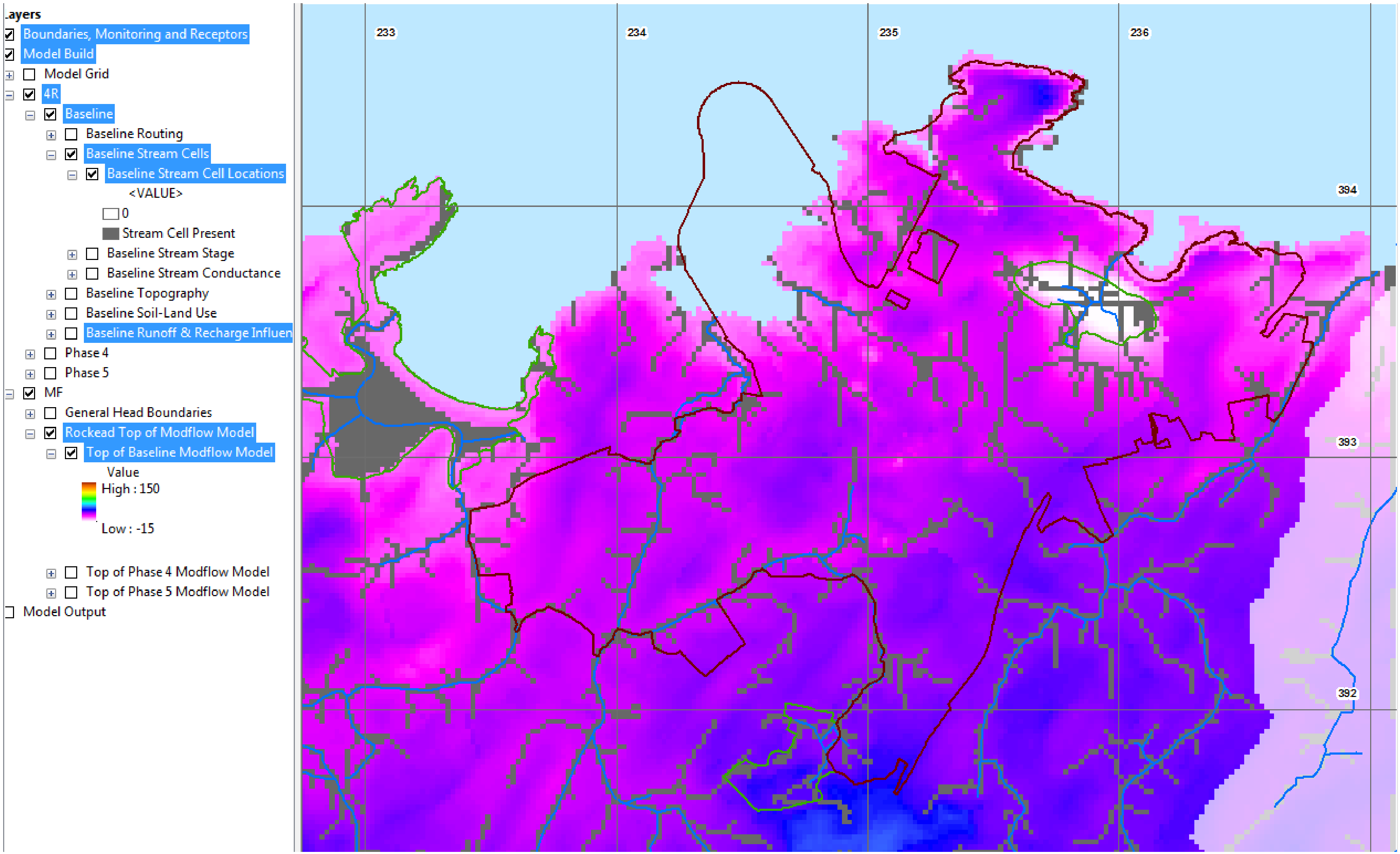

WylDCOGWMod_35989N1403i1 Appendix B, Baseline model build and output plans from 35989X1409Map\WylDCOModelMap.mxd

Baseline rivers, SSSI receptors, Site boundary, MODFLOW General Head Boundary sea bed & Stream cells, top of bedrock layer elevation (rock head) and Inactive cell overlay

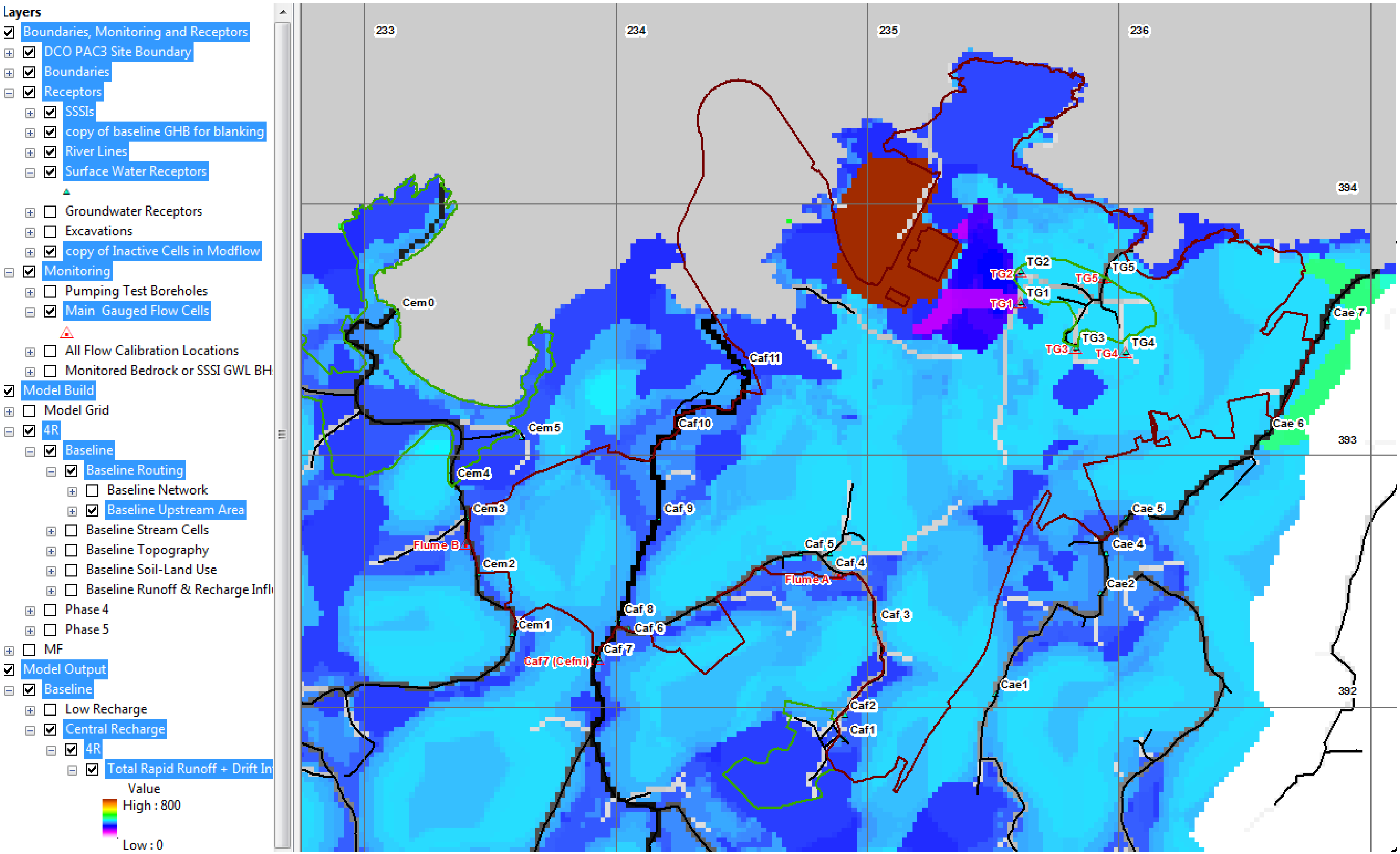

amec foster wheeler

WylDCOGWMod_35989N1403i1 Appendix B, Baseline model build and output plans from 35989X1409Map\WylDCOModelMap.mxd

7

Baseline rivers, SSSI receptors, Site boundary, SW flow receptors & main gauging sites, 4R upstream routed area and Central Model rapid runoff + interflow output, MODFLOW GHB cells and Inactive cell overlay

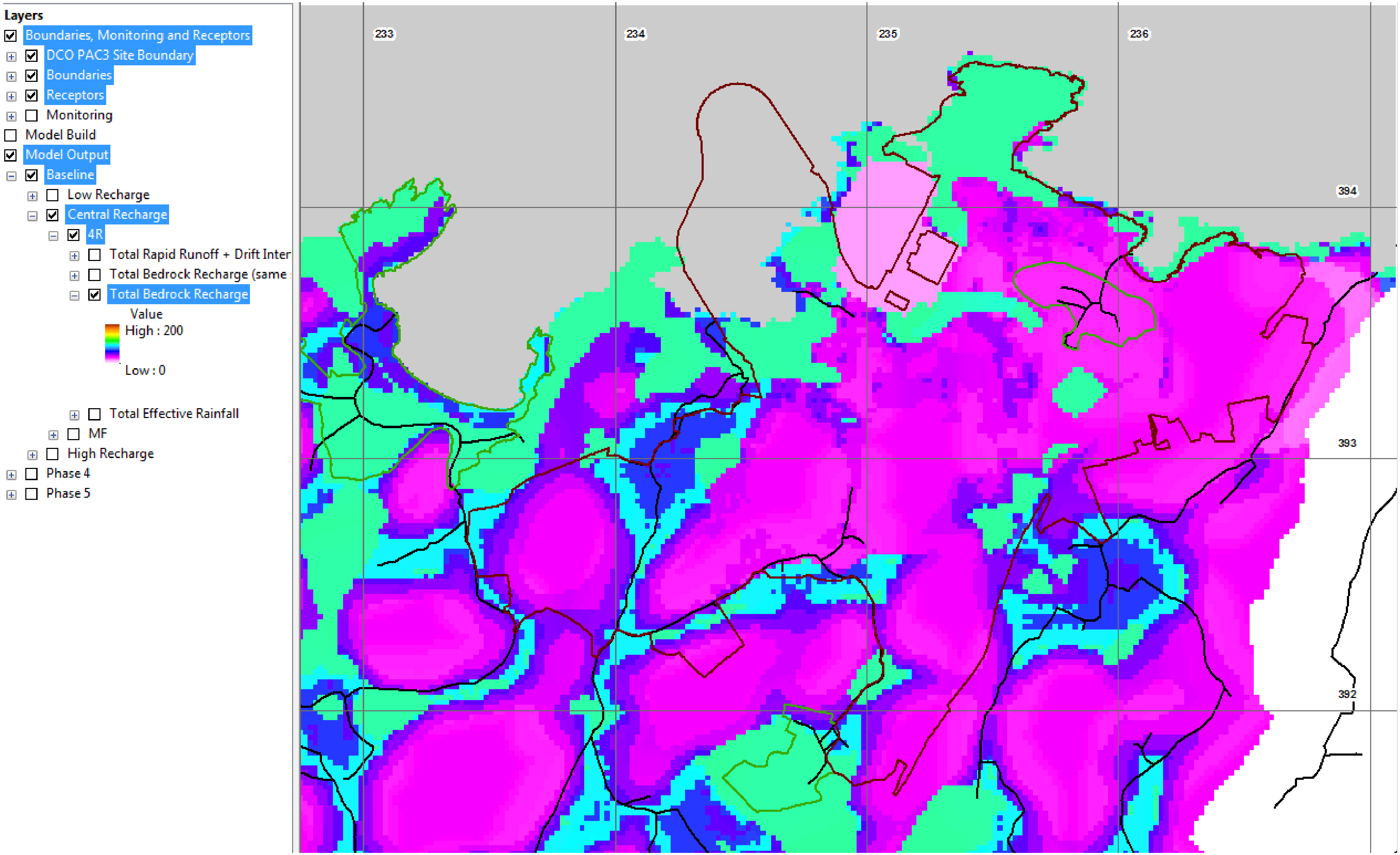

Layers
Boundaries, Monitoring and Receptors
DCO PAC3 Site Boundary
Boundaries
Receptors
Monitoring
Model Build
Model Output
Baseline
Low Recharge
Central Recharge
4R
Total Rapid Runoff + Drift Inter
Total Bedrock Recharge (same
Total Bedrock Recharge
Value
High : 200
Low : 0
Total Effective Rainfall
MF
High Recharge
Phase 4
Phase 5
233
234
235
236
394
393
392

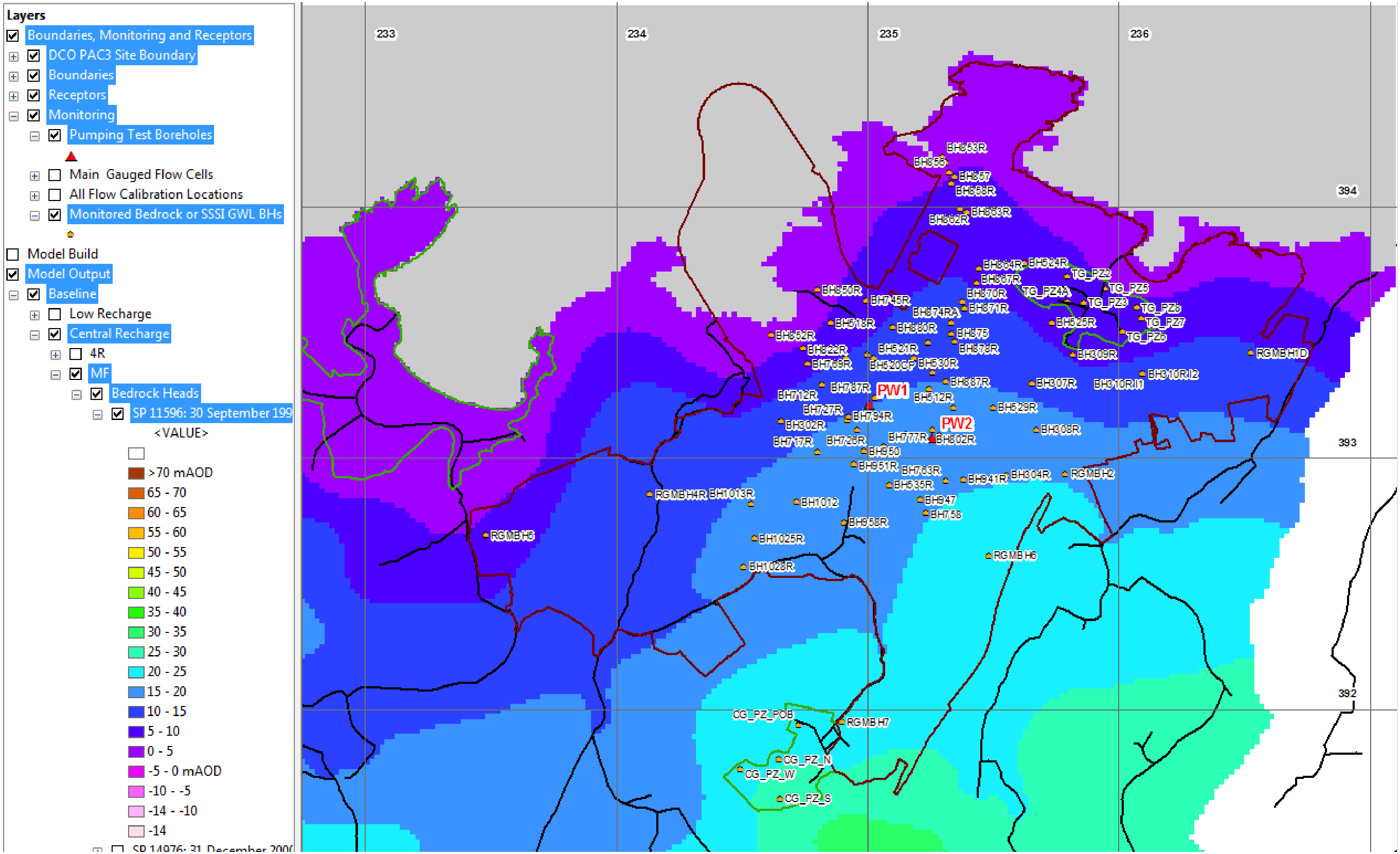

WylDCOGWMod_35989N1403i1 Appendix B, Baseline model build and output plans from 35989X1409Map\WylDCOModelMap.mxd

Baseline rivers, SSSI receptors, Site boundary, monitored bedrock or SSSI boreholes, pumping test boreholes MODFLOW Central Model dry period (30/09/91) bedrock heads with GHB cells and Inactive cell overlay

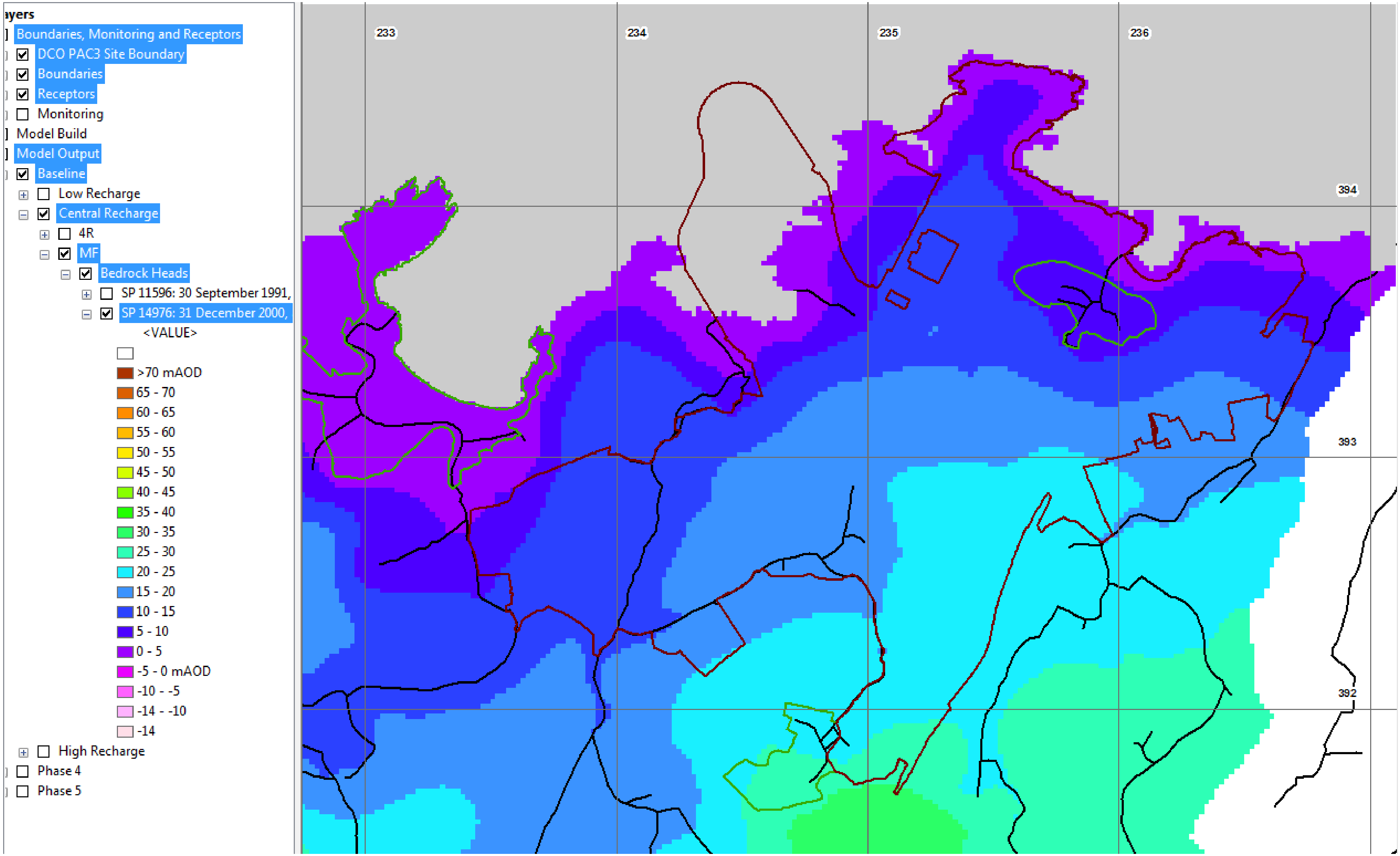

Baseline rivers, SSSI receptors, Site boundary, MODFLOW Central Model wet period (31/12/2000) bedrock heads with GHB cells and Inactive cell overlay

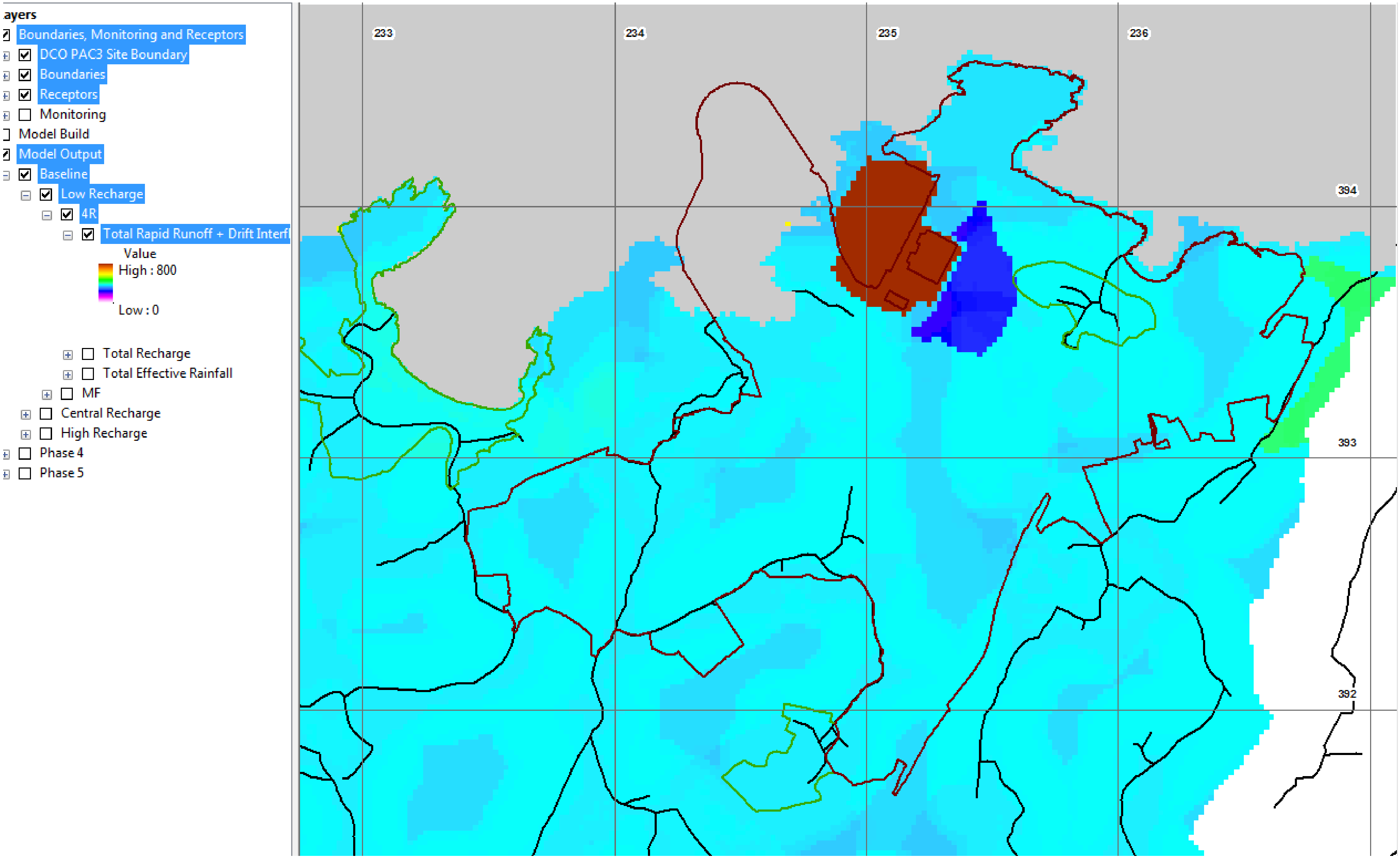

Baseline rivers, SSSI receptors, Site boundary, and 4R Low Model rapid runoff + interflow output, MODFLOW GHB cells and Inactive cell overlay

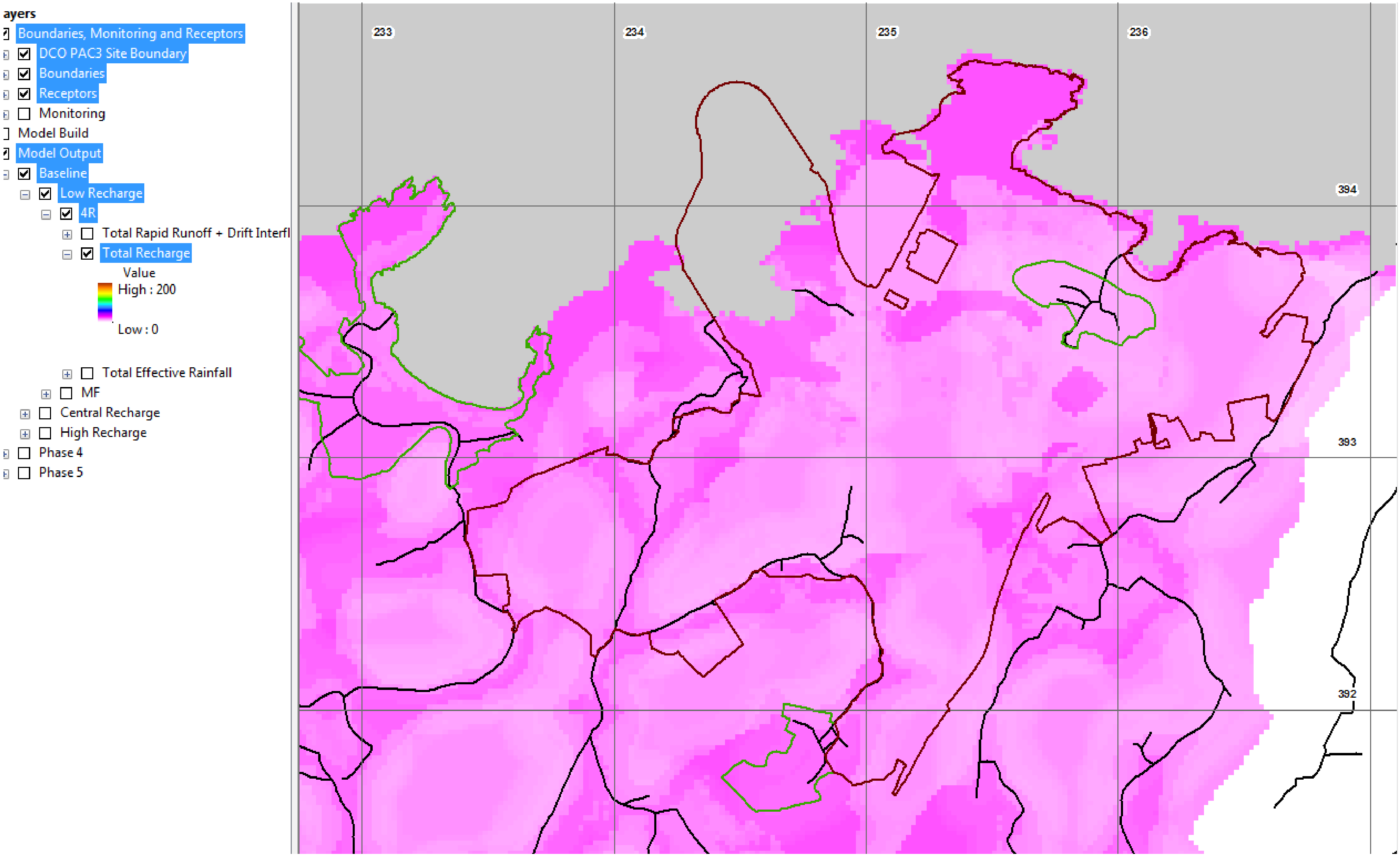

Baseline rivers, SSSI receptors, Site boundary, 4R Low Model bedrock recharge, MODFLOW GHB cells and Inactive cell overlay

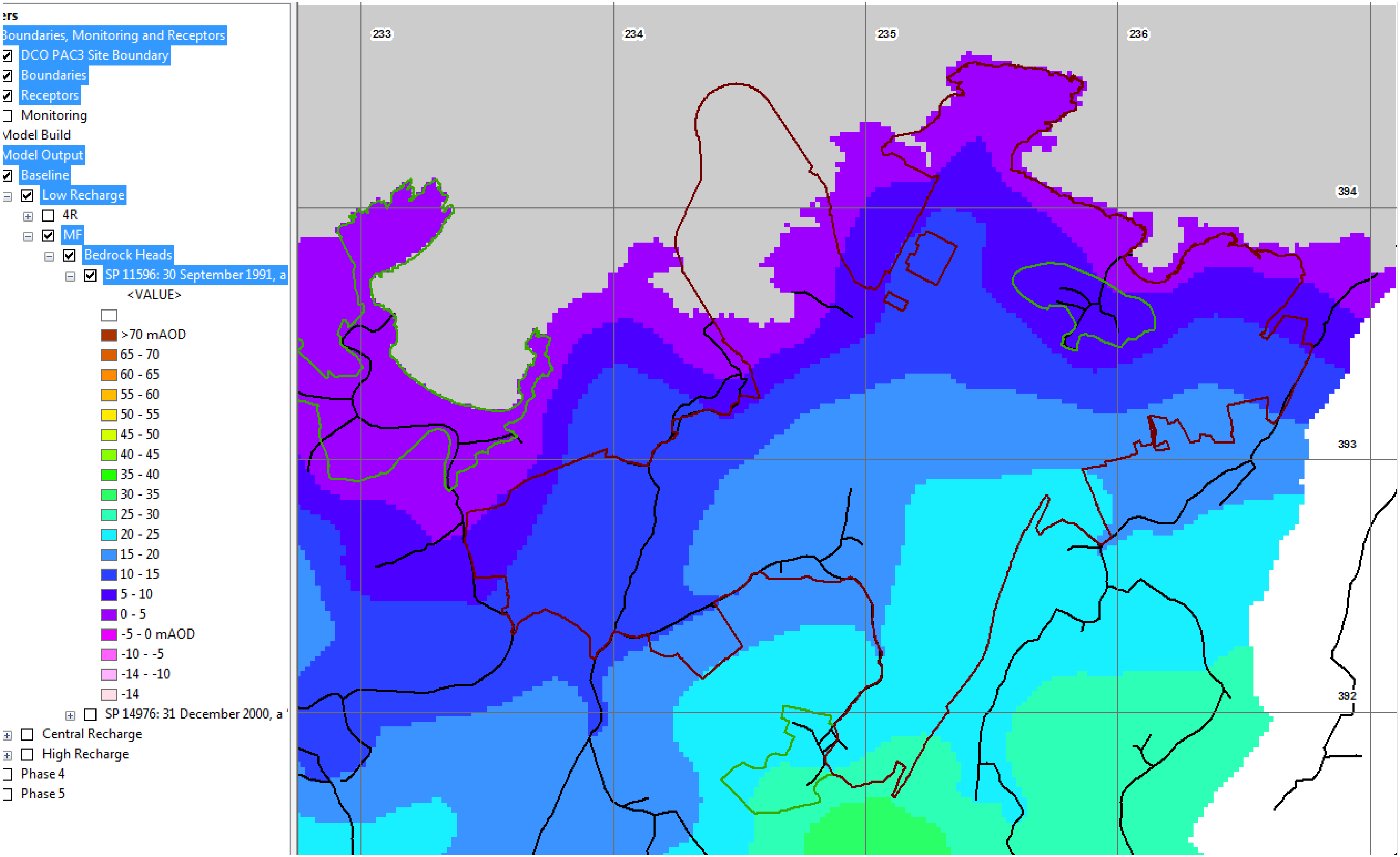

WylDCOGWMod_35989N1403i1 Appendix B, Baseline model build and output plans from 35989X1409Map\WylDCOModelMap.mxd

Baseline rivers, SSSI receptors, Site boundary, and MODFLOW Low Model dry period (30/09/91) bedrock heads with GHB cells and Inactive cell overlay

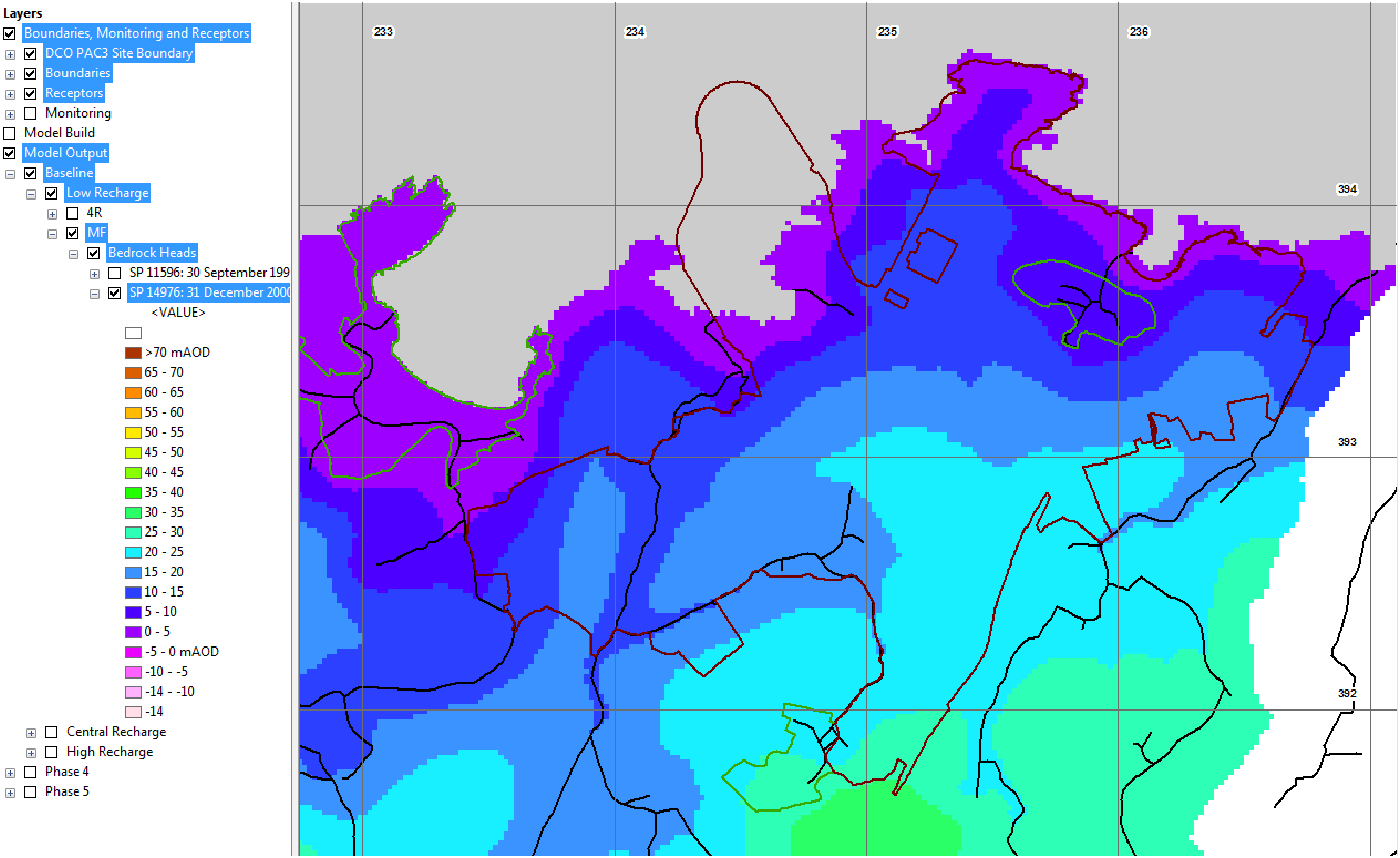

Baseline rivers, SSSI receptors, Site boundary, MODFLOW Low Model wet period (31/12/2000) bedrock heads with GHB cells and Inactive cell overlay

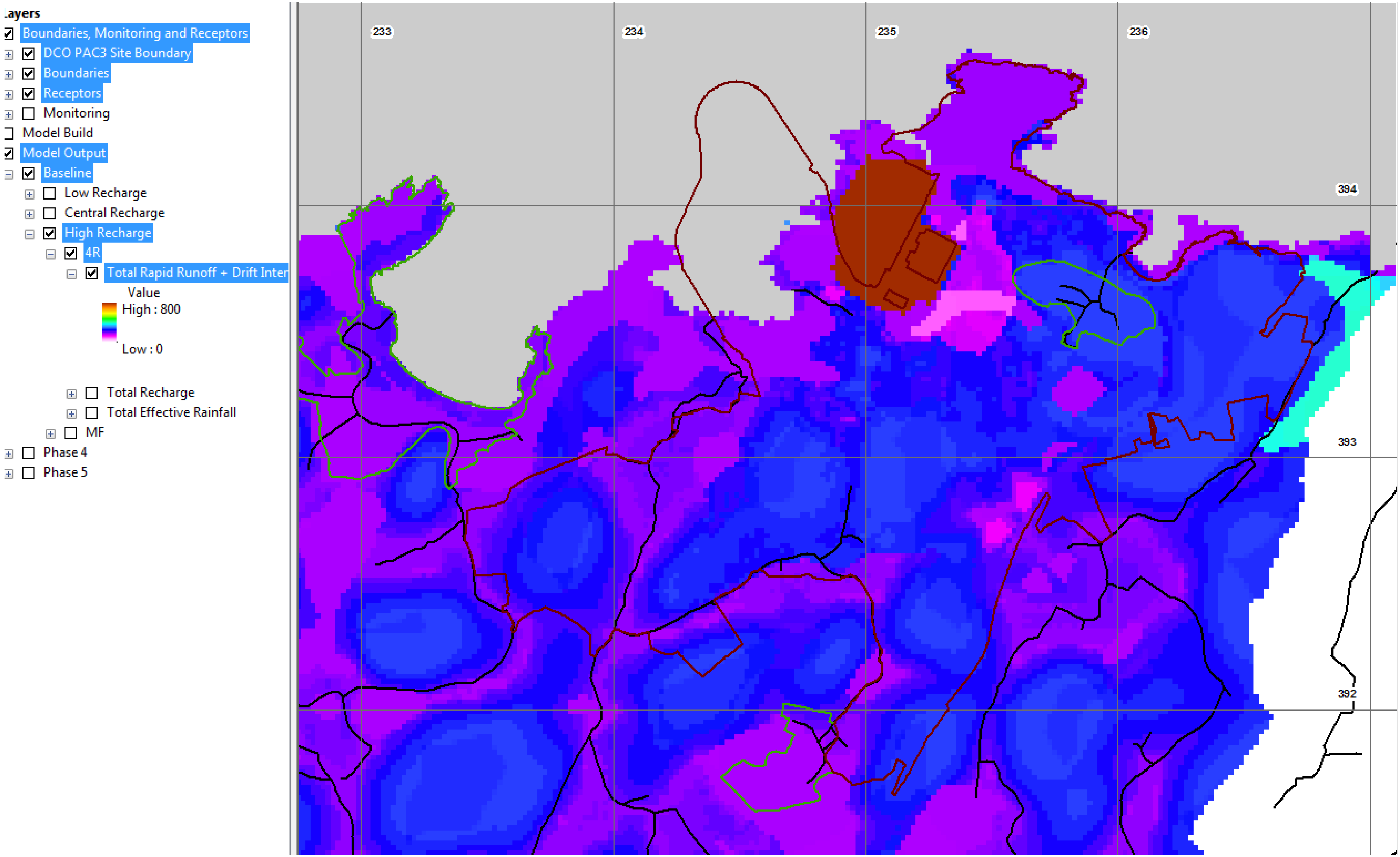

Baseline rivers, SSSI receptors, Site boundary, and 4R High Model rapid runoff + interflow output, MODFLOW GHB cells and Inactive cell overlay

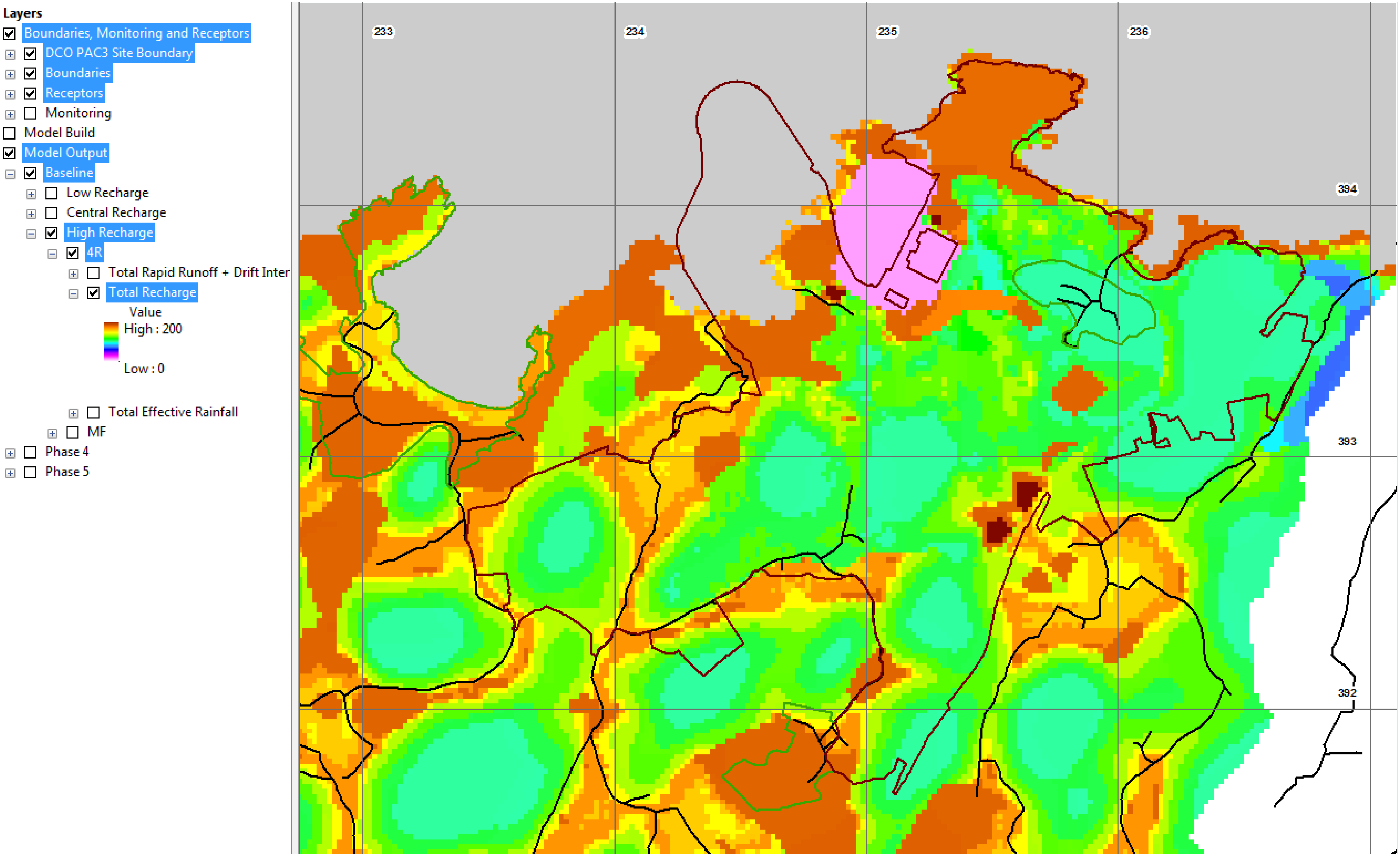

Baseline rivers, SSSI receptors, Site boundary, 4R High Model bedrock recharge, MODFLOW GHB cells and Inactive cell overlay

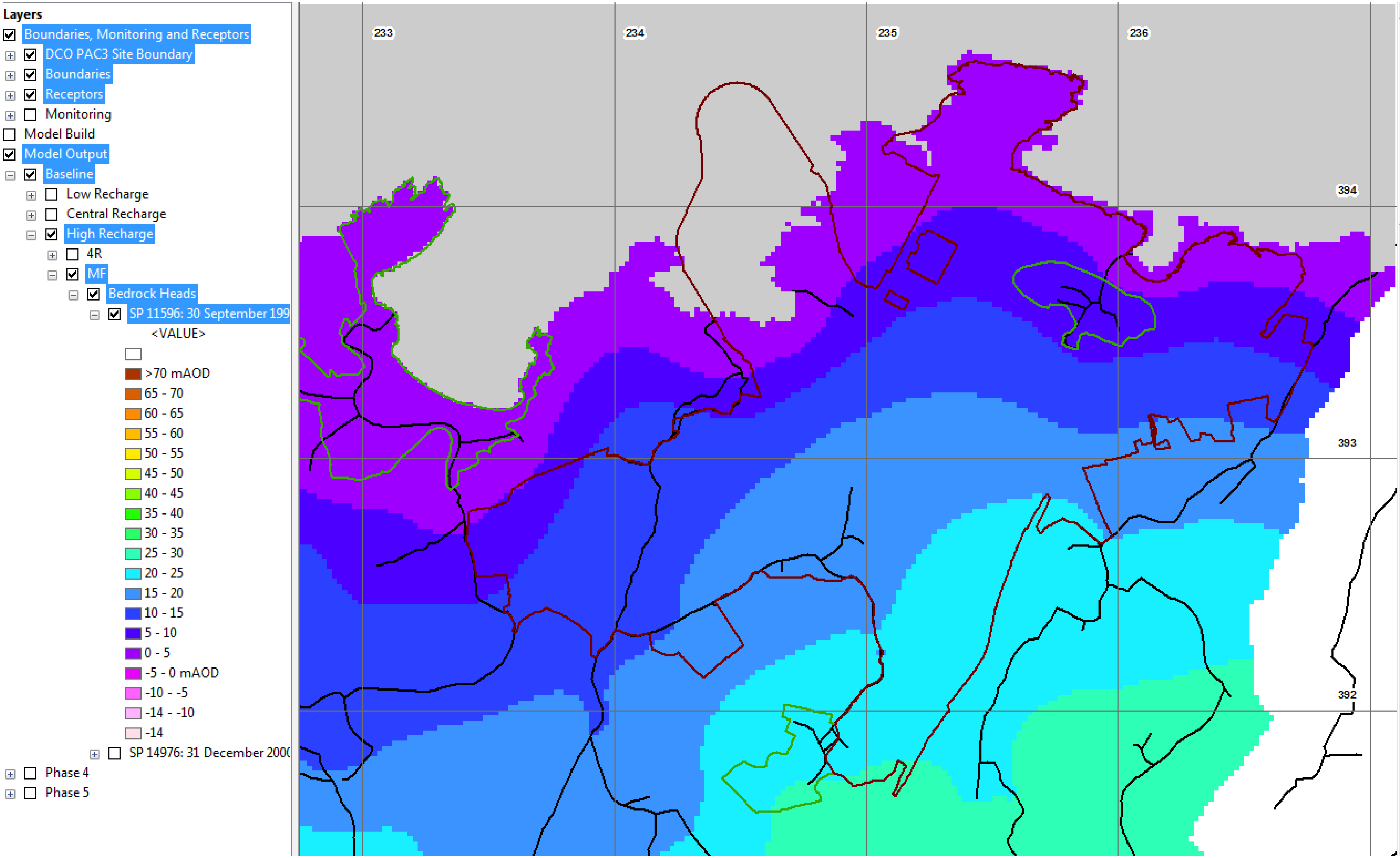

Baseline rivers, SSSI receptors, Site boundary, and MODFLOW High Model dry period (30/09/91) bedrock heads with GHB cells and Inactive cell overlay

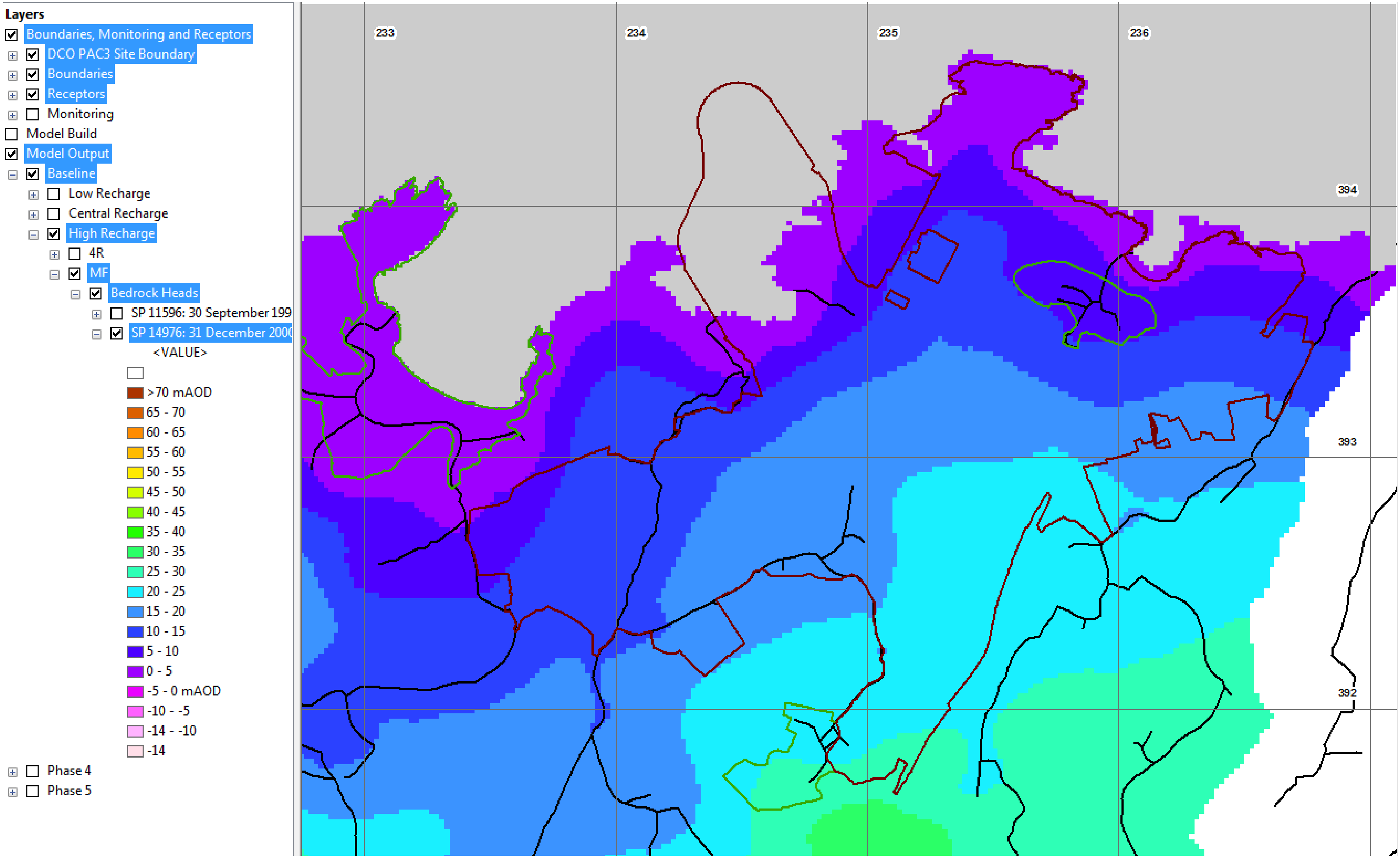

Baseline rivers, SSSI receptors, Site boundary, MODFLOW High Model wet period (31/12/2000) bedrock heads with GHB cells and Inactive cell overlay

Appendix C
Groundwater level and stream flow data with baseline historical model calibration

Borehole	GL mAOD	RH mAOD (SDTM)	Aquifer	Easting	Northing
BH301R	14.77	12.88	Bedrock	234918.2	393397.5
BH302R	21.37	17.65	Bedrock	234655.2	393148.0
BH303R	34.34	19.70	Bedrock	235102.3	393018.7
BH304R	21.65	20.07	Bedrock	235555.6	392932.5
BH305AR	16.57	15.50	Bedrock	235245.2	393272.5
BH305R	16.57	15.50	Bedrock	235245.2	393272.5
BH306R	14.87	13.84	Bedrock	235243.9	393457.5
BH307R	16.24	15.28	Bedrock	235657.3	393296.5
BH308R	21.22	19.68	Bedrock	235671.8	393112.7
BH309R	9.45	8.36	Bedrock	235816.1	393410.5
BH310R I1	11.98	10.81	Bedrock	236096.6	393334.7
BH310R I2	11.98	10.81	Bedrock	236096.6	393334.7
BH512R	18	16.63	Bedrock	235341.8	393197.4
BH516R	15.39	14.18	Bedrock	235258.0	393340.1
BH518R	9.63	7.37	Bedrock	234854.6	393536.1
BH520CP	15.446	13.96	Bedrock	235001.5	393411.4
BH521R	16.55	14.81	Bedrock	235026.0	393395.1
BH523RD	19.74	18.12	Bedrock	235489.3	393971.5
BH524R	9.56	7.45	Bedrock	235623.8	393776.7
BH525R	10.76	9.18	Bedrock	235735.9	393538.1
BH526RD	7.89	4.08	Bedrock	236005.9	393683.2
BH529R	17.087	15.81	Bedrock	235502.6	393199.8
BH530R	14.77	13.74	Bedrock	235185.2	393395.0
BH534RA	30.825	18.56	Bedrock	235153.3	393091.8
BH535R	32.485	19.34	Bedrock	235086.6	392893.2
BH536R	16.732	14.23	Bedrock	234707.7	393238.2
BH712R	17.01	15.26	Bedrock	234818.8	393289.7
BH717R	32.76	16.64	Bedrock	234802.4	393021.4
BH726R	20.88	16.56	Bedrock	234961.1	393109.9
BH727R	20.42	15.84	Bedrock	234922.3	393148.6
BH745R	12.02	9.83	Bedrock	234995.1	393626.6
BH763R	26.91	14.32	Bedrock	235312.3	392907.5
BH769R	12.95	11.84	Bedrock	234761.8	393376.2
BH787R	18.58	15.52	Bedrock	235031.3	393239.7
BH794R	19.67	15.65	Bedrock	234925.1	393165.6
BH801R	26.67	16.30	Bedrock	235287.3	393088.2
BH802R	26.47	17.21	Bedrock	235257.3	393112.5
BH822R	8.88	7.55	Bedrock	234745.6	393438.5
BH850R	5.38	3.40	Bedrock	234804.2	393668.5
BH852R	8.65	6.09	Bedrock	234617.1	393487.8
BH853R	12.98	8.47	Bedrock	235297.7	394197.1
BH856	12.91	11.29	Bedrock	235327.5	394133.8
BH862R	16.62	15.15	Bedrock	235368.6	393992.6
BH863R	17.52	16.07	Bedrock	235394.5	393979.2
BH864R	19.07	14.71	Bedrock	235443.1	393754.4
BH867R	16.81	15.23	Bedrock	235435.3	393695.3

BH870R	21.1	18.90	Bedrock	235377.2	393619.4
BH871R	20.05	16.29	Bedrock	235387.0	393596.7
BH874RA	15.65	13.06	Bedrock	235334.7	393536.3
BH878R	15.06	13.82	Bedrock	235348.2	393462.4
BH880R	20.28	16.34	Bedrock	235099.8	393518.6
BH887R	16.84	15.63	Bedrock	235313.9	393303.7
BH941R	22.23	16.61	Bedrock	235382.4	392915.0
BH951R	20.5	14.37	Bedrock	234949.4	392975.6
BH958R	17.12	14.77	Bedrock	234906.7	392743.0
BH1012	34.59	16.08	Bedrock	234718.6	392823.2
BH1013R	21.67	16.86	Bedrock	234536.6	392818.4
BH1025R	18.33	14.78	Bedrock	234550.7	392679.7
BH1028R	16.7	14.55	Bedrock	234508.3	392566.6
RGMBH1D	21	6.92	Bedrock	236525.5	393417.7
RGMBH2	25.63	23.73	Bedrock	235788.7	392937.3
RGMBH4R	14.84	13.35	Bedrock	234133.3	392855.5
RGMBH5	9.21	7.11	Bedrock	233481.1	392692.8
RGMBH6	25.5	23.01	Bedrock	235484.6	392612.0
RGMBH7	24.65	22.76	Bedrock	234898.6	391949.7
RGMBH13	31.69	29.65	Bedrock	234648.2	391385.5
BH777R	28.1	18.46	Bedrock/Superficial	235064.0	393044.8
BH858R	12.5	11.31	Bedrock/Superficial	235335.8	394090.9
BH758	23.12	16.31		235231.4	392781.5
BH854RA	12.54	10.40	Not specified*	235311.5	394173.7
BH857	12.83	11.43	Not specified*	235346.4	394120.0
BH875	15.11	13.43	Not specified*	235334.0	393494.3
BH947	26.77	15.76	Not specified*	235210.2	392832.1
BH950	21	15.49	Not specified*	234985.2	393027.1
CG_PZ_S	28.12	N/A	Superficial	234650.7	391642.7
CG_PZ_W	23.12	N/A	Superficial	234492.8	391759.7
CG_PZ_N	25.73	N/A	Superficial	234649.1	391799.7
CG_PZ_POB	23.04	N/A	Superficial	234728.5	391936.3
TG_PZ1A	6.4147	N/A	Superficial	235710.0524	393654.115
TG_PZ2	6.3471	N/A	Superficial	235794.0237	393724.1497
TG_PZ3	6.5319	N/A	Superficial	235860.9206	393618.4778
TG_PZ4A	6.7513	N/A	Superficial	235797.5647	393619.7953
TG_PZ5	6.4766	N/A	Superficial	235943.9115	393675.6609
TG_PZ6	7.2749	N/A	Superficial	236014.1209	393502.9293
TG_PZ7	7.0527	N/A	Superficial	236089.1946	393554.0302
TG_PZ8	7.3993	N/A	Superficial	236071.0087	393598.7374
TG_PZ8_unanch	7.2625	N/A	Superficial	236071.0106	393598.74

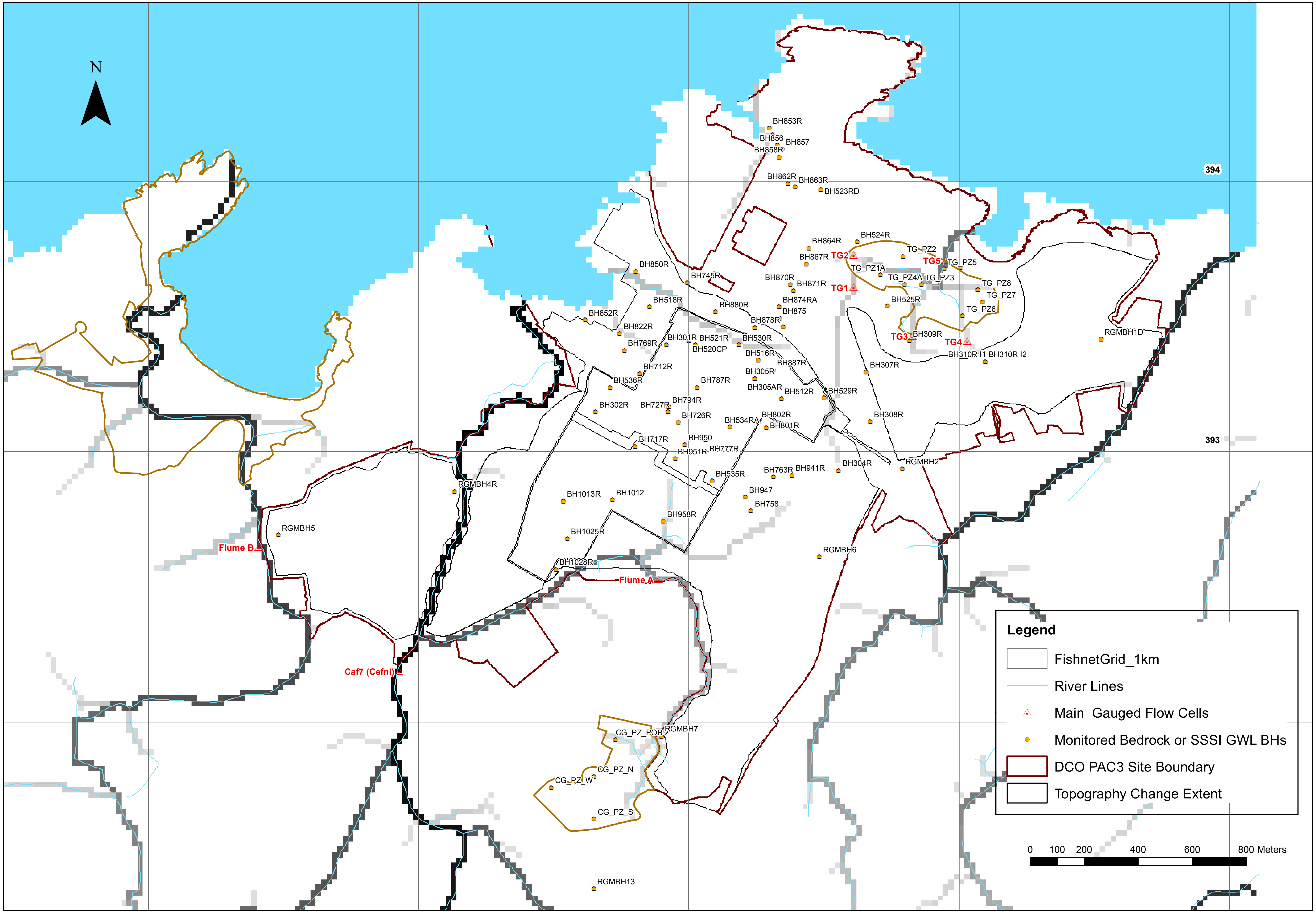

N
394
393
BH853R
BH856
BH857
BH858R
BH862R
BH863R
BH523RD
BH864R
BH524R
BH867R
TG2
TG_PZ2
TG5
TG_PZ5
TG_PZ1A
BH850R
BH745R
BH870R
BH871R
TG1
TG_PZ4A
TG_PZ3
TG_PZ8
TG_PZ7
BH518R
BH880R
BH874RA
BH525R
TG_PZ6
BH852R
BH875
BH878R
BH822R
TG3
BH309R
TG4
RGMBH1D
BH769R
BH301R
BH521R
BH530R
BH520CP
BH516R
BH310R I1
BH310R I2
BH712R
BH887R
BH307R
BH536R
BH787R
BH305R
BH305AR
BH512R
BH529R
BH794R
BH302R
BH727R
BH726R
BH802R
BH308R
BH534RA
BH801R
BH717R
BH950
BH951R
BH777R
BH304R
RGMBH2
BH763R
BH941R
BH535R
RGMBH4R
BH947
BH1013R
BH1012
BH758
BH958R
RGMBH5
BH1025R
Flume B
RGMBH6
BH1028R
Flume A
Caf7 (Cefni)
CG_PZ_POB
RGMBH7
CG_PZ_N
CG_PZ_W
CG_PZ_S
RGMBH13
Legend
FishnetGrid_1km
River Lines
Main Gauged Flow Cells
Monitored Bedrock or SSSI GWL BHs
DCO PAC3 Site Boundary
Topography Change Extent
0
100
200
400
600
800 Meters

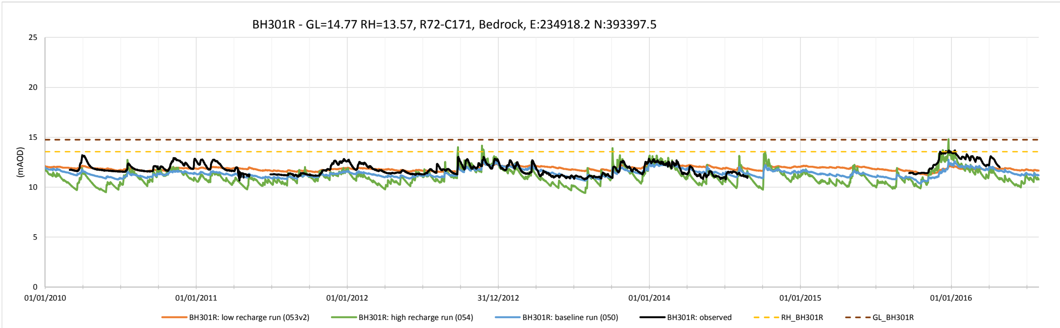
BH301R - GL=14.77 RH=13.57, R72-C171, Bedrock, E:234918.2 N:393397.5
(mAOD)
0
5
10
15
20
25
01/01/2010
01/01/2011
01/01/2012
31/12/2012
01/01/2014
01/01/2015
01/01/2016
BH301R: low recharge run (053v2)
BH301R: high recharge run (054)
BH301R: baseline run (050)
BH301R: observed
RH_BH301R
GL_BH301R

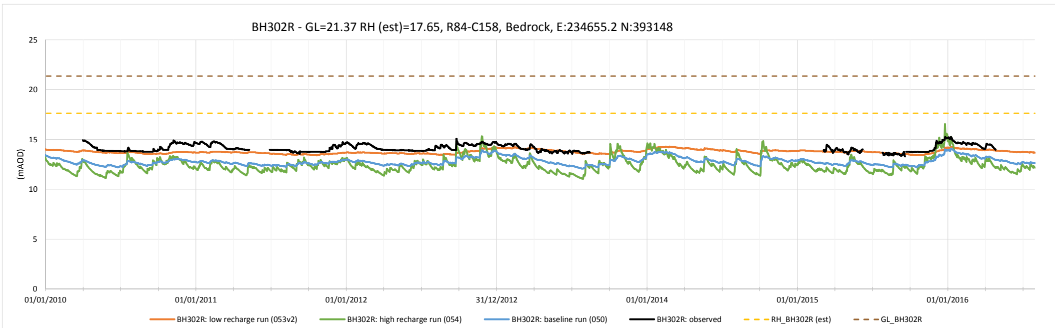
BH302R - GL=21.37 RH (est)=17.65, R84-C158, Bedrock, E:234655.2 N:393148
(mAOD)
0
5
10
15
20
25
01/01/2010
01/01/2011
01/01/2012
31/12/2012
01/01/2014
01/01/2015
01/01/2016
BH302R: low recharge run (053v2)
BH302R: high recharge run (054)
BH302R: baseline run (050)
BH302R: observed
RH_BH302R (est)
GL_BH302R

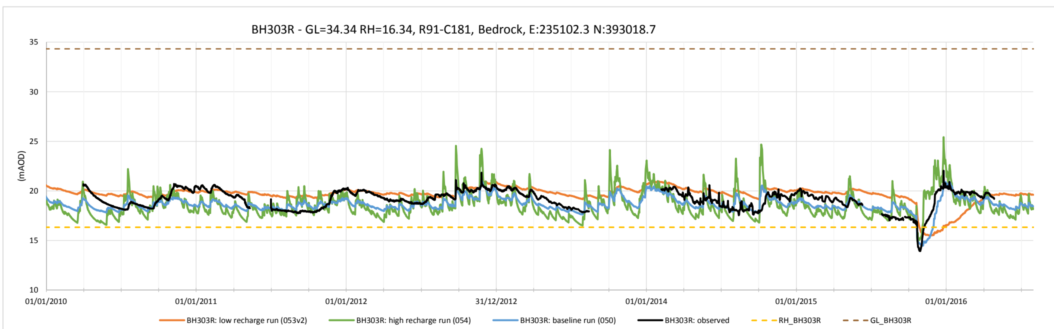
BH303R - GL=34.34 RH=16.34, R91-C181, Bedrock, E:235102.3 N:393018.7
(mAOD)
10
15
20
25
30
35
01/01/2010
01/01/2011
01/01/2012
31/12/2012
01/01/2014
01/01/2015
01/01/2016
BH303R: low recharge run (053v2)
BH303R: high recharge run (054)
BH303R: baseline run (050)
BH303R: observed
RH_BH303R
GL_BH303R

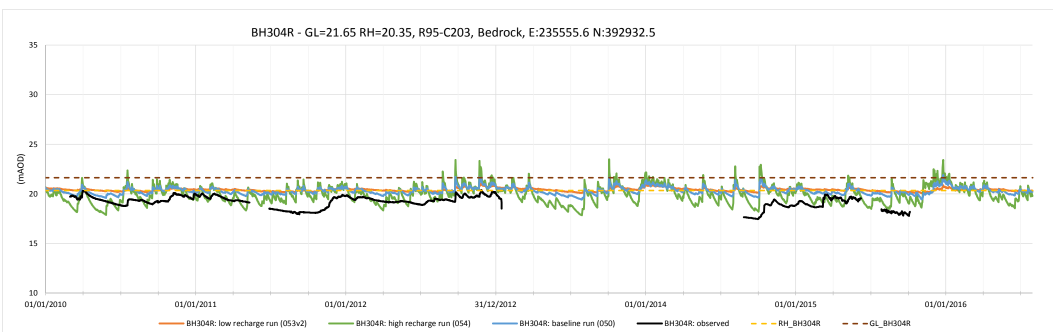
BH304R - GL=21.65 RH=20.35, R95-C203, Bedrock, E:235555.6 N:392932.5
(mAOD)
10
15
20
25
30
35
01/01/2010
01/01/2011
01/01/2012
31/12/2012
01/01/2014
01/01/2015
01/01/2016
BH304R: low recharge run (053v2)
BH304R: high recharge run (054)
BH304R: baseline run (050)
BH304R: observed
RH_BH304R
GL_BH304R

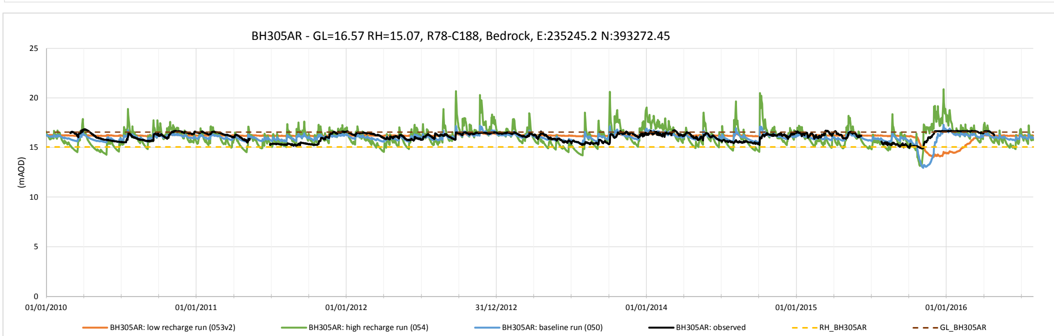
BH305AR - GL=16.57 RH=15.07, R78-C188, Bedrock, E:235245.2 N:393272.45
(mAOD)
0
5
10
15
20
25
01/01/2010
01/01/2011
01/01/2012
31/12/2012
01/01/2014
01/01/2015
01/01/2016
BH305AR: low recharge run (053v2)
BH305AR: high recharge run (054)
BH305AR: baseline run (050)
BH305AR: observed
RH_BH305AR
GL_BH305AR

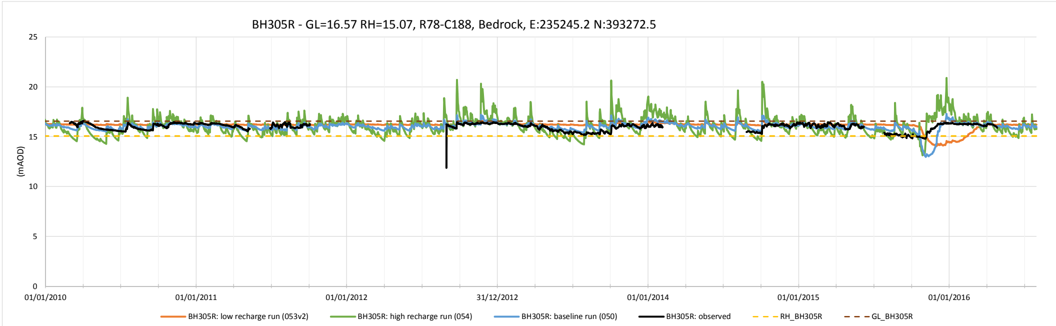
BH305R - GL=16.57 RH=15.07, R78-C188, Bedrock, E:235245.2 N:393272.5
25
20
15
10
5
0
(mAOD)
01/01/2010
01/01/2011
01/01/2012
31/12/2012
01/01/2014
01/01/2015
01/01/2016
BH305R: low recharge run (053v2)
BH305R: high recharge run (054)
BH305R: baseline run (050)
BH305R: observed
RH_BH305R
GL_BH305R

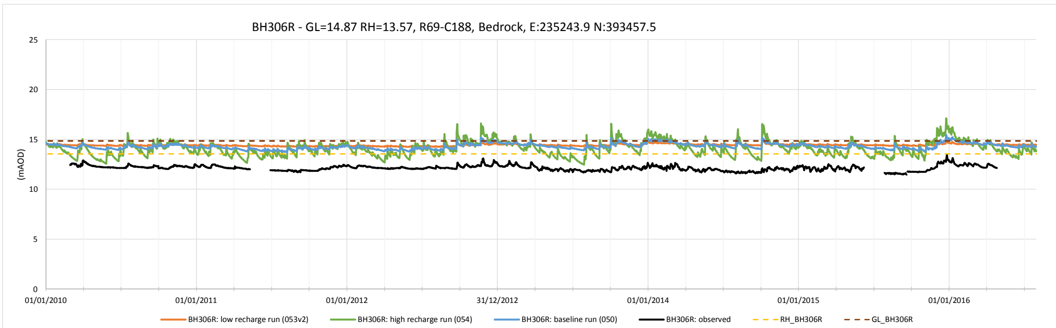
BH306R - GL=14.87 RH=13.57, R69-C188, Bedrock, E:235243.9 N:393457.5
25
20
15
10
5
0
(mAOD)
01/01/2010
01/01/2011
01/01/2012
31/12/2012
01/01/2014
01/01/2015
01/01/2016
BH306R: low recharge run (053v2)
BH306R: high recharge run (054)
BH306R: baseline run (050)
BH306R: observed
RH_BH306R
GL_BH306R

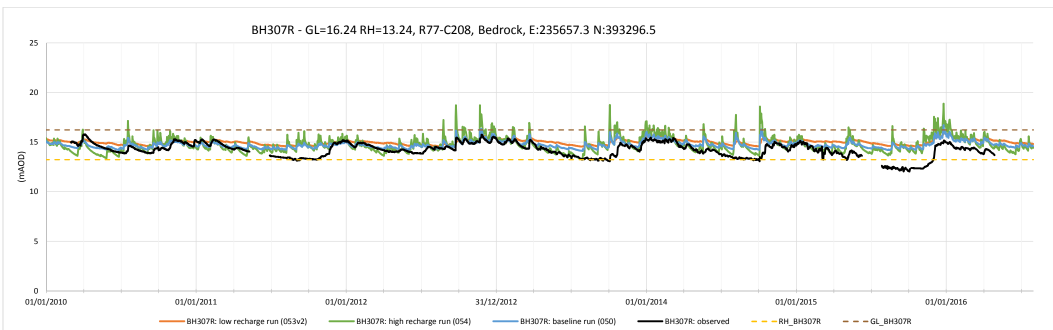
BH307R - GL=16.24 RH=13.24, R77-C208, Bedrock, E:235657.3 N:393296.5
25
20
15
10
5
0
(mAOD)
01/01/2010
01/01/2011
01/01/2012
31/12/2012
01/01/2014
01/01/2015
01/01/2016
BH307R: low recharge run (053v2)
BH307R: high recharge run (054)
BH307R: baseline run (050)
BH307R: observed
RH_BH307R
GL_BH307R

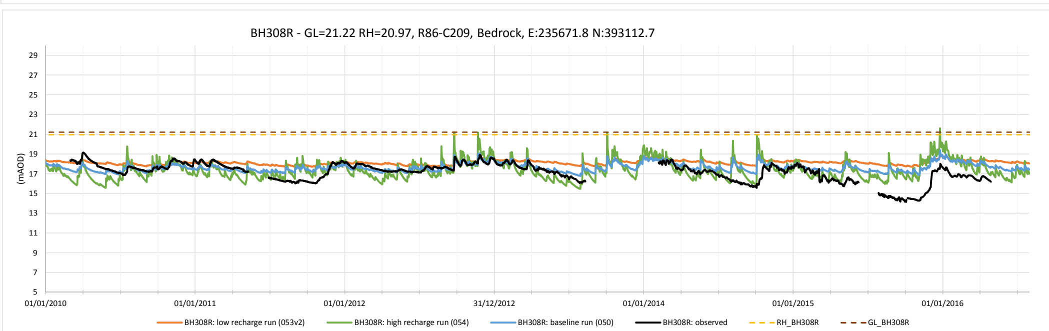
BH308R - GL=21.22 RH=20.97, R86-C209, Bedrock, E:235671.8 N:393112.7
29
27
25
23
21
19
17
15
13
11
9
7
5
(mAOD)
01/01/2010
01/01/2011
01/01/2012
31/12/2012
01/01/2014
01/01/2015
01/01/2016
BH308R: low recharge run (053v2)
BH308R: high recharge run (054)
BH308R: baseline run (050)
BH308R: observed
RH_BH308R
GL_BH308R

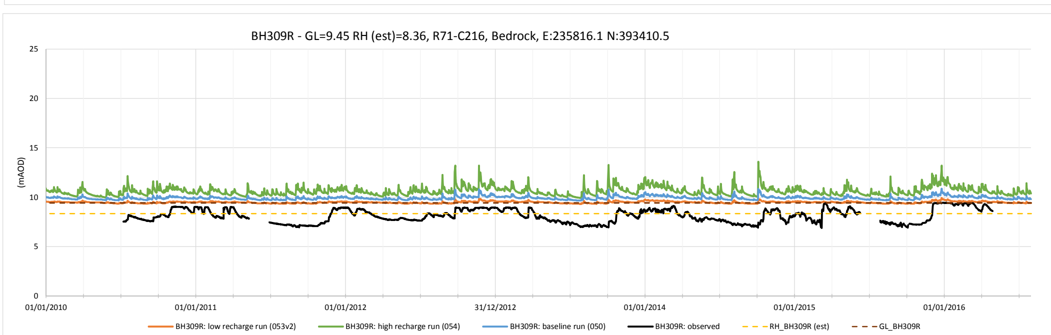
BH309R - GL=9.45 RH (est)=8.36, R71-C216, Bedrock, E:235816.1 N:393410.5
25
20
15
10
5
0
(mAOD)
01/01/2010
01/01/2011
01/01/2012
31/12/2012
01/01/2014
01/01/2015
01/01/2016
BH309R: low recharge run (053v2)
BH309R: high recharge run (054)
BH309R: baseline run (050)
BH309R: observed
RH_BH309R (est)
GL_BH309R

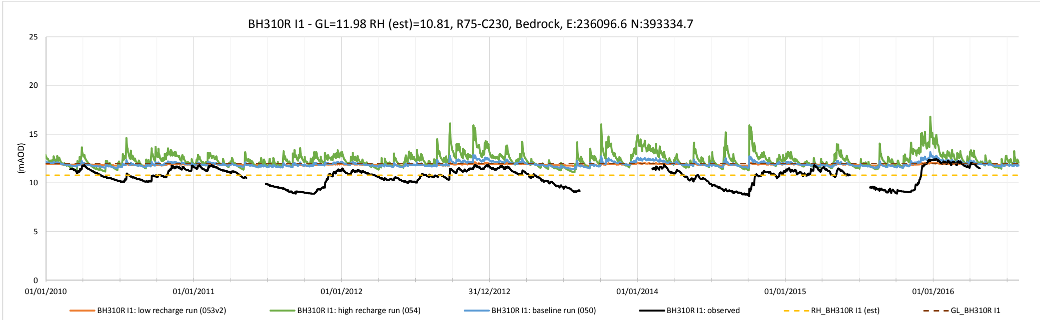
BH310R I1 - GL=11.98 RH (est)=10.81, R75-C230, Bedrock, E:236096.6 N:393334.7
(mAOD)
0
5
10
15
20
25
01/01/2010
01/01/2011
01/01/2012
31/12/2012
01/01/2014
01/01/2015
01/01/2016
BH310R I1: low recharge run (053v2)
BH310R I1: high recharge run (054)
BH310R I1: baseline run (050)
BH310R I1: observed
RH_BH310R I1 (est)
GL_BH310R I1

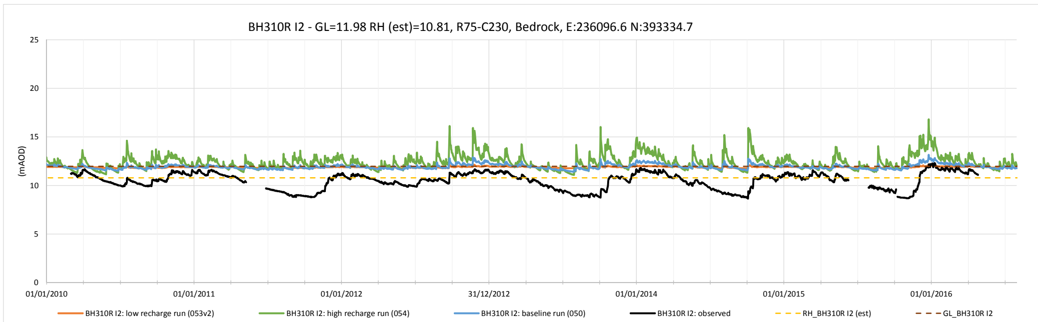
BH310R I2 - GL=11.98 RH (est)=10.81, R75-C230, Bedrock, E:236096.6 N:393334.7
(mAOD)
0
5
10
15
20
25
01/01/2010
01/01/2011
01/01/2012
31/12/2012
01/01/2014
01/01/2015
01/01/2016
BH310R I2: low recharge run (053v2)
BH310R I2: high recharge run (054)
BH310R I2: baseline run (050)
BH310R I2: observed
RH_BH310R I2 (est)
GL_BH310R I2

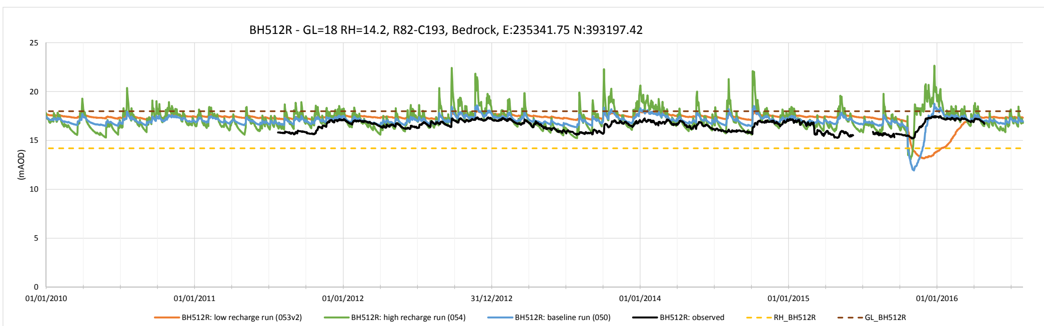
BH512R - GL=18 RH=14.2, R82-C193, Bedrock, E:235341.75 N:393197.42
(mAOD)
0
5
10
15
20
25
01/01/2010
01/01/2011
01/01/2012
31/12/2012
01/01/2014
01/01/2015
01/01/2016
BH512R: low recharge run (053v2)
BH512R: high recharge run (054)
BH512R: baseline run (050)
BH512R: observed
RH_BH512R
GL_BH512R

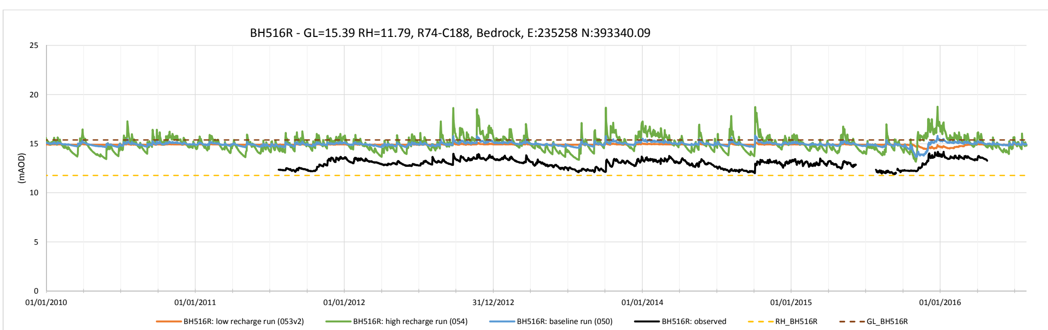
BH516R - GL=15.39 RH=11.79, R74-C188, Bedrock, E:235258 N:393340.09
(mAOD)
0
5
10
15
20
25
01/01/2010
01/01/2011
01/01/2012
31/12/2012
01/01/2014
01/01/2015
01/01/2016
BH516R: low recharge run (053v2)
BH516R: high recharge run (054)
BH516R: baseline run (050)
BH516R: observed
RH_BH516R
GL_BH516R

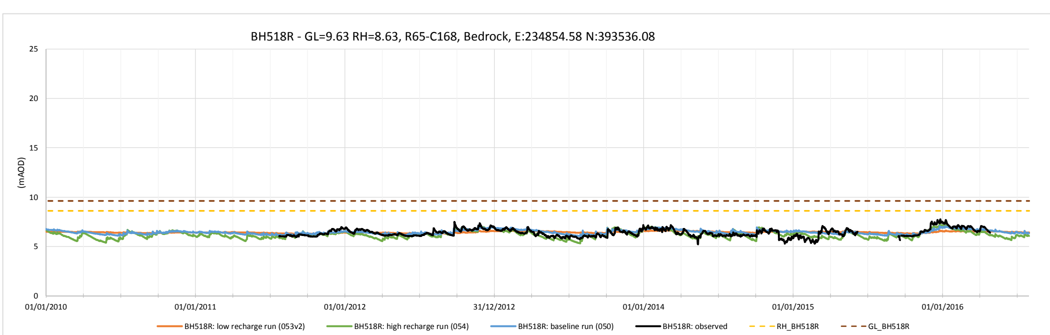
BH518R - GL=9.63 RH=8.63, R65-C168, Bedrock, E:234854.58 N:393536.08
(mAOD)
0
5
10
15
20
25
01/01/2010
01/01/2011
01/01/2012
31/12/2012
01/01/2014
01/01/2015
01/01/2016
BH518R: low recharge run (053v2)
BH518R: high recharge run (054)
BH518R: baseline run (050)
BH518R: observed
RH_BH518R
GL_BH518R

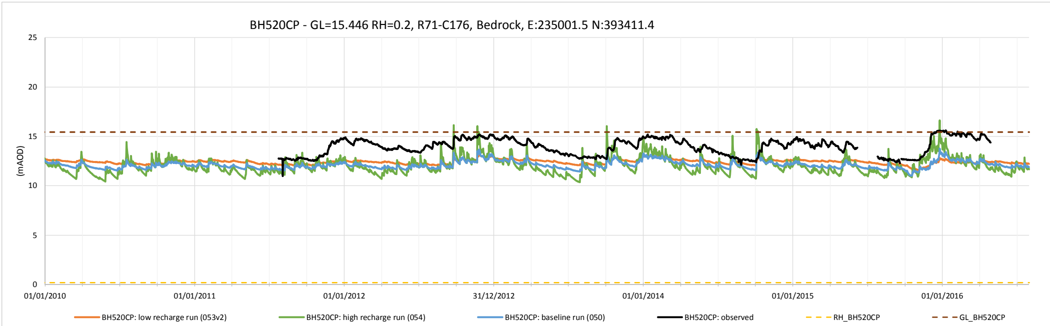
BH520CP - GL=15.446 RH=0.2, R71-C176, Bedrock, E:235001.5 N:393411.4
(mAOD)
BH520CP: low recharge run (053v2)
BH520CP: high recharge run (054)
BH520CP: baseline run (050)
BH520CP: observed
RH_BH520CP
GL_BH520CP

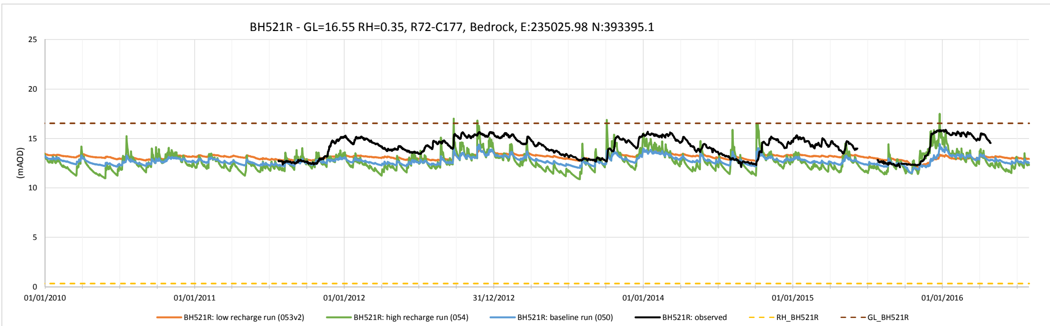
BH521R - GL=16.55 RH=0.35, R72-C177, Bedrock, E:235025.98 N:393395.1
(mAOD)
BH521R: low recharge run (053v2)
BH521R: high recharge run (054)
BH521R: baseline run (050)
BH521R: observed
RH_BH521R
GL_BH521R

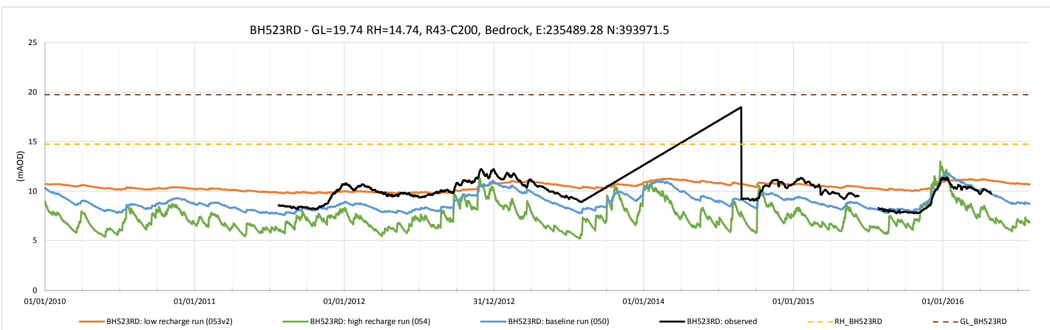
BH523RD - GL=19.74 RH=14.74, R43-C200, Bedrock, E:235489.28 N:393971.5
(mAOD)
BH523RD: low recharge run (053v2)
BH523RD: high recharge run (054)
BH523RD: baseline run (050)
BH523RD: observed
RH_BH523RD
GL_BH523RD

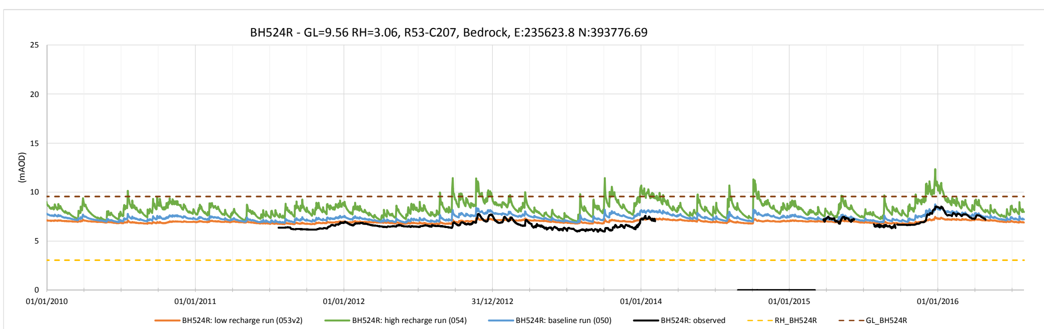
BH524R - GL=9.56 RH=3.06, R53-C207, Bedrock, E:235623.8 N:393776.69
(mAOD)
BH524R: low recharge run (053v2)
BH524R: high recharge run (054)
BH524R: baseline run (050)
BH524R: observed
RH_BH524R
GL_BH524R

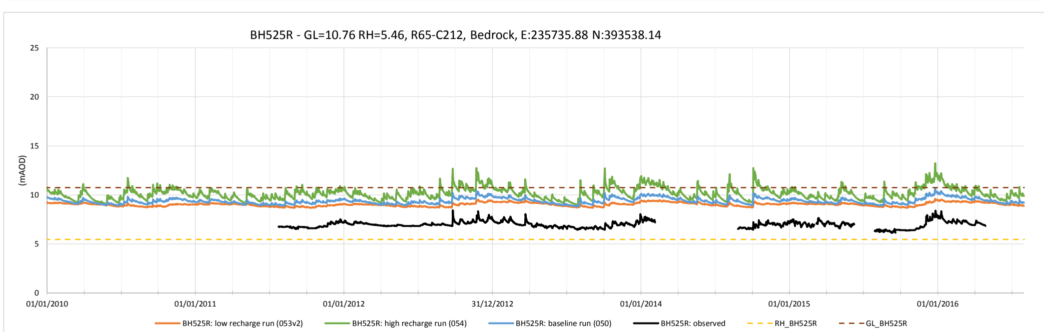
BH525R - GL=10.76 RH=5.46, R65-C212, Bedrock, E:235735.88 N:393538.14
(mAOD)
BH525R: low recharge run (053v2)
BH525R: high recharge run (054)
BH525R: baseline run (050)
BH525R: observed
RH_BH525R
GL_BH525R

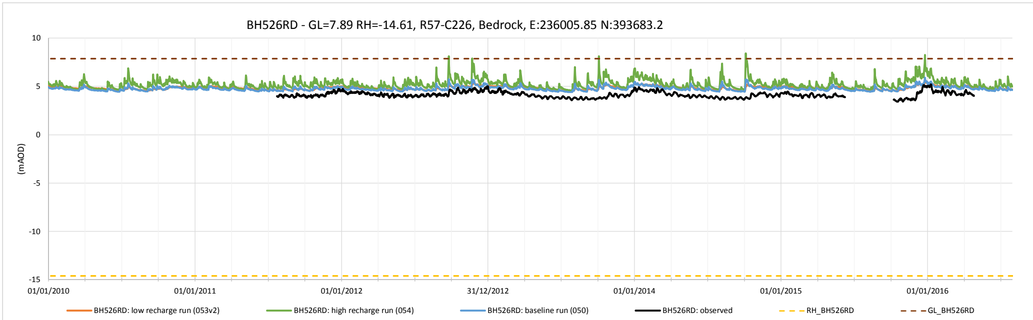
BH526RD - GL=7.89 RH=-14.61, R57-C226, Bedrock, E:236005.85 N:393683.2
(mAOD)
10
5
0
-5
-10
-15
01/01/2010
01/01/2011
01/01/2012
31/12/2012
01/01/2014
01/01/2015
01/01/2016
BH526RD: low recharge run (053v2)
BH526RD: high recharge run (054)
BH526RD: baseline run (050)
BH526RD: observed
RH_BH526RD
GL_BH526RD

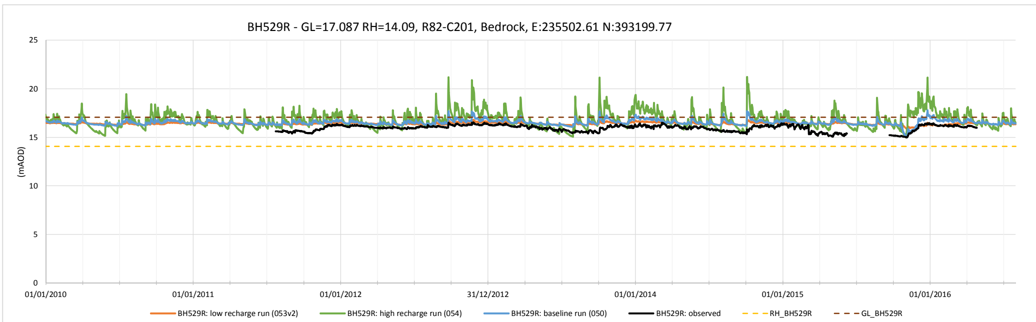
BH529R - GL=17.087 RH=14.09, R82-C201, Bedrock, E:235502.61 N:393199.77
(mAOD)
25
20
15
10
5
0
01/01/2010
01/01/2011
01/01/2012
31/12/2012
01/01/2014
01/01/2015
01/01/2016
BH529R: low recharge run (053v2)
BH529R: high recharge run (054)
BH529R: baseline run (050)
BH529R: observed
RH_BH529R
GL_BH529R

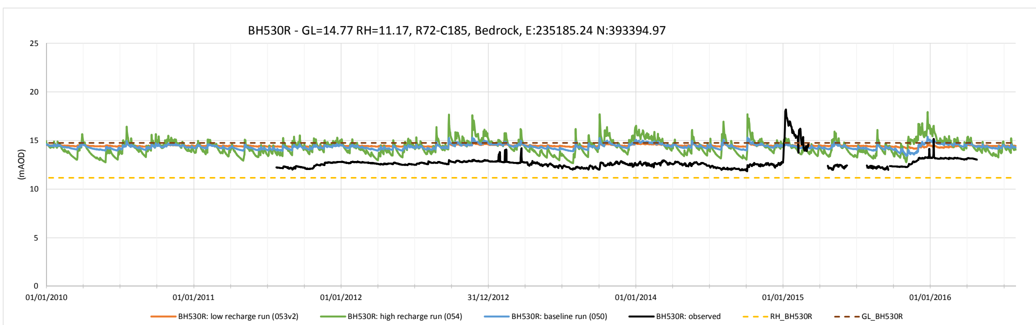
BH530R - GL=14.77 RH=11.17, R72-C185, Bedrock, E:235185.24 N:393394.97
(mAOD)
25
20
15
10
5
0
01/01/2010
01/01/2011
01/01/2012
31/12/2012
01/01/2014
01/01/2015
01/01/2016
BH530R: low recharge run (053v2)
BH530R: high recharge run (054)
BH530R: baseline run (050)
BH530R: observed
RH_BH530R
GL_BH530R

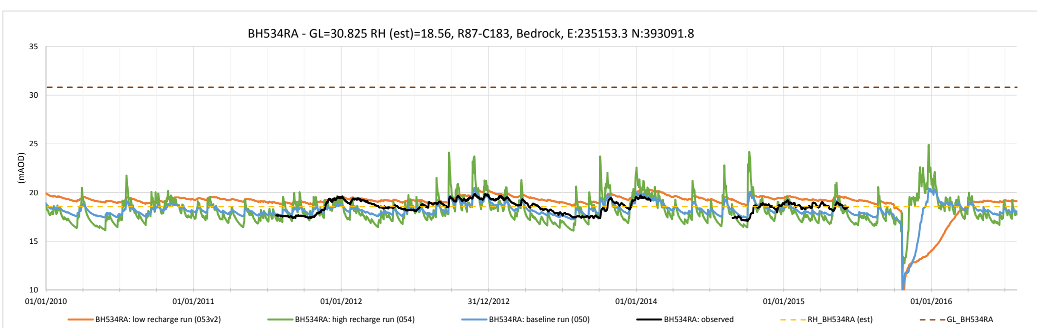
BH534RA - GL=30.825 RH (est)=18.56, R87-C183, Bedrock, E:235153.3 N:393091.8
(mAOD)
35
30
25
20
15
10
01/01/2010
01/01/2011
01/01/2012
31/12/2012
01/01/2014
01/01/2015
01/01/2016
BH534RA: low recharge run (053v2)
BH534RA: high recharge run (054)
BH534RA: baseline run (050)
BH534RA: observed
RH_BH534RA (est)
GL_BH534RA

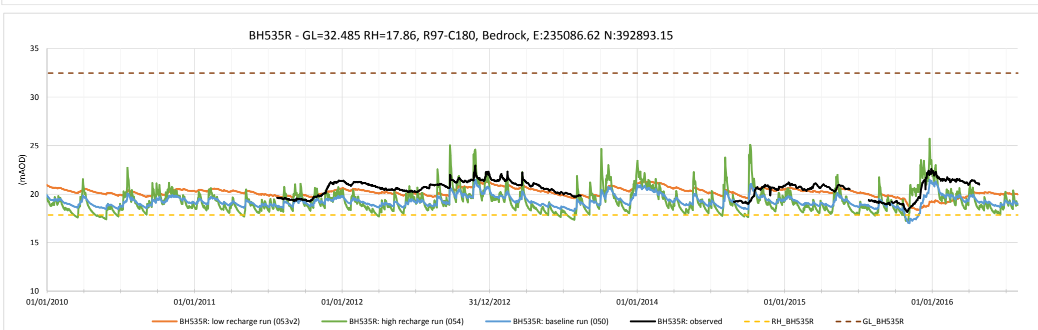
BH535R - GL=32.485 RH=17.86, R97-C180, Bedrock, E:235086.62 N:392893.15
(mAOD)
35
30
25
20
15
10
01/01/2010
01/01/2011
01/01/2012
31/12/2012
01/01/2014
01/01/2015
01/01/2016
BH535R: low recharge run (053v2)
BH535R: high recharge run (054)
BH535R: baseline run (050)
BH535R: observed
RH_BH535R
GL_BH535R

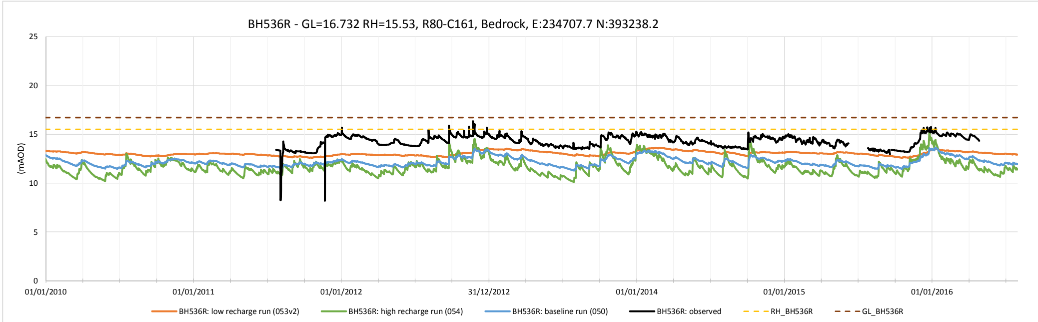
BH536R - GL=16.732 RH=15.53, R80-C161, Bedrock, E:234707.7 N:393238.2
(mAOD)
0
5
10
15
20
25
01/01/2010
01/01/2011
01/01/2012
31/12/2012
01/01/2014
01/01/2015
01/01/2016
BH536R: low recharge run (053v2)
BH536R: high recharge run (054)
BH536R: baseline run (050)
BH536R: observed
RH_BH536R
GL_BH536R

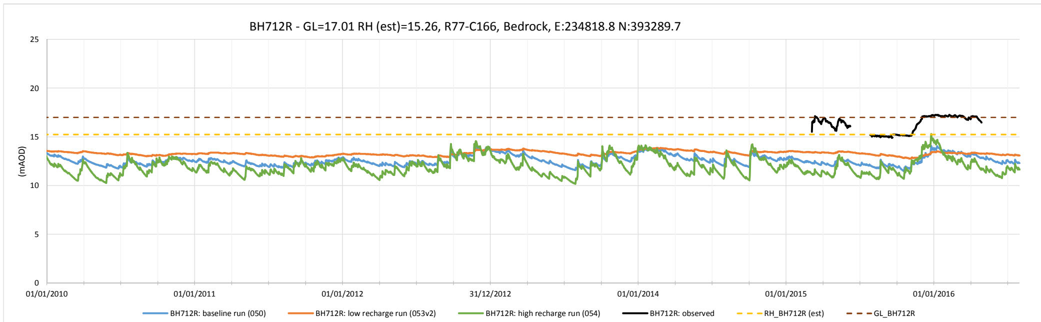
BH712R - GL=17.01 RH (est)=15.26, R77-C166, Bedrock, E:234818.8 N:393289.7
(mAOD)
0
5
10
15
20
25
01/01/2010
01/01/2011
01/01/2012
31/12/2012
01/01/2014
01/01/2015
01/01/2016
BH712R: baseline run (050)
BH712R: low recharge run (053v2)
BH712R: high recharge run (054)
BH712R: observed
RH_BH712R (est)
GL_BH712R

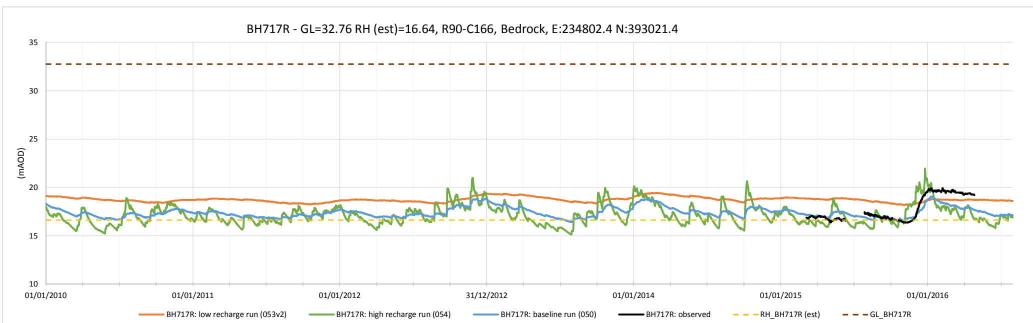
BH717R - GL=32.76 RH (est)=16.64, R90-C166, Bedrock, E:234802.4 N:393021.4
(mAOD)
10
15
20
25
30
35
01/01/2010
01/01/2011
01/01/2012
31/12/2012
01/01/2014
01/01/2015
01/01/2016
BH717R: low recharge run (053v2)
BH717R: high recharge run (054)
BH717R: baseline run (050)
BH717R: observed
RH_BH717R (est)
GL_BH717R

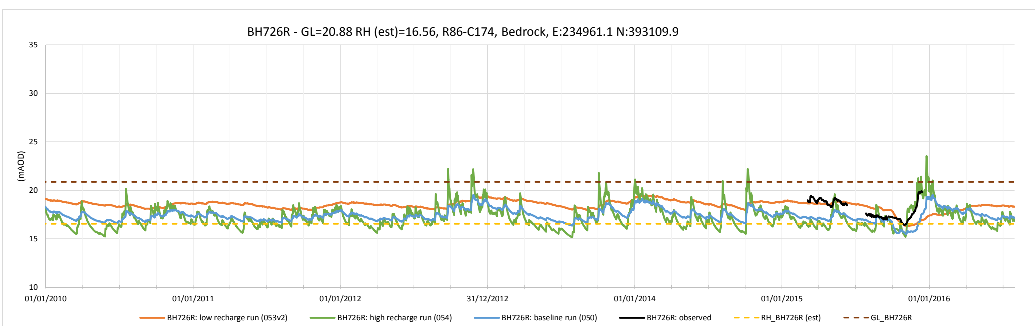
BH726R - GL=20.88 RH (est)=16.56, R86-C174, Bedrock, E:234961.1 N:393109.9
(mAOD)
10
15
20
25
30
35
01/01/2010
01/01/2011
01/01/2012
31/12/2012
01/01/2014
01/01/2015
01/01/2016
BH726R: low recharge run (053v2)
BH726R: high recharge run (054)
BH726R: baseline run (050)
BH726R: observed
RH_BH726R (est)
GL_BH726R

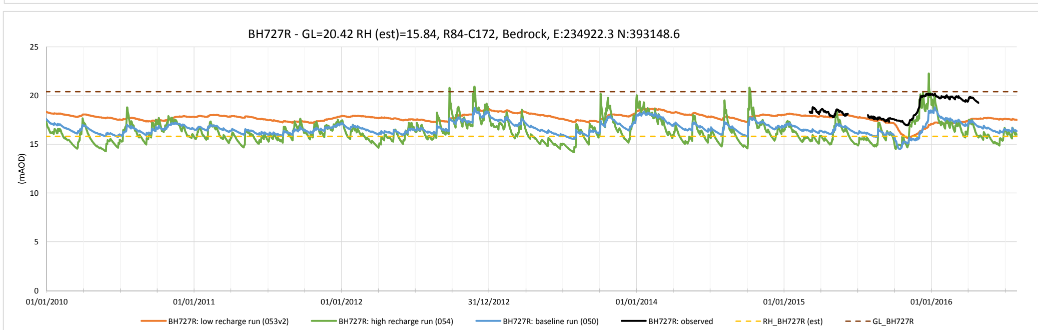
BH727R - GL=20.42 RH (est)=15.84, R84-C172, Bedrock, E:234922.3 N:393148.6
(mAOD)
0
5
10
15
20
25
01/01/2010
01/01/2011
01/01/2012
31/12/2012
01/01/2014
01/01/2015
01/01/2016
BH727R: low recharge run (053v2)
BH727R: high recharge run (054)
BH727R: baseline run (050)
BH727R: observed
RH_BH727R (est)
GL_BH727R

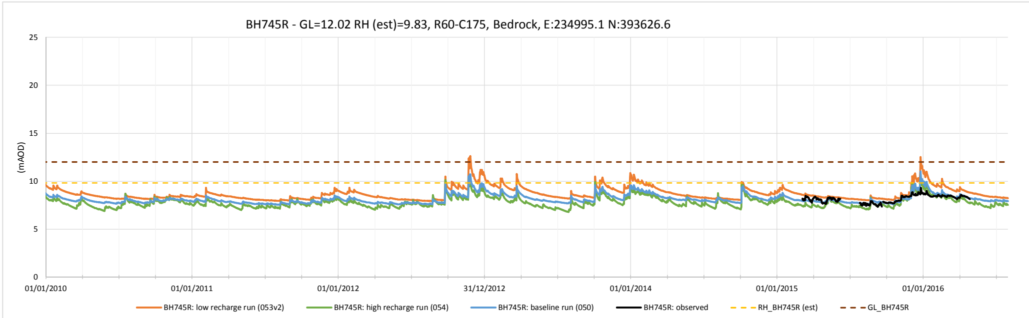
BH745R - GL=12.02 RH (est)=9.83, R60-C175, Bedrock, E:234995.1 N:393626.6
25
20
15
10
5
0
(mAOD)
01/01/2010
01/01/2011
01/01/2012
31/12/2012
01/01/2014
01/01/2015
01/01/2016
BH745R: low recharge run (053v2)
BH745R: high recharge run (054)
BH745R: baseline run (050)
BH745R: observed
RH_BH745R (est)
GL_BH745R

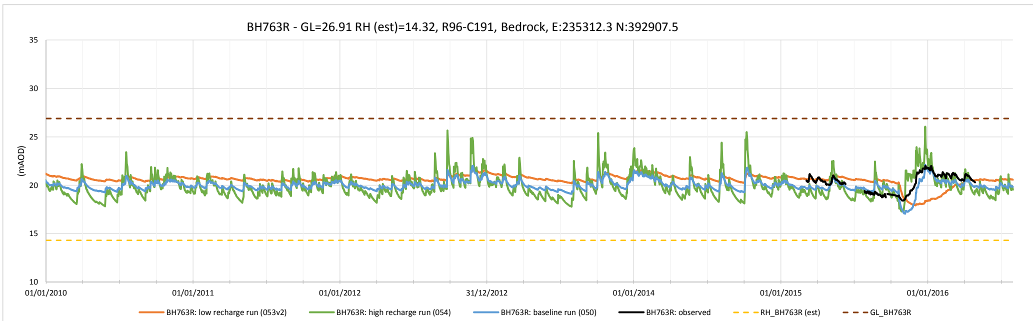
BH763R - GL=26.91 RH (est)=14.32, R96-C191, Bedrock, E:235312.3 N:392907.5
35
30
25
20
15
10
(mAOD)
01/01/2010
01/01/2011
01/01/2012
31/12/2012
01/01/2014
01/01/2015
01/01/2016
BH763R: low recharge run (053v2)
BH763R: high recharge run (054)
BH763R: baseline run (050)
BH763R: observed
RH_BH763R (est)
GL_BH763R

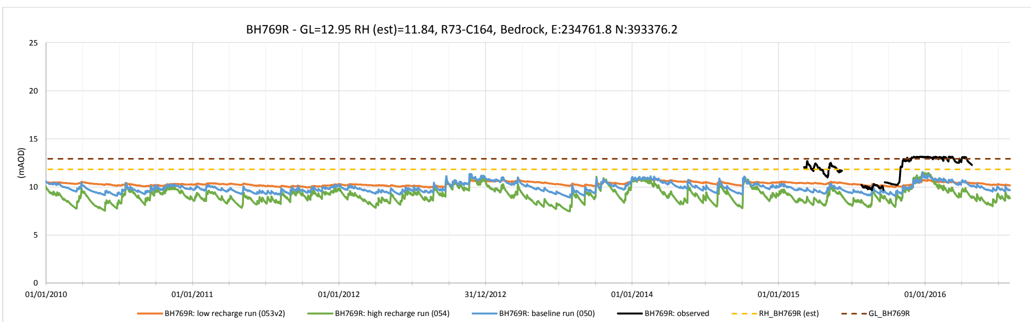
BH769R - GL=12.95 RH (est)=11.84, R73-C164, Bedrock, E:234761.8 N:393376.2
25
20
15
10
5
0
(mAOD)
01/01/2010
01/01/2011
01/01/2012
31/12/2012
01/01/2014
01/01/2015
01/01/2016
BH769R: low recharge run (053v2)
BH769R: high recharge run (054)
BH769R: baseline run (050)
BH769R: observed
RH_BH769R (est)
GL_BH769R

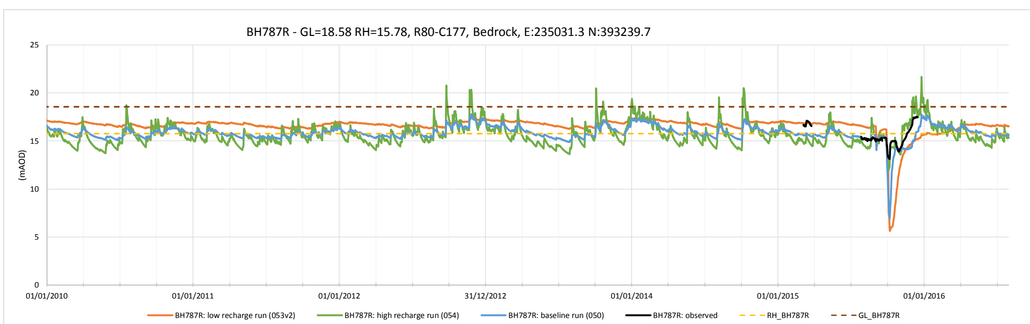
BH787R - GL=18.58 RH=15.78, R80-C177, Bedrock, E:235031.3 N:393239.7
25
20
15
10
5
0
(mAOD)
01/01/2010
01/01/2011
01/01/2012
31/12/2012
01/01/2014
01/01/2015
01/01/2016
BH787R: low recharge run (053v2)
BH787R: high recharge run (054)
BH787R: baseline run (050)
BH787R: observed
RH_BH787R
GL_BH787R

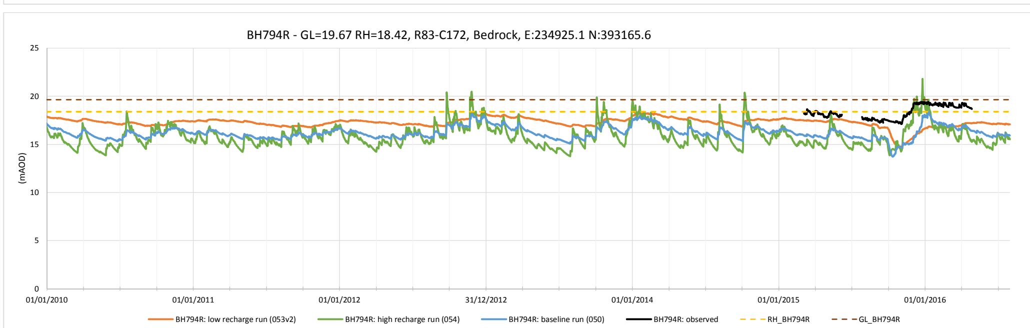
BH794R - GL=19.67 RH=18.42, R83-C172, Bedrock, E:234925.1 N:393165.6
25
20
15
10
5
0
(mAOD)
01/01/2010
01/01/2011
01/01/2012
31/12/2012
01/01/2014
01/01/2015
01/01/2016
BH794R: low recharge run (053v2)
BH794R: high recharge run (054)
BH794R: baseline run (050)
BH794R: observed
RH_BH794R
GL_BH794R

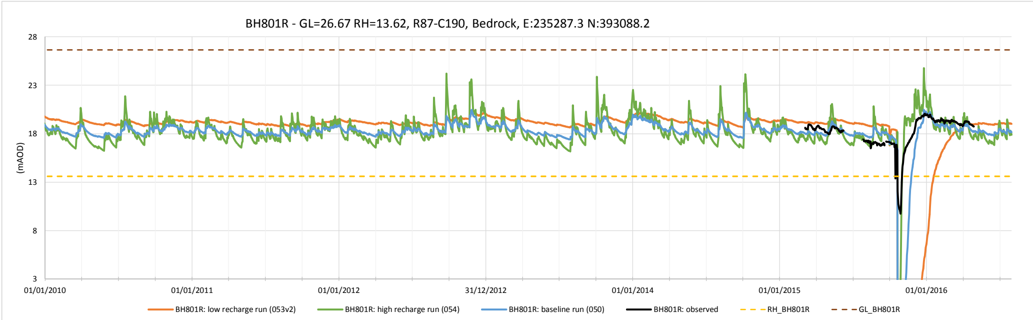
BH801R - GL=26.67 RH=13.62, R87-C190, Bedrock, E:235287.3 N:393088.2
(mAOD)
28
23
18
13
8
3
01/01/2010
01/01/2011
01/01/2012
31/12/2012
01/01/2014
01/01/2015
01/01/2016
BH801R: low recharge run (053v2)
BH801R: high recharge run (054)
BH801R: baseline run (050)
BH801R: observed
RH_BH801R
GL_BH801R

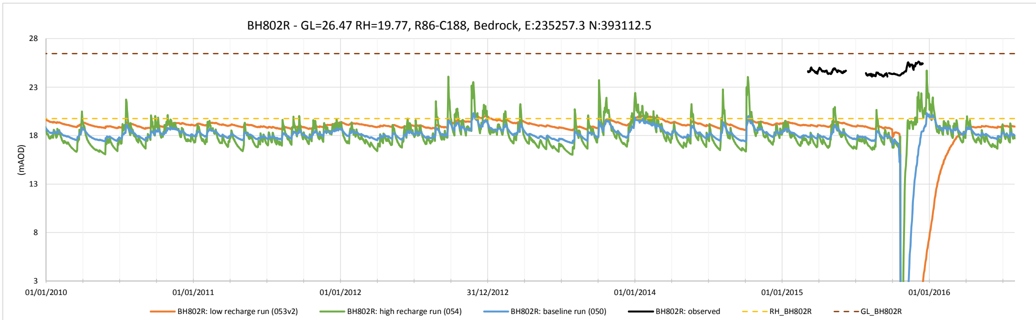
BH802R - GL=26.47 RH=19.77, R86-C188, Bedrock, E:235257.3 N:393112.5
(mAOD)
28
23
18
13
8
3
01/01/2010
01/01/2011
01/01/2012
31/12/2012
01/01/2014
01/01/2015
01/01/2016
BH802R: low recharge run (053v2)
BH802R: high recharge run (054)
BH802R: baseline run (050)
BH802R: observed
RH_BH802R
GL_BH802R

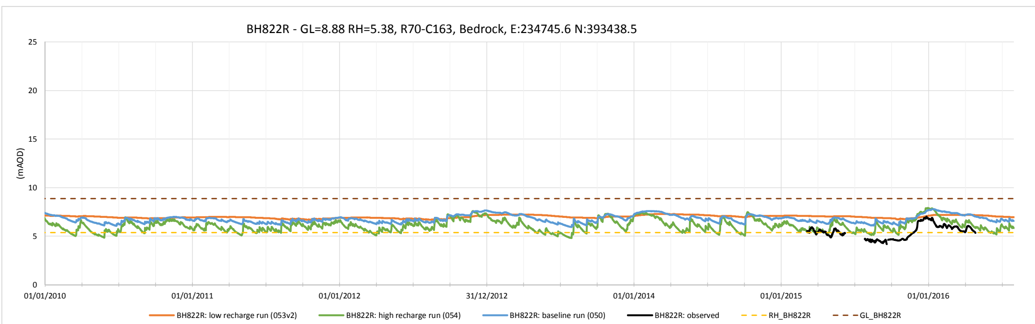
BH822R - GL=8.88 RH=5.38, R70-C163, Bedrock, E:234745.6 N:393438.5
(mAOD)
25
20
15
10
5
0
01/01/2010
01/01/2011
01/01/2012
31/12/2012
01/01/2014
01/01/2015
01/01/2016
BH822R: low recharge run (053v2)
BH822R: high recharge run (054)
BH822R: baseline run (050)
BH822R: observed
RH_BH822R
GL_BH822R

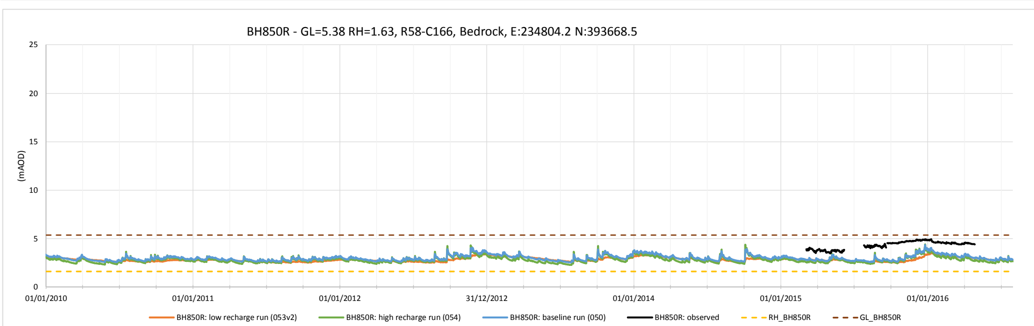
BH850R - GL=5.38 RH=1.63, R58-C166, Bedrock, E:234804.2 N:393668.5
(mAOD)
25
20
15
10
5
0
01/01/2010
01/01/2011
01/01/2012
31/12/2012
01/01/2014
01/01/2015
01/01/2016
BH850R: low recharge run (053v2)
BH850R: high recharge run (054)
BH850R: baseline run (050)
BH850R: observed
RH_BH850R
GL_BH850R

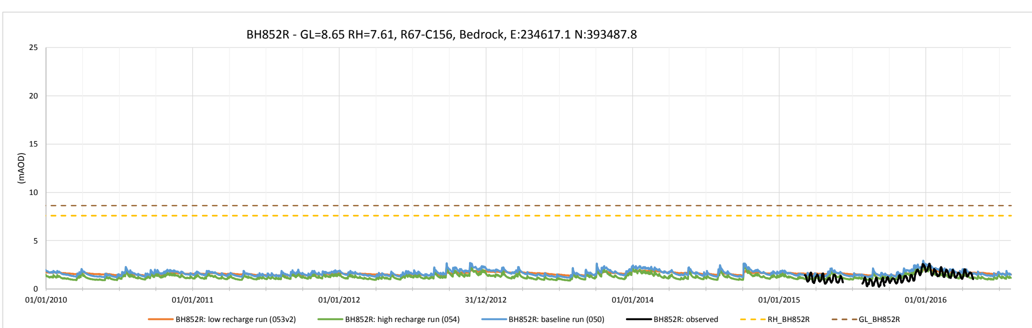
BH852R - GL=8.65 RH=7.61, R67-C156, Bedrock, E:234617.1 N:393487.8
(mAOD)
25
20
15
10
5
0
01/01/2010
01/01/2011
01/01/2012
31/12/2012
01/01/2014
01/01/2015
01/01/2016
BH852R: low recharge run (053v2)
BH852R: high recharge run (054)
BH852R: baseline run (050)
BH852R: observed
RH_BH852R
GL_BH852R

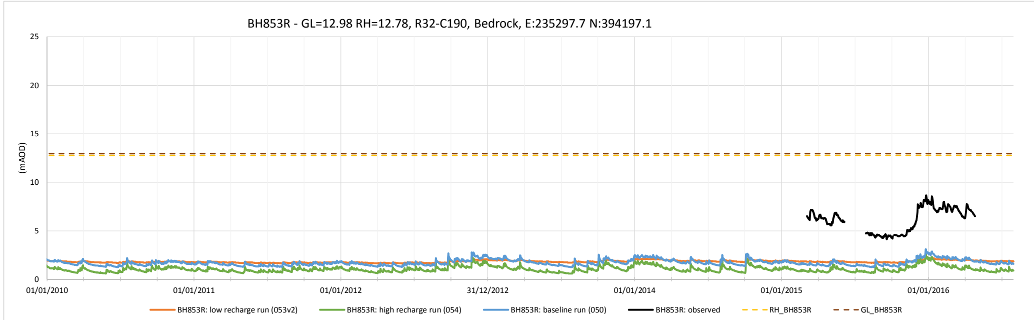
BH853R - GL=12.98 RH=12.78, R32-C190, Bedrock, E:235297.7 N:394197.1
(mAOD)
0
5
10
15
20
25
01/01/2010
01/01/2011
01/01/2012
31/12/2012
01/01/2014
01/01/2015
01/01/2016
BH853R: low recharge run (053v2)
BH853R: high recharge run (054)
BH853R: baseline run (050)
BH853R: observed
RH_BH853R
GL_BH853R

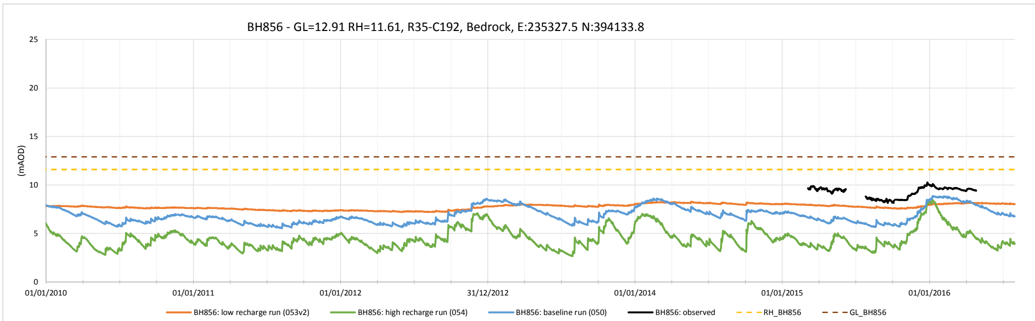
BH856 - GL=12.91 RH=11.61, R35-C192, Bedrock, E:235327.5 N:394133.8
(mAOD)
0
5
10
15
20
25
01/01/2010
01/01/2011
01/01/2012
31/12/2012
01/01/2014
01/01/2015
01/01/2016
BH856: low recharge run (053v2)
BH856: high recharge run (054)
BH856: baseline run (050)
BH856: observed
RH_BH856
GL_BH856

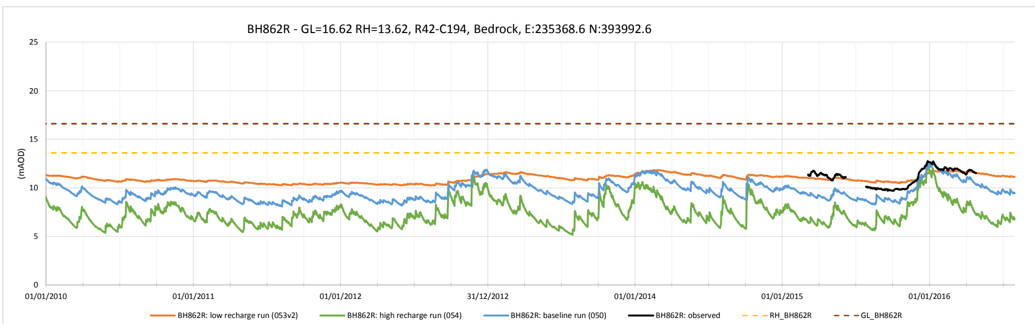
BH862R - GL=16.62 RH=13.62, R42-C194, Bedrock, E:235368.6 N:393992.6
(mAOD)
0
5
10
15
20
25
01/01/2010
01/01/2011
01/01/2012
31/12/2012
01/01/2014
01/01/2015
01/01/2016
BH862R: low recharge run (053v2)
BH862R: high recharge run (054)
BH862R: baseline run (050)
BH862R: observed
RH_BH862R
GL_BH862R

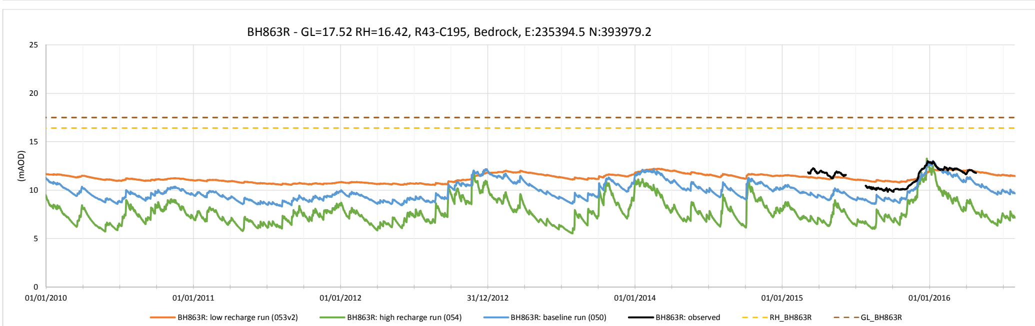
BH863R - GL=17.52 RH=16.42, R43-C195, Bedrock, E:235394.5 N:393979.2
(mAOD)
0
5
10
15
20
25
01/01/2010
01/01/2011
01/01/2012
31/12/2012
01/01/2014
01/01/2015
01/01/2016
BH863R: low recharge run (053v2)
BH863R: high recharge run (054)
BH863R: baseline run (050)
BH863R: observed
RH_BH863R
GL_BH863R

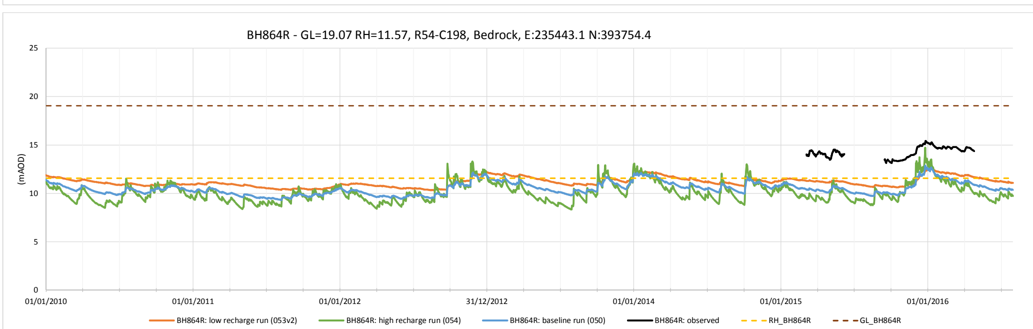
BH864R - GL=19.07 RH=11.57, R54-C198, Bedrock, E:235443.1 N:393754.4
(mAOD)
0
5
10
15
20
25
01/01/2010
01/01/2011
01/01/2012
31/12/2012
01/01/2014
01/01/2015
01/01/2016
BH864R: low recharge run (053v2)
BH864R: high recharge run (054)
BH864R: baseline run (050)
BH864R: observed
RH_BH864R
GL_BH864R

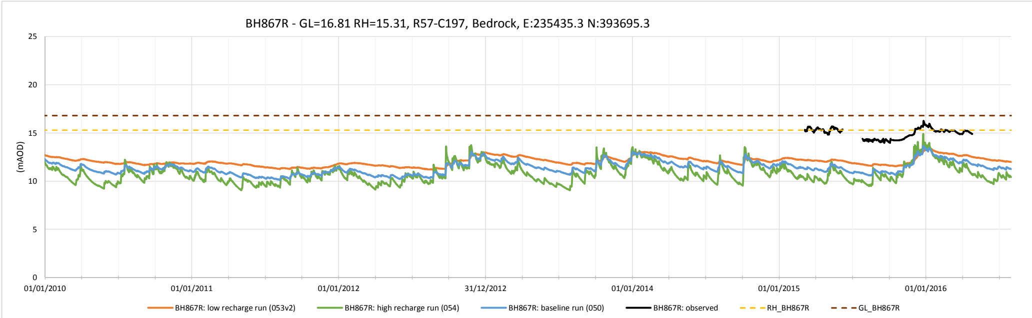
BH867R - GL=16.81 RH=15.31, R57-C197, Bedrock, E:235435.3 N:393695.3
(mAOD)
0
5
10
15
20
25
01/01/2010
01/01/2011
01/01/2012
31/12/2012
01/01/2014
01/01/2015
01/01/2016
BH867R: low recharge run (053v2)
BH867R: high recharge run (054)
BH867R: baseline run (050)
BH867R: observed
RH_BH867R
GL_BH867R

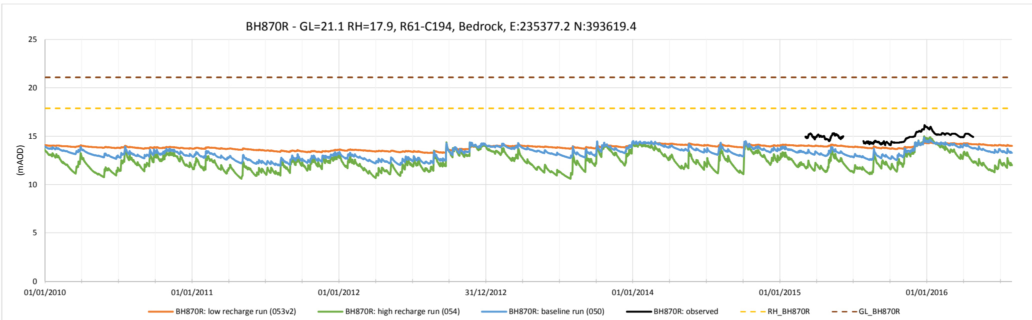
BH870R - GL=21.1 RH=17.9, R61-C194, Bedrock, E:235377.2 N:393619.4
(mAOD)
0
5
10
15
20
25
01/01/2010
01/01/2011
01/01/2012
31/12/2012
01/01/2014
01/01/2015
01/01/2016
BH870R: low recharge run (053v2)
BH870R: high recharge run (054)
BH870R: baseline run (050)
BH870R: observed
RH_BH870R
GL_BH870R

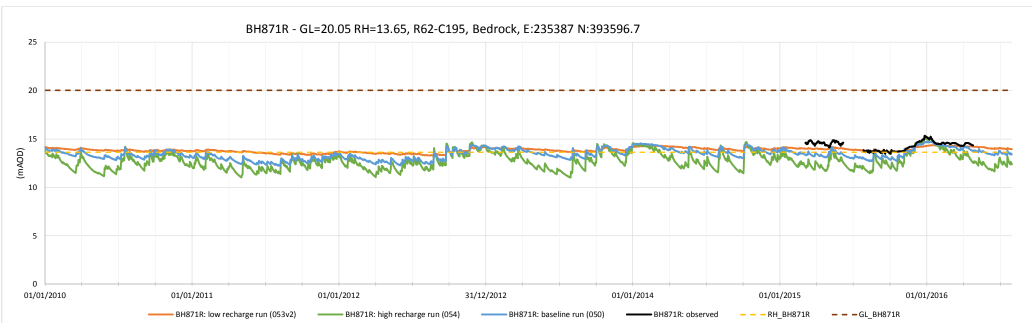
BH871R - GL=20.05 RH=13.65, R62-C195, Bedrock, E:235387 N:393596.7
(mAOD)
0
5
10
15
20
25
01/01/2010
01/01/2011
01/01/2012
31/12/2012
01/01/2014
01/01/2015
01/01/2016
BH871R: low recharge run (053v2)
BH871R: high recharge run (054)
BH871R: baseline run (050)
BH871R: observed
RH_BH871R
GL_BH871R

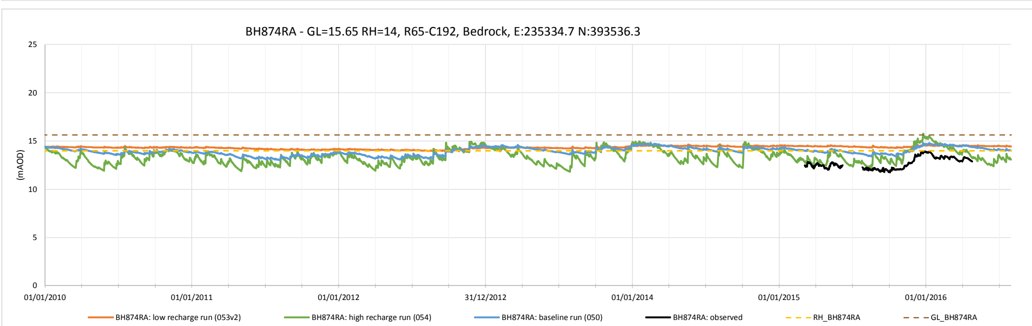
BH874RA - GL=15.65 RH=14, R65-C192, Bedrock, E:235334.7 N:393536.3
(mAOD)
0
5
10
15
20
25
01/01/2010
01/01/2011
01/01/2012
31/12/2012
01/01/2014
01/01/2015
01/01/2016
BH874RA: low recharge run (053v2)
BH874RA: high recharge run (054)
BH874RA: baseline run (050)
BH874RA: observed
RH_BH874RA
GL_BH874RA

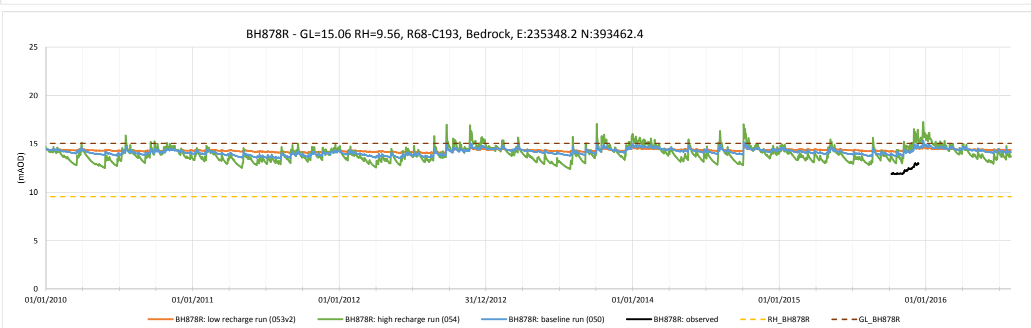
BH878R - GL=15.06 RH=9.56, R68-C193, Bedrock, E:235348.2 N:393462.4
(mAOD)
0
5
10
15
20
25
01/01/2010
01/01/2011
01/01/2012
31/12/2012
01/01/2014
01/01/2015
01/01/2016
BH878R: low recharge run (053v2)
BH878R: high recharge run (054)
BH878R: baseline run (050)
BH878R: observed
RH_BH878R
GL_BH878R

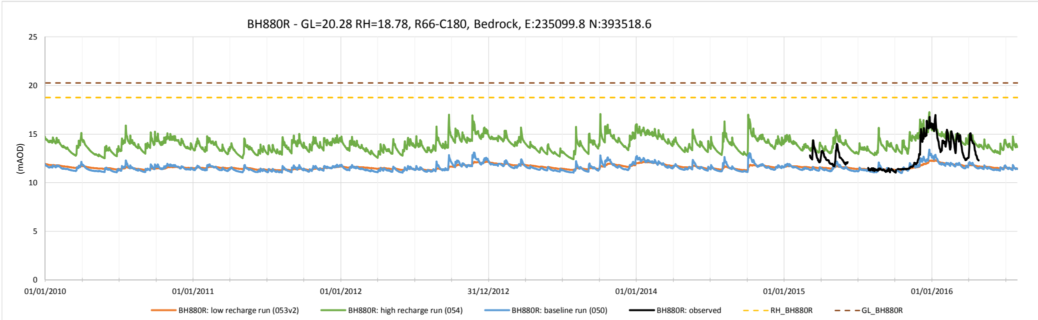
BH880R - GL=20.28 RH=18.78, R66-C180, Bedrock, E:235099.8 N:393518.6
(mAOD)
0
5
10
15
20
25
01/01/2010
01/01/2011
01/01/2012
31/12/2012
01/01/2014
01/01/2015
01/01/2016
BH880R: low recharge run (053v2)
BH880R: high recharge run (054)
BH880R: baseline run (050)
BH880R: observed
RH_BH880R
GL_BH880R

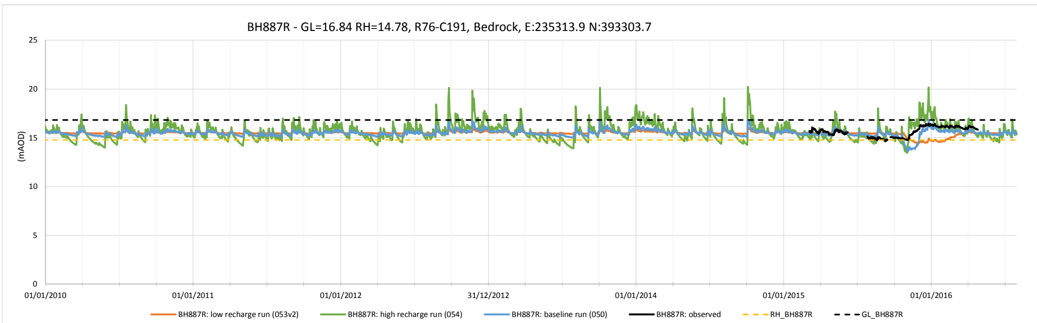
BH887R - GL=16.84 RH=14.78, R76-C191, Bedrock, E:235313.9 N:393303.7
(mAOD)
0
5
10
15
20
25
01/01/2010
01/01/2011
01/01/2012
31/12/2012
01/01/2014
01/01/2015
01/01/2016
BH887R: low recharge run (053v2)
BH887R: high recharge run (054)
BH887R: baseline run (050)
BH887R: observed
RH_BH887R
GL_BH887R

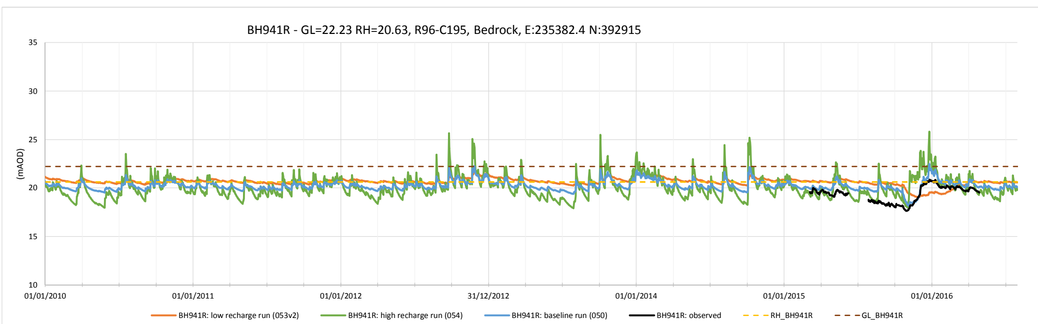
BH941R - GL=22.23 RH=20.63, R96-C195, Bedrock, E:235382.4 N:392915
(mAOD)
10
15
20
25
30
35
01/01/2010
01/01/2011
01/01/2012
31/12/2012
01/01/2014
01/01/2015
01/01/2016
BH941R: low recharge run (053v2)
BH941R: high recharge run (054)
BH941R: baseline run (050)
BH941R: observed
RH_BH941R
GL_BH941R

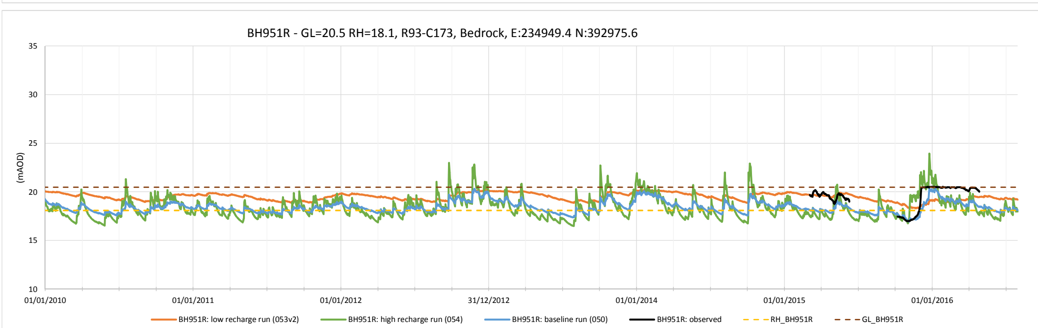
BH951R - GL=20.5 RH=18.1, R93-C173, Bedrock, E:234949.4 N:392975.6
(mAOD)
10
15
20
25
30
35
01/01/2010
01/01/2011
01/01/2012
31/12/2012
01/01/2014
01/01/2015
01/01/2016
BH951R: low recharge run (053v2)
BH951R: high recharge run (054)
BH951R: baseline run (050)
BH951R: observed
RH_BH951R
GL_BH951R

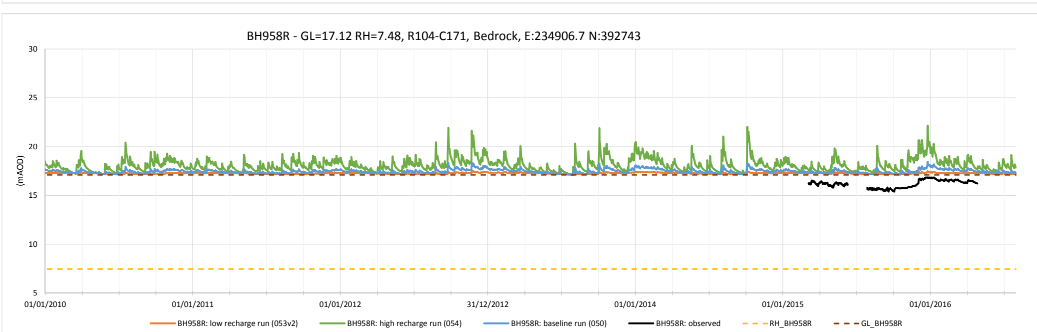
BH958R - GL=17.12 RH=7.48, R104-C171, Bedrock, E:234906.7 N:392743
(mAOD)
5
10
15
20
25
30
01/01/2010
01/01/2011
01/01/2012
31/12/2012
01/01/2014
01/01/2015
01/01/2016
BH958R: low recharge run (053v2)
BH958R: high recharge run (054)
BH958R: baseline run (050)
BH958R: observed
RH_BH958R
GL_BH958R

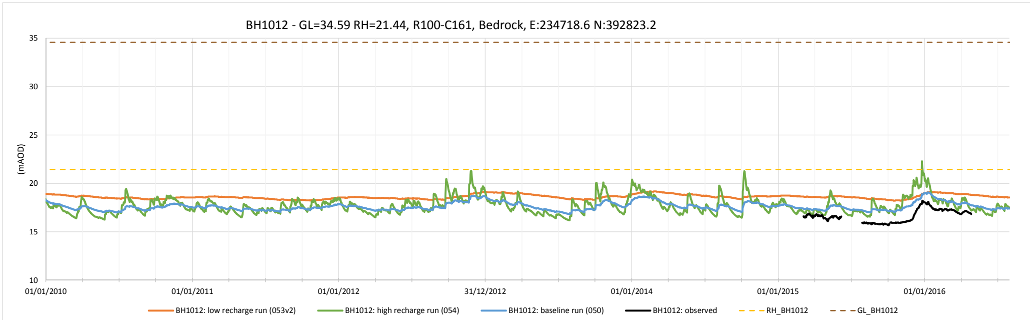
BH1012 - GL=34.59 RH=21.44, R100-C161, Bedrock, E:234718.6 N:392823.2
(mAOD)
35
30
25
20
15
10
01/01/2010
01/01/2011
01/01/2012
31/12/2012
01/01/2014
01/01/2015
01/01/2016
BH1012: low recharge run (053v2)
BH1012: high recharge run (054)
BH1012: baseline run (050)
BH1012: observed
RH_BH1012
GL_BH1012

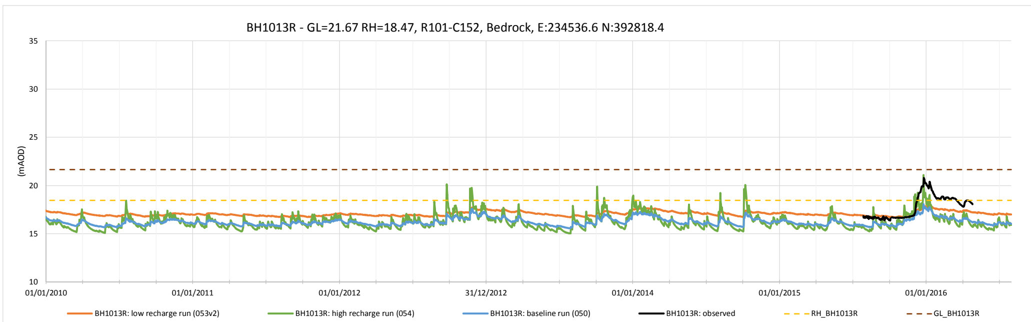
BH1013R - GL=21.67 RH=18.47, R101-C152, Bedrock, E:234536.6 N:392818.4
(mAOD)
35
30
25
20
15
10
01/01/2010
01/01/2011
01/01/2012
31/12/2012
01/01/2014
01/01/2015
01/01/2016
BH1013R: low recharge run (053v2)
BH1013R: high recharge run (054)
BH1013R: baseline run (050)
BH1013R: observed
RH_BH1013R
GL_BH1013R

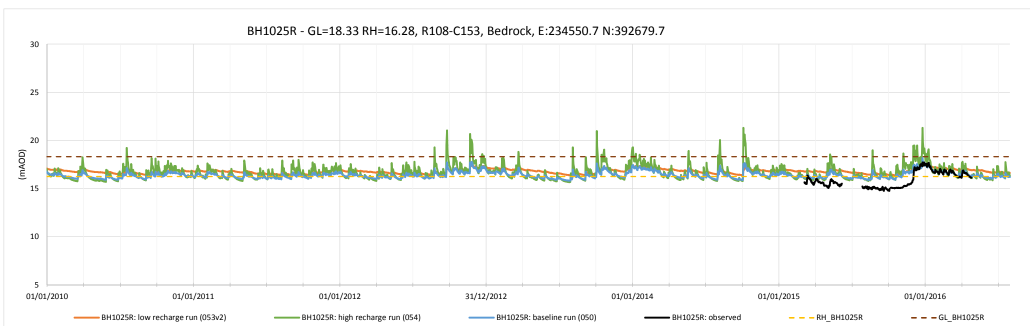
BH1025R - GL=18.33 RH=16.28, R108-C153, Bedrock, E:234550.7 N:392679.7
(mAOD)
30
25
20
15
10
5
01/01/2010
01/01/2011
01/01/2012
31/12/2012
01/01/2014
01/01/2015
01/01/2016
BH1025R: low recharge run (053v2)
BH1025R: high recharge run (054)
BH1025R: baseline run (050)
BH1025R: observed
RH_BH1025R
GL_BH1025R

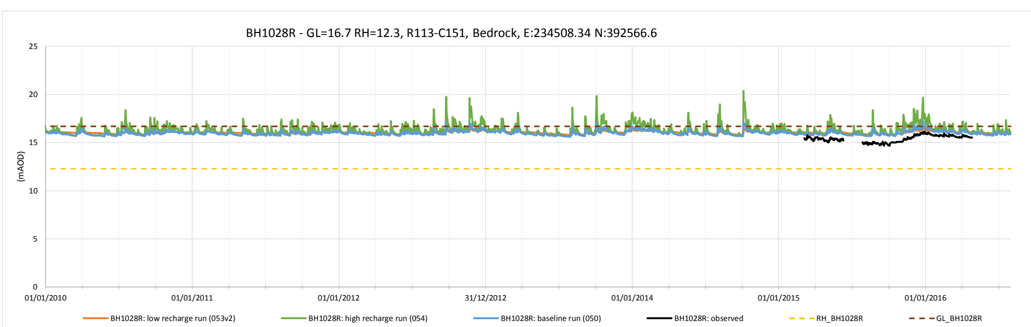
BH1028R - GL=16.7 RH=12.3, R113-C151, Bedrock, E:234508.34 N:392566.6
(mAOD)
25
20
15
10
5
0
01/01/2010
01/01/2011
01/01/2012
31/12/2012
01/01/2014
01/01/2015
01/01/2016
BH1028R: low recharge run (053v2)
BH1028R: high recharge run (054)
BH1028R: baseline run (050)
BH1028R: observed
RH_BH1028R
GL_BH1028R

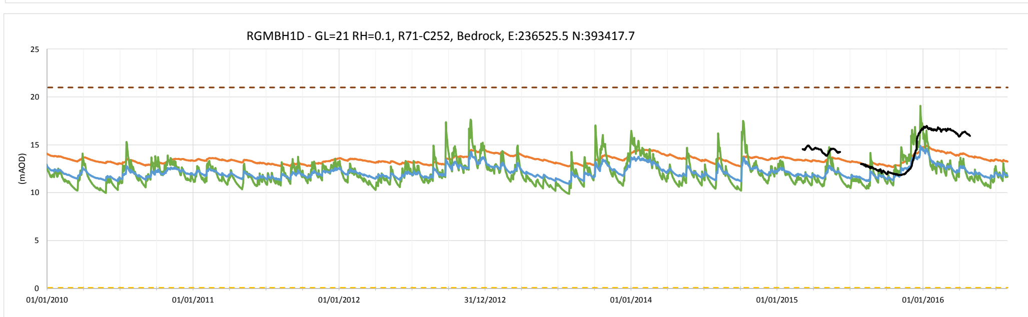
RGMBH1D - GL=21 RH=0.1, R71-C252, Bedrock, E:236525.5 N:393417.7
(mAOD)
25
20
15
10
5
0
01/01/2010
01/01/2011
01/01/2012
31/12/2012
01/01/2014
01/01/2015
01/01/2016
RGMBH1D: low recharge run (053v2)
RGMBH1D: high recharge run (054)
RGMBH1D: baseline run (050)
RGMBH1D: observed
RH_RGMBH1D
GL_RGMBH1D

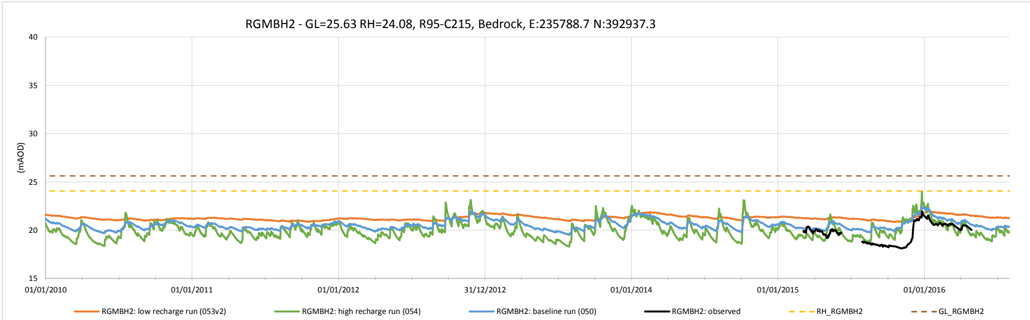
RGMBH2 - GL=25.63 RH=24.08, R95-C215, Bedrock, E:235788.7 N:392937.3
(mAOD)
40
35
30
25
20
15
01/01/2010
01/01/2011
01/01/2012
31/12/2012
01/01/2014
01/01/2015
01/01/2016
RGMBH2: low recharge run (053v2)
RGMBH2: high recharge run (054)
RGMBH2: baseline run (050)
RGMBH2: observed
RH_RGMBH2
GL_RGMBH2

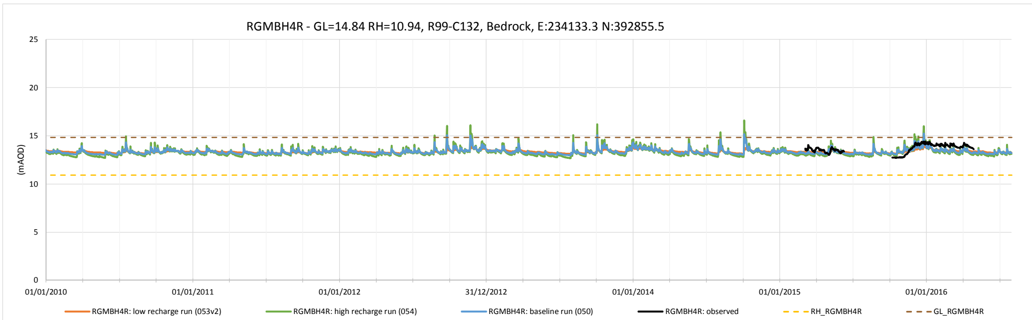
RGMBH4R - GL=14.84 RH=10.94, R99-C132, Bedrock, E:234133.3 N:392855.5
(mAOD)
25
20
15
10
5
0
01/01/2010
01/01/2011
01/01/2012
31/12/2012
01/01/2014
01/01/2015
01/01/2016
RGMBH4R: low recharge run (053v2)
RGMBH4R: high recharge run (054)
RGMBH4R: baseline run (050)
RGMBH4R: observed
RH_RGMBH4R
GL_RGMBH4R

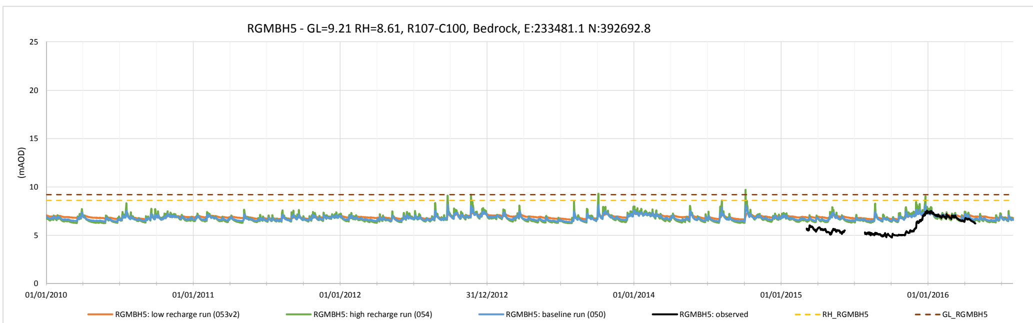
RGMBH5 - GL=9.21 RH=8.61, R107-C100, Bedrock, E:233481.1 N:392692.8
(mAOD)
25
20
15
10
5
0
01/01/2010
01/01/2011
01/01/2012
31/12/2012
01/01/2014
01/01/2015
01/01/2016
RGMBH5: low recharge run (053v2)
RGMBH5: high recharge run (054)
RGMBH5: baseline run (050)
RGMBH5: observed
RH_RGMBH5
GL_RGMBH5

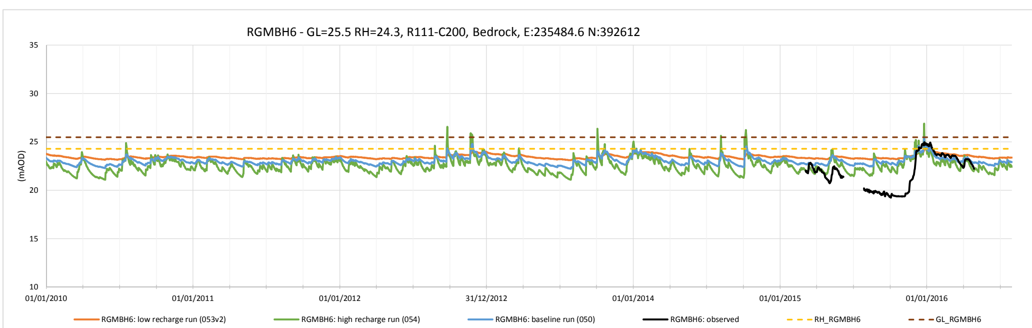
RGMBH6 - GL=25.5 RH=24.3, R111-C200, Bedrock, E:235484.6 N:392612
(mAOD)
35
30
25
20
15
10
01/01/2010
01/01/2011
01/01/2012
31/12/2012
01/01/2014
01/01/2015
01/01/2016
RGMBH6: low recharge run (053v2)
RGMBH6: high recharge run (054)
RGMBH6: baseline run (050)
RGMBH6: observed
RH_RGMBH6
GL_RGMBH6

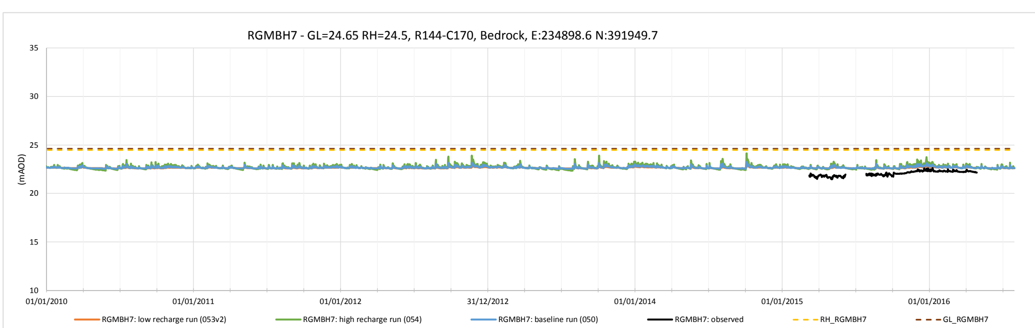
RGMBH7 - GL=24.65 RH=24.5, R144-C170, Bedrock, E:234898.6 N:391949.7
(mAOD)
35
30
25
20
15
10
01/01/2010
01/01/2011
01/01/2012
31/12/2012
01/01/2014
01/01/2015
01/01/2016
RGMBH7: low recharge run (053v2)
RGMBH7: high recharge run (054)
RGMBH7: baseline run (050)
RGMBH7: observed
RH_RGMBH7
GL_RGMBH7

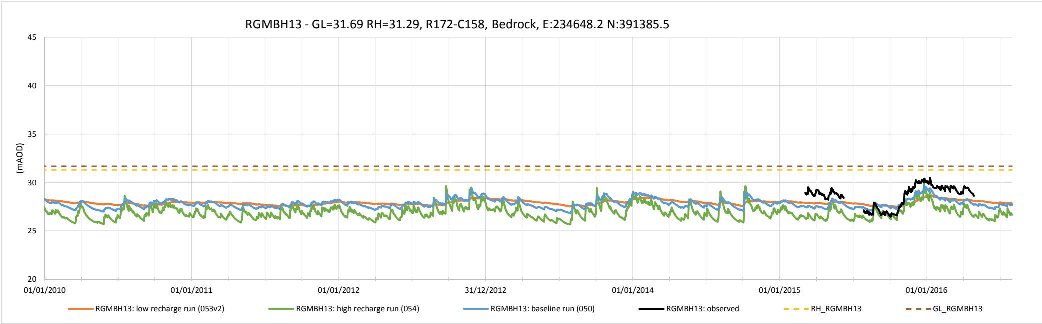
RGMBH13 - GL=31.69 RH=31.29, R172-C158, Bedrock, E:234648.2 N:391385.5
45
40
35
30
25
20
(mAOD)
01/01/2010
01/01/2011
01/01/2012
31/12/2012
01/01/2014
01/01/2015
01/01/2016
RGMBH13: low recharge run (053v2)
RGMBH13: high recharge run (054)
RGMBH13: baseline run (050)
RGMBH13: observed
RH_RGMBH13
GL_RGMBH13

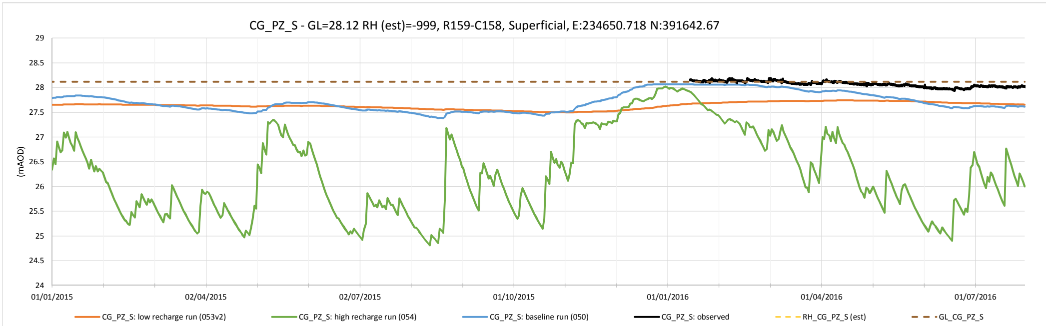
CG_PZ_S - GL=28.12 RH (est)=-999, R159-C158, Superficial, E:234650.718 N:391642.67
(mAOD)
29
28.5
28
27.5
27
26.5
26
25.5
25
24.5
24
01/01/2015
02/04/2015
02/07/2015
01/10/2015
01/01/2016
01/04/2016
01/07/2016
CG_PZ_S: low recharge run (053v2)
CG_PZ_S: high recharge run (054)
CG_PZ_S: baseline run (050)
CG_PZ_S: observed
RH_CG_PZ_S (est)
GL_CG_PZ_S

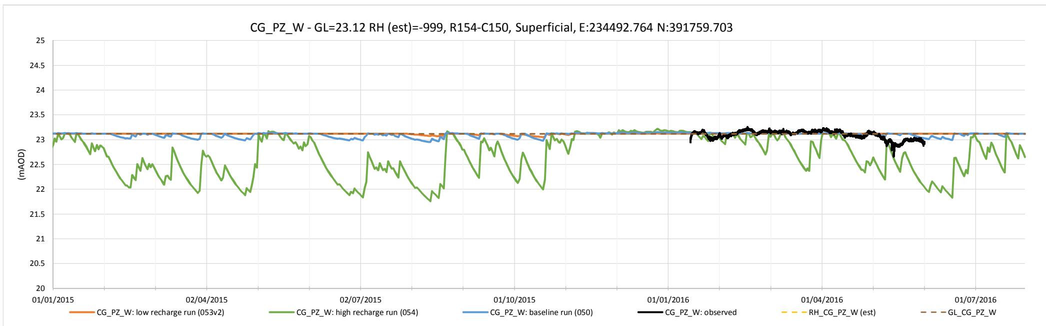
CG_PZ_W - GL=23.12 RH (est)=-999, R154-C150, Superficial, E:234492.764 N:391759.703
(mAOD)
25
24.5
24
23.5
23
22.5
22
21.5
21
20.5
20
01/01/2015
02/04/2015
02/07/2015
01/10/2015
01/01/2016
01/04/2016
01/07/2016
CG_PZ_W: low recharge run (053v2)
CG_PZ_W: high recharge run (054)
CG_PZ_W: baseline run (050)
CG_PZ_W: observed
RH_CG_PZ_W (est)
GL_CG_PZ_W

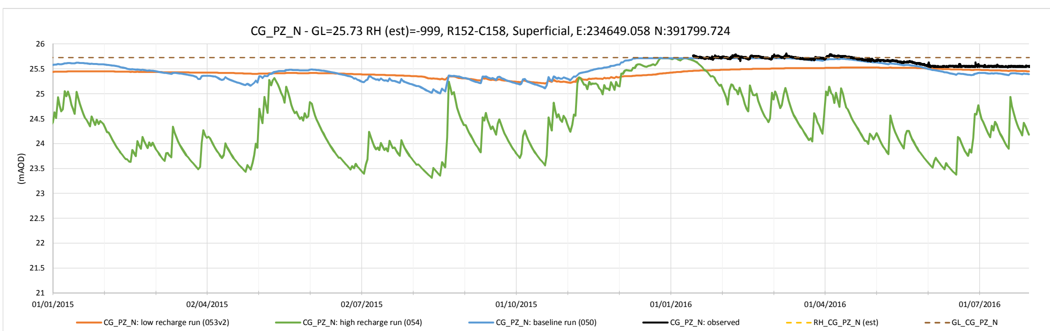
CG_PZ_N - GL=25.73 RH (est)=-999, R152-C158, Superficial, E:234649.058 N:391799.724
(mAOD)
26
25.5
25
24.5
24
23.5
23
22.5
22
21.5
21
01/01/2015
02/04/2015
02/07/2015
01/10/2015
01/01/2016
01/04/2016
01/07/2016
CG_PZ_N: low recharge run (053v2)
CG_PZ_N: high recharge run (054)
CG_PZ_N: baseline run (050)
CG_PZ_N: observed
RH_CG_PZ_N (est)
GL_CG_PZ_N

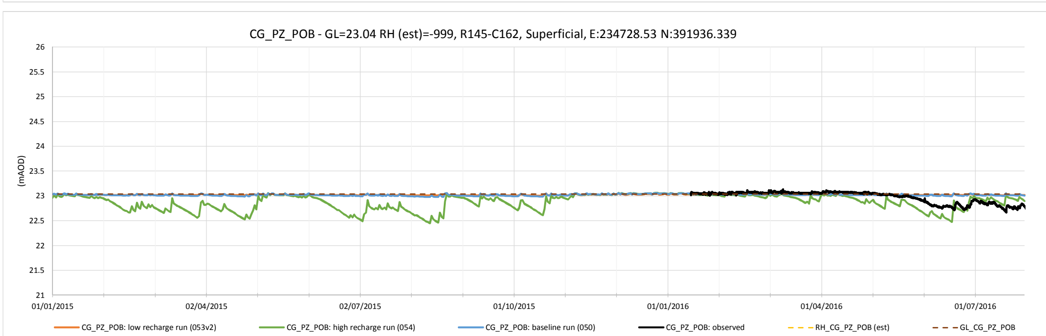
CG_PZ_POB - GL=23.04 RH (est)=-999, R145-C162, Superficial, E:234728.53 N:391936.339
(mAOD)
26
25.5
25
24.5
24
23.5
23
22.5
22
21.5
21
01/01/2015
02/04/2015
02/07/2015
01/10/2015
01/01/2016
01/04/2016
01/07/2016
CG_PZ_POB: low recharge run (053v2)
CG_PZ_POB: high recharge run (054)
CG_PZ_POB: baseline run (050)
CG_PZ_POB: observed
RH_CG_PZ_POB (est)
GL_CG_PZ_POB

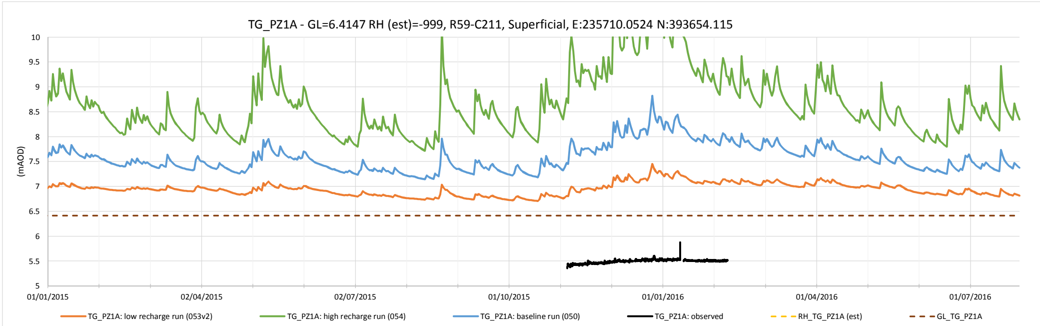
TG_PZ1A - GL=6.4147 RH (est)=-999, R59-C211, Superficial, E:235710.0524 N:393654.115
(mAOD)
01/01/2015
02/04/2015
02/07/2015
01/10/2015
01/01/2016
01/04/2016
01/07/2016
TG_PZ1A: low recharge run (053v2)
TG_PZ1A: high recharge run (054)
TG_PZ1A: baseline run (050)
TG_PZ1A: observed
RH_TG_PZ1A (est)
GL_TG_PZ1A

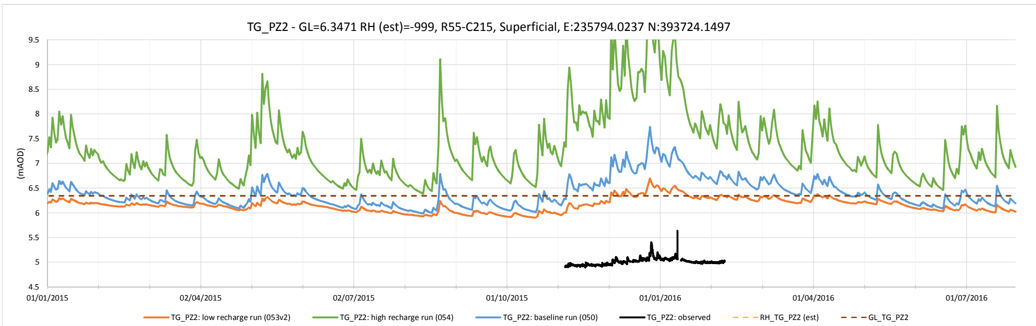
TG_PZ2 - GL=6.3471 RH (est)=-999, R55-C215, Superficial, E:235794.0237 N:393724.1497
(mAOD)
01/01/2015
02/04/2015
02/07/2015
01/10/2015
01/01/2016
01/04/2016
01/07/2016
TG_PZ2: low recharge run (053v2)
TG_PZ2: high recharge run (054)
TG_PZ2: baseline run (050)
TG_PZ2: observed
RH_TG_PZ2 (est)
GL_TG_PZ2

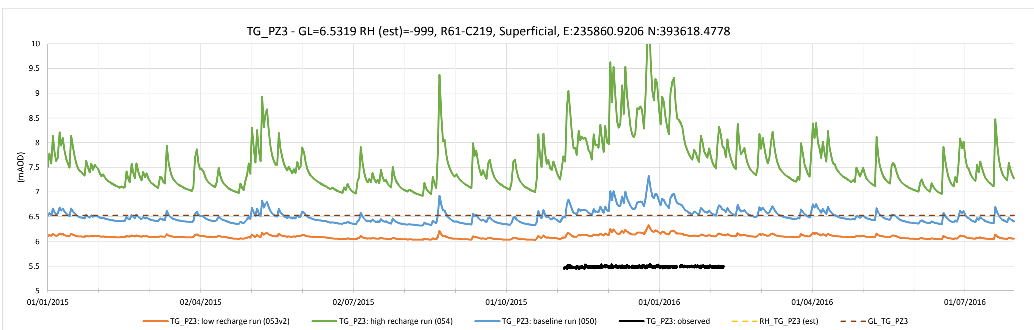
TG_PZ3 - GL=6.5319 RH (est)=-999, R61-C219, Superficial, E:235860.9206 N:393618.4778
(mAOD)
01/01/2015
02/04/2015
02/07/2015
01/10/2015
01/01/2016
01/04/2016
01/07/2016
TG_PZ3: low recharge run (053v2)
TG_PZ3: high recharge run (054)
TG_PZ3: baseline run (050)
TG_PZ3: observed
RH_TG_PZ3 (est)
GL_TG_PZ3

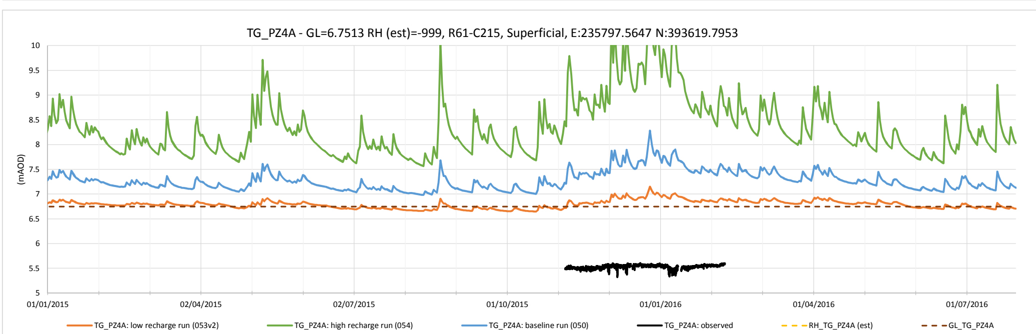
TG_PZ4A - GL=6.7513 RH (est)=-999, R61-C215, Superficial, E:235797.5647 N:393619.7953
(mAOD)
01/01/2015
02/04/2015
02/07/2015
01/10/2015
01/01/2016
01/04/2016
01/07/2016
TG_PZ4A: low recharge run (053v2)
TG_PZ4A: high recharge run (054)
TG_PZ4A: baseline run (050)
TG_PZ4A: observed
RH_TG_PZ4A (est)
GL_TG_PZ4A

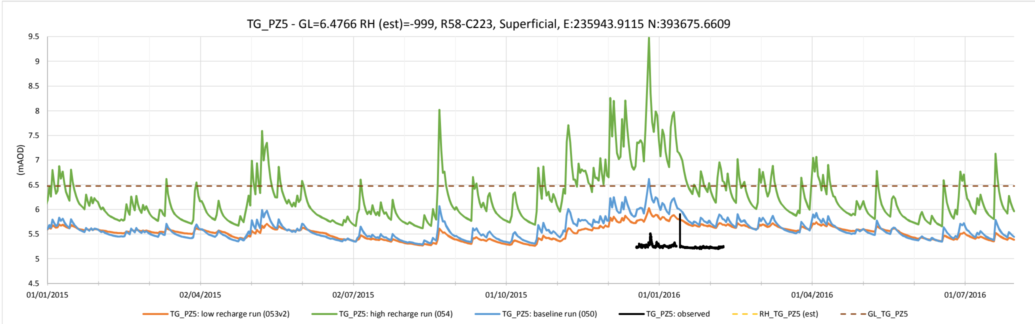
TG_PZ5 - GL=6.4766 RH (est)=-999, R58-C223, Superficial, E:235943.9115 N:393675.6609
(mAOD)
01/01/2015
02/04/2015
02/07/2015
01/10/2015
01/01/2016
01/04/2016
01/07/2016
TG_PZ5: low recharge run (053v2)
TG_PZ5: high recharge run (054)
TG_PZ5: baseline run (050)
TG_PZ5: observed
RH_TG_PZ5 (est)
GL_TG_PZ5

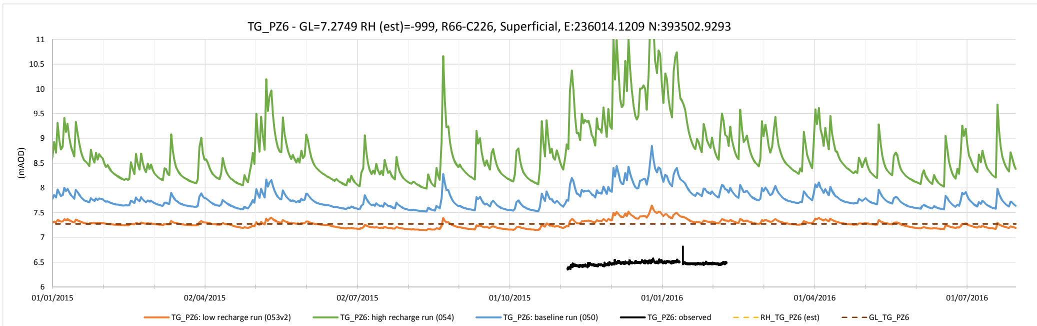
TG_PZ6 - GL=7.2749 RH (est)=-999, R66-C226, Superficial, E:236014.1209 N:393502.9293
(mAOD)
01/01/2015
02/04/2015
02/07/2015
01/10/2015
01/01/2016
01/04/2016
01/07/2016
TG_PZ6: low recharge run (053v2)
TG_PZ6: high recharge run (054)
TG_PZ6: baseline run (050)
TG_PZ6: observed
RH_TG_PZ6 (est)
GL_TG_PZ6

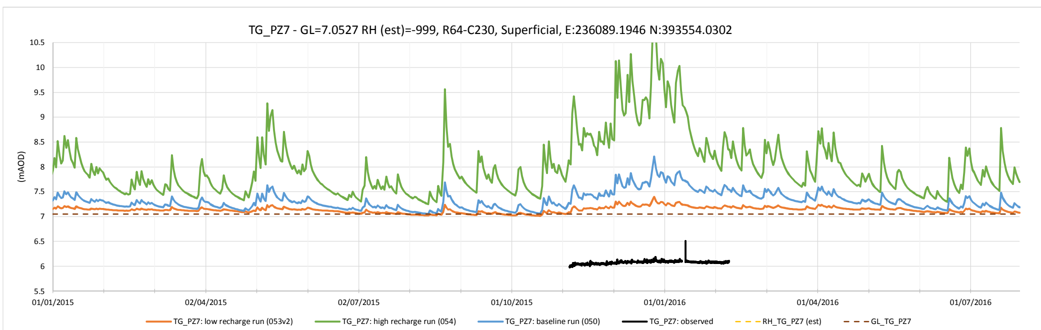
TG_PZ7 - GL=7.0527 RH (est)=-999, R64-C230, Superficial, E:236089.1946 N:393554.0302
(mAOD)
01/01/2015
02/04/2015
02/07/2015
01/10/2015
01/01/2016
01/04/2016
01/07/2016
TG_PZ7: low recharge run (053v2)
TG_PZ7: high recharge run (054)
TG_PZ7: baseline run (050)
TG_PZ7: observed
RH_TG_PZ7 (est)
GL_TG_PZ7

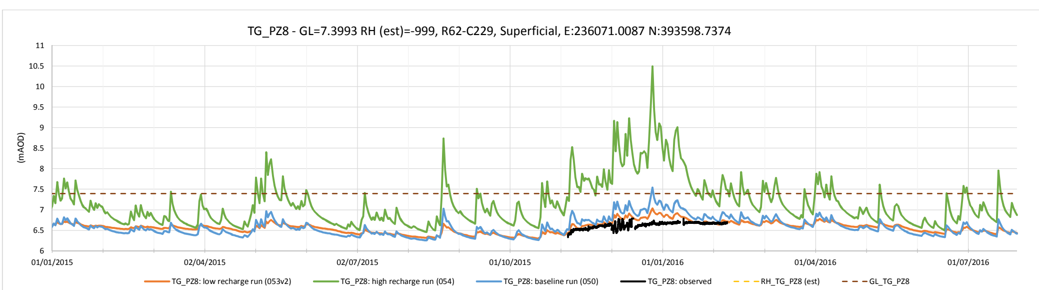
TG_PZ8 - GL=7.3993 RH (est)=-999, R62-C229, Superficial, E:236071.0087 N:393598.7374
(mAOD)
01/01/2015
02/04/2015
02/07/2015
01/10/2015
01/01/2016
01/04/2016
01/07/2016
TG_PZ8: low recharge run (053v2)
TG_PZ8: high recharge run (054)
TG_PZ8: baseline run (050)
TG_PZ8: observed
RH_TG_PZ8 (est)
GL_TG_PZ8

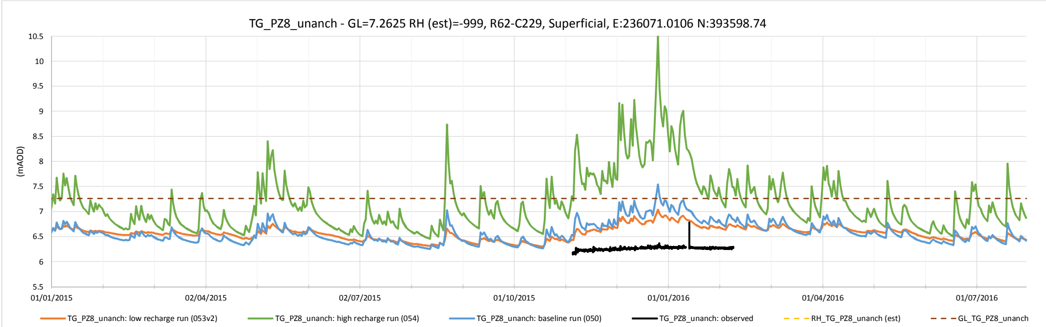
TG_PZ8_unanch - GL=7.2625 RH (est)=-999, R62-C229, Superficial, E:236071.0106 N:393598.74
(mAOD)
10.5
10
9.5
9
8.5
8
7.5
7
6.5
6
5.5
01/01/2015
02/04/2015
02/07/2015
01/10/2015
01/01/2016
01/04/2016
01/07/2016
TG_PZ8_unanch: low recharge run (053v2)
TG_PZ8_unanch: high recharge run (054)
TG_PZ8_unanch: baseline run (050)
TG_PZ8_unanch: observed
RH_TG_PZ8_unanch (est)
GL_TG_PZ8_unanch

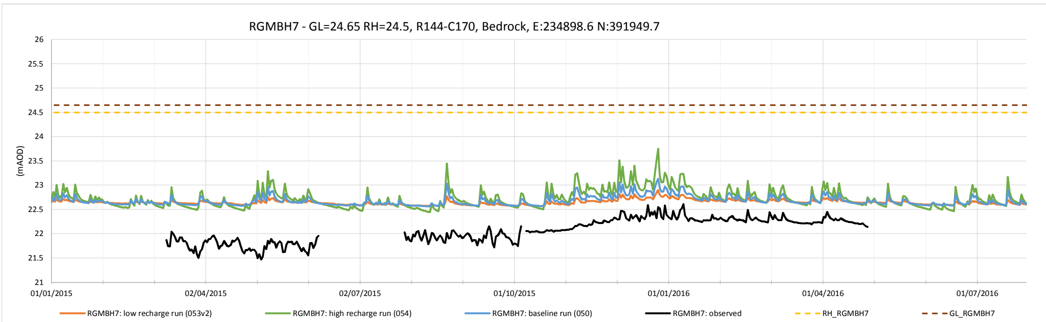
RGMBH7 - GL=24.65 RH=24.5, R144-C170, Bedrock, E:234898.6 N:391949.7
(mAOD)
26
25.5
25
24.5
24
23.5
23
22.5
22
21.5
21
01/01/2015
02/04/2015
02/07/2015
01/10/2015
01/01/2016
01/04/2016
01/07/2016
RGMBH7: low recharge run (053v2)
RGMBH7: high recharge run (054)
RGMBH7: baseline run (050)
RGMBH7: observed
RH_RGMBH7
GL_RGMBH7

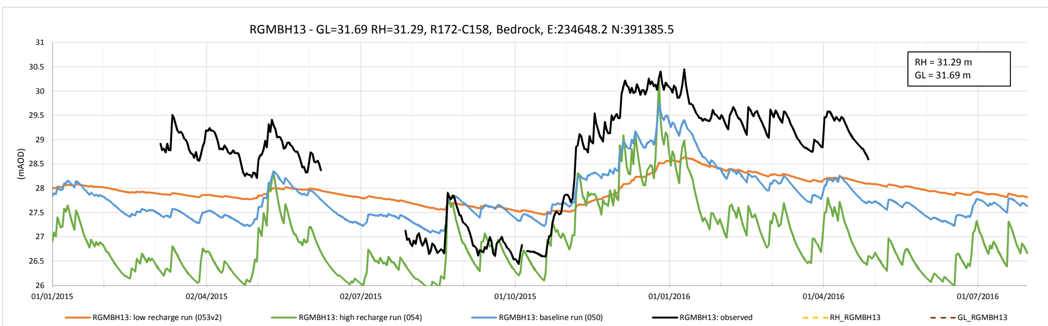
RGMBH13 - GL=31.69 RH=31.29, R172-C158, Bedrock, E:234648.2 N:391385.5
RH = 31.29 m
GL = 31.69 m
(mAOD)
31
30.5
30
29.5
29
28.5
28
27.5
27
26.5
26
01/01/2015
02/04/2015
02/07/2015
01/10/2015
01/01/2016
01/04/2016
01/07/2016
RGMBH13: low recharge run (053v2)
RGMBH13: high recharge run (054)
RGMBH13: baseline run (050)
RGMBH13: observed
RH_RGMBH13
GL_RGMBH13

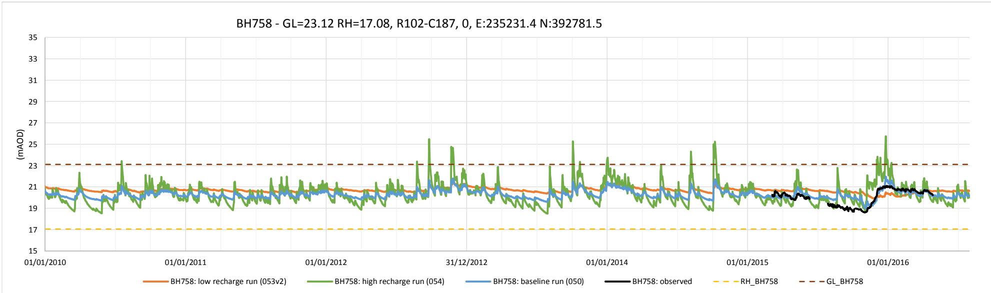
BH758 - GL=23.12 RH=17.08, R102-C187, 0, E:235231.4 N:392781.5
(mAOD)
01/01/2010
01/01/2011
01/01/2012
31/12/2012
01/01/2014
01/01/2015
01/01/2016
BH758: low recharge run (053v2)
BH758: high recharge run (054)
BH758: baseline run (050)
BH758: observed
RH_BH758
GL_BH758

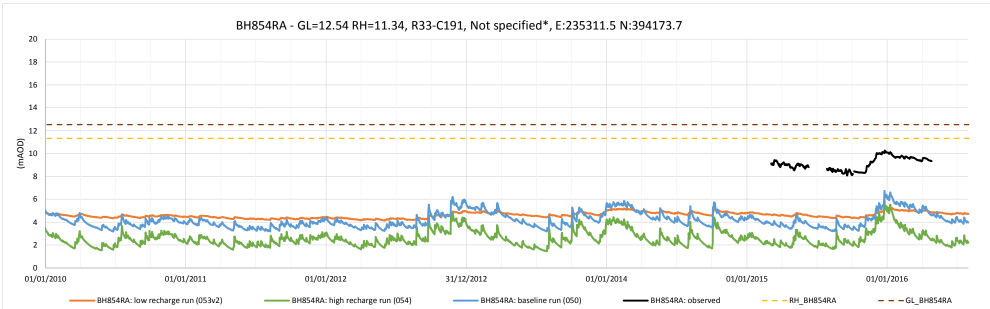
BH854RA - GL=12.54 RH=11.34, R33-C191, Not specified*, E:235311.5 N:394173.7
(mAOD)
01/01/2010
01/01/2011
01/01/2012
31/12/2012
01/01/2014
01/01/2015
01/01/2016
BH854RA: low recharge run (053v2)
BH854RA: high recharge run (054)
BH854RA: baseline run (050)
BH854RA: observed
RH_BH854RA
GL_BH854RA

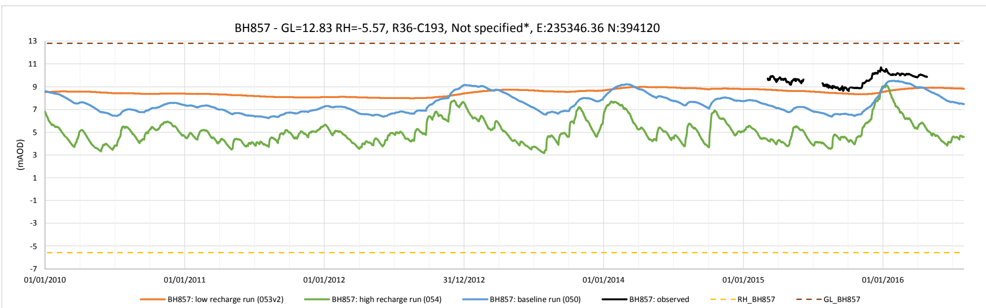
BH857 - GL=12.83 RH=-5.57, R36-C193, Not specified*, E:235346.36 N:394120
(mAOD)
01/01/2010
01/01/2011
01/01/2012
31/12/2012
01/01/2014
01/01/2015
01/01/2016
BH857: low recharge run (053v2)
BH857: high recharge run (054)
BH857: baseline run (050)
BH857: observed
RH_BH857
GL_BH857

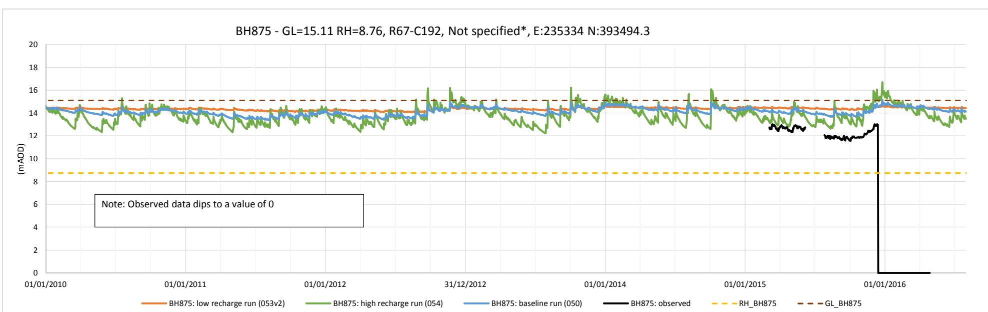
BH875 - GL=15.11 RH=8.76, R67-C192, Not specified*, E:235334 N:393494.3
(mAOD)
Note: Observed data dips to a value of 0
01/01/2010
01/01/2011
01/01/2012
31/12/2012
01/01/2014
01/01/2015
01/01/2016
BH875: low recharge run (053v2)
BH875: high recharge run (054)
BH875: baseline run (050)
BH875: observed
RH_BH875
GL_BH875

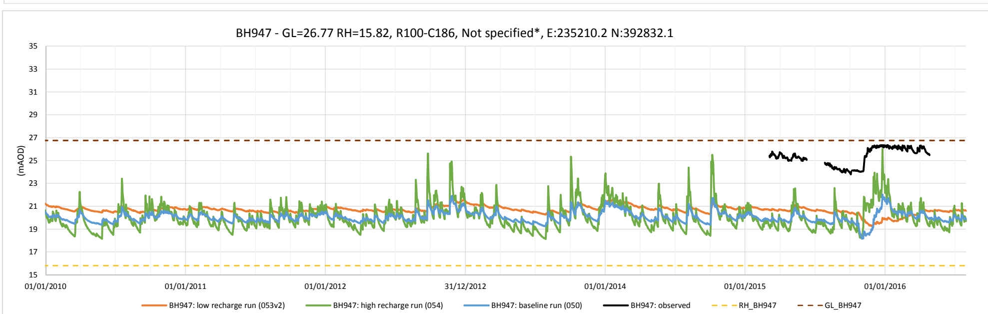
BH947 - GL=26.77 RH=15.82, R100-C186, Not specified*, E:235210.2 N:392832.1
(mAOD)
01/01/2010
01/01/2011
01/01/2012
31/12/2012
01/01/2014
01/01/2015
01/01/2016
BH947: low recharge run (053v2)
BH947: high recharge run (054)
BH947: baseline run (050)
BH947: observed
RH_BH947
GL_BH947

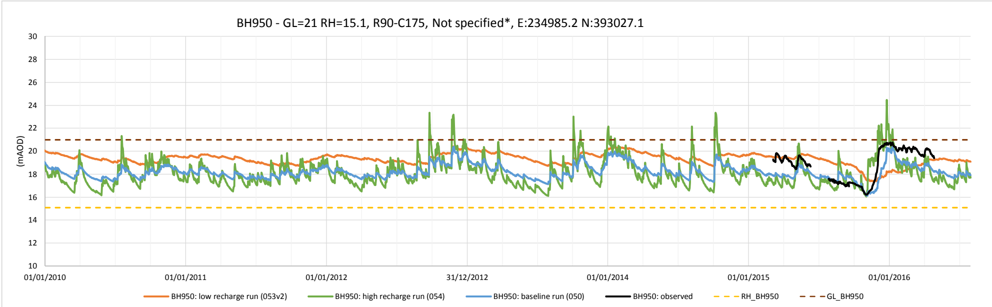
BH950 - GL=21 RH=15.1, R90-C175, Not specified*, E:234985.2 N:393027.1
30
28
26
24
22
20
18
16
14
12
10
(mAOD)
01/01/2010
01/01/2011
01/01/2012
31/12/2012
01/01/2014
01/01/2015
01/01/2016
BH950: low recharge run (053v2)
BH950: high recharge run (054)
BH950: baseline run (050)
BH950: observed
RH_BH950
GL_BH950

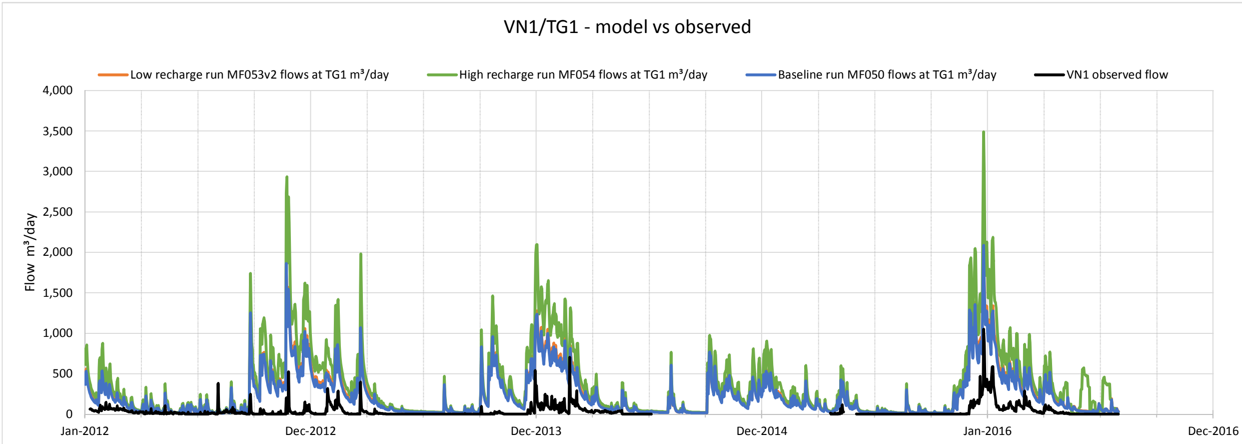
VN1/TG1 - model vs observed
Low recharge run MF053v2 flows at TG1 m³/day
High recharge run MF054 flows at TG1 m³/day
Baseline run MF050 flows at TG1 m³/day
VN1 observed flow
Flow m³/day
4,000
3,500
3,000
2,500
2,000
1,500
1,000
500
0
Jan-2012
Dec-2012
Dec-2013
Dec-2014
Jan-2016
Dec-2016

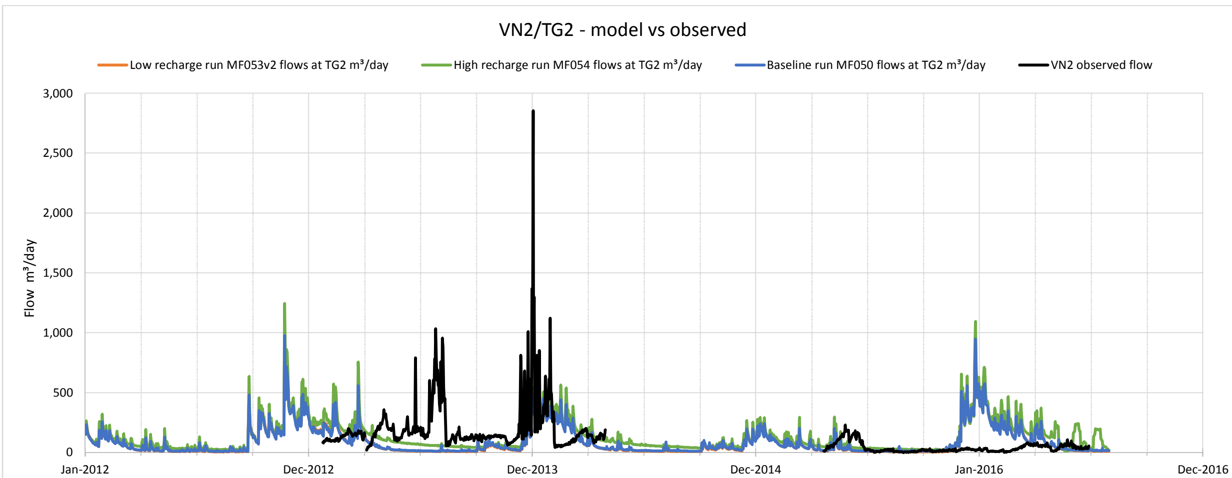
VN2/TG2 - model vs observed
Low recharge run MF053v2 flows at TG2 m³/day
High recharge run MF054 flows at TG2 m³/day
Baseline run MF050 flows at TG2 m³/day
VN2 observed flow
Flow m³/day
3,000
2,500
2,000
1,500
1,000
500
0
Jan-2012
Dec-2012
Dec-2013
Dec-2014
Jan-2016
Dec-2016

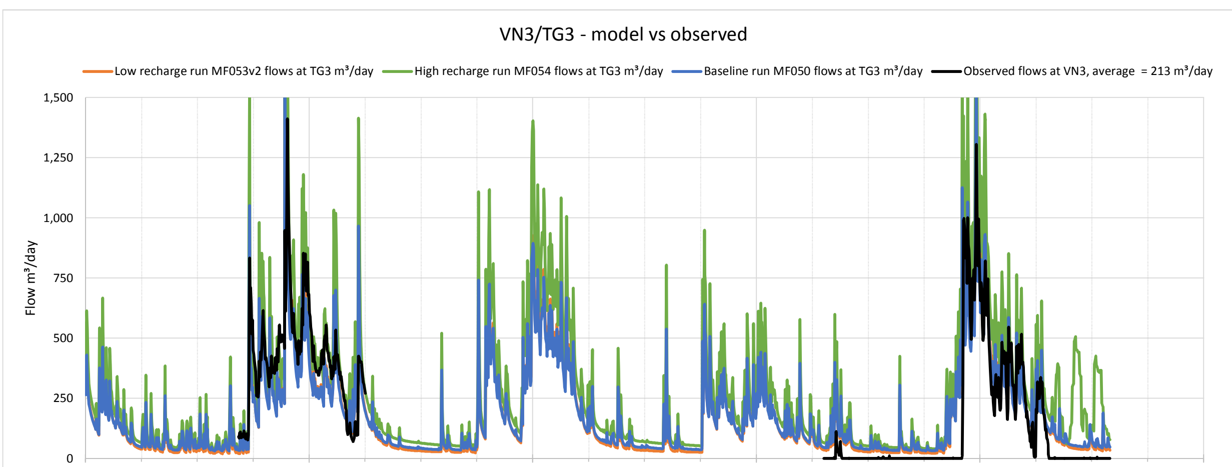
VN3/TG3 - model vs observed
Low recharge run MF053v2 flows at TG3 m³/day
High recharge run MF054 flows at TG3 m³/day
Baseline run MF050 flows at TG3 m³/day
Observed flows at VN3, average = 213 m³/day
Flow m³/day
1,500
1,250
1,000
750
500
250
0

Jan-2012
Dec-2012
Dec-2013
Dec-2014
Jan-2016
Dec-2016

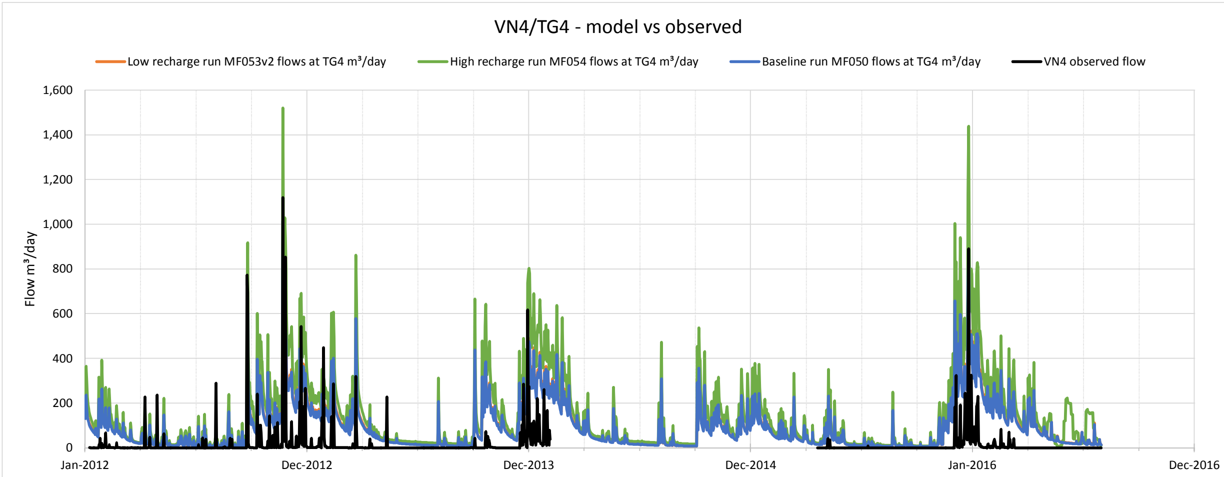
VN4/TG4 - model vs observed
Low recharge run MF053v2 flows at TG4 m³/day
High recharge run MF054 flows at TG4 m³/day
Baseline run MF050 flows at TG4 m³/day
VN4 observed flow
Flow m³/day
1,600
1,400
1,200
1,000
800
600
400
200
0
Jan-2012
Dec-2012
Dec-2013
Dec-2014
Jan-2016
Dec-2016

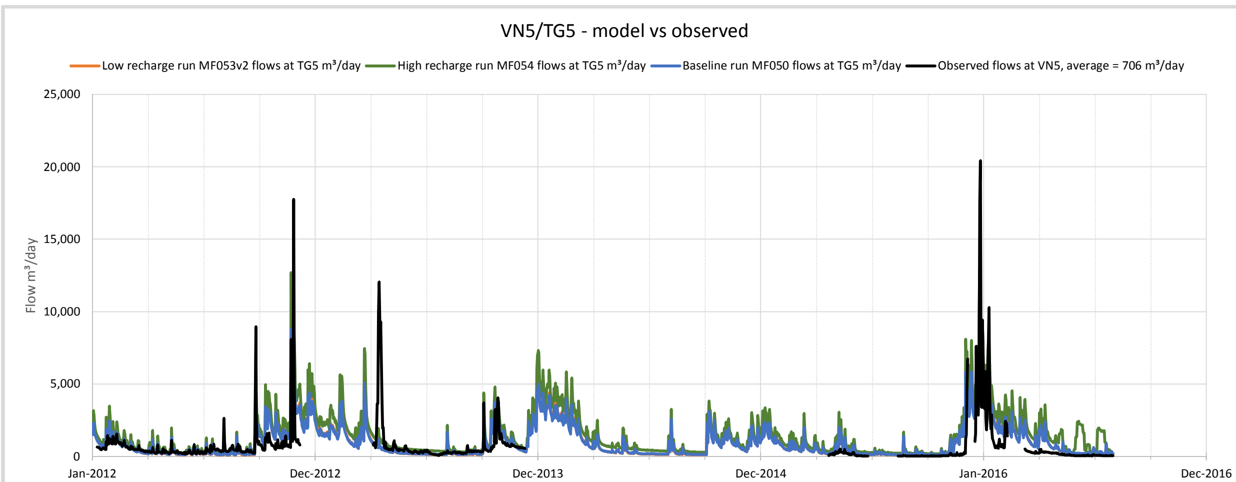
VN5/TG5 - model vs observed
Low recharge run MF053v2 flows at TG5 m³/day
High recharge run MF054 flows at TG5 m³/day
Baseline run MF050 flows at TG5 m³/day
Observed flows at VN5, average = 706 m³/day
Flow m³/day
25,000
20,000
15,000
10,000
5,000
0
Jan-2012
Dec-2012
Dec-2013
Dec-2014
Jan-2016
Dec-2016

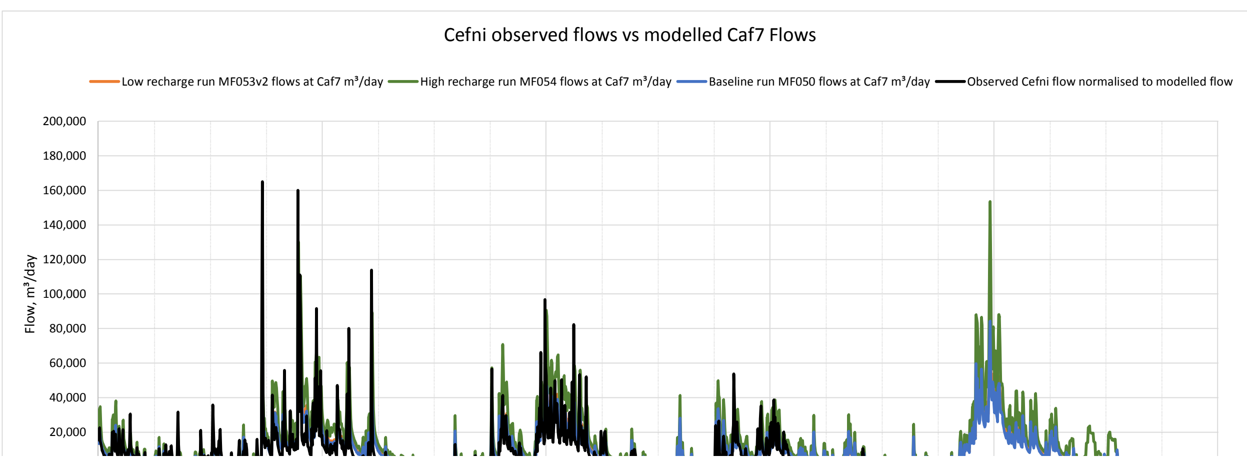
Cefni observed flows vs modelled Caf7 Flows
Low recharge run MF053v2 flows at Caf7 m³/day
High recharge run MF054 flows at Caf7 m³/day
Baseline run MF050 flows at Caf7 m³/day
Observed Cefni flow normalised to modelled flow
Flow, m³/day
200,000
180,000
160,000
140,000
120,000
100,000
80,000
60,000
40,000
20,000

Flume A - model vs observed

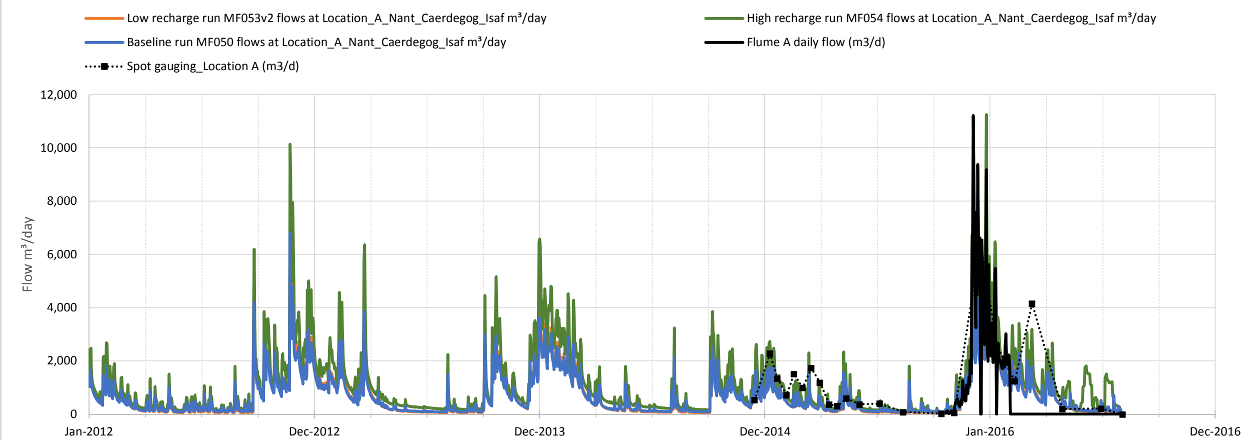

Flume B - model vs observed

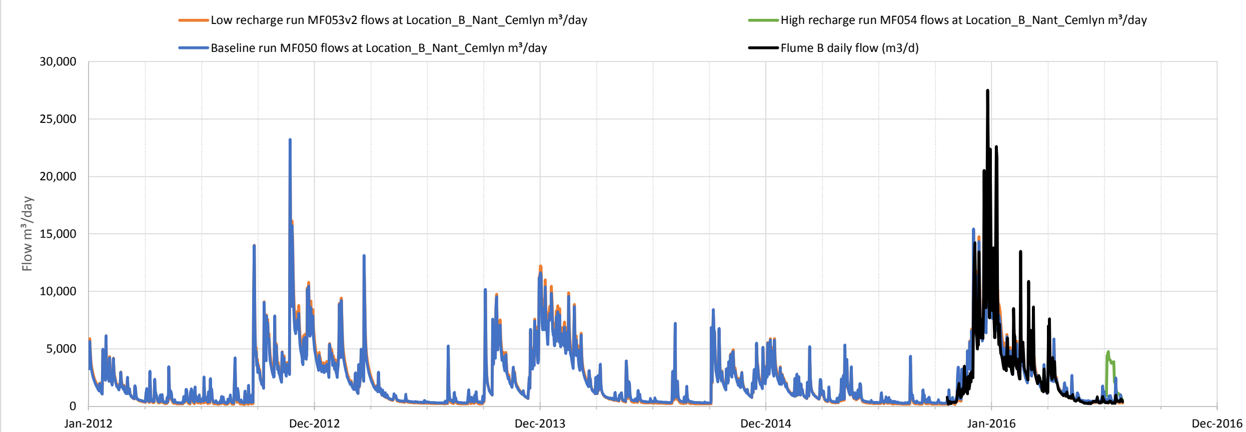

Location B(2) - spot gaugings only - model vs observed

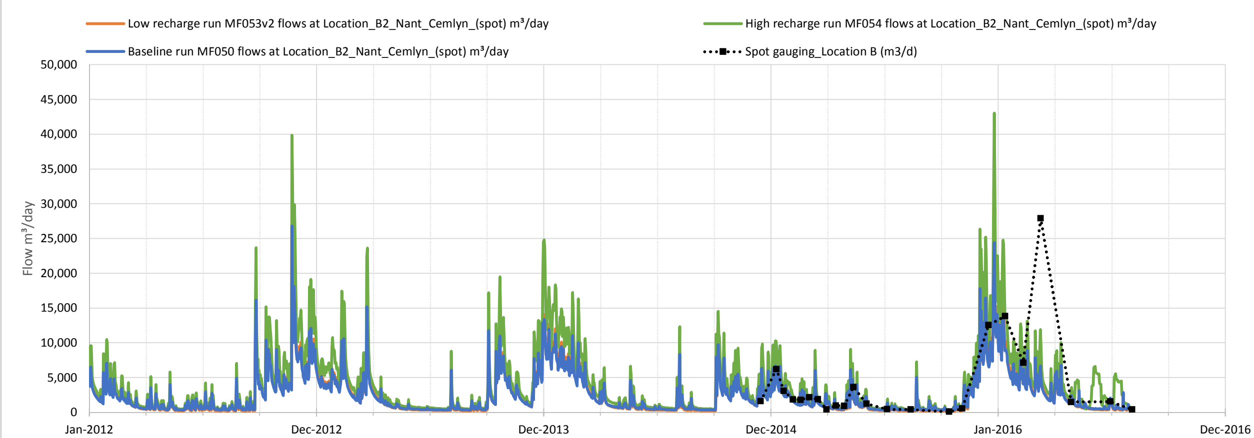

Appendix D
Predictive scenario model plans for Reference Point 4 (construction) and Reference Point 5 (operation)

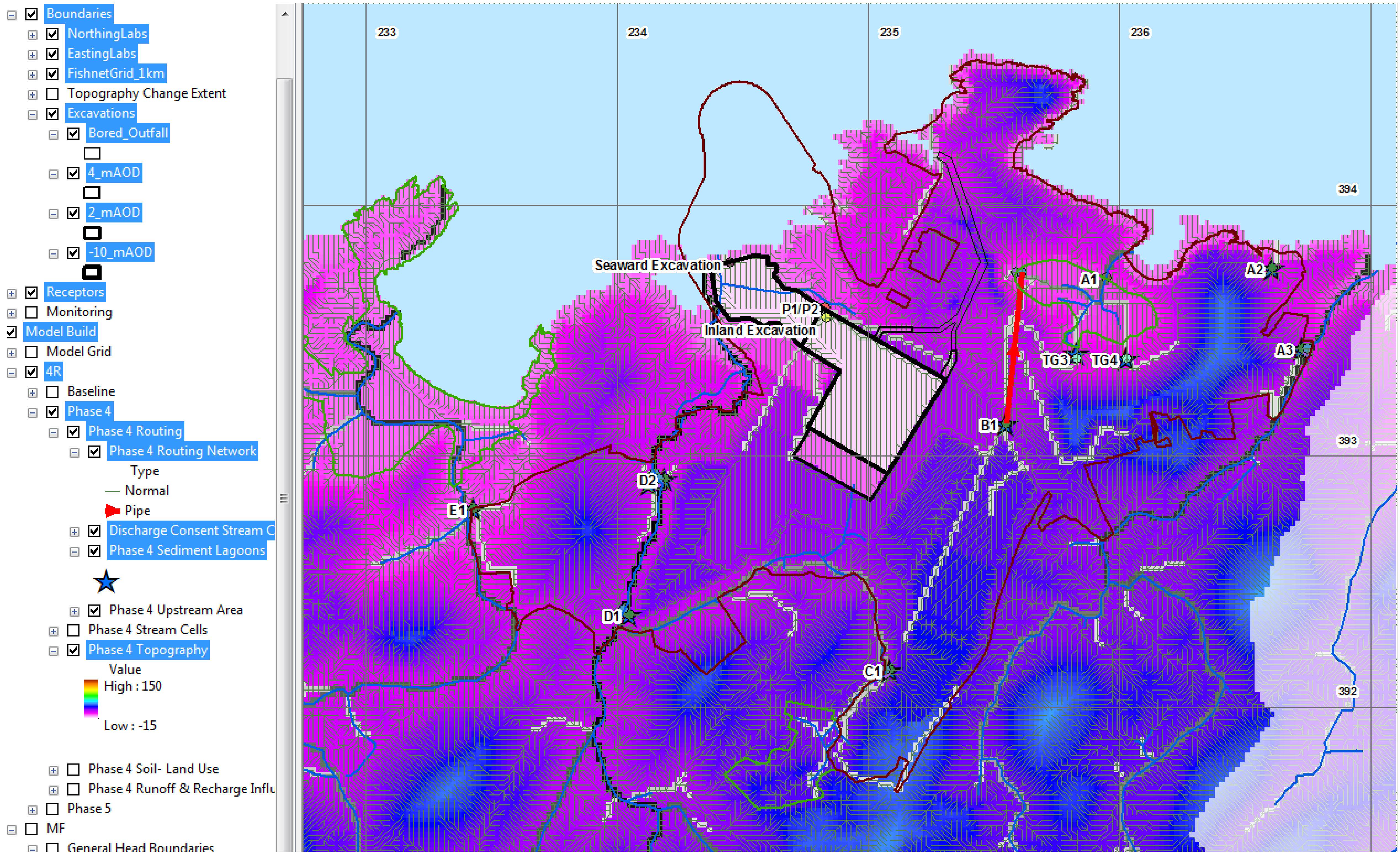

Phase 4 topography, rivers, SSSI receptors, Site boundary, 4R upstream routed area, detailed routing, sediment lagoons, drainage discharge MODFLOW General Head Boundary sea bed, and Inactive cell overlay

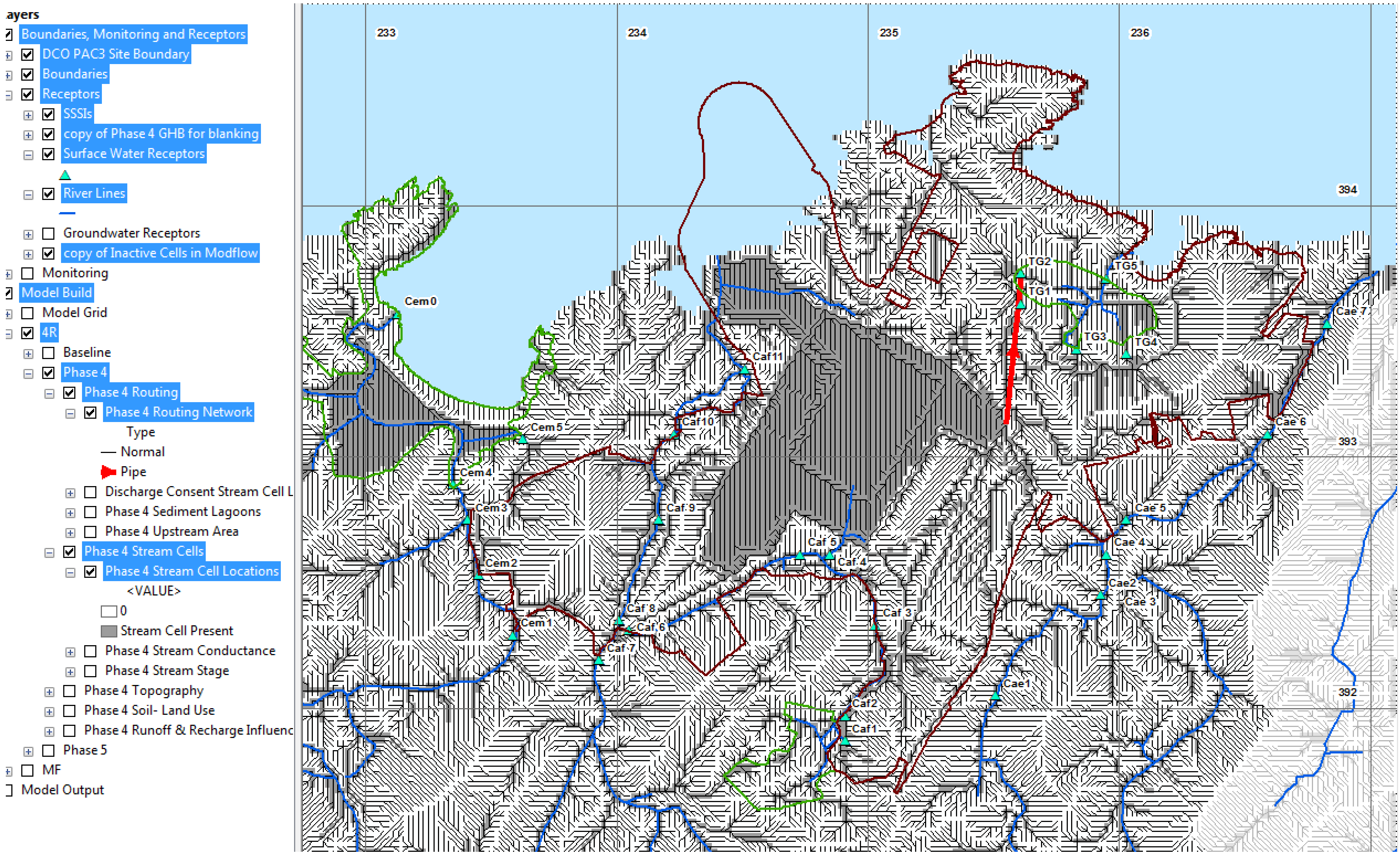

Phase 4 rivers, SSSI receptors, Site boundary, surface water flow receptors, 4R detailed routing, MODFLOW Stream cells, General Head Boundary sea bed, and Inactive cell overlay

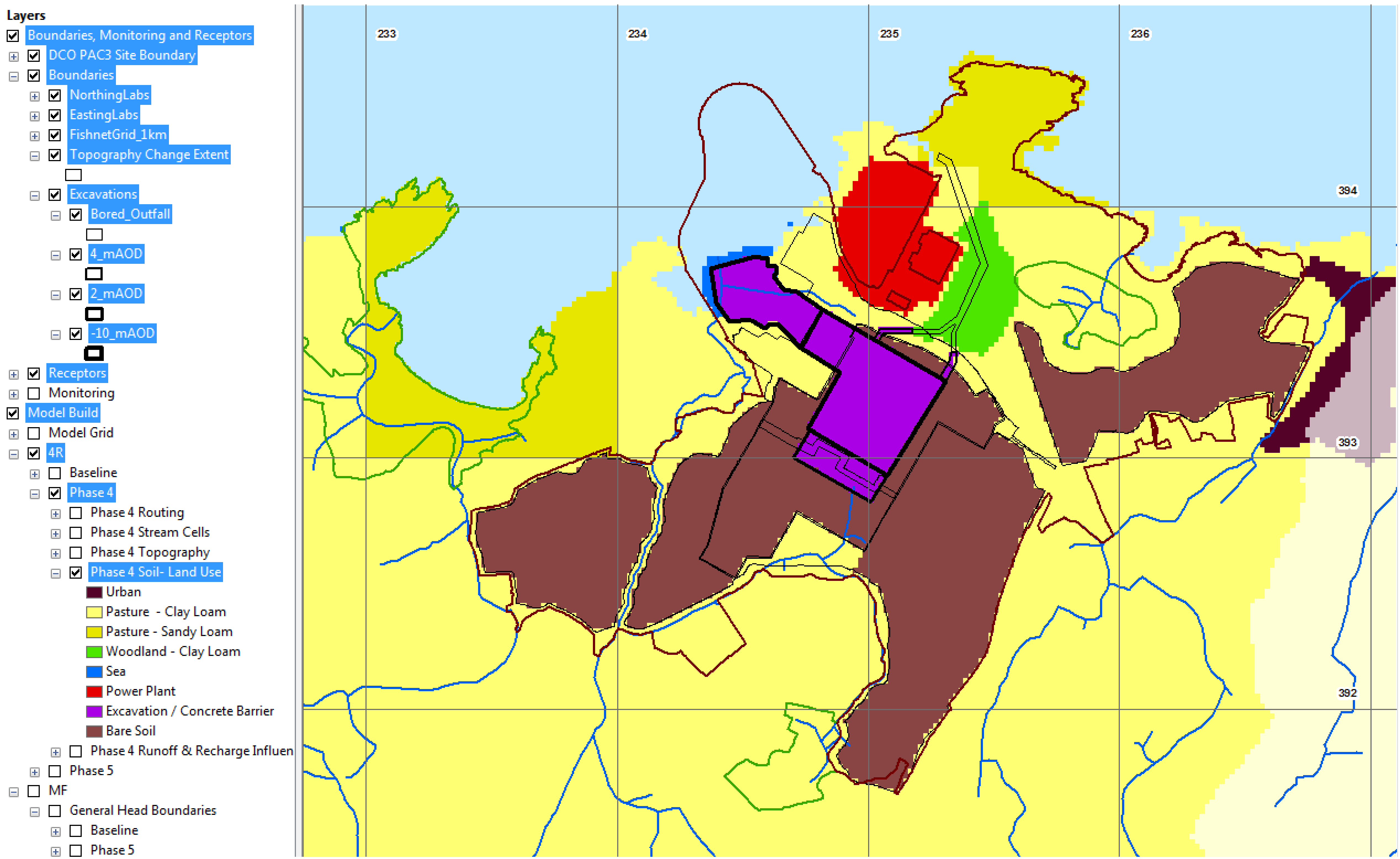

Phase 4 rivers, SSSI receptors, Site boundary, excavation outline, topography change area, 4R soil - land use, MODFLOW General Head Boundary sea bed and Inactive cell overlay

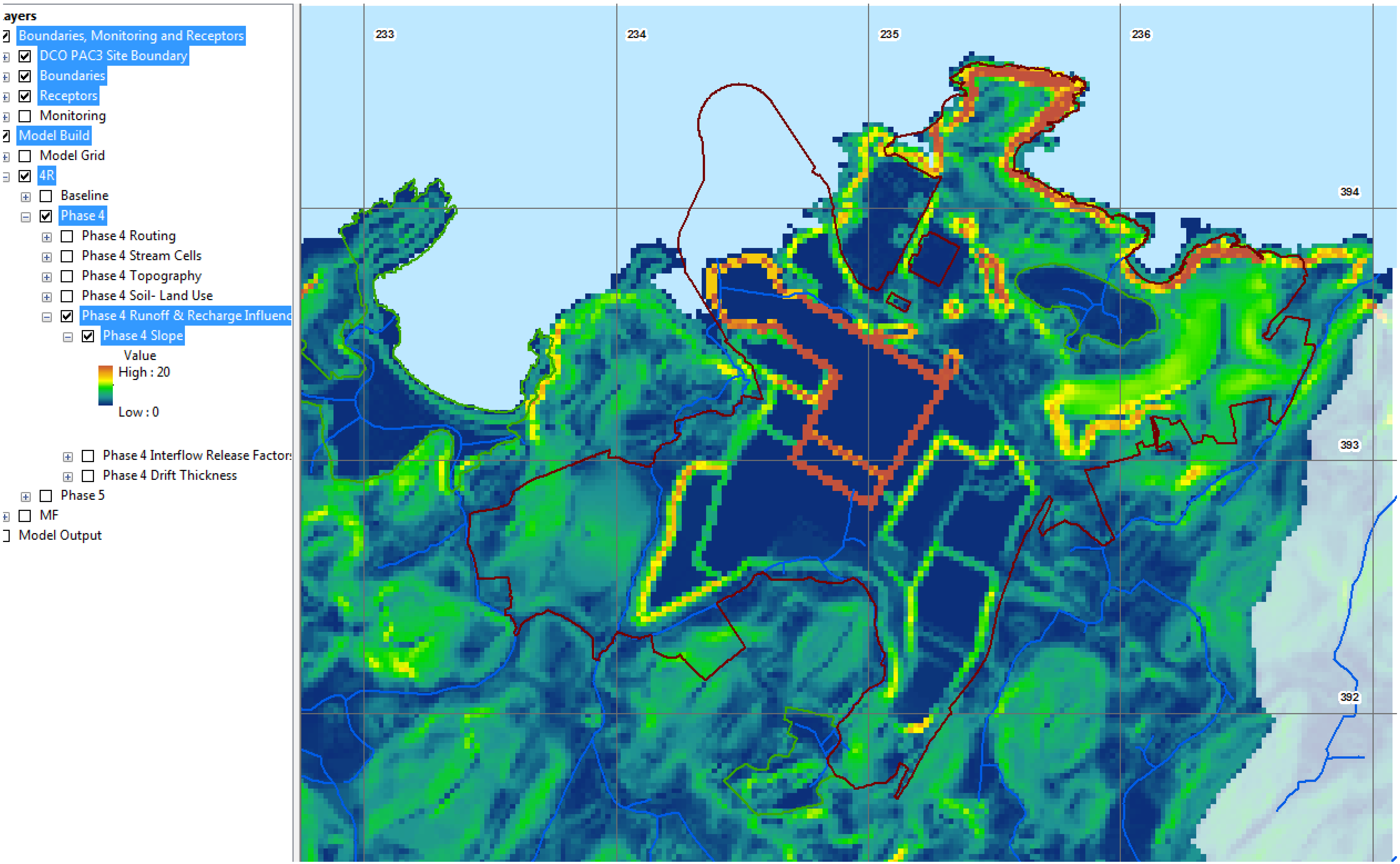

Phase 4 rivers, SSSI receptors, Site boundary, 4R slope, MODFLOW General Head Boundary sea bed, and Inactive cell overlay

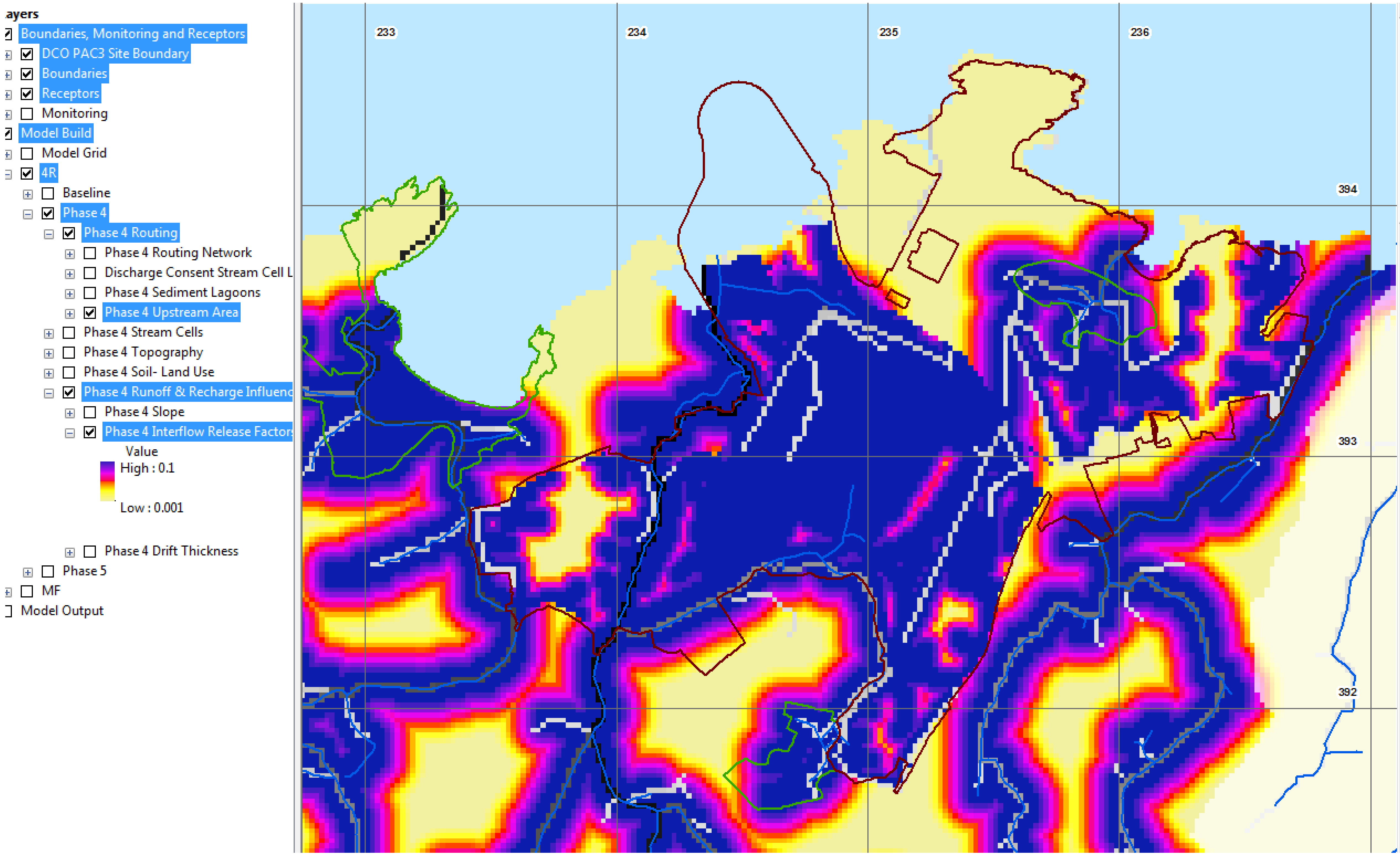

Phase 4 rivers, SSSI receptors, Site boundary, 4R upstream routed area and interflow release factor, MODFLOW General Head Boundary sea bed, and Inactive cell overlay

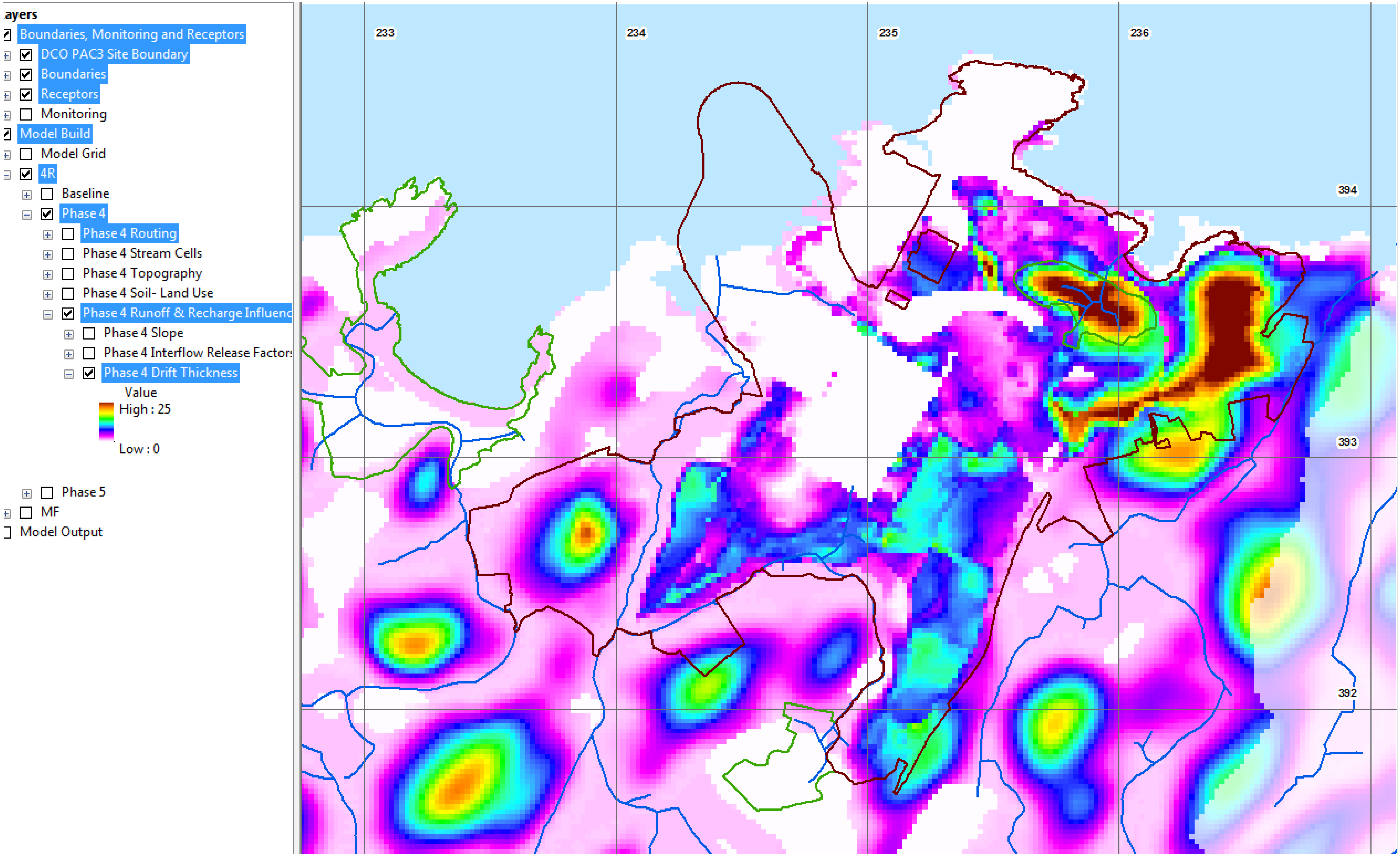

Phase 4 rivers, SSSI receptors, Site boundary, Drift & Mound thickness, MODFLOW General Head Boundary sea bed, and Inactive cell overlay

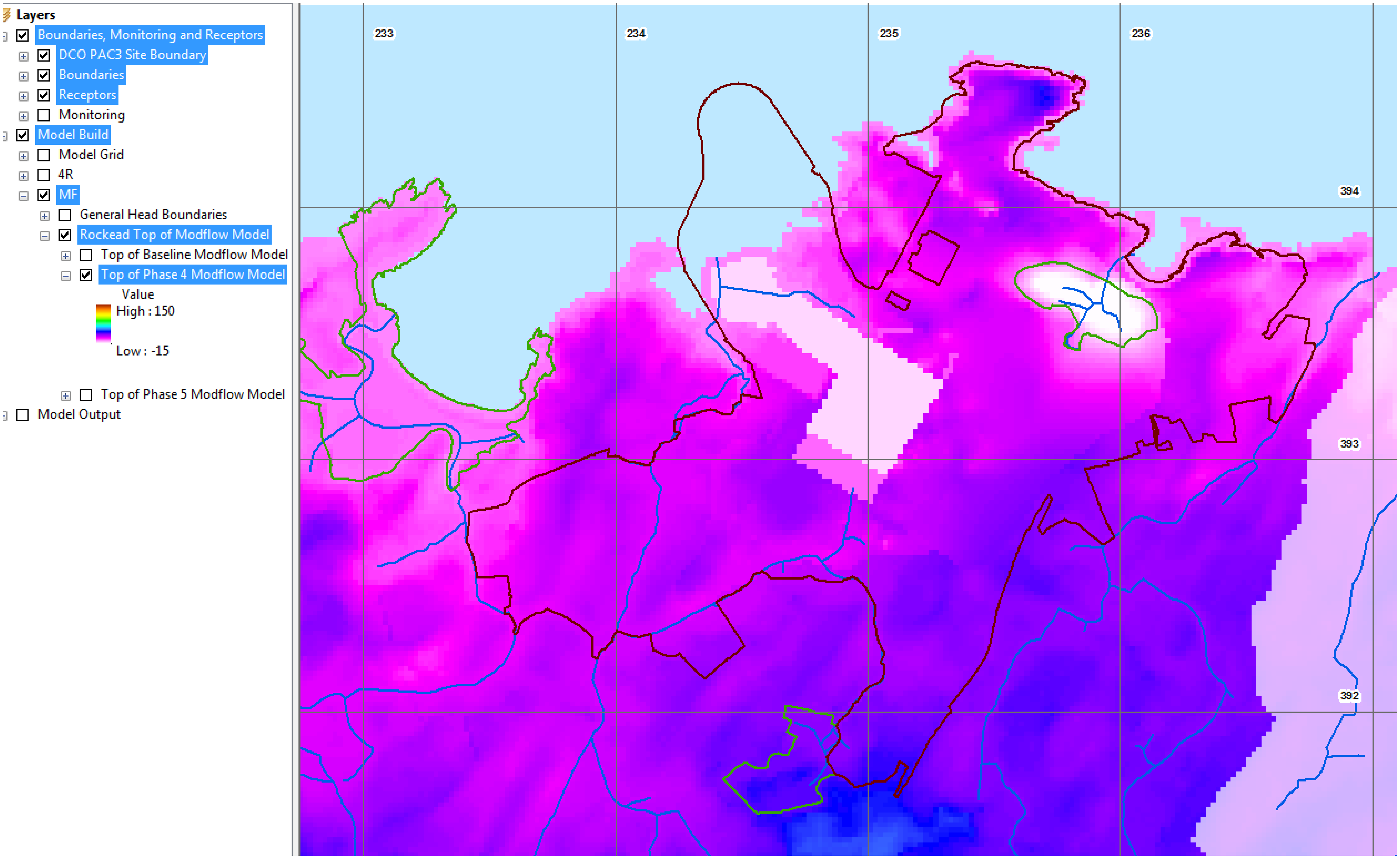

Phase 4 rivers, SSSI receptors, Site boundary, MODFLOW General Head Boundary sea bed cells, top of bedrock layer elevation (rock head) and Inactive cell overlay

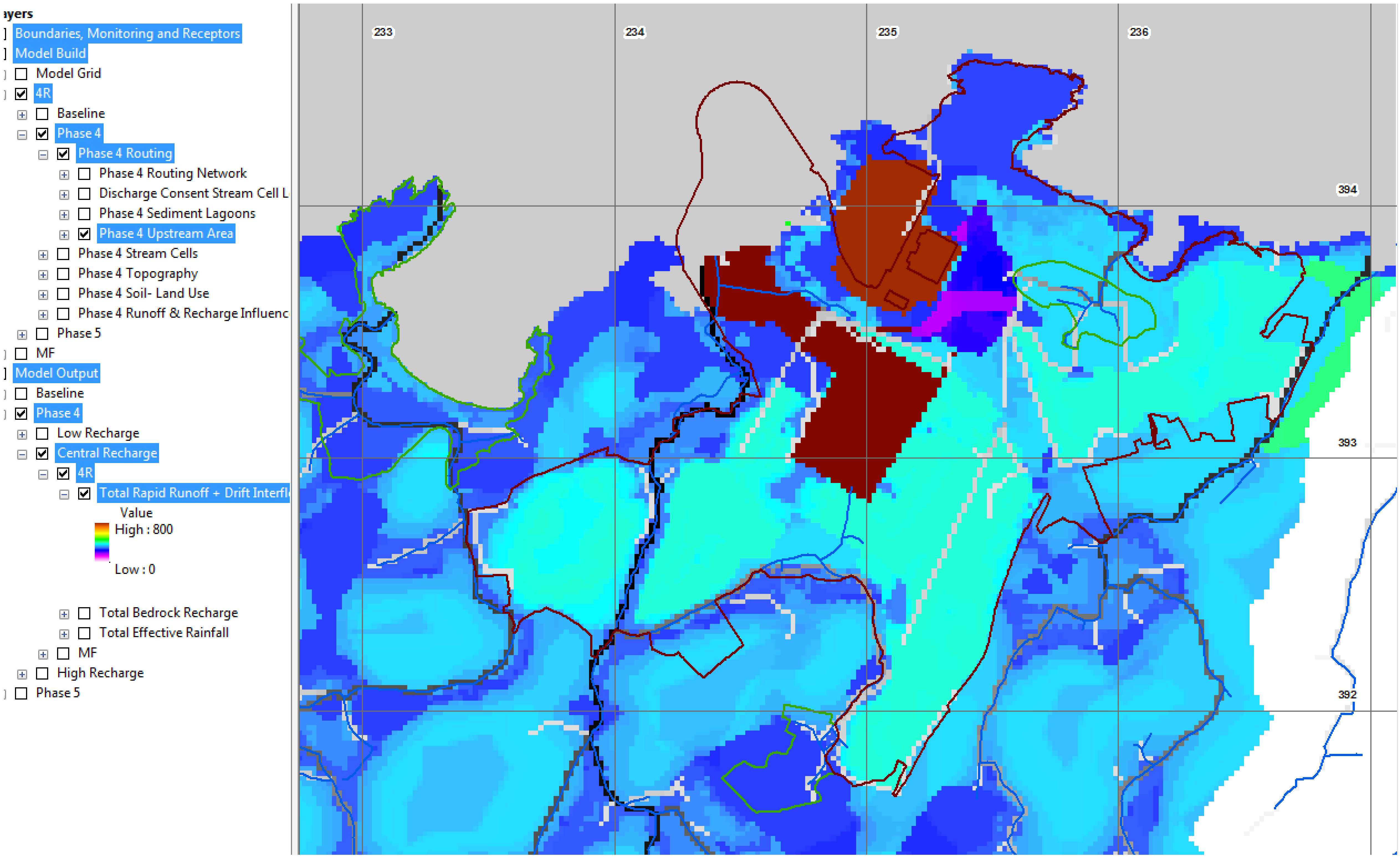

Phase 4 rivers, SSSI receptors, Site boundary, 4R upstream routed area and Central Model rapid runoff + interflow output, MODFLOW GHB cells and Inactive cell overlay

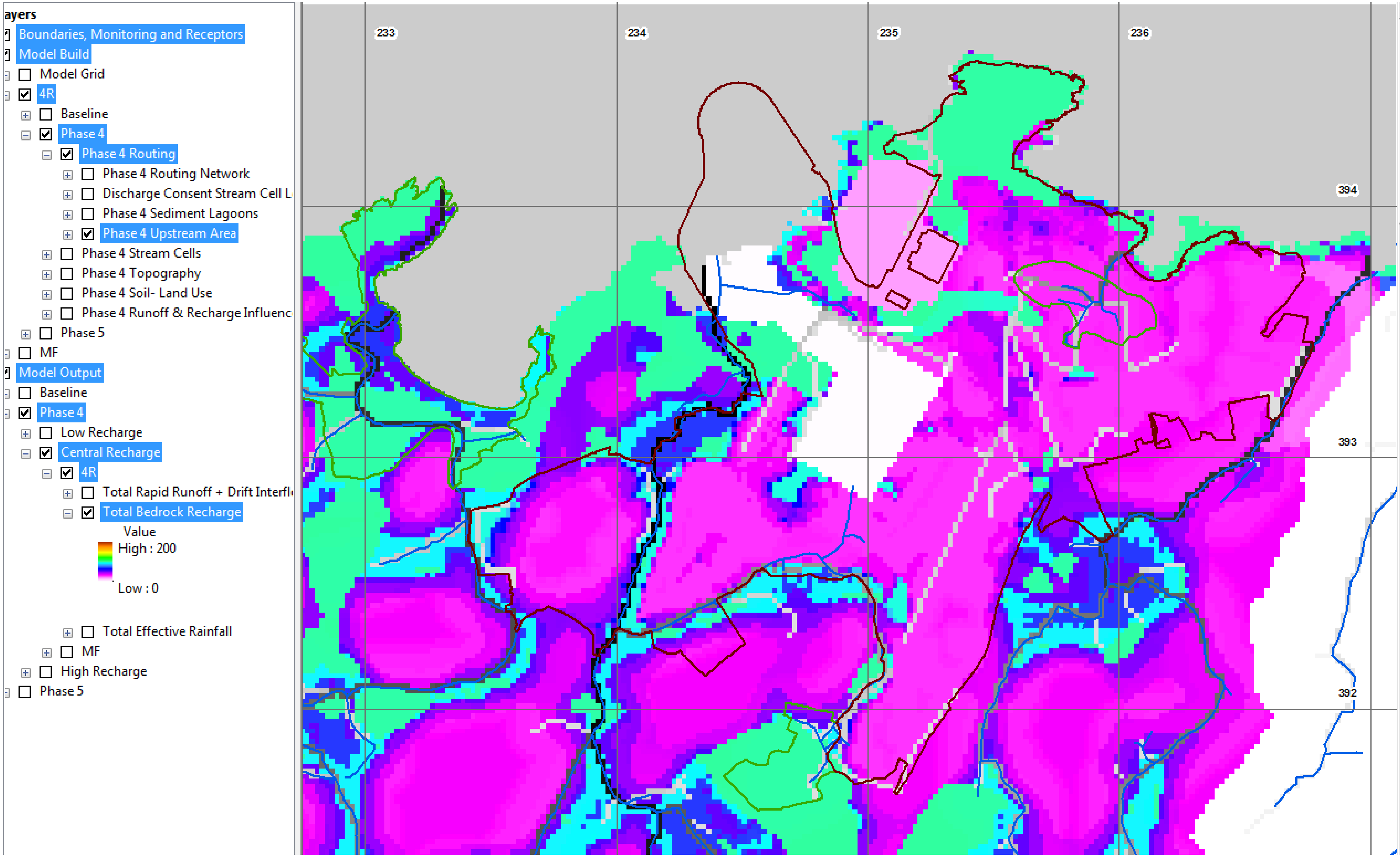

Phase 4 rivers, SSSI receptors, Site boundary, 4R Central Model bedrock recharge, MODFLOW GHB cells and Inactive cell overlay

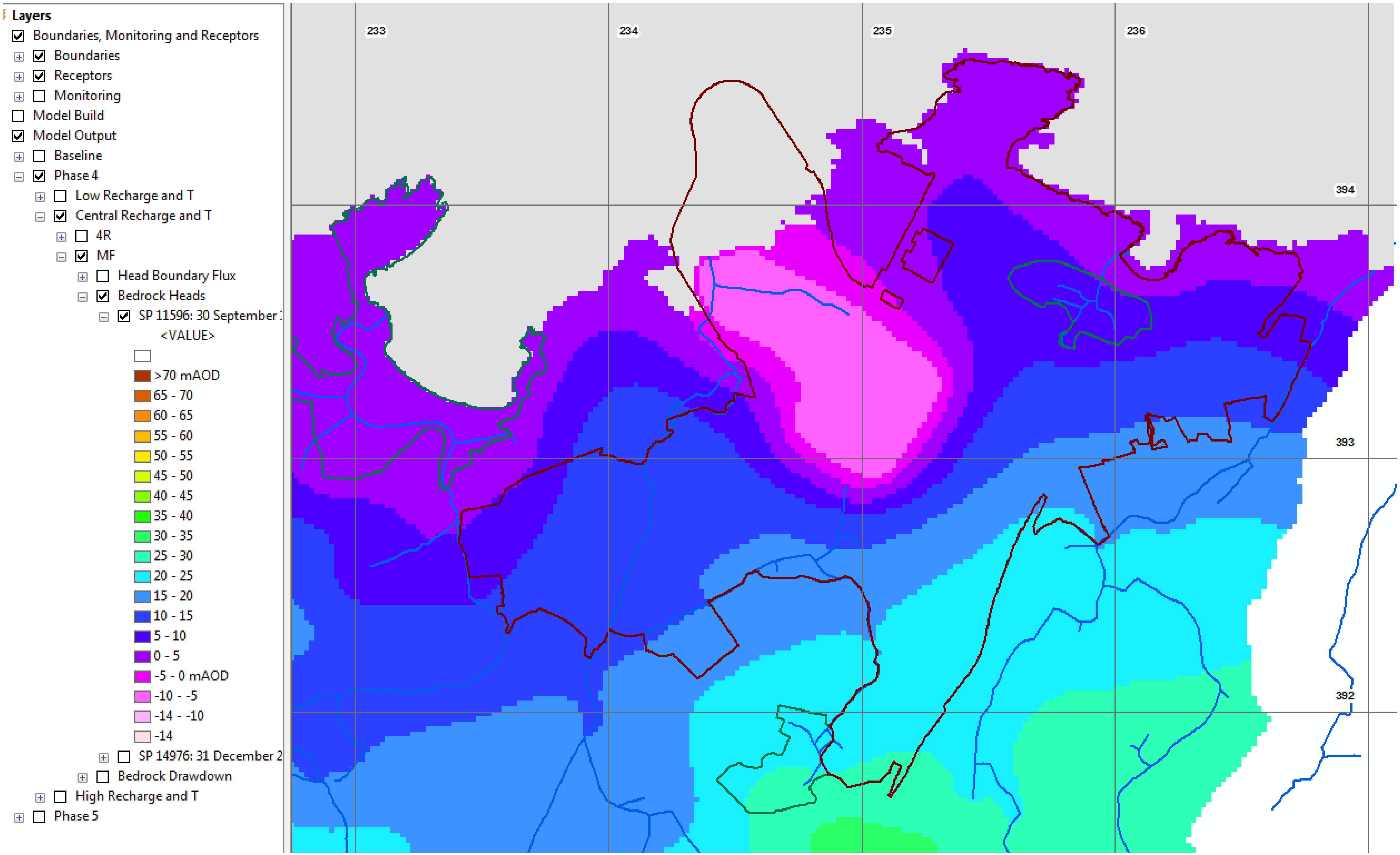

amec foster wheeler

WylDCOGWMod_35989N1403i1 Appendix D, Phases 4 & 5 model build and output plans from 35989X1409Map\WylDCOModelMap.mxd

Phase 4 rivers, SSSI receptors, Site boundary, MODFLOW Central Model dry period (30/09/91) bedrock heads with GHB cells and Inactive cell overlay

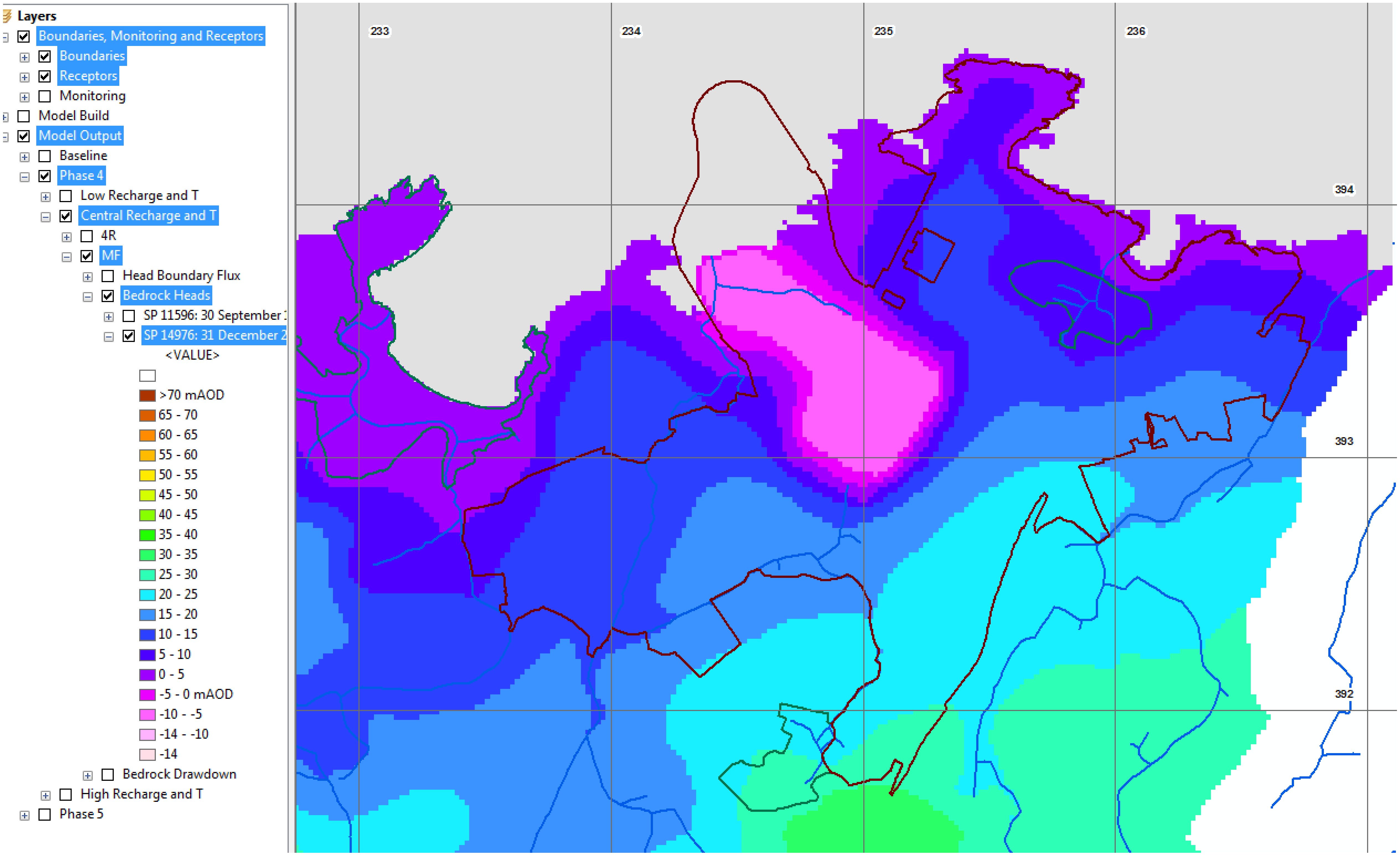

Phase 4 rivers, SSSI receptors, Site boundary, MODFLOW Central Model wet period (31/12/2000) bedrock heads with GHB cells and Inactive cell overlay

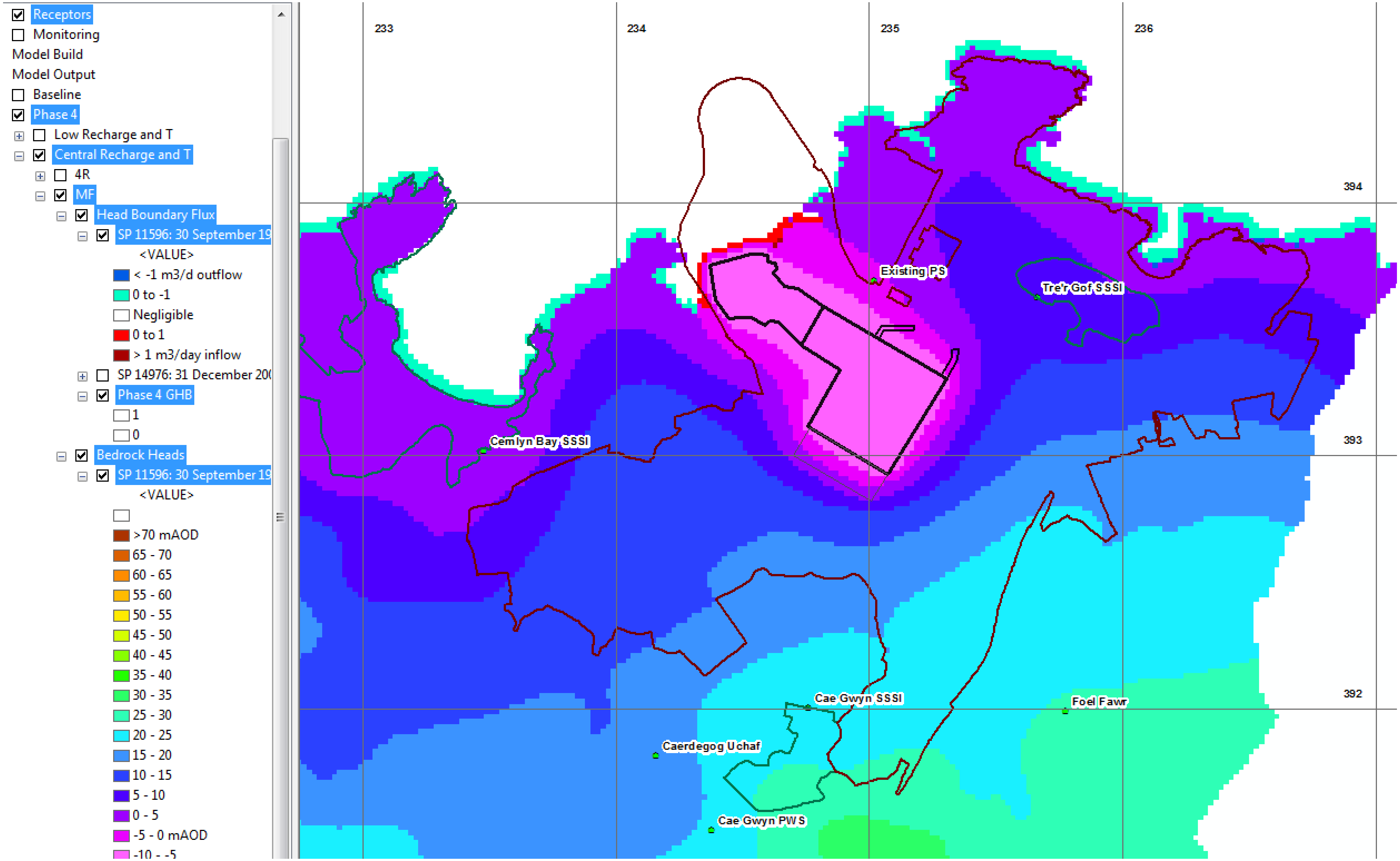

Phase 4 SSSI receptors, Site boundary, excavation, MODFLOW Central Model dry period (31/12/2000) bedrock heads with GHB cells flows and Inactive cell overlay

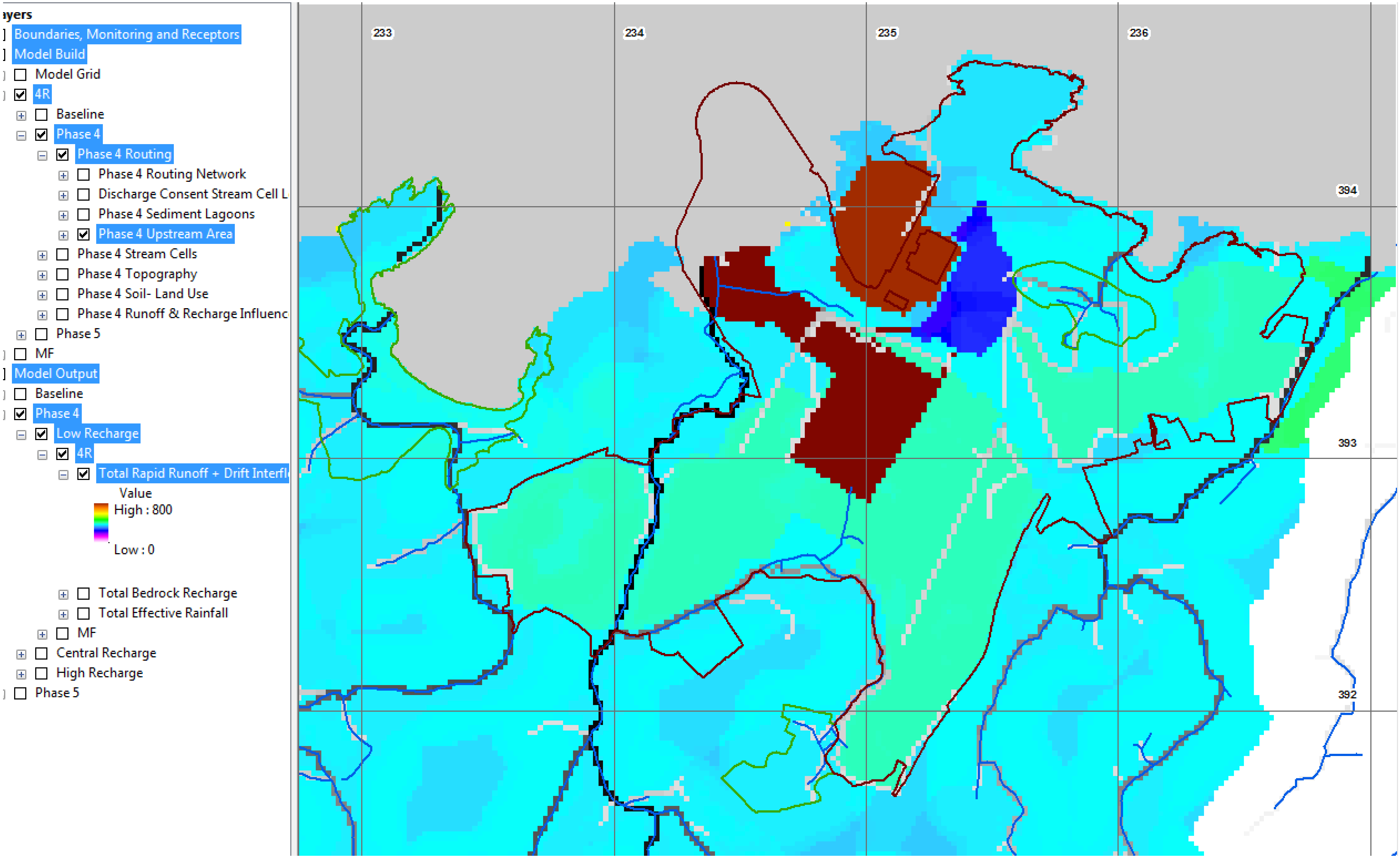

Phase 4 rivers, SSSI receptors, Site boundary, and 4R Low Model rapid runoff + interflow output, MODFLOW GHB cells and Inactive cell overlay

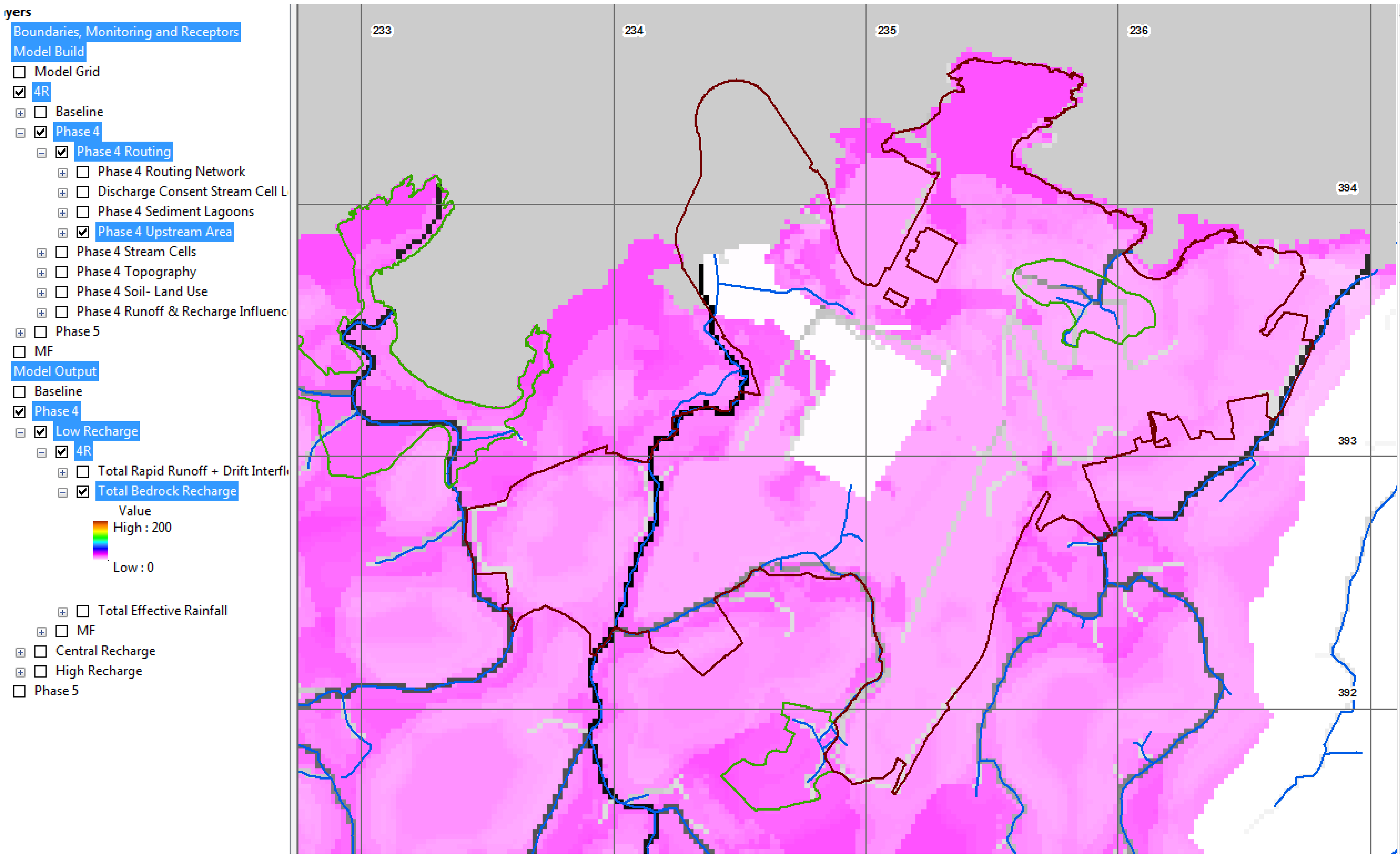

Phase 4 rivers, SSSI receptors, Site boundary, 4R Low Model bedrock recharge, MODFLOW GHB cells and Inactive cell overlay

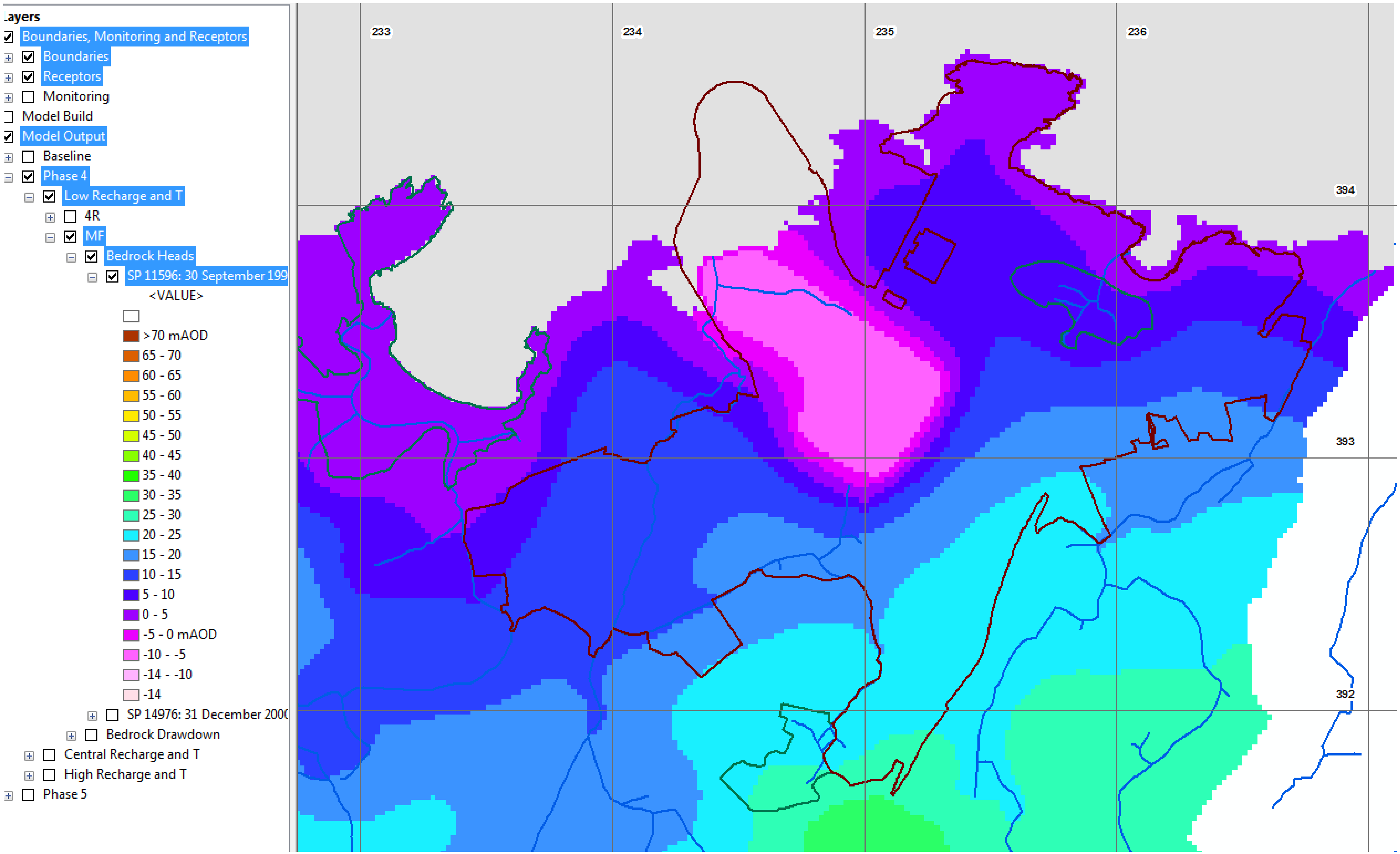

Phase 4 rivers, SSSI receptors, Site boundary, and MODFLOW Low Model dry period (30/09/91) bedrock heads with GHB cells and Inactive cell overlay

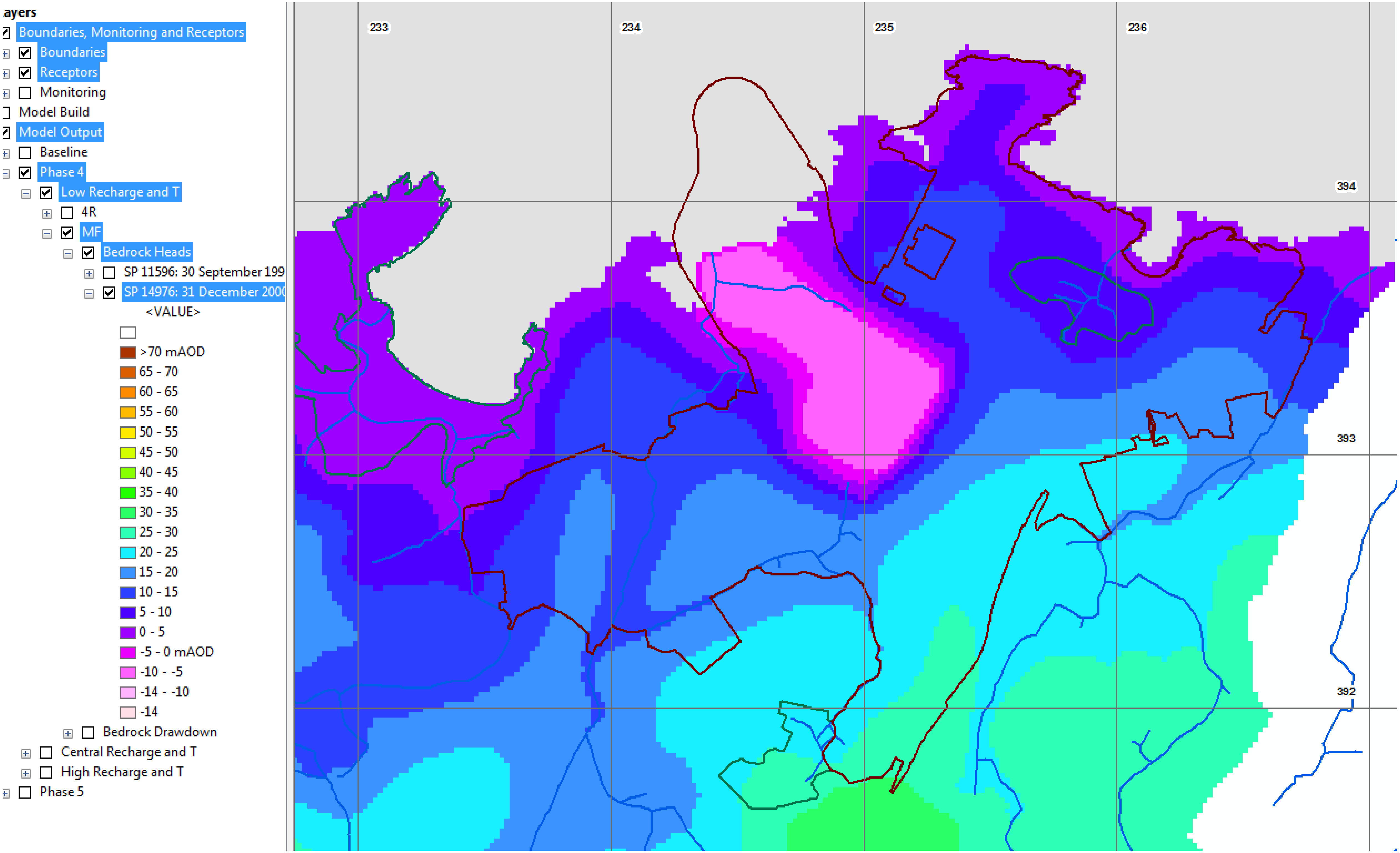

Phase 4 rivers, SSSI receptors, Site boundary, MODFLOW Low Model wet period (31/12/2000) bedrock heads with GHB cells and Inactive cell overlay

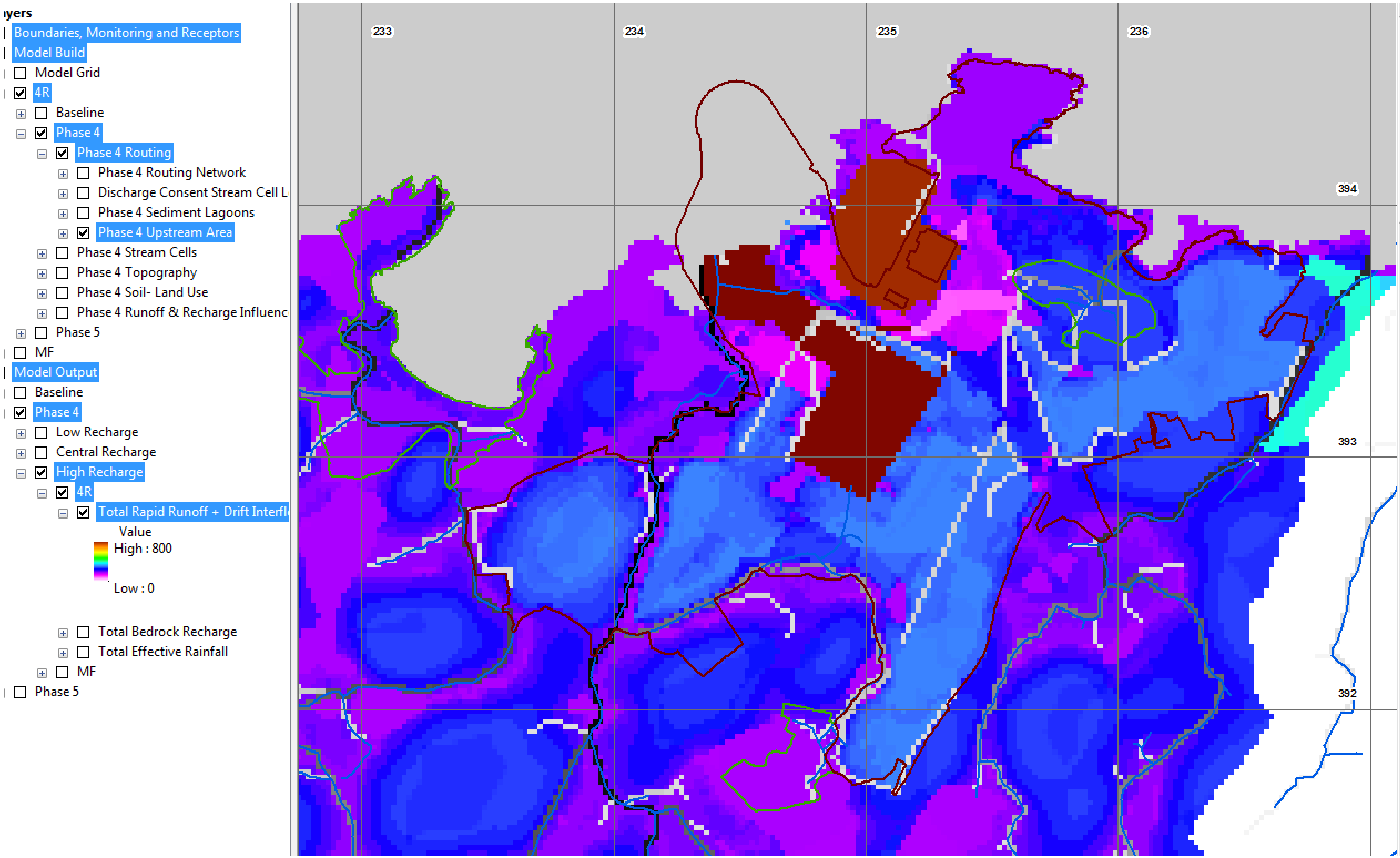

Phase 4 rivers, SSSI receptors, Site boundary, and 4R High Model rapid runoff + interflow output, MODFLOW GHB cells and Inactive cell overlay

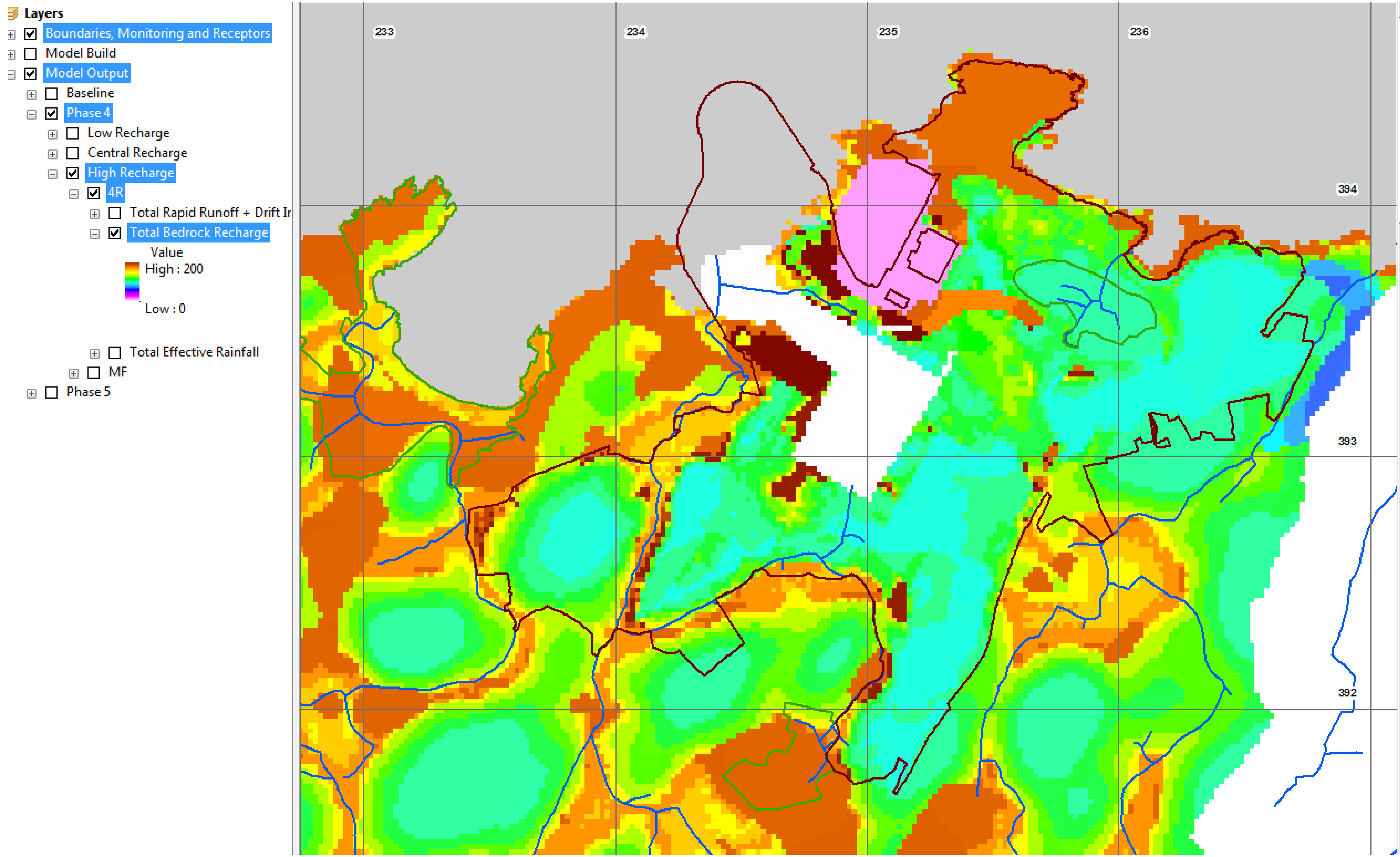

Phase 4 rivers, SSSI receptors, Site boundary, 4R High Model bedrock recharge, MODFLOW GHB cells and Inactive cell overlay

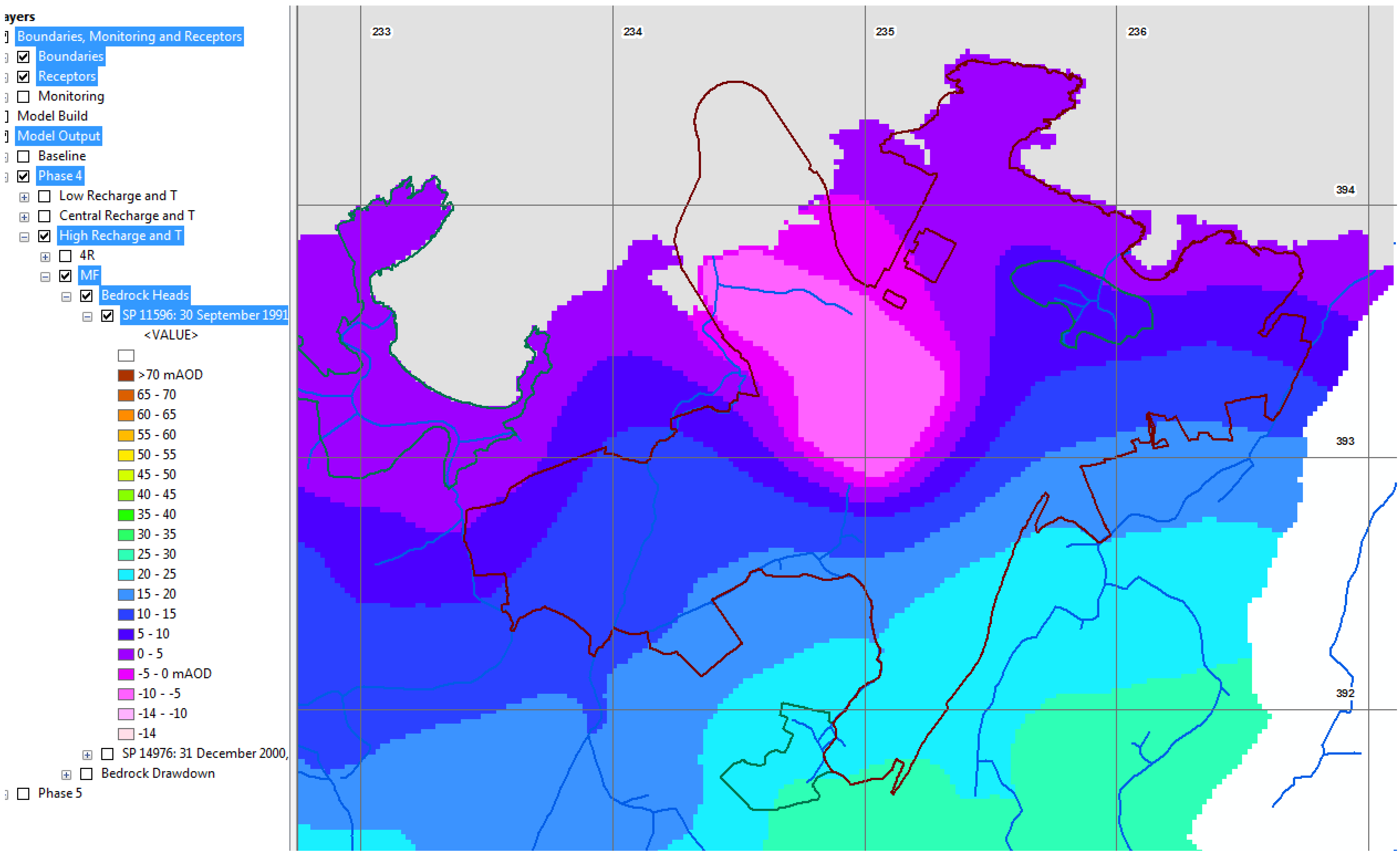

Phase 4 rivers, SSSI receptors, Site boundary, and MODFLOW High Model dry period (30/09/91) bedrock heads with GHB cells and Inactive cell overlay

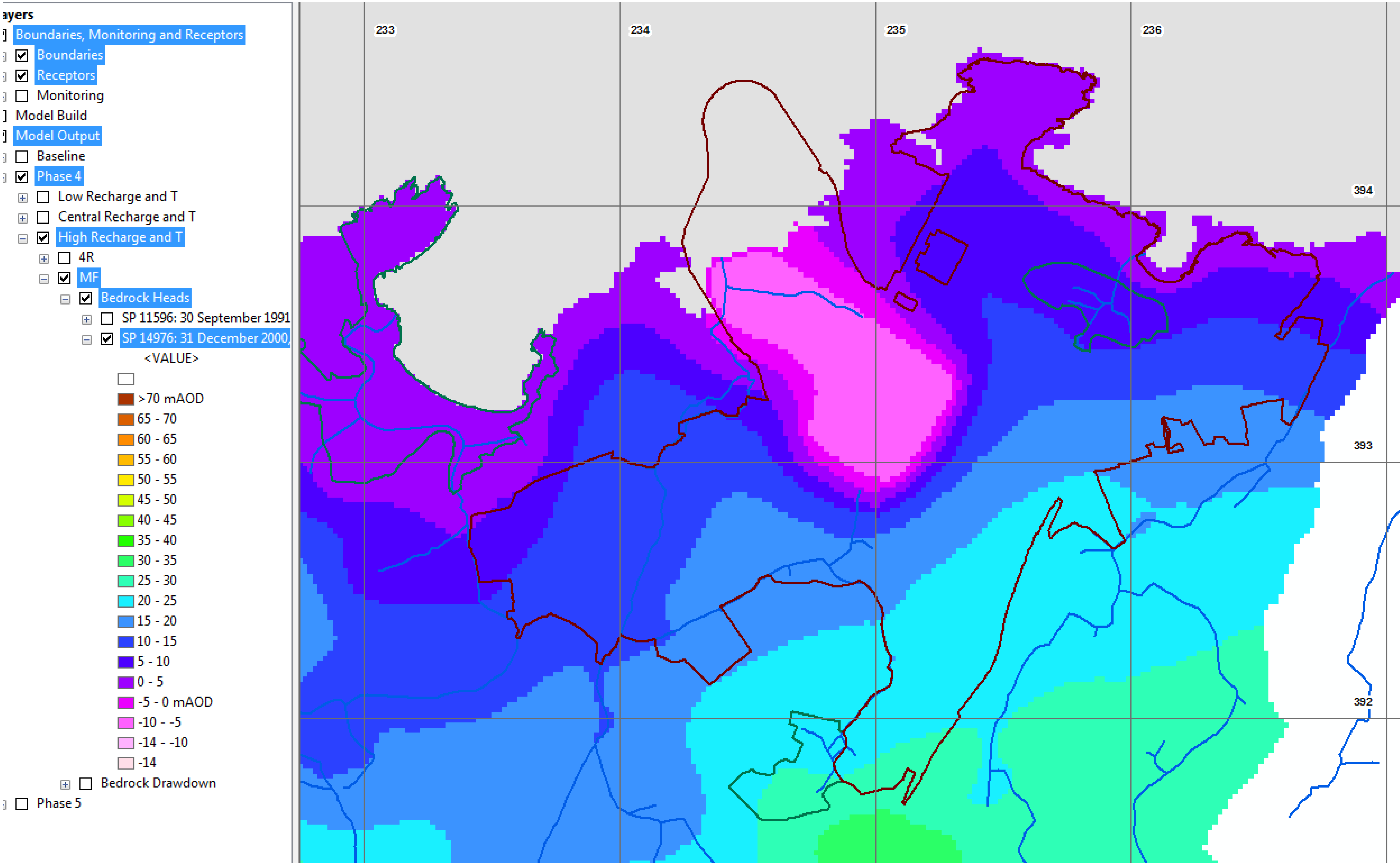

Phase 4 rivers, SSSI receptors, Site boundary, MODFLOW High Model wet period (31/12/2000) bedrock heads with GHB cells and Inactive cell overlay

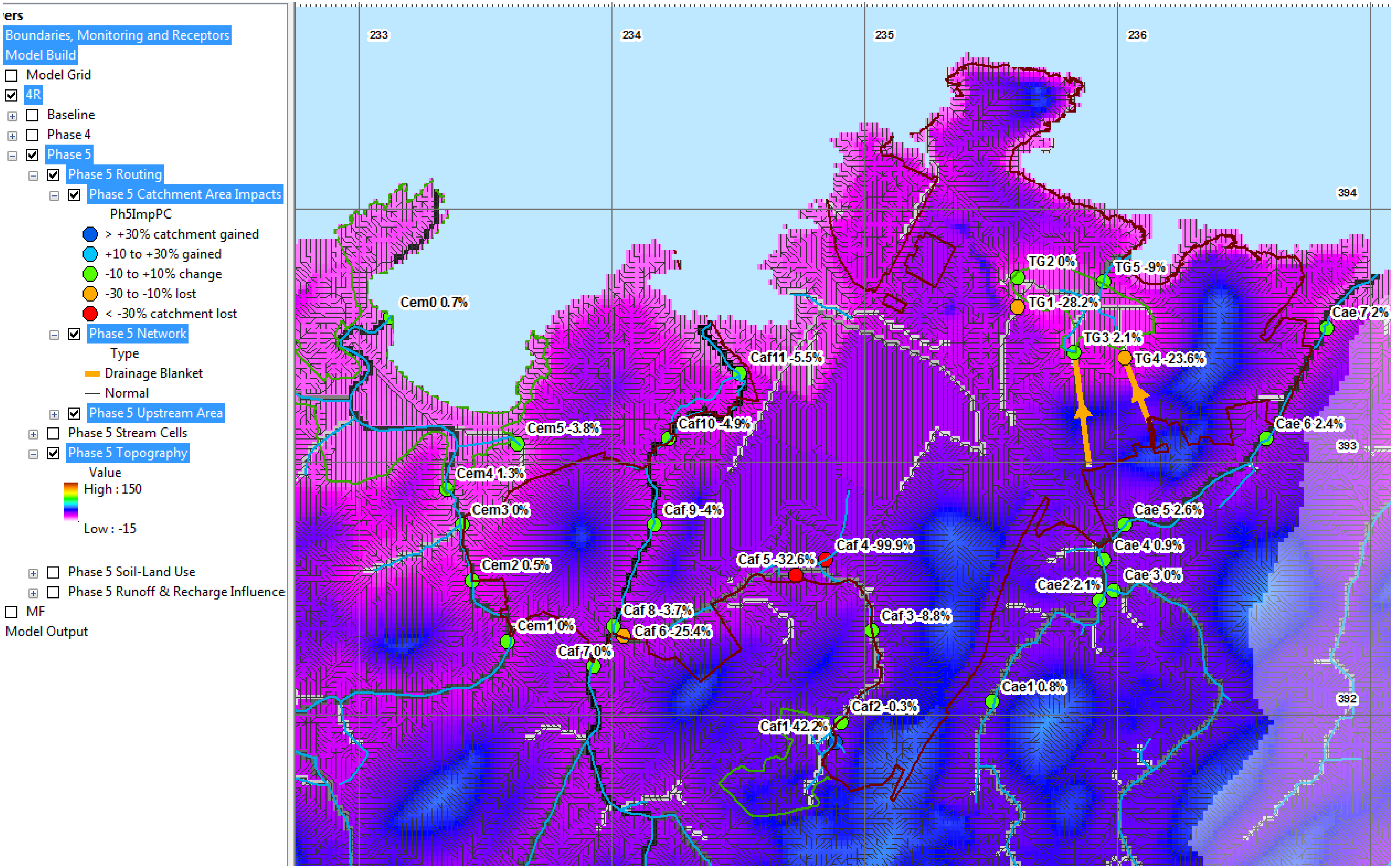

Phase 5 topography, rivers, SSSI receptors, surface water flow receptors with % change in catchment area Site boundary, 4R upstream area, routing, MODFLOW General Head Boundary sea bed, and Inactive cell overlay

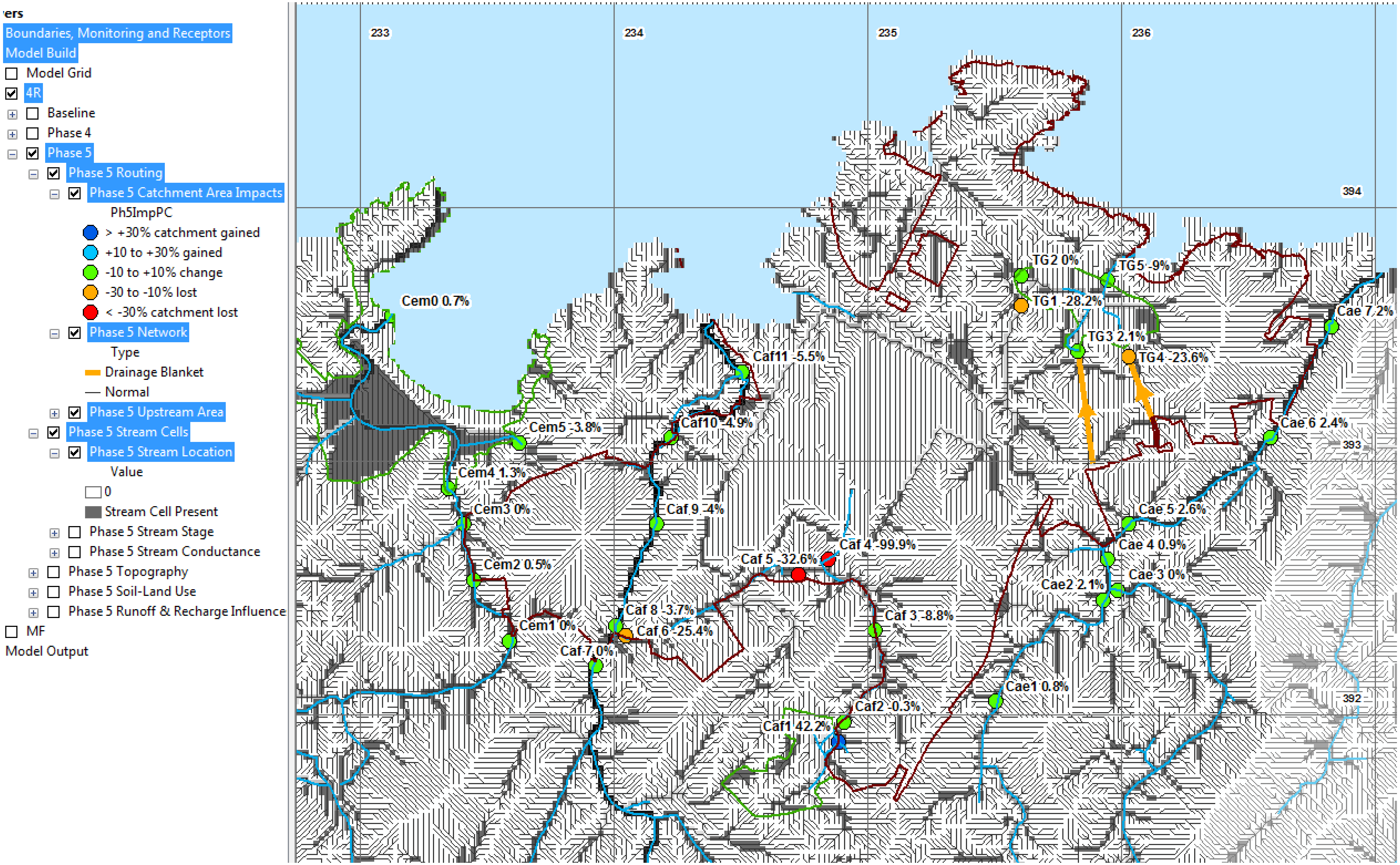

Phase 5 rivers, SSSI receptors, Site boundary, surface water flow receptors with area change labelled, 4R detailed routing, MODFLOW Stream cells, General Head Boundary sea bed, and Inactive cell overlay

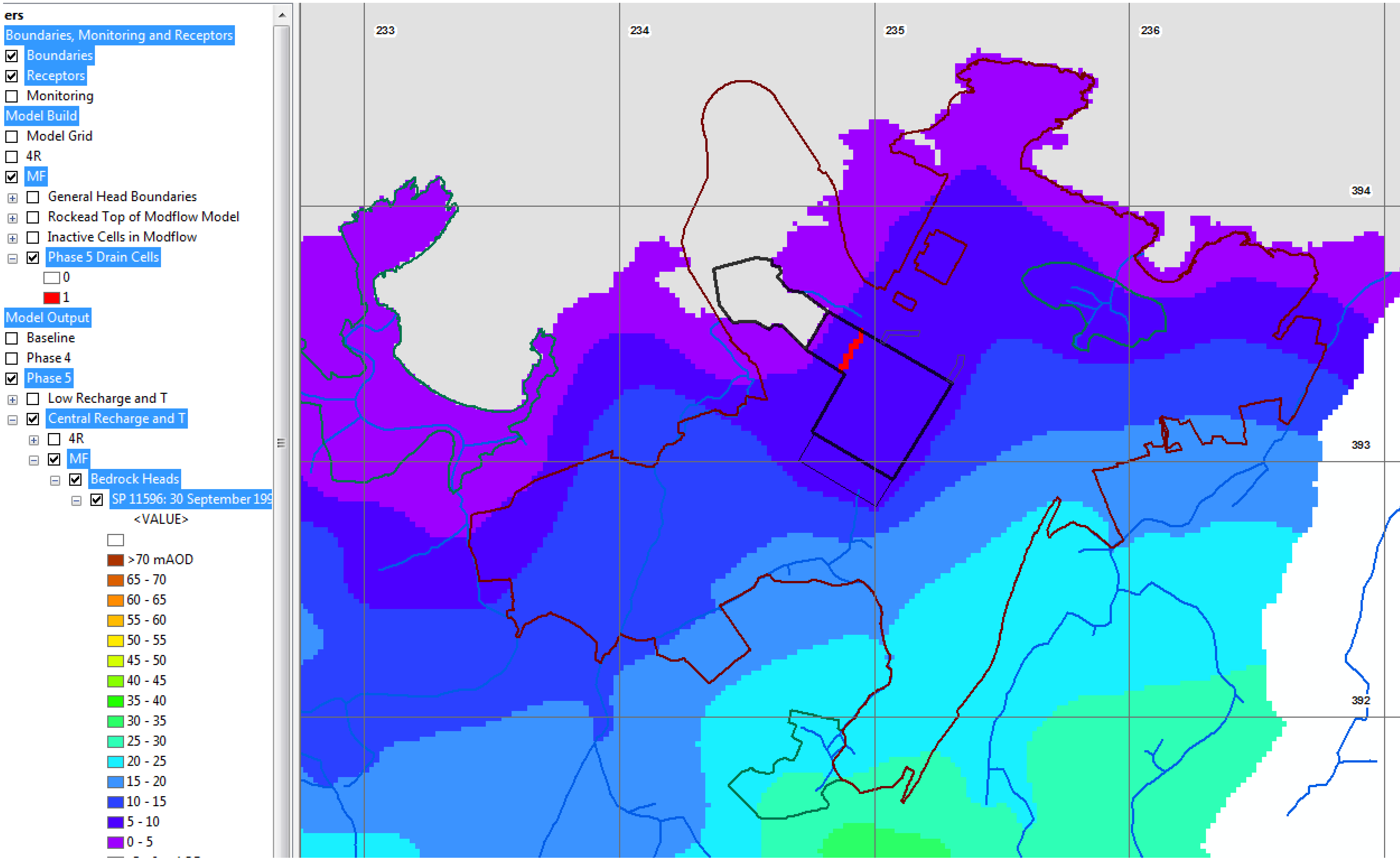

Phase 5 rivers, SSSI receptors, Site boundary, excavation & permeable backfill area, MODFLOW Drain cells (at 6 mAOD), Central Model dry period bedrock heads, General Head Boundary sea bed, and Inactive cell overlay

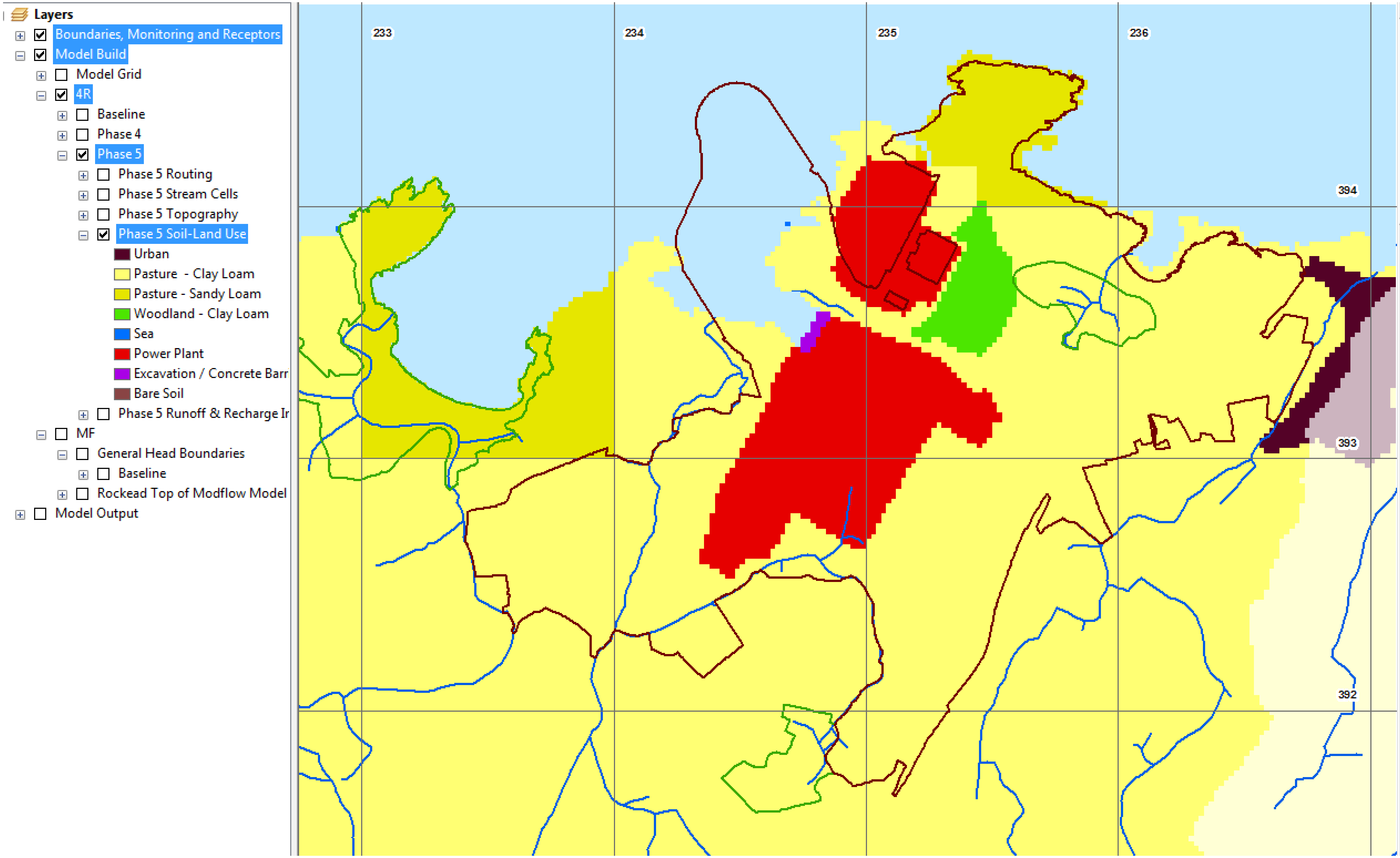

Phase 5 rivers, SSSI receptors, Site boundary, 4R soil - land use including impermeable concrete intake barrier and power station platforms, MODFLOW General Head Boundary sea bed and Inactive cell overlay

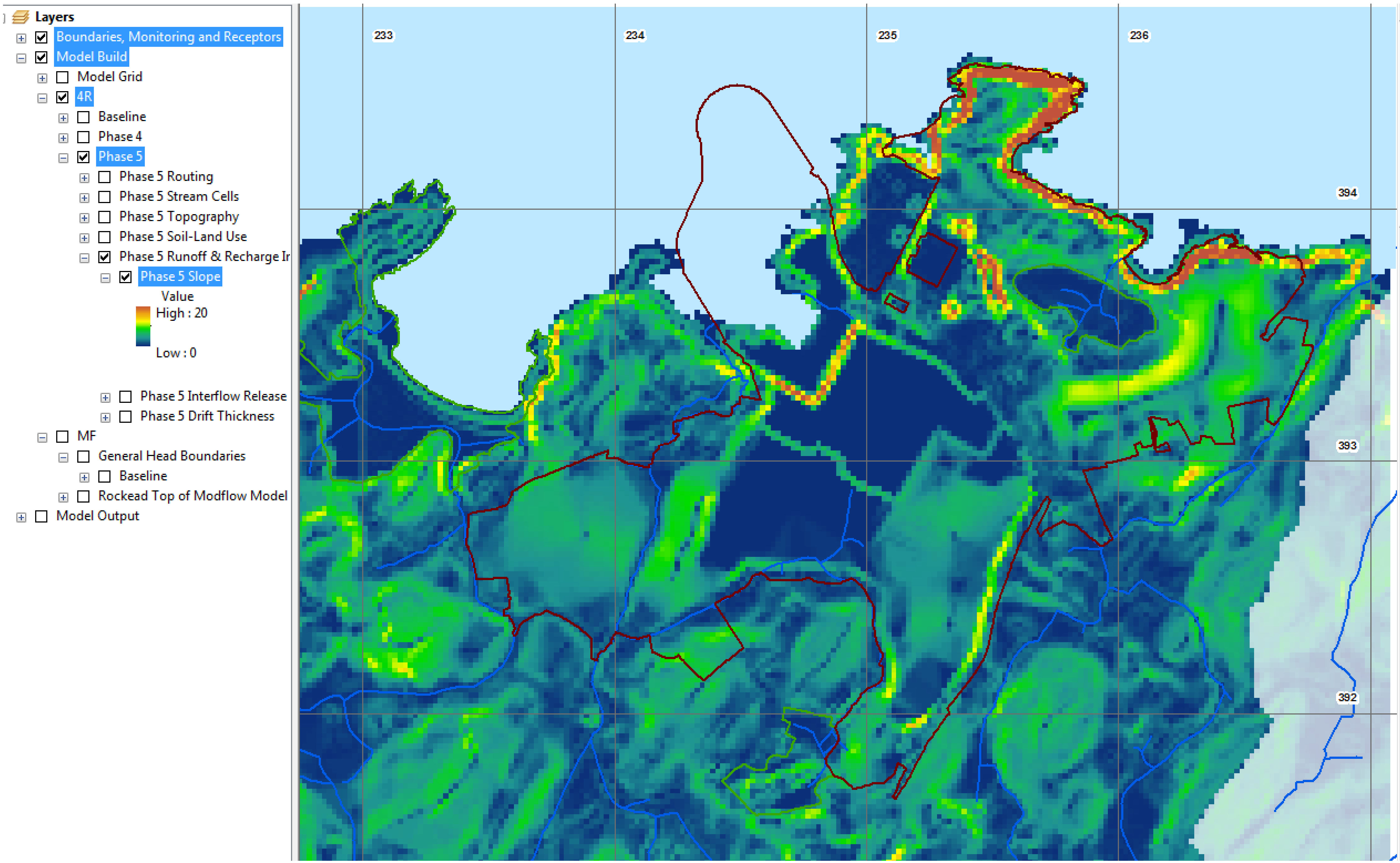

Phase 5 rivers, SSSI receptors, Site boundary, 4R slope, MODFLOW General Head Boundary sea bed, and Inactive cell overlay

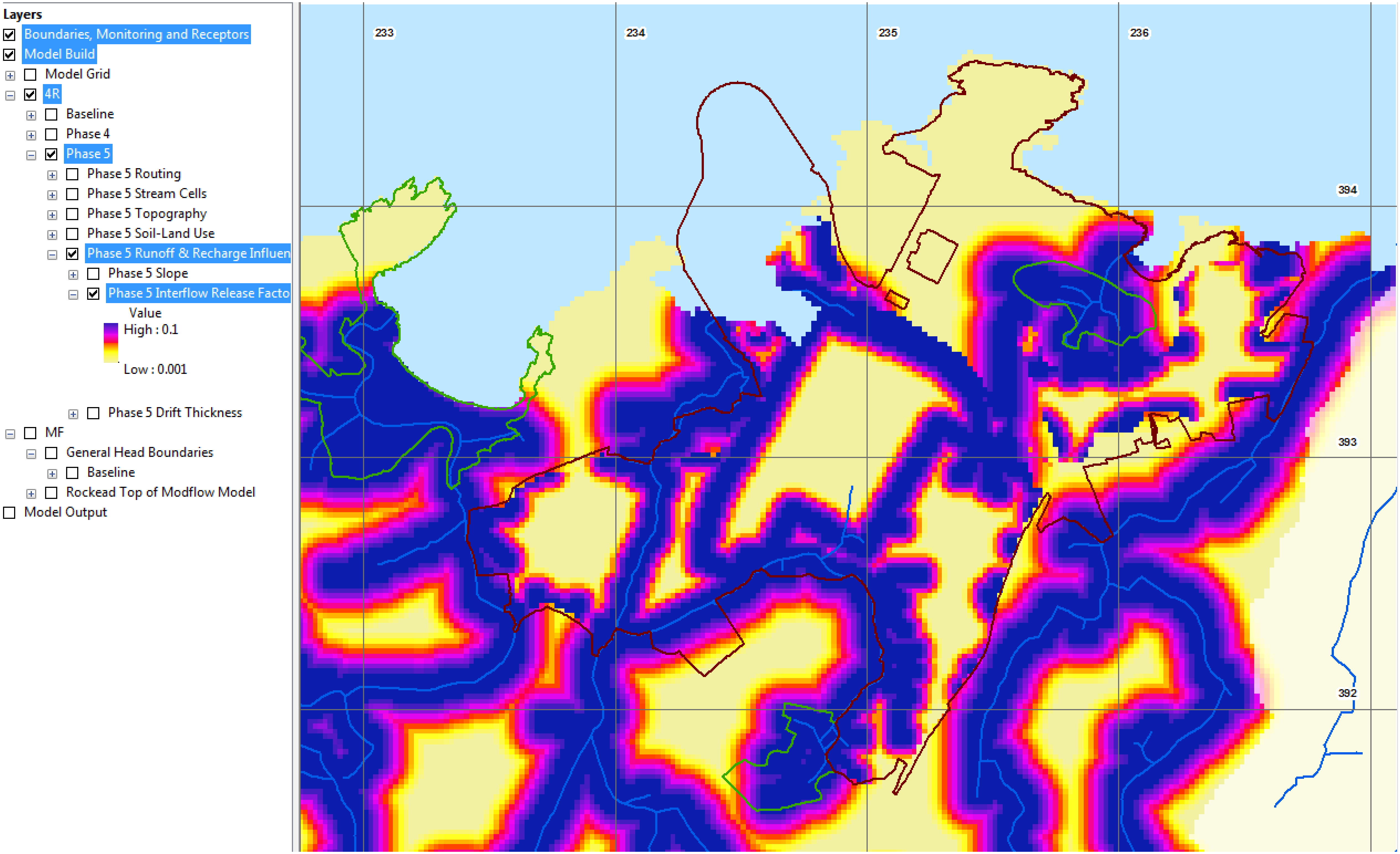

WylDCOGWMod_35989N1403i1 Appendix D, Phases 4 & 5 model build and output plans from 35989X1409Map\WylDCOModelMap.mxd

Phase 5 rivers, SSSI receptors, Site boundary, 4R upstream routed area and interflow release factor, MODFLOW General Head Boundary sea bed, and Inactive cell overlay

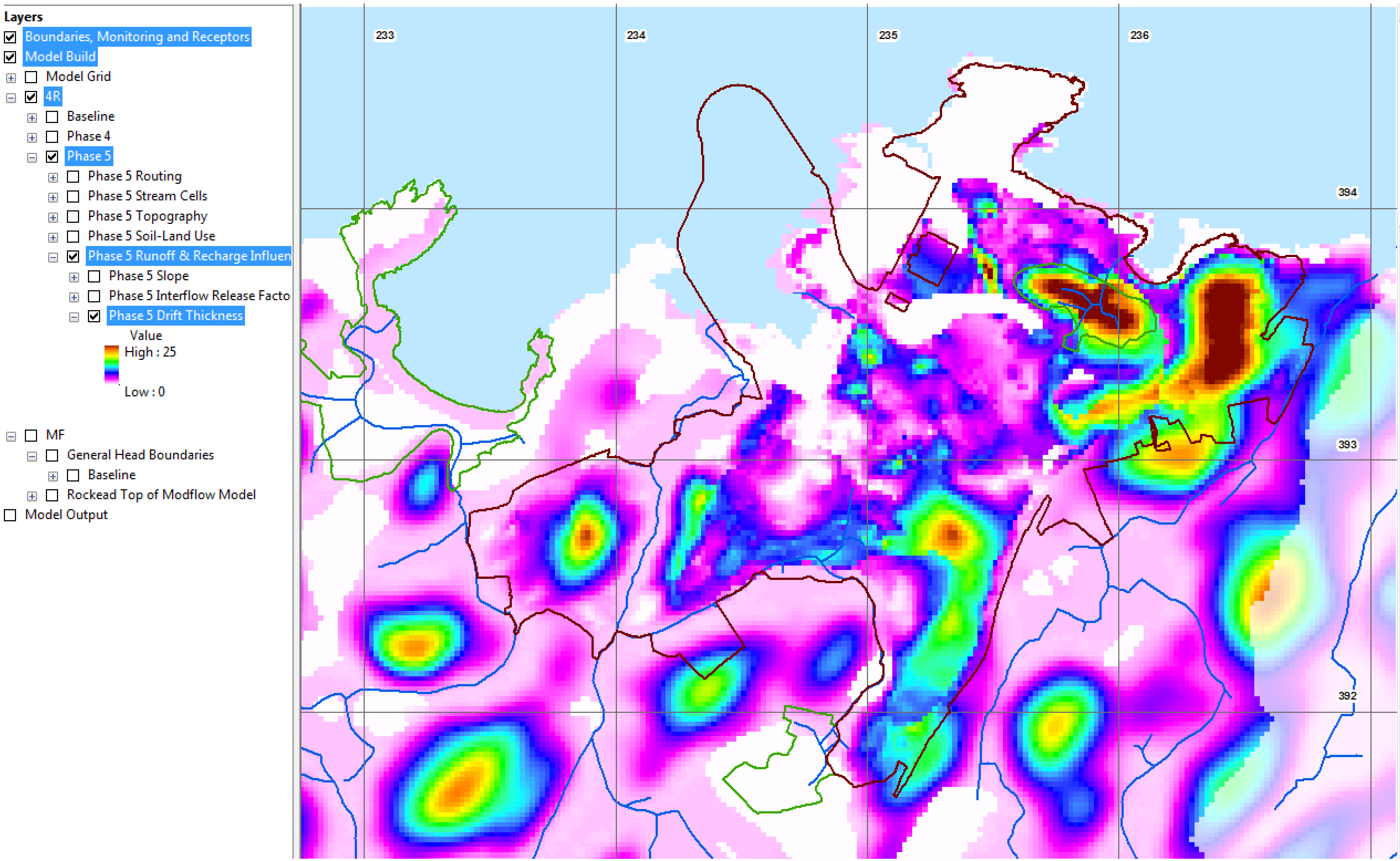

Phase 5 rivers, SSSI receptors, Site boundary, Drift & Mound thickness, MODFLOW General Head Boundary sea bed, and Inactive cell overlay

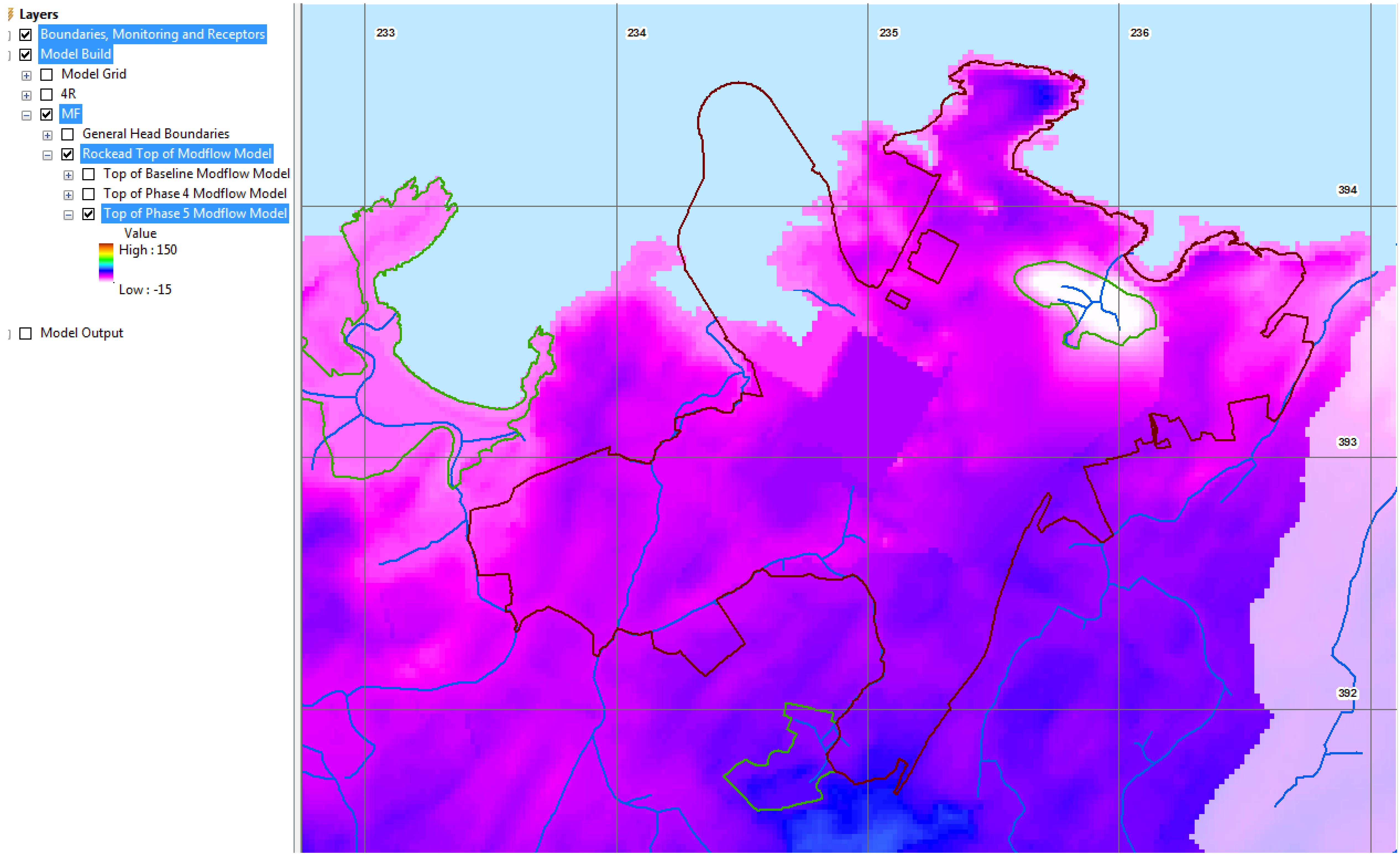

Phase 5 rivers, SSSI receptors, Site boundary, MODFLOW General Head Boundary sea bed cells, top of bedrock layer elevation and Inactive cell overlay

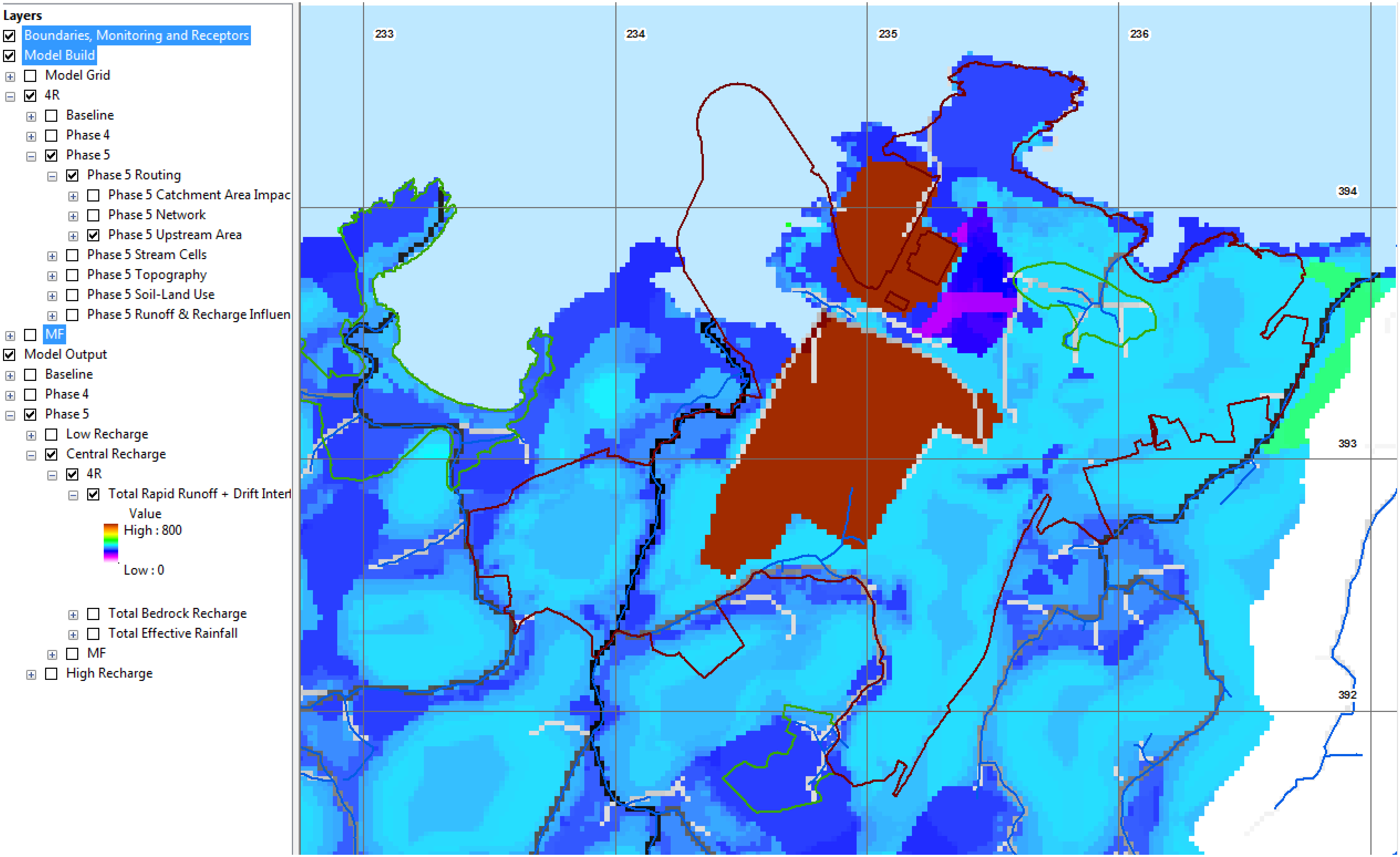

Phase 5 rivers, SSSI receptors, Site boundary, 4R upstream routed area and Central Model rapid runoff + interflow output, MODFLOW GHB cells and Inactive cell overlay

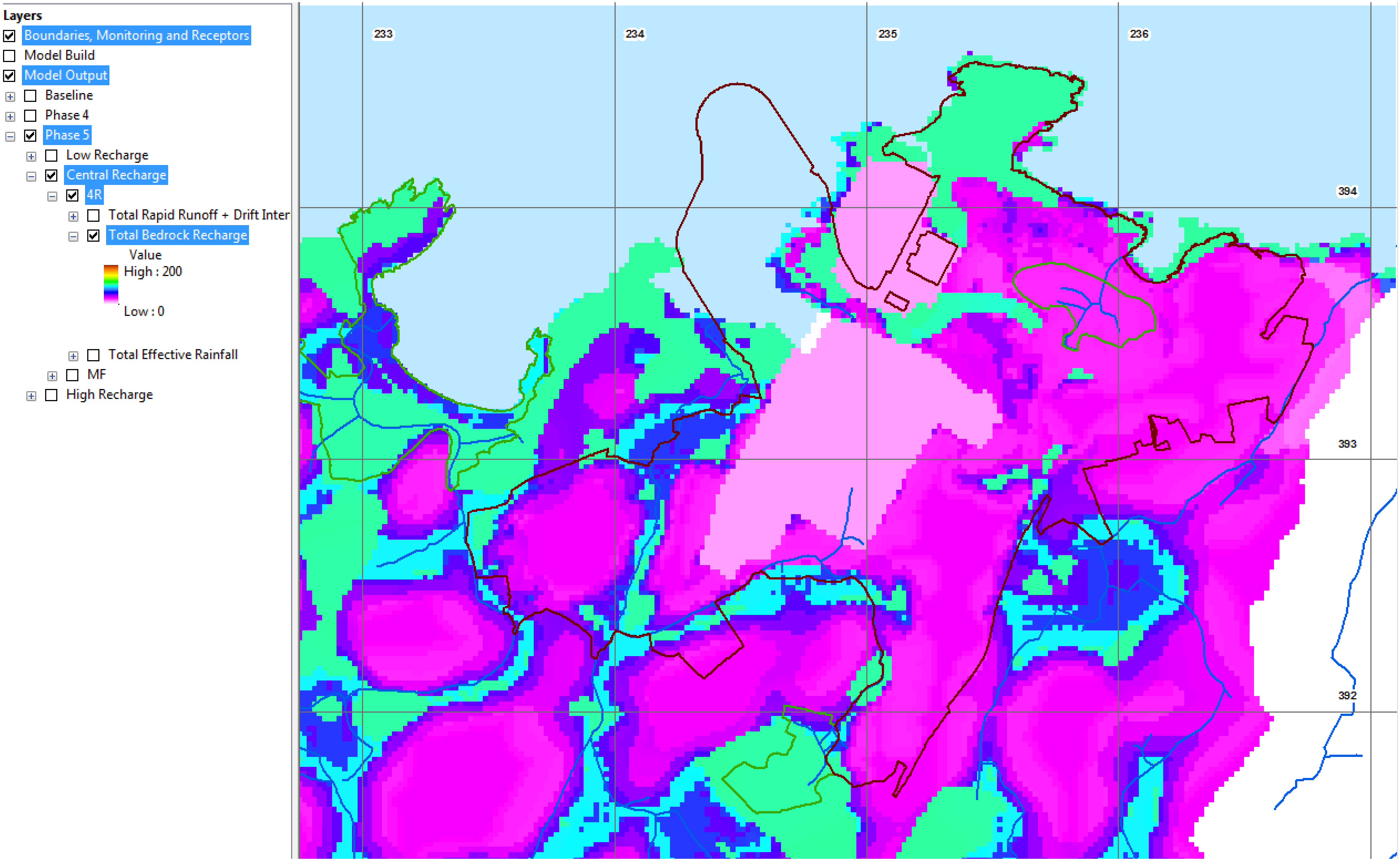

Phase 5 rivers, SSSI receptors, Site boundary, 4R Central Model bedrock recharge, MODFLOW GHB cells and Inactive cell overlay

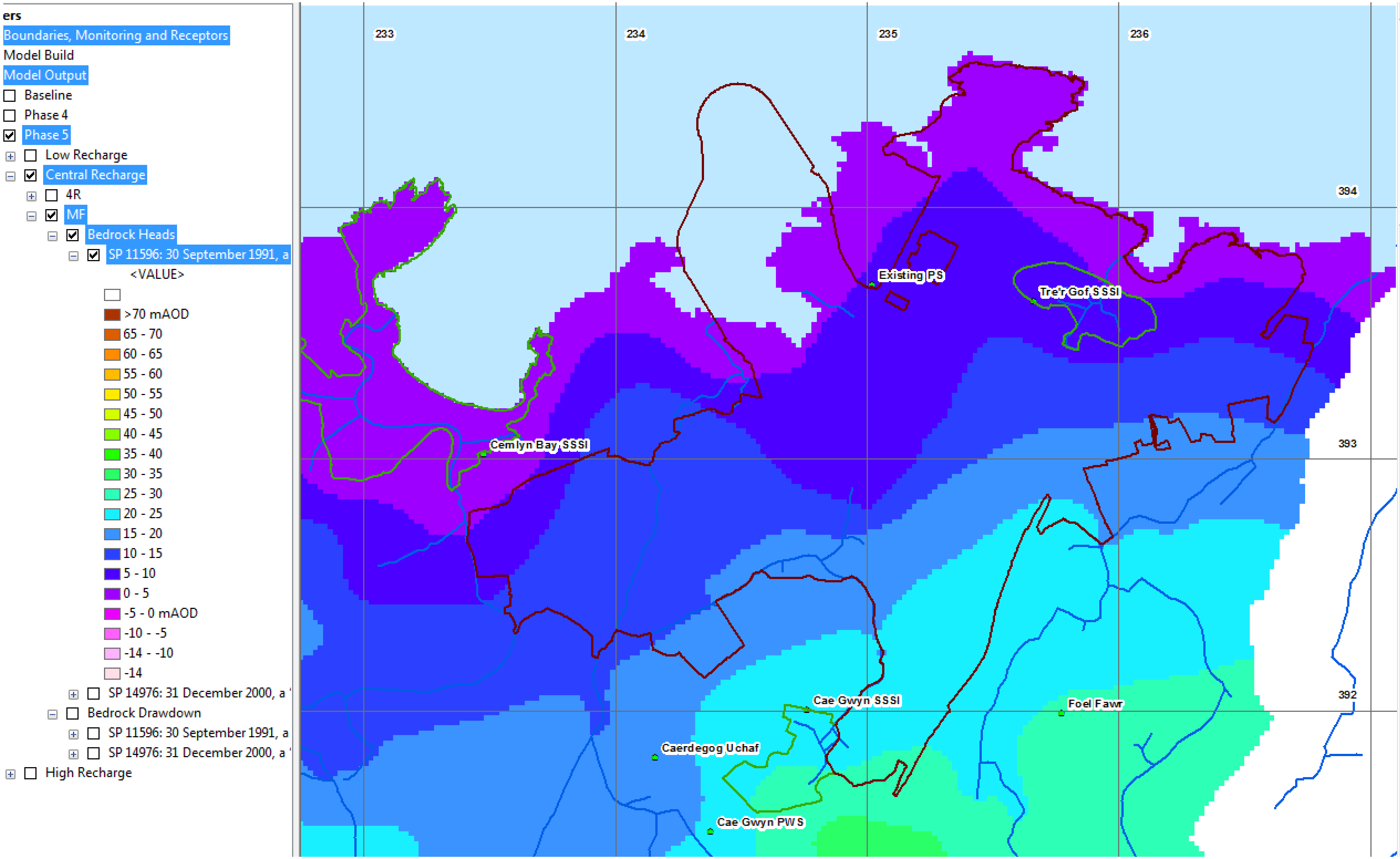

Phase 5 rivers, SSSI receptors, Site boundary, GW receptor cells, and MODFLOW Central Model dry period (30/09/91) bedrock heads with GHB cells and Inactive cell overlay

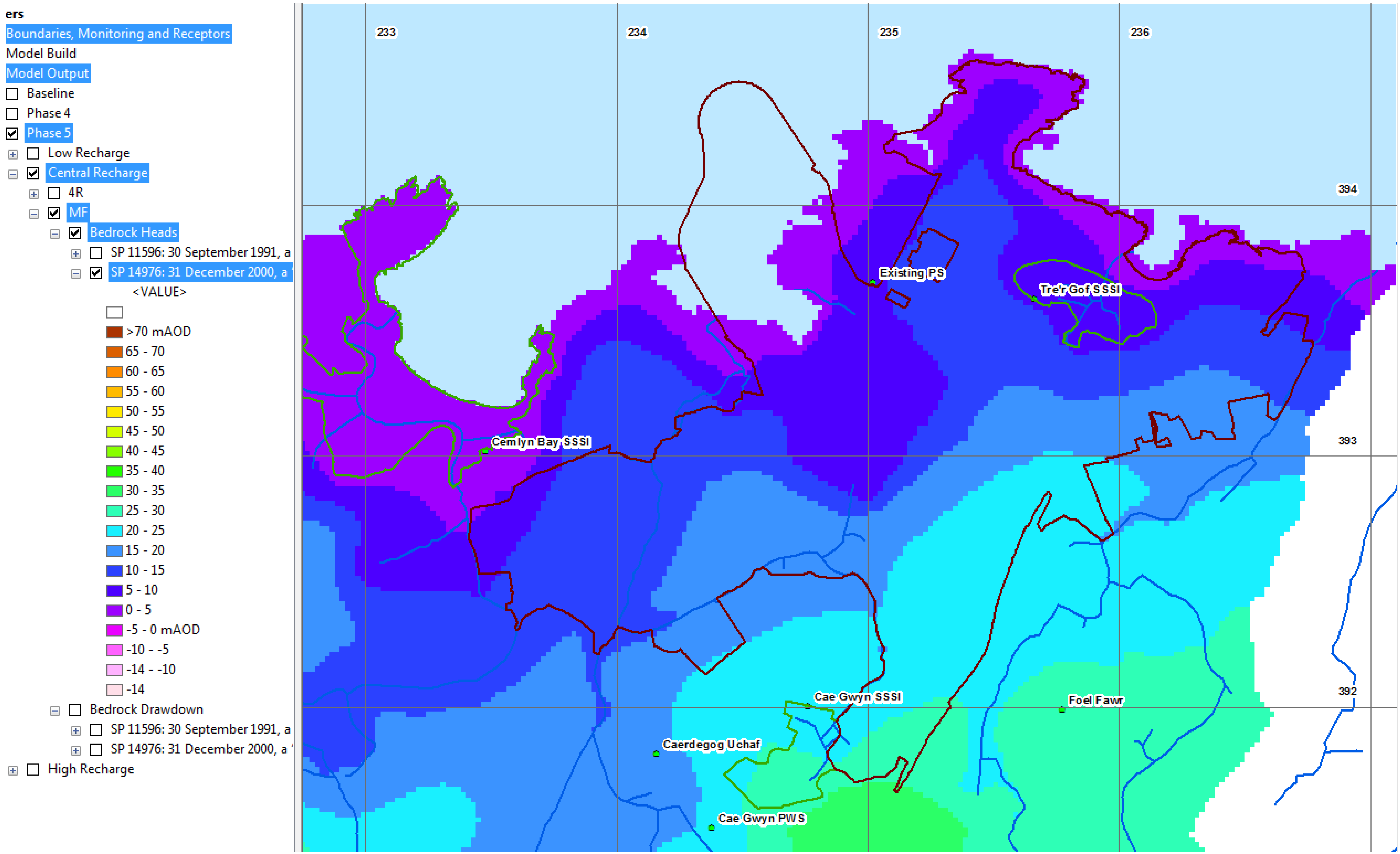

Phase 5 rivers, SSSI receptors, Site boundary, and MODFLOW Central Model wet period (31/12/2000) bedrock heads with GHB cells and Inactive cell overlay

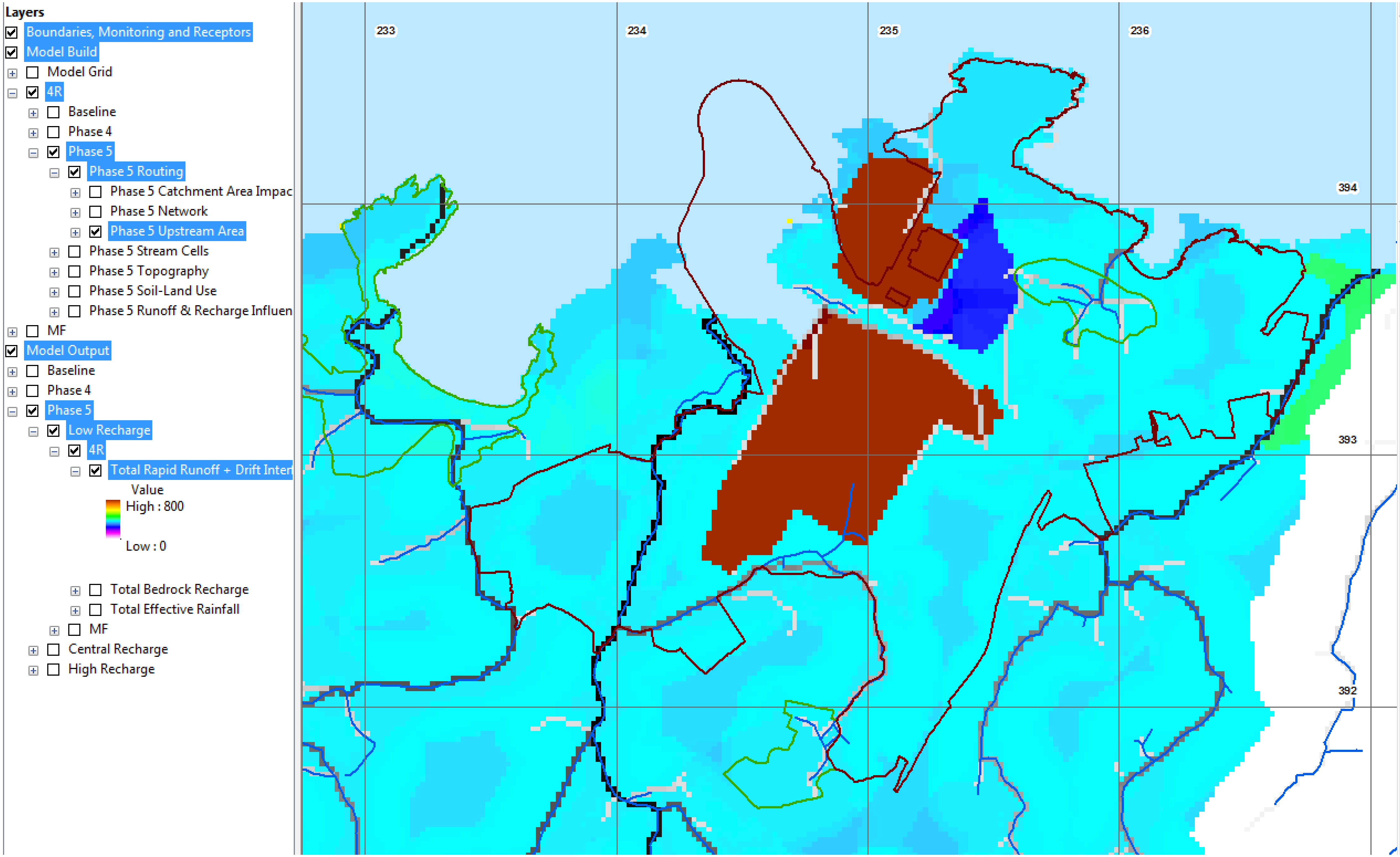

Phase 5 rivers, SSSI receptors, Site boundary, and 4R Low Model rapid runoff + interflow output, MODFLOW GHB cells and Inactive cell overlay

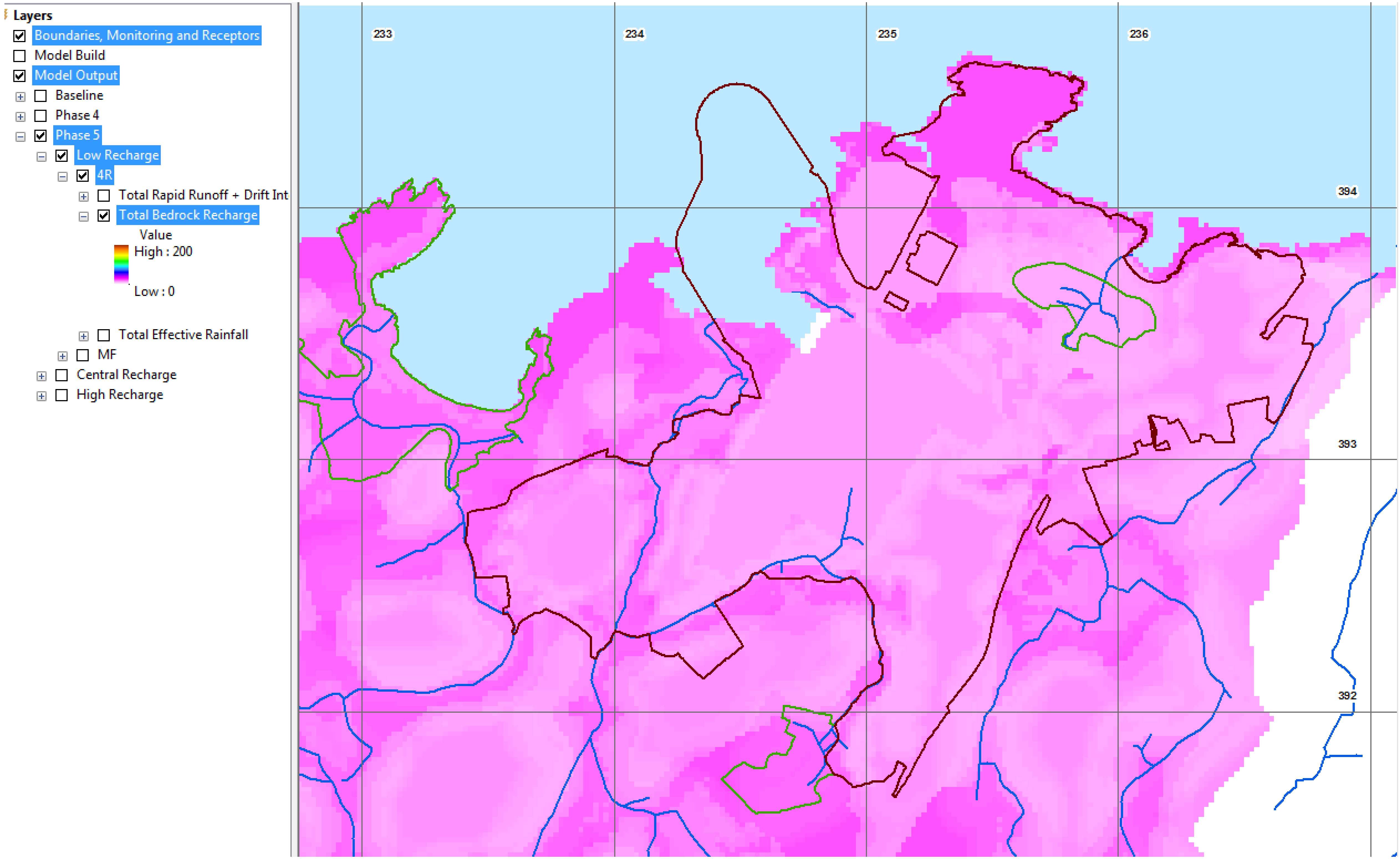

Phase 54 rivers, SSSI receptors, Site boundary, 4R Low Model bedrock recharge, MODFLOW GHB cells and Inactive cell overlay

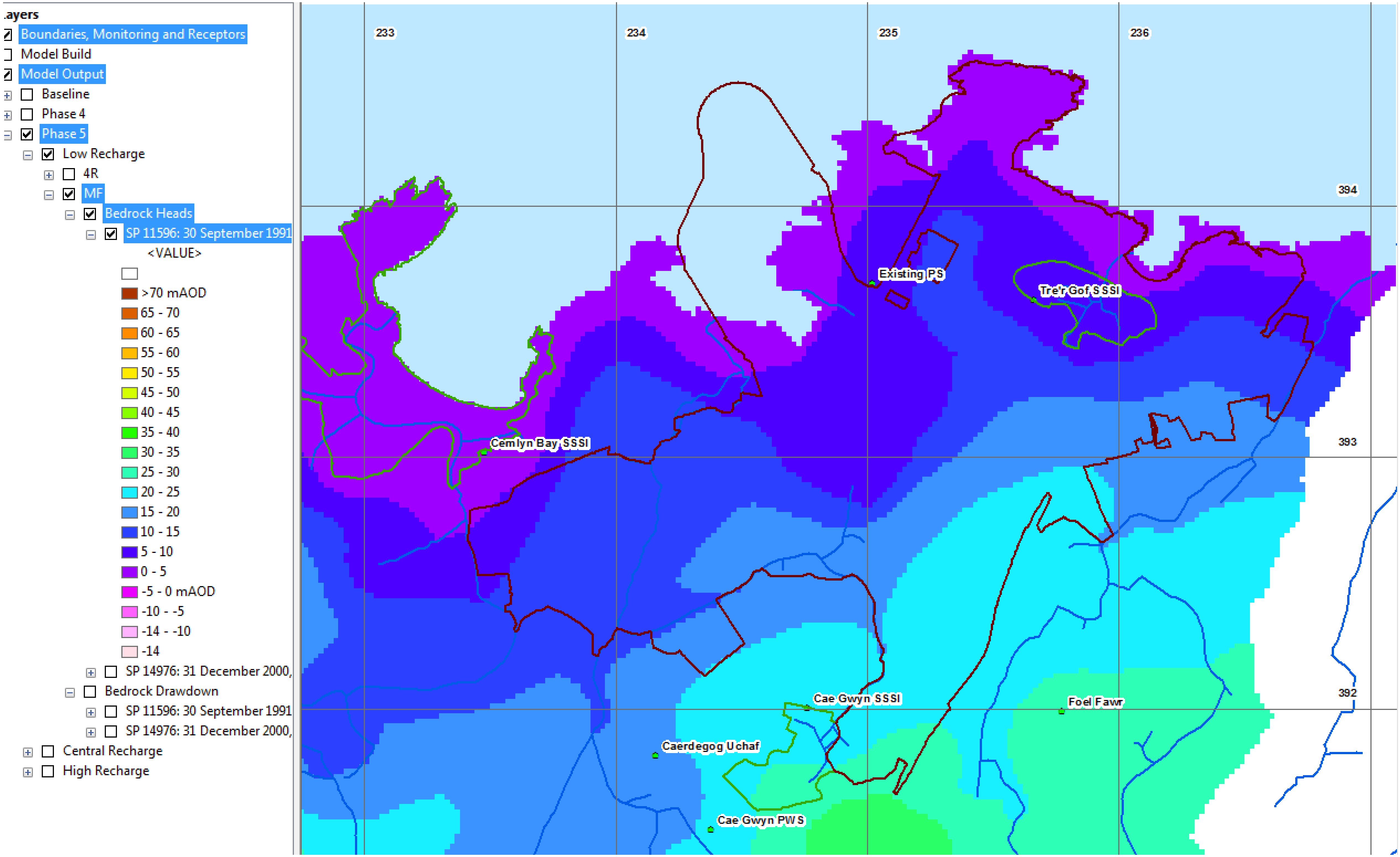

Phase 5 rivers, SSSI receptors, Site boundary, and MODFLOW Low Model dry period (30/09/91) bedrock heads with GHB cells and Inactive cell overlay

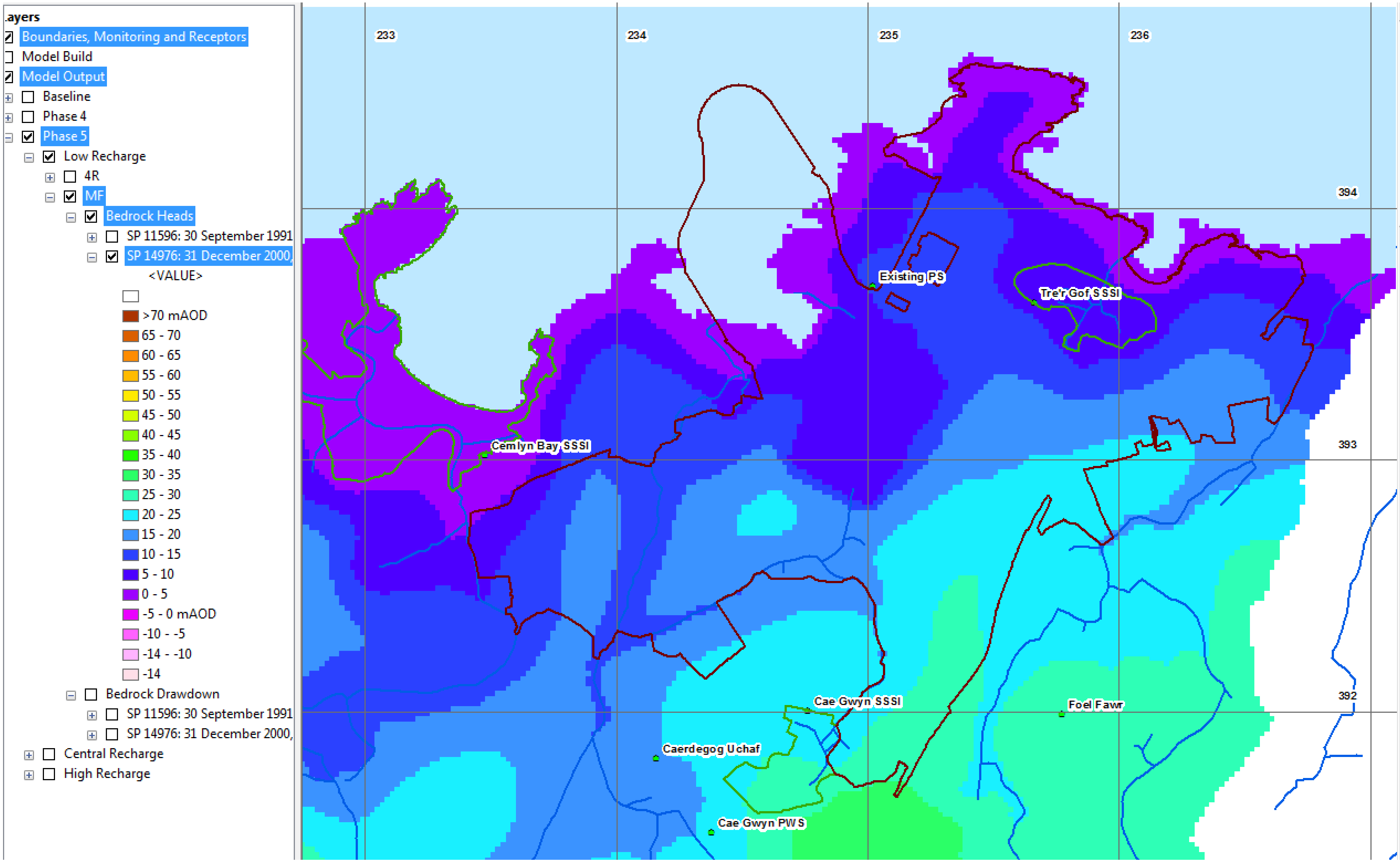

Phase 5 rivers, SSSI receptors, Site boundary, MODFLOW Low Model wet period (31/12/2000) bedrock heads with GHB cells and Inactive cell overlay

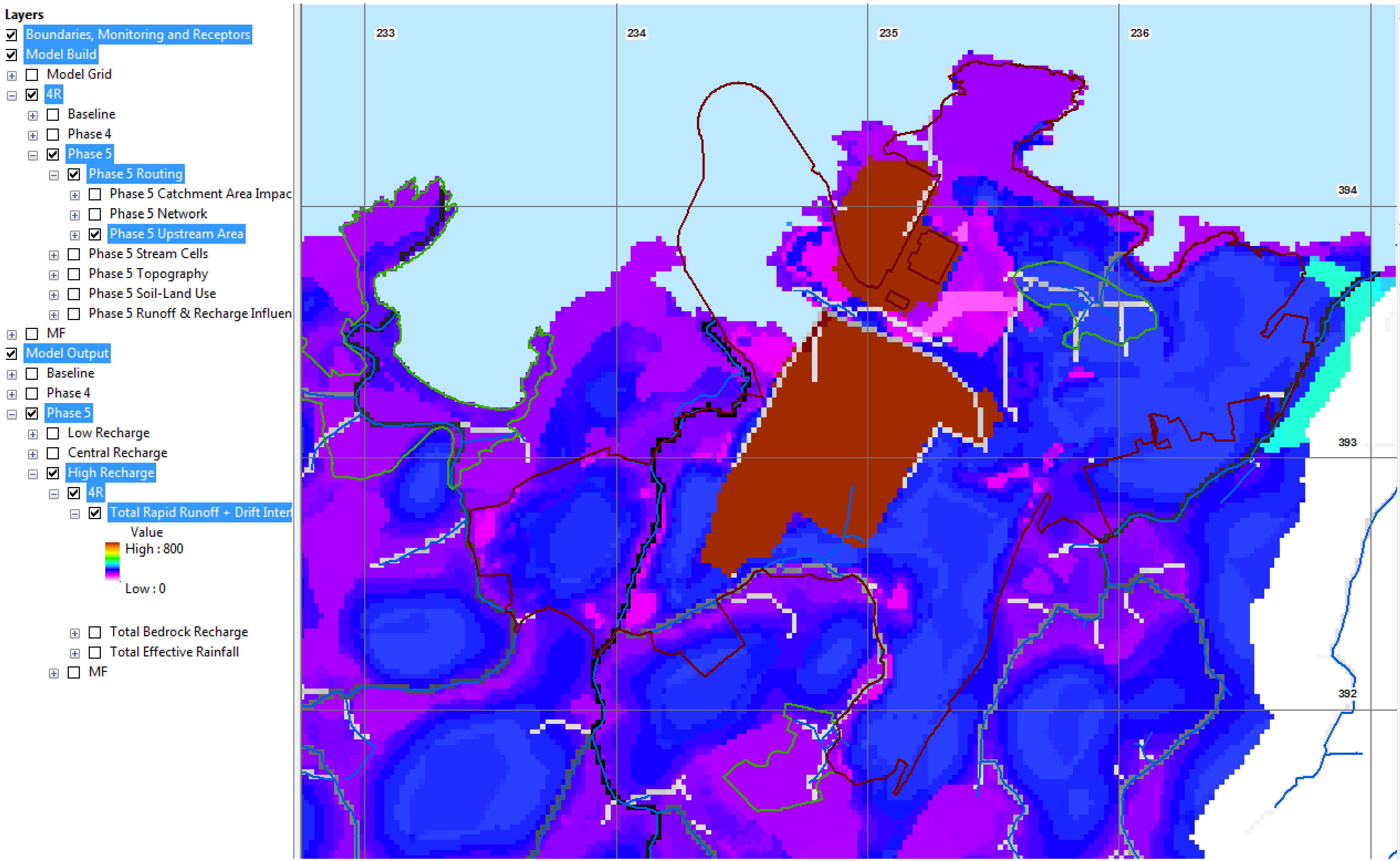

Phase 5 rivers, SSSI receptors, Site boundary, and 4R High Model rapid runoff + interflow output, MODFLOW GHB cells and Inactive cell overlay

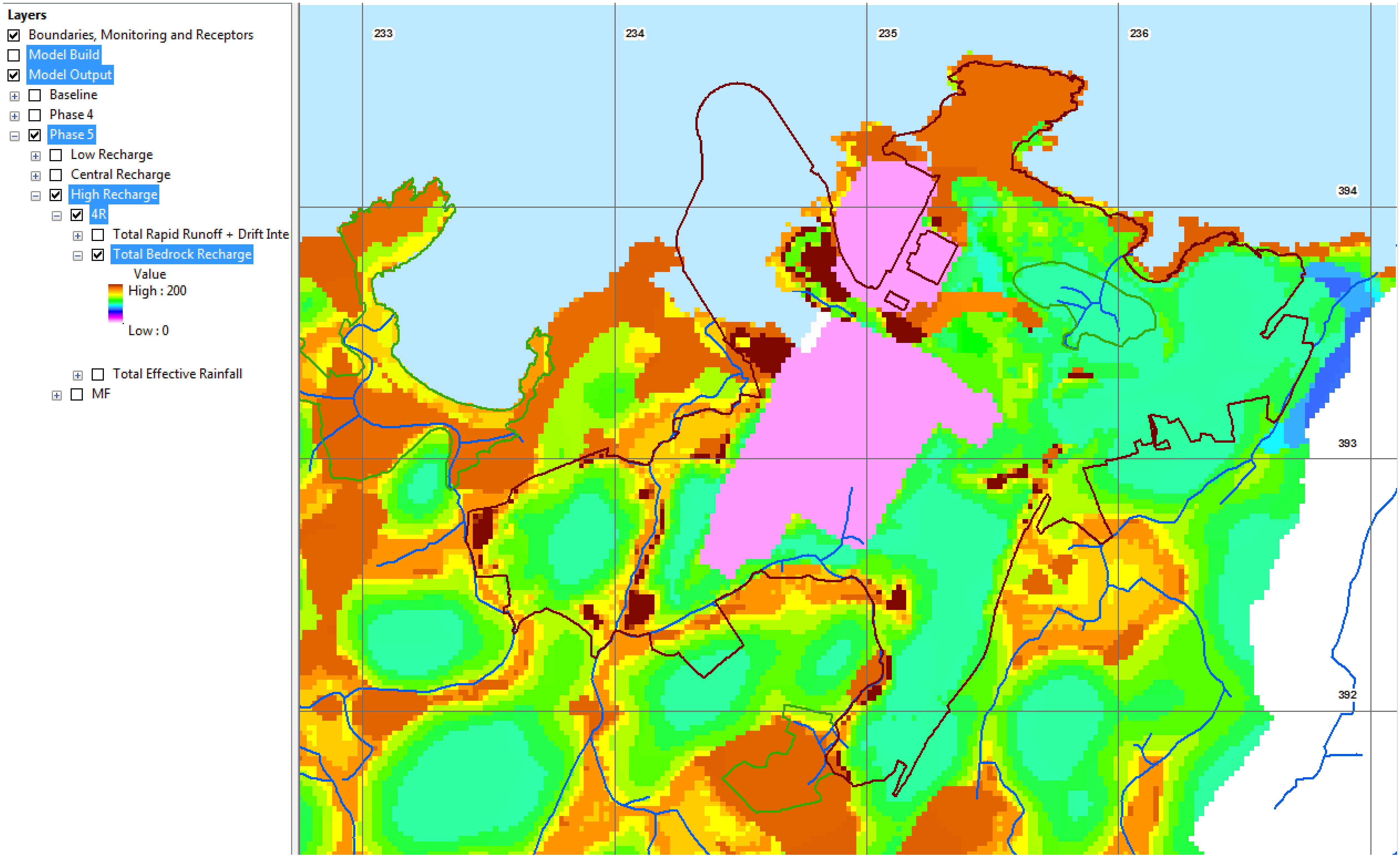

Phase 5 rivers, SSSI receptors, Site boundary, 4R High Model bedrock recharge, MODFLOW GHB cells and Inactive cell overlay

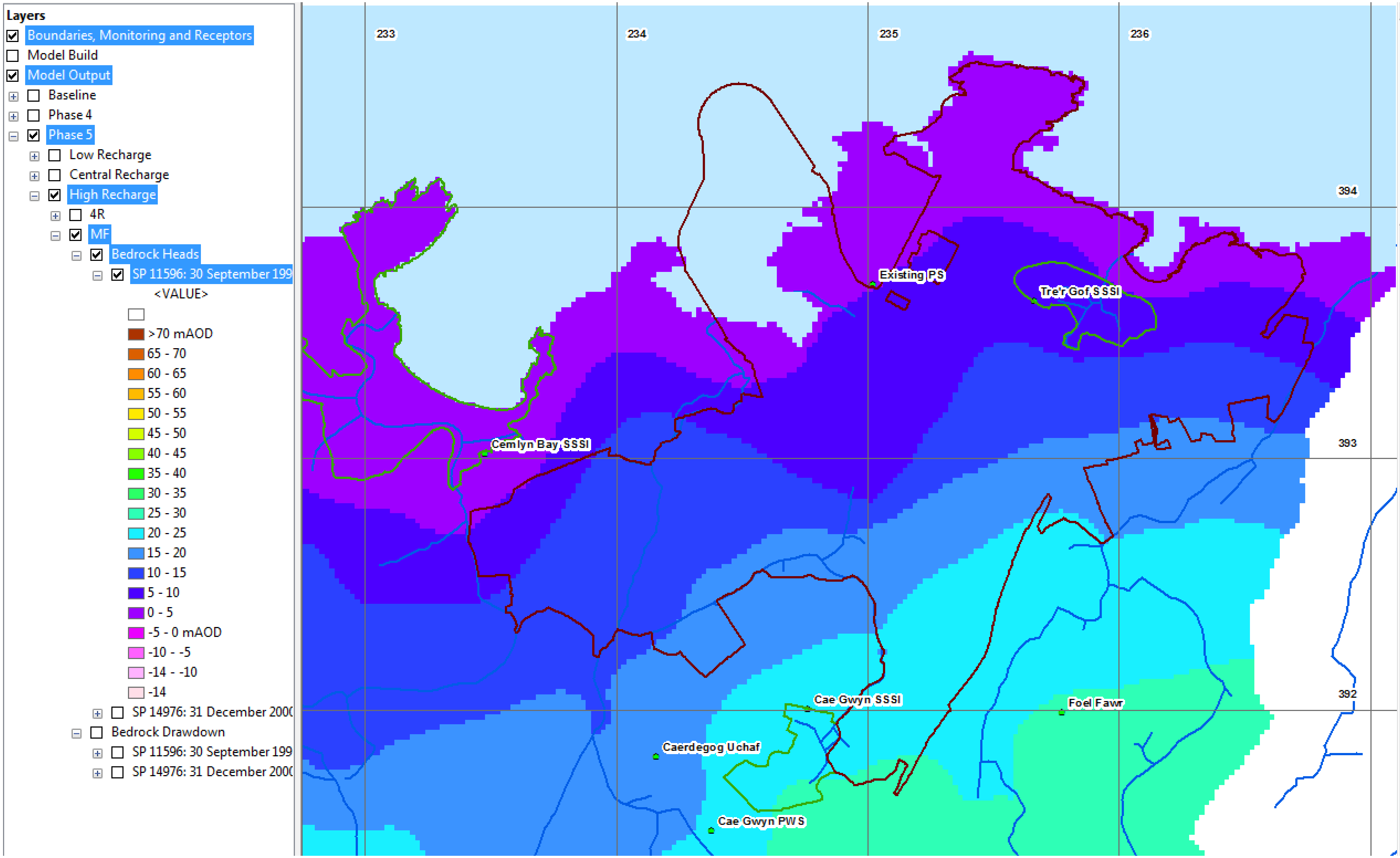

Phase 5 rivers, SSSI receptors, Site boundary, and MODFLOW High Model dry period (30/09/91) bedrock heads with GHB cells and Inactive cell overlay

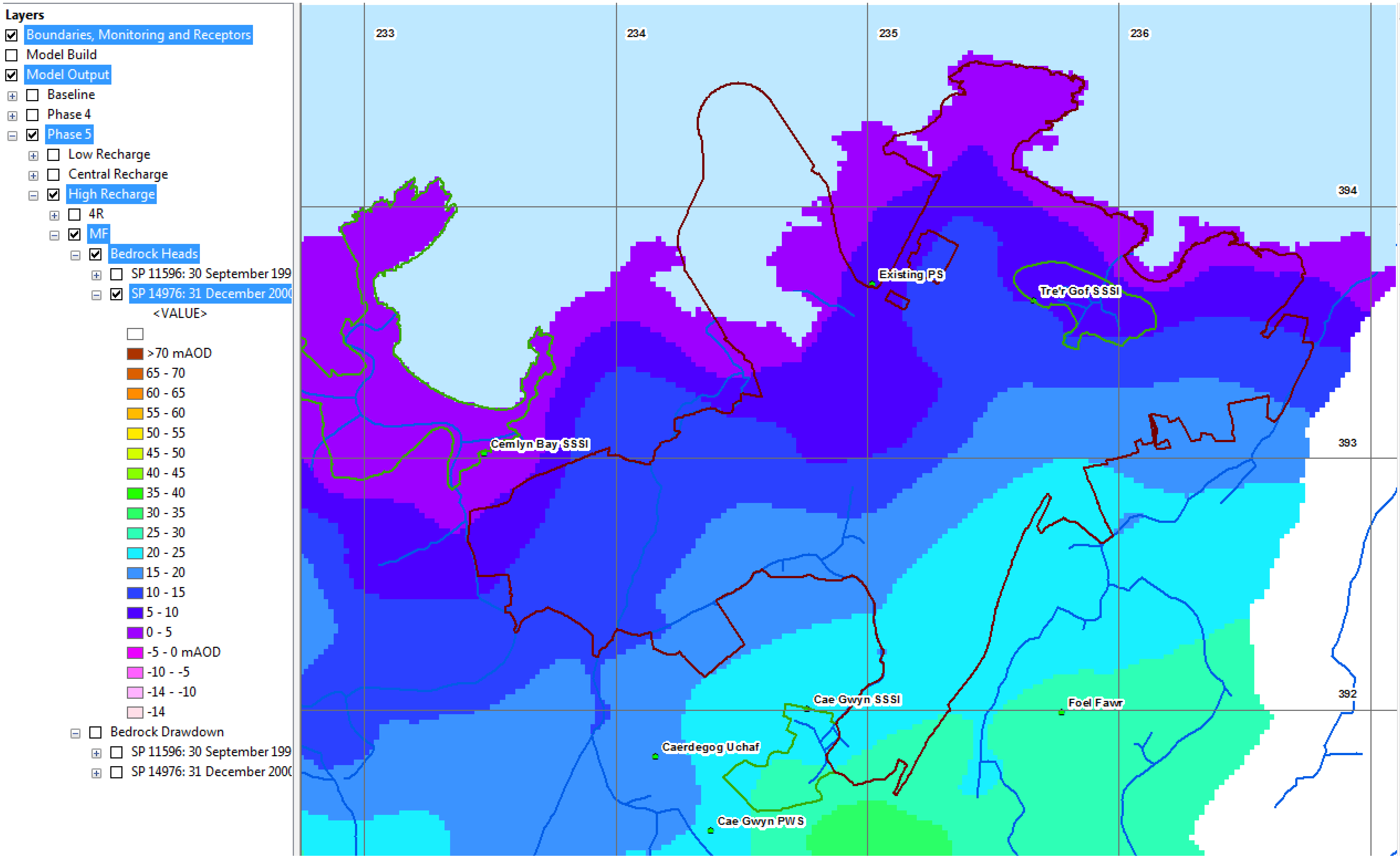

Phase 5 rivers, SSSI receptors, Site boundary, MODFLOW High Model wet period (31/12/2000) bedrock heads with GHB cells and Inactive cell overlay

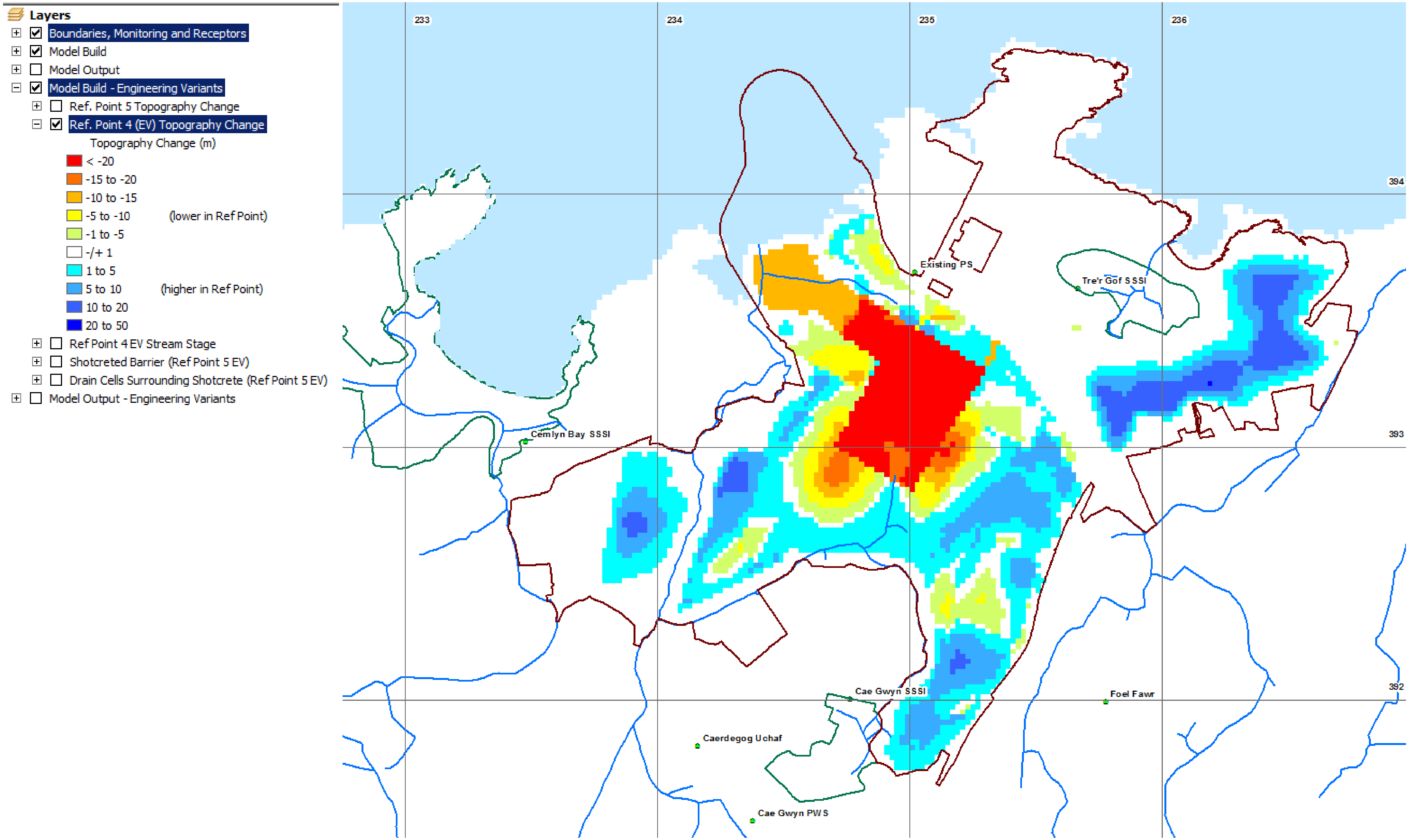

WylDCOGWMod_35989N1403i1 Appendix D, Phases 4 & 5 model build and output plans from 35989X1409Map\WylDCOModelMap.mxd

Ref Point 4 (Engineering Variant) topography change with respect to baseline

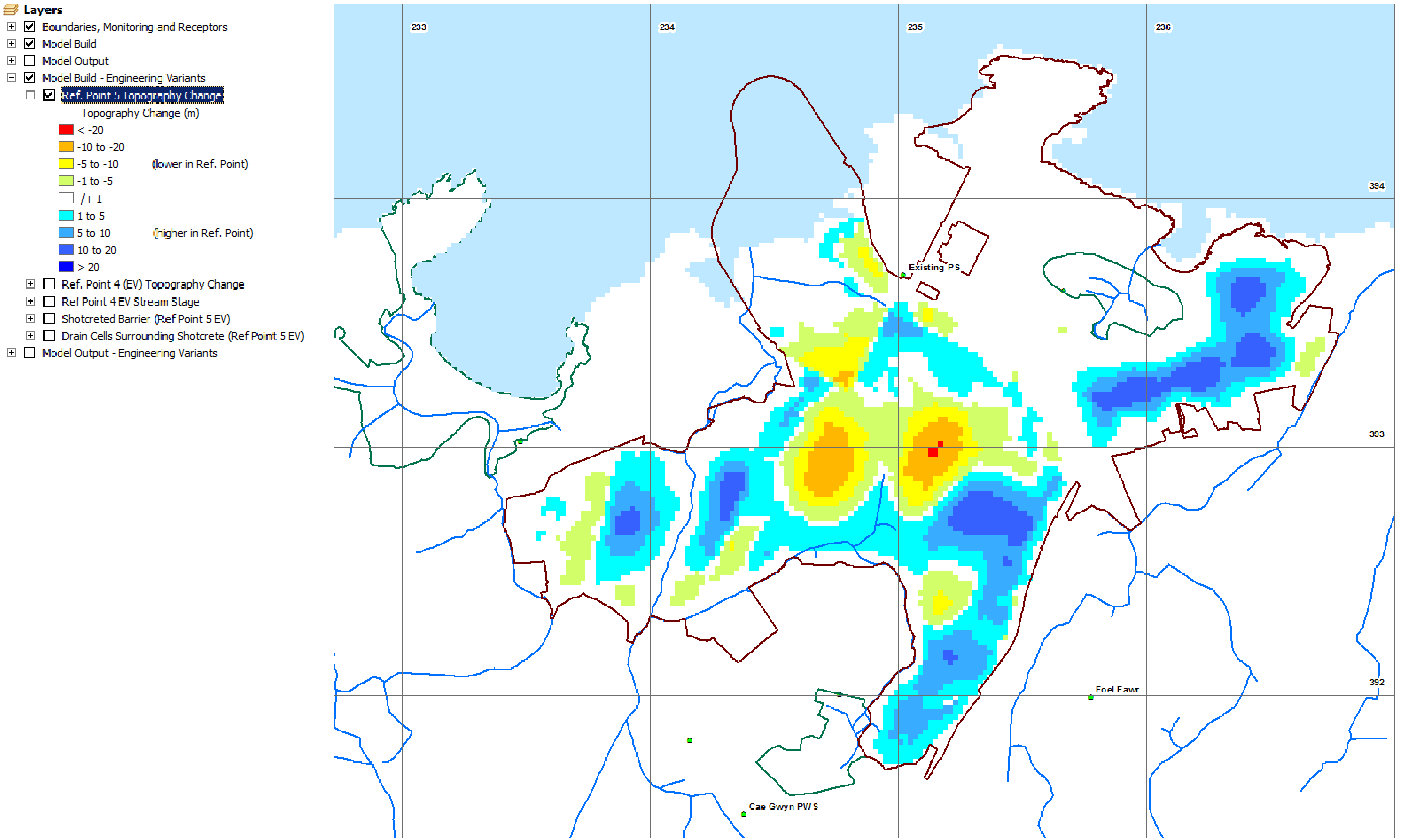

amec foster wheeler

WylDCOGWMod_35989N1403i1 Appendix D, Phases 4 & 5 model build and output plans from 35989X1409Map\WylDCOModelMap.mxd

Ref Point 5 (Engineering Variant) topography change with respect to baseline

Appendix E
Environmental impact predictions – bedrock groundwater level drawdown, and stream flow duration curves

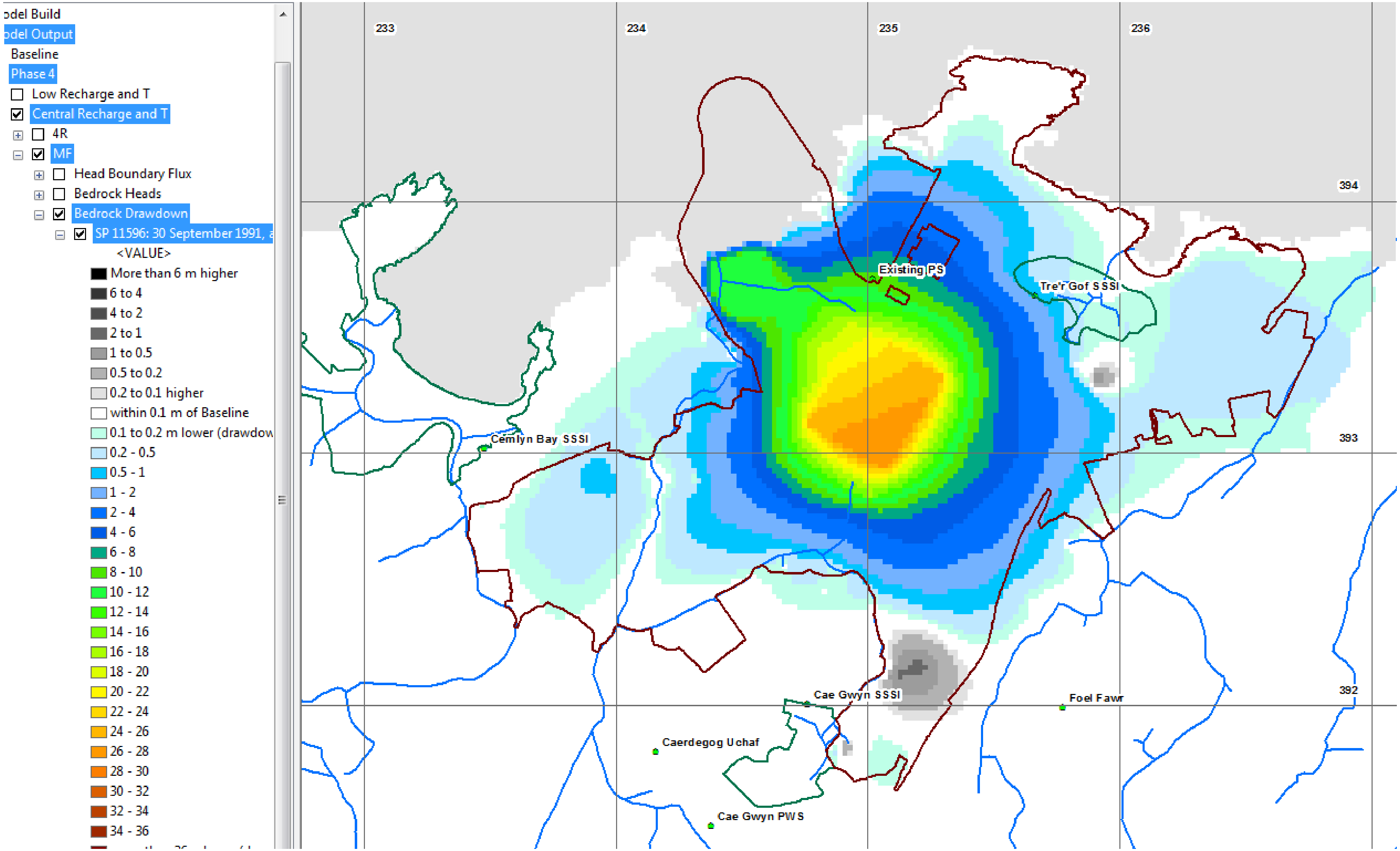

WylDCOGWMod_35989N1403i1 Appendix E, Phases 4 & 5 drawdown plans from 35989X1409Map\WylDCOModelMap.mxd

1

Phase 4 rivers, SSSI receptors, Site boundary, GW receptor cells & MODFLOW Central Model bedrock drawdown (Baseline minus Phase 4 heads), dry period (30/09/1991)

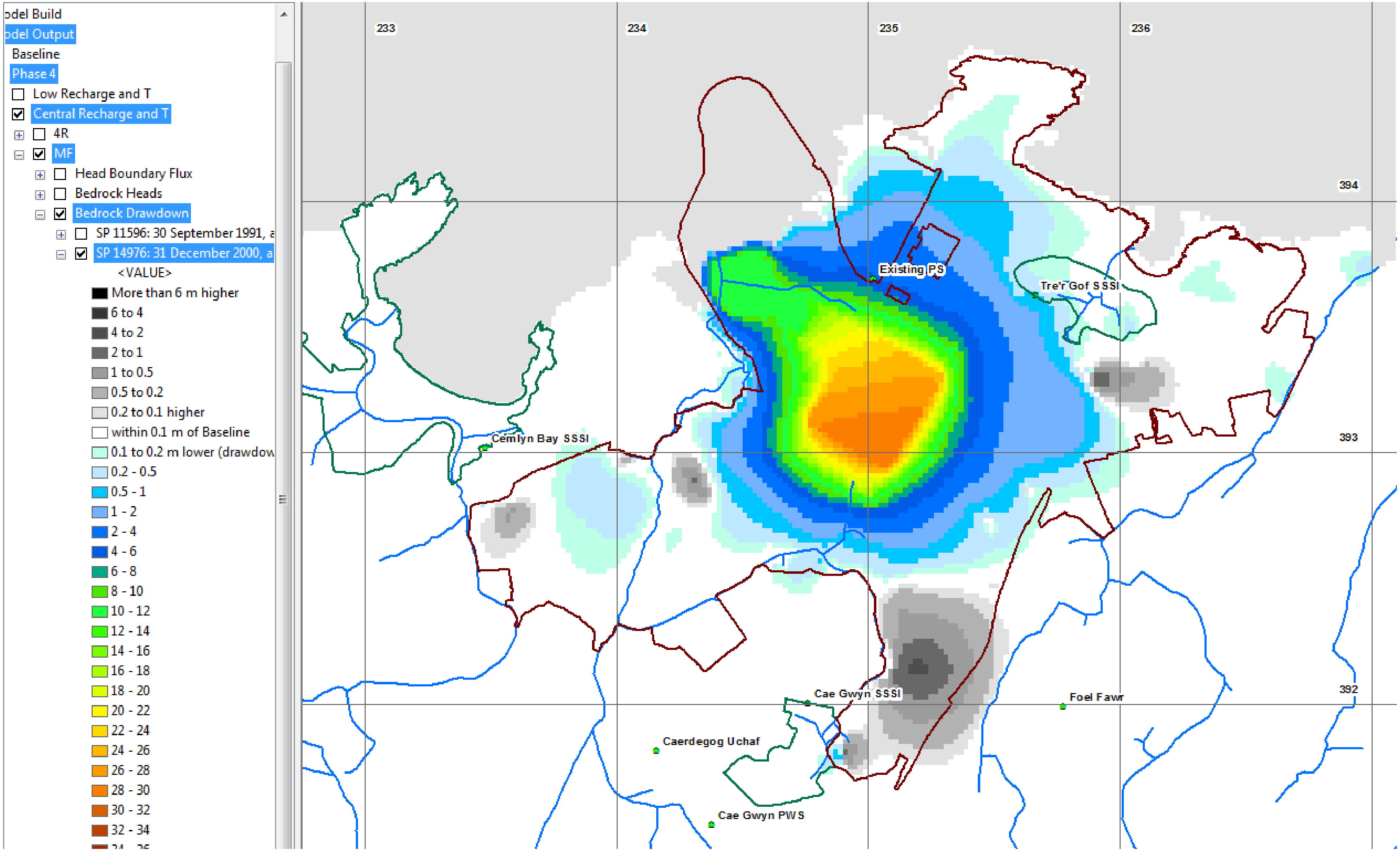

WylDCOGWMod_35989N1403i1 Appendix E, Phases 4 & 5 drawdown plans from 35989X1409Map\WylDCOModelMap.mxd

2 **Phase 4 rivers, SSSI receptors, Site boundary, GW receptor cells & MODFLOW Central Model bedrock drawdown (Baseline minus Phase 4 heads), wet period (31/12/2000)**

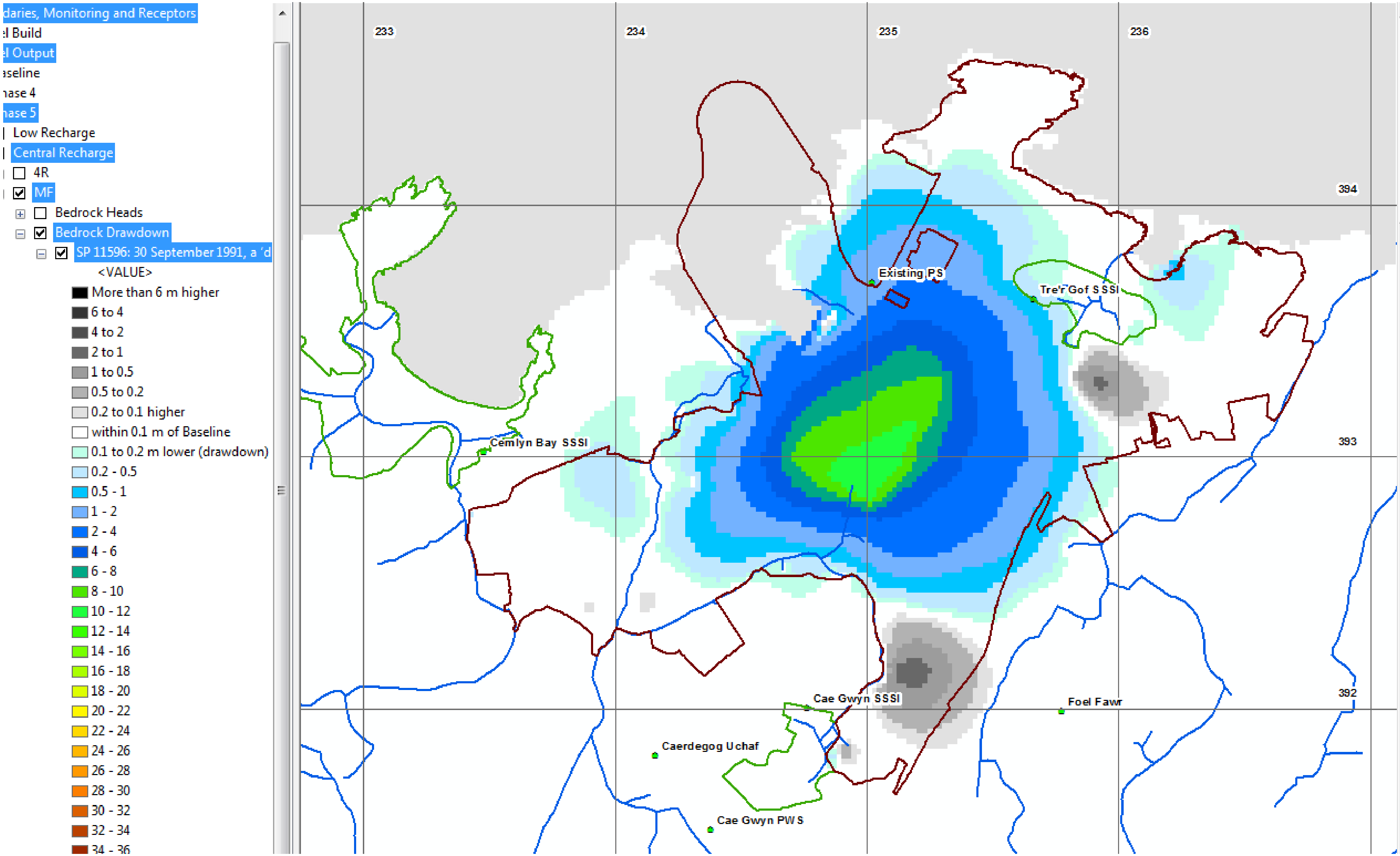

WylDCOGWMod_35989N1403i1 Appendix E, Phases 4 & 5 drawdown plans from 35989X1409Map\WylDCOModelMap.mxd

3

Phase 5 rivers, SSSI receptors, Site boundary, GW receptor cells & MODFLOW Central Model bedrock drawdown (Baseline minus Phase 5 heads), dry period (30/09/1991)

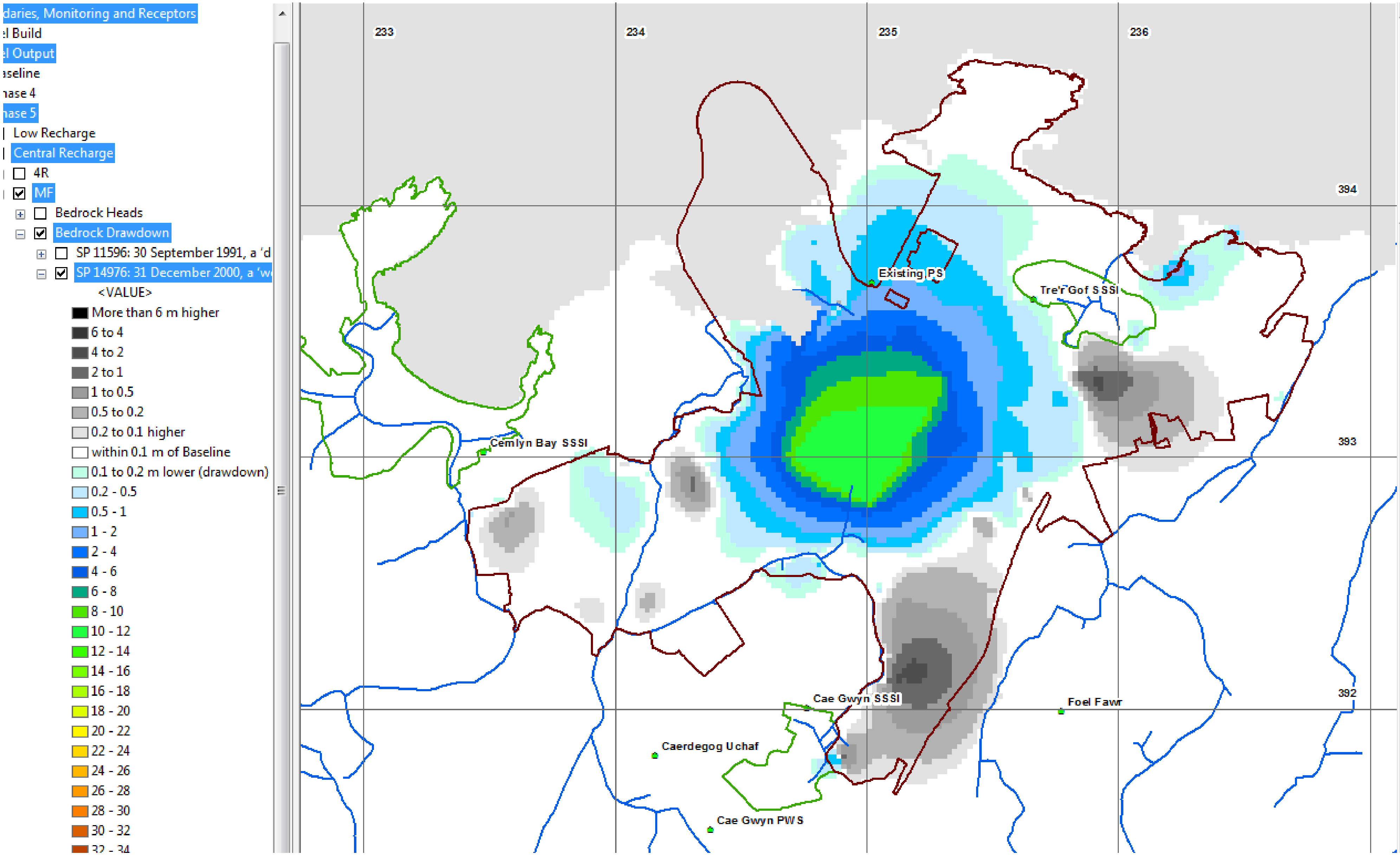

WylDCOGWMod_35989N1403i1 Appendix E, Phases 4 & 5 drawdown plans from 35989X1409Map\WylDCOModelMap.mxd

4

Phase 5 rivers, SSSI receptors, Site boundary, GW receptor cells & MODFLOW Central Model bedrock drawdown (Baseline minus Phase 5 heads), wet period (31/12/2000)

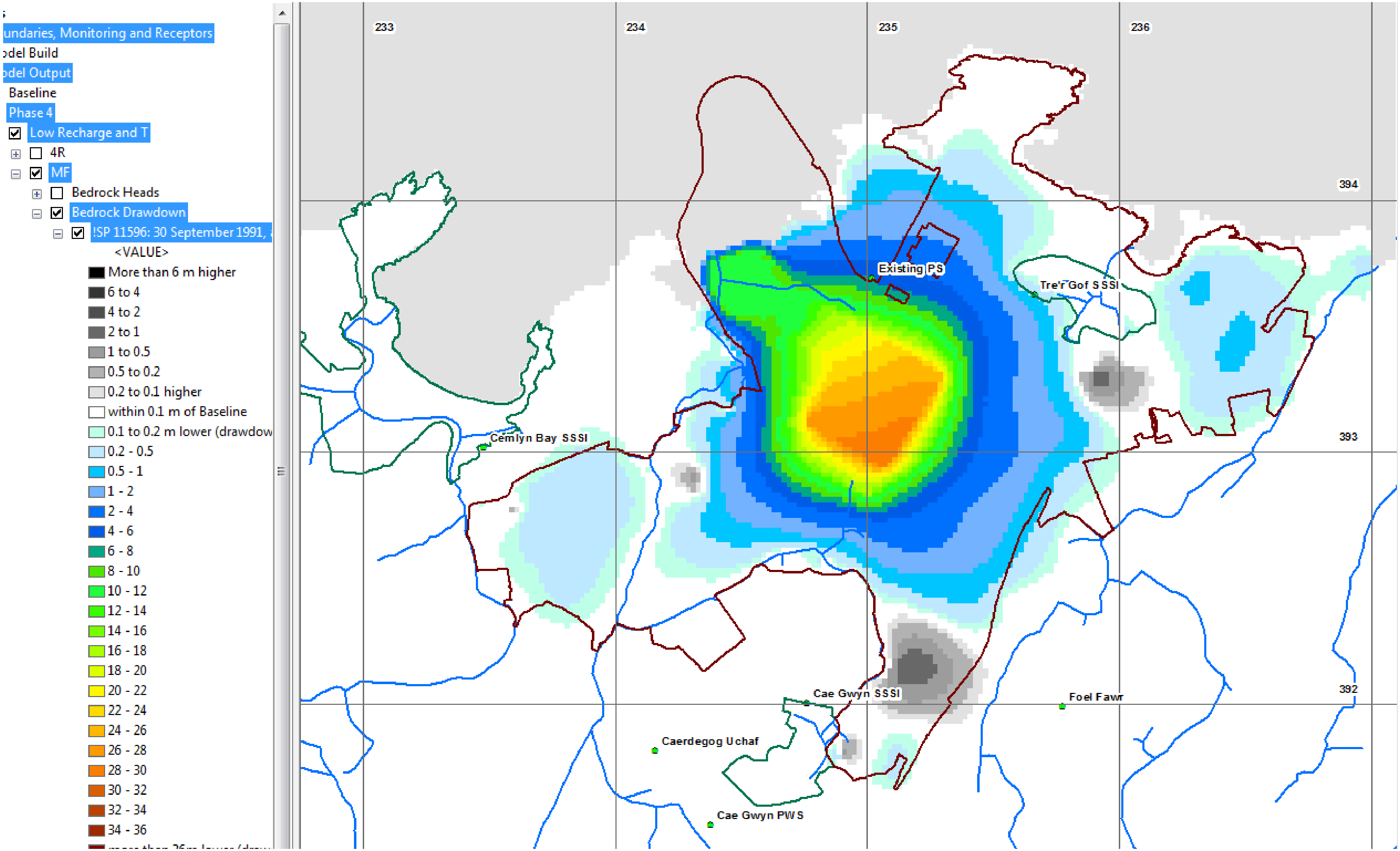

WylDCOGWMod_35989N1403i1 Appendix E, Phases 4 & 5 drawdown plans from 35989X1409Map\WylDCOModelMap.mxd

Phase 4 rivers, SSSI receptors, Site boundary, GW receptor cells & MODFLOW Low Model bedrock drawdown (Baseline minus Phase 4 heads), dry period (30/09/1991)

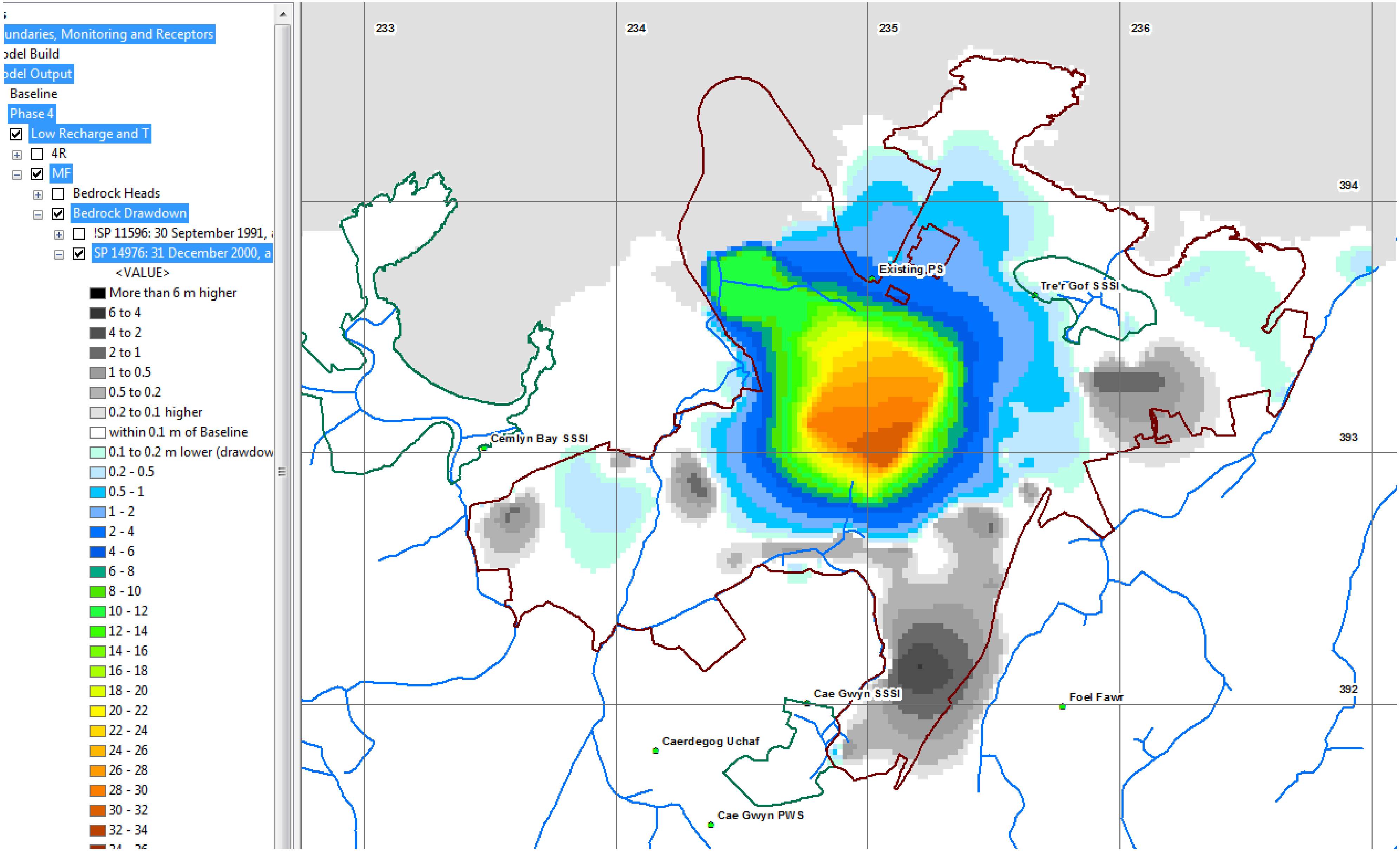

Phase 4 rivers, SSSI receptors, Site boundary, GW receptor cells & MODFLOW Low Model bedrock drawdown (Baseline minus Phase 4 heads), wet period (31/12/2000)

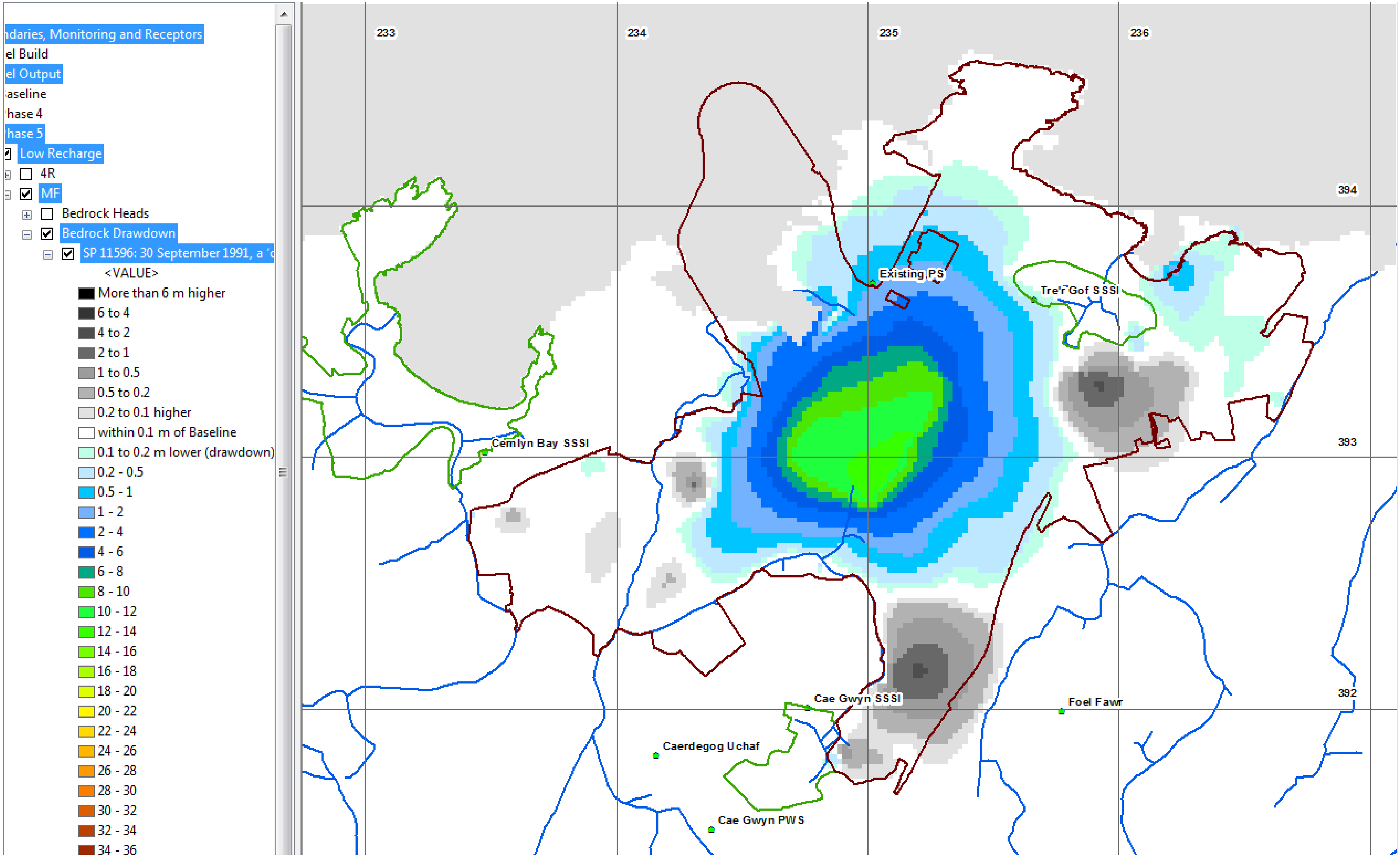

WylDCOGWMod_35989N1403i1 Appendix E, Phases 4 & 5 drawdown plans from 35989X1409Map\WylDCOModelMap.mxd

7

Phase 5 rivers, SSSI receptors, Site boundary, GW receptor cells & MODFLOW Low Model bedrock drawdown (Baseline minus Phase 5 heads), dry period (30/09/1991)

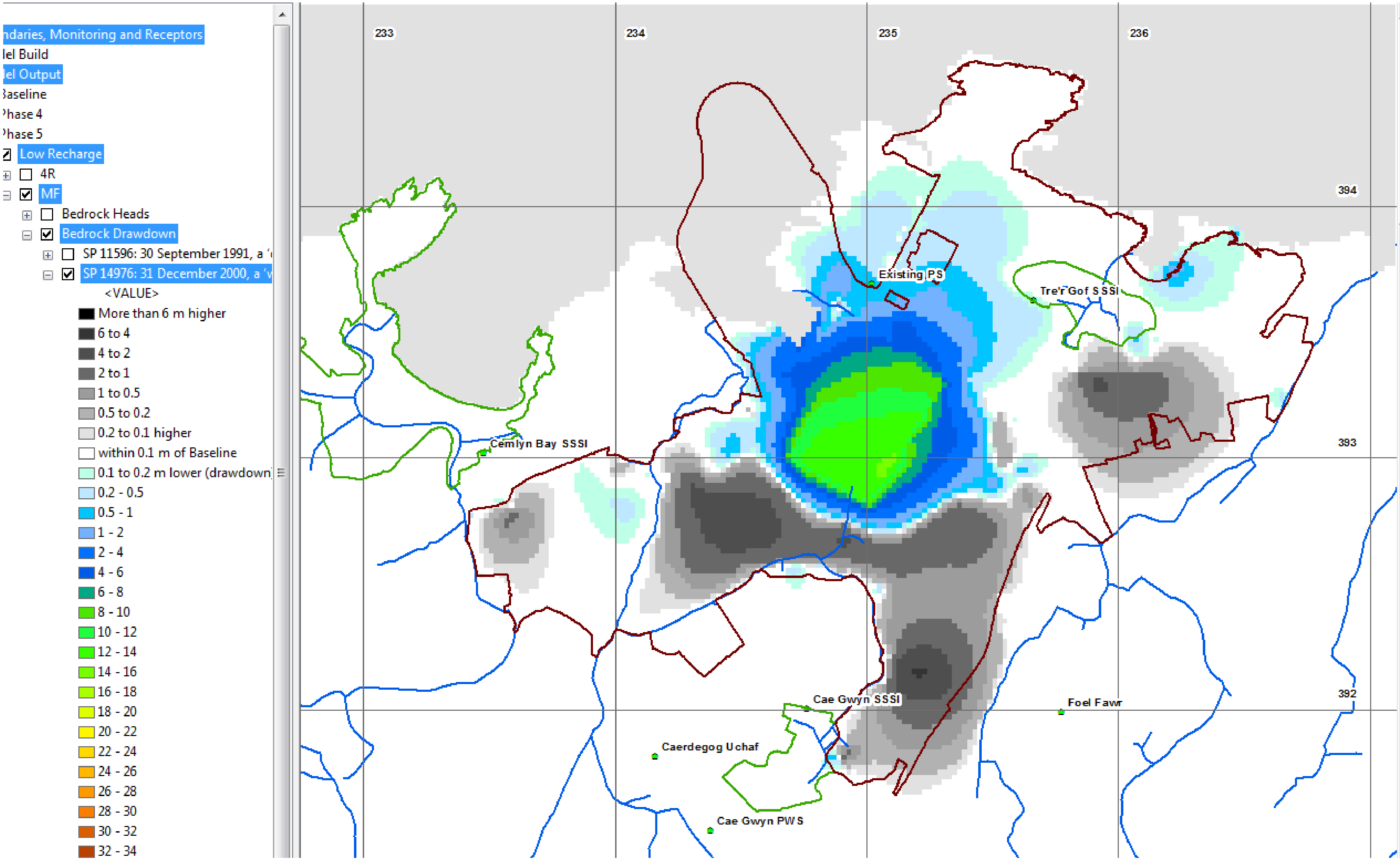

Phase 5 rivers, SSSI receptors, Site boundary, GW receptor cells & MODFLOW Low Model bedrock drawdown (Baseline minus Phase 5 heads), wet period (31/12/2000)

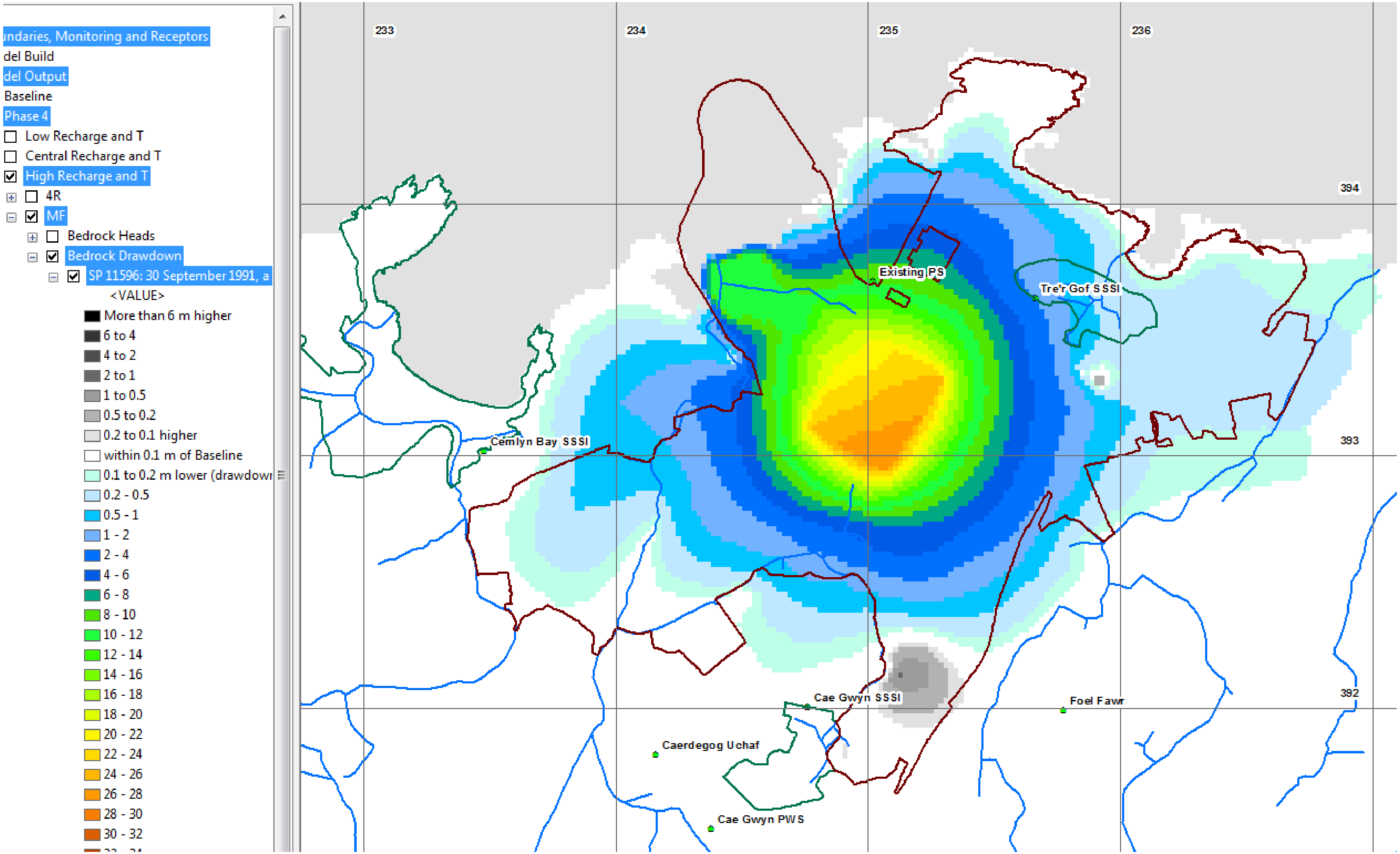

WylDCOGWMod_35989N1403i1 Appendix E, Phases 4 & 5 drawdown plans from 35989X1409Map\WylDCOModelMap.mxd

9 **Phase 4 rivers, SSSI receptors, Site boundary, GW receptor cells & MODFLOW High Model bedrock drawdown (Baseline minus Phase 4 heads), dry period (30/09/1991)**

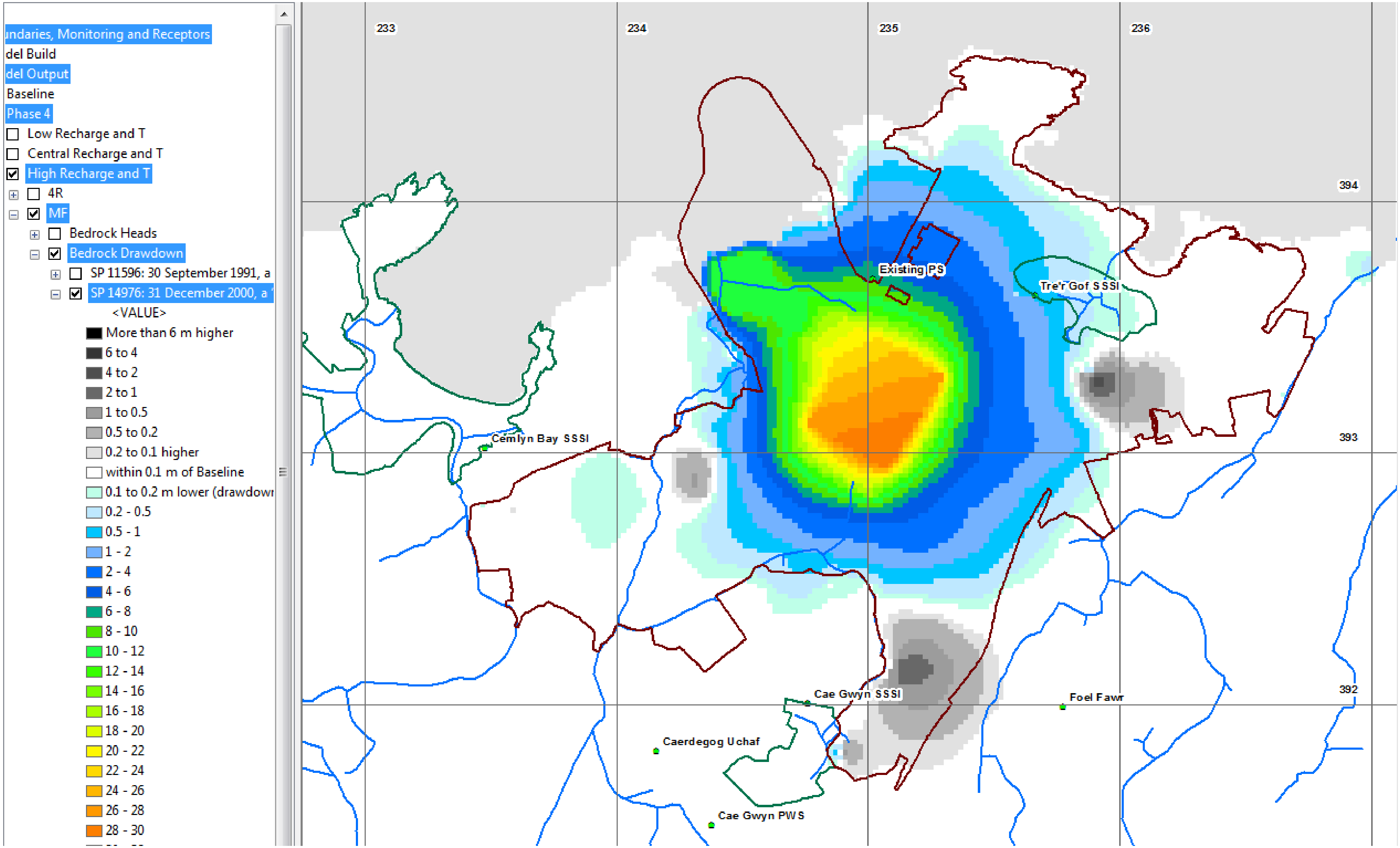

Phase 4 rivers, SSSI receptors, Site boundary, GW receptor cells & MODFLOW High Model bedrock drawdown (Baseline minus Phase 4 heads), wet period (31/12/2000)

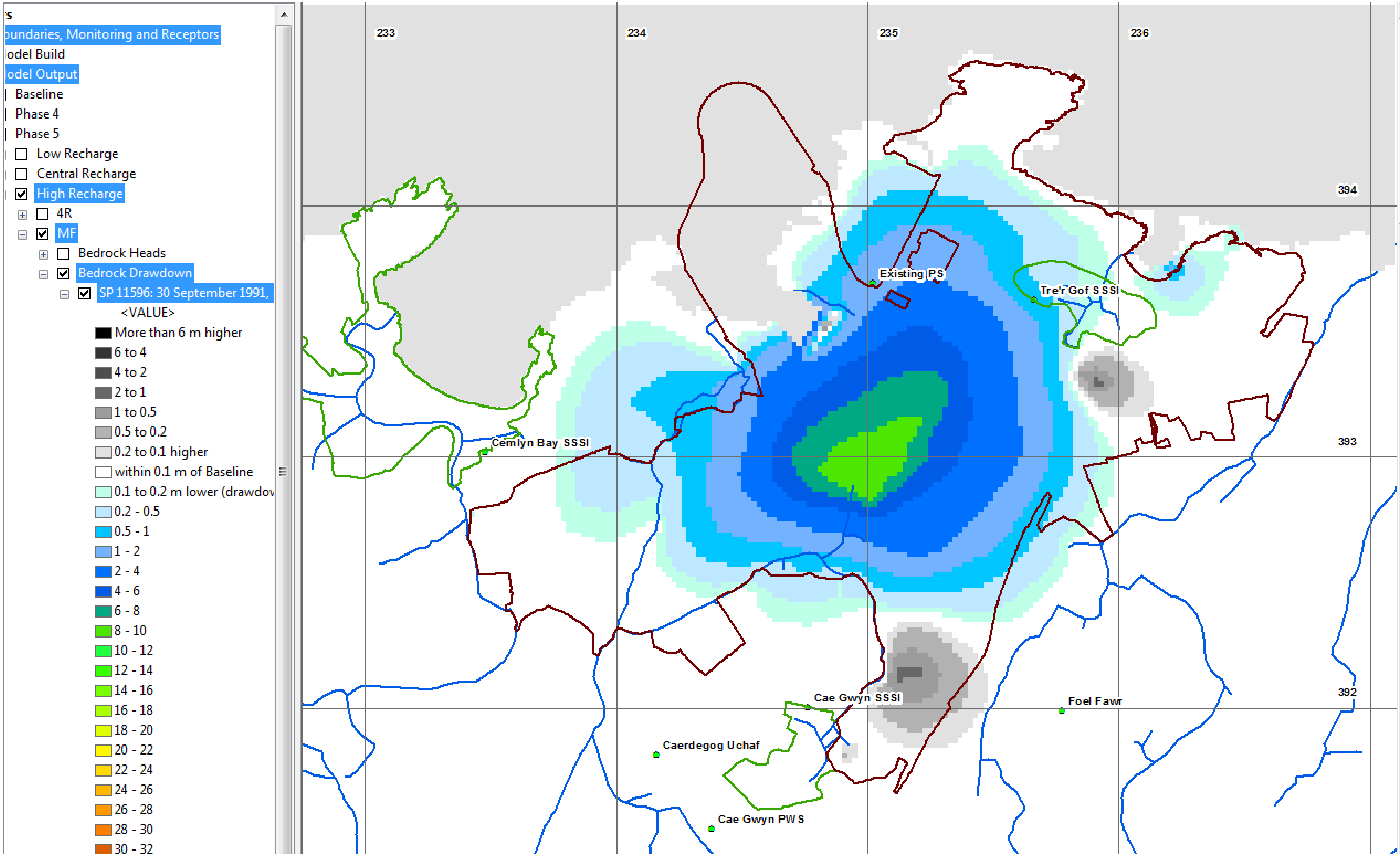

WylDCOGWMod_35989N1403i1 Appendix E, Phases 4 & 5 drawdown plans from 35989X1409Map\WylDCOModelMap.mxd

11

Phase 5 rivers, SSSI receptors, Site boundary, GW receptor cells & MODFLOW High Model bedrock drawdown (Baseline minus Phase 5 heads), dry period (30/09/1991)

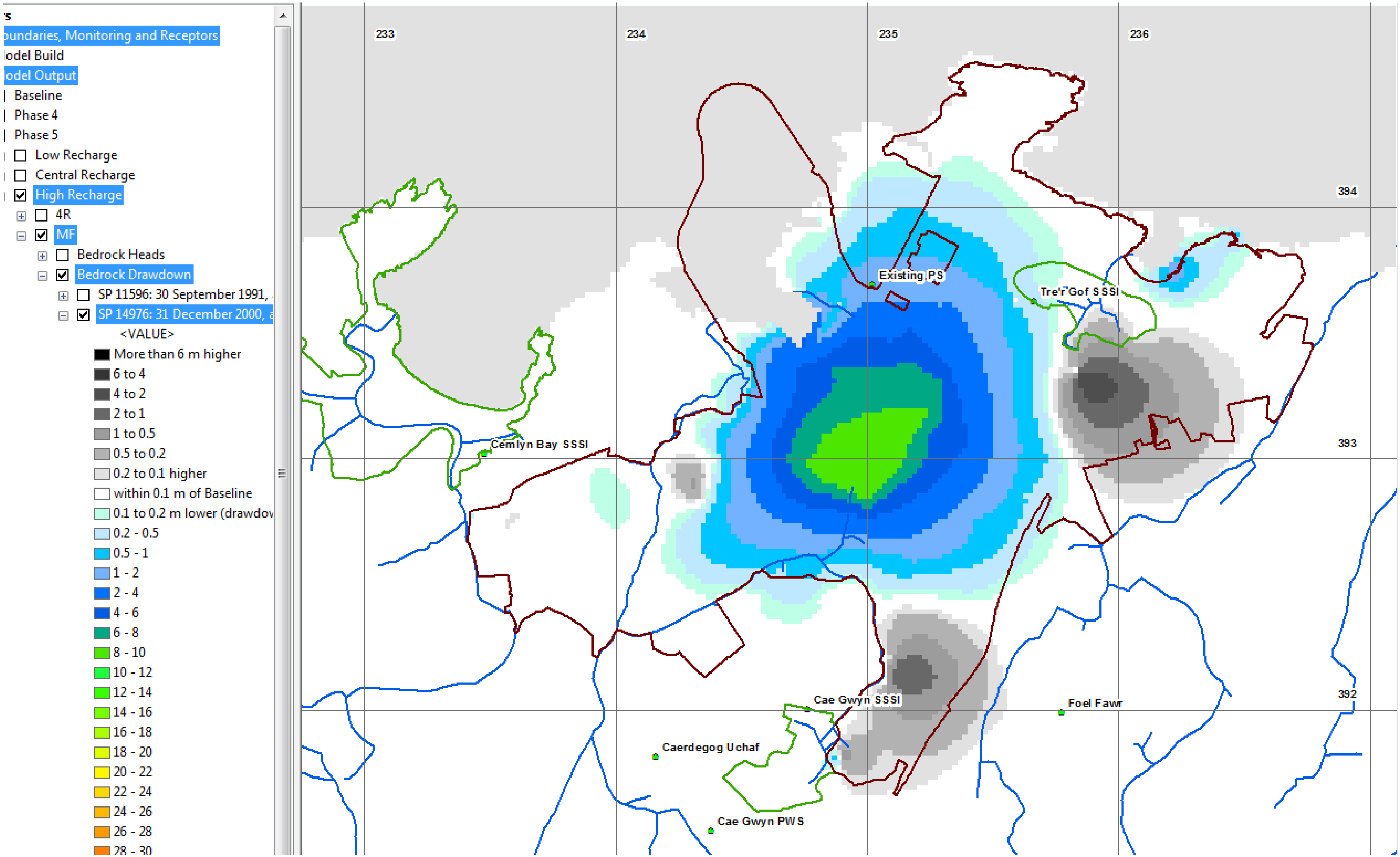

WylDCOGWMod_35989N1403i1 Appendix E, Phases 4 & 5 drawdown plans from 35989X1409Map\WylDCOModelMap.mxd

12 **Phase 5 rivers, SSSI receptors, Site boundary, GW receptor cells & MODFLOW High Model bedrock drawdown (Baseline minus Phase 5 heads), wet period (31/12/2000)**

Bottom of FDC impact plot = Ph5 long term FDC impacts as % of Baseline flows:

< -30%	-30 to -10%	-10 to +10%	+10 to +30%	+30% >	Base.<1m^3/d

RUN: LOW CENTRAL HIGH

CAE1

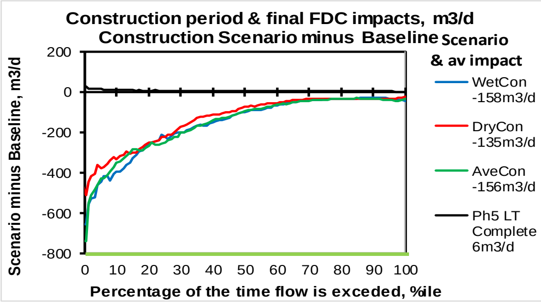

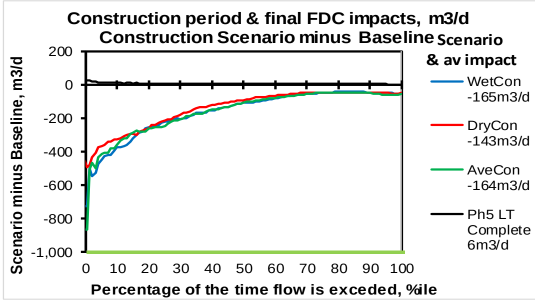

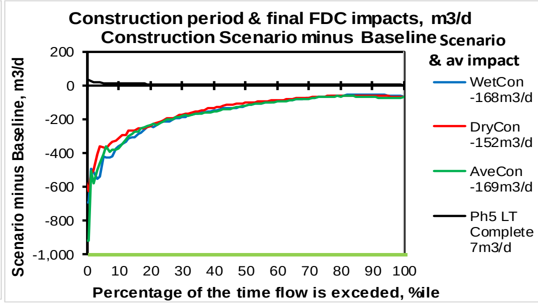

CAE2

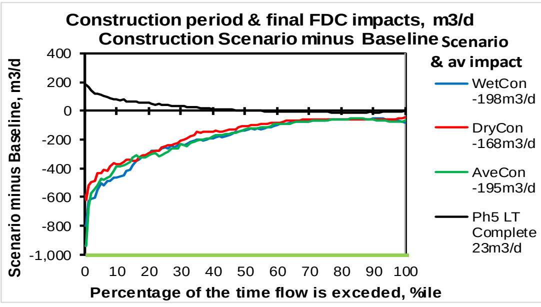

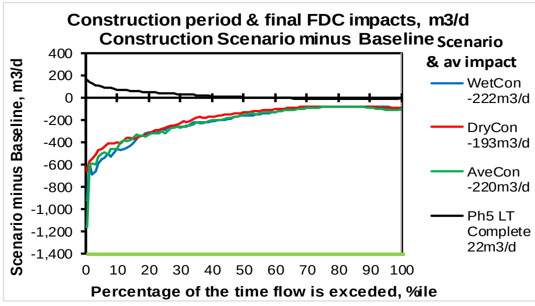

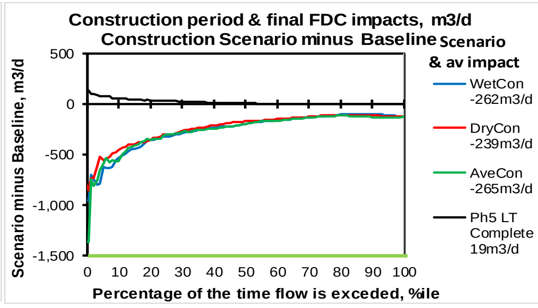

CAE3

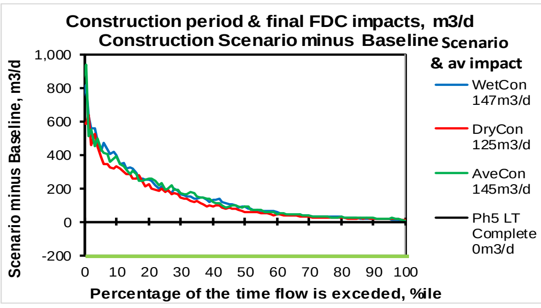

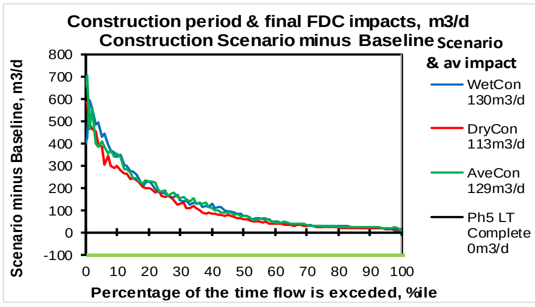

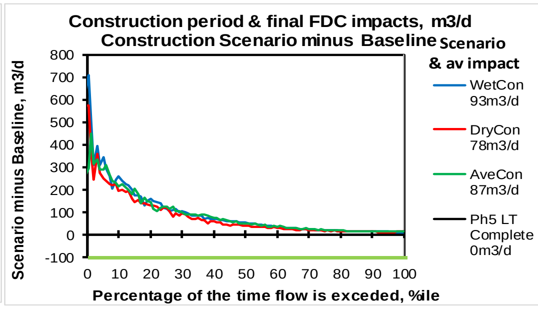

CAE4

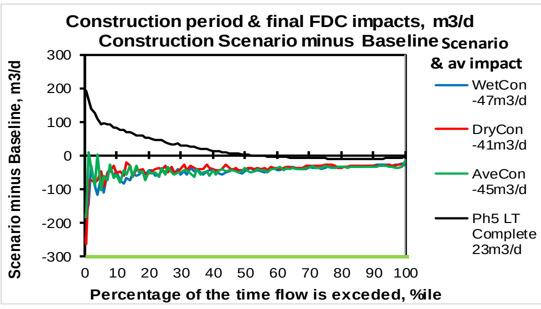

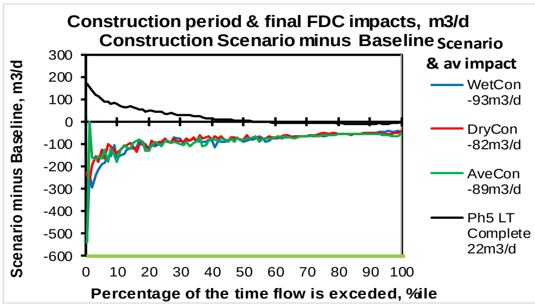

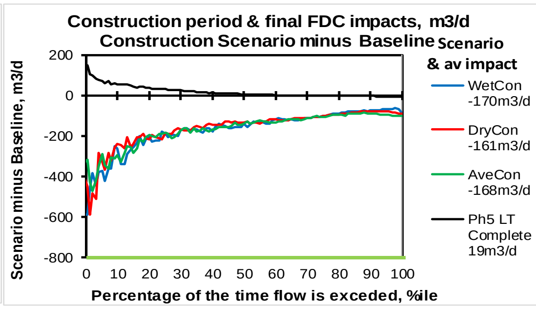

CAE5

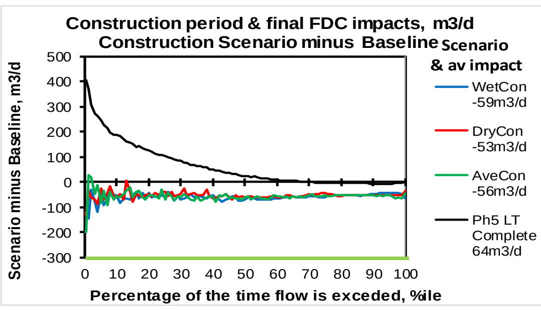

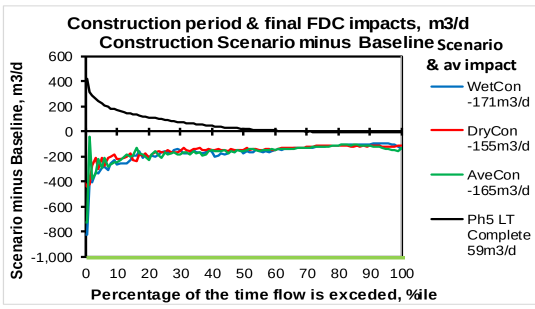

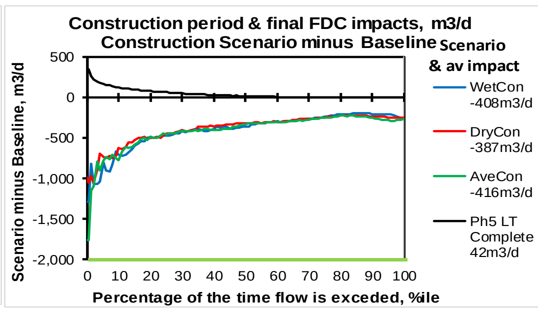

CAE6

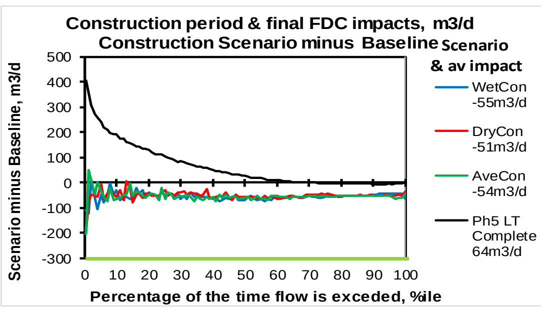

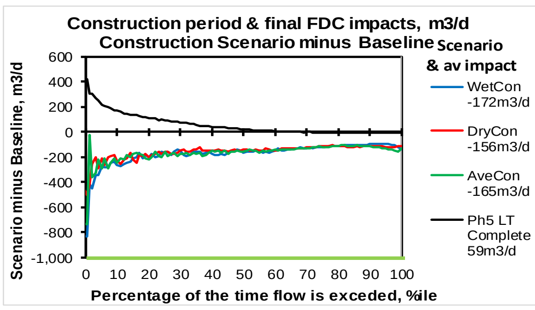

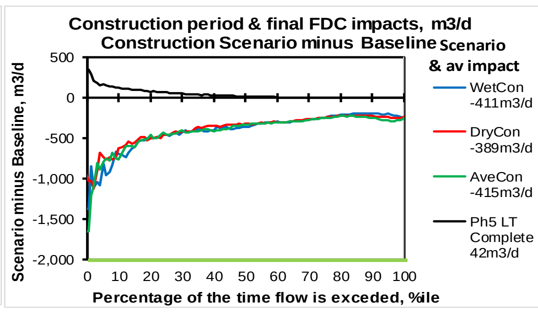

CAE7

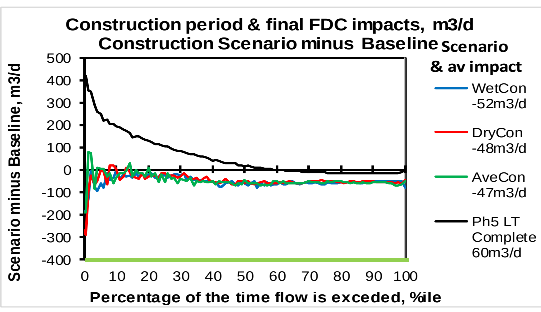

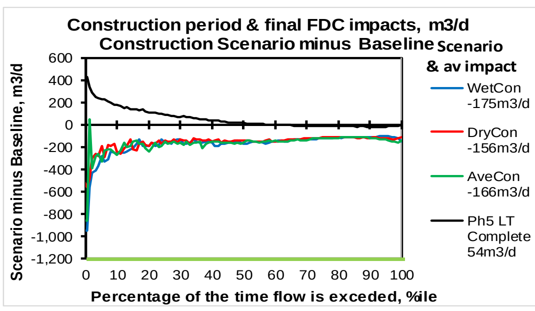

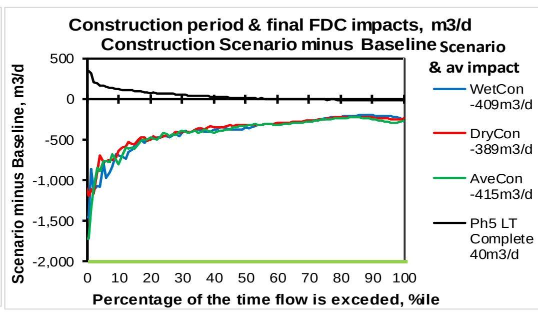

CAF1

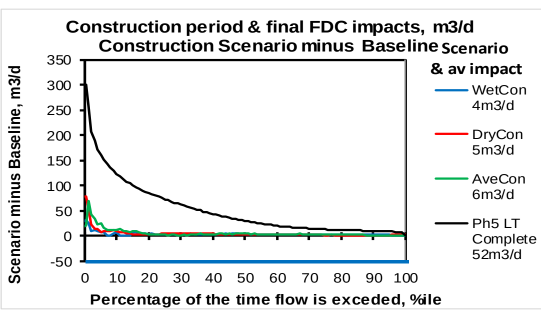

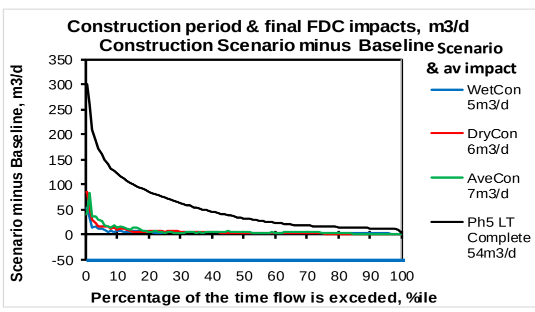

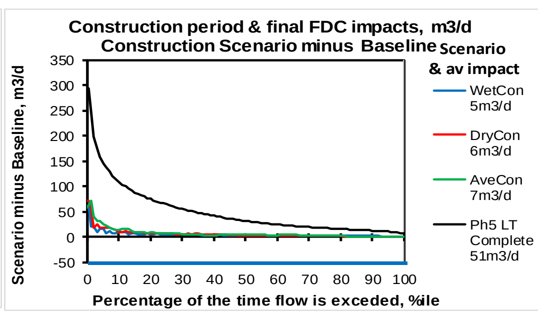

Bottom of FDC impact plot = Ph5 long term FDC impacts as % of Baseline flows:

< -30%	-30 to -10%	-10 to +10%	+10 to +30%	+30% >	Base.<1m³/d

RUN: **LOW** **CENTRAL** **HIGH**

CAF2

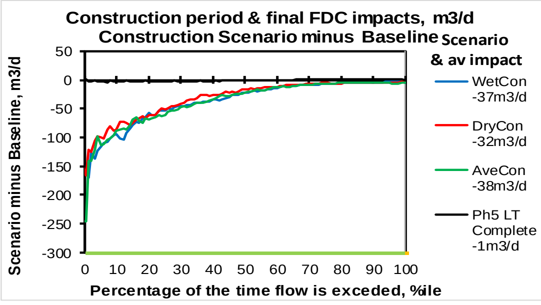

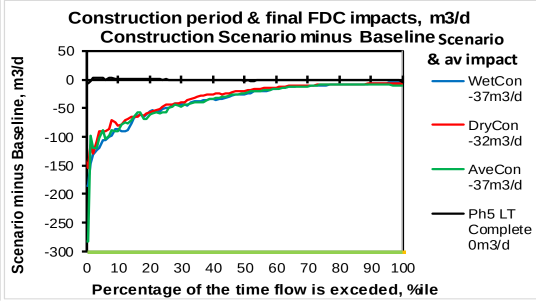

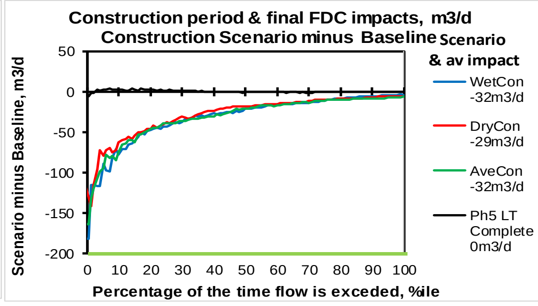

CAF3

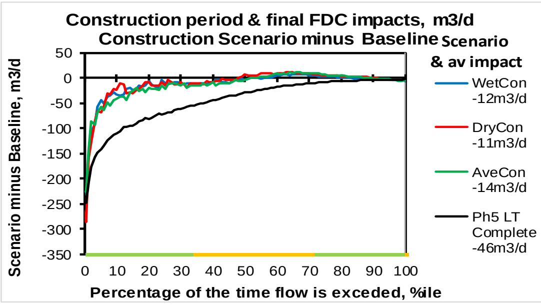

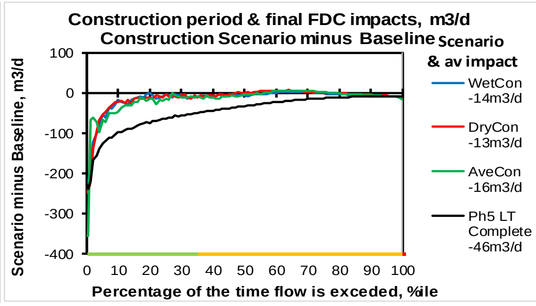

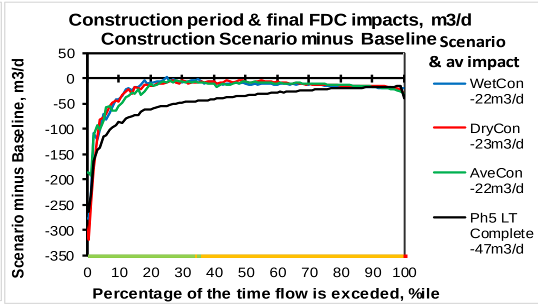

CAF4

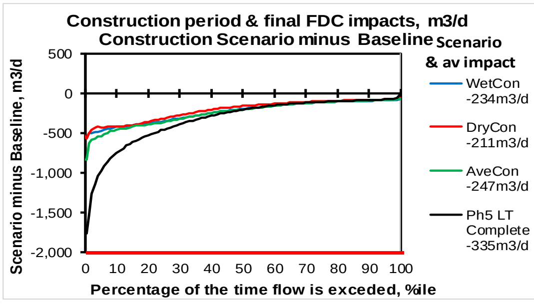

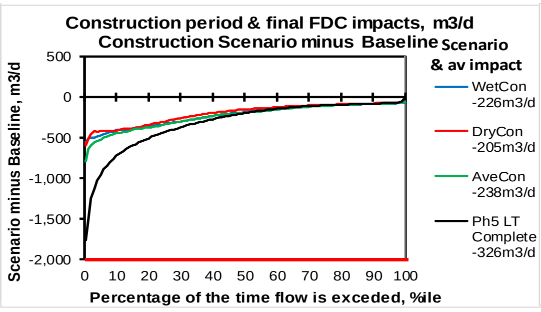

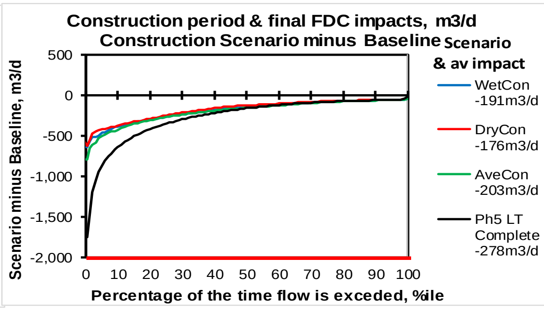

CAF5

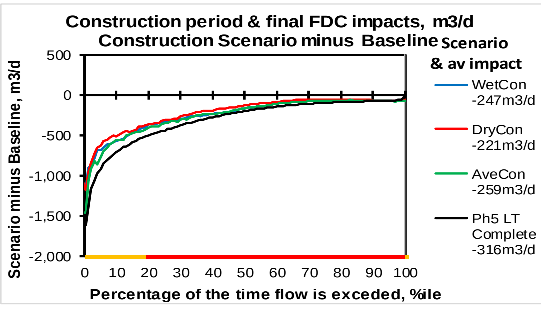

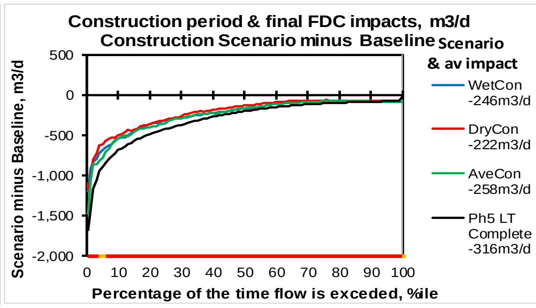

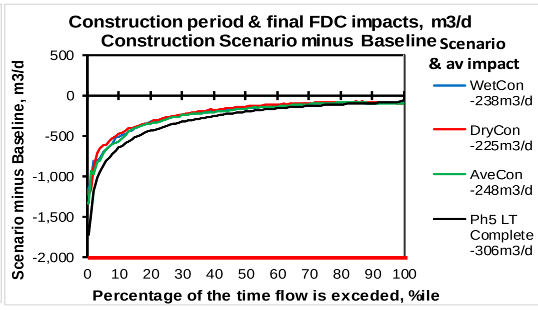

CAF6

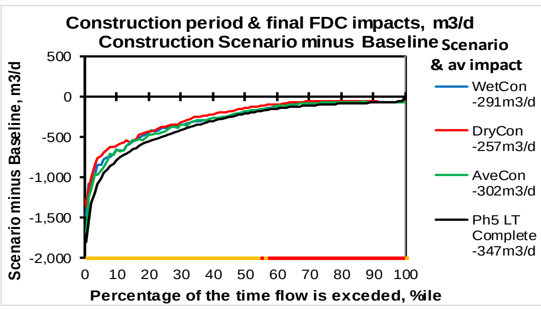

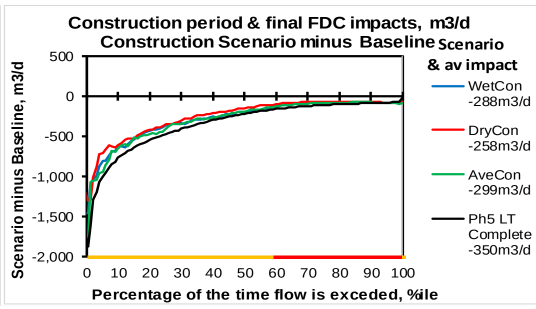

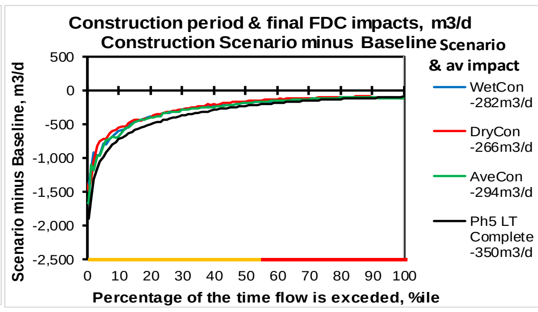

CAF7

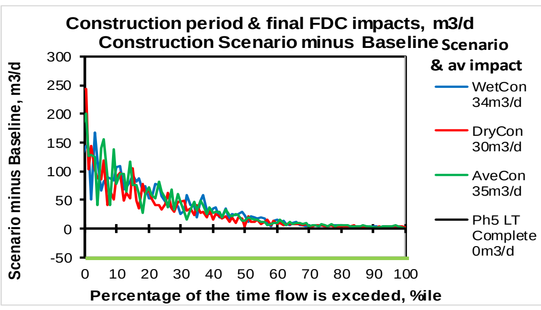

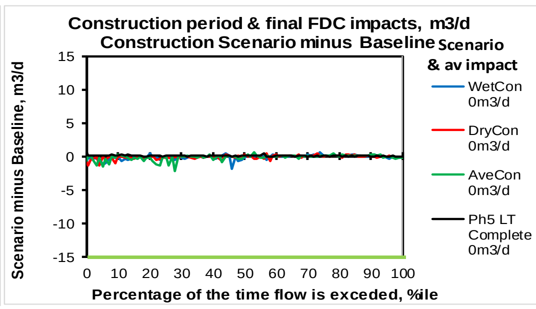

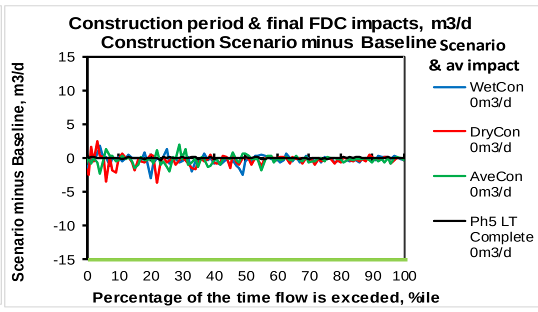

CAF8

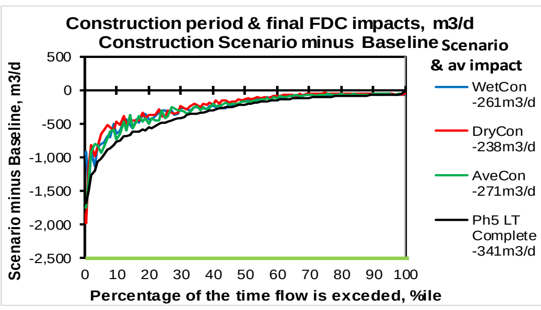

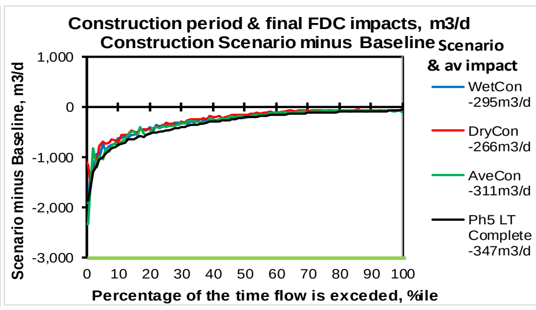

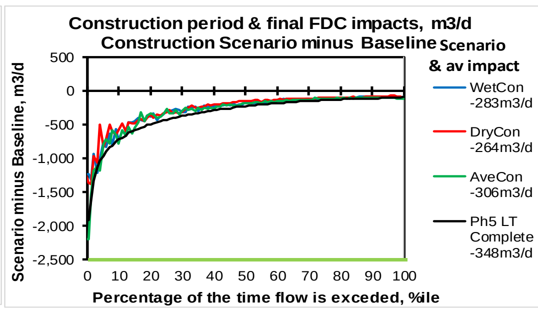

CAF9

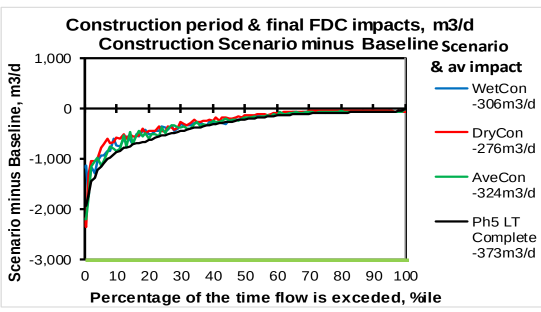

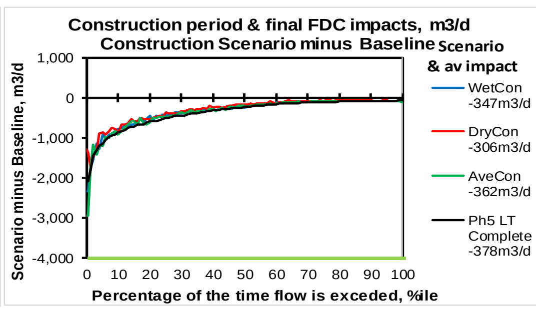

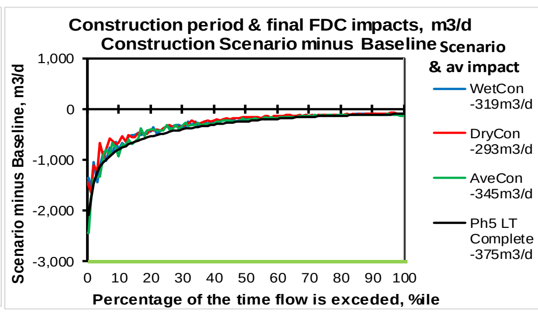

Bottom of FDC impact plot = Ph5 long term FDC impacts as % of Baseline flows:

< -30%	-30 to -10%	-10 to +10%	+10 to +30%	+30% >	Base.<1m^3/d

RUN: **LOW** **CENTRAL** **HIGH**

CAF10

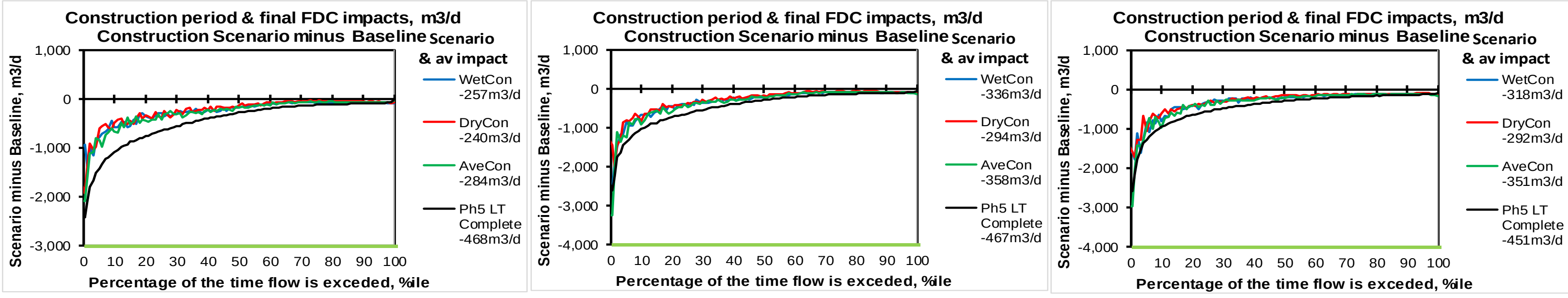

CAF11

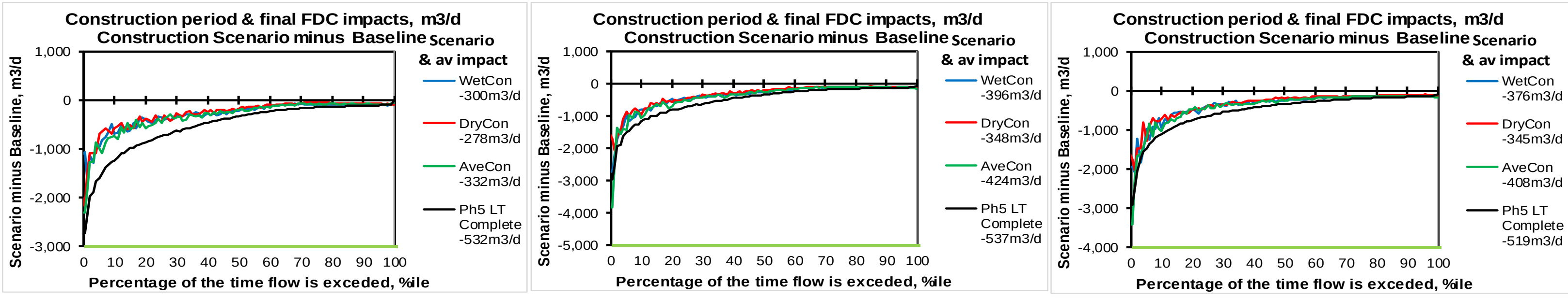

CEM0

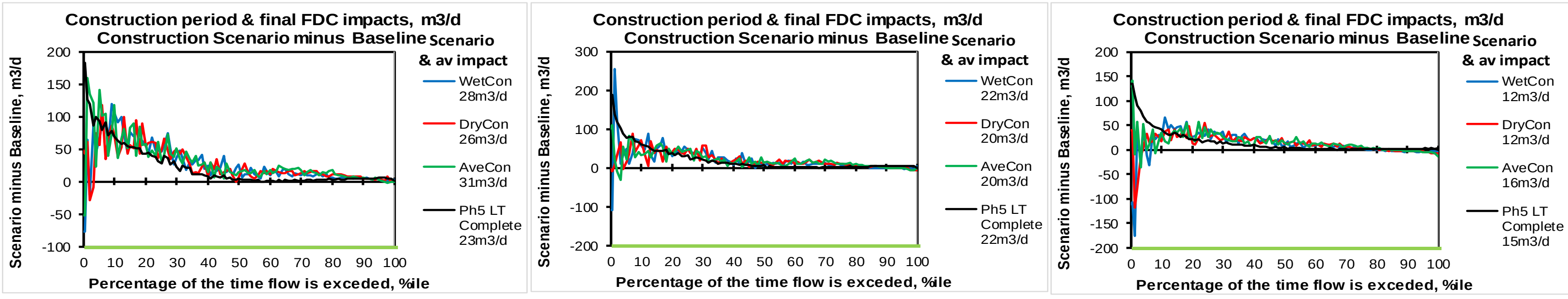

CEM1

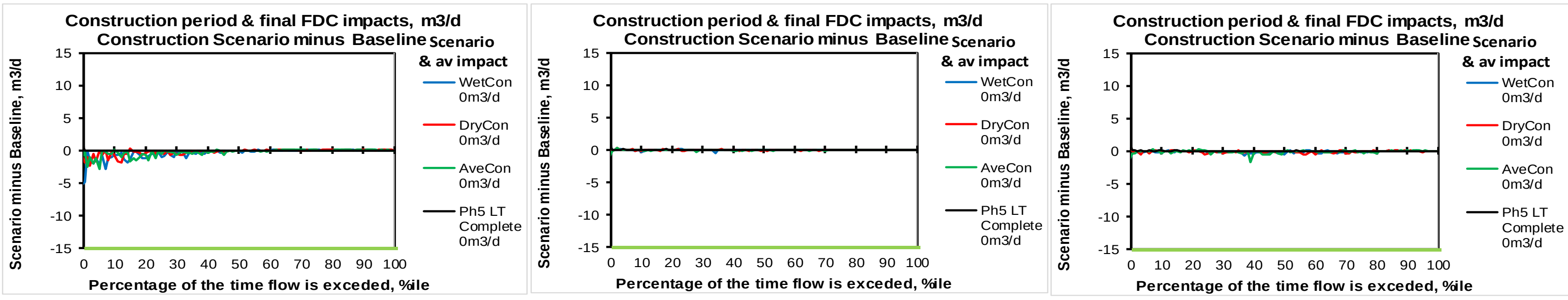

CEM2

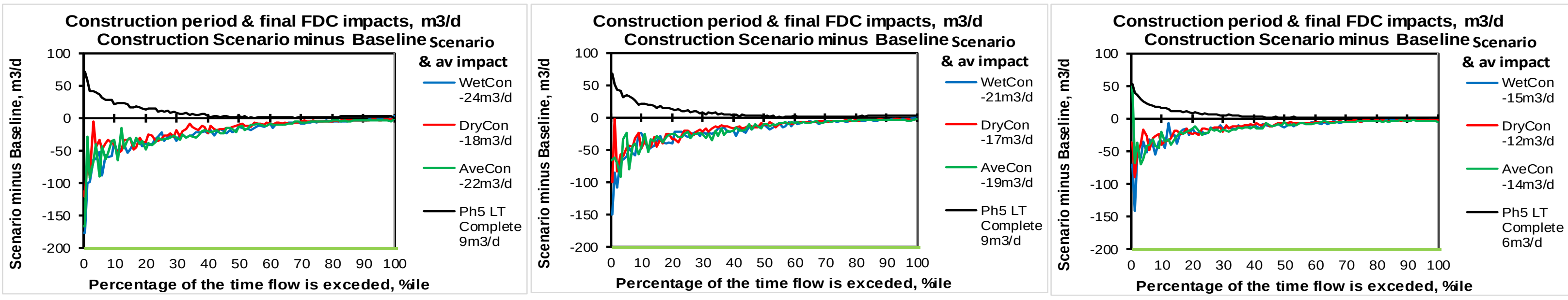

CEM3

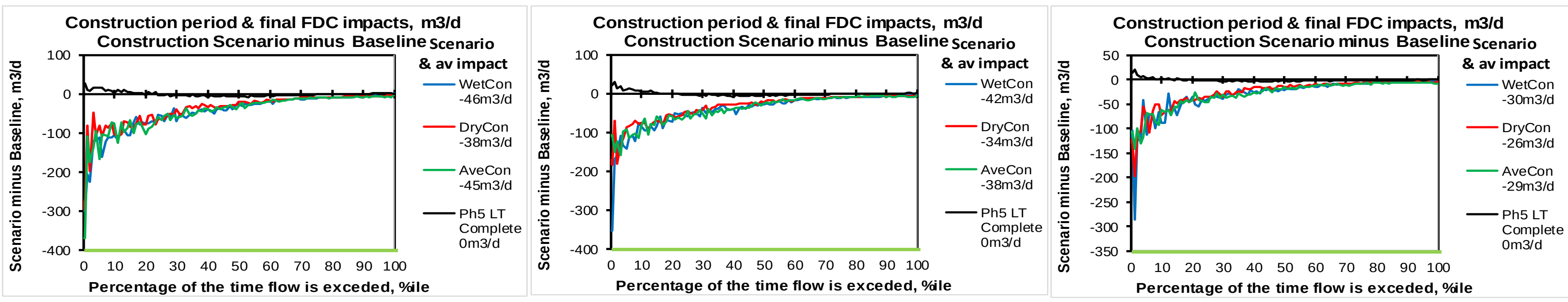

CEM4

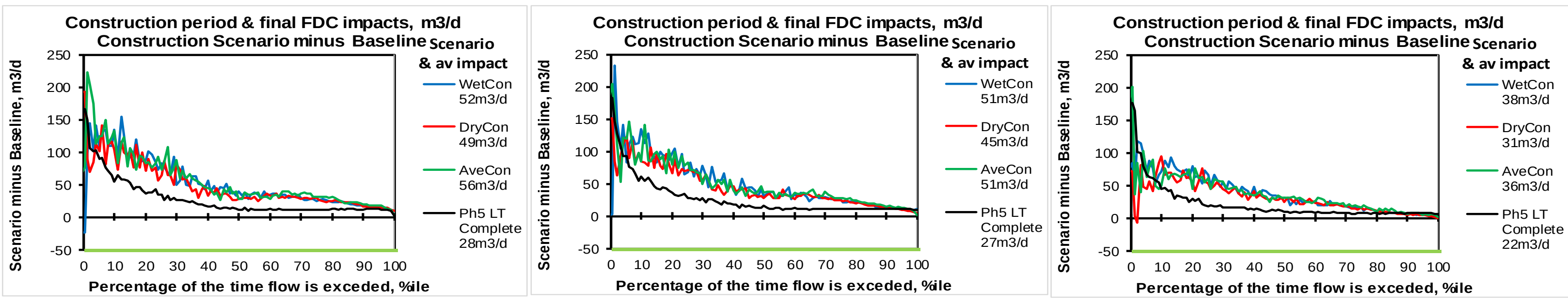

CEM5

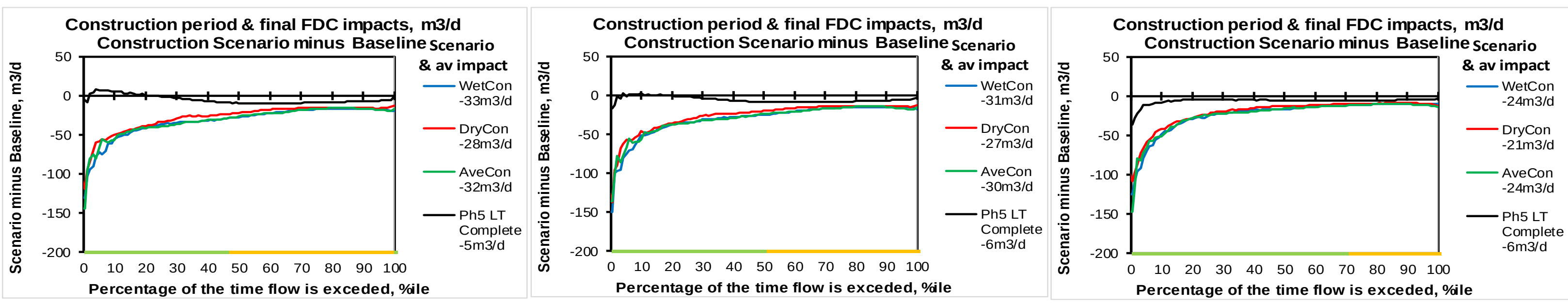

Bottom of FDC impact plot = Ph5 long term FDC impacts as % of Baseline flows: | < -30% | -30 to -10% | -10 to +10% | +10 to +30% | +30% > | Base.<1m^3/d |

RUN: LOW CENTRAL HIGH

LLYN1

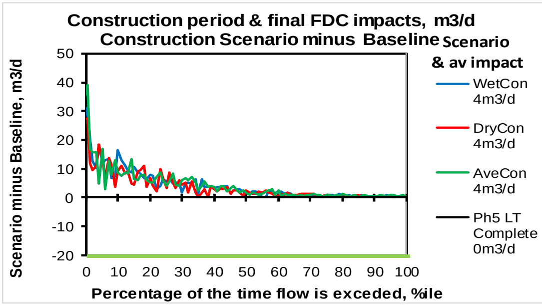

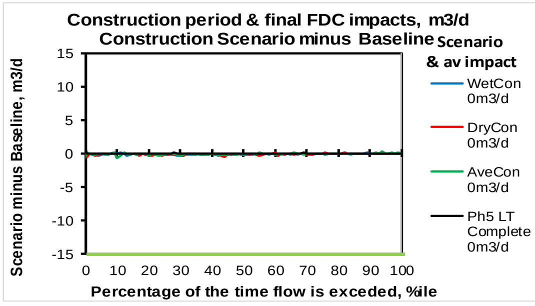

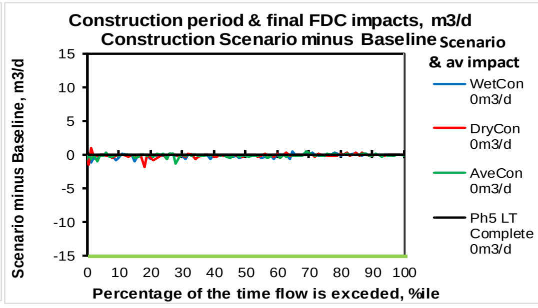

TG1

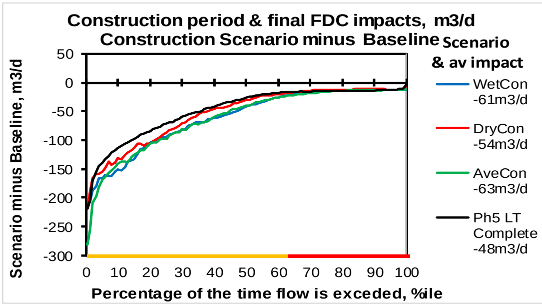

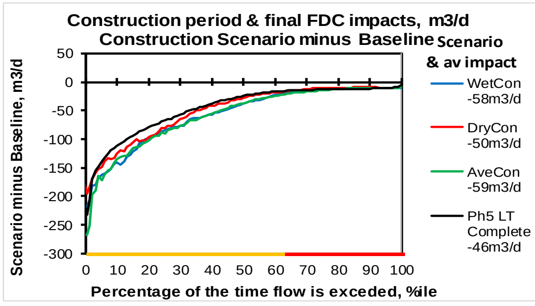

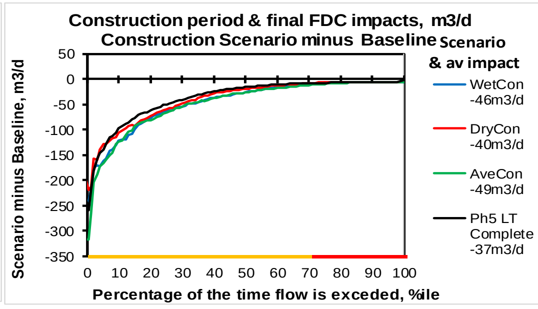

TG2

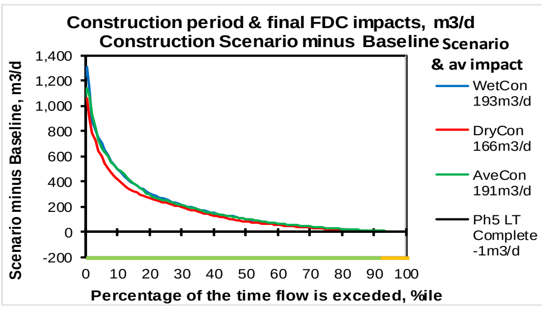

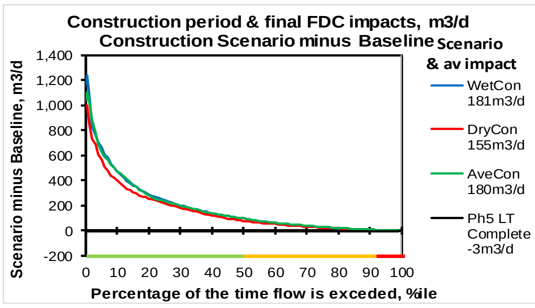

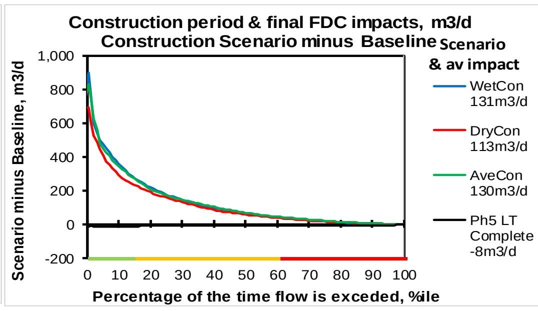

TG3

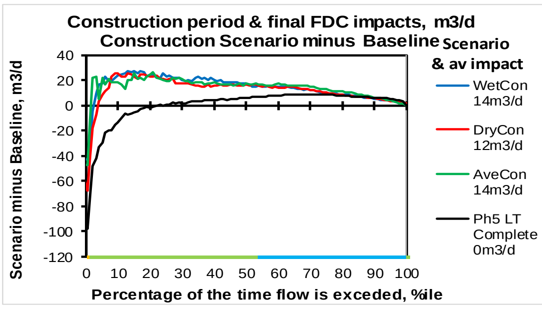

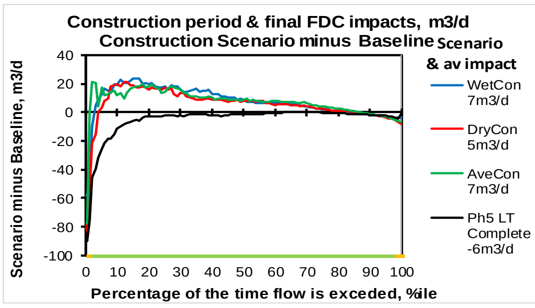

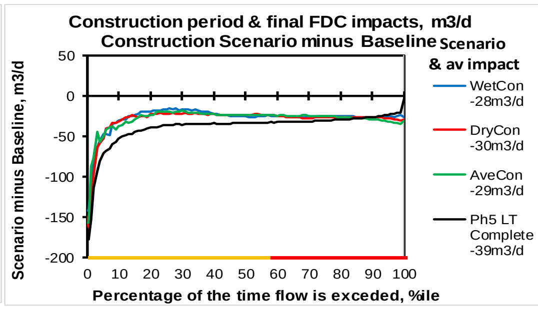

TG4

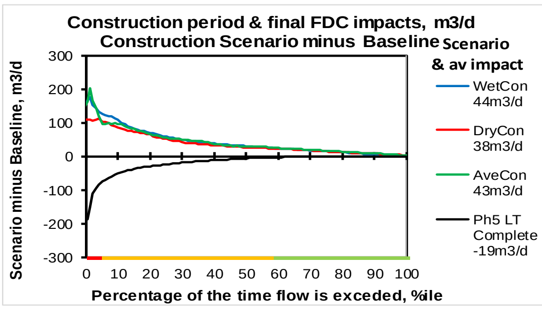

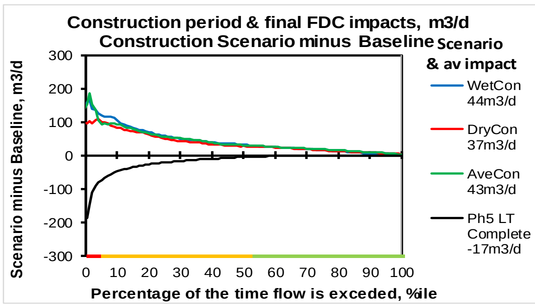

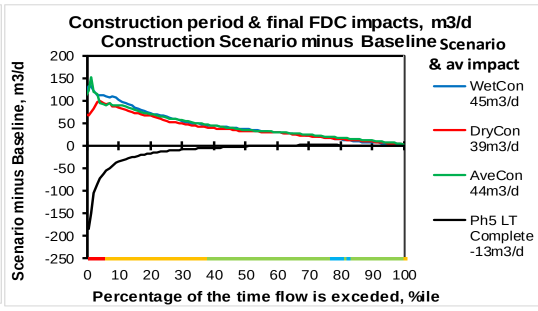

TG5

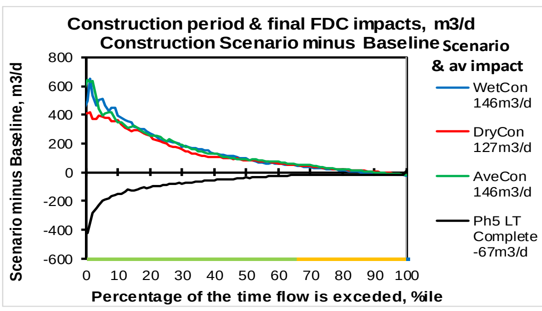

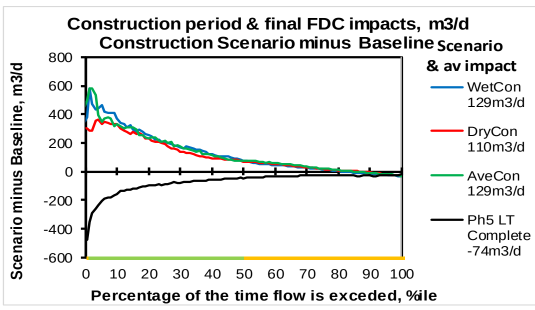

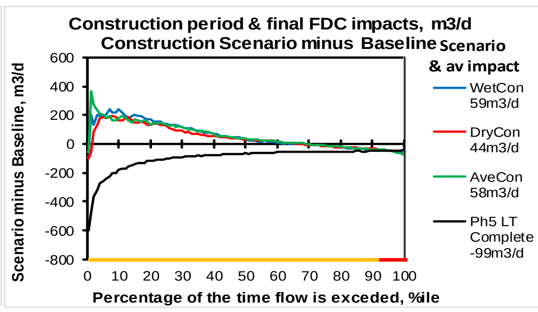

Appendix F
Digital results file listing

NOT PROTECTIVELY MARKED